π-Loaded Rhenium Complexes

A thesis presented in partial fulfilment of the requirements for the degree of

Doctor of Philosophy
in
Chemistry

at Massey University, Palmerston North, New Zealand

Andrew John Steedman
2000

This is dedicated to my life long companion,
Jacqueline Marie

Abstract

A range of rhenium(VII) tris(imido) complexes, $XRe(NR)_3$ (X=Me_3SiO, R=Ar'; X=Cl, R=Ar', mes, Ar), have been synthesized either from $[ReO_4]^-$, RNH_2 (R=Ar', mes, Ar), Et_3N and Me_3SiCl or $Re(NR)_2Cl_3(py)$, RNH_2 (R=Ar', Ar) and Et_3N. An X-ray crystal structure of $Me_3SiORe(NAr')_3$ and $ClRe(NAr)_3$ showed a slightly bent Re-N-C angle (158.8(5)° and 168.8(7)° respectively) and short Re-N distances (1.749(6)Å and 1.758(7)Å). Mixed tris(imido) complexes, $ClRe(NR)_2(NR')$ (R=Ar, R'=Ar, *p*-tol; R=Ar, R'=Ar, *p*-FC_6H_4, *p*-$NO_2C_6H_4$, *p*-tol, AMP, *o*-ClC_6H_4, *m*-ClC_6H_4, *o*-$^tBuC_6H_4$) have been synthesized from $Re(NR)_2Cl_3(py)$ (R=Ar', Ar), $R'NH_2$ (R'= Ar, *p*-tol, Ar', *p*-FC_6H_4, *p*-$NO_2C_6H_4$, AMP, *o*-ClC_6H_4, *m*-ClC_6H_4, *o*-$^tBuC_6H_4$) and Et_3N. An X-ray crystal structure of $ClRe(NAr)_2(NAr')$ showed near linear Re-N-C angles (165(2)-172.5(19)°) and short Re-N distances (1.70(2)-1.766(19)Å). The crystal structure of $ClRe(NAr)_2(N\text{-}o\text{-}^tBu)$ showed 2 near linear Re-N-Ar angles (172.4(2)° and 171.2(2)°) and one bent Re-N-*o*-^{t}Bu angle (160.8(2)°). Intermolecular imido ligand exchange was shown to occur slowly at room temperature between NAr' and Nmes. However, exchange between NAr' and NAr required heating to 60°C for exchange to occur. A chiral tetrahedral complex, $ClRe(NAr')(NAr)(N\text{-}o\text{-}^tBu)$, was synthesized from $Re(NAr')(NAr)Cl_3(py)$, *o*-$^tBuC_6H_4NH_2$ and Et_3N. Alkyl/aryl derivatives of the mixed tris(imido) complexes, $R''Re(NR)_2(NR')$ (R=Ar', Ar, R'=Ar', Ar, R"=Me, *p*-tol, CH_2Ph), have been synthesized from $ClRe(NR)_2(NR')$ (R=Ar, R'=Ar'; R=Ar', R'=Ar) and the Grignard, R"MgX (R"=Me, *p*-tol, X=Br; R"=CH_2Ph, X=Cl). An X-ray crystal structure of $MeRe(NAr)_2(NAr')$ showed near linear Re-N-C angles (168.5(3)-171.2(3)°) and short Re-N lengths (1.753(4)-1.763(4)Å). The Re-N-Ar' angle was found to be ~10° larger than those found for tris(Ar'-imido) Re(VII) tetrahedral complexes. An oxo-bridging species, $[Re(NAr)_2(p\text{-tol})(\mu\text{-}O)]_2$, was isolated presumably from the hydrolysis of *p*-$tolRe(NAr)_3$. The crystal structure of $[Re(NAr)_2(p\text{-tol})(\mu\text{-}O)]_2$ showed the rhenium atoms to be in a distorted square pyramidal geometry, as indicated by the Re-O bond distances (1.948(2) and 1.985(3)Å). Bis(imido) complexes, $Re(NR)(NR')Cl_3(py)$ (R=Ar', R'=Ar', Ar; R=R'=Ar), were synthesized from $ClRe(NR)_2(NR')$ (R=Ar', R'=Ar', Ar; R=Ar, R'=Ar', Ar) and pyHCl. An X-ray crystal structure of $Re(NAr')_2Cl_3(py)$ showed near linear Re-N-C angles (171.8(12) and 174.4(3)°) and short Re-N distances (1.734(18) and 1.760(14)Å). The Cl ligands in the *cis* positions to the imido ligands are bent away from the imido ligands at an angle of 166.10(19)°. Amido complexes, *p*-$tolNHRe(NR)(NR')(NR")$, have been synthesized from $ClRe(NR)(NR')(NR")$

(R=R'=Ar, R"=Ar, *o*-^{t}Bu; R=Ar, R'=Ar', R"=*o*-^{t}Bu) and LiNH*p*-tol. An X-ray crystal structure of *p*-tolNHRe(NAr)$_3$ showed a bent Re-NH-C angle (129.6(3)°) typical of amido nitrogens. A range of Re(V) tris(imido) complexes, $[Re(NR)_2(NR')]^-$ (R=R'=Ar'; R=Ar, R'=Ar', Ar, *o*-^{t}Bu), have been synthesized from $XRe(NR)_2(NR')$ (X=Me_3SiO, Cl) and elemental sodium. These anions were found to be very sensitive both in solution and as solids. An X-ray crystal structure of $[Re(NAr')_3]^-$ showed the complex to possess a 2-fold axis of symmetry through one of the imido ligands. The counter ion was found to be Na^+ with 6 coordinated molecules of thf. The anions were found to react with $ClSnMe_3$ and $ClAuPPh_3$ to form Re-Sn ($Me_3SnRe(NAr)_2(NR)$, R=Ar', Ar, *o*-^{t}Bu) and Re-Au ($Ph_3PAuRe(NR)_2(NR')$, R=R'=Ar'; R=Ar, R'=Ar', Ar) complexes respectively. The crystal structure of $Me_3SnRe(NAr)_3$ and $Me_3SnRe(NAr)_2(NAr')$ showed near linear Re-N-C angles (170.2(5)-172.9(2)°) and short Re-N distances (1.752(6)-1.779(3)Å). Rhenium(VI) dimeric complexes were synthesized from the anion, $[Re(NR)_2(NR')]^-$ (R=R'=Ar'; R=Ar, R'=Ar', Ar, *o*-^{t}Bu) and ferrocenium, $[Cp_2Fe]^+$. Both $Re_2(NAr')_6$ and $Re_2(NAr)_4(NAr')_2$ contain bridging imido ligands, while $Re_2(NAr)_6$ and $Re_2(NAr)_4(N\text{-}o\text{-}^tBu)_2$ contain only terminal imido ligands, as indicated by proton NMR. An X-ray crystal structure of $[Re(NAr')_2(\mu\text{-}NAr')]_2$ showed slightly bent terminal imido angles (156.2(3) to 168.8(3)°), short Re-N(terminal) distances (1.750(4) to 1.763(3)Å) and typical Re-N(bridging) distances of 1.951-1.959(4)Å. The average Re-Re distance of 2.735(4)Å indicates a weak metal-metal interaction. The crystal structure of $Re_2(NAr)_6$ showed the complex adopts an ethane-like geometry with the imido ligands arranged in a staggered orientation. The Re-Re bond lies on a crystallographic S_6 axis. A Re(VII) cation, $[Re(NAr)_3]^+$, is implicated on the basis of formation of a ferrocene complex, $(C_5H_5)Fe(C_5H_4)Re(NAr)_3$.

Acknowledgements

During the course of this work, a number of people have provided contributions, whom I would like to acknowledge. First, I thank my supervisor Prof. Tony Burrell for his guidance and dedication for this research. Second, I would like to thank the people of B403/B406 especially Warwick Belcher (use of Sky TV) and Gavin Collis for their advice. Third, I would like to thank John Allen and his team at the Hort Research Mass Spectrometry Facility and the people of the microanalytical lab at Otago University for elemental analysis data.

A special thanks goes to Steven Kennedy, who provided the much needed distractions over the past few years.

Finally, I would like to thank the Marsden Fund for providing financial support.

Table of Contents

Chapter Two: Synthesis of Re(VII) Complexes 70

Chapter Three: Reactivity of Re(VII) Complexes 115

Appendix I: General experimental procedures, details regarding the instrumentation used and preparation of precursors 197

Appendix II: Tables of selected bond lengths and angles of structurally characterized complexes reported within this thesis 212

List of Figures

List of Tables

List of Schemes

Abbreviations

ada	adamantyl
AMP	2-amino,6-methylpyridine
Ar	2,6-diisopropylphenyl
Ar'	2,6-dimethylphenyl
Ar*	2,6-dichlorophenyl
bipy	2,2'-bipyridine
br	broad
Bu	butyl
Cat	catecholate ($C_6H_4O_2^{2-}$)
Cp	cyclopentadienyl
Cp*	pentamethylcyclopentadienyl
d	doublet
DME	1,2-dimethoxyethane
Et	ethyl
hep	heptet
J	coupling constant in Hz
L	ligand
L_n	n number of ligands
M	metal
m	multiplet
m-Cl	*m*-chlorophenyl
Me	methyl
mes	2,4,6-trimethylphenyl
^{n}Bu	butyl
NMR	nuclear magnetic resonance
Np	neopentyl (CH_2CMe_3)
o-Cl	*o*-chlorophenyl
o-^{t}Bu	*o-tert*-butylphenyl
OTf	triflate ($OSO_2CF_3^-$)
o-tol	*o*-methylphenyl
p-F	*p*-fluorophenyl
Ph	phenyl
p-NO_2	*p*-nitrophenyl
PPN	$[Ph_3P{=}N{=}PPh_3]^+$
p-tol	*p*-methylphenyl

py	pyridine
R	organic group
s	singlet
Si*	Si^tBu_3
t	triplet
^{t}Bu	*tert*-butyl
thf	tetrahydrofuran
TM	transition metal
tmed	N,N,N',N'-tetramethylethylenediamine
TMS	trimethylsiloxy
VB	valance bond
X	anionic ligand

Chapter One

Introduction to the chemistry of π-loaded imido complexes

Introduction

For some years now transition metal imido chemistry has been a rapidly growing area of research.[1] Imido complexes have found application in the catalytic hydroamination of alkynes[2] and the synthesis of various nitrogen heterocycles[3,4] and as support ligands in olefin metathesis.[51,115] Although traditionally considered inert, highly reactive $L_nM{=}NR$ species have been generated that can engage in the activation of C-H bonds[5,6,20] and in cycloaddition reactions with unsaturated organic substrates.[3,4,6-11] One conventional feature of these reactive compounds is a coordination sphere containing multiple π-donor ligands, a feature that has aroused interest in "π-loaded", multiple imido complexes.[12-21]

Imido complexes possess a multiple bond between nitrogen and a metal and formally arise from coordination of nitrene, i.e. $L_nM(NR)$.[1] π-loaded imido chemistry has attracted interest for two reasons. First, the imido ligand (NR^{2-}) allows stabilization of high formal oxidation states. Second, putting sufficient electron density on the imido nitrogen boosts the reactivity of these typically inert ligands.[1,20-22] Oxo ligands also stabilize high oxidation states and can activate C-H bonds, but the imido ligand has the advantage in that varying the electronic and steric nature of R gives exquisite control over the properties of the resulting complex.

One new strategy for novel imido chemistry involves repeated coordination of imido ligands to a single metal center for which Wigley has coined the term "π-loading".[14] Multiple coordination of hard ligands such as NR^{2-} should help to further stabilize high oxidation states. Additionally, coordination of more than one strongly π-bonding ligand will lead to increased competition for metal dπ-Npπ bonding and hence weakened π-bonding. Since many reactions of imidos proceed through cleavage of the M-N π-bond one can propose that π-loaded poly(imido) complexes may possess greater potential reactivity versus mono(imido) analogues. Wolczanski[23] and Horton[24] have studied d^0

bis(imido) complexes of tantalum and vanadium, respectively, and demonstrated their ability to activate methane. Cundari has compared methane activation by d^0 3-coordinate group IVB bis(amido)imido and group VB amidobis(imido) complexes.[25] The results are inconclusive about the efficacy of π-loading for yielding more potent methane activators, but suggest that further π-loading beyond that in a bis(imido) complex may yield interesting chemistry.

Tris(imido) Complexes

The logical extension of the π-loading strategy is coordination of 3 imido ligands to a single metal. To date no one has isolated a 3-coordinate, d^0 tris(imido) complex, although Wigley has isolated a PPh_2Me adduct of $W(NAr)_3$[14] and PMe_3 adduct of $Mo(NAr)_3$.[28] Three coordinate, d^2 tris(imido) complexes have been isolated. Schrock *et al.* have structurally characterized $Os(NAr)_3$,[26,27] and the anion, $[Re(NAr)_3]^-$.[19,12] The technetium analogue of the anion has also been studied and displays higher reactivity but was not structurally characterized.[17] Four coordinate complexes of the form $XM(NR)_3$, where X is typically a univalent ligand, are well known. The majority of these complexes incorporate metals from the manganese triad. Herrmann *et al.* have recently studied oxo/imido complexes of heptavalent rhenium,[1c,21] also Wilkinson and coworkers have published extensively on the synthesis, reactivity and structure of rhenium tris(imido)[29,30] and manganese tris(imido) complexes.[31,32] The Bryan group has studied the chemistry of technetium tris(imido) complexes.[17,33,16]

Studying $XM(NR)_3$ compounds allows , in essence, investigation of "trapped" tris(imido) transients of potential interest as methane activating complexes.

Synthetic methods

Isocyanates have been oberved to react with M=O in metathesis reactions to introduce imido ligands (Equ. 1 and Equ. 2).[22,26]

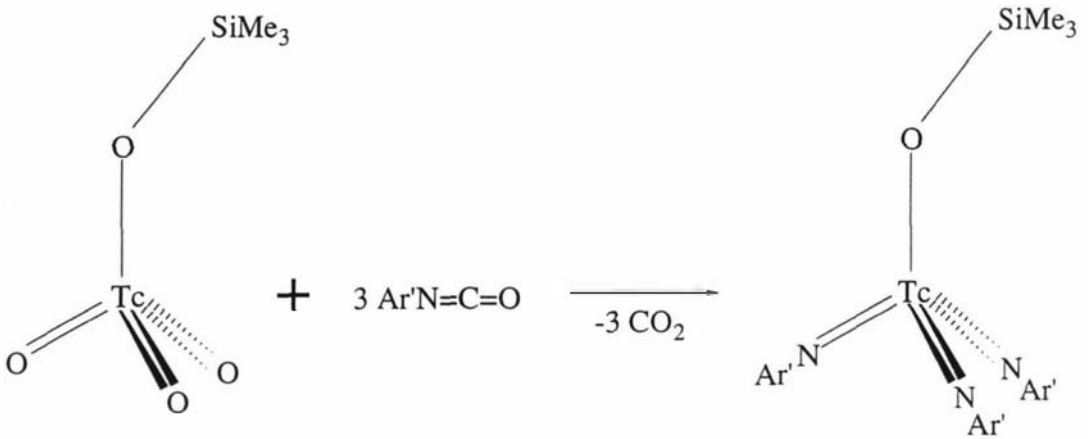

Equation 1

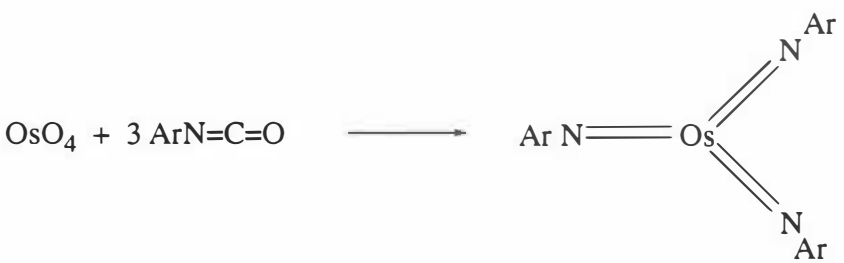

Equation 2

However, this reaction can be problematic as some imido complexes react with isocyanates. Thus, the synthesis of $Me_3SiOTc(NAr')_3$ can be complicated by the formation of the urylene complex shown in Figure 1.

Careful control of the reation conditions is required to avoid formation of the urylene complex. However, reaction of ArNCO with $Me_3SiOTcO_3$ produces only the tris(imido) complex, $Me_3SiOTc(NAr)_3$, suggesting that the steric bulk about the nitrogen is critical to the success of this reaction.[22] The reaction of ArNCO with OsO_4 formed the first example of a 3-coordinate d^2 tris(imido) complex, $Os(NAr)_3$. An X-ray study showed the complex to be of planar trigonal geometry.[26]

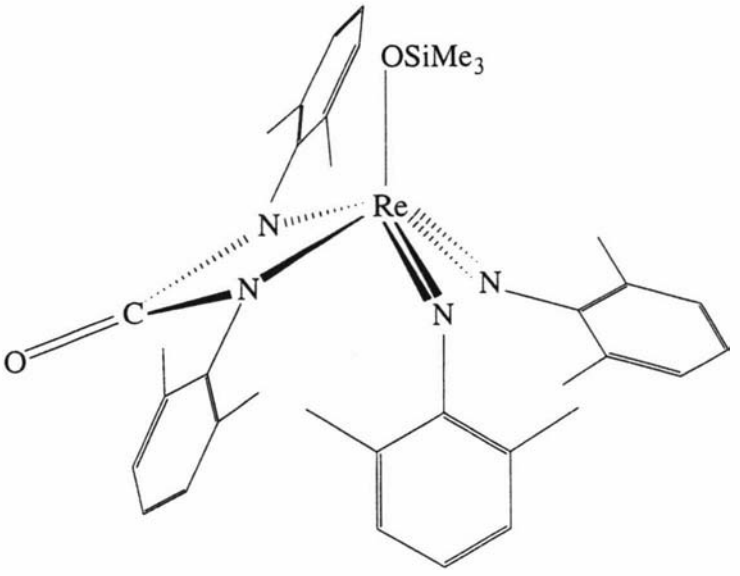

Figure 1

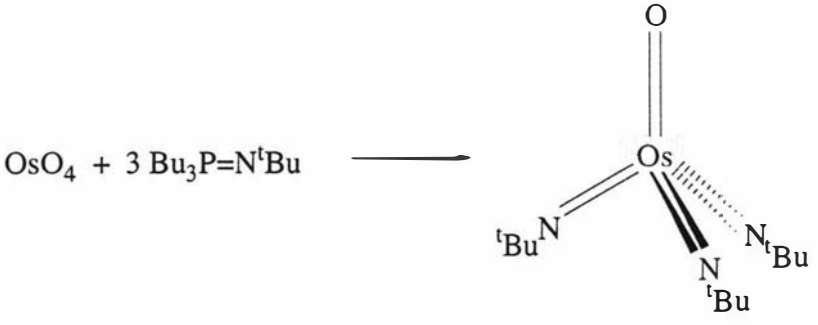

Equation 3

Another reaction of OsO_4 is with a phosphinimine, $Bu_3P{=}N^tBu$, to result in a tris(^{t}Buimido)oxo osmium(VIII) complex (Equ. 3). This complex was found to react with monosubstituted and trans-disubstitiuted olefins to give *cis* vicinal diamines as the major products (Fig. 2).[34]

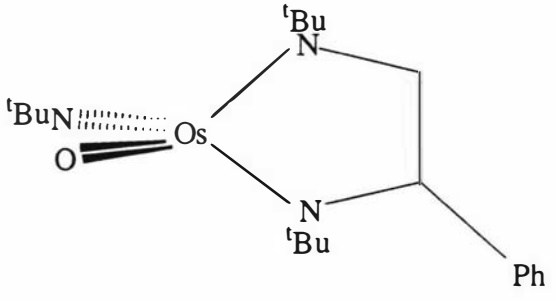

Figure 2

Use of 4 equivalents of LiNHmes towards a Cr bis(imido) complex leads to an amidotris(imido) complex. Interaction of $(mesN)_2CrCl_2$ with 4 equivalents of LiNHmes (Equ. 4) affords $[Cr(Nmes)_3(NHmes)][Li(Et_2O)_2]$ in moderate yields as red-brown air sensitive crystals.[103]

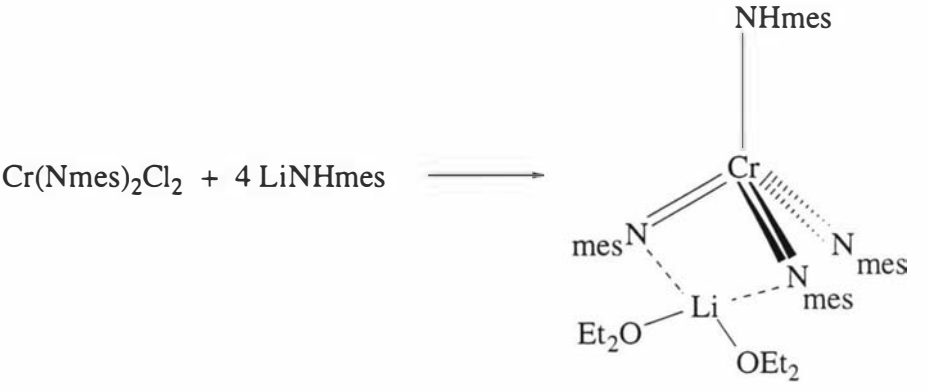

Equation 4

Upon reaction of $W(NAr)_2Cl_2(thf)_2$ with 2 equivalents of LiNHAr in thf, yellow $[Li(thf)_4][W(NAr)_3Cl]$ is obtained in high yield (Equ. 5). The structure of the $[W(NAr)_3Cl]^-$ anion reveals that the tungsten atom is tetrahedrally coordinated with three essentially identical imido nitrogen atoms.[14]

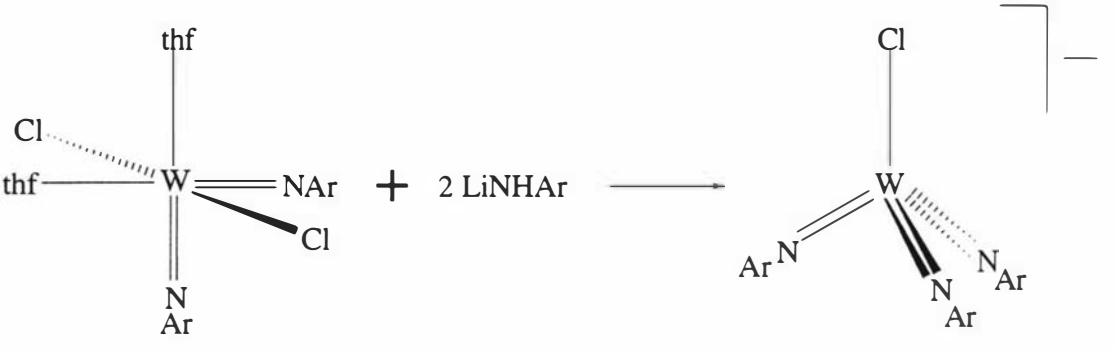

Equation 5

Interaction off a purple solution of $MnCl_3$ in acetonitrile, obtained from an oxoacetate and Me_3SiCl solution, with $^tBuNHSiMe_3$ at -35°C gives a low yield of green crystals of $MnCl(N^tBu)_3$ (Equ. 6).[31] The compound is stable towards air and water and the compounds thermal stability is remarkably different from that of $MnClO_3$ which detonates above 0°C.[14]

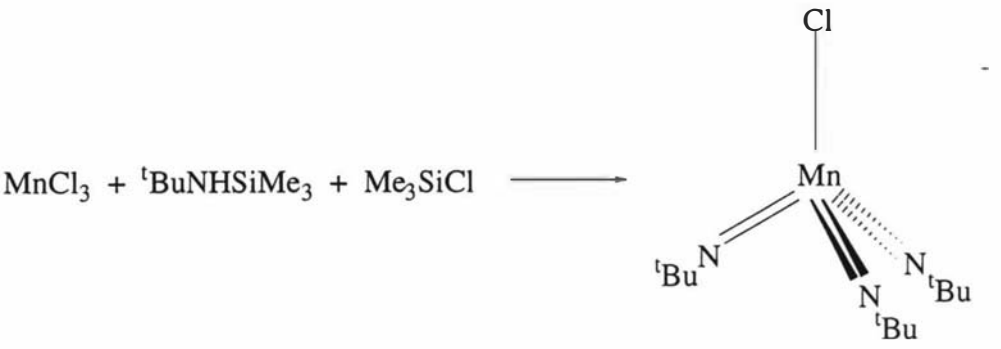

Equation 6

Deprotonation of an amido ligand to form the imido ligand is used in the synthesis of $[Nb(NAr)_3(NHAr)]^{2-}$.[44] Reaction of $[Nb(NAr)_2(NHAr)_2]^-$ with ^{t}BuLi afforded the amidotris(imido) complex (Equ. 7).

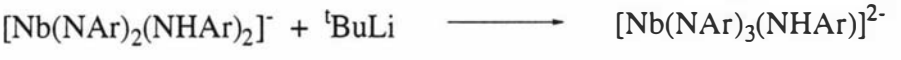

Equation 7

Recently, Wolczanski and Schafer II produced an amidobis(imido) complex of formulation $(^tBu_3SiN)_2(^tBu_3SiNH)WH$ from $NaW_2Cl_7(thf)_5$ and 6 equivalents of $^tBu_3SiNHLi$. This complex was then able to be deprotonated with excess KH to produce a now tris(imido) anion, $[(^tBu_3SiN)_3WH]K$ and H_2 (Equ. 8). The reactivity of primary halides with $[(^tBu_3SiN)_3WH]K$ provided evidence of alkane complexation.[20]

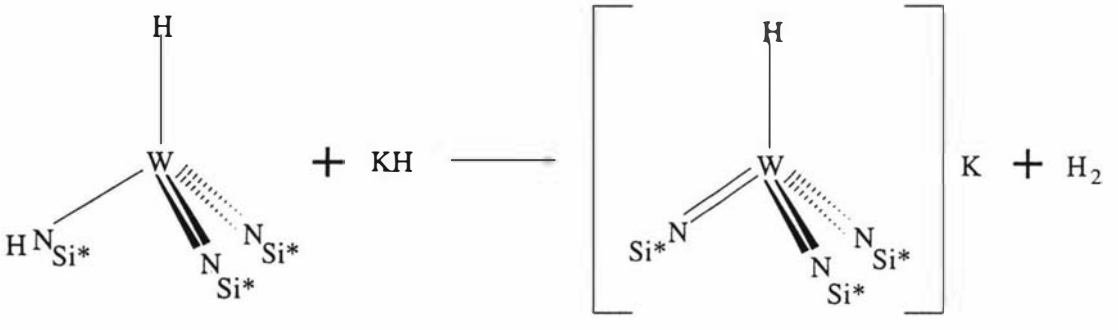

Equation 8

Structure and bonding

The imido ligand can be considered to bond to a transition metal with one σ and either one or two π interactions. Limiting valence bond (VB) description of this interaction is presented in figure 3, where the hybridization about the nitrogen and the metal ligand bond order are suggested to impose certain structural parameters on the imido ligand.[1a]

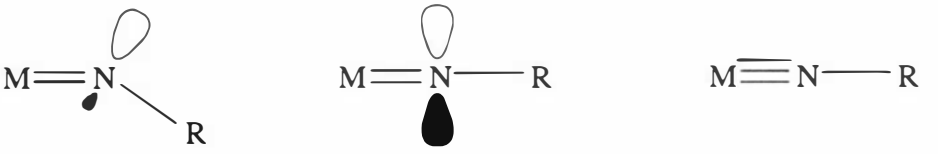

A	B	C
$N(sp^2)$	N(sp)	N(sp)
4 e^- donor	4 e^- donor	6 e^- donor

Figure 3

Structure A depicts an sp^2 hybridized nitrogen leading to a M=N double bond ($1\sigma,1\pi$) and a bent M-N-R linkage with the lone pair residing on the $N(sp^2)$ orbital. In the closed shell formalism, the imido dianion [NR^{2-}] behaves as a four electron donor. In structure B, the M=N double bond ($1\sigma,1\pi$) is maintined if symmetry restrictions (or perhaps a severe energetic mismatch with available metal orbitals) do not allow lone-pair donation. However, in most systems lone-pair p(π)-M(d) donation is very effective leading to a linear structure depicted in C and a M≡N bond order of three. In this case the imido dianion [NR^{2-}] is a formal six electron $1\sigma,2\pi$ donor to the metal.

Using these simple VB arguments, imido M-N bond lengths and M-N-R angles might be assumed to reflect the closest limiting structure from the localised bonding description. However, it has become apparent in recent years that attempts to correlate these structural parameters with M-N bond order or the number of electrons donated by these ligands is tenuous (see page 308). A MO approach is often required to understand simple structural preferences, M-N bond order, and other bonding features in imido compounds, particularly those with multiple strong π donor ligands.

Consider, for example, the trigonal planar molecule $Os(NAr)_3$, which contains Os-N-C angles of 178.0(5)Å and 180(3)Å.[26] Linear imido ligands are often taken as an indication that the ligands are donating their full complement of electrons to the metal, which would make $Os(NAr)_3$ a 20-electron complex. However, symmetry considerations reveal that one combination of nitrogen pπ orbitals (composed of the "in plane" set of π

orbitals) has a'_2 symmetry, and therefore has no corresponding metal d orbital with which to interact. The $Os(NAr)_3$ molecule is best considered an 18-electron complex and the maximum M-N bond order in this molecule is therefore 2.67 [i.e. $(3\sigma+5\pi)/3$].

Several theoretical studies of imido complexes have been reported. Investigations by Cundari and co-workers[35] have pointed to tris(imido) complexes that may display exceptional reactivity and potentially enable the isolation of a complex containing a coordinated methane. Seven model tris(imido) complexes ($Mo(NH)_3$, $W(NH)_3$, $[Ta(NH)_3]^-$, $[Tc(NH)_3]^+$, $[Re(NH)_3]^+$, $[Tc(NH)_3]^-$ and $Os(NH)_3$) were investigated to probe the effects of metal, charge and d orbital occupation on the potential energy surface (PES) for methane activation.[35] In the 20-electron d^2 tris(imido) complexes ($Os(NH)_3$ and $[Tc(NH)_3]^-$) a pair of electrons is located in a ligand based non-bonding MO for a planar coordination geometry; hence the preferred 18-electron arrangement about the metal is maintained (Fig. 4, 1a). The d^0 complexes are 18-electron complexes thus, there is no impertus to remain planar and they can pyramidalize (Fig. 4,1b). However if there is a weaker π-bonding ligand in a d^0 tris(imido), the electronic driving force for pyramidalization is lessened and steric preferences shift the energetic balance towards a planar geometry. This is seen in the d^o $[Ta(NH)_3]^-$ complex.[36,37]

1a 1b

Figure 4

The product of $[2\sigma+2\pi]$ addition to $M(NH)_3$ is $M(NH)_2(NH_2)(CH_3)$. Analysis of the molecular and electronic structure of the products (Fig. 5) and comparison with ECP data for tris(imido) reactants (Fig. 4) lead to two conclusions. First, metal-imido bonding in 2 (Fig. 5) is stronger than in 1 (Fig. 4). Second, metal-imido bonding is stronger in d^0 than in d^2 complexes. It would be differcult to quantify these effects, although it seems clear that conversion of an imido ligand in the activating complex to an amido in the product reduces competition for $d\pi$-$p\pi$ bonding. Thus the calculations suggest that π-loading may provide extra driving force for methane activation not only by reducing the π-bond energy of the metal imido bond in the reactant which cleaves the C-H bond, but also by affording a relatively greater strengthening of the spectator imido ligands in reactants.

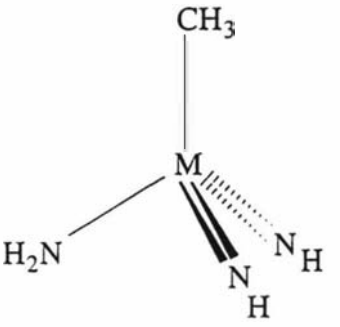

2

Figure 5

The combination of metric and wavefunction data suggest that methane will coordinate more strongly to a heavier transition metal (3rd transition series) and a complex with a positive charge. As seen previously[38] d^2 tris(imido) complexes do not bind methane, although the metal is highly electrophilic.

It is reasonable to question whether methane can coordinate to a realistic experimental model such as $[M(NAr)_3]^+$ given the steric requirements in $[M(NH)_3...HCH_3]^+$ and $[M(NAr)_3...HCH_3]^+$ are obviously very different. After successfully modeling $TcMe(NAr)_3$ (using computational methods calculated against X-ray data for $TcMe(NAr)_3$[39]) a methane adduct of $[Tc(NAr)_3]^+$ was investigated. The results showed that coordination of methane to a cationic tris(imido) complex of technetium is feasible from both an electronic and steric point of view. Given their similar properties a related rhenium complex would also appear to be a worthwhile experimental target for a relatively stable d^0 methane adduct.

A study of tris(imido) complexes (focusing on Tc-tris(imido) complexes of the formulation, $TcX(NR)_3$) is reported in which X-ray crystallography and computation methods are combined to probe the bonding in heavily π-loaded transition metal complexes.[39] Several interesting conclusions resulted from the work. The bonding in the tris(imido) complex is very sensitive to the X group. The metric parameter which is the best gauge for changes in electronic structure of the complex is the X-Tc-N imido angle. Subtle experimental variations are accurately reproduced by calculations for an entire series of X ligands from hard nucleophiles to soft metal electrophiles to 3-coordinate complexes in which no X ligand is present. X exerts the majority of its influence on the bonding in $MX(NR)_3$ through the σ framework.

The effects of π-loading can be observed in the structure of $Me_3SiOTc(NAr)_3$ and $ITc(NAr)_3$. All the Tc-N-C angles in $Me_3SiOTc(NAr)_3$ (<Tc-N-Cav=155.8Å) and $ITc(NAr)_3$ (>Tc-N-Cav=166.6Å) are bent significantly from 180°, falling within the range often obsered for complexes with multiple π-donors.[1b,14,16,29,48] The iodo complex is

closer to being linear at nitrogen than the siloxy complex, and $Me_3SiOTc(NAr)_3$ is very close to tetrahedral about technetium, $ITc(NAr)_3$ is distorted towards a trigonal based pyramid where the iodide occupies the apex. These differences are probably due to the greater electronic dominance of the imido ligands in $ITc(NAr)_3$ where there is less competition from the more weakly donating I^-.[22] Similar comparison of the structure for $Me_3SiOTc(NAr)_3$ and the urylene complex, shown in figure 6, suggest that replacement of an imido ligand with a urylene ligand allows the remaining imido ligands to donate more strongly.

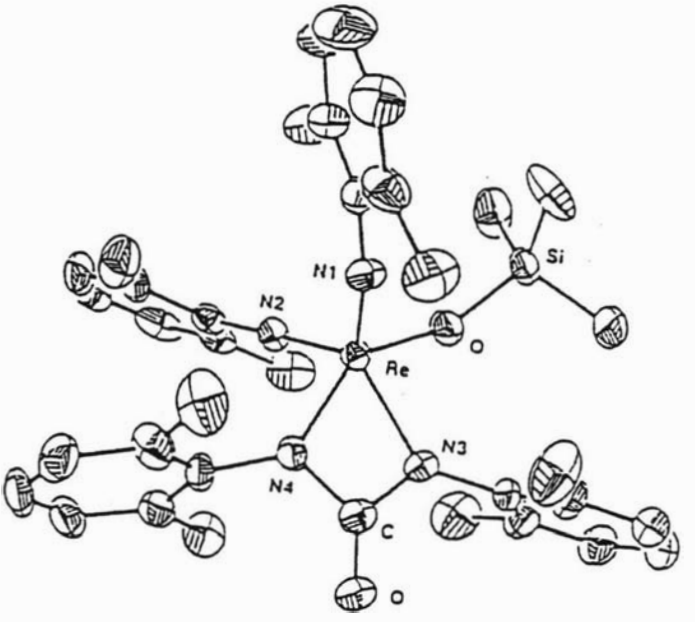

Figure 6

These three structures suggest that the imido ligands moderate their donor ability depending on donor strength of the other ligands.[22]

Reactivity

The reactivity of an imido ligand is a function of the metal, its oxidation state, the ancillary ligands and steric factors that may influence certain modes of reactivity. Despite their notoriety as inert ligands, highly reactive early transition metal[lb] moieties may be generated, even involving C-H activation[6,90] if sufficient electron density resides on the imido nitrogen.[90] For example $Zr(NHSi^tBu_3)_2(NSi^tBu_3)$ can activate C-H bonds as shown in Equation 9.

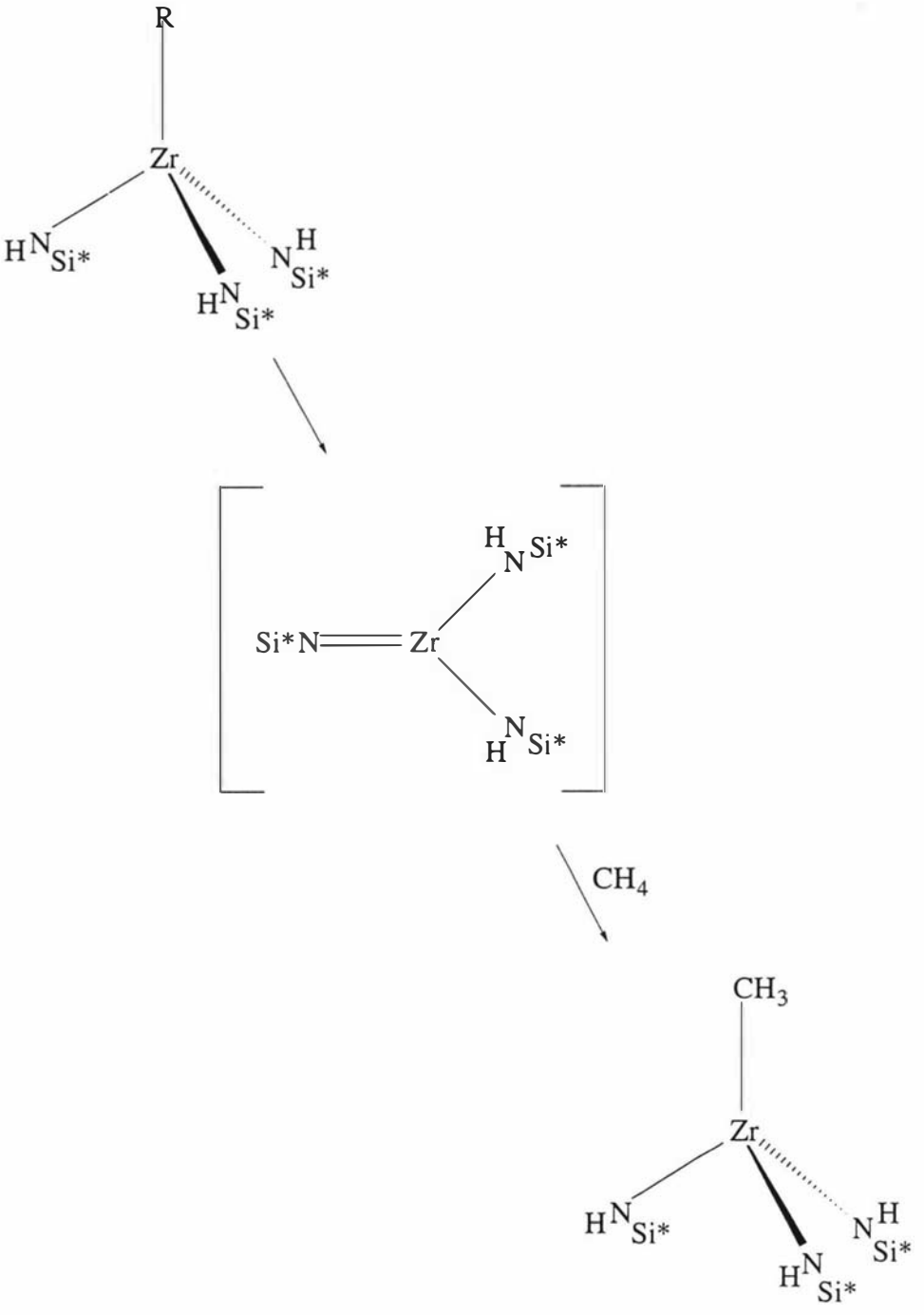

Equation 9

Reactions in which the imido ligands are spectators involve deprotonations and nucleophilic substitution. Wigley *et al.* expected BuLi to act as a base but instead the lithium reagent acted as a nucleophile, eliminating NHmes from the complex (Equ. 10).[44] However a stronger base, ^{t}BuLi, does deprotonate $[Nb(Nmes)_3(NHmes)]^{2-}$ to give the expected tetrakis(imido) complex (Equ. 11).[1a, page303]

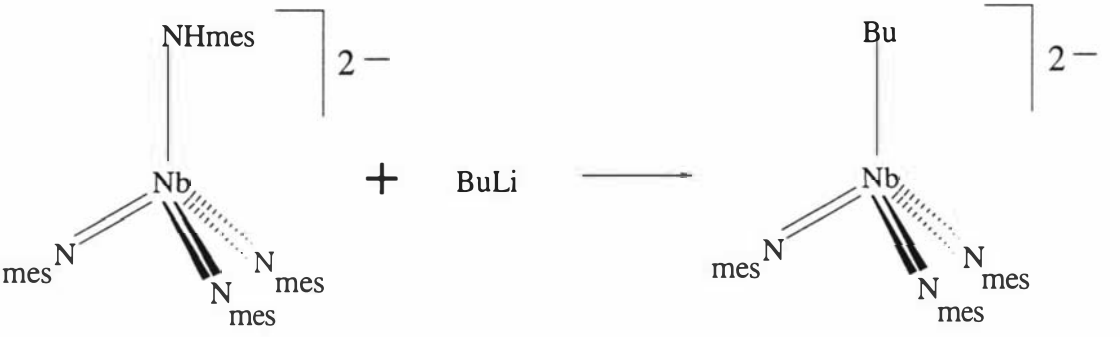

Equation 10

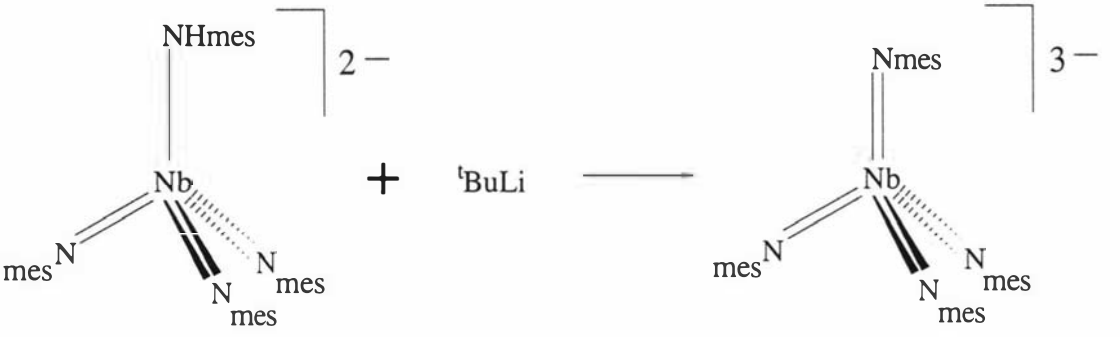

Equation 11

Protonation of an imido ligand by aniline resulting in imido/amido complexes (Equ. 12) is thought to be achieved by first displacement of Cl^- followed by an intramolecular α-H transfer (Equ. 13).[28] Reaction time is crucial for the successful isolation of the tris(imido) complex as H_2NAr is a by product of its synthesis.

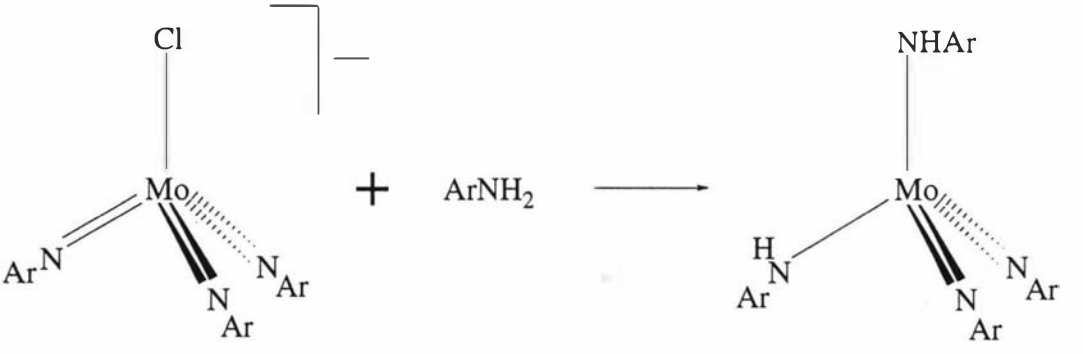

Equation 12

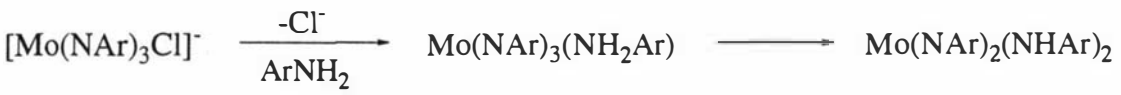

Equation 13

The chloride ion in $[Mo(NAr)_3Cl]^-$ is subject to nucleophilic displacement. Thus, $Mo(NAr)_3R$ can be obtained from reaction of $[Mo(NAr)_3Cl]^-$ with PMe_3, MeLi and $[Bu_4N]Br$ (Scheme 1).[28]

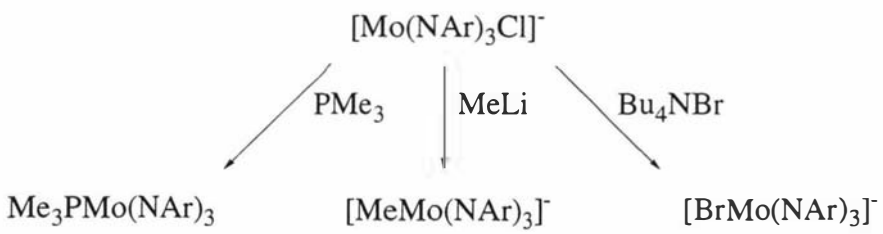

Scheme 1

The imido ligands of $[Mo(NAr)_3Cl]^-$ and $Mo(NAr)_3PMe_3$ are susceptible to electrophilic attack (Equ. 14 and Equ. 15).

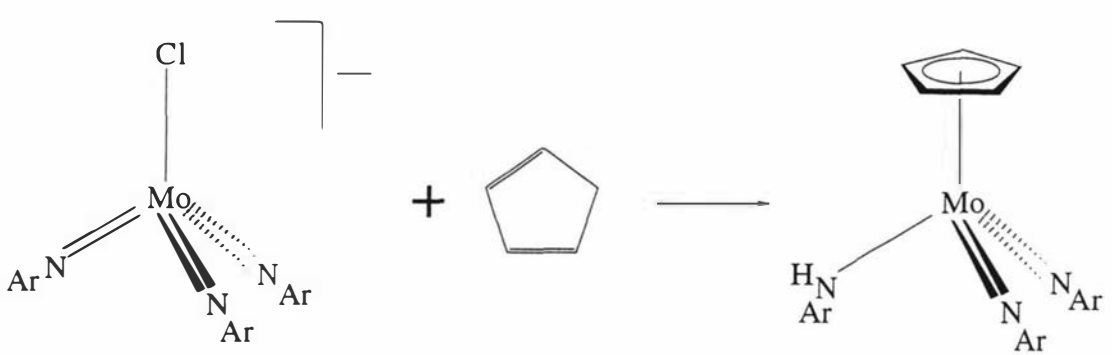

Equation 14

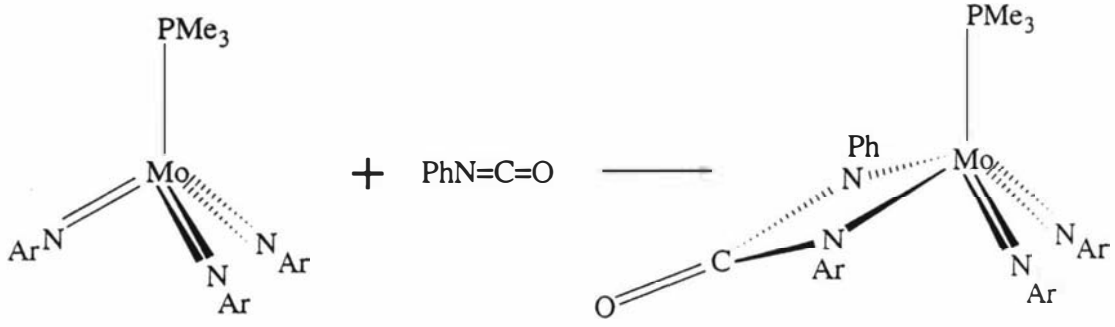

Equation 15

The cycloaddition reaction between PhNCO and a Mo=NAr bond in $Mo(NAr)_3PMe_3$ is observed to afford the metallacyclic complex given in Equation 15. Although excess PhNCO is used only one imido ligand reacted. The active proton of the cyclopentadiene monomer is also observed to attack an imido ligand (Equ. 14).[28] Since the imido dianion $[NR^{2-}]$ and the cyclopentadienyl anion $[C_5H_5^-]$ may both be described as $\sigma+2\pi$ donors, the metal center in $(ArN)_2Mo(NHAr)(Cp)$ appears to be π-loaded in much the same fashion as $[Mo(NAr)_3Cl]^-$. Therefore electronic restrictions seem to prevent the amido ligand in $(Cp)Mo(NAr)_2(NHAr)$ from effectively π-donating to this metal center.

Displacement of an imido ligand by HO^{t}Bu is observed in the reaction of $Mo(NAr)_3PMe_3$ with HO^{t}Bu (Equ. 16). This reaction presumably proceeds via $[Mo(NAr)_2(NHAr)(O^tBu)$, hence the amido ligand is more susceptible to electrophilic attack than the imido ligands in the same molecule.[40]

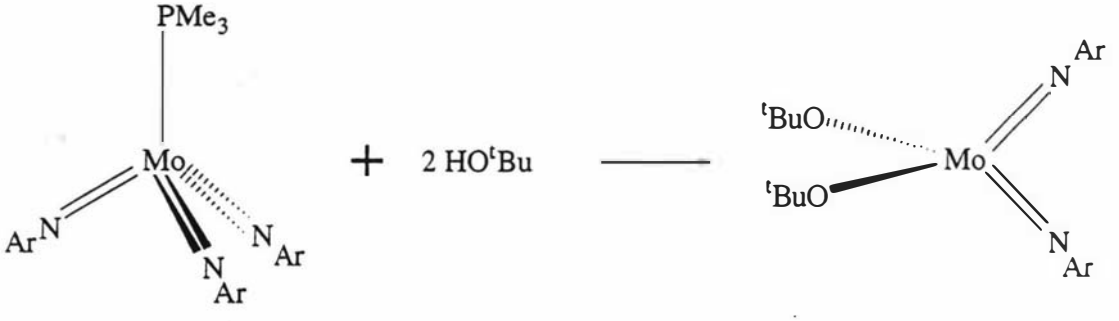

Equation 16

Metal-carbon bonds in early metal alkyl complexes are typically susceptible to electrophilic attack. Reaction of $[Mo(NAr)_3(CH_2{}^tBu)]^-$ with $[HNMe_3]BPh_4$ (Equ. 17) formed $Mo(NAr)_2(NHAr)(CH_2{}^tBu)$, hence the imido ligand is protonated, not the alkyl ligand.[28]

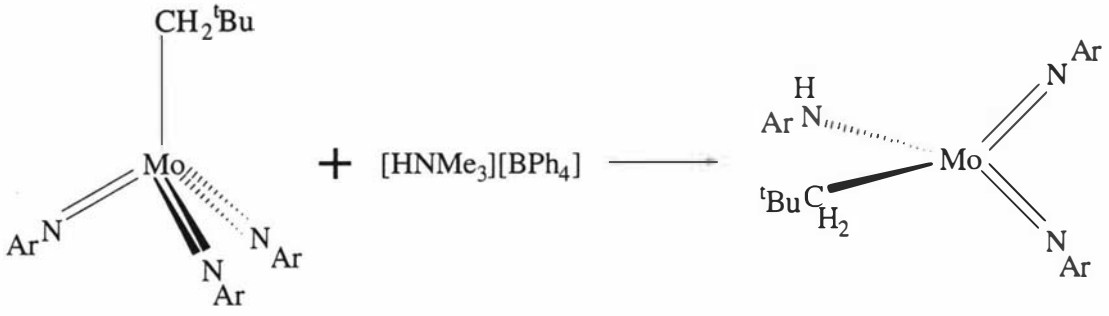

Equation 17

These reactions suggest that π-loading enhances the polarity of the Mo-N bonds in $[Mo(NAr)_3Cl]^-$ and renders the imido ligands more prone to electrophilic cycloadditions. $CpMo(NAr)_2(NHAr)$ constitutes one of a series of $M(\sigma+2\pi)_3$ compounds with 3-fold $\sigma+2\pi$ orbital symmetry. Evidence has been presented that suggests this combination of three $\sigma+2\pi$ ligands contributes 2 electrons less than the maximum possible, despite the loss of overall 3-fold molecule symmetry.[12,13] Accordingly the $[CpMo(NAr)_2]^+$ fragment is more properly described as a 16-electron species which restricts the $[NHR]^-$ ligand to σ bonding with this fragment.

One-electron reductions of d^0 $M(NR)_3X$ (M=Mn,Tc,Re) complexes results in d^1-d^1 dimers. Reactions of $MnCl(N^tBu)_3$ with NaHg lead to a brown dimer, $[(^tBuN)_2Mn(\mu\text{-}N^tBu)]_2$ (Fig. 7).[31]

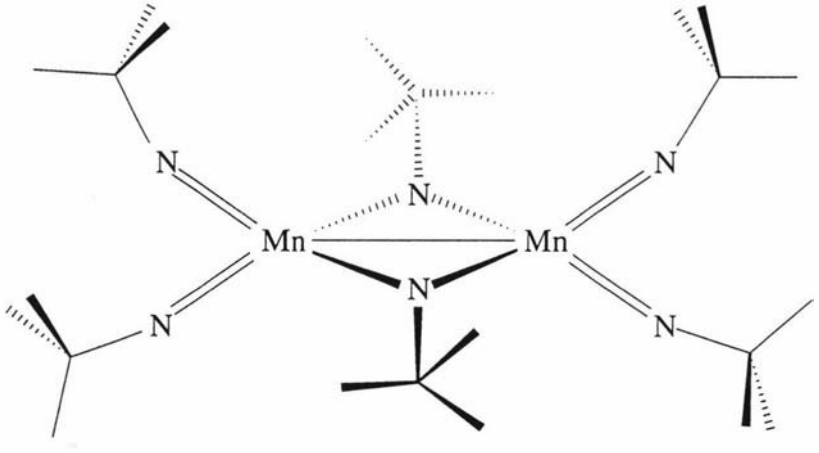

Figure 7

The tris(imido)iodo technetium(VII) complex, $ITc(NAr')_3$, is reduced by one equivalent of elemental sodium to give $Tc_2(NAr')_4(\mu\text{-}NAr')_2$ (Fig. 8), confirmed by X-ray structural analysis.[17]

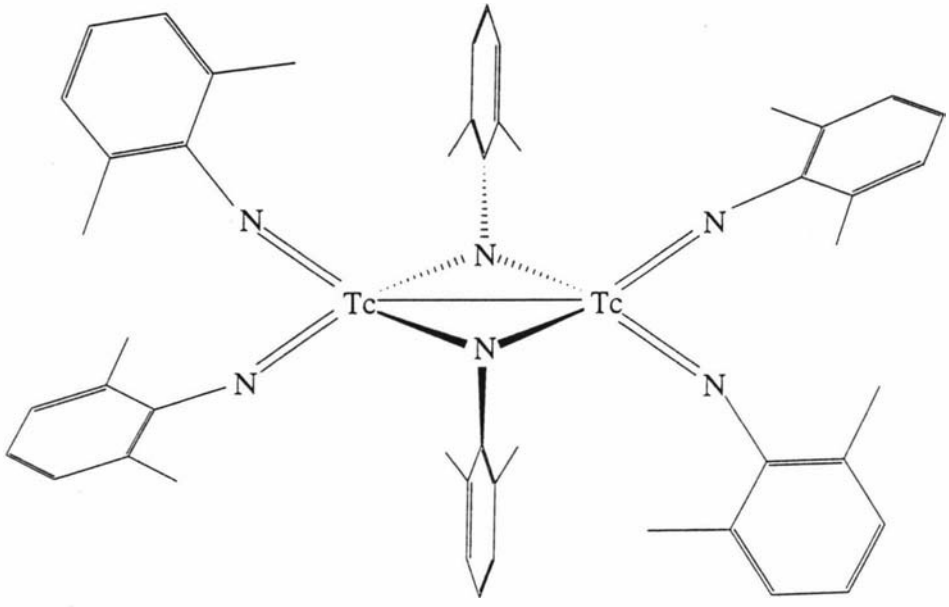

Figure 8

Use of a more sterically demanding ligand, such as 2,6-diisopropylphenylimido, forms a d^1-d^1 dimer as before. However the X-ray structural analysis revealed a technetium(VI) dimer with a staggered ethane-like geometry (Fig. 9).[17]

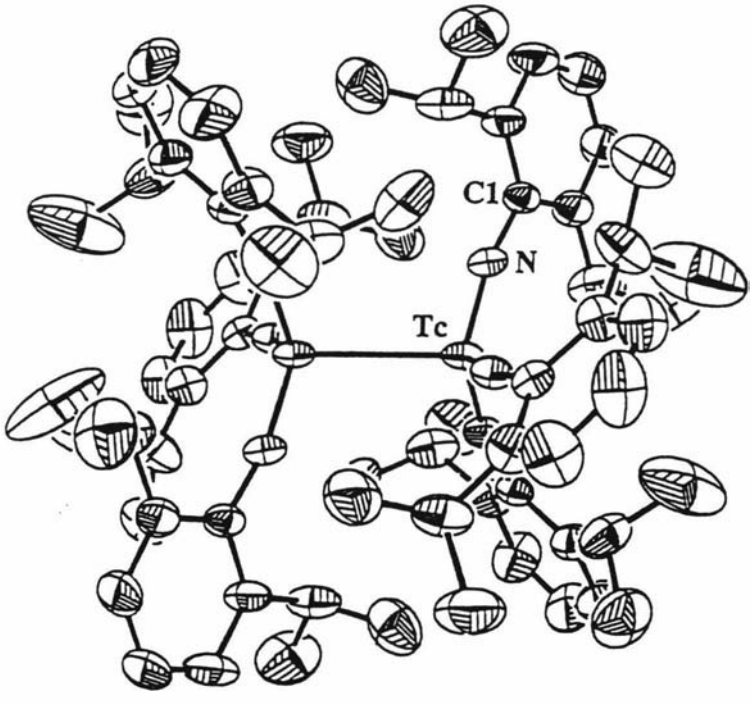

Figure 9

Nucleophilic attack on $Me_3SiOTc(NAr)_3$ by RMgCl resulting in $RTc(NAr)_3$ occurs readily for R=Me, Et, η^1-C_3H_5 and CH_2SiMe_3.[22] Since the trimethylsiloxy ligand in $Me_3SiOTc(NAr)_3$ is a good π-donor in a π-loaded complex, it may also exhibit nucleophilic character at oxygen. This is observed in the reaction of Me_3SiI with $Me_3SiOTc(NAr)_3$ (Equ. 18).[16,22]

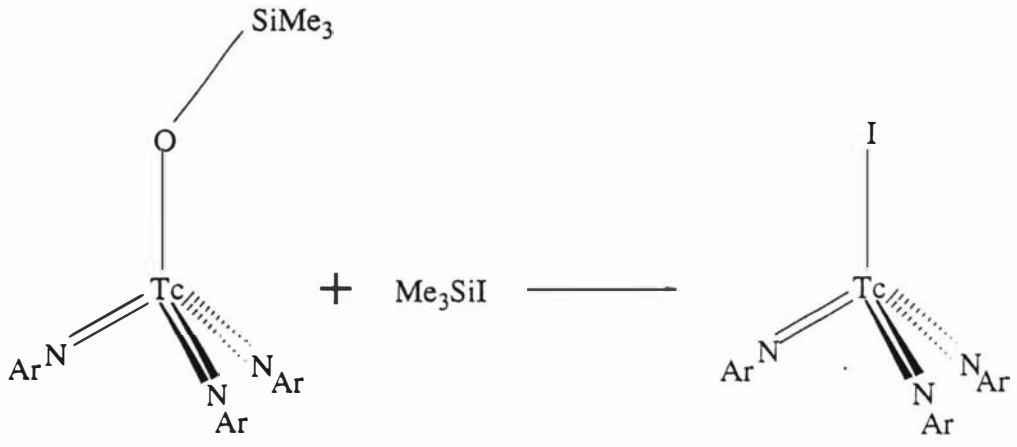

Equation 18

The reaction of equation 18 can be thought of as electrophilic attack of Me_3Si^+ at the siloxy oxygen.[22]

The tris(imido) fragment "$[Tc(NAr)_3]^{+n}$" imparts a high degree of stability to the normally oxidizing technetium(VII) center. For instance, electrochemical studies on tris(imido) complexes demonstrate that they are differcult to reduce. Also, the tris(imido)siloxy and tris(imido)alkyl complexes are stable towards air as solids for extended periods. The technetium tris(imido) fragment is even capable of stabilizing iodide, a ligand that is quite susceptible to oxidation.[1b,51] All of this contrasts strongly with known oxotechnetium(VII) complexes, which are generally more sensitive to moist air and unstable towards reduction.[45]

The coordination of multiple π-donors to a metal centre (π-loading) can result in increased stability of high valent metal centers and/or increased nucleophilicity of relatively inert ligands.[1b,44,46,15,27] This can be seen in $Me_3SiOTc(NAr)_3$ and its reactions.

The iodide in $ITc(NAr)_3$ can be displaced by Cp (from KCp) to produce $CpTc(NAr)_3$. It is believed due to the strong donor ability of the imido ligands, the Cp is η^1-coordinated.[41,42] The η^1 nature of the cyclopentadienyl ligand was conclusively demonstrated by X-ray structural analysis (Fig. 10).[16]

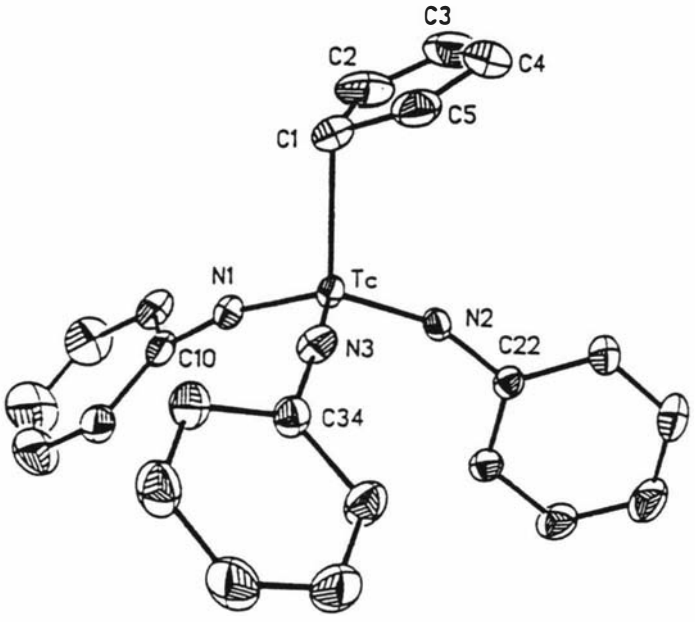

Figure 10

The d^2 monomer $[Tc(NAr)_3]^-$ is produced from $ITc(NAr)_3$ with 2 equivalents of Na or $Tc_2(NAr)_6$ with 1 equivalent of sodium per technetium.[17] Reactions of $[Tc(NAr)_3]^-$ with electrophiles are quite facile. Scheme 2 illustrates these reactions.

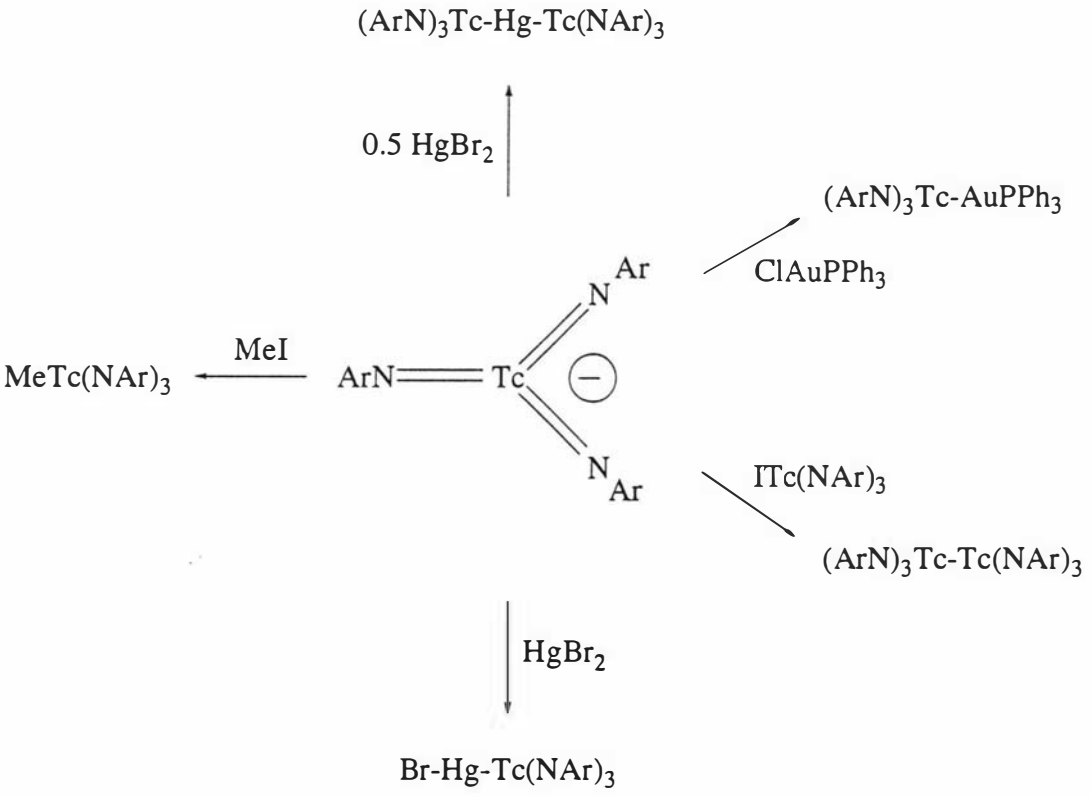

Scheme 2

Attempts to prepare the tris(arylimido) hydride complex "$(ArN)_3TcH$" from $[Tc(NAr)_3]^-$ and protic sources were unsuccessful. Treatment of $ITc(NAr')_3$ with 2 equivalents of sodium or $Tc_2(NAr')_4(\mu\text{-}NAr')_2$ with 1 equivalent of sodium (per technetium) leads to uncharacterized products.[17]

These complexes contain several strong π-donor ligands as such they are heavily "π-loaded". As a result of the competition between strong π-donor ligands, the imido ligands in these complexes are best represented by resonance structure A of Figure 11, where the metal-nitrogen bond order is lowered, bending at nitrogen maybe observed and electron density is displaced from the metal-nitrogen bond to the nitrogen atom making the imido ligand more nucleophilic at the nitrogen.[1b,44,46,15,27]

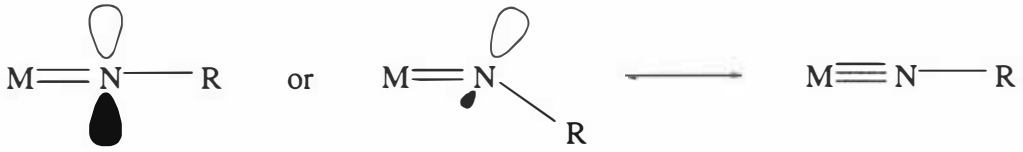

A B

Figure 11

π-loading can also be used to rationalize some of the reactivity illustrated here. Extra-electron density at the imido nitrogen is observed in the formation of the urylene complexes (Equ. 15 and reference 22) if the reaction is viewed as nucleophilic attack by an imido nitrogen on the isocyanate carbon.[49,50] Subsequent reaction of the remaining imido ligands with isocyanate, forming additional urylene ligands, is probably inhibited because the imido ligands in the urylene complex have less competition for π-electron density, are able to donate to technetium more strongly and are therefore less nucleophilic at nitrogen.[49]

The terminal imido ligands of $Tc_2(NAr')_4(\mu\text{-}NAr')_2$ can be substituted with methyl groups. Treatment of $Tc_2(NAr')_4(\mu\text{-}NAr')_2$ with 2 equivalents of MeMgCl results in the formation of $TcMe_2(NAr')(\mu\text{-}NAr')_2Tc(NAr')_2$ (Scheme 3). Further treatment with 2 equivalents of MeMgCl results in substitution of another terminal imido ligand.[43]

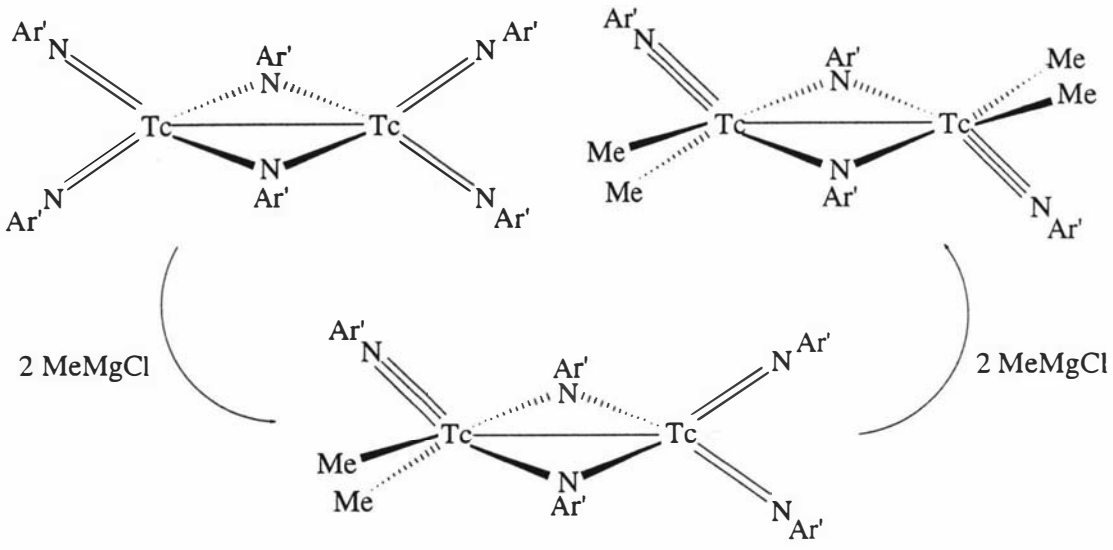

Scheme 3

Reductive elimination of an imido ligand was observed in the reaction of $Os(NAr)_3$ with PMe_2Ph to give $Os(NAr)_2(PMe_2Ph)_2$ and $ArN{=}PMe_2Ph$.[26] $Os(NAr)_3$ also reacts with Me_3NO to give $OsO(NAr)_3$ which can form a Os(VI) diamide complex with ethylene (Fig. 12), norbornene and cyclopentene.[26]

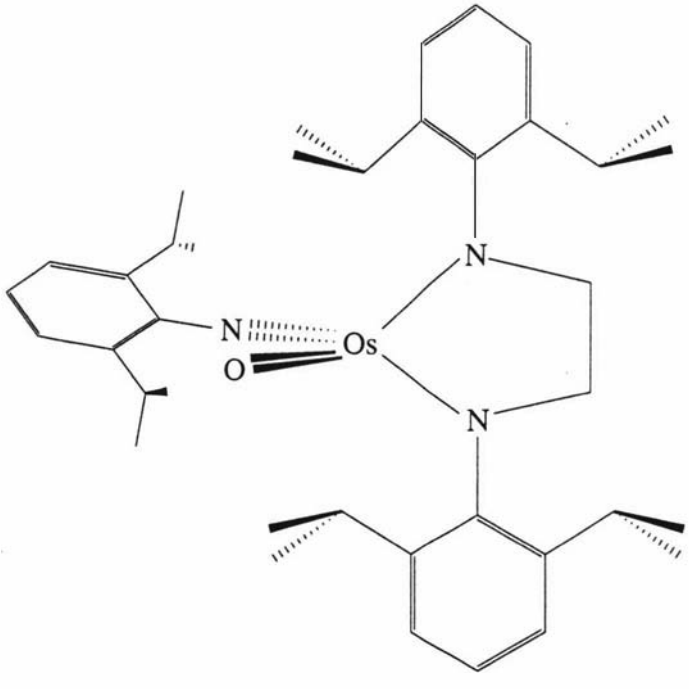

Figure 12

Sharpless and coworkers illustrated in 1977 the pronounced tendence for C-N bond formation in preference to C-O bond formation with the reaction of $OsO(N^tBu)_3$ with $PhCH{=}CH_2$ (Equ. 19).[34]

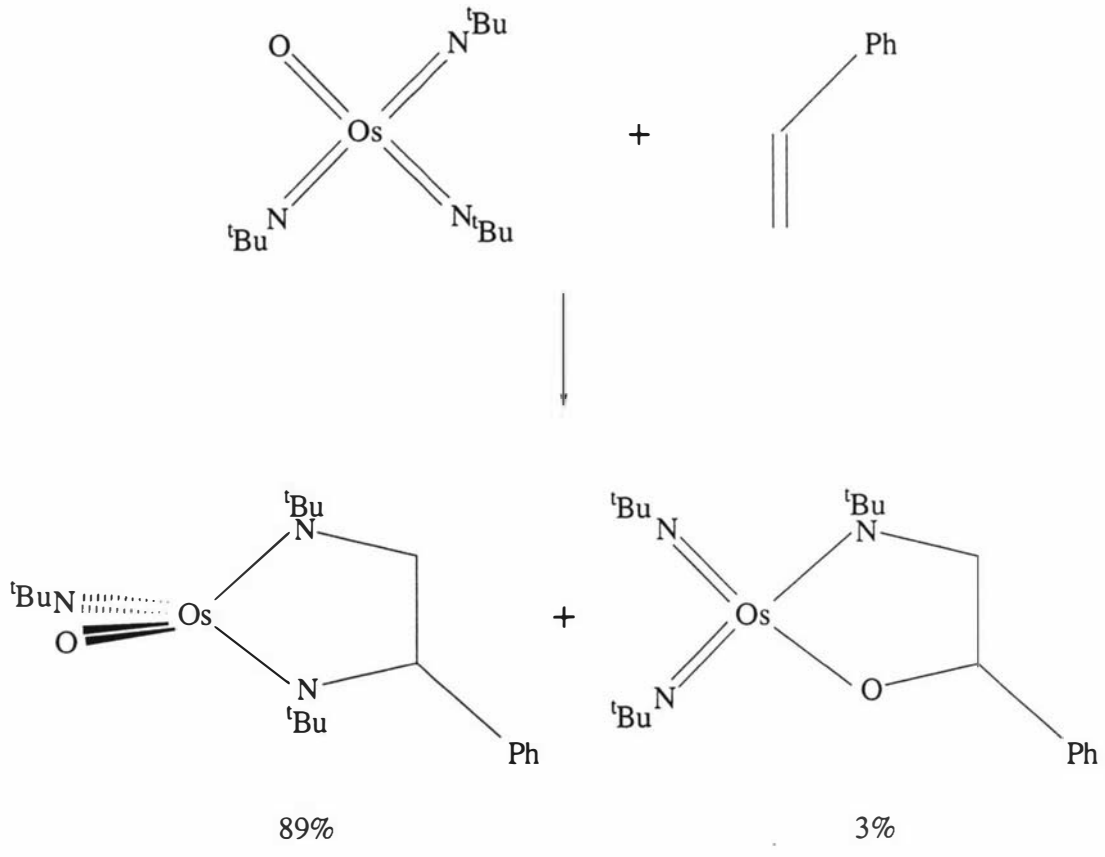

Equation 19

Steric considerations

Imido ligands have found an extensive use in high oxidation state transition metal inorganic and organometallic chemistry due in part to their variable steric requirements, ability to bridge more than one metal center and variable π-bonding capabilities.[1a,1b]

The one electron reduction of $ITc(NR)_3$ (R=Ar' or Ar) results in homoleptic arylimido complexes that can be formulated as $Tc_2(NR)_6$.[17] Examples of structurally characterized complexes of the general formula M_2E_6, where E is a dianionic ligand such as O^{2-}, S^{2-}, Se^{2-} or NR^{2-}, exhibit an edge-bridged tetrahedral dimeric structure (Fig.13).[30,52,53,54]

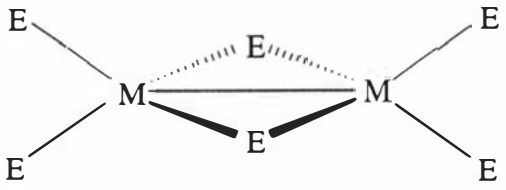

Figure 13

In contrast, M_2X_6 complexes, where X is a monoanionic ligand, typically adopt an ethane-like structure for bulky X (Fig.14) and an edge-bridged tetrahedral dimeric structure for non-bulky X.[55,56]

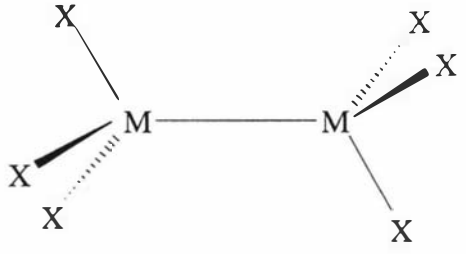

Figure 14

The dimeric complex, $Tc_2(NAr')_6$ was found to adopt the edge-bridged tetrahedral structure. Use of the sterically more demanding 2,6-diisopropylphenylimido (NAr) ligand provides similar reaction chemistry, but reveals somewhat different spectroscopic properties. X-ray structural analysis of a single crystal of $Tc_2(NAr)_6$ revealed a technetium(VI) dimer with a staggered ethane-like geometry.[17] This is the first ethane-like structure observed for a M_2E_6 complex. This result is suggestive that the bulky NAr ligand favours the non-bridging structure. The oberved Tc-Tc bond lengths for $[Tc(NAr)_3]_2$ (2.744(1)Å) are longer than that observed in $[Tc(NAr')_2(\mu\text{-}NAr')]_2$ (2.68(2)Å). This may be due to steric congestion between the imido groups around the ethane-like structure or to the technetium atoms being bridged.[17]

These results suggest that steric requirements may determine if d^1-d^1 M_2E_6 complexes will adopt an edge-bridged tetrahedral or ethane-like dimeric structures. Similar steric constraints imposed by the bulky 2,6-diisopropylphenylimido ligand have been observed in related imido complexes. For example, $Os(NAr)_3$ is a monomeric species,[26] whereas the less sterically demanding ligand *tert*-butylimido analogue exists as a dimer (Fig. 15).[54]

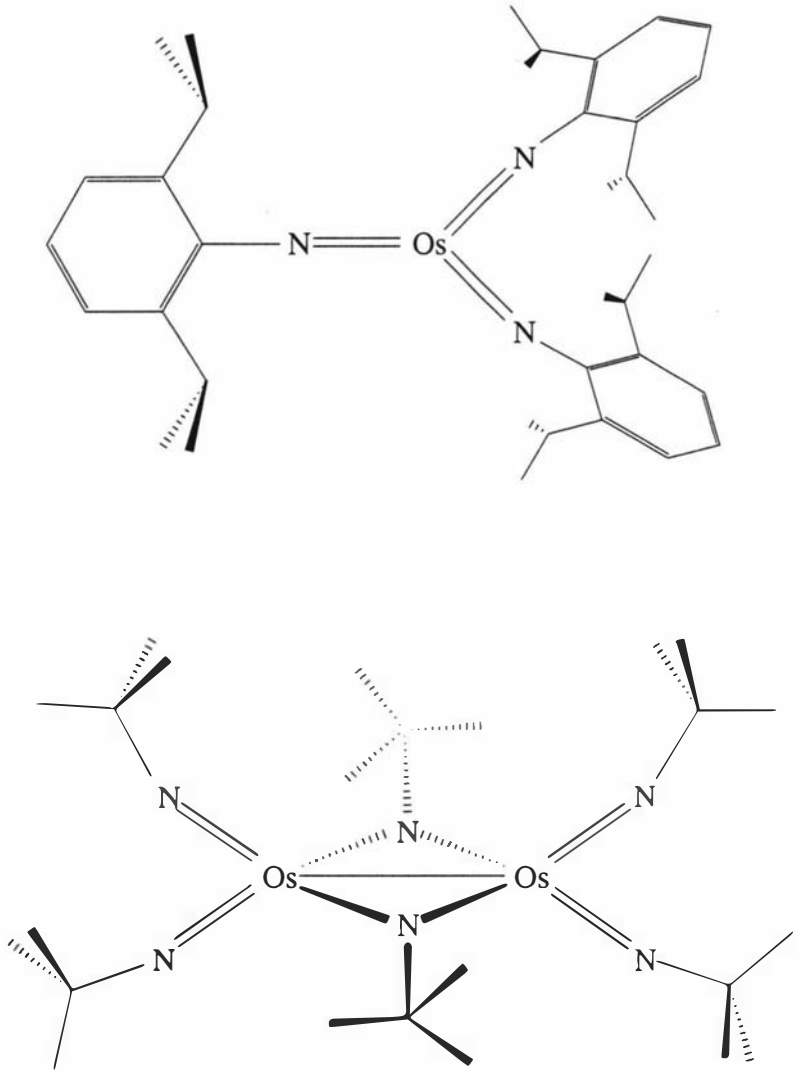

Figure 15

$Os(NAr)_3$ would not exist as a discrete monomeric complex without ligands that provide significant steric congestion.

This is not to say that the NAr ligand is incapable of bridging. There are at least three examples of complexes containing a bridging 2,6-diisopropylphenylimido ligand.[57,58,60] The complexes, $Tc_2(NAr')_6$ and $Tc_2(NAr)_6$ both contain arylimido ligands and are therefore essentially electronically identical. Hence the factors influencing the formation of either ethane-like or the more common edge-bridging tetrahedral dimer configurations appear to be purely steric.[17]

Sterics can play a role in the reactivity of complexes. The steric bulk of the arylimido ligand of $(\eta^5\text{-}Cp^*)_2U(N\text{-}2,4,6\text{-}tri\text{-}^tBu_3C_6H_2)$ affects both the observed structure and the chemical behaviour of the complex. The lact of reactivity of these complexes may simple be due to steric congestion.[59] Reactions of $(\eta^5\text{-}Cp^*)_2UMe_2$ with anilines (H_2NR) form 3 different structural products (Scheme 4) depending on the size of R.

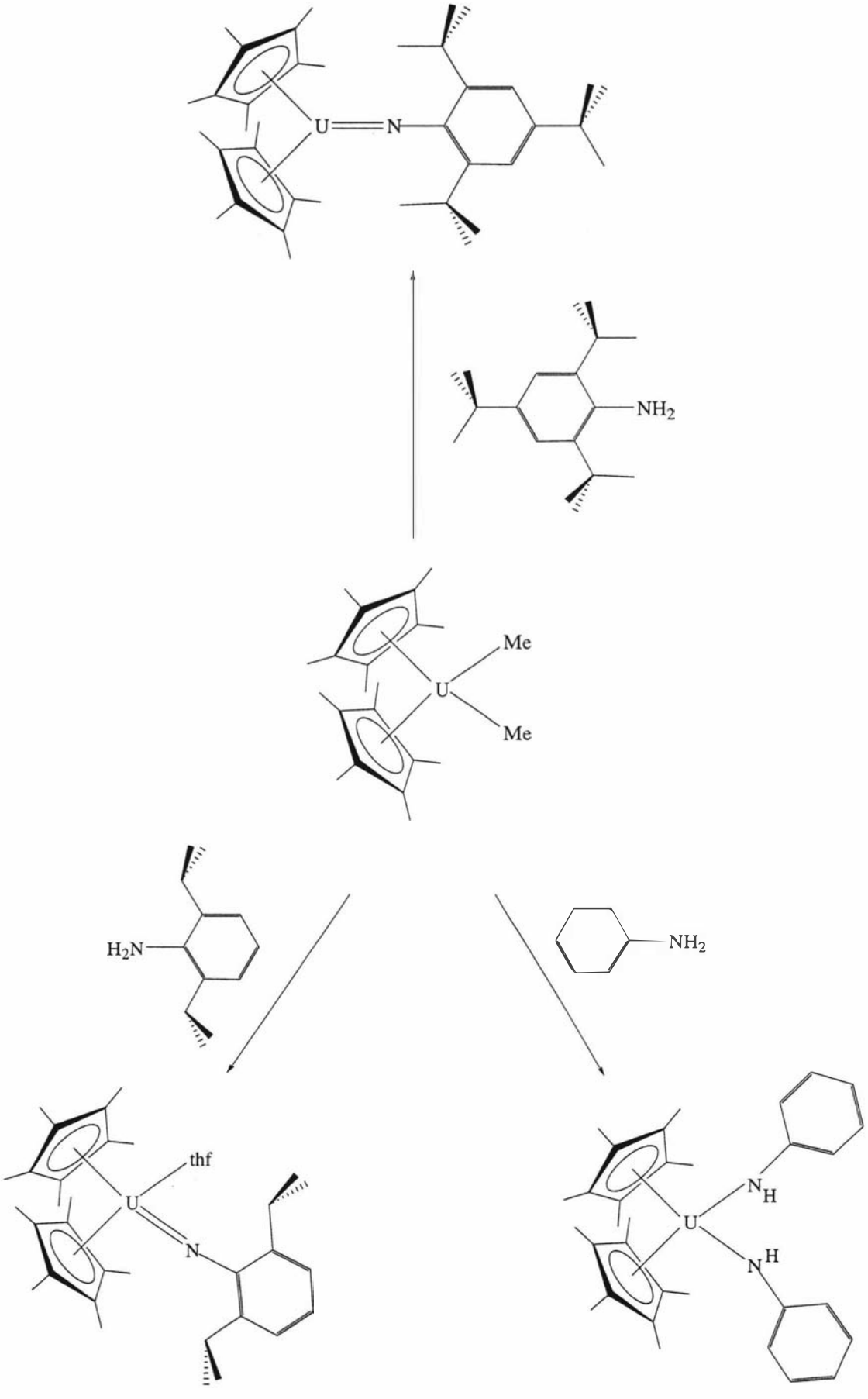

Scheme 4

Concluding remarks

There are many synthetic precedures for the formation of imido complexes.[1a] However, only a fraction of these can be used to synthesize tris(imido) complexes. Most commonly, reactions involve the use of a bis(imido) complex that with the appropiate reagent can incorporate a third imido ligand.[14,20,44] It is possible to start with an oxo complex and to replace the oxo ligands for imido ligands using isocyanates or phosphinimines.[22,26,34] As a result of competition between the imido ligands for π-donation to the metal center, the imido ligand in tris(imido) complexes are best represented by structure A or B of figure 16. Bending at the imido nitrogen is most likely due to the decreased ability of the imido ligand to π-donate due to competition of the other strong π-donor ligands.[22] In several cases the formulation of a complex indicates a 20-electron compound, however it has been found due to a mismatch of orbital symmetry that these complexes are in fact 18-electron compounds.[26,35,28,14] Cundari and coworkers have suggested that π-loading may provide extra driving force for methane activation.[35] Coordination of methane to a cationic tris(imido) complex of technetium is feasible from both an electronic and steric point of view.[39]

A B

Figure 16

The X ligand in the tris(imido) complexes, $XM(NR)_3$ can be substituted by nucleophilic attack of R^-. The action of Grignards on $Me_3SiOTc(NAr)_3$ resulted in alkyl complexes of formulation $RTc(NAr)_3$.[22] The one-electron reductions of $Mn(N^tBu)_3Cl$ and $ITc(NR)_3$ (R=Ar' or Ar) lead to d^1-d^1 dimers. Due to the steric differences of the NR' (R'=^{t}Bu and Ar') and NAr imido ligands, edge-bridged dimers were obtained for the NR' imido ligand and the ethane-like dimer was obtained with the NAr imido ligand.[17,31] Two-electron reductions of $Mn(NR)_3Cl$ and $ITc(NAr')_3$ failed to result in solvable compounds. However, reduction of $ITc(NAr)_3$ resulted in a trigonal planar d^2 anion,

$[Tc(NAr)_3]^-$. This complex was found to react with electrophiles to form new 4-coordinate complexes.[17]

Sterics play an important role in the structure and reactivity of imido complexes. Monomeric[26] vs edge-bridged dimers[54,17] vs ethane-like dimers[17] are formed depending on the steric nature of the imido ligand employed. Reduced reactivity and increased stability may simple be due to steric congestion about the metal.[17,59,71]

Rhenium Tris(imido) Complexes

One of the earliest multiple imido compounds reported was the tris(imido) rhenium species, $Me_3SiORe(N^tBu)_3$, described by Nugent and Harlow[61] as yellow needles obtained from the reaction of $Me_3SiOReO_3$ with excess Me_3SiNH^tBu. Over the past 20 years a vast number of rhenium tris(imido) complexes have appeared in the literature.[1a] These complexes range from d^0 $XRe(NR)_3$, to d^1-d^1 $Re_2(NR)_6$ dimers and d^2 $[Re(NR)_3]^-$ anions. There have been a number of investigations into the chemistry of $XRe(NR)_3$ complexes.[33,17,16,22,51,12,29,30,62] These inquires have provided a wealth of diverse chemistry, but have only scratched the surface of the potential chemistry available. Recent theoretical investigations by Cundari and coworkers[35] have pointed to tris(imido) rhenium complexes that may display exceptional reactivity and potentially enable the isolation of a complex containing a coordinated methane. These calculations suggest that $[Re(NR)_3]^+$ should form a sufficiently stable methane adduct to permit experimental isolation. To date $[Re(NR)_3]^+$ has not been reported.

Synthetic methods

As was seen in technetium tris(oxo)[22] and osmium tetrakis(oxo)[26] chemistry, reaction with isocyanates form tris(imido) complexes. Along these lines tris(imido) rhenium complexes can be synthesized from the oxo derivatives and isocyanates (Equ. 20 and Equ. 21).[41,51] The complexes, $Ph_3SiORe(NR)_3$ (R=Ar, Ar', 'Bu) is prepared in an analogous manner to that of $Me_3SiORe(NAr)_3$.[104]

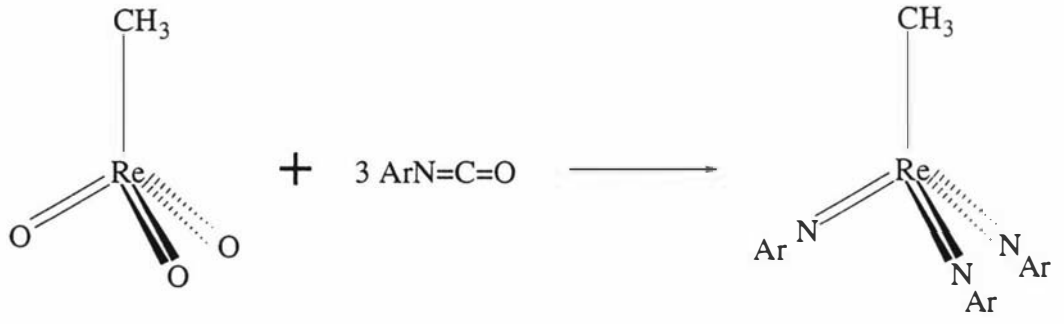

Equation 20

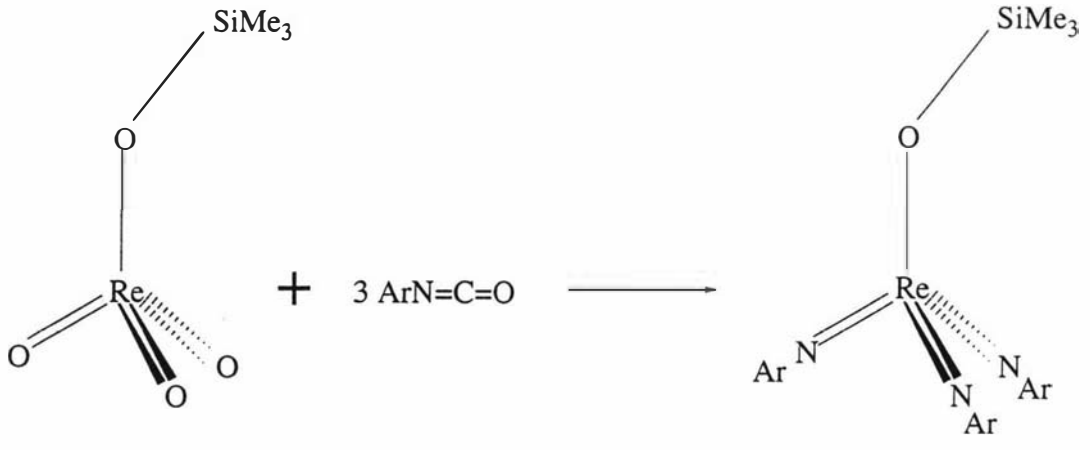

Equation 21

The tris(imido) complex $MeRe(NAr')_3$ can also be synthesized with Ar'NCO and the methyl tris(oxo) complex.[63] Herrmann *et al.* found that a dinuclear complex (Fig. 17) was formed if the reaction of Equation 20 is carried out in dme.[41]

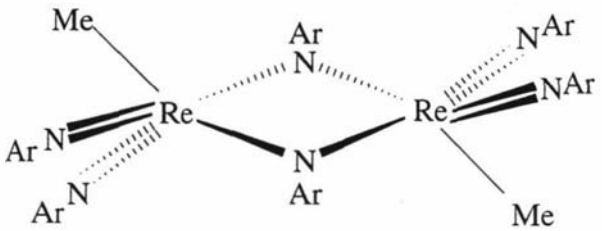

Figure 17

This lead to the tentative conclusion that the monomer converts to the dimer in the more polar solvent since other effects (temperature, time) had been ruled out experimentally. However in a recent paper, Herrmann found that the influence of the polarity of the solvent is not significant.[21] The dimeric derviative turned out to be a mixture of the monomeric compounds and decomposition products caused by the reaction of the monomer with trace amounts of water.

The reaction of $Me_3SiOReO_3$ with ArNCO is proposed to proceed in a stepwise fashion, forming a bis(oxo)imido then a oxobis(imido) and finally with the third equiv. of ArNCO, the tris(imido) complex.[51]

Substitution of oxo ligands for imido ligands can be also achieved with cleavage of the Si-N bond in silylamides. The first Re(VII) tris(imido) complex was synthesized in this way (Equ. 22). Use of an insufficient amount of $^tBuNHSiMe_3$ yielded a yellow, low-melting solid analysing for $Re_3(N^tBu)_4O_5(OSiMe_3)_3$.[61]

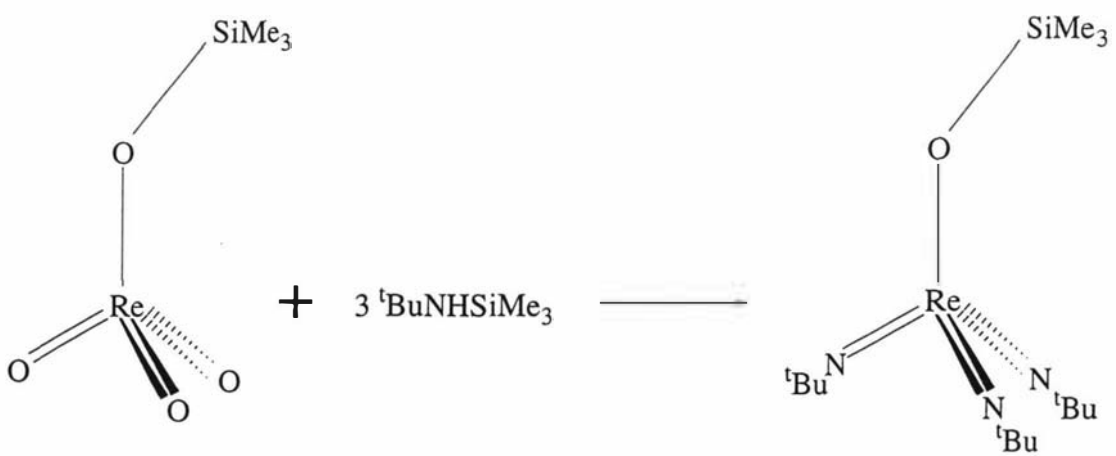

Equation 22

New to the synthesis of tris(imido) complexes is the one-step, high yield reactions from Re_2O_7. Upon adding ^{t}Bu amine and trimethylchlorosilane to a suspension of rhenium heptoxide in dichloromethane, a bright, lemon-yellow colour is generated and flocculent white ^{t}BuNH$_3$Cl precipitates immediately. If the reaction is filtered after 20 minutes, $Me_3SiORe(N^tBu)_3$ can be recovered from the filtrate in >90% yield (Equ. 23).[64]

$$0.5\ Re_2O_7 + 9\ ^tBuNH_2 + 6\ Me_3SiCl \longrightarrow Re(N^tBu)_3(OSiMe_3) + 6\ ^tBuNH_3Cl + 2.5\ (Me_3Si)_2O$$

Equation 23

This procedure is an improvement over Nugent and Harlow's synthesis of $Me_3SiORe(N^tBu)_3$ (Equ. 22)[61] in which the yield was 64% and the reaction took 48 hours. This reaction scheme can also be used to synthesize $Re(NAr)_3Cl$ (Equ. 24) in 99% yield.[12]

$$0.5\ Re_2O_7 + 3\ ArNH_2 + 6\ NEt_3 + 7\ Me_3SiCl \longrightarrow Re(NAr)_3Cl + 6\ Et_3NHCl + 3.5\ (Me_3Si)_2O$$

Equation 24

Notice in Equation 23 that 6 equivalents of ^{t}BuNH$_2$ (out of nine) acts as the base, but in the synthesis of $Re(NAr)_3Cl$, 6 equivalents of triethylamine is used as the base.

Structure and bonding

The effect of π-loading on the coordination of X ligands in $XRe(NR)_3$ complexes has been investigated by an analysis of several X-ray structures. On the basis of the structure of $Me_3SiORe(N^tBu)_3$,[30] all ligands are participating in π-bonding to some extent. Not surpriseingly however, the siloxide, for which the Re-O bond at 1.90Å only slightly shorter than a normal single bond would seem to contribute least. The η^1-coordination mode of the allyl ligand in the complex, $(^tBuN)_3Re(CH_2CH=CH_2)$[41] maybe the result of the high electron density at the metal provided by the three imido ligands. Although orbital symmetry reasons also exist as argued for the related complex $(\eta^1\text{-}C_3H_5)ReO_3$.[65,66]

The geometry of d^2 tris(imido) complexes are expected to be trigonal planar (see page 8). This is consistent for the experimental data of $[Re(NAr)_3]$.[12] A d^0 complex cation, for example $[Re(NR)_3]^+$, would be expected to be pyramidal. The d^0 systems are 18-electron complexes and thus there is no electronic impertus for remaining planar and the complexes pyramidalizes to minimize competition for dπ-Npπ bonding.[39]

Reactions

As in the case of $Mn(N^tBu)_3Cl$[31] and $ITc(NR)_3$ (R=Ar',Ar),[17] 1-electron reductions with sodium amalgam are possible for the $XRe(NR)_3$ complexes. Reaction of $Me_3SiORe(N^tBu)_3$ with NaHg leads to the edge-bridged dimer, $[Re(N^tBu)_2(\mu\text{-}N^tBu)]_2$[30] in 20% yield (Equ. 25).[30] Recently an improved synthesis involving the iodo complex, $IRe(N^tBu)_3$ and NaHg increased the yield to 65%.[67]

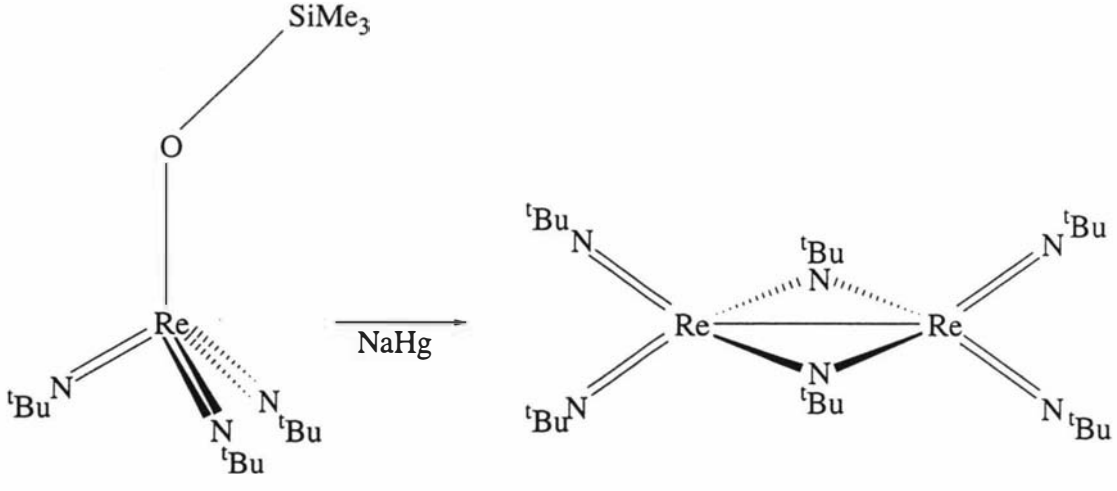

Equation 25

Interestingly the 1-electron reduction of $ClRe(NAr)_3$ with NaHg resulted in a mercury-bridged species (Equ. 26).[12] Its formation is suggested to occur from reduction by mercury of the monomeric Re(VI) radical or radical anion forming $Hg[Re(NAr)_3]_2$.[17]

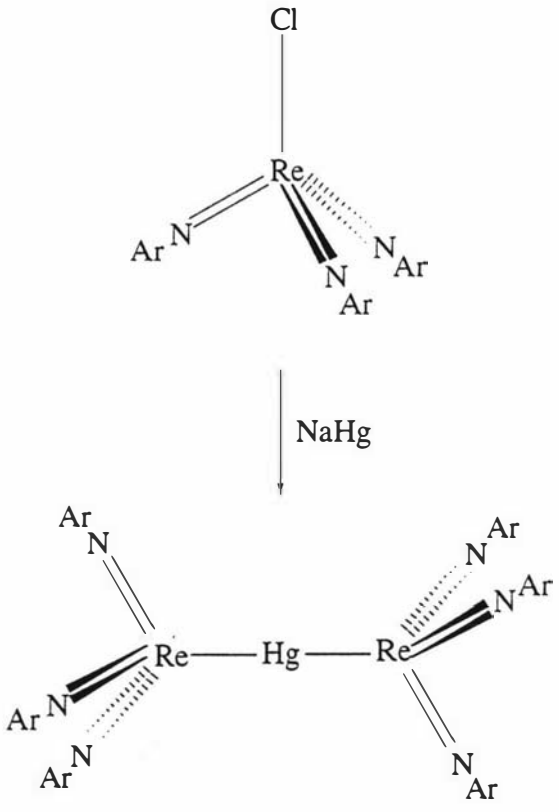

Equation 26

As for technetium, d^2 trigonal planar rhenium anions can be formed from reduction of $ClRe(NAr)_3$ with 2 equivalents of NaHg affording $[Re(NAr)_3]^-$.[12] The anion, $[Mo(NAr)_3(CH_2C^tBu_3)]^-$, can be protonated at the imido.[28] In a similar reaction $[Re(NAr)_3]^-$ can be protonated with $[Et_2NH_2]OTf$ to afford (Equ. 27) what is formulated as the hydride. However formulation of the hydride as $Re(NAr)_2(NHAr)$ was not ruled out entirely.[12]

The deprotonation of amido ligands to the corresponding imido ligand to form tetrakis(imido) complexes as seen for $[Nb(Nmes)_3(NHmes)]^{2-}$ with reaction of a strong base, ^tBuLi,[1a] is also possible in rhenium chemistry. Similar reaction occurs with $Re(N^tBu)_3(NH^tBu)$ and MeLi to give the tetrakis(imido) complex, $[Re(N^tBu)_4]^-$.[30]

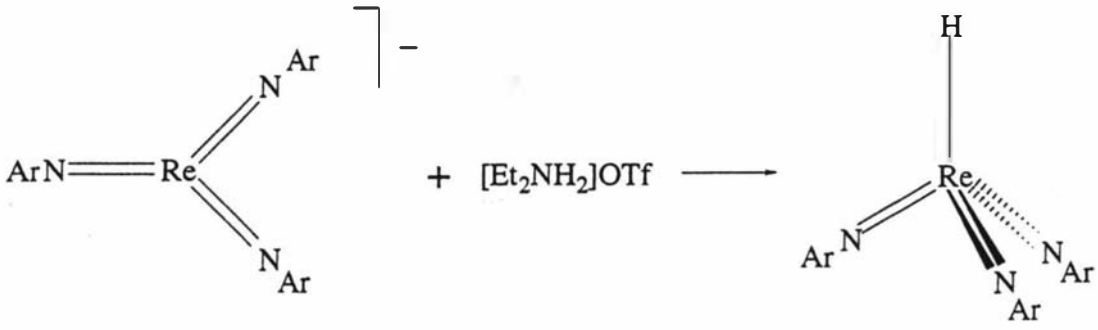

Equation 27

Protonation of a terminal imido ligand in the edge-bridged dimer, $[Re(N^tBu)_2(\mu\text{-}N^tBu)]_2$ can be achieved with CF_3SO_3H, forming the unsymmetrical dimer, $[(Bu^tN)_2Re(\mu\text{-}N^tBu)_2Re(N^tBu)(NH^tBu)]^+$ (Fig. 18).[67] This result mirrors that found for the manganese dimer.[68]

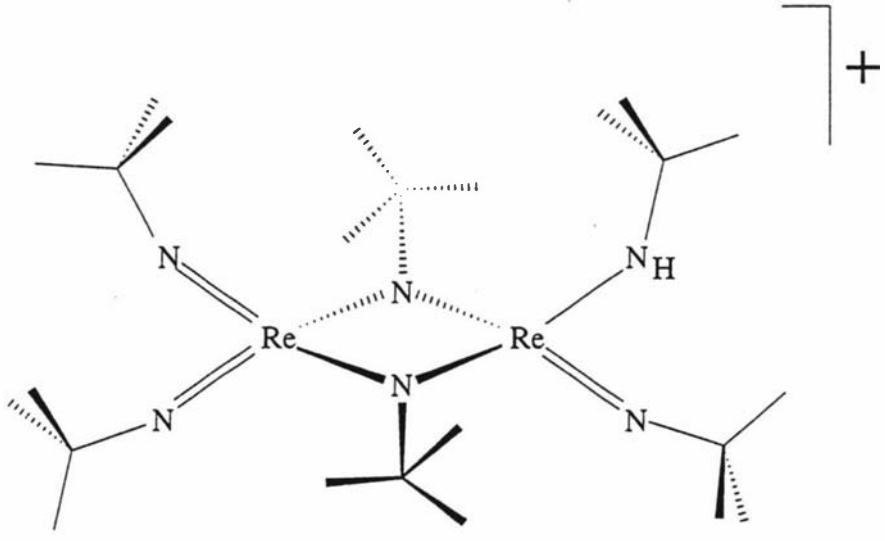

Figure 18

The action of $AgOSO_2CF_3$ and $CuO_3SCF_3.0.5C_6H_6$ on $[Re(N^tBu)_2(\mu\text{-}N^tBu)]_2$ results in the $Re_2(N^tBu)_6$ moiety coordinated in bidentate fashion from a bent N^tBu group on each rhenium atom (Fig. 19 and Fig. 20).[67] In these cases the chemistry here has not been reported for manganese.

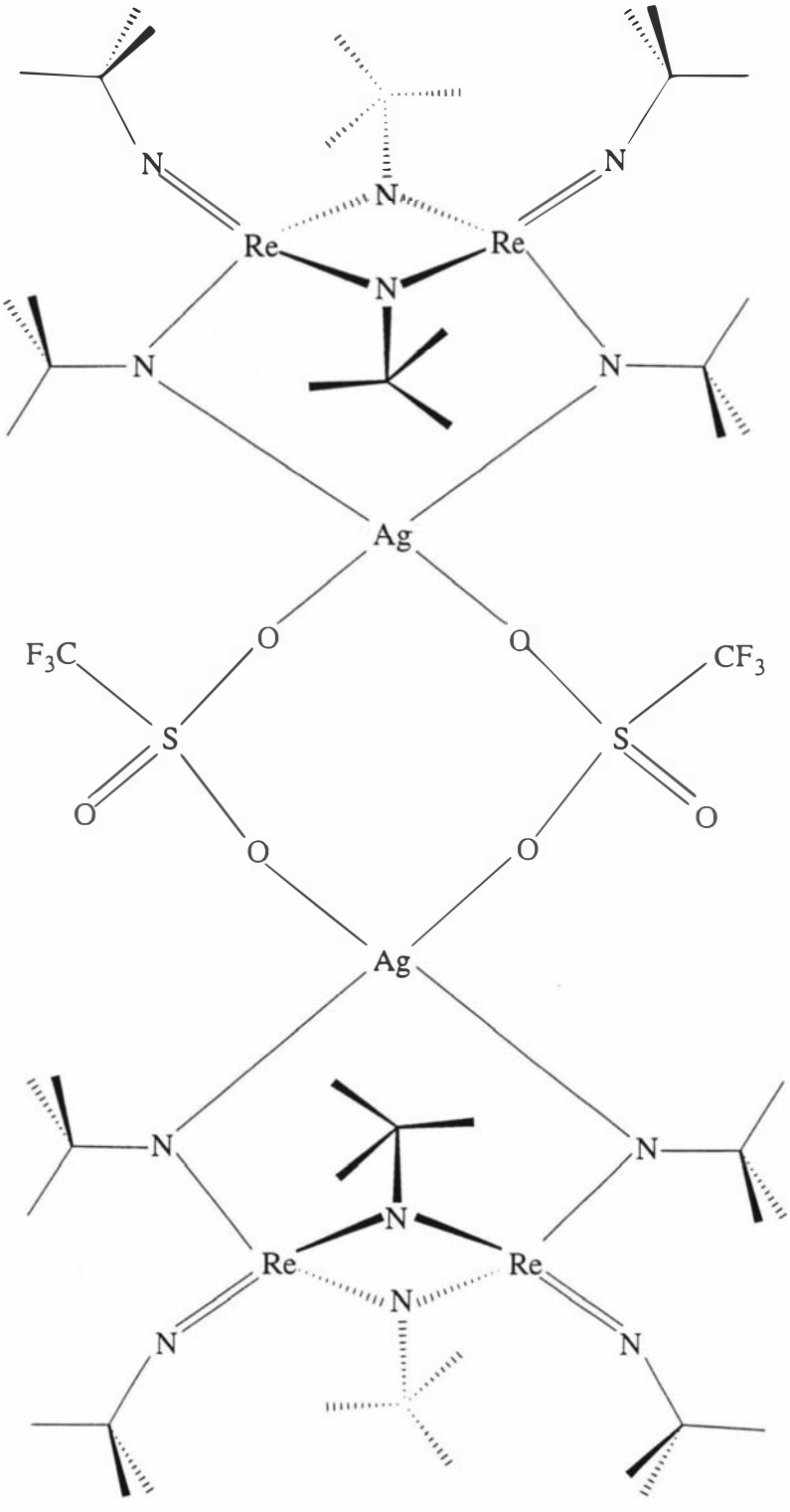

Figure 19

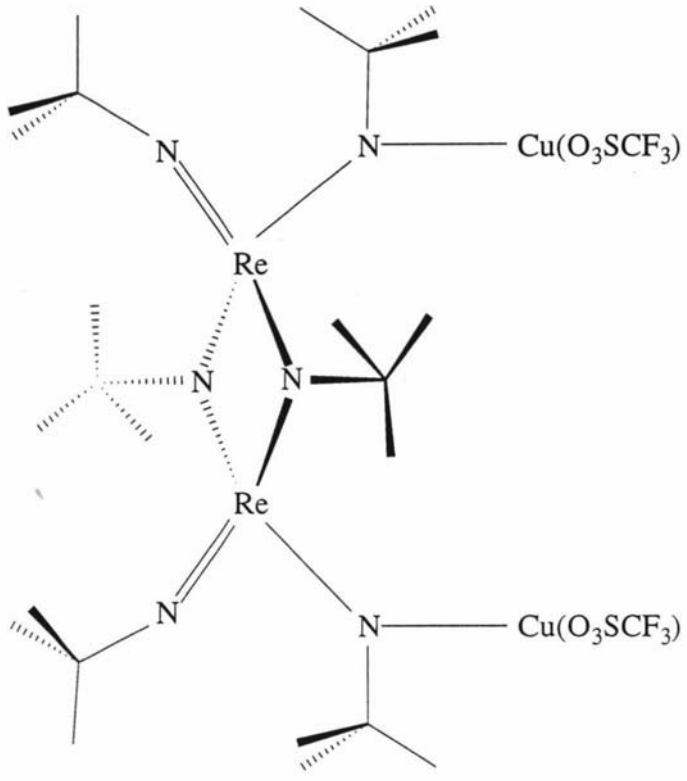

Figure 20

Trifluoromethanesulphonic acid can also be used to protonate $Re(N^tBu)_3(NH^tBu)$ to give the amine cation, $[Re(N^tBu)_3(NH_2{}^tBu)]^+$.[29] The basicity of the amido nitrogen will be greater than that of the imido nitrogens since the lone pairs on the latter are involved in π-bonding to a greater extent than for $NH_2{}^tBu$. Similar behaviour has been observed for $W(N^tBu)_2(NH^tBu)_2$.[69,70]

Phosphido and amido complexes containing the $[Re(N^tBu)_3]$ core are prepared in moderate yields (Scheme 5) from the appropiate lithium reagent.[29]

Formation of amidotris(imido) complexes using $LiNH^tBu$ or $LiCH_2{}^tBu$ reagents respectively have produced $Re(N^tBu)_3(NH^tBu)$[30] and $Re(N^tBu)_3(CH_2{}^tBu)$.[51] A similar reaction with $LiNH^tBu$ was seen for manganese forming $Mn(N^tBu)_3(NH^tBu)$.[1a]

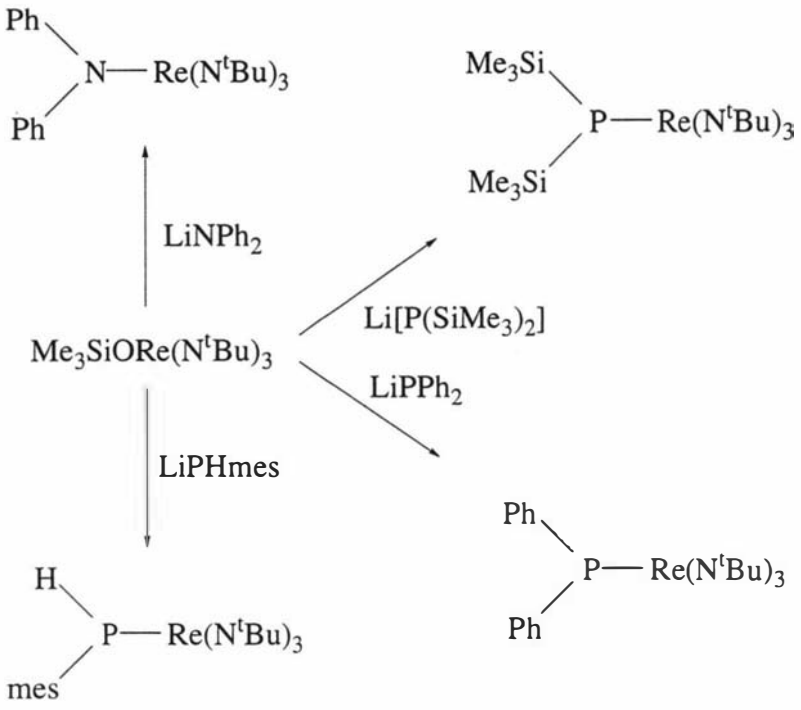

Scheme 5

Action of HCl towards tris(imido) complexes leads to bis(imido) complexes as seen in Equations 28, 29 and 30.[71,63,72] The formation of an anion (Equ. 29) as opposed to a neutral complex can be justified on steric grounds.[63]

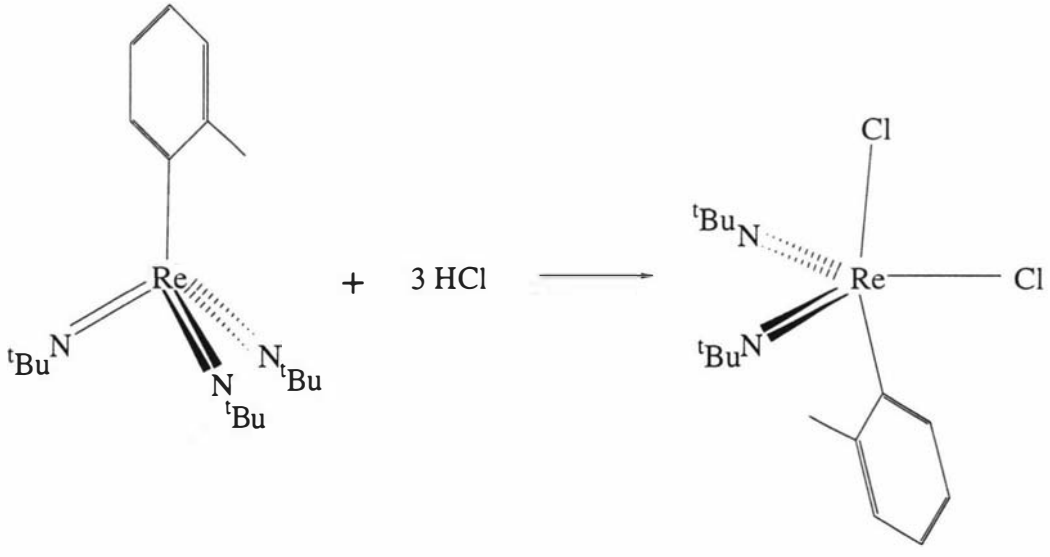

Equation 28

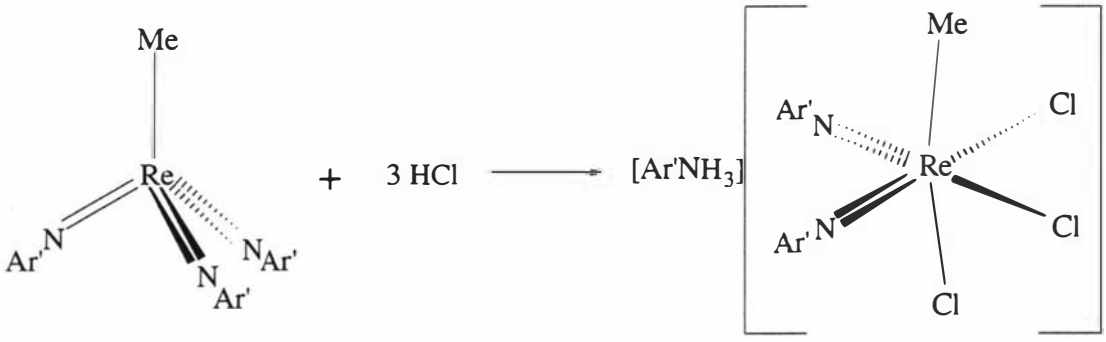

Equation 29

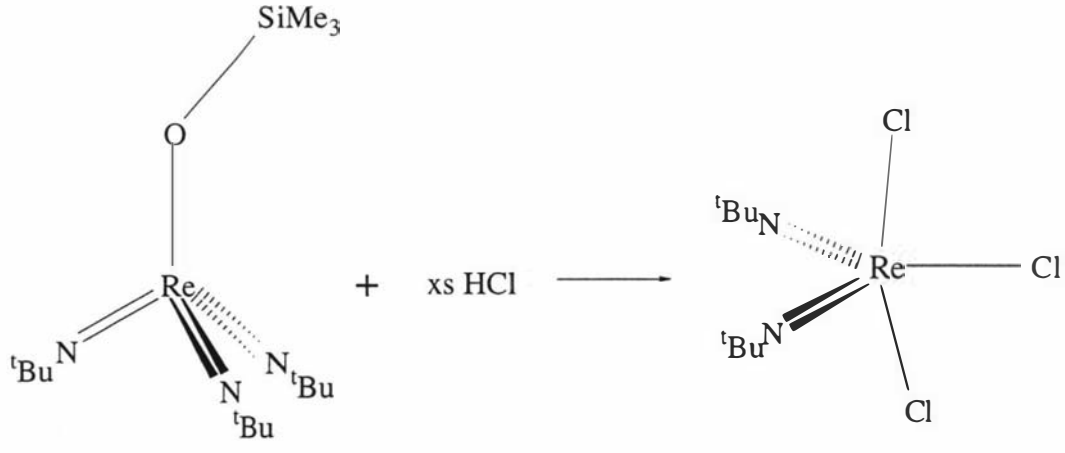

Equation 30

It has been previously seen that R^- can displace the siloxy group of $Me_3SiOTc(NAr)_3$ to form a number of alkyl tris(imido) complexes, $RTc(NAr)_3$.[22] Reaction of Grignards with $Me_3SiORe(N^tBu)_3$ forms the expected alkyl complexes (Scheme 6).[41,71] Similar reaction of $Me_3SiORe(N^tBu)_3$ with PhCCLi formed the alkyldyne complex, $PhCCRe(N^tBu)_3$ (Scheme 6).[41] Wide use of Grignard reagents illustrates that Re(VII) imido complexes are much more resistant to reduction then their oxo analogues.[1a]

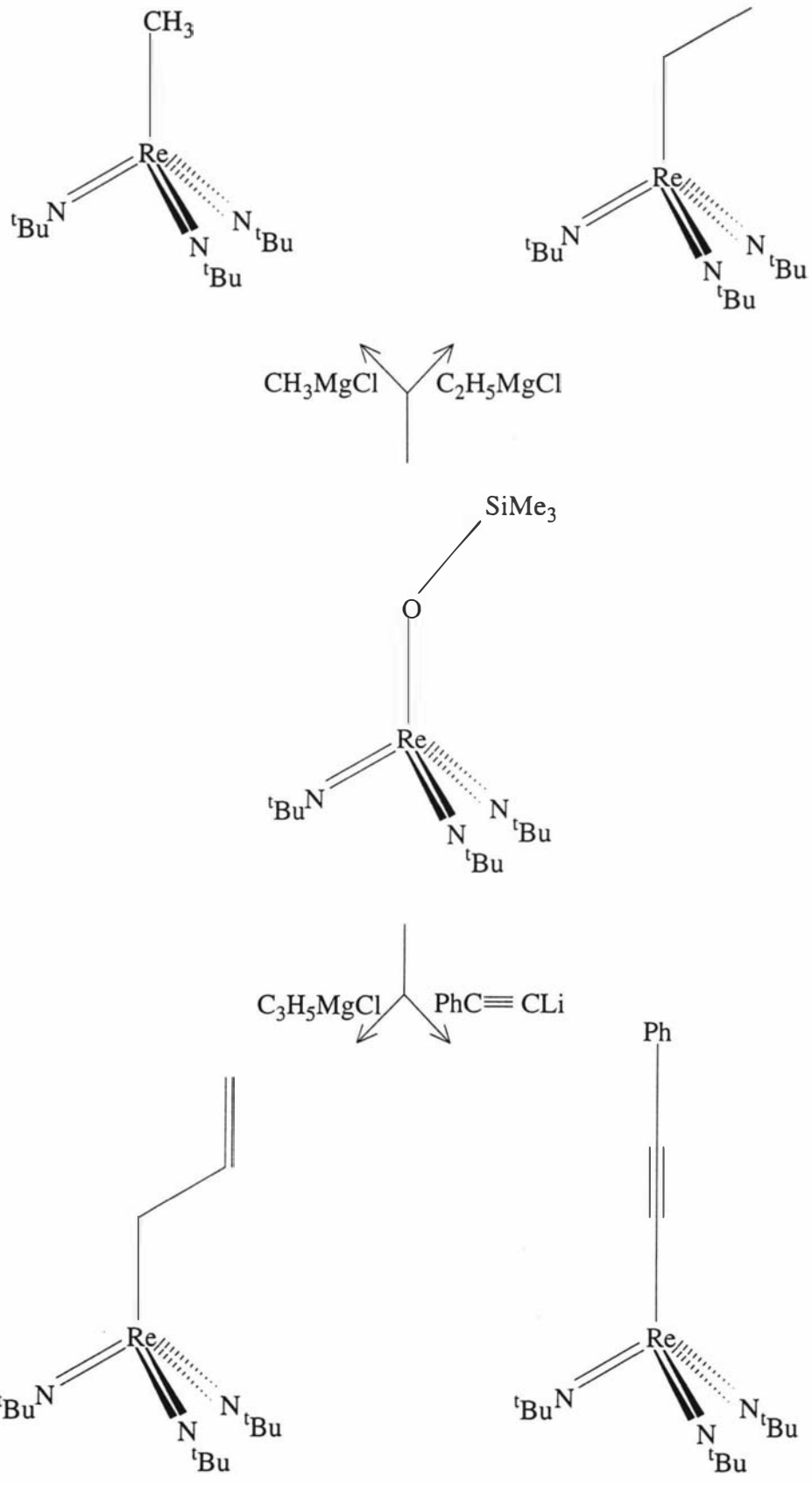
CH3
Re
tBuN
N tBu
N
tBu
CH3MgCl
C2H5MgCl
SiMe3
O
C3H5MgCl
PhC≡ CLi
Ph

Scheme 6

Illustration of a reaction involving a Grignard resulting in a reduction is seen with a trichlorobis(imido) Re(VII) complex (Equ. 31). Reaction of Grignards to $Re(N^tBu)_2Cl_3$ usually results in formation of trialkylbis(imido) complexes, $Re(N^tBu)_2R_3$. However with mesMgBr a reduction occurs giving high yields of a paramagnetic Re(VI) compound.[30]

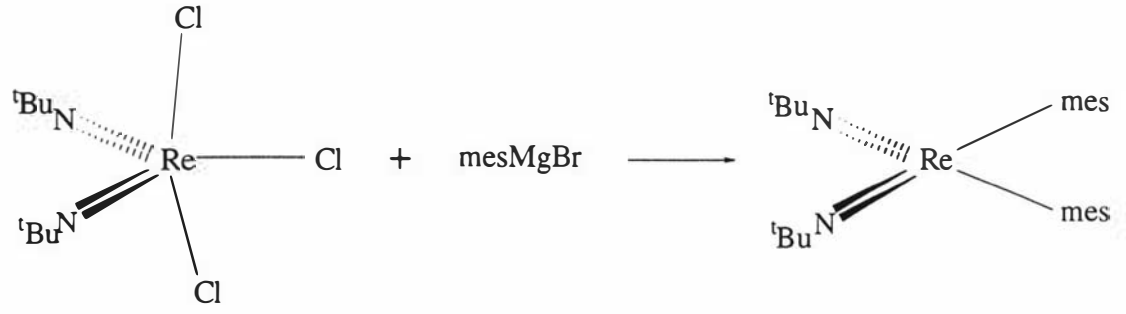

Equation 31

The oxygen atom in $Me_3SiORe(N^tBu)_3$ may exhibit nucleophilic character as is the case for $Me_3SiOTc(NAr)_3$.[22] This is indeed the case as Me_3SiI reacts with $Me_3SiORe(N^tBu)_3$ to give the iodo complex, $IRe(N^tBu)_3$.[67]

The complex, $(\eta^1\text{-Cp})Tc(NAr)_3$ is synthesized simply from $ITc(NAr)_3$ and KCp in good yield.[16] Reaction of $ClRe(N^tBu)_3$ with NaC_5H_5 lead to a compound containing a $C_5H_4^{2-}$ and oxo bridging groups (Fig. 21).[29,102] Interestingly all attempts to react $Me_3SiORe(N^tBu)_3$ with C_5H_5M (M=Na, Tl, $SnBu_3$) or C_5Me_5M (M=K, MgCl, Li) were unsuccessful.[41]

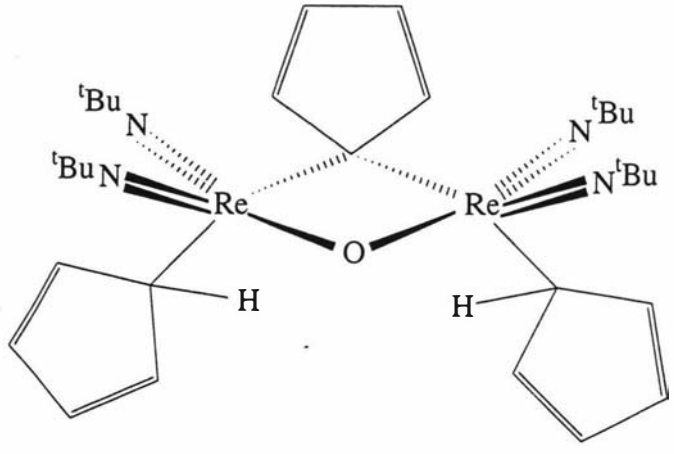

Figure 21

Displacement of the X ($XRe(NR)_3$) by phosphines has been observed in molybdenum and tungsten chemistry.[14] The amine ligand of $[Re(N^tBu)_3(NH_2{}^tBu)]^+$ can be displaced by PPh_3 to give $[Re(N^tBu)_3(PPh_3)]^+$.[29] There are no examples of X displacement for PR_3 where X is a monoanionic ligand. Reductive elimination of an imido ligand by phosphines as seen with $Os(NAr)_3$ has not been observed with rhenium.[26]

Intermolecular oxo/imido exchange is quite common.[1a,21] $MeReO_2(NAr)$ can be synthesized by mixing the tris(imido) complex with the tris(oxo) complex in the correct stoichiometry (Equ. 32).[21]

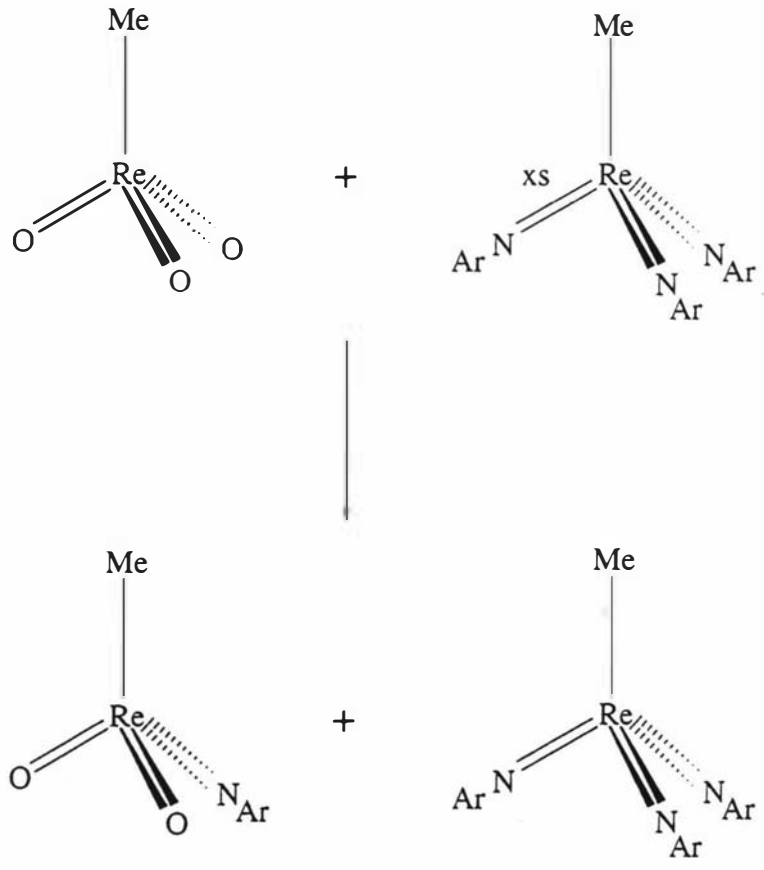

Equation 32

Reactions of tris(imido) complexes with unsaturated molecules are rare. The reaction of PhNCO and $Mo(NAr)_3PMe_3$ to yield the urylene complex[28](see page 14) is the only example excluding rhenium. A technetium urylene complex was synthesized,[22] however the starting material was the tris(oxo) complex, $Me_3SiOTcO_3$. As in the molybdenum case, reaction of Ar'NCO with $Me_3SiORe(NAr')_3$ lead to the urylene complex (Fig. 22).[22] In each case only one imido ligand is reacted even though excess isocyanate is used. A possible explanation for this is that replacement of an imido ligand

for an urylene ligand allows the remaining imido ligands to donate more strongly and thus be less reactive towards isocyanates.[22]

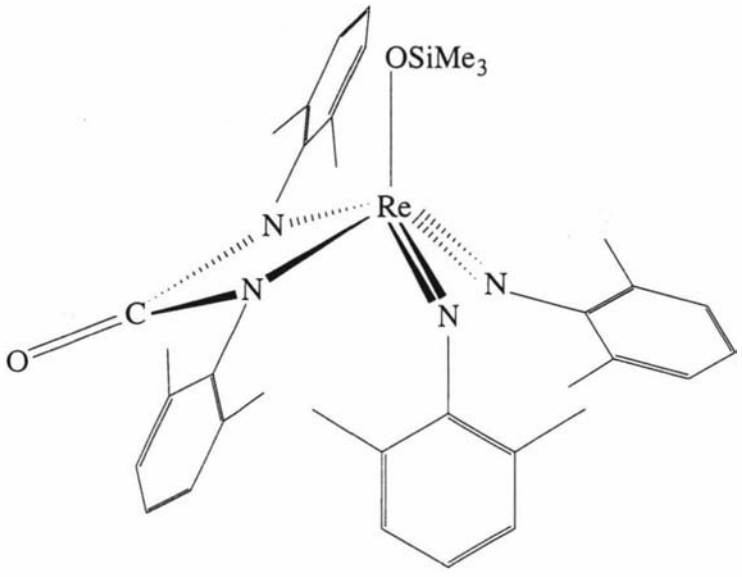

Figure 22

The Re(V) tris(imido)hydride complex is shown to bind unsaturated compounds in a η^2 fashion (Equ. 33). The ligand, L, can be C_2H_2, C_2Me_2, $OCHCMe_3$, C_2H_4 or norbornene.[12]

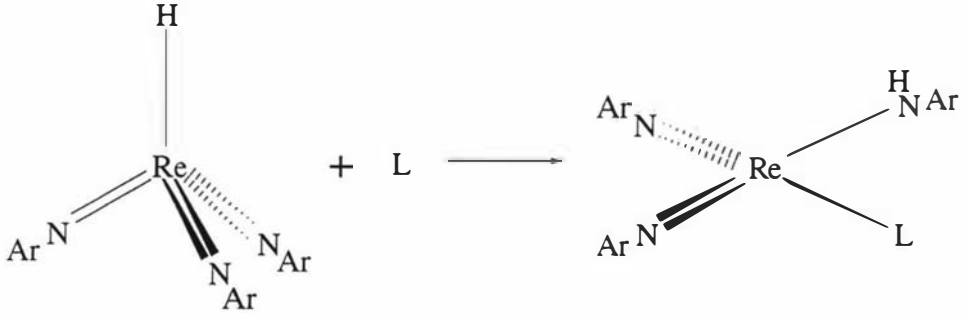

Equation 33

The oxotris(imido) Os(VIII) complexes react with alkenes to form mainly diamide complexes (Equ. 34).[34]

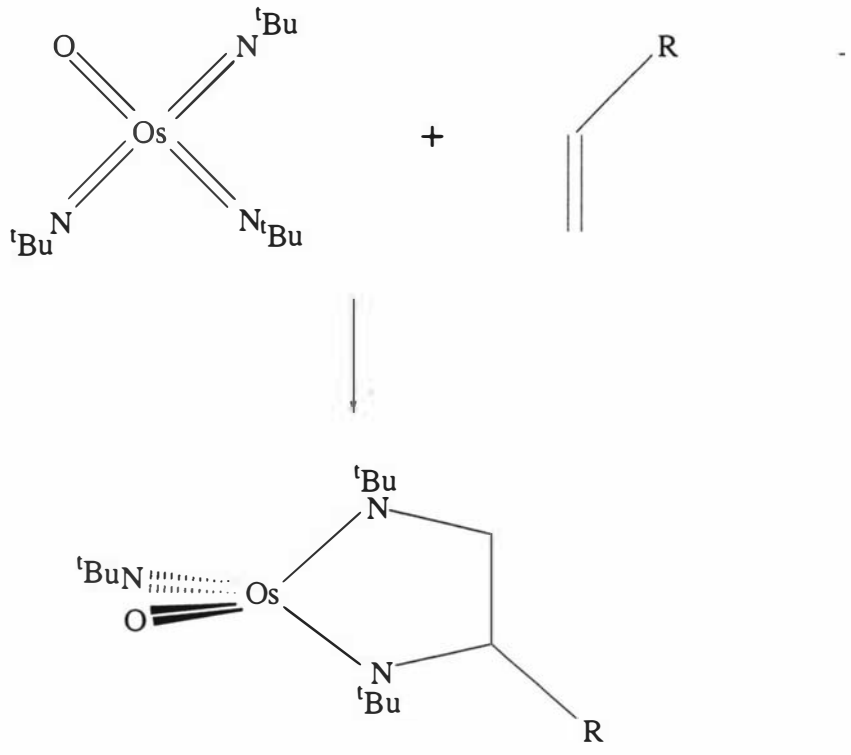

Equation 34

Interestingly in the reaction of alkynes with mono(imido) and bis(imido) complexes, $Cp_2Zr(NAr')(thf)$,[2] $Cp^*Ir(N^tBu)$[9] and $(OEt_2)V(NR)_2(NHR)$[60] (R=$^tBu_3Si$), cycloaddition reactions occur (Equ. 35, 36 and 37).

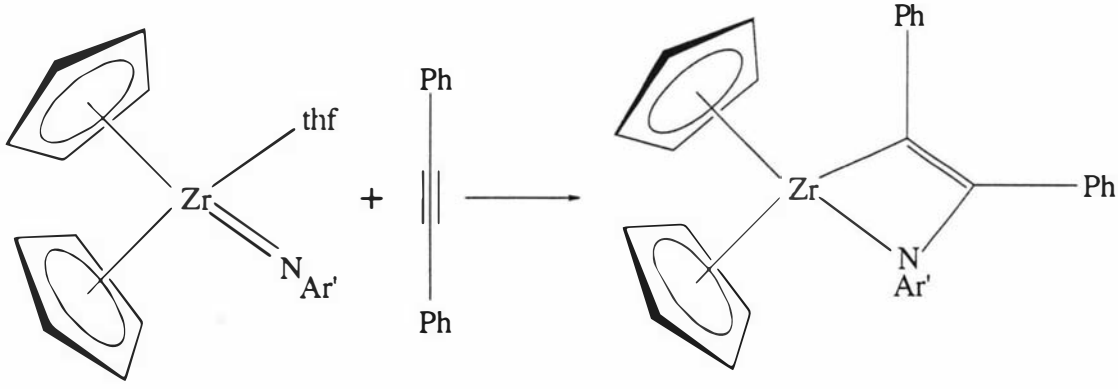

Equation 35

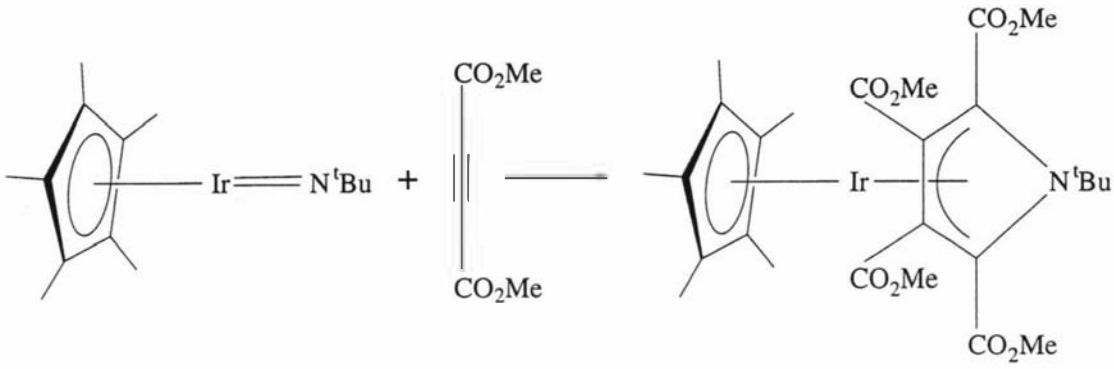

Equation 36

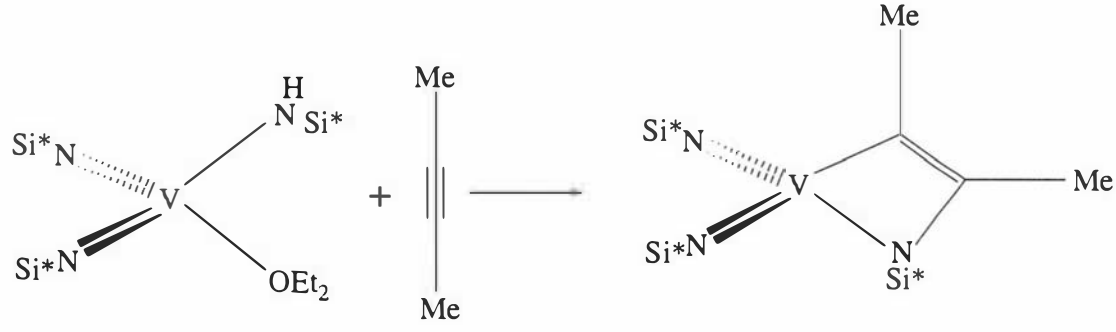

Equation 37

Reactions involving the loss of an imido ligand as the amine resulting in bis(imido) complexes are known for molybdenum[28] and osmium.[27] Protonolysis of one of the imido ligands in $Re(NAr)_3Cl$ with pyridinium chloride affords $Re(NAr)_2Cl_3(py)$ and $ArNH_2$. The reaction can be reversed by adding NEt_3.[12] A high yielding route for alkylbis(halide)bis(imido) pyridine complexes involves the reaction of the alkyltris(imido) complex with 2 equiv of pyHCl or 2 equiv of pyHBr (Equ. 38).[63]

Also $MeRe(NAr')_3$ reacts with 2 HSPh with loss of $Ar'NH_2$ to form $Re(NAr')_2Me(SPh)_2$. Catechol reacts with $MeRe(NAr')_3$ in the presence of pyridine to form $MeRe(NAr')_2(py)(cat)$ (Fig. 23) with loss of $Ar'NH_2$.[63]

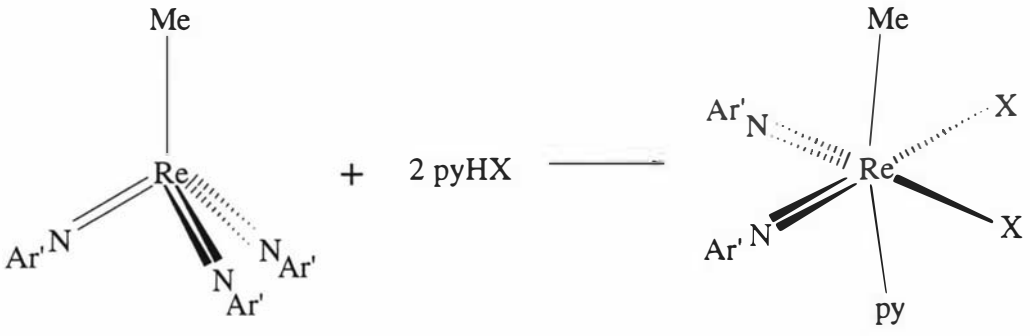

Equation 38

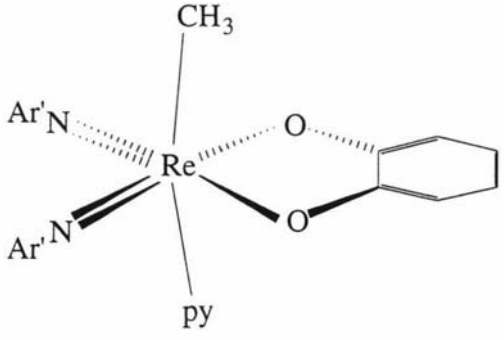

Figure 23

The nucleophilic nature of the Re(V) tris(imido) anion closely parallels that of the technetium complex,[17] $[Tc(NAr)_3]^-$. Hence reaction of MeI and $[Re(NAr)_3]^-$ yields the alkyl tetrahedral complex $MeRe(NAr)_3$. Dichloromethane was also found to react with the anion forming $Re(NAr)_3(CH_2Cl)$ in 85% yield (Equ. 39).[12] Loss of 2 imido ligands as $ArNH_2$ occurs on reaction with 4 equiv of pyHCl (Equ. 40), to form a mono(imido) complex.[12]

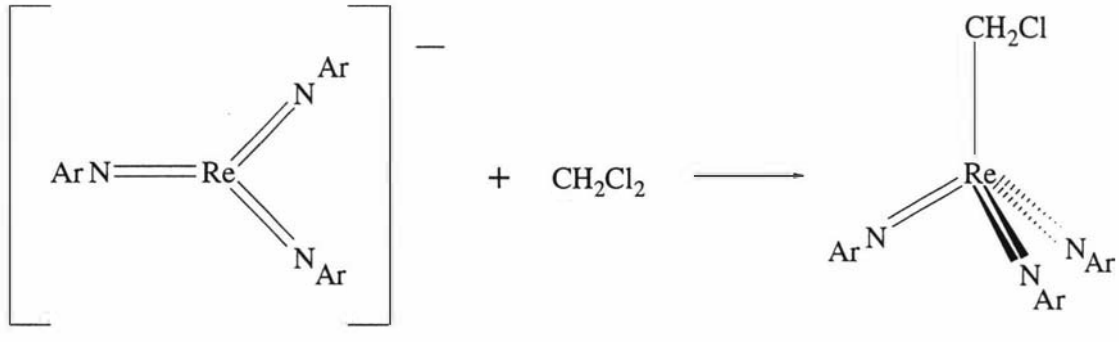

Equation 39

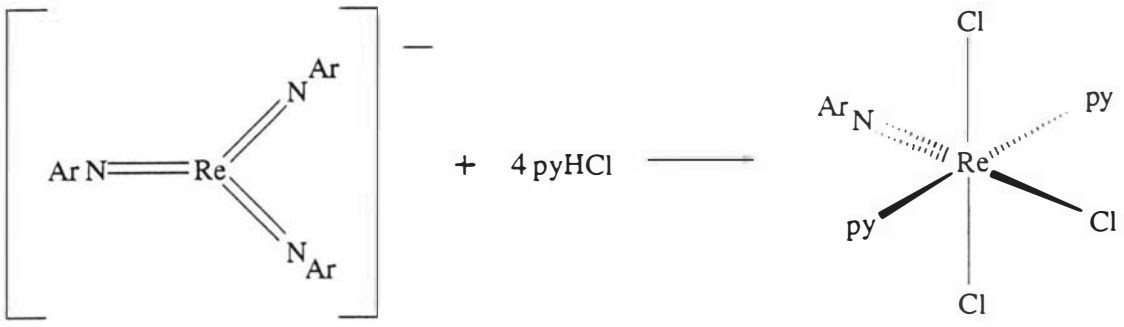

Equation 40

Finally, calculations by Cundari *et al.*[35] suggest that methane can coordinate to a d^0 tris(imido) complex whether it is neutral, anionic or cationic. Two possible routes to $[Re(CH_4)(NR)_3]^+$ are shown in scheme 7.

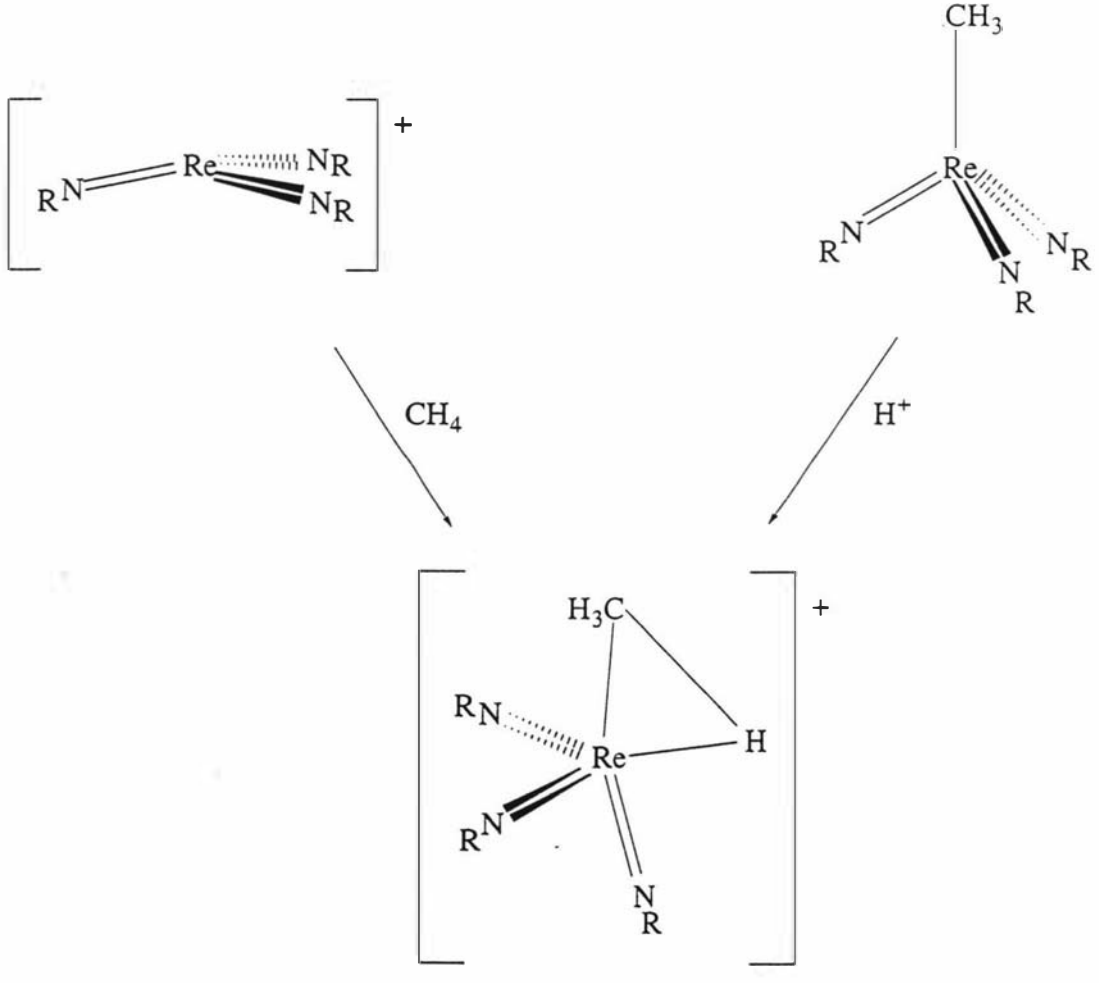

Scheme 7

Steric considerations

Attempts to synthesize a half-sandwich complex via $Me_3SiORe(N^tBu)_3$ with cyclopentadienyl or pentamethylcyclopentadienyl reagents have failed. It is believed that the ring tranfer reagents are too bulky for reaction with the highly sterically hindered starting material. However, an electronic argument can also be employed.[41] The successful interaction of NaC_5H_5 with $Re(N^tBu)_3Cl$ leading to a dimeric structure (Fig. 21) is believed to occur because of the lowered crowding in the chloride compared to the siloxide, coupled with the formation of NaCl rather than $NaOSiMe_3$.[29] A technetium cyclopentadienyl complex was formed from the iodo and KCp. Similar arguments can be used for its formation.

It is thought that formation of the cation, $[Re(N^tBu)_3(NH_2^tBu)]^+$,[29] is the result of reluctance of the Re(VII) to be five or six-coordinate when three bulky N^tBu groups are present. This was put forward as the protonation with trifluoromethanesulphonic acid of the bis(amido)bis(imido) tungsten complex, $W(N^tBu)_2(NH^tBu)_2$ gives rise to a complex containing η^1-OTf ligands, $W(N^tBu)_2(\eta^1\text{-}OTf)_2(NH_2^tBu)_2$.[70] Whereas protonation of $Re(N^tBu)_3(NH^tBu)$ lead to the tetrahedral cation, $[Re(N^tBu)_3(NH_2^tBu)][O_3SCF_3]$.

In the imido/oxo exchange chemistry shown by Herrmann *et al.* it is believed the steric bulk of the imido ligands effects the rate of exchange.[21]

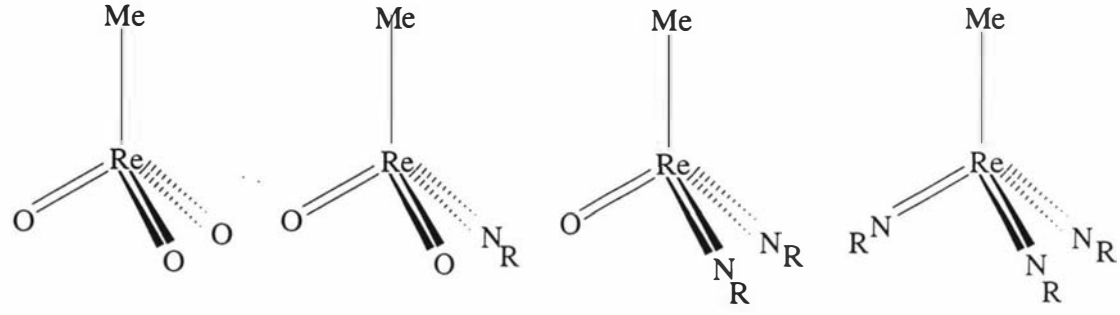

Figure 24

In reference to figure 24 it was found that 3 reacts more readily with 1 compared to the reaction of 4 with 1. The reaction between 1 and 3 to generate 2 is much faster than that between 1 and the tris(imido) derivative 4. This is thought to indicate that the increased steric bulk of $MeRe(NR)_3$ compared with $MeReO(NR)_2$ significantly impends the process of oxo/imido exchange.[21]

The dimerization seen in mixed oxo-imido complexes (Fig. 25) lead to the conclusion that the presence of a higher number of bulky imido ligands is helpful for the

dimerization of the complexes by oxo bridges (A and B of Fig. 25) and that the steric bulk of the imido ligands probably prevents the dimerization of the methyltris(imido) complex (C of Fig. 25). Additionally imido groups are generally stronger donors than oxygen atoms. Thus, three imido groups in one molecule may be sufficient to provide steric and electronic saturation of the metal center.[21]

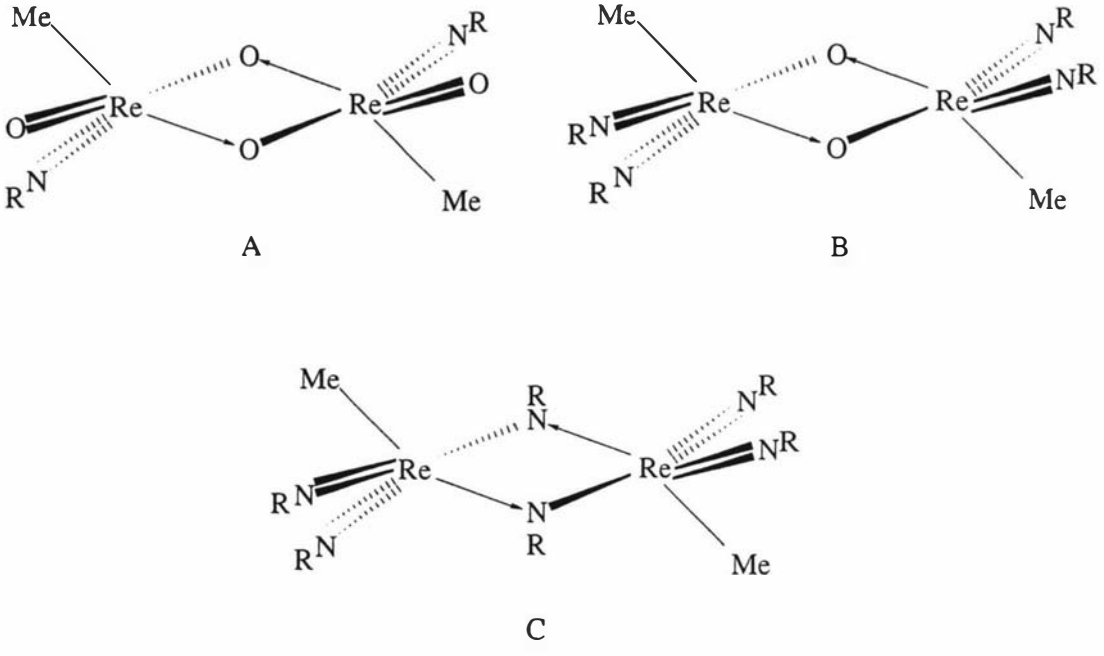

Figure 25

The steric bulk of the aryl substituents is an important factor in the stabilization of $[Re(NAr)_3]^-$. For instance, reduction of $ClRe(NAr')_3$ using NaHg results in the formation of $[Re(NAr')_2(\mu\text{-}NAr')]_2$, which does not undergo further reduction.[12,73] Likewise, reduction of $Me_3SiORe(N^tBu)_3$ with excess NaHg resulted in only the dimeric species.[30] Hence $[Re(NAr')_3]^-$ and $[Re(N^tBu)_3]^-$ have as yet not been synthesized.

Concluding remarks

Heptavalent rhenium has received considerable attention in the past 10 years in both inorganic and organometallic chemistry. There are more rhenium-imido complexes than for any other metal, they range from oxidation states Re(III) to Re(VII) and even include examples of Re(I). The compound, $Me_3SiORe(N^tBu)_3$ has served as an useful entry into tris(imido) complexes.

The reaction of rhenium tris(oxo) species and isocyanates afford monomeric tris(imido) complexes. Derivatives of $XRe(NR)_3$ can be prepared by a number of routes, including (i) metathesis reactions from $Re(NR)_3(OSiR_3)$ or $Re(NR)_3Cl$ (ii) electrophilic attack on the d^2 anion, $[Re(NR)_3]^-$ or (iii) reactions of an electrophile with an existing $Re(NR)_3X$ compound. Tetrahedral Re(VII) tris(imido) complexes can also be synthesized in greater yield and less reaction time from a convenient one-pot method using Re_2O_7. Reductions of $XRe(NR)_3$ complexes results in either dimeric d^1-d^1 complexes or Re(V) tris(imido) anions. The use of NaHg to reduce $ClRe(NAr)_3$ by 1 electron produced a mercury bridged species, instead of the expected Re(VI) dimer.

The steric nature of the ancillary and imido ligands imparts on both the structure and reactivity of rhenium tris(imido) complexes. It is believed that NaCp reacts with $ClRe(N^tBu)_3$ due to the lower crowding in the chloride, as the same reaction with $Me_3SiORe(N^tBu)_3$ is unsuccessful. Dimerization of complexes by oxo bridges is promoted if their is a presence of a high number of bulky imido ligands while bridging of imido ligands is hindered if the imido ligands contain bulky organic substituents. Herrmann *et al.* synthesized a bis(oxo)imido complex by imido/oxo exchange with a tris(imido) and tris(oxo) complex. It was found that the reaction of the tris(oxo) with bis(imido)oxo was much faster due to the steric bulk of the imido ligands. The steric bulk of the 2,6-diisopropylphenylimido ligand is in part thought to stabilize the d^2 tris(imido) complex, $[Re(NAr)_3]^-$, and is perhaps why $[Re(NR)_3]^-$ ($R=^tBu$, Ar') have not been isolated and finally, molecular orbital calculations suggest that the steric protection of the imido ligands can assist with the formation of a methane adduct of $[Re(NAr)_3]^+$.

Mixed Tris(imido) Complexes

While numerous imido complexes containing more than one imido ligand are known. Derivatives containing different imido ligands at the same metal center remain rare.

The presence of electronically and sterically disparate imido groups at the same metal center would allow the opportunity to probe the bonding in such complexes, where the ligands necessarily engage in competition for available metal dπ-symmetry orbitals.[1a,74] Producing tris(imido) complexes with differing degrees of steric congestion without having a dramatic effect electronically can be achieved by the synthesis of mixed-tris(imido) complexes as shown in figure 26.

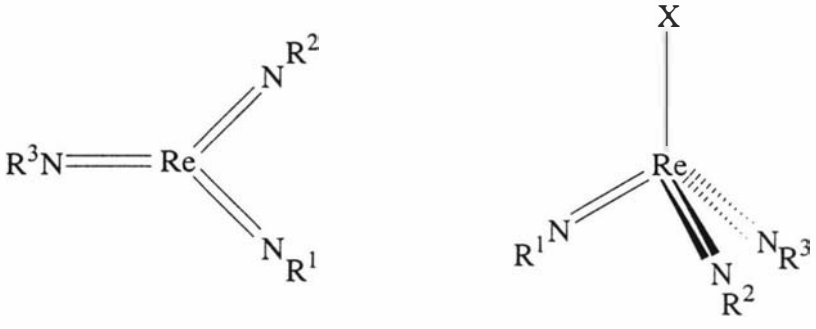

Figure 26

Synthetic methods

The synthesis of mixed imido complexes of molybdenum and tungsten involve dimeric complexes, with bridging imido ligands and terminal imido ligands. The action of *p*-tolylisocyanate towards $[Mo(C_5H_4Me)(NPh)(\mu\text{-}NPh)]_2$ results in exchange of the terminal phenylimido ligands for p-tolyl (Equ. 41).[75,76]

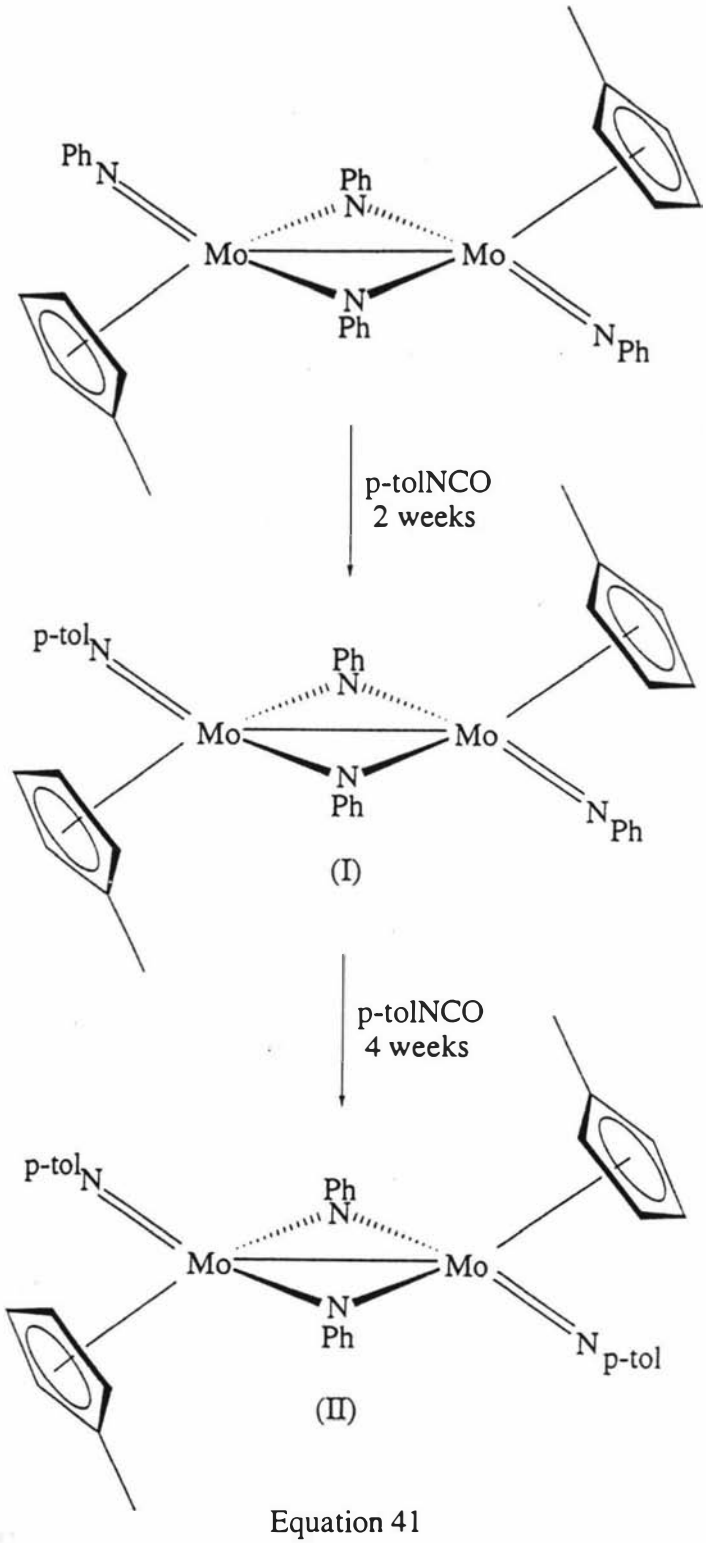
Ph
N
Ph
N
Mo
Mo
N
Ph
N
Ph
p-tolNCO
2 weeks
p-tol
N
Ph
N
Mo
Mo
N
Ph
N
Ph
(I)
p-tolNCO
4 weeks
p-tol
N
Ph
N
Mo
Mo
N
Ph
N
p-tol
(II)

Equation 41

No substitution of the bridging imido ligands was observed. Alternatively complex I and II of Equation 41 can be formed from the oxo dimers and *p*-tolNCO (Equ. 42 and 43).[75,76]

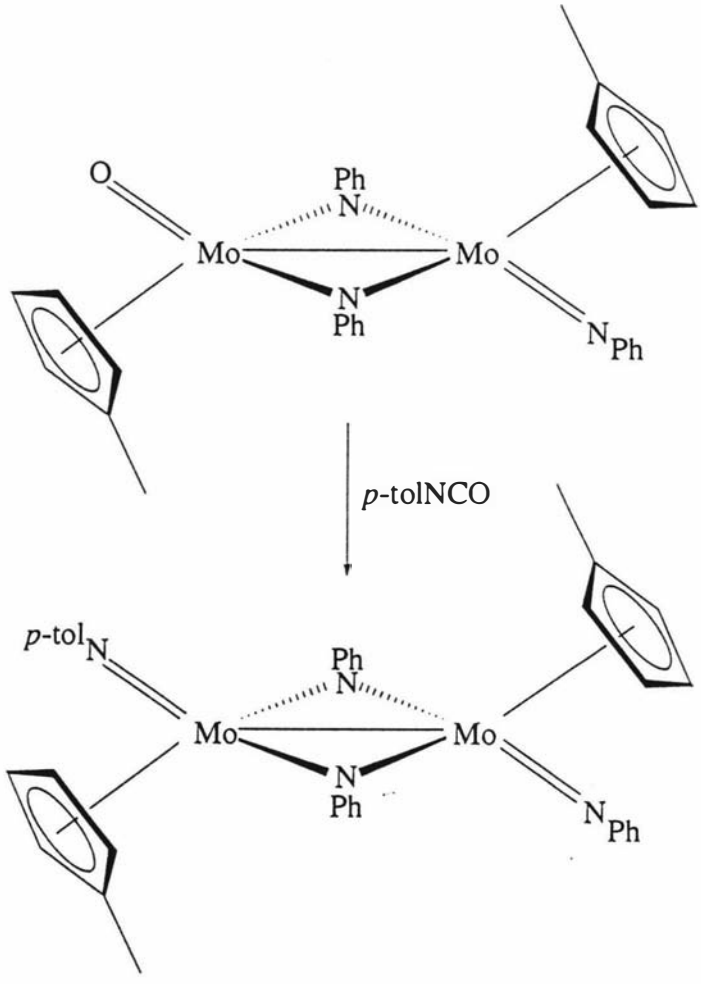

Equation 42

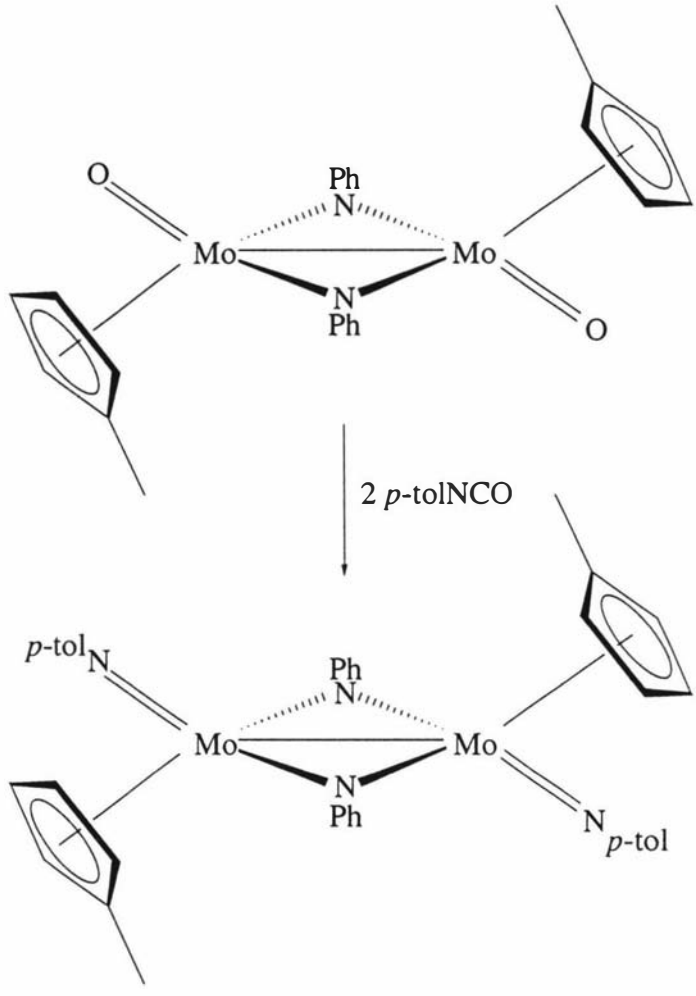

Equation 43

Reaction of the dimeric imido complex, $[WCl_4(NPh)]_2$ with Me_3SiNH^tBu results in a dimeric compound with bridging phenylimido ligands and terminal ^{t}Bu imido ligands (Equ. 44).[77]

Monomeric mixed bis(imido) complexes of tungsten are also available. Reaction of the amine-*tert*-butyldichloro-*tert*-butylimido(μ-phenylimido)tungsten(VI) complex with PMe_3 or bipy yields mixed bis(imido) complexes (Equ. 45 and 46).[78] Notice that the chloro ligands can be *cis* or *trans* depending on the requirements of the new ligand employed.

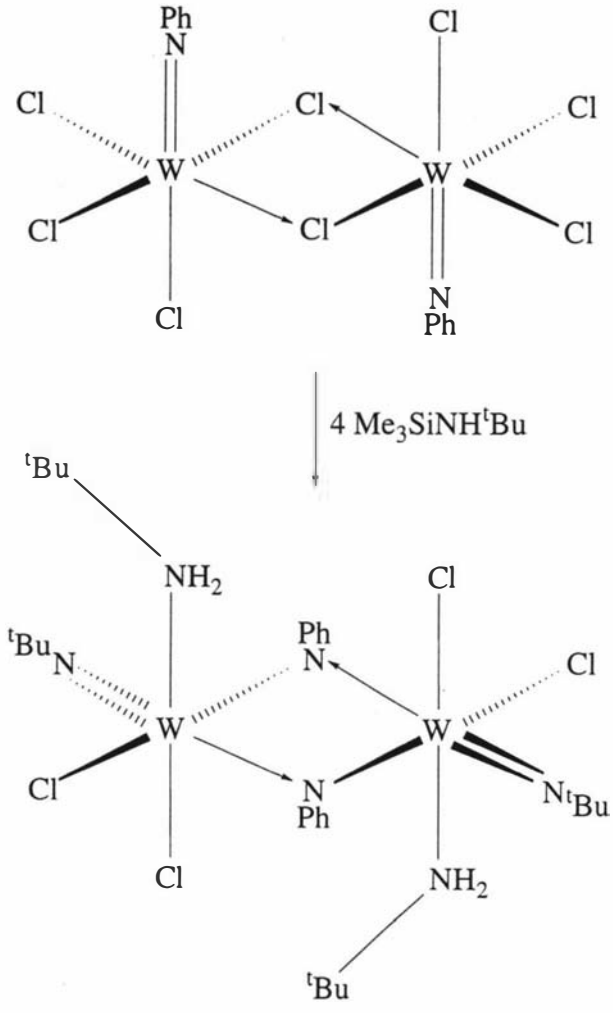

Equation 44

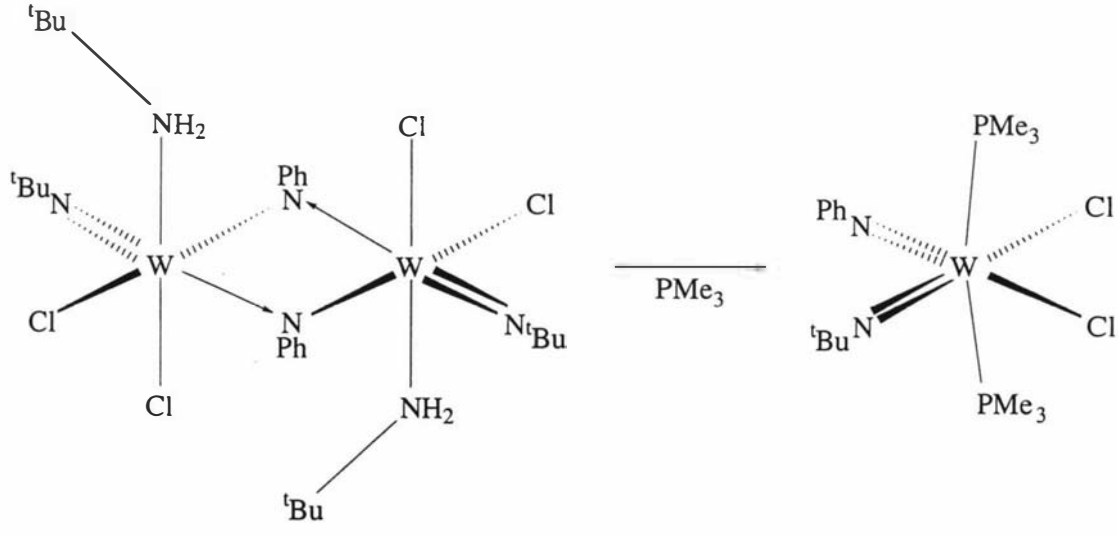

Equation 45

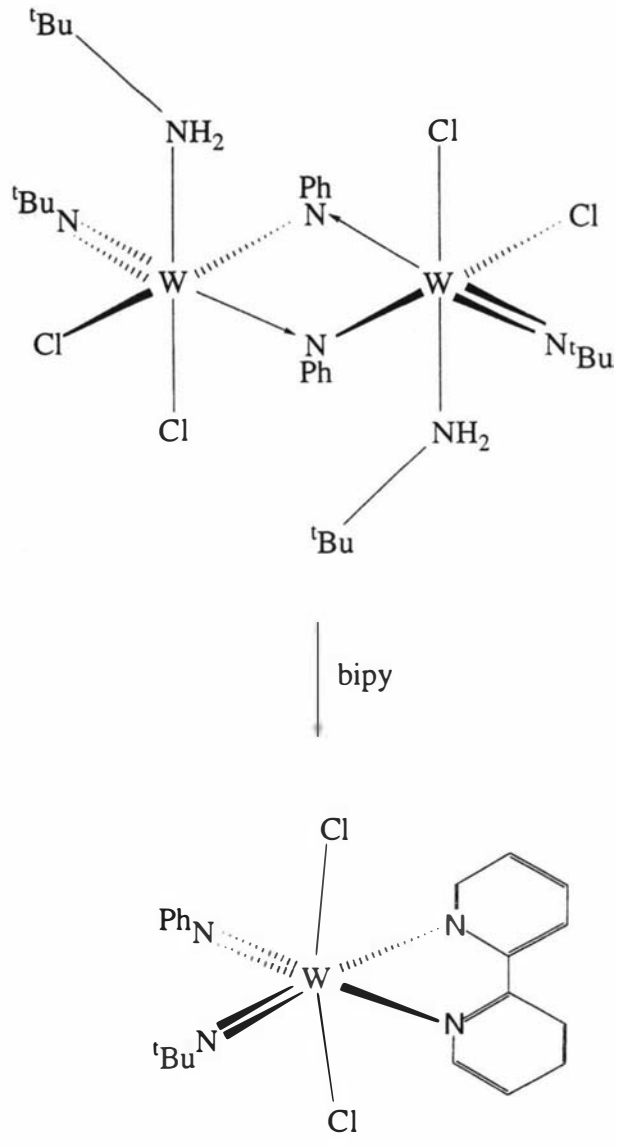

Equation 46

An alternative synthesis for the bipy mixed bis(imido) complex is with $[WCl_4(NPh)]_2$ and *p*-tolN$(SiMe_3)_2$ in the presence of bipy (Equ. 47).

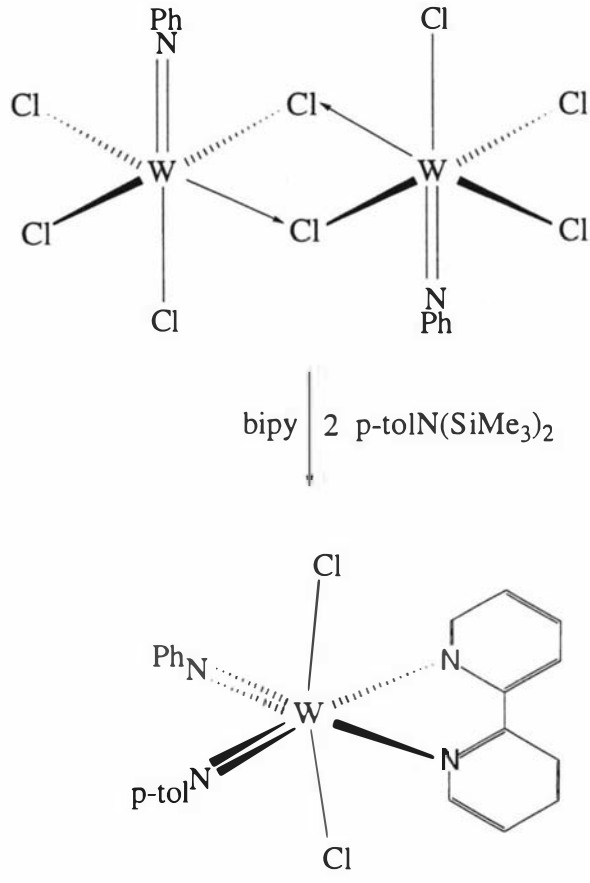

Equation 47

The 4-coordinate complexes $Mo(N^tBu)_2(O^tBu)_2$ undergo imido ligand exchange with $ArNH_2$ (Equ. 48). It is believed this reaction is likey to proceed via a trigonal bipyramidal base adduct (Scheme 8), which then must undergo a proton transfer to give a bis(amide) intermediate.[86]

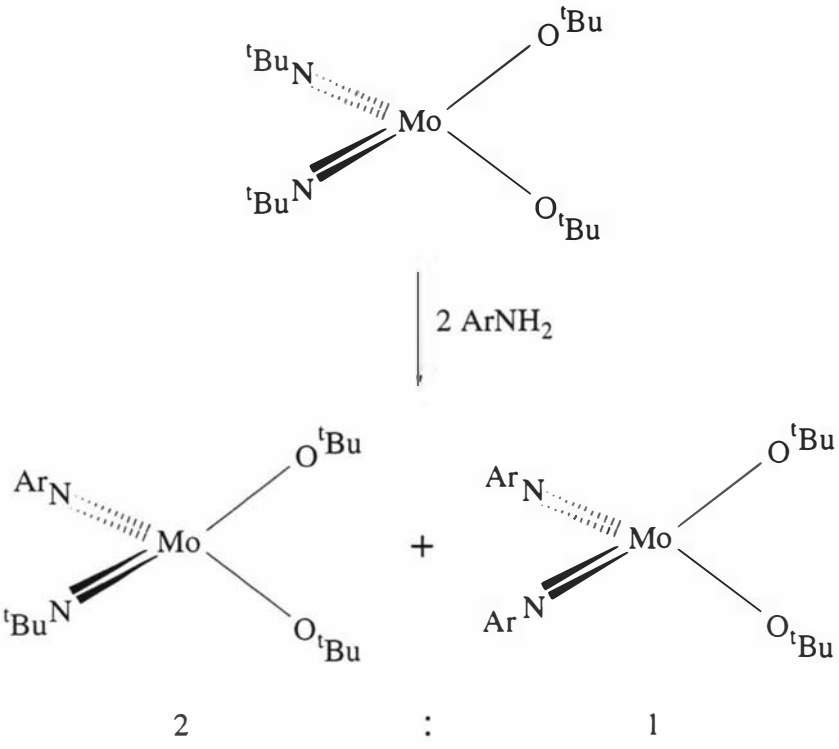

Equation 48

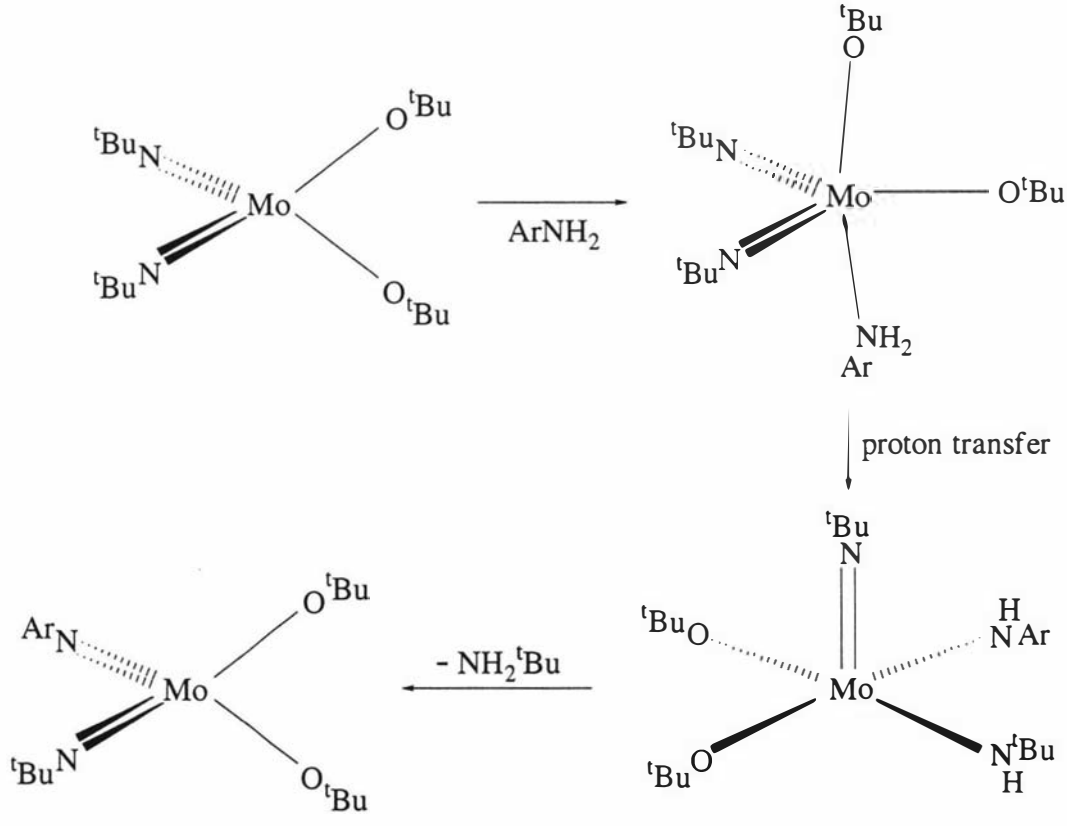

Scheme 8

Also imido ligand exchange reactions occur readily between coordinatively unsaturated centers of $Mo(NR)_2(O^tBu)_2$ and $Nb(\eta^5\text{-}C_5H_5)(O^tBu)_2(N^tBu)$ (Equ. 49 and 50).[87] This exchange may procced via a 4-center transition state (Fig. 27).

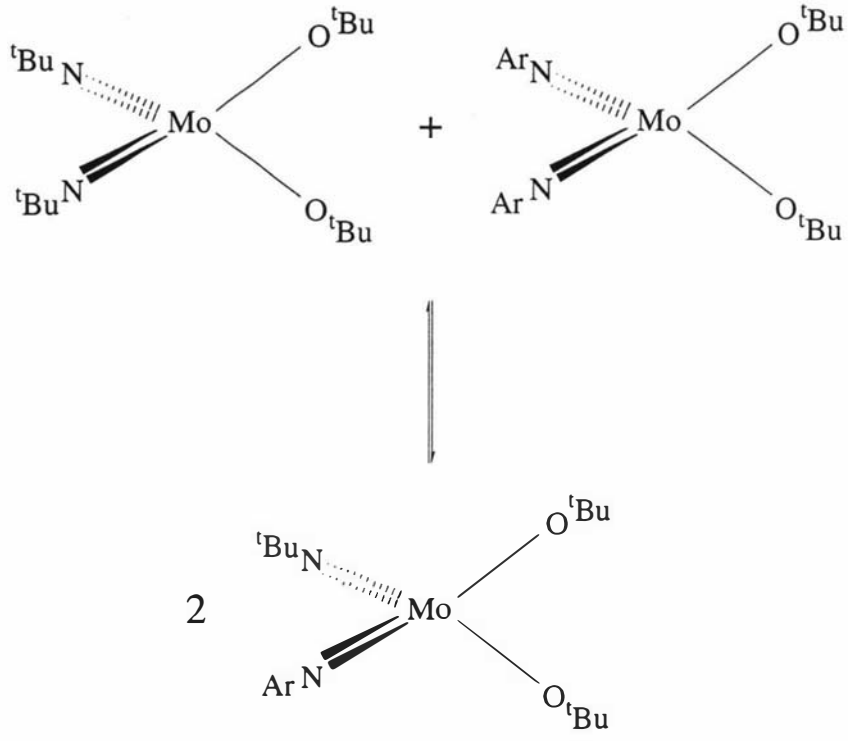

Equation 49

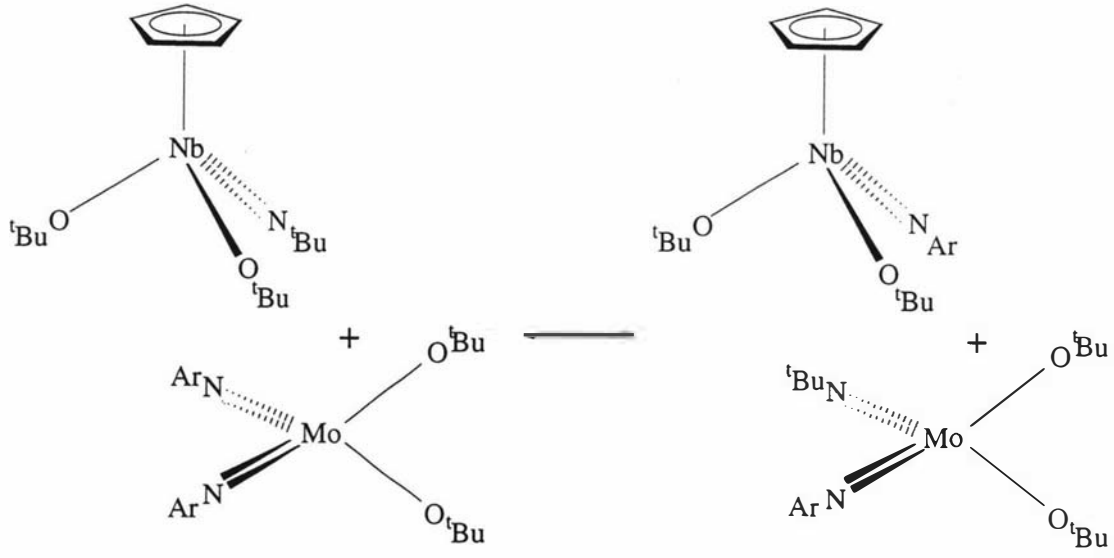

Equation 50

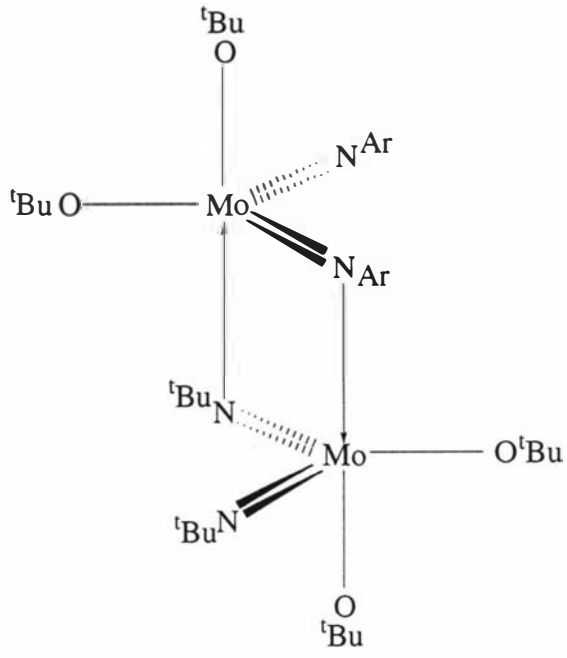

Figure 27

Sharpless *et al.* synthesized bis(imido)bis(oxo) and tris(imido)oxo complexes of Os(VIII) with use of the appropiate oxo complex and a phosphinimine. Using this methodology the only example of a mixed tris(imido) complex was synthesized (Equ. 51).[34]

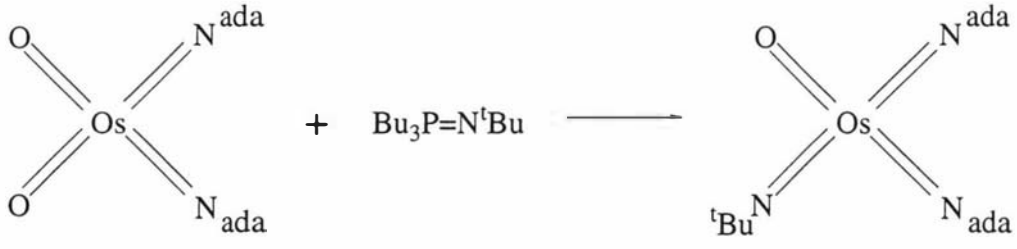

Equation 51

In a attempt to synthesize a Re(VI) mixed bis(imido) complex analogue to $[WCl_2(N^tBu)(\mu\text{-}NPh)(NH_2{}^tBu)]_2$ with Me_3SiNH^tBu, a Re(V) mono(imido) complex was obtained (Equ. 52).[79]

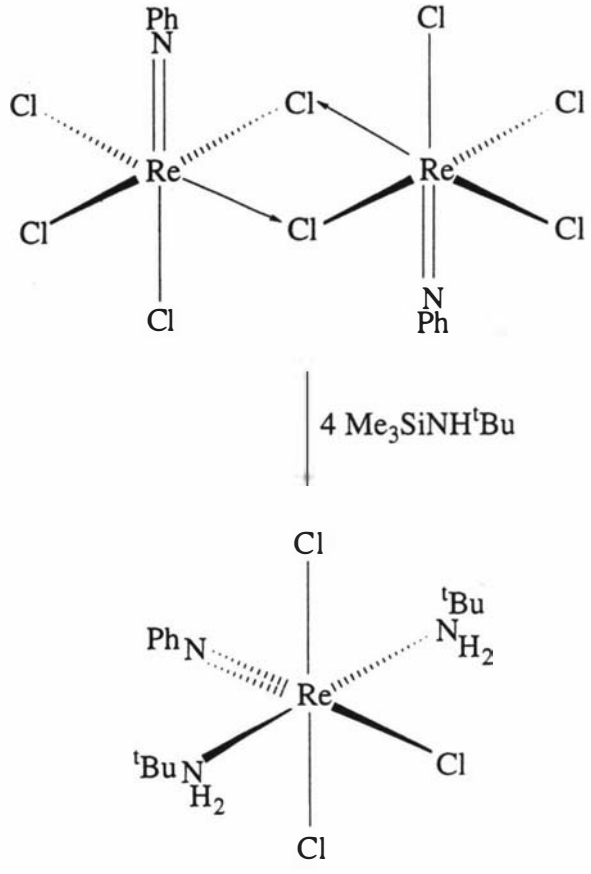

Equation 52

Although the reaction of alkenes with complexes of the type, $OsO_{4-n}(NR)_n$ (n=0, 1, 2) have been shown to form bis(amide) complexes (see pages 4, 20 and 21), the mixed imido complexes, $OsO_2(NR^1)(NR^2)$ and $OsO(Nada)_2(N^tBu)$, were not reported with regard to their reaction with alkenes.[34]

Imido complexes of uranium bear illustration to unique modes of bis(imido) formation.[59] The use of an assymmetric 1,2-diarylhydrazide leads to a mixed bis(imido) U(VI) complex (Equ. 53). This is the first example of reductive cleavage of a hydrazo compound yielding two organoimido functional groups at a single metal.[59]

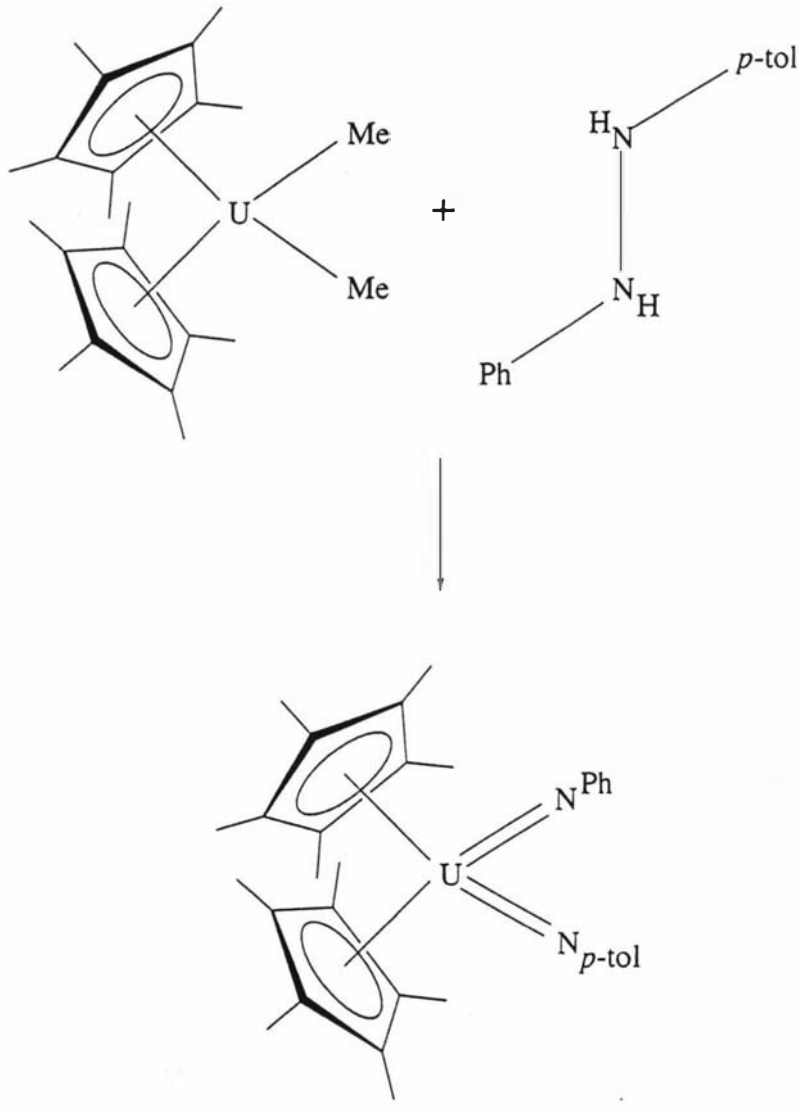

Equation 53

A reaction similar to the one used to prepare $Re(NAr)_3Cl$ (Re_2O_7, $ArNH_2$, NEt_3 and chlorotrimethylsilane[12]) can also be applied to the synthesis of bis(imido) complexes of molybdenum (Scheme 9).[80] Using 1 equivalent of $ArNH_2$ and 1 equivalent of $^tBuNH_2$ leads to a mixture of 3 complexes, the bis(imido) complexes $(N^tBu)_2MoCl_2(dme)$, $(NAr)_2MoCl_2(dme)$ and the mixed bis(imido) complex, $(N^tBu)(NAr)MoCl_2(dme)$. Recrystallization of the mixture results in the isolation of the mixed imido complex in 35% yield.

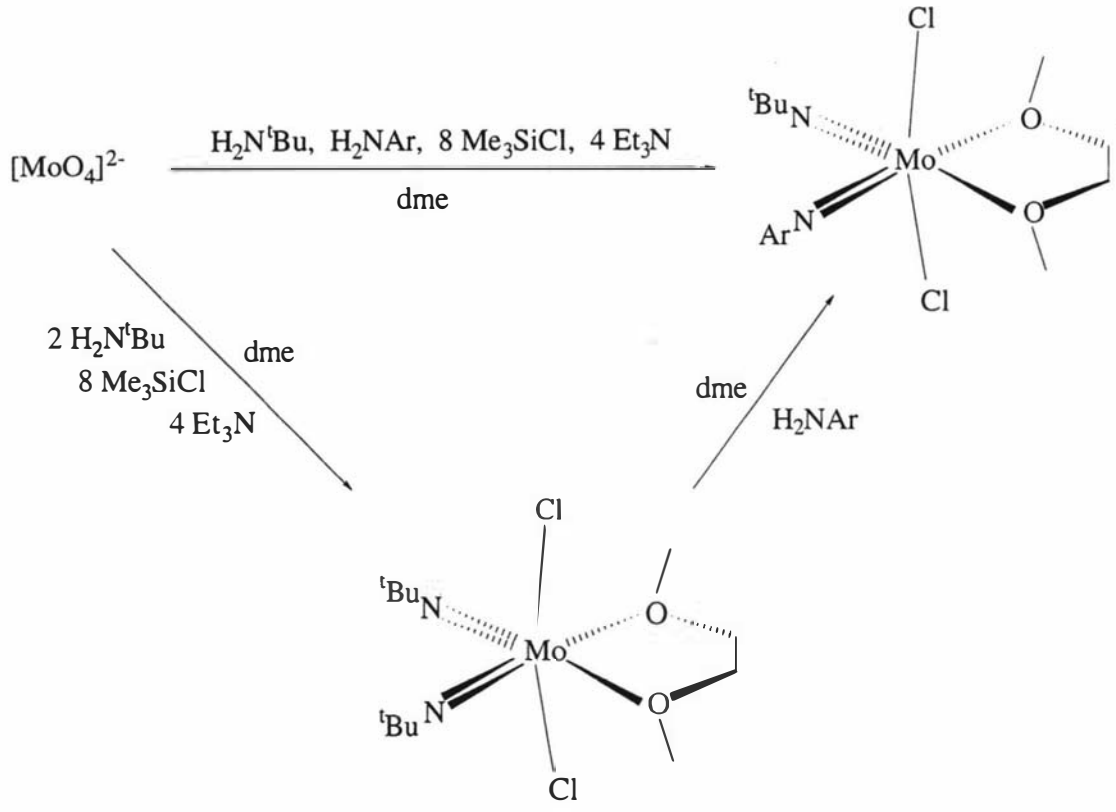

Scheme 9

Alternatively the bis(imido) complex, $(N^tBu)_2MoCl_2(dme)$ can be treated with 1 equiv of $ArNH_2$ in refluxing dme for one hour to afford $(N^tBu)(NAr)MoCl_2(dme)$ in 60% yield (Scheme 9).[81,82] The second method is limited to producing only mixed imido complexes of the type $(N^tBu)(NR)MoCl_2(dme)$, as imido ligand exchange only occurs appreciately with the *tert*-butyl imido ligand.

Structure and bonding

Structural investigations of mixed imido complexes have been limited. However in the case of octahedral Mo(VI) mixed bis(imido) complexes, where crystal structures have been obtained, the effect of different imido substituents can be seen.

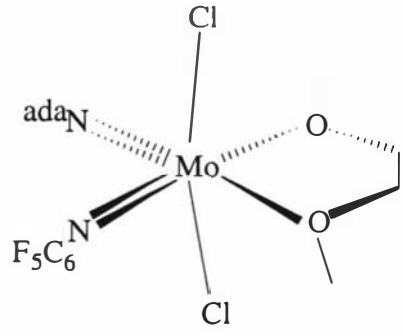

Figure 28

The mixed bis(imido) molybdnum complex shown in figure 28 has been structurally characterized.[82] The Mo-N distances for the adamantylimido ligand are 1.716(3)Å and 1.715(3)Å, while those for pentafluorophenylimido are longer at 1.759(3)Å and 1.775(3)Å. This is thought to occur as the more electron releasing adamantylimido ligand would be expected to be capable of forming stronger π-interactions with metal dπ-symmetry orbitals and the metal-nitrogen π-interactions in the Mo-N(C_6F_5) fragment are likely to be diminished due to π-bonding between the nitrogen and the *ipso*-carbon of the aromatic ring.

The effect of having one imido ligand with a substituent that contains an *ipso* - carbon and one that does not is nicely illustrated in the complex shown in figure 29. The Mo-NAr distance of 1.753(2)Å is slightly longer than Mo-N^{t}Bu at 1.728(2)Å. This is believed to occur due to the π-overlap between the nitrogen and *ipso*-carbon of the aryl ring, which effectively places the metal and *ipso*-carbon in competition for one of the nitrogen p-orbitals.[83]

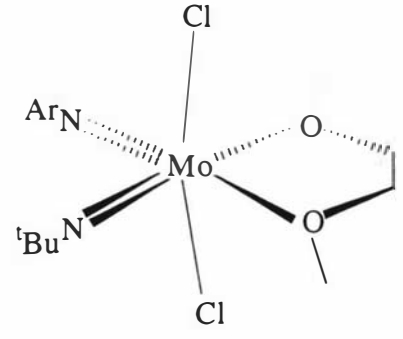

Figure 29

Each of the imido nitrogen atoms can form one strong π-bond unencumbered by competition (Fig. 30). The π-interaction in the xy plane however results in competition

between the p orbitals on N(1) and N(2) for the only suitable orientated metal dπ orbital d_{xy} as shown in Figure 30.

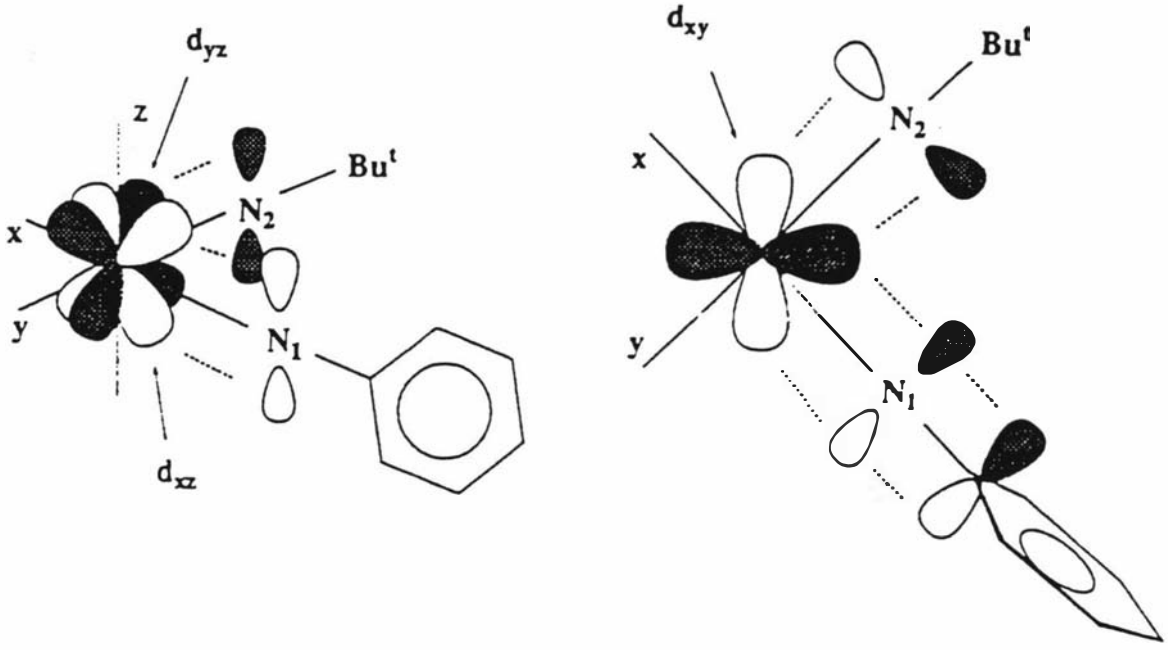

Figure 30

If the substituents on the imido ligands are the same, then the stength of the metal-nitrogen π-bonds would be identical. However, the differing imido substituents present in Mo(N^{t}Bu)(NAr)Cl_2(dme) remove the degeneracy and allow one of the nitrogens to form a stronger π-interaction in the xy plane. This is indicated by the orientation of the phenyl ring, which is positioned in the d_{xz} plane so as to allow the p orbital on the *ipso*-phenyl carbon to interact with the N(1) p_y orbital, thereby diminishing the M-N(1) dπ-pπ interaction. Such an orientation thus allows N(2) to form a stronger π-bond to the metal in the d_{xy} plane and thus give rise to an electronic preference for the phenyl ring orientation. A similar argument can be used for W(N^{t}Bu)(NPh)Cl_2(bipy) where the W-N^{t}Bu distance is 1.754(10)Å is shorter than W-NPh at 1.774(8)Å (Fig. 31).[79] The bis(imido) containing 2 phenylimido ligands, W(NPh)$_2$$Cl_2$(bipy) has W-NPh lengths of 1.775(9)Å and 1.782(9)Å (Fig. 32).[78] Also the 4-coordinate complex, Mo(NAr)(N^{t}Bu)(CH_2^{t}Bu)$_2$ has Mo-N^{t}Bu length of 1.737(2)Å, shorter than the Mo-NAr length of 1.759(2)Å.[81]

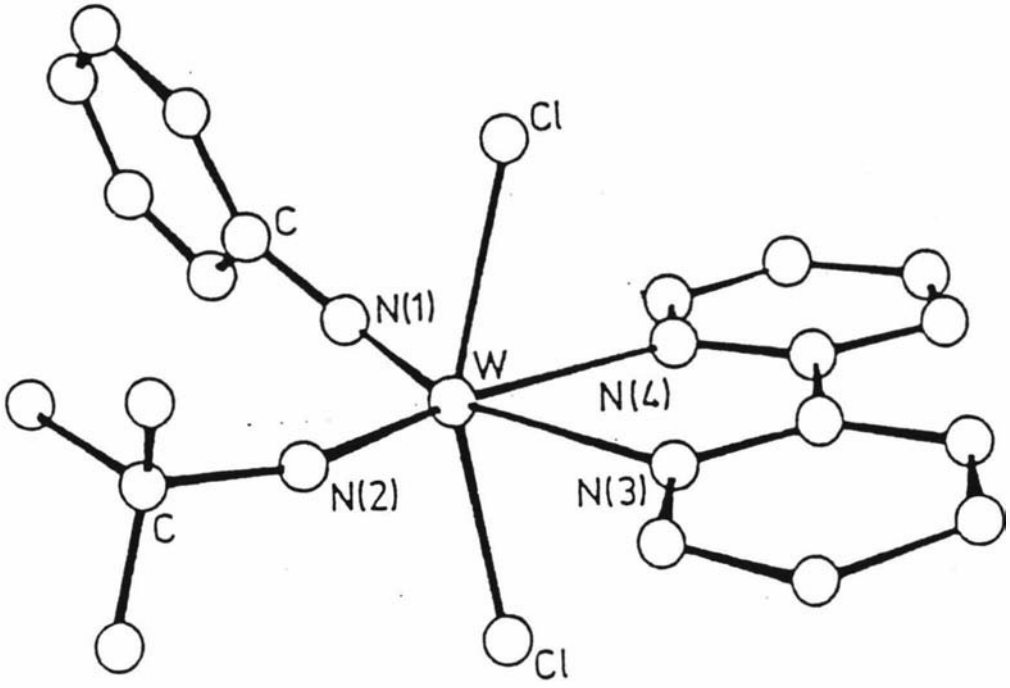

Figure 31

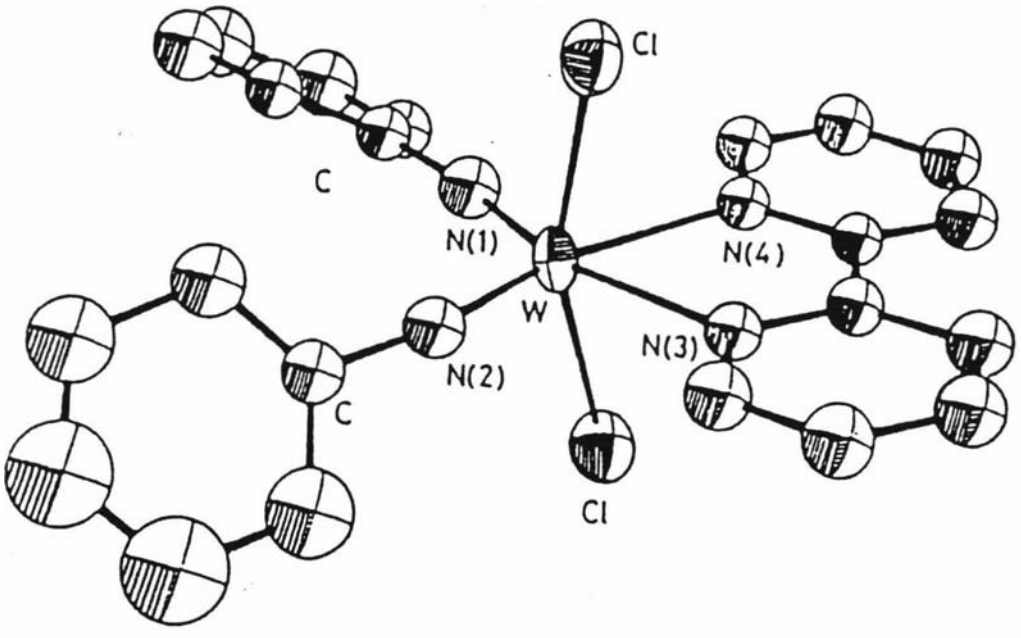

Figure 32

Reactions

The metathesis reaction of isocyanate and metal oxo complexes leading to formation of metal imido complexes has previously been mentioned. The formation of $[Mo(C_5H_4Me)(N\text{-}p\text{-tol})(\mu\text{-}NPh)]_2$ involves the metathesis of *p*-tolylisocyanate and a terminal phenylimido ligand (Equ. 54).[75,76]

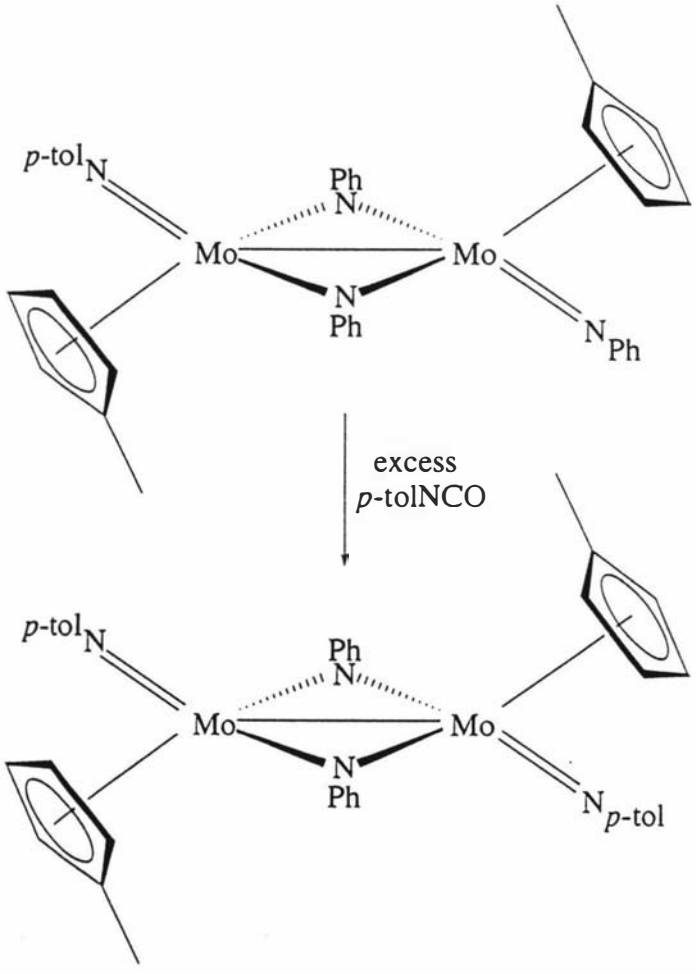

Equation 54

While mechanistic details of the exchange are not known, the reaction is assumed to proceed via a Wittig-like (2+2)π transformation (Scheme 10),[76] similar to that postulated for the exchange of oxo for imido ligands upon reaction with isocyanates.[84]

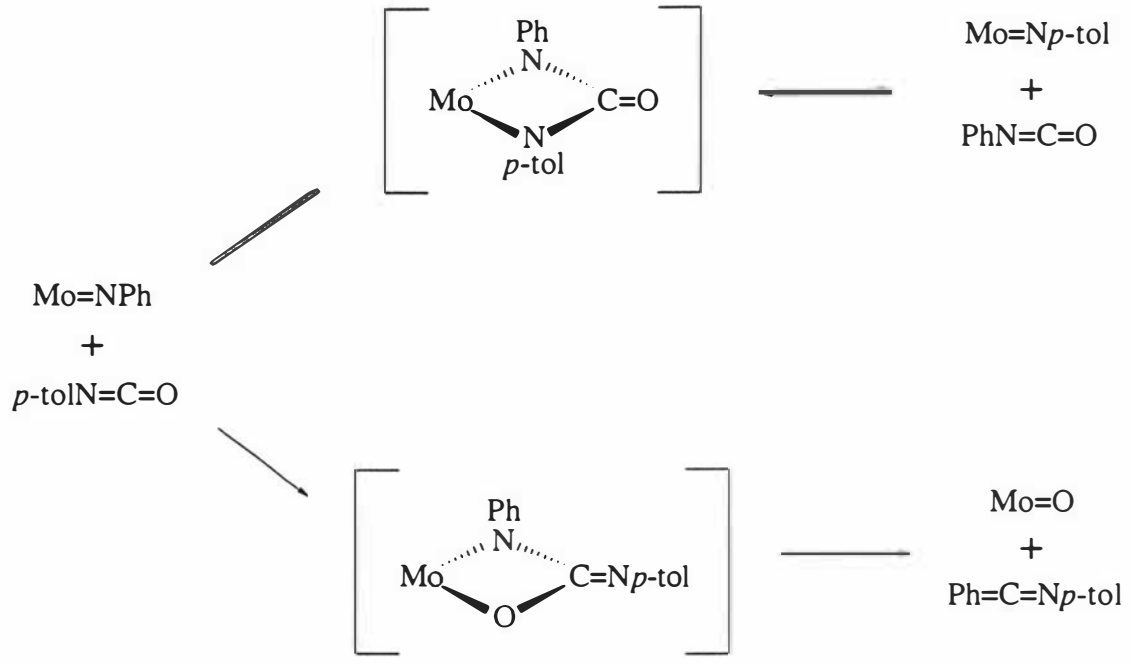

Scheme 10

The presence of excess *p*-tolylisocyanate would drive the reaction to completion (Equ. 54). The formation of a carbodi-imide and a molybdum oxide cannot be ruled out. Of course the Mo=O would react further with *p*-tolylisocyanate to give the *p*-tolylimido ligand.[84]

Treatment of Mo(N^{t}Bu)(NAr)Cl_2(dme) with 2 equivalents of neopentylmagnesium chloride in diethyl ether affords a 4-coordinate dialkyl complex, Mo(N^{t}Bu)(NAr)($CH_2{}^t$Bu)$_2$ (Equ. 55).

The more basic ***tert***-butylimido ligand is protonated upon reaction of HOC_6F_5 with Mo(N^{t}Bu)(NAr)($CH_2{}^t$Bu)$_2$ (Equ. 56). There is no evidence of protonation at the less basic arylimido ligand.[81]

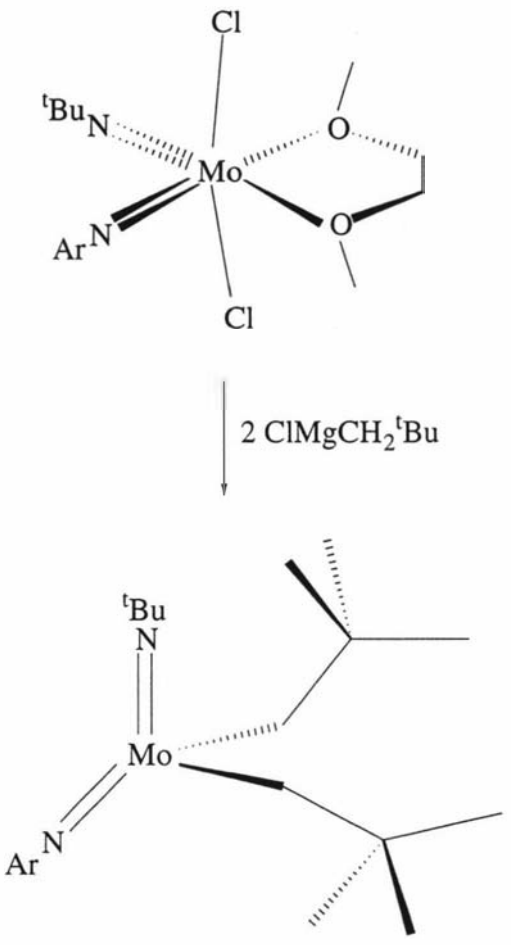

Equation 55

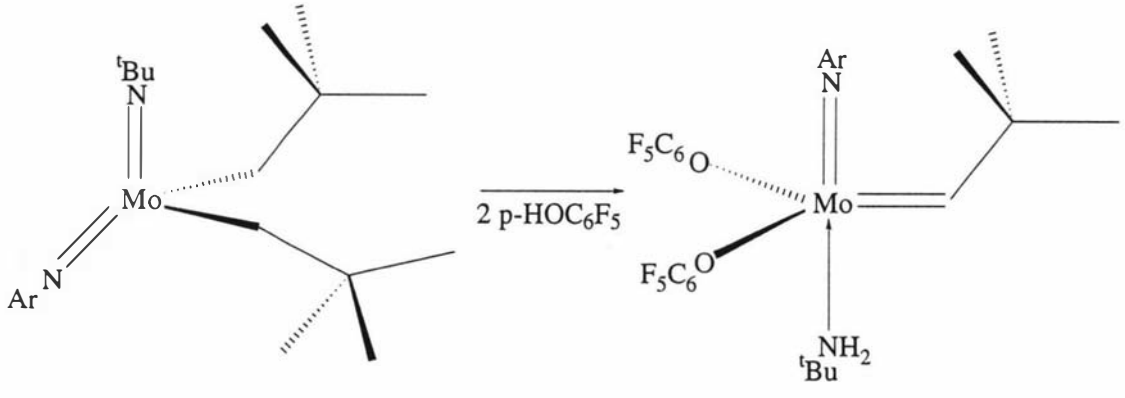

Equation 56

Uranium(IV) bis(amido) complexes can be synthesized from the U(VI) bis(imido) complexes (Equ. 57).[59] The homolytic cleavage of dihydrogen by imido complexes has not been previously observed.

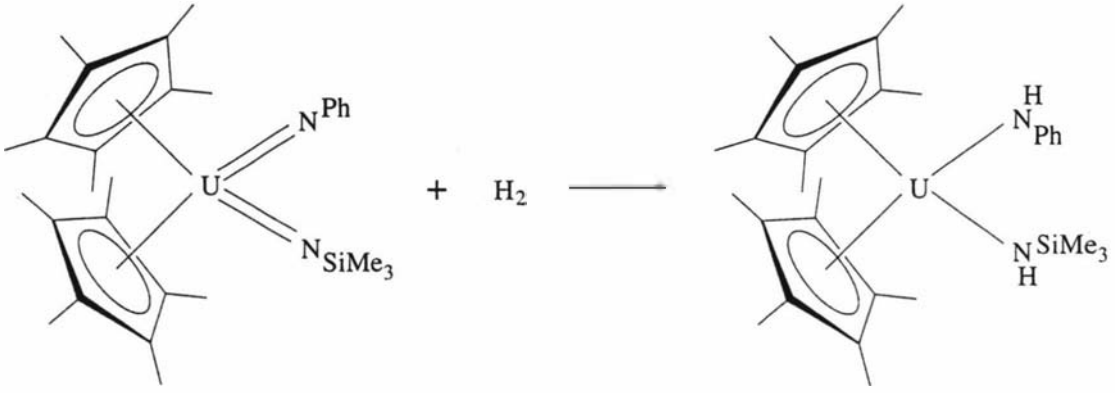

Equation 57

Concluding remarks

Investigations into the chemistry of mixed imido complexes has been limited. Examples have been observed only with molybdenum, tungsten, osmium and uranium. The molybdenum and tungsten mixed imido complexes are dimeric or 6-coordinate bis(imido) monomeric species. The monomers are synthesized with reaction of neutral molecules such as PMe_3 and bipy with the dimeric species or from MoO_4^{2-} yielding statistical mixtures. Interestingly an attempt to synthesize a mixed bis(imido) complex of Re(VI) failed. The synthesis of tetrahedral monomeric mixed bis(imido) complexes of molybdenum used either imido liagnd exchange with anilines or between another metal center.

The utility of oxo ligands to form imido ligands was shown in the tetrahedral Os(VIII) complexes. Displacement of the oxo ligand with reaction of phosphinimines (R_3P=NR) to form new imido ligands allowed the formation of the only known example of a mixed tris(imido) complex. The use of a 1,2-disubstituted hydrazine in the synthesis of a mixed bis(imido) U(VI) complex is the first such example.

The orientation of the phenyl ring in 6-coordinate molybdenum(VI) species has been explained in terms of competition between M-N dπ-pπ interactions. Thus the presence of an alkylimido ligand has given rise to an electronic preference for the phenyl ring orientation.

Reactions involving the imido ligands of mixed imido complexes are extremely rare. The homolytic cleavage of H_2 by the uranium complex (Cp*)U(NPh)($NSiMe_3$) to form the bis(amido) complex also occurs with the bis(phenylimido) complex, (Cp*)U($NPh)_2$. However, the protonation reaction of Mo(NAr)(N^{t}Bu)($CH_2{}^t$Bu)$_2$ with HOC_6F_5 showed that the more basic imido ligand is protonated as expected. Hence preferential reactivity at one imido ligand can be selected for by synthesizing complexes containing imido ligands with different substituents (Fig. 33).

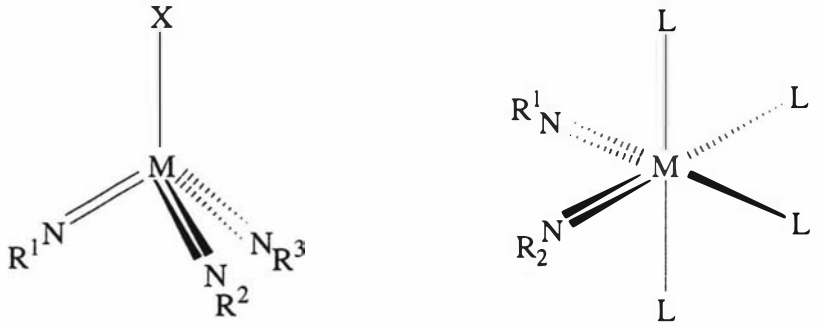

Figure 33

Conclusion

Limiting valence bond (VB) descriptions of imido ligand bonding can lead to tenous conclusions, especially where the complex contains multiple imido ligands. As such a MO approach is often required to understand bonding features in tris(imido) complexes. Many 20-electron imido complexes have now been shown to be best described as 18-electron complexes due to a mismatch of symmetry on the N pπ orbitals, for example $Os(NAr)_3$.[26] The effects of π-loading have been observed in the structures of $ITc(NAr)_3$ compared with $Me_3SiOTc(NAr)_3$[22] and in the bonding mode of Me_3SiO^- in $Me_3SiORe(N^tBu)_3$,[30] and of $CH_2{=}CHCH_2^-$ in $Re(N^tBu)_3(\eta^1\text{-}CH_2CH{=}CH_2)$.[41] Highly reactive transition metal moieties that can activate C-H bonds can be generated if sufficient electron density resides on the imido nitrogen.[90] The cycloaddition reactions of $[Mo(NAr)_3Cl]^-$ suggest that the Mo-N polarity is enhanced via π-loading.[28] The coordination of multiple π-donors can result in increased stabilization of high valent metal centres and increased nucleophilicity of the ligands.[1b,44,46,15,27] The tris(imido) technetium fragment is even capable of stabilizing iodide, a ligand that is quite susceptible to oxidation.[1b,51]

Competition between strong π-donor ligands results in the imido ligands of tris(imido) complexes to have a lowered bond order and bending at the nitrogen may be observed. Electron density is displaced from the metal-nitrogen bond to the nitrogen atom making the imido ligand more nucleophilic at nitrogen.[1b,44,46,15,27] The structure of 6-coordinate mixed bis(imido) complexes containing an alkylimido ligand and an arylimido ligand suggested that the orientation of the aryl ring is electronically determined.[83] Interestingly the reaction of the d^2 rhenium tris(imido) complex, $Re(NAr)_3H$ with alkynes leads to η^2-alkyne complexes,[12] while with mono and bis(imido) early transition metal[2,60] complexes and low valent iridium mono(imido) complexes[9] cycloaddition products are observed. Also diamide complexes result with $OsO(N^tBu)_3$ and alkenes.[34] Why is there no cycloaddition or indeed diamide formation with $Re(NAr)_3H$ or $XRe(NR)_3$ and

alkenes/alkynes? The simple substitution of an imido ligand for 2 methyl ligands in the reaction of $[Tc(NAr')_2(\mu\text{-}NAr')]$ with MeMgCl[43] illustrates the unexpected reactivity π-loaded complexes can exhibit.

The structures of dimeric d^1 tris(imido) species is largely controlled by the steric bulk of the imido ligands.[31,17,30] Therefore if the bulk of the imido ligand is increased from 2,6-diisopropylphenyl to a bulkier imido ligand then it may be possible to isolate a monomeric d^1 tris(imido) complex.

The only example of a mixed tris(imido) complex is that of osmium, $OsO(Nada)_2(N^tBu)$,[34] however there are many examples of mixed bis(imido) complexes (see pages 51-60). As the protonation of $Mo(NAr)(N^tBu)(CH_2{}^tBu)_2$ illustrated, each imido ligand can have different reactivities.[81] The presence of electronically and sterically disparate imido ligands in tris(imido) complexes at the same metal centre should show interesting and diverse chemistry.

The literature methods of synthesizing tetrahedral tris(imido) complexes do not allow for the inclusion of an imido ligand containing an organic substituent different from those of the other imido ligands. In the next chapter complexes of this type, $XRe(NR)_2(NR')$, i.e mixed imido complexes will be synthesized using a readily viable method.

Chapter Two

Synthesis of Re(VII) Complexes

Introduction

This chapter describes the synthesis of tetrahedral rhenium(VII) tris(imido) complexes. The methodology developed incorporates the modification of prexisting procedures and development of a new procedure for viable formation of mixed imido species and a chiral complex.

The synthesis of rhenium tris(imido) complexes from the oxo species has generally involved the use of isocyanates[41,51,63] or silylamides. [61] However, a simple one-pot synthesis has been developed for bis(imido) complexes.[91,92,93] Here we have modified a procedure used to prepare tris(imido) complexes[12,64,80] and used it to prepare mixed tris(imido) compounds.

Synthesis from ReO_4^-

Toreki *et al.* reported an improved synthesis of $Re(NR)_2Cl_3(py)$ (R=Ar', Ar) and $Me_3SiORe(N^tBu)_3$ (Equ. 58 and 59),[64] using only the amine or aniline as the imido source.

$$0.5\ Re_2O_7 + 2\ ArNH_2 + 7\ Me_3SiCl + xs\ py \longrightarrow Re(NAr)_2Cl_3(py) + 4\ pyHCl + 3.5\ (Me_3Si)_2O$$

Equation 58

$$0.5\ Re_2O_7 + 9\ ^tBuNH_2 + 6\ Me_3SiCl$$

$$\downarrow$$

$$Re(N^tBu)_3(OSiMe_3) + 6\ ^tBuNH_3Cl + 2.5\ (Me_3Si)_2O$$

Equation 59

Complexes of this type were previously prepared via the reaction of the tris(oxo) species and the isocyanate[51] or silylamide.[61,94] The most important step in this new reaction (Equ. 59) probably involves attack of the aniline at the metal followed by proton transfer to an oxo ligand giving the imido ligand and water. The water then reacts with Me_3SiCl to give hexamethyldisiloxane and HCl. The HCl is removed from the reaction as $^tBuNH_3Cl$, thereby driving what would otherwise likely be an equilibrium to the right.[64]

$$0.5\ Re_2O_7 + 3\ ArNH_2 + 6\ NEt_3 + 7\ Me_3SiCl$$

$$\downarrow$$

$$Re(NAr)_3Cl + 6\ Et_3NHCl + 3.5\ (Me_3Si)_2O$$

Equation 60

This methodology was also applied to the synthesis of the rhenium tris(arylimido) complex, $Re(NAr)_3Cl$ (Equ. 60).[12] In this case NEt_3 was used as the HCl trap. Notice the odd behaviour of the reactions of equations 59 and 60. One product contains the siloxy group, the other the chloro. The reason for this is not known, however it is tempting to suggest the steric bulk of the imido ligands plays a part. We will see later (see page 73) that the situation is not so clear.

Synthesis from bis(imido) complexes

The one-pot synthesis described above (Equ. 59 and 60) is not suitable for formation of mixed tris(imido) complexes, $ClRe(NR)_2(NR')$, as such a new method is

required. Converting bis(imido) complexes ($Re(NR)_2Cl_3L$) to tris(imido) complexes should allow such complexes to be synthesized.

The formation of tris(imido) compounds from bis(imido) complexes involves deprotonation of an amido ligand using LiNHR reagents[44,14] or in the case of a tungsten amidobis(imido) complex reaction with KH forming H_2 and the tris(imido) compound.[20] There are however no examples of this type of reaction involving rhenium amidobis(imido) complexes. Although the deprotonation of a Re(VII) amidotris(imido) complex with LiMe(tmed) to form the tetrakis(imido) complex was reported in 1989,[62] no such reaction with an amidobis(imido) complex has been reported.

$$Re(NAr)_3Cl \xrightarrow[2\ NEt_3]{2\ pyHCl} Re(NAr)_2Cl_3(py) + ArNH_2$$

Equation 61

The reaction shown in equation 61 was only briefly described in a paper by Williams and Schrock.[12] Reaction of pyHCl towards the tris(imido) complex, $Re(NAr)_3Cl$, results in a bis(imido) complex and aniline. The fact that triethylamine reverses this reaction provides not only a route to Re(VII) tris(imido) complexes, but a viable methodology for the preparation of mixed tris(imido) complexes (Equ. 62, R=aryl).

$$Re(NAr)_2Cl_3(py) + RNH_2 + 2\ NEt_3$$

$$\downarrow$$

$$Re(NAr)_2(NR)Cl + 2\ Et_3NHCl + py$$

Equation 62

Results and Discussion

Synthesis of tris(imido) complexes

When the anilines (RNH_2), and triethylamine were added to a suspension of $[ReO_4][NH_4]$ followed by addition of Me_3SiCl at –40°C, the Re(VII) tris(imido) complexes (Scheme 11) were isolated in good yield.

$$ReO_4^- + 3\,RNH_2 + 7\,Et_3N + 8\,Me_3SiCl \longrightarrow XRe(NR)_3$$

R	X	Complex
Ar'	Me_3SiO	$Me_3SiORe(NAr')_3$
mes	Cl	$ClRe(Nmes)_3$
Ar	Cl	$ClRe(NAr)_3$

Scheme 11

The synthesis of $Re(NAr)_3Cl$ is analogous to that reported by Schrock and Williams.[12] The only difference being the source of rhenium where, Re_2O_7 was used previously $[ReO_4][NH_4]$ (or $[ReO_4][NBu_4]$) was used here. The complex $Me_3SiORe(NAr')_3$ has been previously reported,[51] however was prepared from the isocyanate, Ar'NCO, and $Me_3SiOReO_3$.

It is interesting to note that the reaction with $Ar'NH_2$ leads to a siloxide complex while with $ArNH_2$ and $mesNH_2$, chloro complexes are formed. It is not known why such a difference occurs. However, it is not purely due to the steric bulk of the imido ligands. You would expect the Nmes ligand to be sterically similar to the NAr' ligand and hence the tris(Nmes) complex to contain the siloxy group, this is not the case.

Another route to chlorotris(imido) complexes is shown in Scheme 12.

$$Re(NR)_2Cl_3(py) + RNH_2 + 2\,Et_3N \longrightarrow ClRe(NR)_3$$

R	Complex
Ar'	$ClRe(NAr')_3$
Ar	$ClRe(NAr)_3$

Scheme 12

Although this synthetic method produces only moderate yields it does provide an alternative method to synthesize the chloro complex, $ClRe(NAr')_3$. This complex was previously reported by reaction of $Me_3SiOReO_3$ with Ar'NCO and HCl to form what is believed to be $[Ar'NH_3]$ $[Re(NAr')_2Cl_4]$ which then can be reacted with NEt_3 producing finally $ClRe(NAr')_3$.[51] The real advantage of this method is the ability to use a variety of anilines to form tris(imido) complexes that contain mixed imido ligands with different organic substituents.

X-ray structure of $Me_3SiORe(NAr')_3$

X-ray quality crystals of $Me_3SiORe(NAr')_3$ were obtained from a concentrated hexane solution cooled to -35°. The final structure is shown in figure 34. Tables containing complete bond lengths and angles, atomic coordinate and equivalent isotropic displacement parameters, anisotropic displacement parameters and calculated H-atom positions are presented in appendix V.

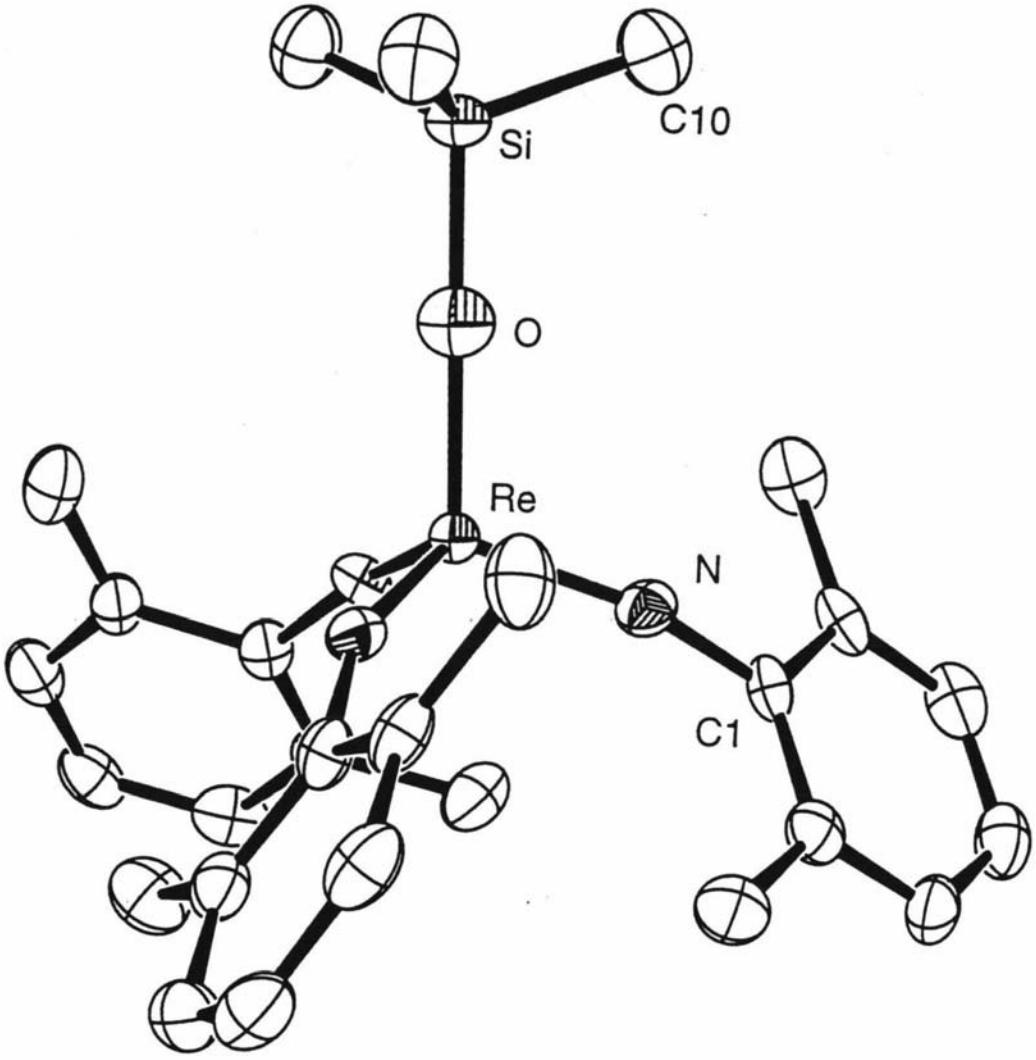

Figure 34

Tables 1 and 2 show selected bond lengths and angles for $Me_3SiORe(NAr')_3$ and 3 other rhenium(VII) tris(imido) siloxy complexes. The molecule has a distorted tetrahedral geometry with angles at the rhenium atom of 109.1(2)° and 109.87(19)°. The Re-O-Si angle is exactly linear as was found for $Ph_3SiORe(NAr)_3$.[104] The complexes $Me_3SiORe(N^tBu)_3$ and $Ph_3SiORe(NAr')_3$ have bent Re-Si-O angles of 138.2(4)° and 139.7(2)° respectively.[30,104] The substituents on the Si and Re have an eclipsed conformation. This conformation was also found for $Ph_3SiORe(NAr)_3$[104] (out of 3 independent structures, 2 were found in the staggered conformation, while one

was eclipsed). The Re-N-C bond is slightly bent at 158.8(5)° and compares with $Ph_3SiORe(NAr')_3$ with a Re-N-C angle of 158.4(3)°.[104] The Re-N distance of 1.749(6)Å falls within the range for known rhenium(VII) tris(imido) siloxy complexes at 1.706(9) to 1.754(5)Å (see table 2 and appendix III and IV). The Re-O distance may give an indication of the extent of π-bonding the siloxide is involved in. In fact the Re-O distance of 1.840(12)Å is on the shorter side compared with the complexes of table 2 which range from 1.880(11) to 1.902(3)Å, suggesting the siloxide contributes some degree of π-bonding.

Complex	#	X-Re-N(#)	Re-N(#)-C	N(1)-Re-N(#)	Ref.	Comments
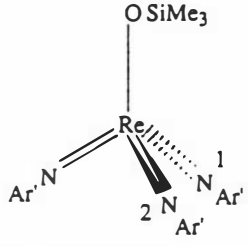	1	109.87(19)	158.8(5)		-	O-Si-C
	2			109.1(2)		107.8(3)
						Re-O-Si
						180.0(1)
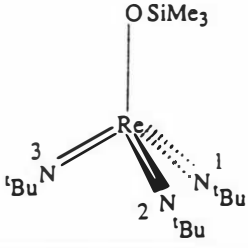	1	109.7(4)	164.8(8)		30	Distorted tetrahedral
	2	110.4(5)	160.6(9)	111.1(6)		Re-O-Si 138.2(4)
	3	108.0(4)	157.7(8)	109.0(6)		N(2)-Re-N(3)
						108.7(6)
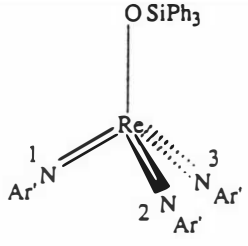	1	106.0(1)	158.4(3)		104	Distorted tetrahedral
	2	108.6(1)		112.0(1)		Re-O-Si 139.7(2)
	3	107.0(1)		110.5(2)		N(2)-Re-N(3)
						112.4(2)
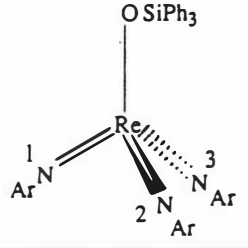	1	109.3(2)			104	N(2)-Re-N(3)
	2	109.3(2)		109.6(2)		109.6(2)
	3	109.3(2)		109.6(2)		Re-O-Si 180.0(1)
						Average values

Table 1: Selected bond angles(°) for $Me_3SiORe(NAr')_3$ and 3 other Re(VII) tris(imido)-siloxy complexes

Complex	Re-X	Re-N(1)	Re-N(2)	Re-N(3)	Ref.	Comments
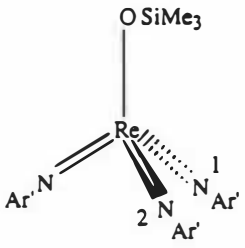	1.840(12)	1.749(6)			-	Si-O 1.671(12)
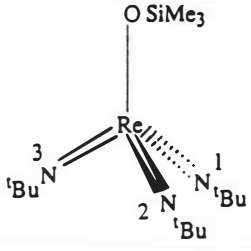	1.899(7)	1.706(9)	1.704(11)	1.740(10)	30	Si-O 1.624(8)
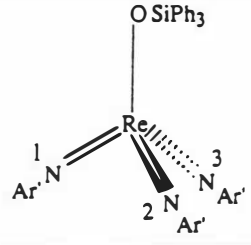	1.902(3)	1.743(3)	1.750(3)	1.726(3)	104	Si-O 1.652(3)
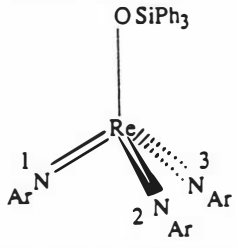	1.880(11)	1.753(5)	1.753(6)	1.754(5)	104	Si-O 1.625(11) Average values

Table 2: Selected bond lengths(Å) for $Me_3SiORe(NAr')_3$ and 3 other Re(VII)tris-(imido)siloxy complexes

X-ray structure of $ClRe(NAr)_3$

X-ray quality crystals of $ClRe(NAr)_3$ were obtained from evaporation of a hexane solution. The final structure is shown in Figure 35. Tables containing complete bond lengths and angles, atomic coordinate and equivalent isotropic displacement parameters, anisotropic displacement parameters and calculated H-atom positions are presented in appendix VI.

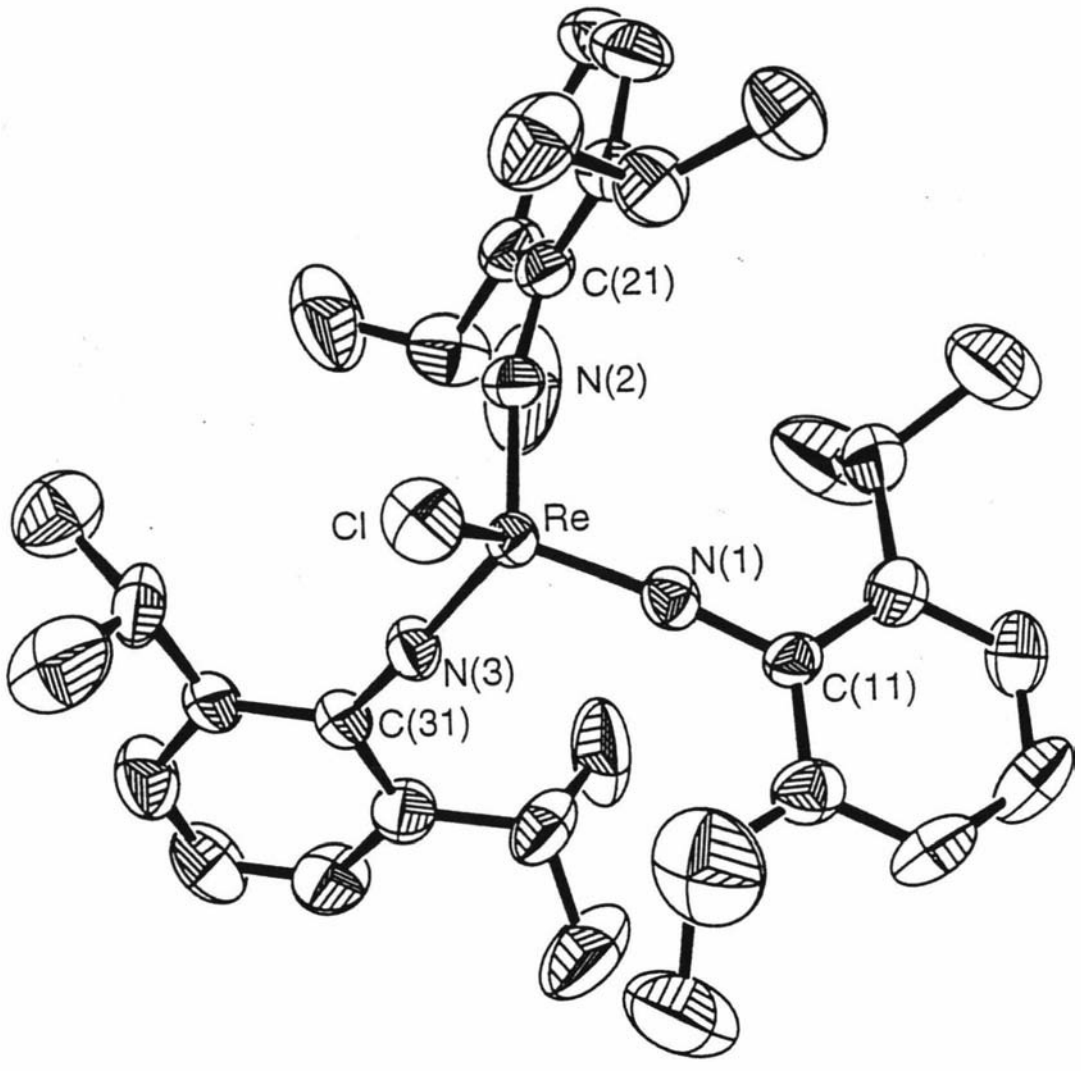

Figure 35

Tables 3 and 4 show selected bond lengths and angles for $ClRe(NAr)_3$ and 3 other related rhenium(VII) tris(imido) complexes. The rhenium atom is in an approximately tetrahedral environment. The Re-N-C bond is slightly bent at 168.8(7)° (average) and compares with complexes of table 3, as does the short Re-N bond length of 1.758Å (average). The Re-Cl bond length compares well with that of $ClRe(NAr)_2(NAr')$ at 2.292(2) and 2.272(9)Å respectively.

Complex	#	X-M-N(#)	M-N(#)-C	N(1)-M-N(#)	Ref.	Comments
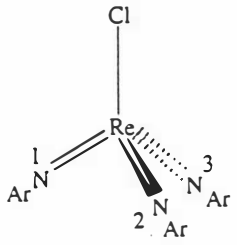	1	106.0(2)	168.9(5)		-	N(2)-Re-N(3)
	2	106.0(2)	165.9(7)	111.2(3)		113.5(3)
	3	106.7(3)	171.5(7)	112.8(3)		
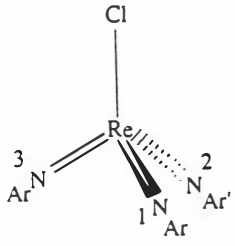	1	107.2(8)	165(2)		-	2 independent
		107.7(8)	166.6(19)			structures
	2	106.9(8)	165(2)	112.2(10)		N(2)-Re-N(3)
		107.1(7)	170.6(18)	110.0(9)		112.4(8)
	3	107.4(8)	172.5(19)	110.4(10)		113.5(10)
		106.7(8)	162.1(19)	111.6(10)		
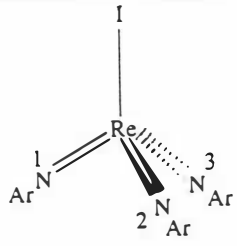	1	106.7(2)	165.7(6)		39	Approximately
	2	105.9(2)	169.9(6)	113.8(3)		tetrahedral
	3	105.4(2)	167.5(5)	112.1(3)		N(2)-Re-N(3)
						112.2(3)
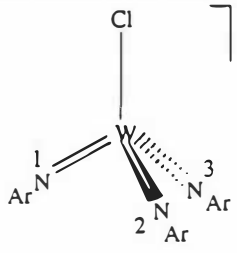	1	106.0(6)	173.4(15)		14	Tetrahedral
	2	104.7(5)	167.7(14)	112.5(7)		N(2)-W-N(3)
	3	107.2(6)	171.4(15)	113.5(7)		112.1(7)

Table 3: Selected bond angles(°) for $ClRe(NAr)_3$ and 3 other related complexes of the type, $XM(NAr)_3$

Complex	M-X	M-N(1)	M-N(2)	M-N(3)	Ref.	Comments
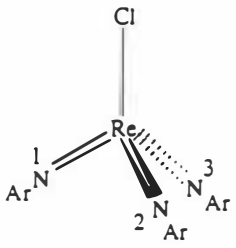	2.292(2)	1.749(6)	1.757(6)	1.769(7)	-	
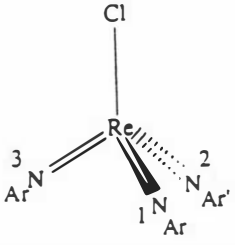	2.271(9) 2.272(9)	1.70(2) 1.72(2)	1.725(18) 1.766(19)	1.71(2) 1.73(2)	-	2 independent structures
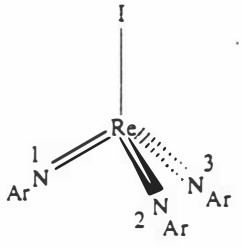	2.664(1)	1.770(7)	1.767(6)	1.765(6)	39	
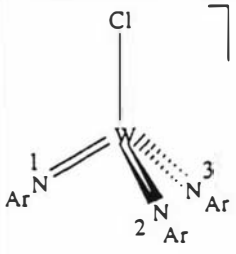	2.343(6)	1.777(15)	1.763(15)	1.805(18)	14	

Table 4: Selected bond lengths(Å) for $ClRe(NAr)_3$ and 3 other related complexes of the type, $XM(NAr)_3$

Synthesis of mixed tris(imido) complexes

Moderate yields of mixed tris(imido) complexes, $ClRe(NR)_2(NR')$, can be synthesized via the bis(imido) complex, $Re(NR)_2Cl_3(py)$, the aniline ($R'NH_2$) and triethylamine as shown in scheme 13.

$$Re(NR)_2Cl_3(py) + R'NH_2 + 2\,Et_3N \longrightarrow ClRe(NR)_2(NR')$$

R	R'	Complex
Ar'	Ar	$ClRe(NAr')_2(NAr)$
Ar'	*p*-tol	$ClRe(NAr')_2(N\text{-}p\text{-tol})$
Ar	Ar'	$ClRe(NAr)_2(NAr')$
Ar	*p*-F	$ClRe(NAr)_2(N\text{-}p\text{-F})$
Ar	*p*-NO_2	$ClRe(NAr)_2(N\text{-}p\text{-}NO_2)$
Ar	*p*-tol	$ClRe(NAr)_2(N\text{-}p\text{-tol})$
Ar	AMP	$ClRe(NAr)_2(N\text{-AMP})$
Ar	*o*-Cl	$ClRe(NAr)_2(N\text{-}o\text{-Cl})$
Ar	*m*-Cl	$ClRe(NAr)_2(N\text{-}m\text{-Cl})$
Ar	*o*-^{t}Bu	$ClRe(NAr)_2(N\text{-}o\text{-}^t\text{Bu})$

Scheme 13

The complexes of scheme 13 are the only examples of d^0 Re tris(imido) complexes that contain imido ligands with different organic substituents.

Imido ligand exchange

With the successful synthesis of mixed tris(imido) complexes completed, the question of imido ligand exchange in solution needs to be investigated.

Intermolecular oxo/imido exchange is quite common (see page 39).[1a,21] The exchange of imido ligands has been restricted to that of N^{t}Bu (see pages 56 and 60).[81,82,87] The imido/imido exchange of arylimido ligands is not thought to occur appreciately.

The intermolecular imido/imido exchange of the 2 complexes of figure 36 was investigated by nmr.

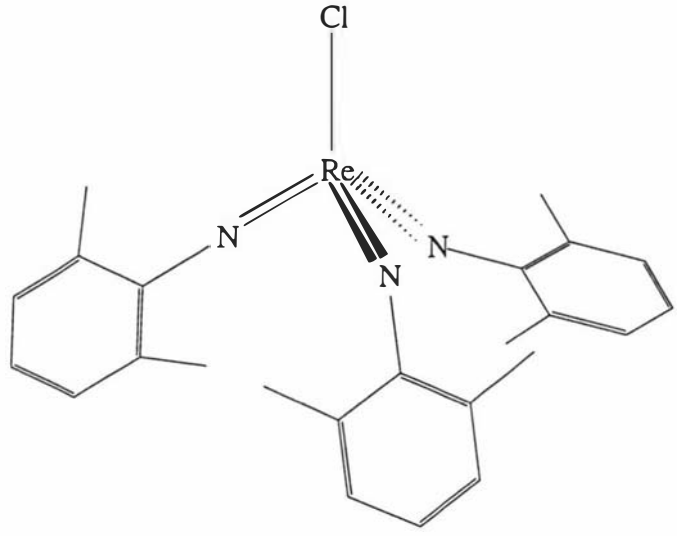

$ClRe(NAr')_3$

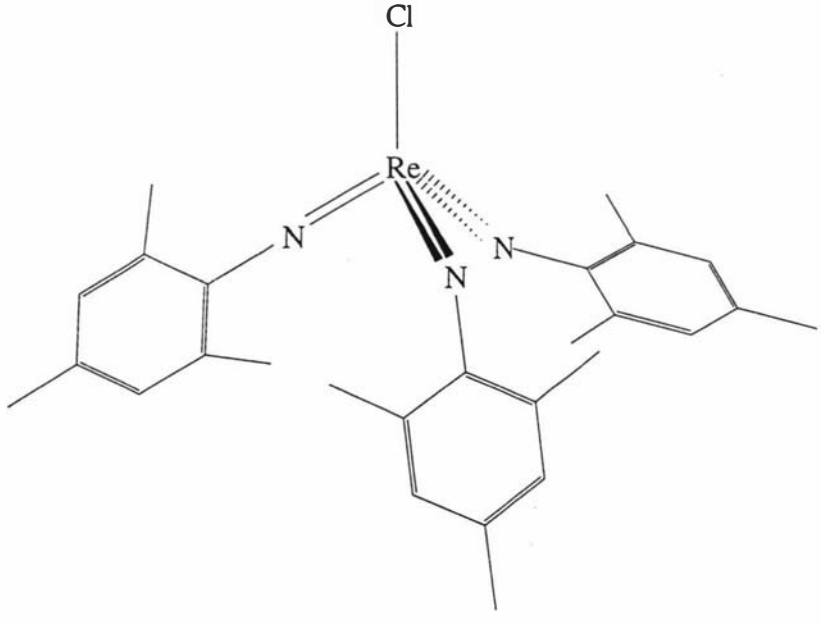

$ClRe(Nmes)_3$

Figure 36

Equal molar amounts of each complex was weighed into separate nmr tubes. Deuterated benzene was used as the solvent. The ^1H nmr was obtained of $ClRe(NAr')_3$ (Fig. 37) and $ClRe(Nmes)_3$ (Fig. 38).

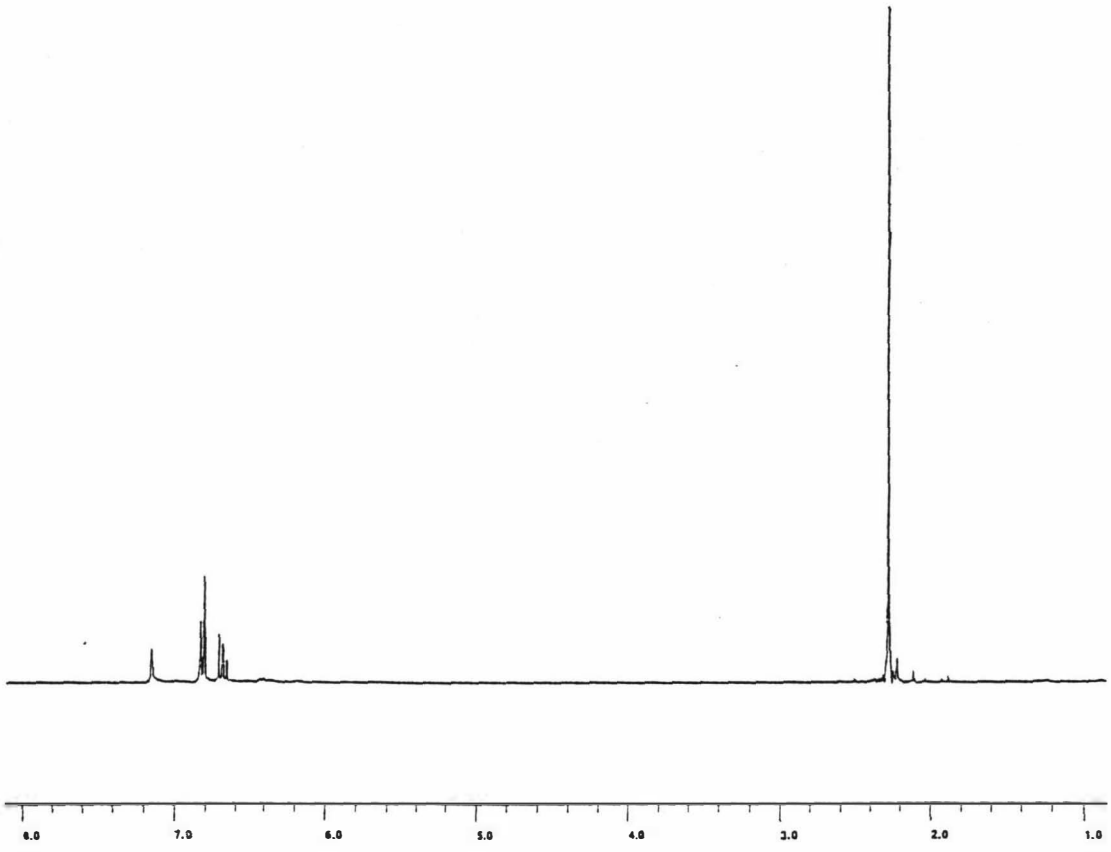

Figure 37

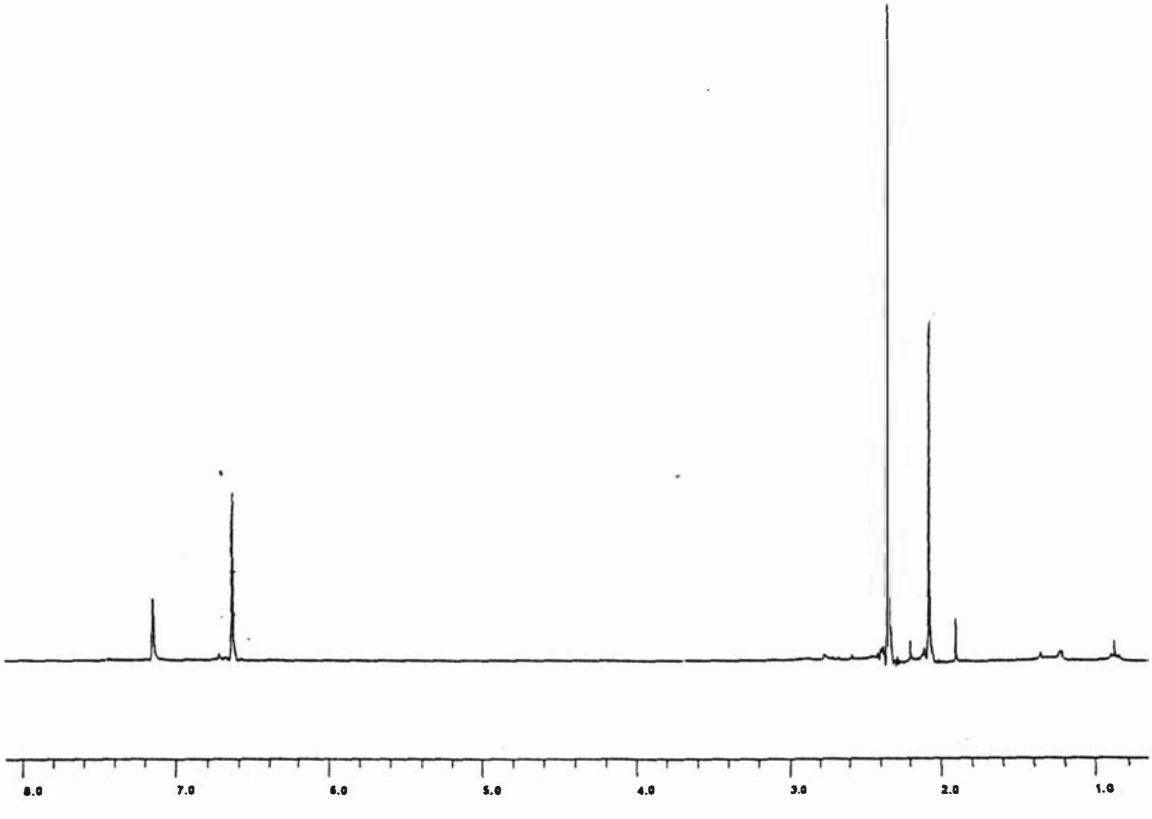

Figure 38

To observe if intermolecular imido/imido exchange occurs, the 2 nmr samples were mixed together, then the ^1H nmr spectrum was recorded at 3 minutes, 40 minutes, 20 hours and 3 days after mixing at room temperature. After 40 minutes there was no indication of exchange (Fig. 39).

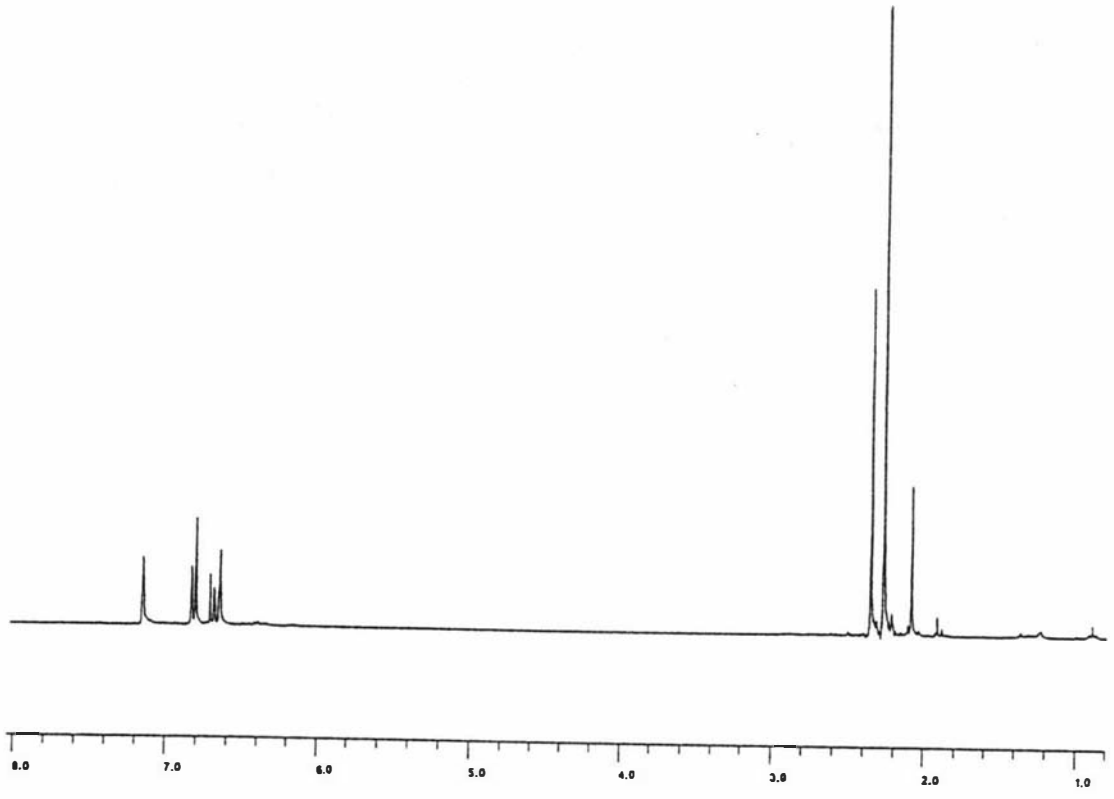

Figure 39

However, after 20 hours, 3 new peaks emerged (Fig. 40) and after 3 days the new signals dominate, although $ClRe(NAr')_3$ and $ClRe(Nmes)_3$ are still present (Fig. 41).

The new signals are presumably due to the mixed imido complexes, $ClRe(NAr')_2(Nmes)$ and $ClRe(NAr')(Nmes)_2$.

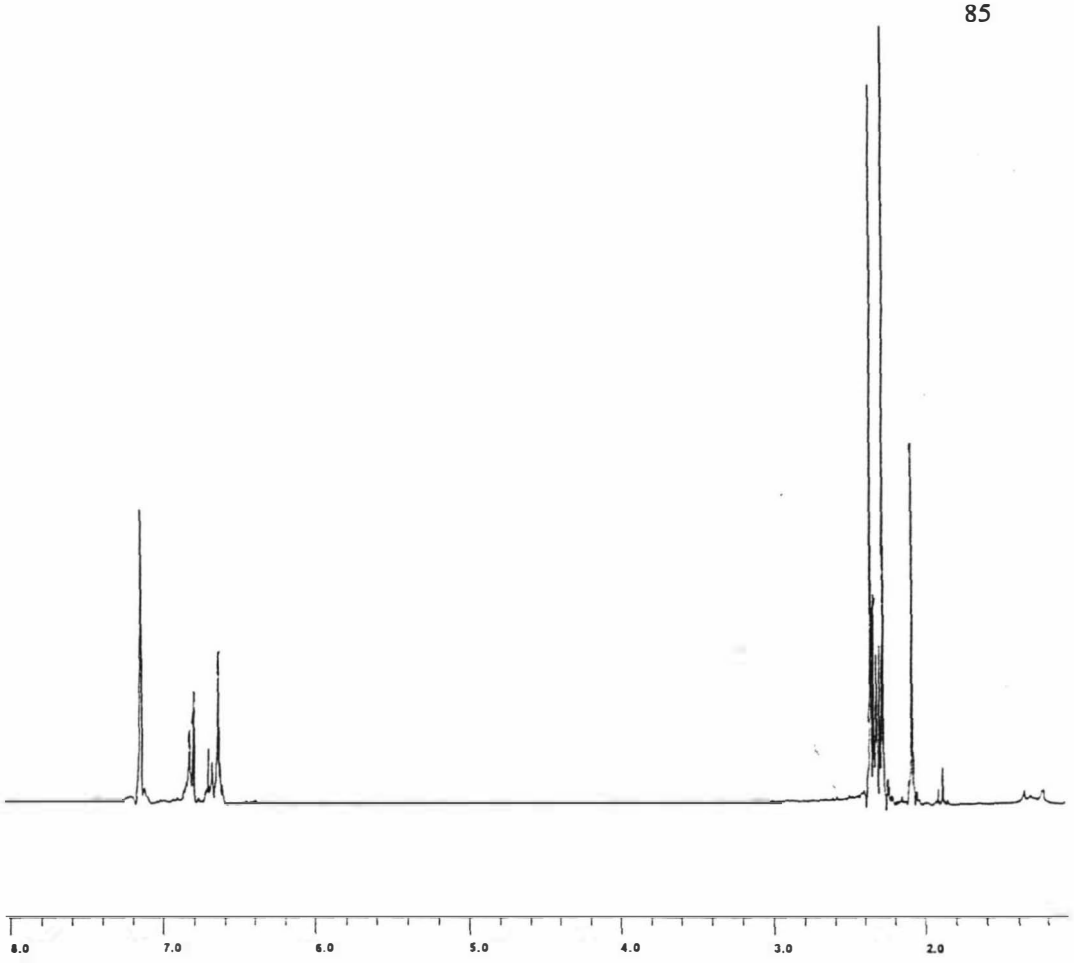

Figure 40

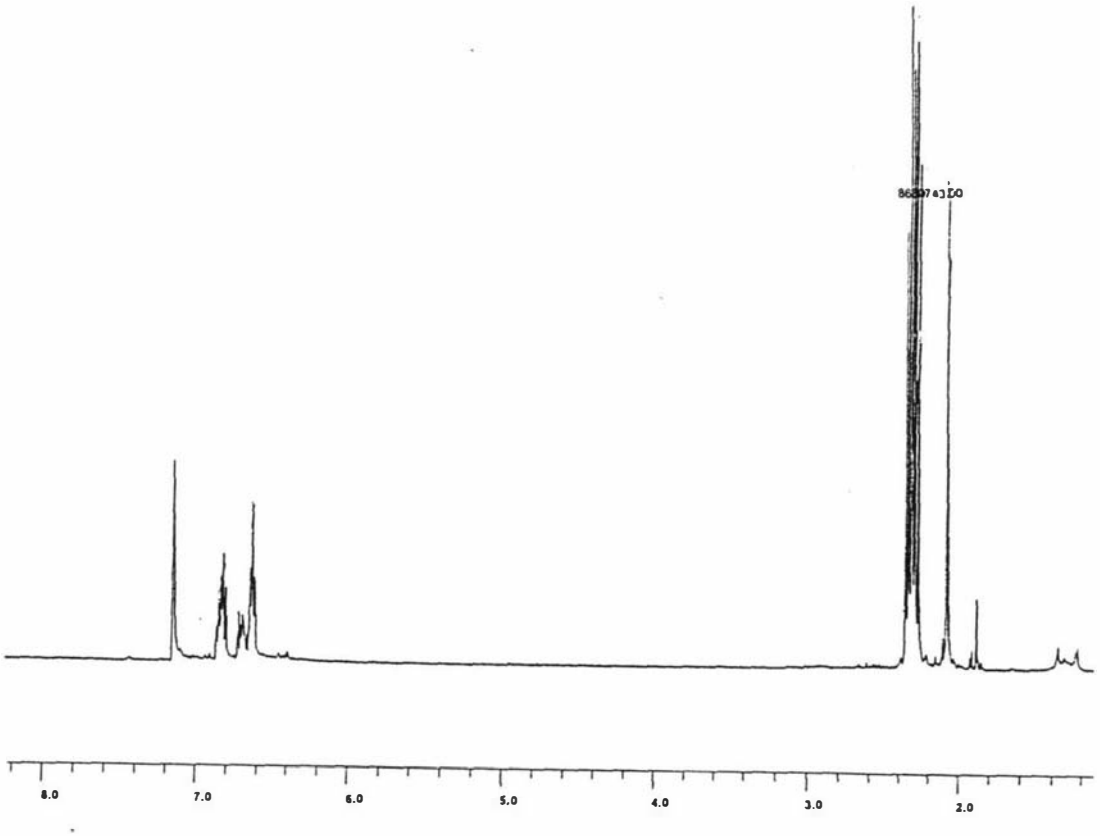

Figure 41

The procedure was also carried out with the complexes of figure 42.

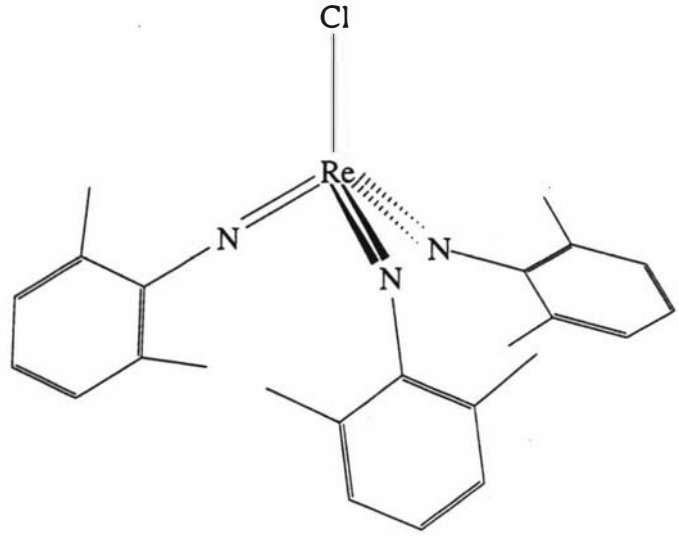

$ClRe(NAr')_3$

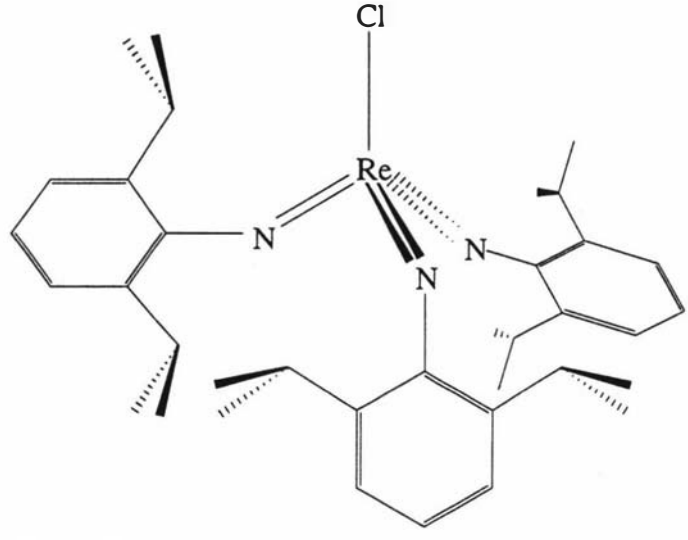

$ClRe(NAr)_3$

Figure 42

The ^1H nmr of $ClRe(NAr')_3$ is shown in figure 37 and for $ClRe(NAr)_3$, figure 43.

After 3 days at room temperature and then 2 hours at 60°C there was no indication of imido ligand exchange (Fig. 44).

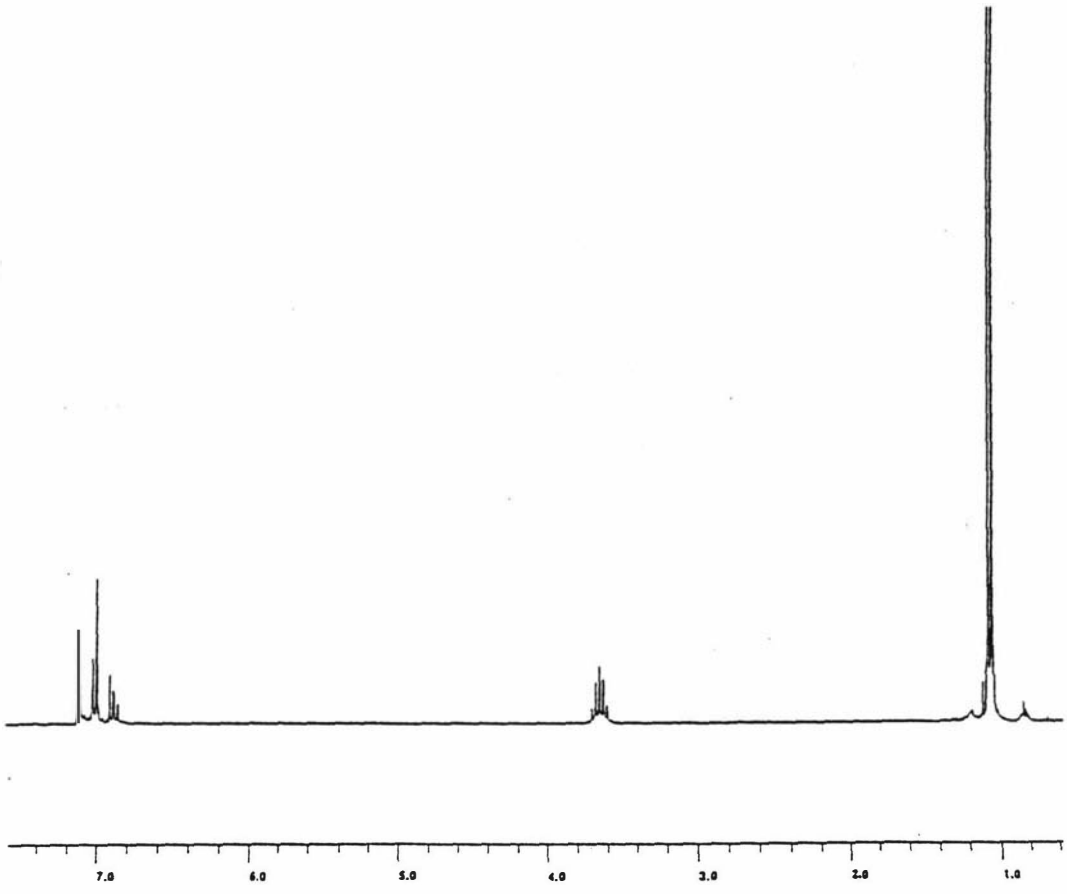

Figure 43

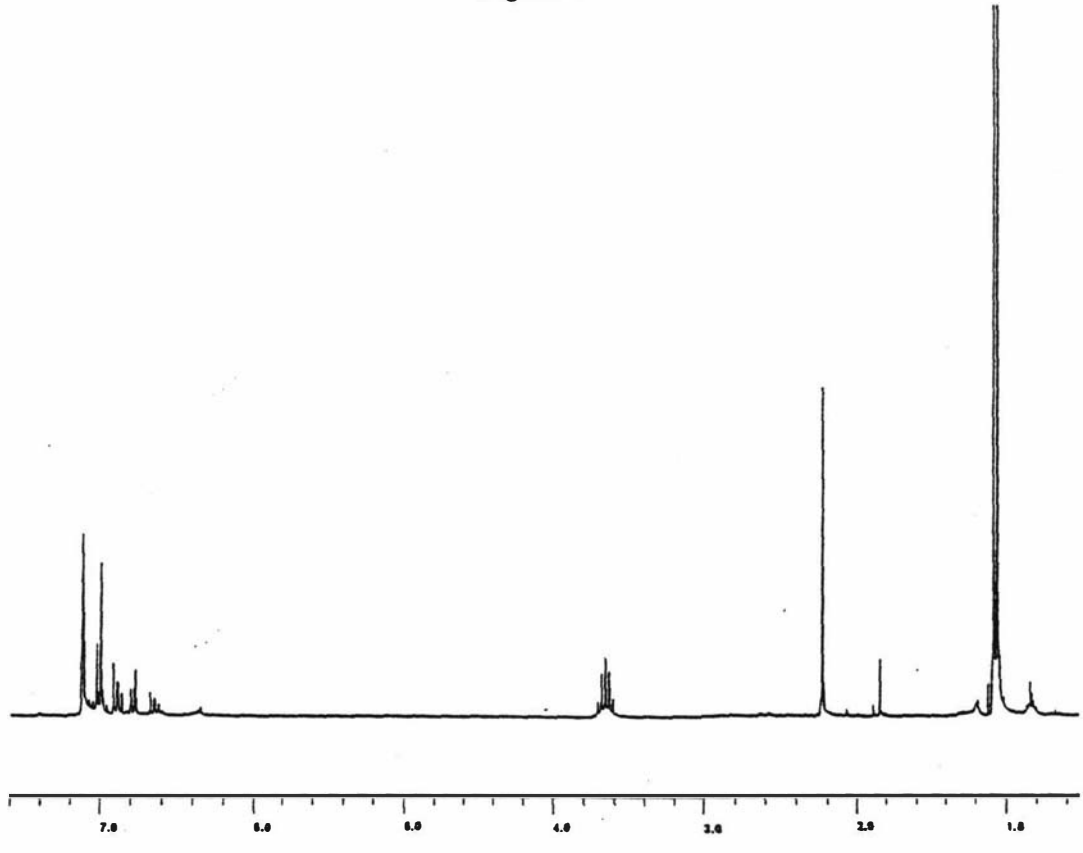

Figure 44

However, after a further 24 hours at 60°C two singlets and a doublet began to appear (Fig. 45). The singlets are very close to each other, presumably these new signals are due to the mixed imido complexes, $ClRe(NAr)_2(NAr')$ and $ClRe(NAr)(NAr')_2$.

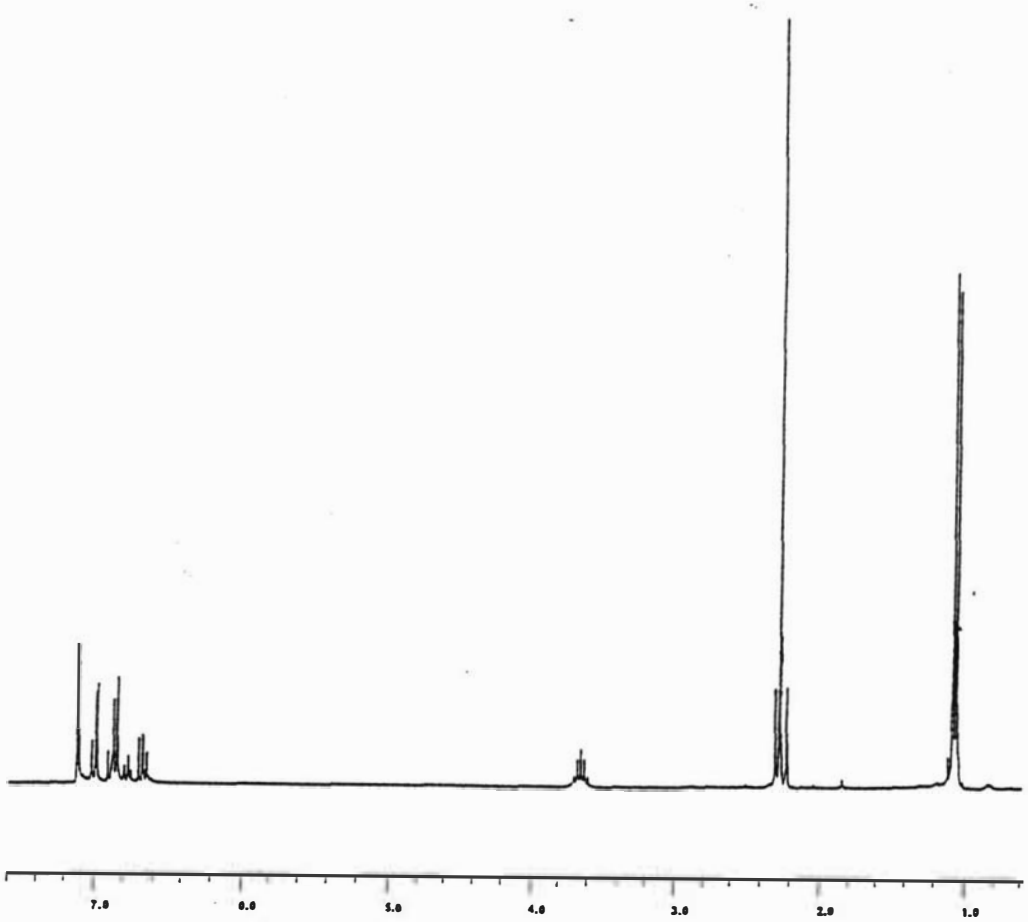

Figure 45

Heating for another 24 hours at 60°C results in loss of $ClRe(NAr')_3$ and formation of $Ar'NH_2$ (Fig. 46), presumably via hydrolysis. However, the solution still contains $ClRe(NAr)_3$, $ClRe(NAr)_2(NAr')$ and $ClRe(NAr)(NAr')_2$.

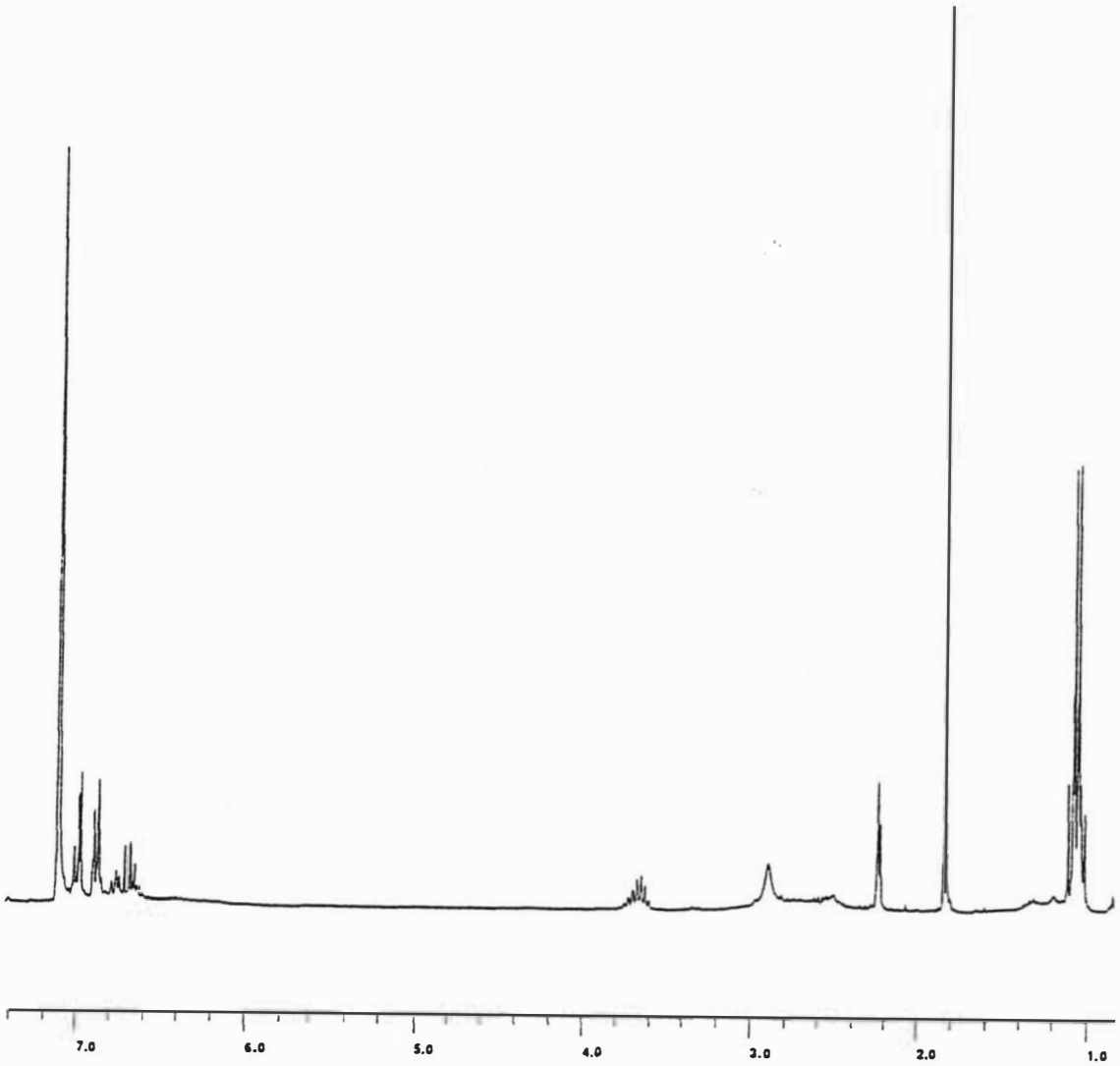

Figure 46

From these results it is clear that arylimido intermolecular exchange does occur in solution. It was shown that the exchange between NAr' and Nmes occurs slowly at room temperature. The exchange between NAr' and NAr does not occur at room temperature (after 3 days), however, at higher temperatures some exchange does occur.

X-ray structure of $ClRe(NAr)_2(NAr')$

X-ray quality crystals of $ClRe(NAr)_2(NAr')$ were obtained from evaporation of a hexane solution. The final structure is shown in figure 47. Tables containing complete bond lengths and angles, atomic coordinate and equivalent isotropic displacement parameters, anisotropic displacement parameters and calculated H-atom positions are presented in appendix VII.

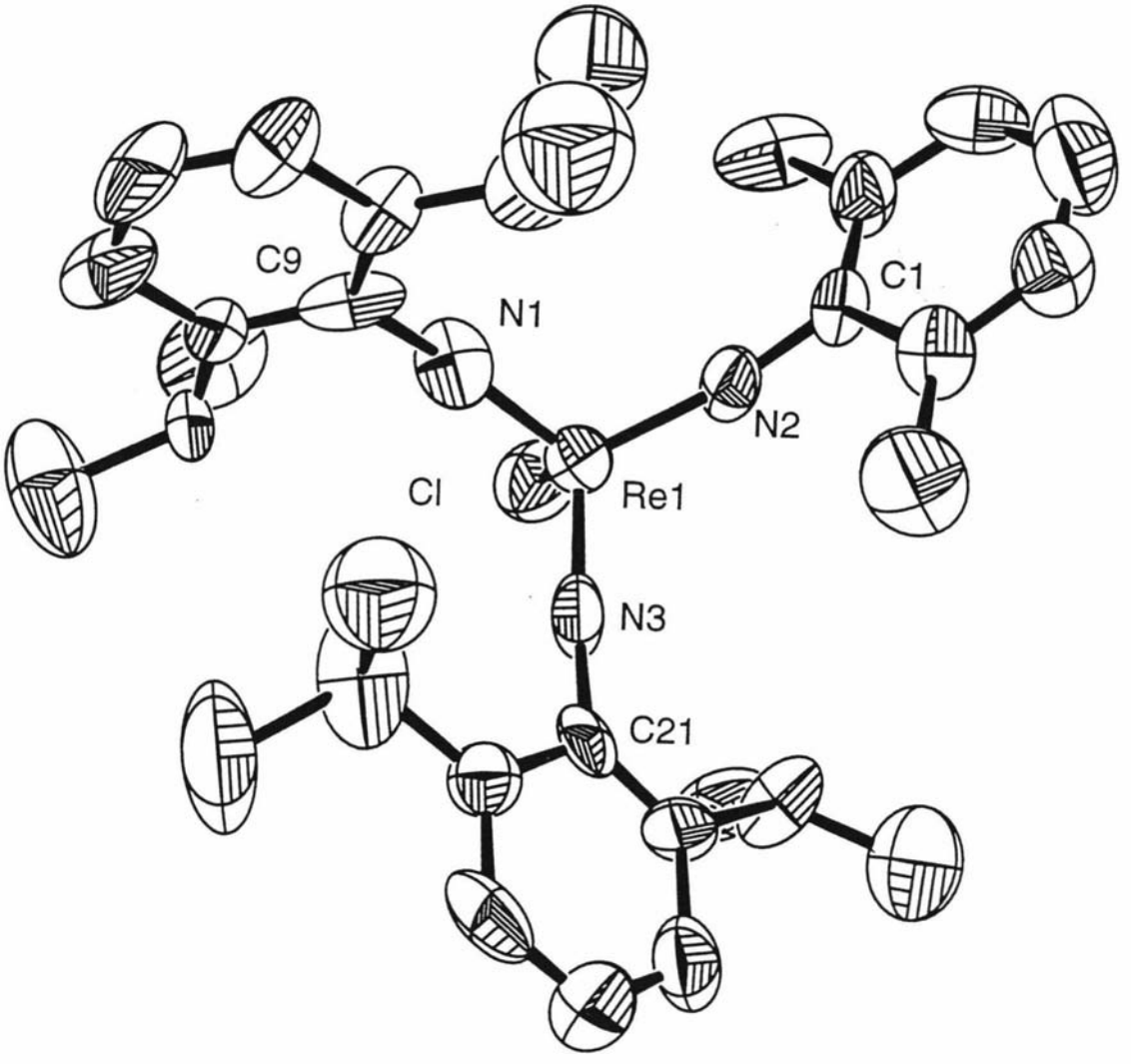

Figure 47

Tables 5 and 6 show selected bond lengths and angles for $ClRe(NAr)_2(NAr')$ and the methyl mixed imido complex, $CH_3Re(NAr)_2(NAr')$, $IRe(NAr)_3$ and $[ClW(NAr)_3]^-$. The rhenium atom is approximately tetrahedrally coordinated. The Re-N-C angles are close to linear ranging from 165(2) to 172.5(19)°, typical for pseudo tetrahedral tris(imido) complexes (see appendix IV). The average Re-N bond length is

1.725(19)Å and is significantly shorter than the complexes of table 6 where $CH_3Re(NAr)_2(NAr')$, $IRe(NAr)_3$ and $[ClW(NAr)_3]^-$ have average M-N bond distances of 1.758(4), 1.767(7) and 1.782(18)Å respectively.[39,14] The X-M-N angles of $ClRe(NAr)_2(NAr')$ compare well with both $IRe(NAr)_3$ and $ClW(NAr)_3$ (see table 5), but they are significantly greater than those of $CH_3Re(NAr)_2(NAr')$. This is expected as the extent of polarization ($X^{\delta-}$-$M(NR)_3^{\delta+}$) experienced in the methyl complex should be less then if X is Cl^- or I^-, as such the H_3C-Re-N angle is smaller.[39] The Re-Cl distance of 2.272(9)Å is comparable with $ClRe(NAr)_2(NO^tBu)$ where the Re-Cl bond length is 2.2990(8)Å (see page 96) and is in the expected range for complexes containing metal-chloride bonds (see appendix III).

Complex	#	X-M-N(#)	M-N(#)-C	N(1)-M-N(#)	Ref.	Comments
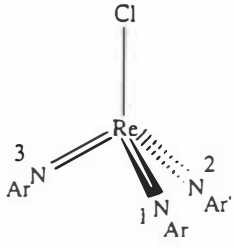	1	107.2(8)	165(2)		-	2 independent
		107.7(8)	166.6(19)			structures
	2	106.9(8)	165(2)	112.2(10)		N(2)-Re-N(3)
		107.1(7)	170.6(18)	110.0(9)		112.4(8)
	3	107.4(8)	172.5(19)	110.4(10)		113.5(10)
		106.7(8)	162.1(19)	111.6(10)		
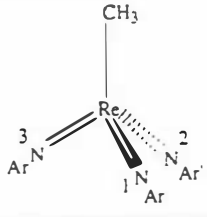	1	103.9(2)	169.1(3)		-	N(2)-Re-N(3)
	2	102.81(19)	168.5(3)	115.23(18)		115.63(17)
	3	101.85(19)	171.2(3)	114.75(17)		
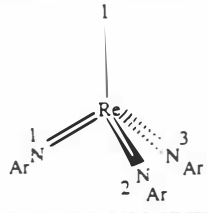	1	106.7(2)	165.7(6)		39	N(2)-Re-N(3)
	2	105.9(2)	169.9(6)	113.8(3)		112.2(3)
	3	105.4(2)	167.5(5)	112.1(3)		
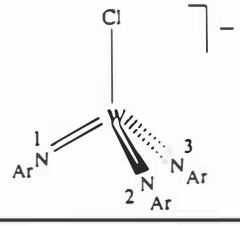	1	106.0(6)	173.4(15)		14	Tetrahedral
	2	104.7(5)	167.7(14)	112.5(7)		N(2)-W-N(3)
	3	107.2(6)	171.4(15)	113.5(7)		112.1(7)

Table 5: Selected bond angles(°) for $ClRe(NAr)_2(NAr')$, $CH_3Re(NAr)_2(NAr')$, $IRe(NAr)_3$ and $[ClW(NAr)_3]^-$

Complex	M-X	M-N(1)	M-N(2)	M-N(3)	Ref.	Comments
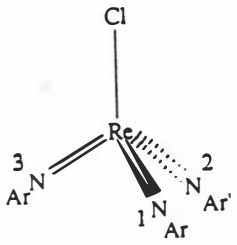	2.271(9) 2.272(9)	1.70(2) 1.72(2)	1.725(18) 1.766(19)	1.71(2) 1.73(2)	-	2 independent structures
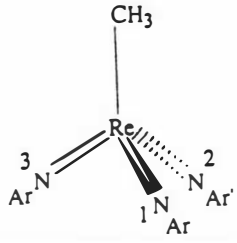	2.113(5)	1.763(4)	1.753(4)	1.757(3)		
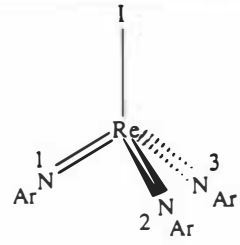	2.664(1)	1.770(7)	1.767(6)	1.765(6)	39	
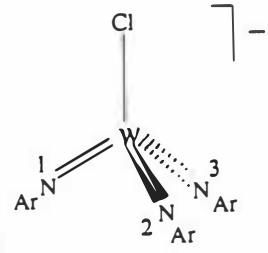	2.343(6)	1.777(15)	1.763(15)	1.805(18)	14	

Table 6: Selected bond lengths(Å) for $ClRe(NAr)_2(NAr')$,$CH_3Re(NAr)_2(NAr')$, $IRe(NAr)_3$ and $[ClW(NAr)_3]^-$

X-ray structure of $ClRe(NAr)_2(N\text{-}o\text{-}^tBu)$

X-ray quality crystals of $ClRe(NAr)_2(N\text{-}o\text{-}^tBu)$ were obtained from a concentrated hexane solution cooled to -35°. The final structure is shown in figure 49. Tables containing complete bond lengths and angles, atomic coordinate and equivalent isotropic displacement parameters, anisotropic displacement parameters and calculated H-atom positions are presented in appendix VIII.

Tables 7 and 8 show selected bond lengths and angles for $ClRe(NAr)_2(N\text{-}o\text{-}^tBu)$, $ClRe(NAr)_2(NAr')$ and $IRe(NAr)_3$. The geometry about the rhenium atom is approximately tetrahedral with angles about the Re ranging from 107.37(8) to 111.46(13)°. Two of the imido ligands are essentially linear at 172.4(2)° for N(1) and 171.2(2)° for N(2), however the imido ligand containing the *o*-^{t}Bu group is bent at 160.8(2)°. There are two possible reasons why bending occurs at only one imido ligand (ignoring electronic considerations), there maybe repulsion between the *o*-^{t}Bu group on the *ortho* carbon of the phenyl ring with the Cl or the absense of an organic group on the second *ortho* position of the phenyl ring may allow room for bending at the nitrogen. In all structurally characterized tetrahedral tris(arylimido) complexes the greatest difference in the M-N-C angles are less than 6°. However, $ClRe(NAr)_2(N\text{-}o\text{-}^tBu)$ with 10° is not the only exception. The Tc(VII) tris(imido) complex, $(\eta^1\text{-}Cp)Tc(NAr)_3$, has Tc-N-C angles of 166.2(2) (Tc-N(1)-C), 157.3(2) (Tc-N(2)-C) and 162.0(1)° (Tc-N(3)-C). Hence there is a difference of 8.9° between N(1) and N(2). The greater bend at N(2) maybe the result of repulsion between the iso-propyl group at the ortho position of the phenyl ring and the Cp ring (figure 48).[16] Given that both ortho positions of the phenyl ring at N(2) of $(\eta^1\text{-}Cp)Tc(NAr)_3$, contain an iso-propyl group, then the bending of N(3) of $ClRe(NAr)_2(N\text{-}o\text{-}^tBu)$ (see figure 49) maybe due to the repulsion of the ortho and Cl rather than to the absence of an organic group on the second ortho position. The average Re-N bond length is 1.751(3)Å and compares well with $CH_3Re(NAr)_2(NAr')$ and $IRe(NAr)_3$ at 1.758(4) (table 4) and 1.767(7)Å,[39] respectively. The Re-N(3) distance of the bent imido ligand is not significantly longer than the Re-N(2) distance. However, the Re-N(1) distance of 1.744(3)Å is significantly shorter then the other two at 1.757(3)Å for Re-N(3) and 1.751(3)Å for Re-N(2).

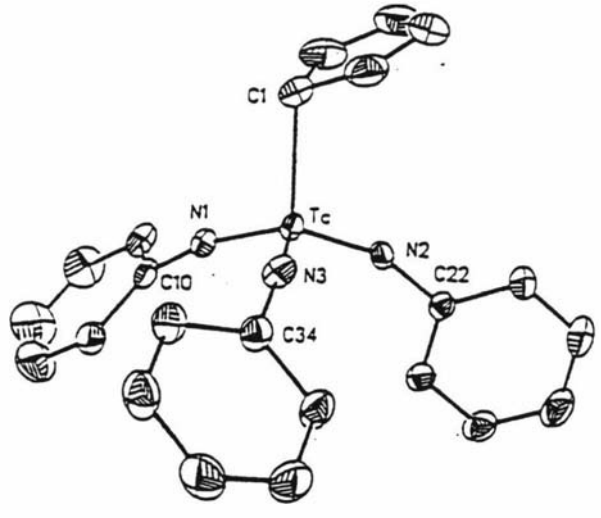

Figure 48

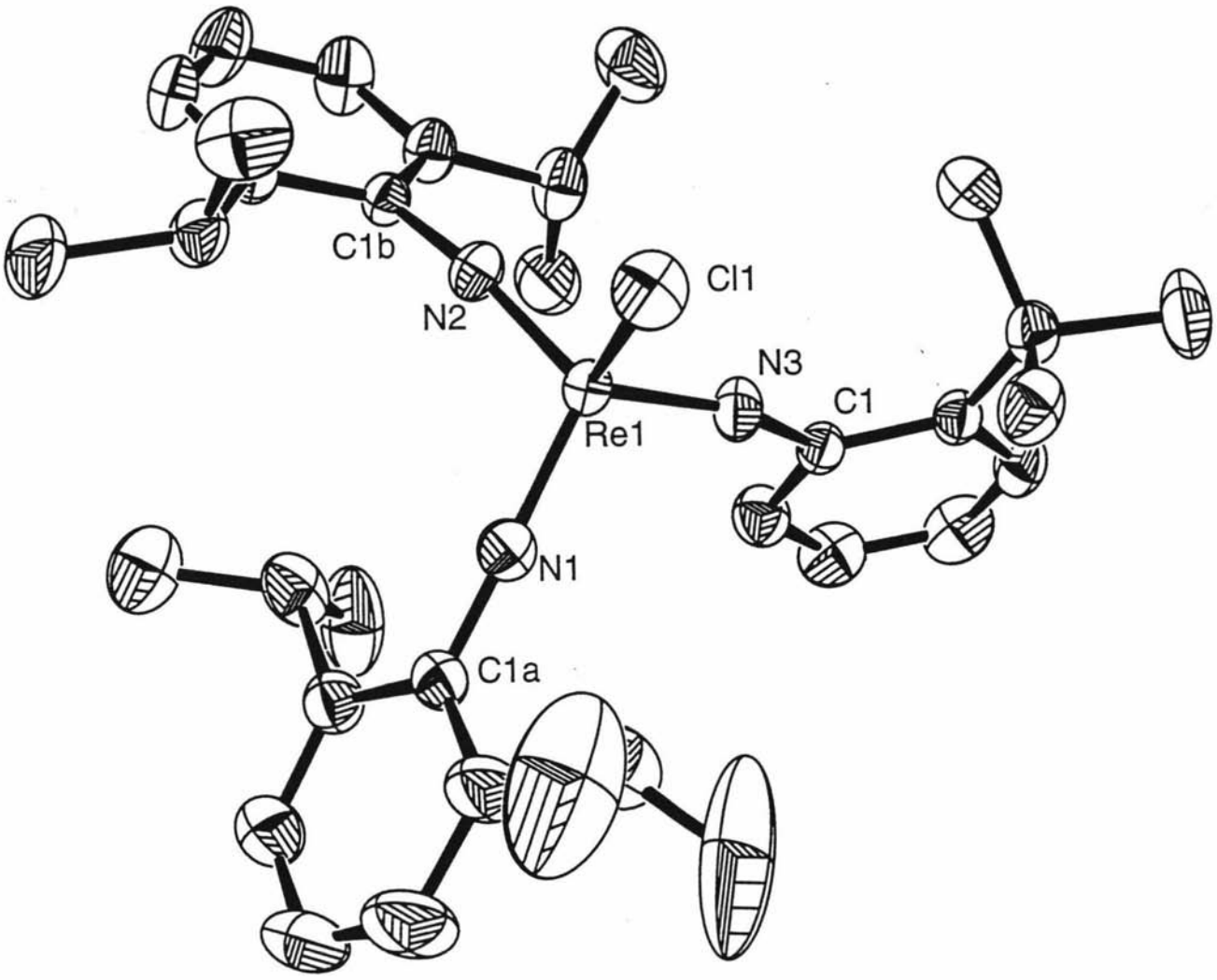

Figure 49

Complex	#	X-Re-N(#)	Re-N(#)-C	N(1)-Re-N(#)	Ref.	Comments
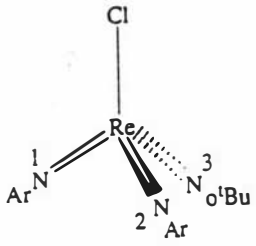	1	107.59(9)	172.4(2)		-	N(2)-Re-N(3)
	2	107.37(8)	171.2(2)	111.46(13)		111.62(12)
	3	108.10(9)	160.8(2)	110.56(13)		
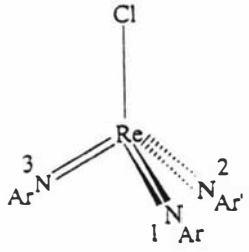	1	107.2(8)	165(2)		-	2 independent
		107.7(8)	166.6(19)			structures
	2	106.9(8)	165(2)	112.2(10)		N(2)-Re-N(3)
		107.1(7)	170.6(18)	110.0(9)		112.4(8)
	3	107.4(8)	172.5(19)	110.4(10)		113.5(10)
		106.7(8)	162.1(19)	111.6(10)		
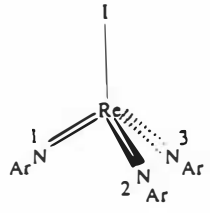	1	106.7(2)	165.7(6)		39	Approximately
	2	105.9(2)	169.9(6)	113.8(3)		tetrahedral
	3	105.4(2)	167.5(5)	112.1(3)		N(2)-Re-N(3)
						112.2(3)

Table 7: Selected bond angles(°) for $ClRe(NAr)_2(N\text{-}o\text{-}^tBu)$, $ClRe(NAr)_2(NAr')$ and $IRe(NAr)_3$

Complex	Re-X	Re-N(1)	Re-N(2)	Re-N(3)	Ref
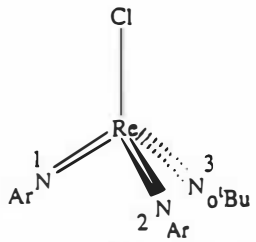	2.2990(8)	1.744(3)	1.751(3)	1.757(3)	-
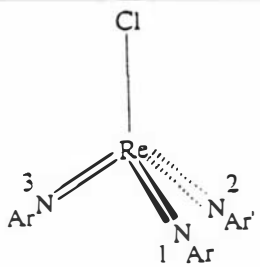	2.271(9) 2.272(9)	1.70(2) 1.72(2)	1.725(18) 1.766(19)	1.71(2) 1.73(2)	-
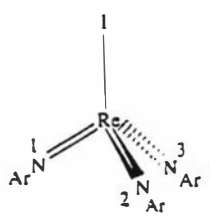	2.664(1)	1.770(7)	1.767(6)	1.765(6)	39

Table 8:Selected bond lengths(Å) for $ClRe(NAr)_2(N\text{-}o\text{-}^tBu)$, $ClRe(NAr)_2(NAr')$ and $IRe(NAr)_3$

Synthesis of a chiral tris(imido) complex

The methodology shown in scheme 13 can be used to synthesize a tris(imido) complex containing 4 different ligands only if the bis(imido) complex itself contains two different imido ligands (Equation 63).

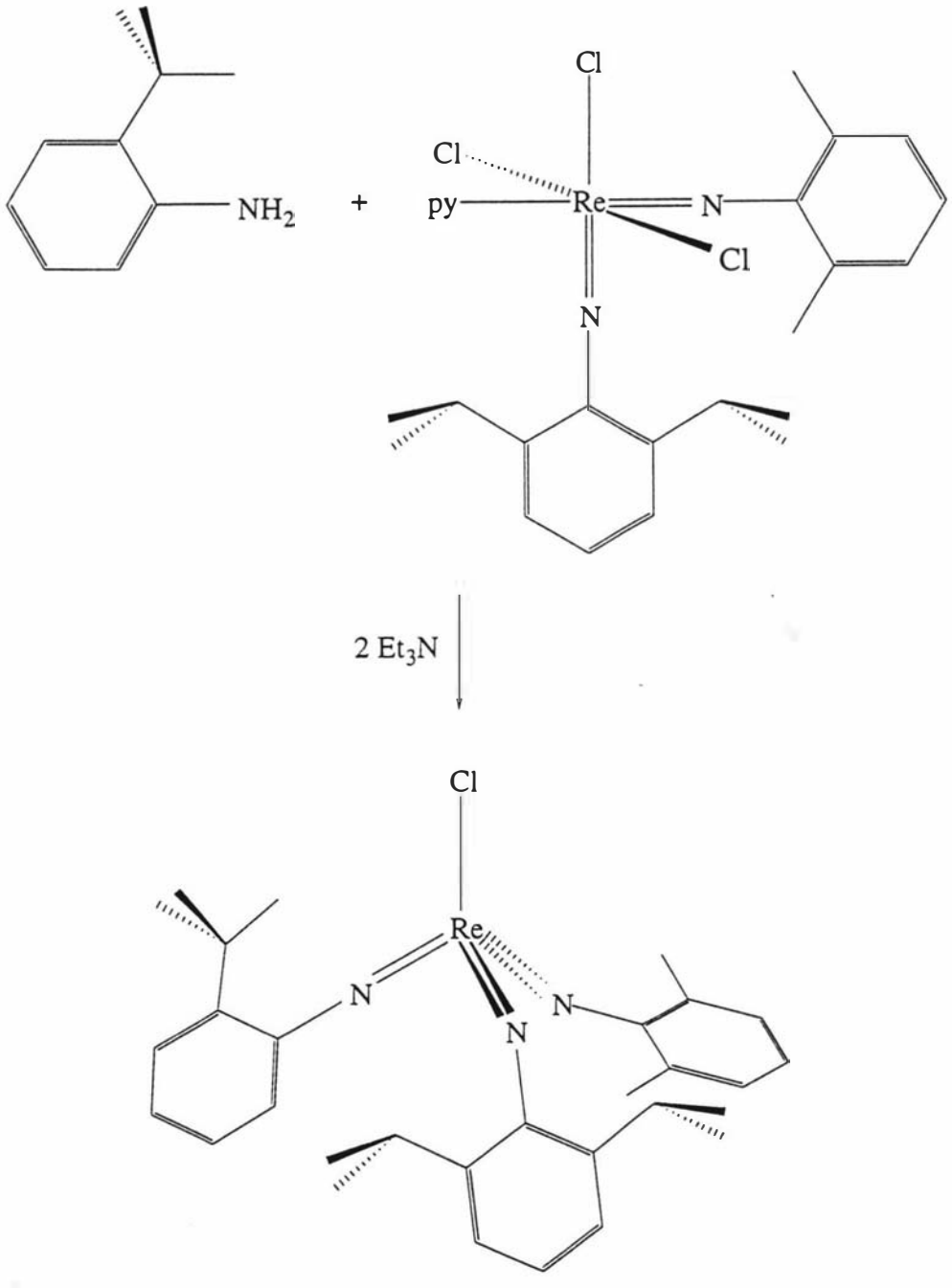

Equation 63

The synthesis of $Re(NAr)(NAr')Cl_3(py)$ will be described in chapter 3 (page 130).

Conclusions

The simple one pot synthesis of Re(VII) tris(imido) complexes was found to give high yields, however this method is not convenient for the synthesis of mixed tris(imido) species. This can be overcome by addition of an imido ligand to a complex that already contains two imido ligands.

Experimental section

General

General experimental procedures and details regarding the instrumentation used are given in appendix I. ^{1}H NMR were recorded in d_6-benzene and referenced to benzene at 7.15ppm. ^{13}C NMR were recorded in d_6-benzene and referenced to benzene at 128ppm. Deuterated benzene was purchased from Acros and freeze pumped thawed 3 times before use. Triethylamine and liquid anilines were purchased from Aldrich and vacuum distilled. Solid anilines were purchased from Aldrich and were used as obtained. $[ReO_4][NH_4]$ was purchased from Strem. Toluene was distilled from sodium/benzophenone and CH_2Cl_2 was distilled from CaH_2. $Re(NAr)_2Cl_3(py)$ and $Re(NAr')_2Cl_3(py)$ were prepared from literature methods.[64] The synthesis of $Re(NAr')(NAr)Cl_3(py)$ is described in chapter 3, page 130. Me_3SiCl was purchased from Aldrich.

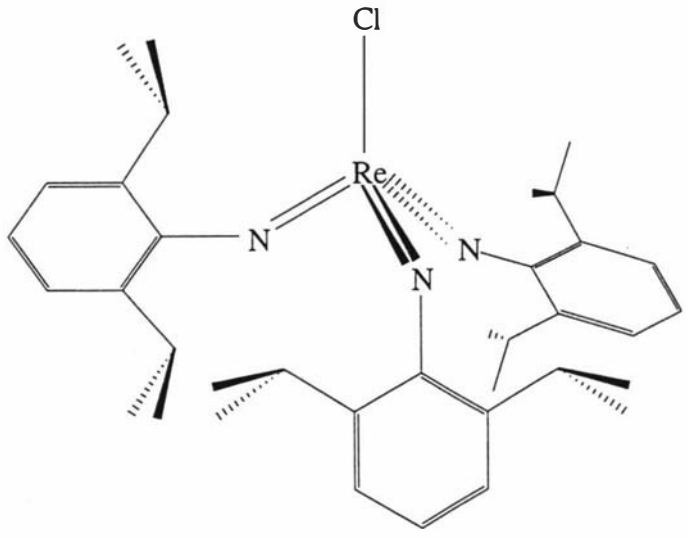

Procedure 1:

$ClRe(NAr)_3$

A solution of $Re(NAr)_2Cl_3(py)$ (0.250g, 0.35mmol), $ArNH_2$ (0.061g, 0.34mmol) and Et_3N (0.076g, 0.75mmol) in toluene was stirred for 6 hours. The reaction mixture was reduced to dryness *in vacuo* and hexane (6mL) was then added. The resulting suspension was filtered through celite, which was then washed with hexane (2x5mL). The filtrates were pumped to dryness, yielding 0.120g (47%) of a red solid. Further purification can be achieved by silica column in hexane.

^1H NMR (C_6D_6) : 7.04(d, 6, J=7.1, Ar), 6.92(t, 3, J=7.1, Ar), 3.68(sept, 6, J=6.8, $C\underline{H}Me_2$), 1.09(d, 36, J=7.0, $CHC\underline{H}_3$).

$^{13}C\{^1H\}$ NMR (C_6D_6) : 153.0(Ar), 142.7(Ar), 133.0(Ar), 121.4(Ar), 28.3($\underline{C}HCH_3$), 23.3($CH\underline{C}H_3$).

Found: C, 58.21 ; H, 6.74 ; N, 5.46
Calc: C, 57.85 ; H, 6.88 ; N, 5.62

Procedure 2: This was prepared by modification of the literature method.[12]

$[ReO_4][NH_4]$ (0.500g, 1.86mmol) was added to 100mL of dichloromethane and the slurry was chilled to -40°C. To this slurry was added sequentially at -40°C, $ArNH_2$ (0.995g, 5.61mmol), NEt_3 (1.330g, 13.1mmol) and slowly Me_3SiCl (1.90mL, 15mmol). The reaction mixture was allowed to warm to room temperature and was stirred under nitrogen for 3 days. The solution was reduced to dryness *in vacuo* and the resulting solid was transferred to an inert atmosphere drybox. The maroon solid was extracted with benzene (200mL). The mixture was filtered through celite and the precipitate washed with benzene until the filtrate was no longer red. The solvent was removed *in vacuo*, and the resulting solid was washed with cold pentane to afford 1.185g (85%) of a red solid.

Found: C, 58.26 ; H, 6.94 ; N, 5.60
Calc: C, 57.85 ; H, 6.87 ; N, 5.62

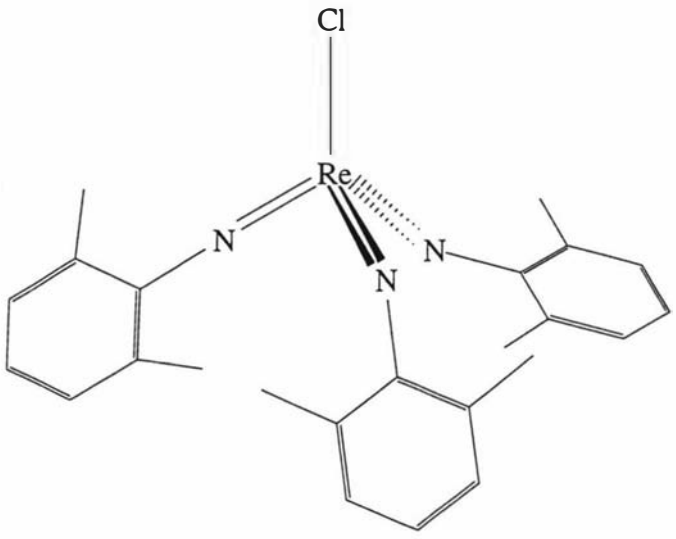

$ClRe(NAr')_3$

A solution of $Re(NAr')_2Cl_3(py)$ (0.250g, 0.41mmol), $Ar'NH_2$ (0.049g, 0.40mmol) and Et_3N (0.088g, 0.87mmol) in toluene was stirred for 3 hours. The reaction mixture was reduced to dryness *in vacuo* and hexane (6mL) was then added. The resulting suspension was filtered through celite, which was then washed with hexane (2x5mL). The filtrates were pumped to dryness, yielding 0.100g (43%) of a red solid. Further purification can be achieved by silica column in hexane.

^1H NMR (C_6D_6) : 6.81(d, 6, J=7.1, Ar'), 6.66(t, 3, J=7.1, Ar'), 2.26(s, 18, Me).

$^{13}C\{^1H\}$ NMR (C_6D_6) : 153.4(Ar'), 136.4(Ar'), 127.2(Ar'), 122.2(Ar'), 18.4(Me).

Found: C, 50.18 ; H, 4.68 ; N, 7.01
Calc: C, 49.77 ; H, 4.70 ; N, 7.26

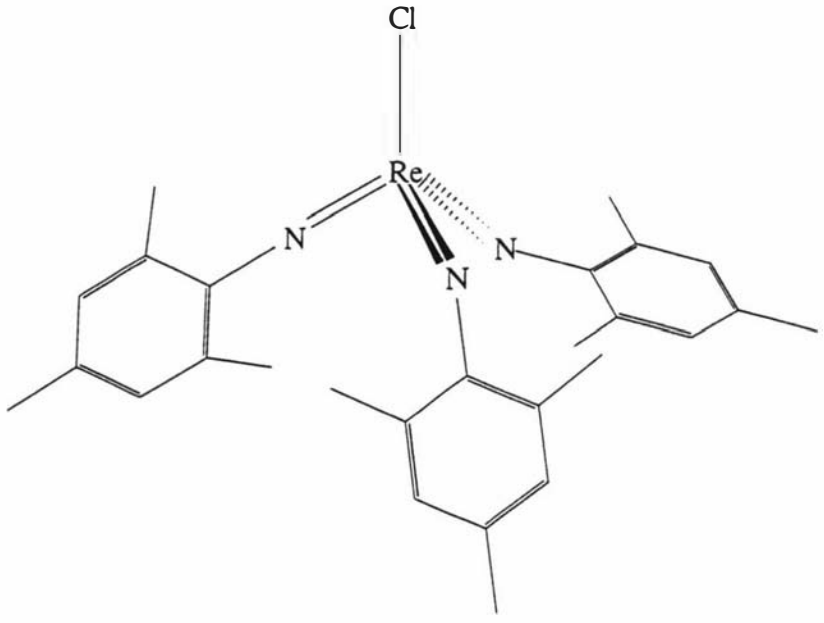

$ClRe(Nmes)_3$

$[ReO_4][NH_4]$ (0.500g, 1.86mmol) was added to 100mL of dichloromethane and the slurry was chilled to -40°C. To this slurry was added sequentially at -40°C, $mesNH_2$ (0.758g, 5.61mmol), NEt_3 (1.330g, 13.1mmol) and slowly Me_3SiCl (1.90mL, 15mmol). The reaction mixture was allowed to warm to room temperature and was stirred under nitrogen for 3 days. The solution was reduced to dryness *in vacuo* and the resulting solid was transferred to an inert atmosphere drybox. The maroon solid was extracted with benzene (200mL). The mixture was filtered through celite and the precipitate washed with benzene until the filtrate was no longer red. The solvent was removed *in vacuo*, and the resulting solid was washed with cold pentane to afford 0.231g (20%) of a red solid.

^1H NMR (C_6D_6) : 6.61(s, 6, mes), 2.33(s, 18, *o*-Me), 2.07(s, 9, *p*-Me).

$^{13}C\{^1H\}$ NMR (C_6D_6) : 152.6(mes), 142.4(mes), 125.7(mes), 121.2(mes), 20.3($C_6H_4\underline{C}H_3$), 17.6($C_6H_3(\underline{C}H_3)_2$).

Found: C, 52.95 ; H, 5.04 ; N, 7.12
Calc: C, 52.20 ; H, 5.35 ; N, 6.76

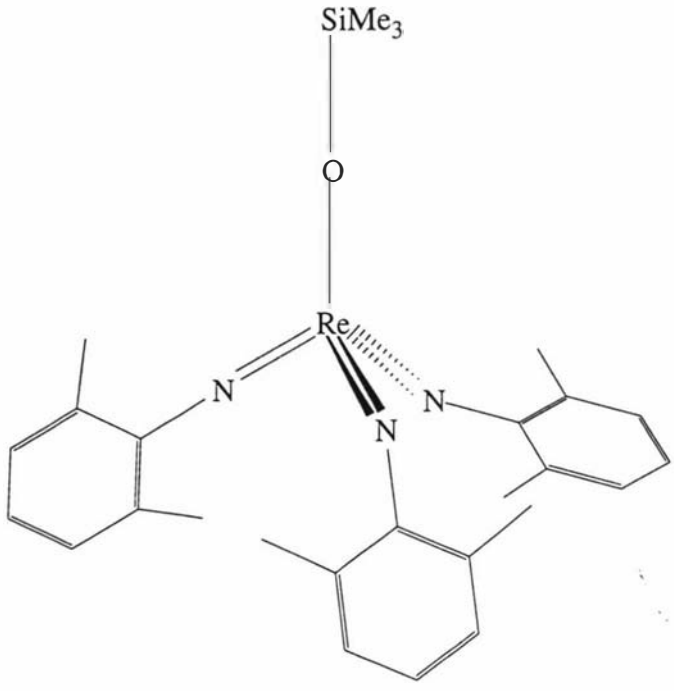

$Me_3SiORe(NAr')_3$

This was prepared by modification of the literature method.[64]

$[ReO_4][NBu_4]$ (2.032g, 4.12mmol) was added to 100mL of dichloromethane and the slurry was chilled to -40°C. To this slurry was added sequentially at -40°C, $Ar'NH_2$ (2.30g, 12.4mmol), NEt_3 (2.93g, 28.9mmol) and slowly Me_3SiCl (4.19mL, 33mmol). The reaction mixture was allowed to warm to room temperature and was stirred under nitrogen for 3 days. The solution was reduced to dryness *in vacuo* and the resulting solid was transferred to the inert atmosphere drybox. The maroon solid was extracted with benzene (250mL). The mixture was filtered through celite and the precipitate washed with benzene until the filtrate was no longer red. The solvent was removed *in vacuo*, and the resulting solid was washed with cold pentane to afford 2.385g (91%) of a red solid.

^1H NMR (C_6D_6) : 6.83(d, 6, J=7.1, Ar'), 6.68(t, 3, J=7.1, Ar'), 2.23(s, 18, Me), 0.41(s, 9, $OSi(C\underline{H}_3)_3$).

$^{13}C\{^1H\}$ NMR (C_6D_6) : 153.2(Ar'), 135.9(Ar'), 127.8(Ar'), 122.6(Ar'), 18.1($C_6H_3(\underline{C}H_3)_2$), 1.8($OSi(\underline{C}H_3)_3$).

Found: C, 52.64 ; H, 5.61 ; N, 6.93; Calc: C, 51.24 ; H, 5.73 ; N, 6.64

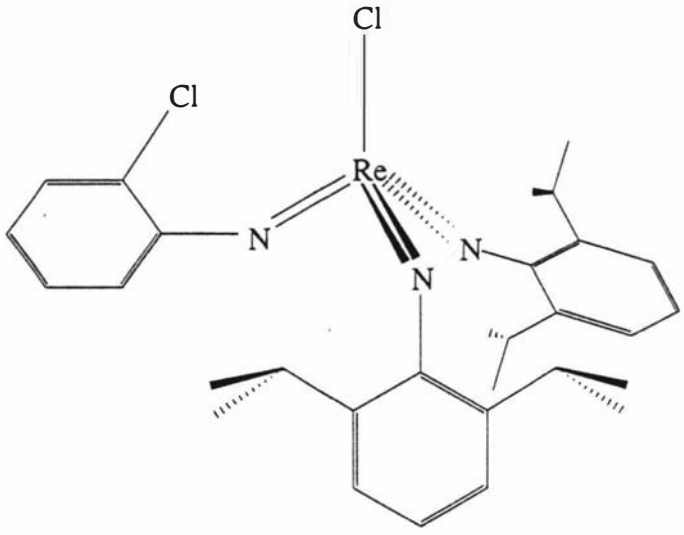

$ClRe(NAr)_2(N\text{-}o\text{-}Cl)$

A solution of $Re(NAr)_2Cl_3(py)$ (0.215g, 0.30mmol), *o*-chloroaniline (0.038g, 0.30mmol) and triethylamine (0.064g, 0.63mmol) in toluene was stirred for 3 hours. The reaction mixture was reduced to dryness *in vacuo* and hexane (6mL) was then added. The resulting suspension was filtered through celite, which was then washed with hexane (2x5mL). The filtrates were pumped to dryness, yielding 0.083g (40%) of a deep red solid. Recrystallisation can be achieved by cooling to –35°C with a minimal amount of either hexane or hexamethyldisiloxane.

^1H NMR (C_6D_6): 7.61 (d, 1, J=7.2, *o*-chlorophenyl), 7.02 (m, 5, *o*-chlorophenyl /Ar), 6.91 (m, 3, *o*-chlorophenyl /Ar), 6.42 (t, 1, J=7.0, *o*-chlorophenyl), 3.70 (sept, 4, J=6.8, $C\underline{H}Me_2$), 1.08 (d, 24, J=7.0, $CHC\underline{H}_3$).

^{13}C NMR: (C_6D_6); 154.1 (Ar), 147.8 ($\underline{C}_6H_4Cl$), 141.9 (Ar), 141.8 ($\underline{C}_6H_4Cl$), 128.8 (Ar), 128.6 ($\underline{C}_6H_4Cl$), 127.8 ($\underline{C}_6H_4Cl$), 127.4 (C_6H_4Cl), 122.1 (Ar), 122.0 ($\underline{C}_6H_4Cl$), 28.2 ($\underline{C}CH_3$), 22.7 ($C\underline{C}H_3$).

Found: C, 51.92 ; H, 5.87 ; N, 6.48
Calc: C, 51.64 ; H, 5.49 ; N, 6.02

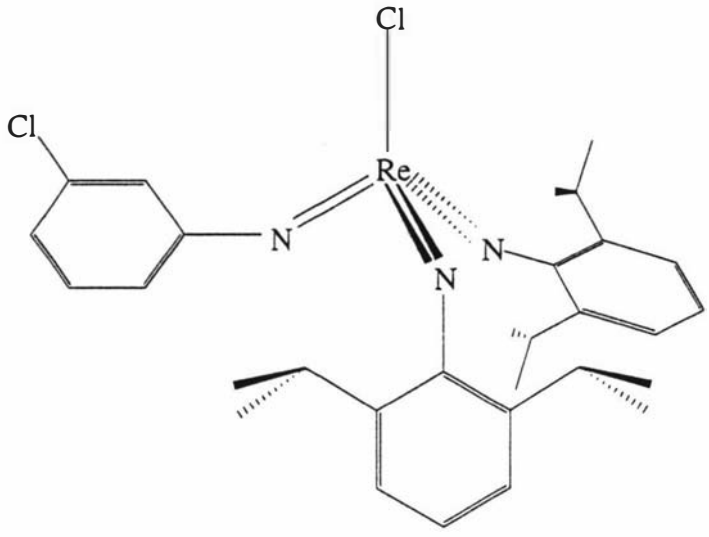

$ClRe(NAr)_2(N\text{-}m\text{-}Cl)$

A solution of $Re(NAr)_2Cl_3(py)$ (0.239g, 0.33mmol), *m*-chloroaniline (0.042g, 0.33mmol) and triethylamine (0.070g, 0.69mmol) in toluene was stirred for 3 hours. The reaction mixture was reduced to dryness *in vacuo* and hexane (6mL) was then added. The resulting suspension was filtered through celite, which was then washed with hexane (2x5mL). The filtrates were pumped to dryness, yielding 0.090g (39%) of a deep red solid. Recrystallisation can be achieved by cooling to –35°C with a minimal amount of either hexane or hexamethyldisiloxane.

^1H NMR (C_6D_6): 7.20-6.51 (m, 10, *m*-chlorophenyl /Ar), 3.63 (sept, 4, J=6.8, $C\underline{H}Me_2$), 1.04 (d, 24, J=7.0, $CHC\underline{H}_3$).

^{13}C NMR (C_6D_6): 152.8 (Ar), 152.6 ($\underline{C}_6H_4Cl$), 142.6 (Ar), 142.2 ($\underline{C}_6H_4Cl$), 130.2 ($\underline{C}_6H_4Cl$), 129.5 (Ar), 128.9 ($\underline{C}_6H_4Cl$), 126.9 ($\underline{C}_6H_4Cl$), 122.4 (Ar), 122.3 ($\underline{C}_6H_4Cl$), 29.1 ($\underline{C}CH_3$), 23.1 ($C\underline{C}H_3$).

Found: C, 51.92 ; H, 5.94 ; N, 5.45
Calc: C, 51.64 ; H, 5.49 ; N, 6.02

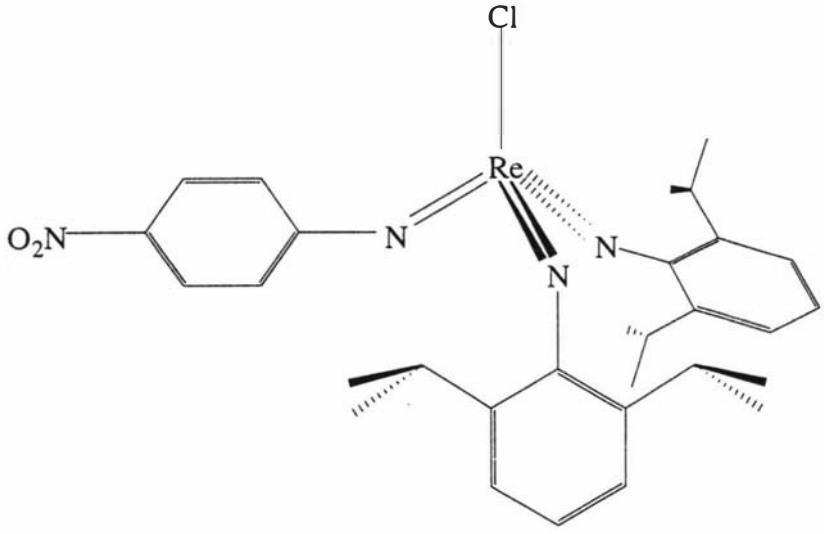

$ClRe(NAr)_2(N\text{-}p\text{-}NO_2)$

A solution of $Re(NAr)_2Cl_3(py)$ (0.262g, 0.36mmol), *p*-nitroaniline (0.050g, 0.36mmol) and triethylamine (0.077g, 0.76mmol) in toluene was stirred for 3 hours. The reaction mixture was reduced to dryness *in vacuo* and hexane (6mL) was then added. The resulting suspension was filtered through celite, which was then washed with hexane (2x5mL). The filtrates were pumped to dryness, yielding 0.087g (34%) of a deep red solid. Recrystallisation can be achieved by cooling to –35°C with a minimal amount of either hexane or hexamethyldisiloxane.

^1H NMR (C_6D_6): 7.90 (d, 2, J=7.2, *p*-nitrophenyl), 7.01 (d, 4, J=7.0, Ar), 6.87 (t, 2, J=7.0, Ar), 6.75 (d, 2, J=7.2, *p*-nitrophenyl), 3.61 (sept, 4, J=6.8, $C\underline{H}Me_2$), 1.03 (d, 24, J=7.0, $CHC\underline{H}_3$).

^{13}C NMR (C_6D_6); 152.1 (Ar), 151.8 ($\underline{C}_6H_4NO_2$), 142.6 (Ar), 141.9 ($\underline{C}_6H_4NO_2$), 128.2 (Ar), 124.6 ($\underline{C}_6H_4NO_2$), 122.0 (Ar), 117.6 ($\underline{C}_6H_4NO_2$), 28.2 ($\underline{C}CH_3$), 23.1 ($C\underline{C}H_3$).

Found: C, 50.33 ; H, 5.02 ; N, 7.95
Calc: C, 50.87 ; H, 5.41 ; N, 7.91

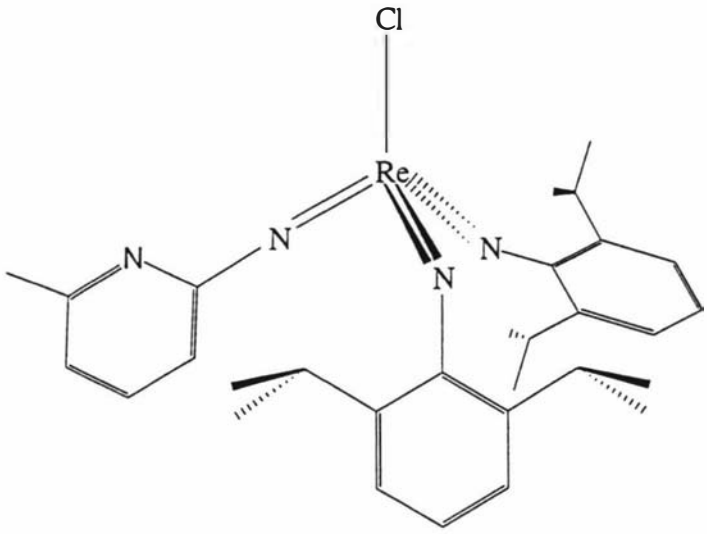

ClRe(NAr)$_2$(N-AMP)

A solution of Re(NAr)$_2$Cl$_3$(py) (0.271g, 0.38mmol), 2-amino-6-methyl pyridine (0.041g, 0.38mmol) and triethylamine (0.081g, 0.080mmol) in toluene was stirred for 3 hours. The reaction mixture was reduced to dryness *in vacuo* and hexane (6mL) was then added. The resulting suspension was filtered through celite, which was then washed with hexane (2x5mL). The filtrates were pumped to dryness, yielding 0.096g (37%) of a deep red solid. Recrystallisation can be achieved by cooling to –35°C with a minimal amount of either hexane or hexamethyldisiloxane.

^{1}H NMR (C_6D_6); 7.02 (m, 5, Ar/pyridyl), 6.87 (t, 2, J=7.1, Ar), 6.59 (d, 1, J=7.2, pyridyl), 6.25 (d, 1, J=7.2, pyridyl), 3.72 (sept, 4, J=6.8, C$\underline{H}$Me$_2$), 2.21 (s, 3, $C_5NC\underline{H}_3$), 1.02 (d, 24, J=7.0, CHC$\underline{H}_3$).

^{13}C NMR (C_6D_6); 152.5 (Ar), 152.2 ($\underline{C}_5H_3NCH_3$), 141.9 (Ar), 141.5 ($\underline{C}_5H_3NCH_3$), 137.1 ($\underline{C}_5H_3NCH_3$), 126.2 (Ar), 122.8 ($\underline{C}_5H_3NCH_3$), 121.9 ($\underline{C}_5H_3NCH_3$), 121.8 (Ar), 28.6 (C$\underline{C}$H3), 24.0 (C$\underline{C}$H3), 22.7 ($C_5H_3N\underline{C}H_3$).

Found: C, 54.14 ; H, 5.68 ; N, 7.67
Calc: C, 53.12 ; H, 5.94 ; N, 8.26

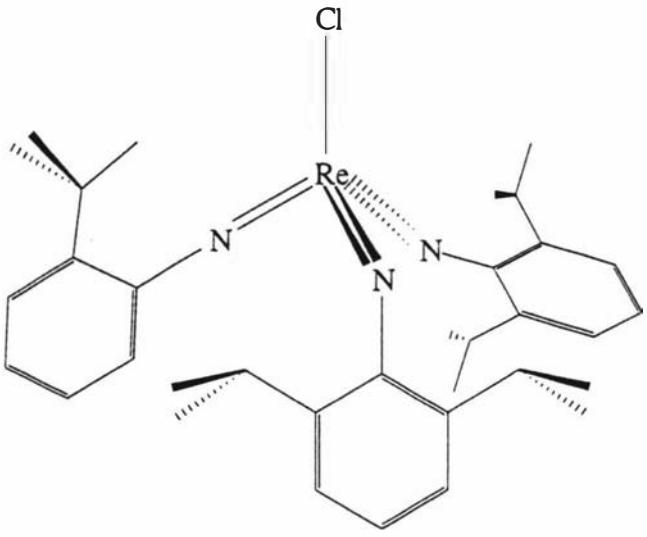

$ClRe(NAr)_2(N\text{-}o\text{-}^tBu)$

A solution of $Re(NAr)_2Cl_3(py)$ (0.305g, 0.47mmol), *o-tert*-butylaniline (0.063g, 0.42mmol) and triethylamine (0.090g, 0.89mmol) in toluene was stirred for 3 hours. The reaction mixture was reduced to dryness *in vacuo* and hexane (6mL) was then added. The resulting suspension was filtered through celite, which was then washed with hexane (2x5mL). The filtrates were pumped to dryness, yielding 0.156g (52%) of a deep red solid. Recrystallisation can be achieved by cooling to –35°C with a minimal amount of either hexane or hexamethyldisiloxane.

^1H NMR (C_6D_6); 7.19 (d, 1, J=7.2, *o-t*-butylphenyl), 7.01 (d, 4, J=7.0, Ar), 6.64-6.91 (m, 5, Ar/*o-t*-butylphenyl), 3.72 (sept, 4, J=6.8, C$\underline{H}Me_2$), 1.48 (s, 9, *t*-butyl), 1.04 (d, 24, J=7.0, CHC$\underline{H}_3$).

^{13}C NMR (C_6D_6); 155.2 (Ar), 151.9 ($\underline{C}_6H_5C(CH_3)_3$), 143.0 (Ar), 142.9 ($\underline{C}_6H_5C(CH_3)_3$), 128.6 ($\underline{C}_6H_5C(CH_3)_3$), 125.4 (Ar), 125.1 ($\underline{C}_6H_5C(CH_3)_3$), 125.0 ($\underline{C}_6H_5C(CH_3)_3$), 124.8 ($\underline{C}_6H_5C(CH_3)_3$), 122.6 (Ar), 35.2 ($C_6H_5\underline{C}(CH_3)_3$), 30.6 ($C_6H_5C(\underline{C}H_3)_3$), 27.6 ($\underline{C}CH_3$), 23.1 ($C\underline{C}H_3$).

Found: C, 56.15 ; H, 6.86 ; N, 5.94
Calc: C, 56.76 ; H, 6.59 ; N, 5.84

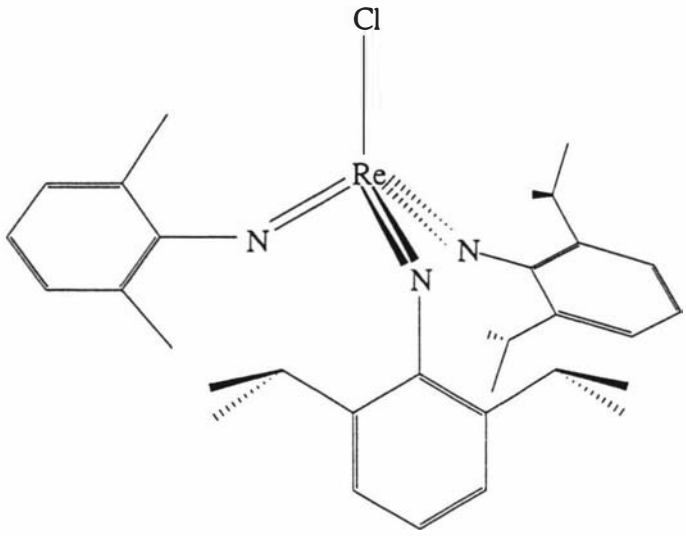

$ClRe(NAr)_2(NAr')$

A solution of $Re(NAr)_2Cl_3(py)$ (0.203g, 0.28mmol), $Ar'NH_2$ (0.034g, 0.28mmol) and Et_3N (0.060g, 0.59mmol) in toluene was stirred for 2 hour. The reaction mixture was reduced to dryness *in vacuo* and hexane (6mL) was then added. The resulting suspension was filtered through celite, which was then washed with hexane (2x5mL). The filtrates were pumped to dryness, yielding 0.126g (65%) of a deep red solid. Further purification can be achieved by silica column in hexane.

^1H NMR (C_6D_6) : 7.10(d, 4, J=7.1, Ar), 6.96(t, 2, J=7.1, Ar), 6.88(d, 2, J=7.1, Ar'), 6.72(t, 1, J=7.1, Ar'), 3.84(sept, 4, J=6.8, C<u>H</u>Me_2), 2.32(s, 6, <u>C</u>H_3), 1.13(d, 24, J=7.0, CHC<u>H</u>$_3$).

$^{13}C\{^1H\}$ NMR (C_6D_6) : 152.8(Ar), 152.7(Ar'), 143.0(Ar), 142.5(Ar'), 132.1(Ar), 127.1(Ar'), 122.5(Ar), 122.4(Ar'), 28.1(<u>C</u>HCH_3), 23.5(CH<u>C</u>H_3), 17.9(<u>C</u>H_3).

Found: C, 55.97 ; H, 6.12 ; N, 5.96
Calc: C, 55.59 ; H, 6.27 ; N, 6.08

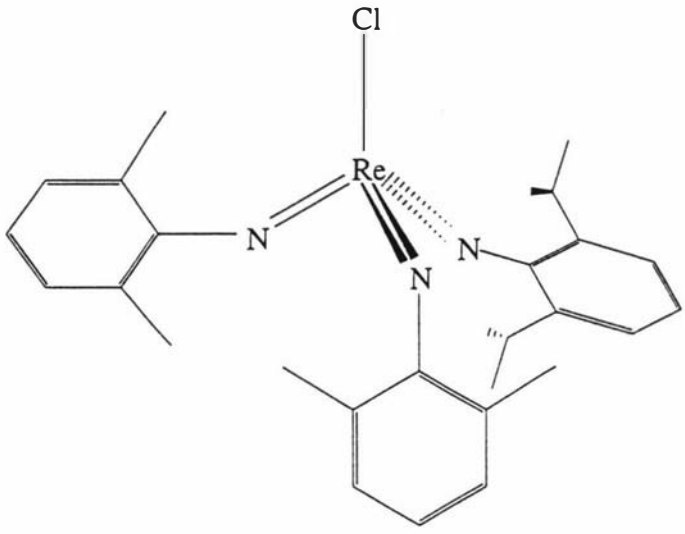

$ClRe(NAr')_2(NAr)$

A solution of $Re(NAr')_2Cl_3(py)$ (0.200g, 0.33mmol), $ArNH_2$ (0.058g, 0.33mmol) and Et_3N (0.071g, 0.70mmol) in toluene was stirred for 6 hours. The reaction mixture was reduced to dryness *in vacuo* and hexane (6mL) was then added. The resulting suspension was filtered through celite, which was then washed with hexane (2x5mL). The filtrates were pumped to dryness, yielding 0.094g (45%) of a deep red solid. Further purification can be achieved by silica column in hexane.

^1H NMR (C_6D_6) : 7.03(d, 2, J=7.1, Ar), 6.89(t, 1, J=7.1, Ar), 6.79(d, 4, J=7.1, Ar'), 6.65(t, 2, J=7.1, Ar'), 3.79(sept, 2, J=6.7, C<u>H</u>Me_2), 2.25(s, 12, C<u>H</u>$_3$), 1.10(d, 12, J=7.0, CHC<u>H</u>$_3$).

$^{13}C\{^1H\}$ NMR (C_6D_6) : 159.2(Ar), 152.2(Ar'), 142.9(Ar), 142.6(Ar'), 132.2(Ar), 126.9(Ar'), 121.9(Ar), 121.8(Ar'), 28.1(<u>C</u>HCH_3), 23.0(CH<u>C</u>H_3), 17.8(<u>C</u>H_3).

Found: C, 53.57 ; H, 6.01 ; N, 6.10
Calc: C, 52.94 ; H, 5.55 ; N, 6.61

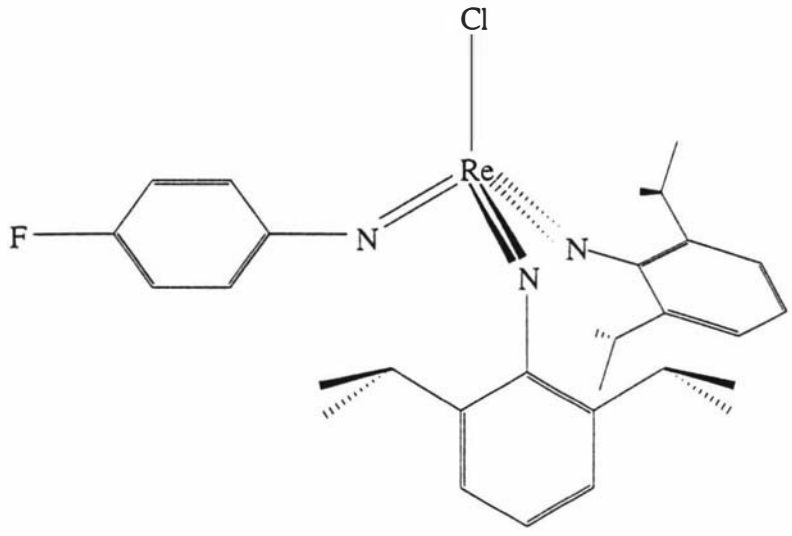

$ClRe(NAr)_2(N\text{-}p\text{-}F)$

A solution of $Re(NAr)_2Cl_3(py)$ (0.264g, 0.37mmol), *p*-fluoroaniline (0.040g, 0.36mmol) and Et_3N (0.079g, 0.78mmol) in toluene was stirred for 4 hours. The reaction mixture was reduced to dryness *in vacuo* and hexane (7mL) was then added. The resulting suspension was filtered through celite, which was then washed with hexane (2x6mL). The filtrates were pumped to dryness, yielding 0.125g (51%) of a deep red solid. Further purification can be achieved by silica column in hexane.

^1H NMR (C_6D_6) : 7.07(d, 4, J=7.1, Ar), 7.04(d, 4, J=7.2, *p*-fluorophenyl), 6.94(t, 2, J=7.1, Ar), 3.70(sept, 4, J=6.8, C<u>H</u>Me_2), 1.03(d, 24, J=7.0, CHC<u>H</u>$_3$).

$^{13}C\{^1H\}$ NMR (C_6D_6) : 157.9(Ar), 157.6(<u>C</u>$_6H_4F$), 142.1(Ar), 141.7(<u>C</u>$_6H_4F$), 128.1(Ar), 127.0(<u>C</u>$_6H_4F$), 122.2(Ar), 119.2(<u>C</u>$_6H_4F$), 28.5(<u>C</u>HCH_3), 23.1(CH<u>C</u>H_3).

Found: C, 53.42 ; H, 6.02 ; N, 5.98
Calc: C, 52.89 ; H, 5.62 ; N, 6.17

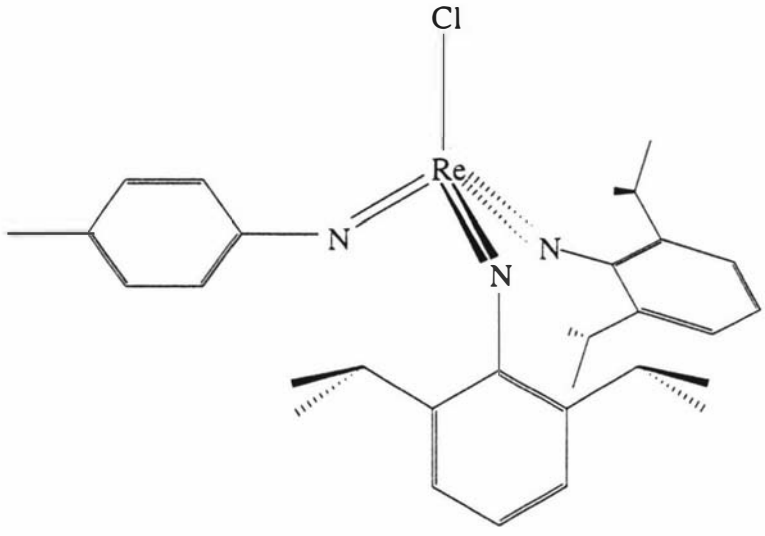

$ClRe(NAr)_2(N\text{-}p\text{-}tol)$

A solution of $Re(NAr)_2Cl_3(py)$ (0.298g, 0.41mmol), *p*-$tolNH_2$ (0.044g, 0.41mmol) and Et_3N (0.087g, 0.86mmol) in toluene was stirred for 4 hours. The reaction mixture was reduced to dryness *in vacuo* and hexane (7mL) was then added. The resulting suspension was filtered through celite, which was then washed with hexane (2x6mL). The filtrates were pumped to dryness, yielding 0.141g (50%) of a deep red solid. Further purification can be achieved by silica column in hexane.

^1H NMR (C_6D_6) : 7.12(d, 4, J=7.1, Ar), 7.01(d, 4, J=7.2, $C_6\underline{H}_4CH_3$), 6.99(t, 2, J=7.1, Ar), 3.75(sept, 4, J=6.8, $C\underline{H}Me_2$), 2.08(s, 3, $C_6H_4C\underline{H}_3$), 1.02(d, 24, J=7.0, $CHC\underline{H}_3$).

$^{13}C\{^1H\}$ NMR (C_6D_6) : 157.8(Ar), 157.5($\underline{C}_6H_4CH_3$), 142.5(Ar), 142.2($\underline{C}_6H_4CH_3$), 128.2(Ar), 126.2($\underline{C}_6H_4CH_3$), 121.9(Ar), 118.1($\underline{C}_6H_4CH_3$), 28.1($\underline{C}HCH_3$), 22.9($CH\underline{C}H_3$), 20.1($C_6H_4\underline{C}H_3$).

Found: C, 55.46 ; H, 6.62 ; N, 5.76
Calc: C, 54.97 ; H, 6.10 ; N, 6.20

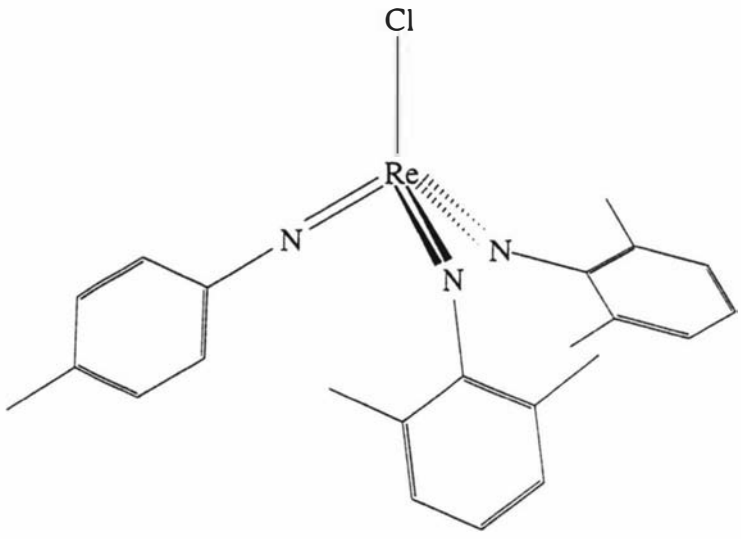

ClRe(NAr')$_2$(N-*p*-tol)

A solution of Re(NAr')$_2$Cl$_3$(py) (0.200g, 0.33mmol), *p*-tolNH$_2$ (0.035g, 0.33mmol) and Et$_3$N (0.071g, 0.70mmol) in toluene was stirred for 6 hours. The reaction mixture was reduced to dryness *in vacuo* and hexane (6mL) was then added. The resulting suspension was filtered through celite, which was then washed with hexane (2x5mL). The filtrates were pumped to dryness, yielding 0.078g (42%) of a deep red solid. Further purification can be achieved by silica column in hexane of from a hexane solution at -36°C.

^{1}H NMR (C_6D_6) : 6.98(d, 4, J=7.2, *p*-tol), 6.78(d, 4, J=7.1, Ar'), 6.62(t, 2, J=7.1, Ar'), 2.32(s, 3, $C_6H_4C\underline{H}_3$), 2.22(s, 12, $C_6H_3(C\underline{H}_3)_2$).

^{13}C{^{1}H} NMR (C_6D_6) : 156.8(p-tol), 153.0(Ar'), 143.1(Ar'), 142.0(p-tol), 127.0(Ar'), 125.9(p-tol), 122.3(Ar'), 117.9(p-tol), 20.4($C_6H_4\underline{C}H_3$), 17.8($C_6H_3(C\underline{H}_3)_2$).

Found: C, 49.23 ; H, 4.56 ; N, 6.95
Calc: C, 48.88 ; H, 4.46 ; N, 7.44

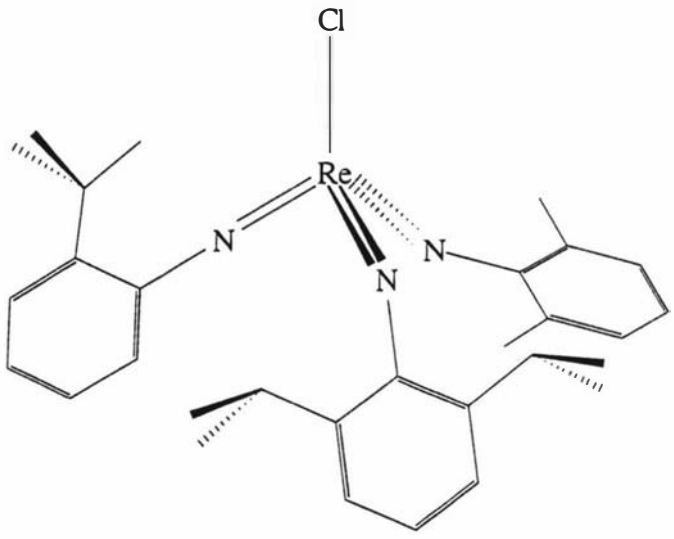

ClRe(NAr)(NAr')(N-*o*-^{t}Bu)

A solution of Re(NAr')(NAr)Cl_3(py) (0.152g, 0.28mmol), *o-tert*-butylaniline (0.034g, 0.23mmol) and Et_3N (0.050g, 0.49mmol) in toluene was stirred for 3 hours. The reaction mixture was reduced to dryness *in vacuo* and hexane (5mL) was then added. The resulting suspension was filtered through celite, which was then washed with hexane (2x5mL). The filtrates were pumped to dryness, yielding 0.053g (35%) of a deep red solid. Further purification can be achieved by silica column in hexane.

^{1}H NMR (C_6D_6) : 7.21(d, 1, J=7.2, *t*-butyl), 7.02(d, 2, J=7.0, Ar), 6.61-6.92(m, 7, Ar/*t*-butyl), 3.78(sept, 2, J=6.8, C$\underline{H}Me_2$), 2.29(s, 6, $\underline{C}H_3$), 1.48(s, 9, *t*-butyl), 1.05(d, 12, J=7.0, CHC$\underline{H}_3$)

^{13}C{^{1}H} NMR (C_6D_6) : 155.8(Ar), 154.6(Ar'), 152.1($\underline{C}_6H_4CMe_3$), 143.2(Ar), 143.0($\underline{C}_6H_4CMe_3$), 142.4(Ar'), 133.2(Ar), 129.9(Ar'), 128.0($\underline{C}_6H_4CMe_3$), 127.4($\underline{C}_6H_4CMe_3$), 126.4($\underline{C}_6H_4CMe_3$), 126.2($\underline{C}_6H_4CMe_3$), 125.4(Ar), 122.8(Ar'), 35.4($\underline{C}Me_3$), 30.2(C($\underline{C}H_3$)$_3$), 28.6($\underline{C}HCH_3$), 23.0(CH$\underline{C}H_3$), 18.2($\underline{C}H_3$).

Found: C, 55.92 ; H, 5.70 ; N, 6.85
Calc: C, 56.90 ; H, 6.21 ; N, 6.64

Chapter Three

Reactivity of Re(VII) Complexes

Introduction

This chapter describes the reactions of tetrahedral rhenium(VII) tris(imido) complexes towards Grignards, pyHCl and LiNHR.

The X^- group in the complexes $XM(NR)_3$ are readily substituted by Grignard reagents of which there are many examples.[41,71,51,30] The action of pyHCl on tris(imido) complexes was first described by Schrock and Horton to form bis(imido) complexes.[51] Similar reactions have been carried out with $MeRe(NAr')_3$,[63] $Re(NAr)_3Cl$[12] and $Os(NAr)_3$.[27] Although there are many examples of reactions involving LiNHR reagents forming amido species,[1a,b] there is only one example for tris(imido) complexes.[30]

Reactions with Grignards

The arylimido complexes of formulation $Re(N^tBu)_3(aryl)$ were prepared from $Me_3SiORe(N^tBu)_3$ by the reaction shown in Equation 64 (aryl=o-tol, Ar', mes).

$$Me_3SiORe(N^tBu)_3 + (aryl)MgBr \longrightarrow (aryl)Re(N^tBu)_3 + Mg(OSiMe_3)Br$$

Equation 64

The products were found to be air-stable, although on prolonged exposure they appear to be reactive with water.[71] Herrmann *et al.* Subsequently showed that a variety of alkyl/allyl derivatives can be synthesized from RMgCl (Scheme 14).[41]

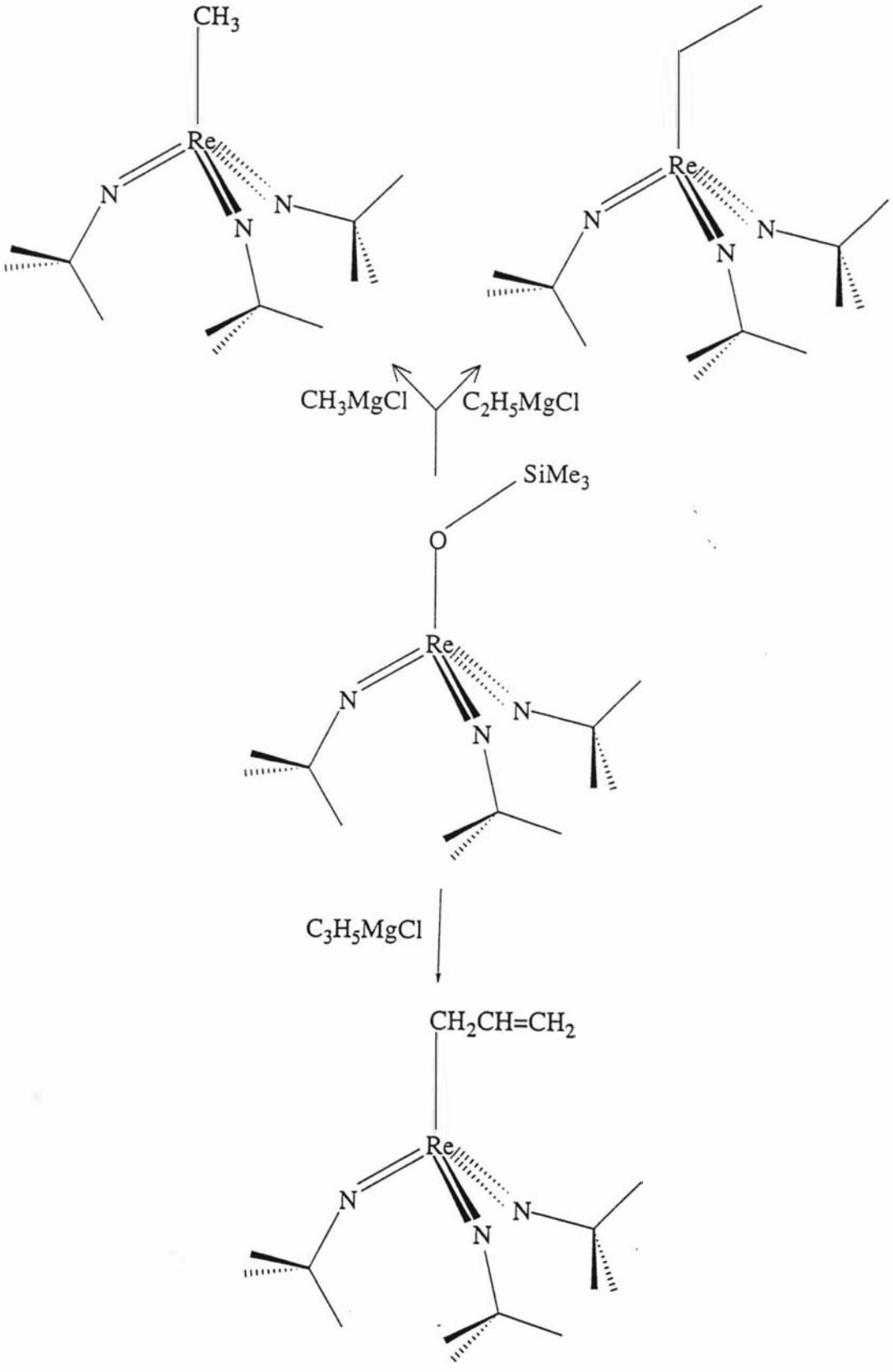

Scheme 14

However, the synthesis of $PhRe(N^tBu)_3$ cannot be achieved with PhMgCl (Scheme 15). The Me_3SiO^- ligand is lost as expected but also lost is an imido ligand which is replaced with 2 Cl^- ligands. The product is obtained in only 30% yield.[30]

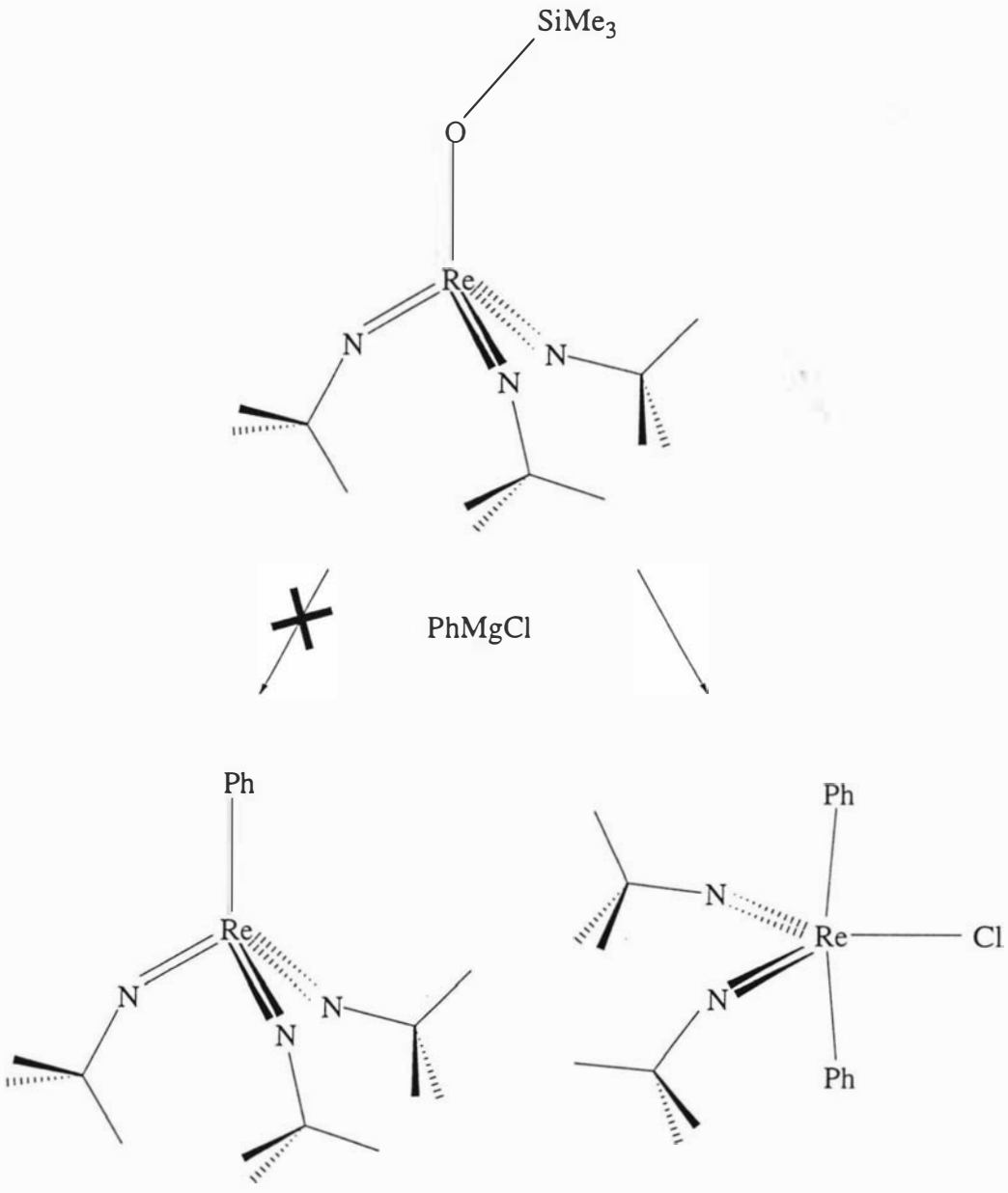

Scheme 15

The only examples of Re(VII) tris(arylimido) complexes reacting with Grignards was shown by Schrock and Horton in 1988.[51] They prepared neopentyl derivatives in high yield (Equ. 65). They also prepared $Re(NAr')_3(CH_2{}^tBu)$ from the chloro, $Re(NAr')_3Cl$, and $^tBuCH_2MgCl$ in high yield. Interestingly formation of

$Re(NAr)_3(CH_2{}^tBu)$ requires the use of $LiCH_2{}^tBu$, presumably the bulky NAr imido ligand impedes the Grignard reagent in some way.[51]

$$Me_3SiORe(NR)_3 + {}^tBuCH_2MgCl \longrightarrow {}^tBuCH_2Re(NR)_3$$

R= Ar', Ar*

Equation 65

Reaction with pyHCl

The loss of an imido ligand from reaction of pyHCl with tris(imido) complexes has been illustrated with rhenium[51,12,63] and osmium.[27] Schrock *et al.* prepared $Re(NR)_2Cl_3(py)$ by either a two step reaction with $Me_3SiOReO_3$ using an isocyanate and then pyHCl or from $Me_3SiORe(NAr^*)_3$ and 3 equivalents of pyHCl (Equ. 66 and 67).[51]

$$Me_3SiOReO_3 \xrightarrow[\text{ii) pyHCl}]{\text{i) RNCO}} Re(NR)_2Cl_3(py)$$

R= Ar', Ar

Equation 66

$$Me_3SiORe(NAr^*)_3 + 3\ pyHCl \longrightarrow Re(NAr^*)_2Cl_3(py)$$

Equation 67

Five years later Schrock *et al.* described an alternative synthesis of $Re(NAr)_2Cl_3(py)$ from $Re(NAr)_3Cl$ (Equ. 68).[12] It was shown that the reaction can be reversed by addition of NEt_3, however no experimental details were given.

$$ClRe(NAr)_3 \xrightarrow[ii)\ 2\ NEt_3]{i)\ 2\ pyHCl} Re(NAr)_2Cl_3(py) + ArNH_2$$

Equation 68

This type of reaction not only works for chloro and siloxy tris(imido) complexes but also the methyl derivative (Equ. 69). It was also shown that pyHBr can also be used to produce the bromide complexes.[63]

$$MeRe(NAr')_3 + 2\ pyHX \longrightarrow Re(NAr')_2MeX_2(py)$$

X= Cl, Br

Equation 69

Not only can bis(imido) complexes be synthesized in this manner, but also mono(imido)complexes. Williams and Schrock[12] synthesized $Re(NAr)Cl(\eta^2\text{-}NpCCNp)_2$ via reduction of $Re(NAr)Cl_3(py)_2$ which they obtained by the reaction shown in equation 70.

$$[Re(NAr)_3]^- + 4\ pyHCl \longrightarrow Re(NAr)Cl_3(py)_2 + 2\ ArNH_2$$

Equation 70

Reaction with LiNHR

The only example of a LiNHR reaction with a Re(VII) tris(imido) complex was described in 1988.[30] The tetrakis(imido) complex $[Li(tmed)][Re(N^tBu)_4]$ was synthesized in 3 steps from $Me_3SiORe(N^tBu)_3$. One of these steps involved the formation of $Re(N^tBu)_3(NH^tBu)$ from the chloro complex $Re(N^tBu)_3Cl$ (Equ. 71).

$$ClRe(N^tBu)_3 + LiNH^tBu \longrightarrow {}^tBuNHRe(N^tBu)_3$$

Equation 71

This reaction gives good yields if the reagents are slowly mixed at low temperature and then allowed to warm slowly to room temperature.[30]

Results and Discussion

Synthesis of $MeRe(NAr')_2(NAr)$ and $RRe(NAr)_2(NAr')$ complexes

The reaction of $Re(NR)_2(NR')Cl$ with one equivalent of a diethyl ether solution containing MeMgBr, *p*-TolMgBr or $PhCH_2MgCl$ in THF forms the alkyl and aryl tris(imido) complexes in good yield (Scheme 16)

$$ClRe(NR)_2(NR') + R''MgX \longrightarrow R''Re(NR)_2(NR')$$

X	R	R'	R''	Complex
Br	Ar	Ar'	Me	$MeRe(NAr)_2(NAr')$
Br	Ar'	Ar	Me	$MeRe(NAr')_2(NAr)$
Br	Ar	Ar'	*p*-tol	*p*-$tolRe(NAr)_2(NAr')$
Cl	Ar	Ar'	$PhCH_2$	$PhCH_2Re(NAr)_2(NAr')$

Scheme 16

In the reaction of *p*-tolMgBr with $ClRe(NAr)_2(NAr')$ the complex, *p*-$tolRe(NAr)_2(NAr')$ was formed as expected, however on recrystallization from hexamethyldisiloxane, a new complex was formed, $[Re(NAr)_2(p\text{-tol})(\mu\text{-}O)]_2$, containing bridging oxo groups. The formation of this dimer was presumably due to the presence of water in the recrystallization solvent (Equ. 72). The methyl analogue, $[Re(NAr)_2(Me)(\mu\text{-}O)]_2$, is synthesized from the oxo, $MeReO_3$ and 2 equivalents of the isocyanate, ArNCO.[21]

$ClRe(NAr)_2(NAr')$ + *p*-tolMgBr

↓

p-tol$Re(NAr)_3$

↓ $Me_3SiOSiMe_3$, wet

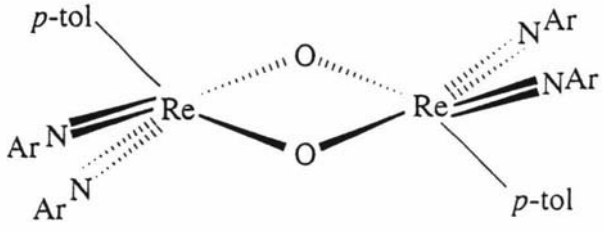

Equation 72

X-ray structure of $MeRe(NAr)_2(NAr')$

Crystals of $MeRe(NAr)_2(NAr')$ were obtained from a concentrated hexamethyldisiloxane solution cooled to -35°C and were used to acquire the molecular structure. The final structure is shown in figure 50. Tables containing complete bond lengths and angles, atomic coordinates and equivalent isotropic displacement parameters, anisotropic displacement parameters and calculated H-atom positions are presented in appendix IX.

Tables 9 and 10 show selected bond lengths and angles for $MeRe(NAr)_2(NAr')$ and 3 related compounds for comparison. The methyl complex is approximately tetrahedral about the metal and contains short metal-nitrogen multiple bond lengths of 1.763(4)Å (Re-N(1)), 1.757(3)Å (Re-N(2)) and 1.753(4)Å (Re-N(3)). The Re-C distance of 2.113(5)Å is within agreement of other known examples, $MeRe(NAr)_3$;Re-C= 2.109(5)Å[21], $MeTc(NAr)_3$;Tc-C= 2.136(17)Å[39] and $CH_3Re(O)_2(1,2\text{-}O_2C_6H_4)(NC_5H_5)$; Re-C=2.101(5)Å.[113] All the C-Re-N angles compare well with $MeRe(NAr)_3$ and $MeTc(NAr)_3$ (Table 9) as do the essentially linear Re-N-C angles.

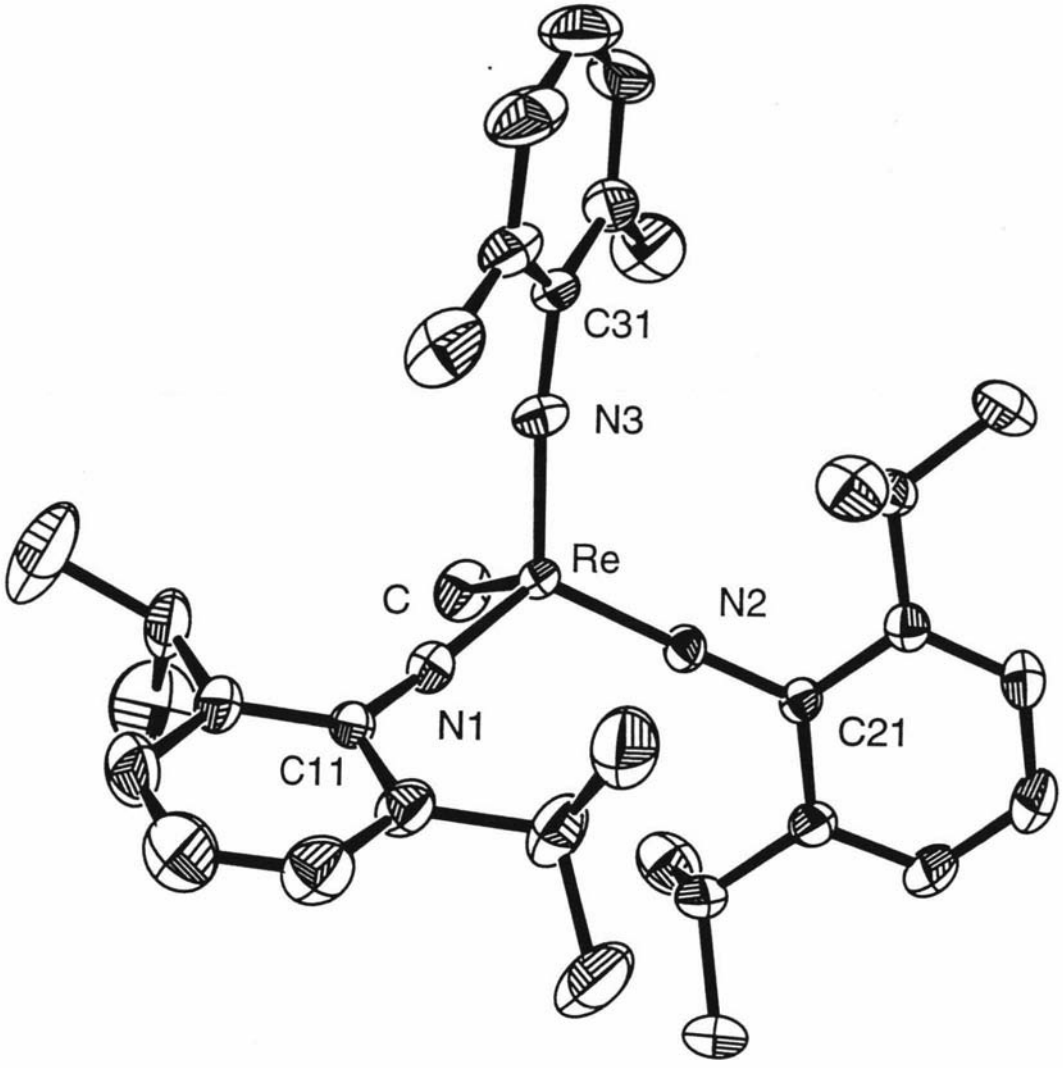

Figure 50

Complex	#	X-M-N(#)	M-N(#)-C	N(1)-M-N(#)	Ref	Comments
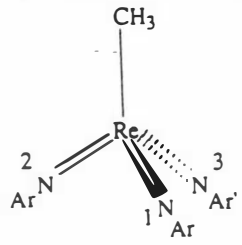	1	103.9(2)	169.1(3)		-	N(2)-Re-N(3)
	2	101.85(19)	171.2(3)	114.75(17)		115.63(17)
	3	102.81(19)	168.5(3)	115.23(18)		
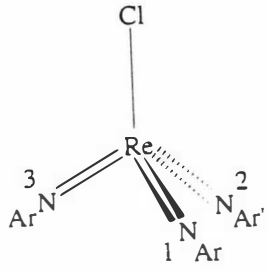	1	107.2(8)	165(2)		-	2 independent
		107.7(8)	166.6(19)			structures
	2	106.9(8)	165(2)	112.2(10)		N(2)-Re-N(3)
		107.1(7)	170.6(18)	110.0(9)		112.4(8)
	3	107.4(8)	172.5(19)	110.4(10)		113.5(10)
		106.7(8)	162.1(19)	111.6(10)		
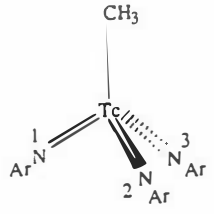	1	101.8(6)	167.0(11)		39	Approximately
	2	102.9(6)	163.9(10)	116.6(6)		tetrahedral
	3	101.4(6)	168.0(9)	115.7(5)		N(2)-Tc-N(3)
						115.0(5)
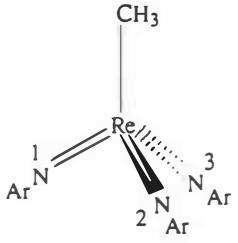	1	102.4(2)	166.3(3)		21	Distorted
	2	101.8(2)	168.8(3)	114.8(2)		tetrahedral
	3	103.0(2)	169.5(3)	116.2(2)		N(2)-Re-N(3)
						115.6(2)

Table 9: Selected bond angles(°) for $CH_3Re(NAr)_2(NAr')$ and 3 related complexes

Complex	M-X	M-N(1)	M-N(2)	M-N(3)	Ref	Comments
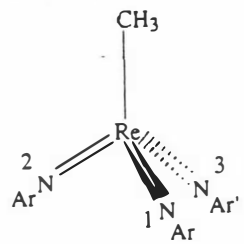	2.113(5)	1.763(4)	1.757(3)	1.753(4)	-	
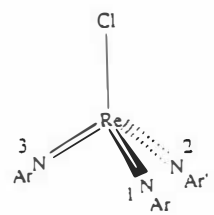	2.271(9) 2.272(9)	1.70(2) 1.72(2)	1.725(18) 1.766(19)	1.71(2) 1.73(2)	-	2 independent structures
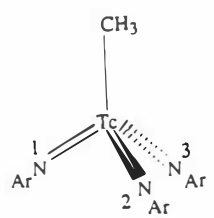	2.136(17)	1.738(11)	1.749(13)	1.743(10)	39	Short Tc-N bond length
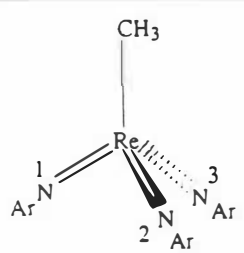	2.109(5)	1.766(3)	1.748(3)	1.758(4)	21	

Table 10: Selected bond lengths(Å) for $CH_3Re(NAr)_2(NAr')$ and 3 related complexes

Table 11 compares the Re-N-Ar' bond angles of four Re(VII) tris(imido) complexes. The complexes containing 2 NAr imido ligands and 1 NAr' imido ligand contain Re-N-Ar' angles of 168.5° and 167.8°. The tris(NAr') imido complexes contain Re-N-Ar' angles of 158.4° and 158.8°, 10° less than the mixed imido complexes (Table 11).

The steric bulk of the NAr imido ligand is much greater than NAr'. It is possible the bending at the nitrogen of the NAr' imido ligand is more restricted in the complexes containing NAr imido ligands. The bending at the nitrogen of the NAr

imido ligand appears uneffected by the presence of the NAr' imido ligand in the mixed imido complexes (see appendix IV).

Complex	Re-N-Ar'	Ref
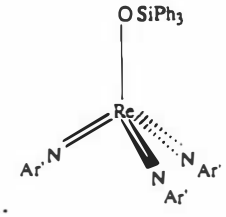	158.4(3)	104
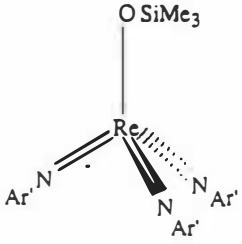	158.8(5)	-
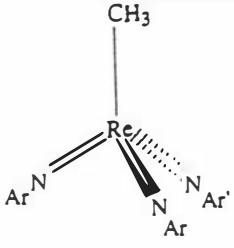	168.5	-
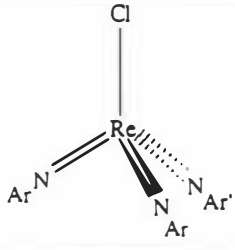	167.8(18)	-

Table 11: Comparison of the Re-N-Ar' bond angles(°) of 4 tetrahedral tris(arylimido) complexes

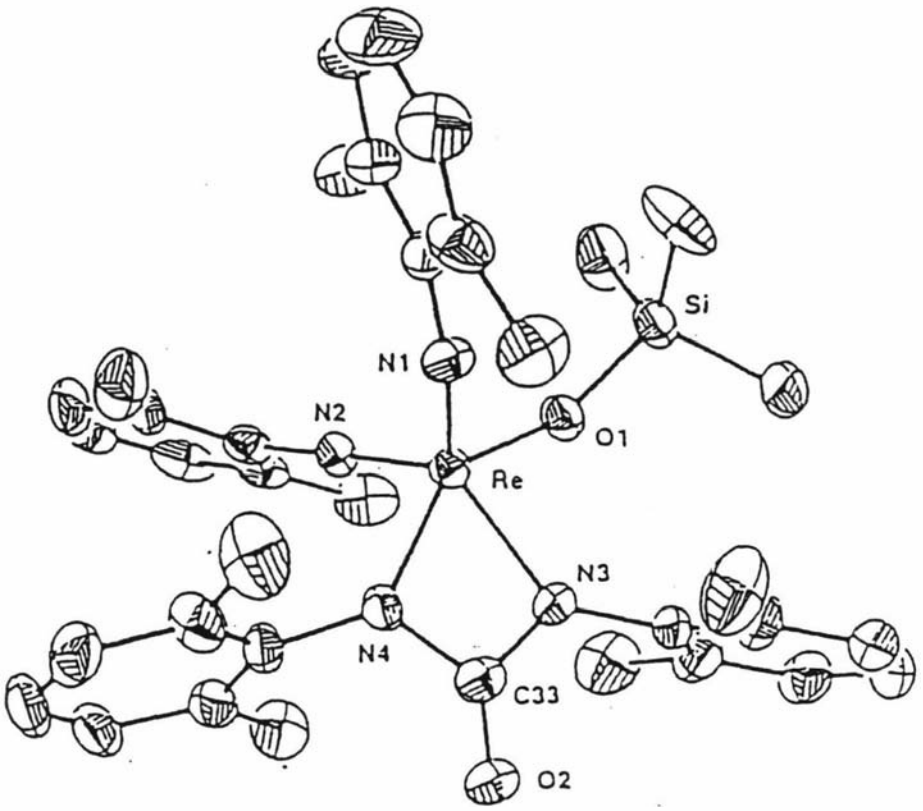

Figure 51

The same argument can be used for the complex shown in figure 51. Here the Re-N-Ar' terminal imido angles are 165.8(6)° and 175.5(6)°,[22] similar to those for the mixed imido complexes. The complex has a distorted square based pyramidal geometry with N(1) at the apex. Due to crowding about the rhenium the Re-N-Ar' terminal angles are not as small as would be expected. Note the value of 165.8(6)° is for the terminal imido ligand which occupies the apex.

X-ray structure of $[Re(NAr)_2(p\text{-tol})(\mu\text{-}O)]_2$

A X-ray structural analysis was carried out of the oxo bridged dimer, $[Re(NAr)_2(p\text{-tol})(\mu\text{-}O)]_2$. The final structure is shown in figure 52. Tables containing complete bond lengths and angles, atomic coordinates and equivalent isotropic displacement parameters, anisotropic displacement parameters and calculated H-atom positions are presented in appendix X.

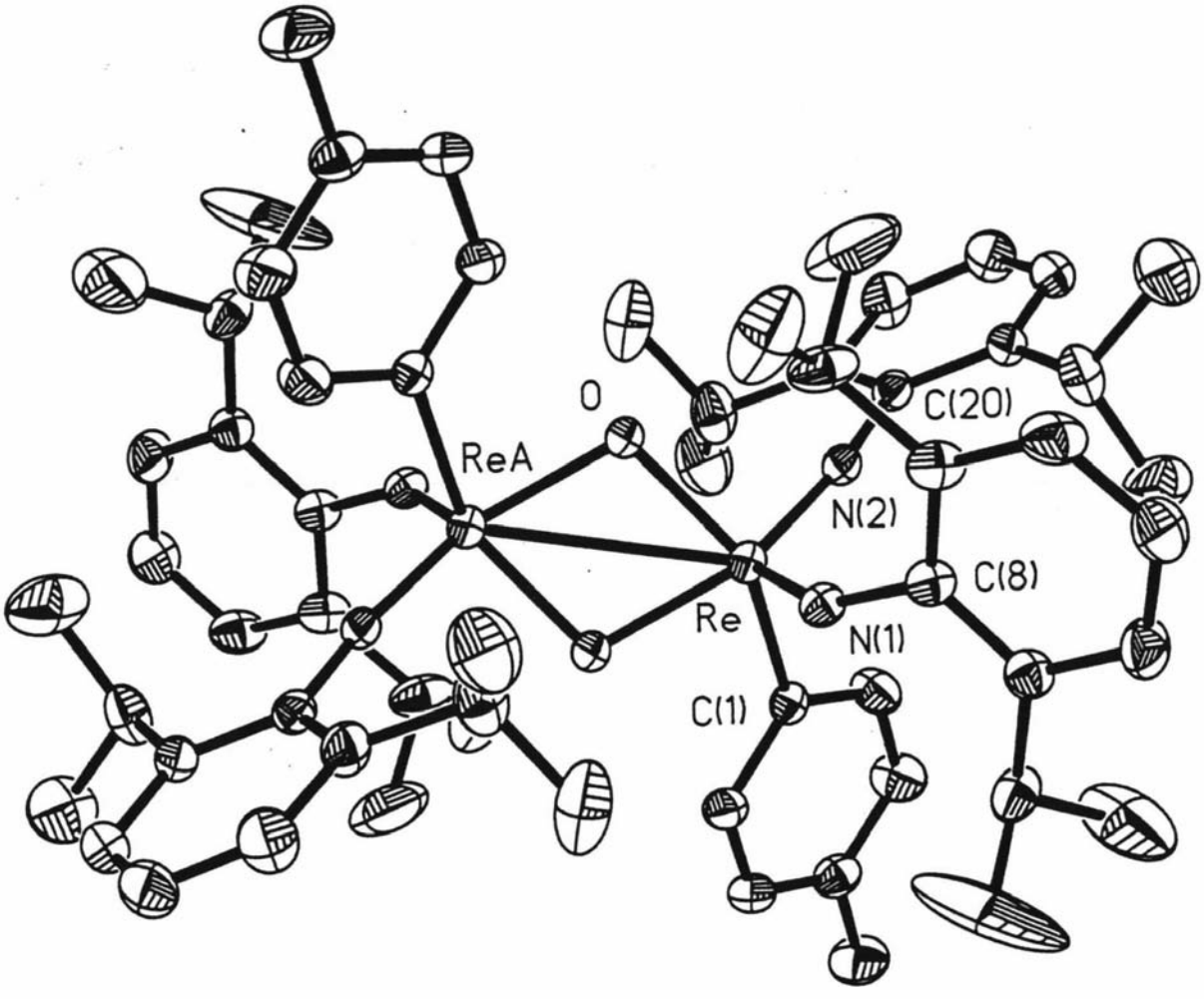

Figure 52

Tables 12 and 13 show selected bond lengths and angles for $[Re(NAr)_2(p\text{-tol})(\mu\text{-O})]_2$ and three other oxo bridging dimers previously structurally characterized.[21,48] The geometry about each Re is distorted square pyramidal with N(1) at the apex. The dimer is centrosymmetric with only slightly unsymmetric oxo bridges. The difference between the equatorial and axial Re-O distances is only 0.037Å. This differs remarkably from other known examples which range from 0.105Å for $[Re(NAr)(O)(Me)(\mu\text{-O})]_2$[21] to 0.573Å for $[Re(N^tBu)(O)(mes)(\mu\text{-O})]_2$.[48] The lengthening of the axial Re-O bond is throught to be caused by the trans influence of the imido group.[48] Why this lengthening for $[Re(NAr)_2(p\text{-tol})(\mu\text{-O})]_2$ is very small maybe related to the geometry about the Re atom.

Complex	#	Re-N(#)-C	N(1)-M-N(#) [O(1)-Re-N(#)]	C(1)-Re-N(#) [C(1)-Re-O(#)]	Ref.	Comments
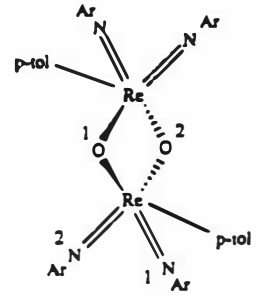	1	145.5(3)	[112.48(13)]	103.12(14) [140.74(13)]	-	N(1)-Re-O(2) 102.77(13)
	2	166.7(3)	107.82(15) [93.72(13)]	90.59(14) [82.17(12)]		N(2)-Re-O(2) 149.41(13) O(1)-Re-O(2) 74.52(12) Re-O(1)-Re 105.48(12)
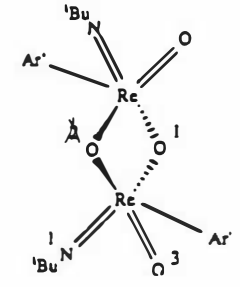	1	173.8(7)	[161.0(4)]	89.4(4) [79. 4(4)]	48	O(1)-Re-O(3) 75.8(4)
	3			[137.1(3)]		N(1)-Re-O(3) 101.4(5) Re-O(1)-Re 107.7(4)
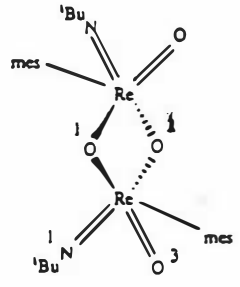	1	153.7(7)	[105.5(4)]	95.6(4) [115.3(4)]	48	O(1)-Re-O(3) 74.2(4)
	3			[79.2(4)]		N(1)-Re-O(3) 173.8(4) Re-O(1)-Re 105.8(4)
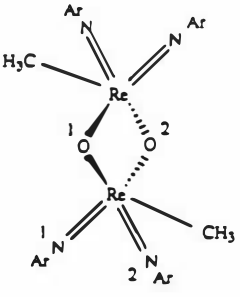	1	172.1(4)	[98.8(2)]	[137. 4(2)]	21	O(2)-Re(1)-N(1) 147.4(2)
	2	157.7(4)	[114.5(2)]	[77.2(2)]		O(2)-Re(1)-N(2) 102.6(2) Re-O(1)-Re 105.9(2)

Table 12: Selected bond angles(°) for $[Re(NAr)_2(p\text{-tol})(\mu\text{-}O)]_2$ and 3 other oxo-bridging dimers

Complex	#	Re-O	Re-N(#)	Re-C(1)	Re-Re	Ref.	Comments
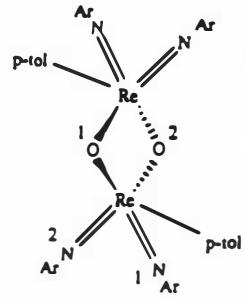	1	1.948(2)	1.751(3)	2.163(4)	3.1307(3)	-	Re*-O(1) 1.985(3)
	2	1.985(3)	1.759(3)				
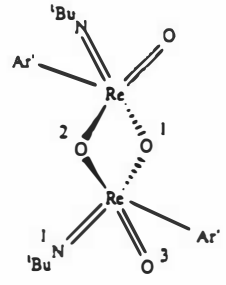	1	2.081(8)	1.722(9)	2.147(10)	3.118(3)	48	Re(1)-O(3) 1.708(9)
	2	1.867(8)					
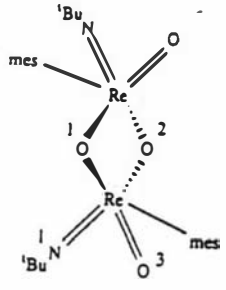	1	1.791(7)	1.741(8)	2.090(10)	3.332(4)	48	Re(1)-O(3) 1.704(8)
	2	2.364(7)					
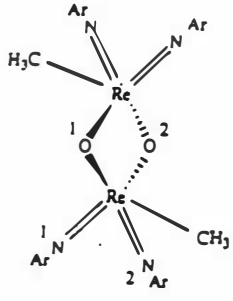	1	1.885(4)	1.740(4)	2.141(6)	3.1190(3)	21	
	2	2.022(3)	1.730(4)				

Table 13: Selected bond lengths(Å) for $[Re(NAr)_2(p\text{-tol})(\mu\text{-}O)]_2$ and 3 other oxo-bridging dimers

For $[Re(N^tBu)(O)(mes)(\mu\text{-}O)]_2$ and $[Re(N^tBu)(O)(xyl)(\mu\text{-}O)]_2$ the difference in Re-O bridging lengths is 0.573 and 0.214 and they have approximately trigonal bipyramidal geometries. While for $[Re(NAr)(O)(Me)(\mu\text{-}O]_2$, $[Re(NAr)_2(Me)(\mu\text{-}O)]_2$ and $[Re(NAr)_2(p\text{-}tol)(\mu\text{-}O)]_2$ the geometries are more distorted square pyramidal and they have smaller values of 0.137, 0.105 and 0.037Å respectively. The Re-N bond lengths are slightly larger then previously seen with Re(VII) oxo-bridging dimers but are typical for Re-NR multiple bonds (see appendix III). The Re-Re distance is rather long and indicates only a very weak bonding interaction. The Re-N(2)-C angle is slightly bent at 166.7(3)° while the Re-N(1)-C angle is some 21.2° smaller at 145.5(3)°. A similar situation is seen with $[Re(NAr)_2(Me)(\mu\text{-}O)]_2$ where the axial imido ligand is essentially linear at 172.1(4)°, while the equatorial imido ligand is bent at 157.7(4)°.[21]

Synthesis of bis(imido) complexes

As expected bis(imido) complexes were formed with the addition of 2 equivalents of pyHCl to the chloro tris(imido) complexes as shown in Scheme 17.

$$ClRe(NR')_2(NR'') + 2\ pyHCl \longrightarrow Re(NR')(NR'^{\ or\ ''})Cl_3(py)$$

R'	R''	Complex
Ar'	Ar'	$Re(NAr')_2Cl_3(py)$
Ar	Ar	$Re(NAr)_2Cl_3(py)$
Ar	Ar'	$Re(NAr)_2Cl_3(py)$
Ar'	Ar	$Re(NAr)(NAr')Cl_3(py)$

Scheme 17

It was previously shown that $[Re(NAr)_3]^-$ loses 2 imido ligands upon reaction with 4 equivalents of pyHCl.[12] In an attempt to remove 2 imido ligands from $ClRe(NAr')_3$ to form $Re(NAr')Cl_5$, it was reacted with 4 equivalents of pyHCl. No complex of formulation $Re(NR)X_5$ is known. The product isolated was however the bis(imido) complex, $Re(NAr')_2Cl_3(py)$, not the mono(imido) compound. These reactions show that loss of the NAr' imido ligand is preferred over loss of NAr. This preference enabled the formation of a mixed bis(imido)complex, $Re(NAr)(NAr')Cl_3(py)$, which is the precursor to the chiral tris(imido) complex

Re(NAr)(NAr')(N-*o*-^{t}Bu)Cl (see page 96). This is the first example of a mixed rhenium bis(imido) complex.

X-ray Structure of $Re(NAr')_2Cl_3(py)$

For the complex, $Re(NAr')_2Cl_3(py)$, the crystals that could be obtained were not of good quality, however the general features of the bis(imido) complex are clear. The final structure is shown in figure 53. Tables containing complete bond lengths and angles, atomic coordinates and equivalent isotropic displacement parameters, anisotropic displacement parameters and calculated H-atom positions are presented in appendix XI.

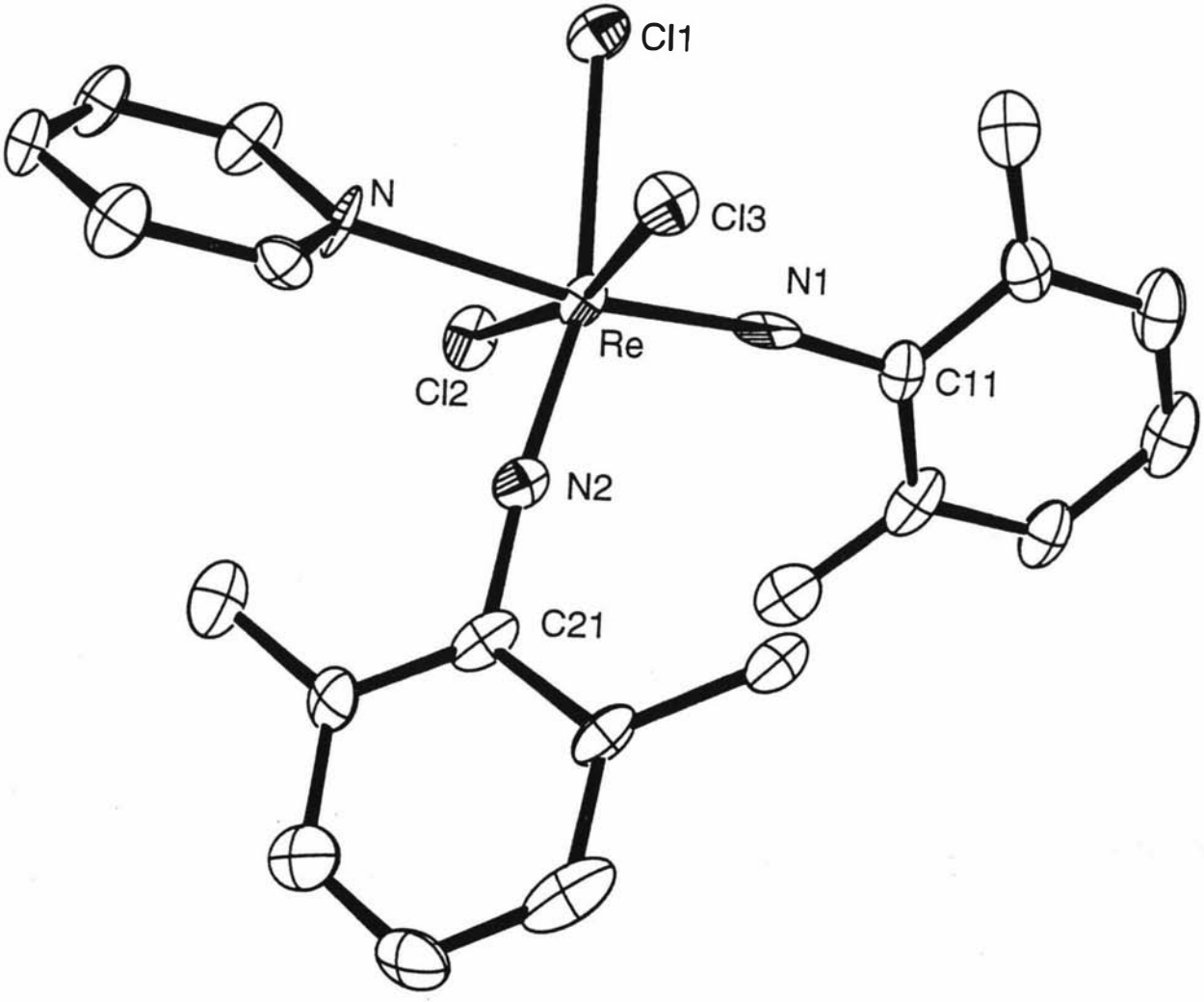

Figure 53

Table 14 shows selected bond lengths and angles for $Re(NAr')_2Cl_3(py)$. The Re atom adopts a distorted octahedral geometry comprising *cis*-orientated aryl imido groups with pyridine and Cl(1) trans to the imido ligands. The aryl imido bond lengths of 1.734(18)Å and 1.760(14)Å lie within the range (see appendix III) for terminal bis(arylimido) complexes. The Re-N-C angles are essentially linear at 171.8(12) and 174.4(13)° and compare well with those found for $Re(NAr')_2Cl_3(Me)$ at 169.2(5) and 170.5(5)°.[63] The Cl(2)-Re-Cl(3) angle is 166.10(19)° and is bent away from the *cis* imido ligands. The bending of the ligands in the *cis* positions to the imido ligands has been previously observed in $W(NPh)_2Cl_2(bipy)$,[105] $W(NPh)(N^tBu)Cl_2(bipy)$,[79] $Mo(Nada)(NC_6F_5)Cl_2(dme)$,[82] $Mo(NAr)(N^tBu)Cl_2(dme)$[83] and $[Re(NAr')_2Cl_3(Me)]^-$.[63] The orientation of the aryl ring of the mixed bis(imido) complexes is approximately orthogonal to the MN_2 plane.[79,82,83] This is thought to arise by competition between the 2 *cis* multiply-bonded ligands for metal-ligand π-bonds (see bonding page 61). This preferred orientation may not be observed if the 2 imido ligands are both aryl groups. The structure of $Re(NAr')_2Cl_3(py)$ shows that the aryl rings are some way off from being orthogonal to the ReN_2 plane. The aryl rings of the complexes $W(NPh)_2Cl_2(bipy)$[105] and $[Re(NAr')_2Cl_3(Me)][Ar'NH_3]$[63] compare well with those of $Re(NAr')_2Cl_3(py)$.

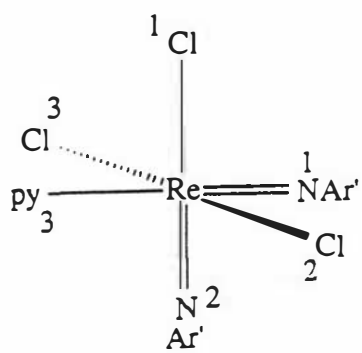

Re-N(1)-C	171.8(12)	Re-Cl(1)	2.456(5)
Re-N(2)-C	174.4(13)	Re-Cl(2)	2.358(5)
N(1)-Re-N(2)	106.2(7)	Re-Cl(3)	2.357(5)
N(1)-Re-N	171.6(6)	Re-N(1)	1.734(18)
N(2)-Re-Cl(1)	164.8(5)	Re-N(2)	1.760(14)
N(2)-Re-Cl(3)	94.4(4)	Re-N	2.305(14)
Cl(2)-Re-Cl(3)	166.10(19)		

Table 14: Selected bond angles(°) and lengths(Å) for $Re(NAr')_2Cl_3(py)$

Synthesis of amido complexes

The amido tris(imido) complexes are synthesized at –36°C with slow addition of LiNH*p*-tol to the chloro tris(imido) complex (Scheme 18).

$$ClRe(NR)(NR')(NR'') + LiNHp\text{-tol} \longrightarrow p\text{-tolNHRe}(NR)(NR')(NR'')$$

R	R'	R''	Complex
Ar	Ar	Ar	p-tolNHRe$(NAr)_3$
Ar	Ar	o-^{t}Bu	p-tolNHRe$(NAr)_2$(N-o-^{t}Bu)
Ar	Ar'	o-^{t}Bu	p-tolNHRe(NAr)(NAr')(N-o-^{t}Bu)

Scheme 18

X-ray Structure of p-tolNHRe$(NAr)_3$

Crystals of Re$(NAr)_3$(NHp-tol) were obtained from a concentrated hexamethyldisiloxane solution cooled to -35°C and were used to acquire the molecular structure. The final structure is shown in figure 54. Tables containing complete bond lengths and angles, atomic coordinates and equivalent isotropic displacement parameters, anisotropic displacement parameters and calculated H-atom positions are presented in appendix XII.

Tables 15 and 16 show selected bond lengths and angles for Re$(NAr)_3$(NHp-tol) and the previously structurally characterized amidotris(imido) complex, [Cr$(Nmes)_3$(NHmes)][Li$(OEt_2)_2$], the amidobis(imido) complex, Cr$(NAr)_2$(NHAr)Cl and the bis(amido)bis(imido) complex, Mo$(NAr)_2(NHAr)_2$.[112] The ReN_4 geometry around the Re atom is distorted tetrahedral with essentially linear imido ligands ranging from 168.8(3) to 174.5(3)°. The Re-NH-C angle of 129.6(3)° compares well with Cr$(NAr)_2$(NHAr)Cl at 135.6(2)°, [Cr$(Nmes)_3$(NHmes)]$^-$ at an average of 129.6(3)° and Mo$(NAr)_2(NHAr)_2$ at 134.3(2) and 123.4(2)°. The Re-N distances of 1.754(3), 1.769(3) and 1.757(3)Å are typical for terminal imido ligands (see appendix III) and compare well with Mo$(NAr)_2(NHAr)_2$ at 1.764(2) and 1.753(2)Å, but are larger than those found for Cr$(NAr)_2$(NHAr)Cl and [Cr$(Nmes)_3$(NHmes)]$^-$ (Table 16).[99,103]

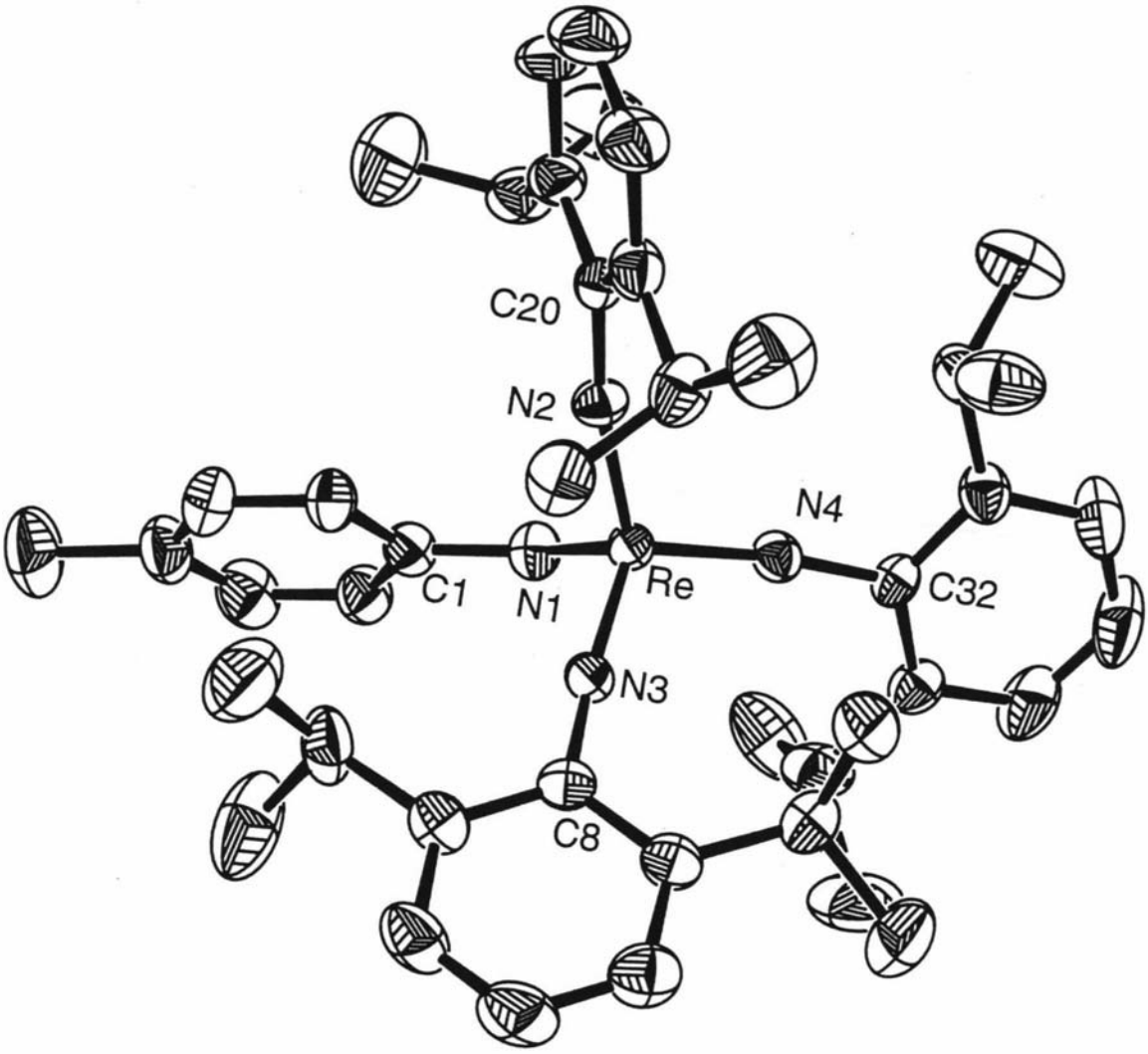

Figure 54

Complex	#	X-M-N(#)	M-N(#)-C	N(1)-M-N(#)	Ref	Comments
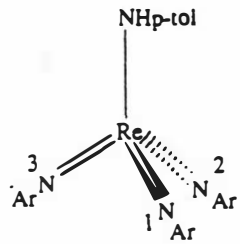	1	100.35(14)	168.8(3)		-	N(2)-Re-N(3)
	2	107.15(14)	169.8(3)	114.01(15)		112.48(15)
	3	108.12(14)	174.5(3)	113.63(15)		Re-N(4)-C
						129.6(3)
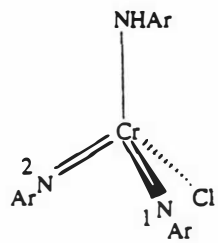	1	108.73(12)	157.3(2)		99	Distorted
	2	105.34(13)	172.7(2)	114.69(13)		tetrahedral
						Cr-N(3)-C
						135.6(2)
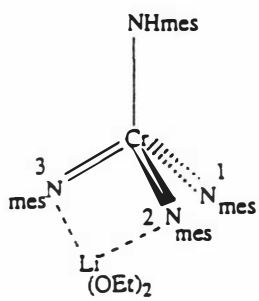	1	103.0(2)	165.6(3)		103	Distorted tetra.
		103.5(2)	174.2(3)			N(2)-Cr-N(3)
	2	105.3(2)	149.9(3)	118.2(2)		103.9(2)
		106.7(2)	137.8(3)	115.8(2)		104.0(2)
	3	110.5(2)	132.0(3)	115.6(2)		Cr-N(4)-C
		110.3(2)	146.5(3)	116.2(2)		132.4(3)
						126.8(3)
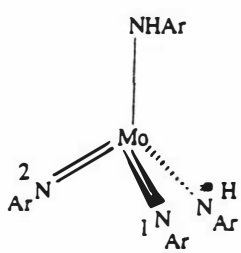	1	110.3(1)	155.7(3)		112	Mo-NH-C
		106.1(1)*				134.3(2)
	2	105.4(1)	172.3(3)	114.4(1)		Mo-NH*-C
		105.4(1)				123.4(2)
						Tetrahedral

Table 15: Selected bond angles for $Re(NAr)_3(NHp\text{-tol})$, $[Cr(Nmes)_3(NHmes)]^-$, $Cr(NAr)_2(NHAr)Cl$ and $Mo(NAr)_2(NHAr)_2$

Complex	M-N	M-N(1)	M-N(2)	M-N(3)	Ref.	Comments
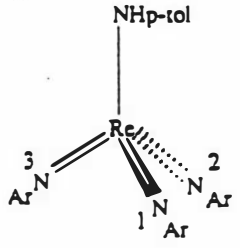	1.969(3)	1.754(3)	1.769(3)	1.757(3)	-	
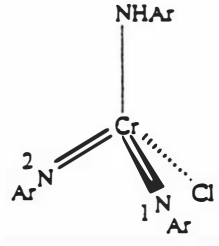	1.843(3)	1.657(3)	1.651(3)		99	Distorted tetrahedral Cr-Cl 2.2287(10)
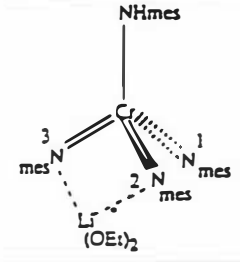	1.933(4) 1.927(3)	1.669(3) 1.654(3)	1.711(3) 1.745(3)	1.756(3) 1.735(3)	103	Two independent molecules
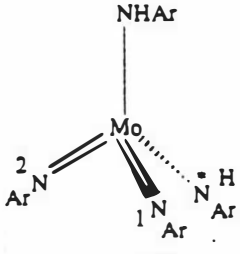	1.987(2) 1.975(2)*	1.764(2)	1.753(2)		112	

Table 16: Selected bond lengths(Å) for $Re(NAr)_3(NHp\text{-tol})$, $[Cr(Nmes)_3(NHmes)]^-$, $Cr(NAr)_2(NHAr)Cl$ and $Mo(NAr)_2(NHAr)_2$

Conclusions

Replacement of the chloro ligand of Re(VII) tris(imido) complexes was achieved using Grignard reagents to form alkyl and aryl complexes or with $LiNHp$-tol to form amido complexes. The use of Grignard reagents to displace Cl^- from the tris(imido) complex $Re(NAr)_2(NAr')Cl$ is a first. The p-tol$Re(NAr)_2(NAr')$ complex

was hydrolysed to a bridging oxo dimer during recrystallization, presumably due to the presence of water in the recrystallization solvent.

The use of pyHCl allowed the synthesis a mixed bis(imido) complex and illustrated that loss of NAr' is preferred over NAr. There are only two other mixed bis(arylimido) complexes known, W(NPh)(N-*p*-tol)Cl_2(bipy)[79] and $(Cp^*)_2$U(NPh)(N-*p*-tol).[59]

The structure of MeRe$(NAr)_2(NAr')$ is comparable to MeRe$(NAr)_3$ and MeTc$(NAr)_3$ despite the presence of an imido ligand containing a different functionality. The presence of the two NAr imido ligands appears to determine the structure regardless if the third imido ligand is NAr or NAr'.

The difference of the Re-O(bridging) length may give an indication of the geometry about the rhenium atom in complexes of the type, $[Re(NR)_2(R')(\mu\text{-}O)]_2$ and $[Re(NR)(O)(R')(\mu\text{-}O)]_2$ where R', R= alkyl or aryl groups. High values i.e. >0.2 may indicate a distorted trigonal bipyramidal structure, while values <0.2 maybe distorted square pyramidal.

The structure of $Re(NAr')_2Cl_3(py)$ showed similar features to other known octahedral bis(imido) complexes. Re(NH*p*-tol)$(NAr)_3$ represents the only fully structurally characterized amido tris(imido) rhenium complex but is comparable to $[Cr(NHmes)(Nmes)_3][Li(OEt_2)_2]$.[103]

Experimental Section

General

General experimental procedures and details regarding the instrumentation used are given in appendix I. ^{1}H NMR were recorded in d_6-benzene and referenced to benzene at 7.15ppm. ^{13}C NMR were recorded in d_6-benzene and referenced to benzene at 128ppm. Deuterated benzene was purchased from Acros and freeze pumped thawed 3 times before use. Toluene and THF was distilled from sodium/benzophenone. MeMgBr, *p*-tolMgBr and $PhCH_2MgCl$ were purchased from Aldrich and came in 3.0M, 1.0M and 1.0M in Et_2O respectively. LiNH*p*-tol is synthesized from *p*-tolNH_2 and neat ^{n}BuLi in benzene.

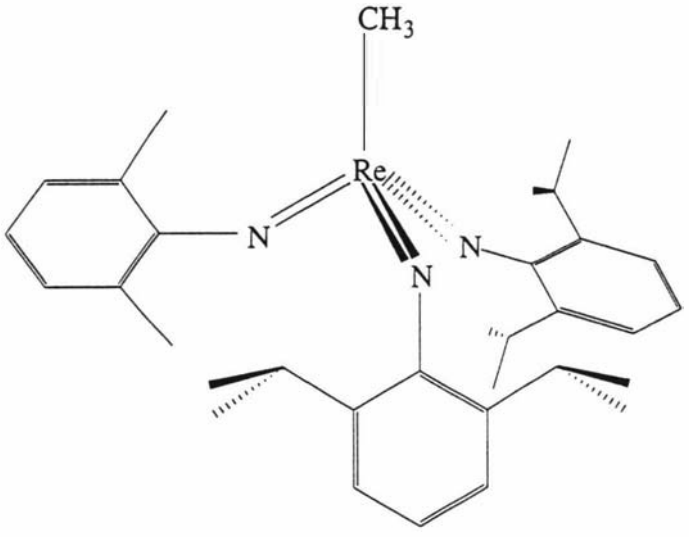

$CH_3Re(NAr)_2(NAr')$

A solution of $ClRe(NAr)_2(NAr')$ (0.137g, 0.20mmol) and MeMgBr (3.0M in diethyl ether, 0.068g, 0.20mmol) in THF was stirred overnight. The reaction mixture was reduced to dryness *in vacuo* and hexane (6mL) was then added. The resulting suspension was filtered through celite, which was then washed with hexane (2x5mL). The filtrates were pumped to dryness, yielding 0.082g (62%) of a red solid.

^1H NMR (C_6D_6) : 7.11(d, 4, J=7.1, Ar), 7.02(t, 2, J=7.1, Ar), 6.96(d, 2, J=7.1, Ar'), 6.81(t, 1, J=7.1, Ar'), 3.82(sept, 4, J=6.8, C<u>H</u>Me_2), 2.68(s, 3, C<u>H</u>$_3$), 2.29(s, 6, Ar'C<u>H</u>$_3$), 1.08(d, 24, J=7.0, CHC<u>H</u>$_3$).

$^{13}C\{^1H\}$ NMR (C_6D_6) : 156.2(Ar), 152.9(Ar'), 141.9(Ar), 141.7(Ar'), 129.5(Ar), 125.6(Ar'), 123.1(Ar), 122.8(Ar'), 28.8(<u>C</u>HCH$_3$), 23.1(CH<u>C</u>H$_3$), 18.6(Ar'<u>C</u>H$_3$), 7.6(Re<u>C</u>H$_3$).

Found: C, 59.47 ; H, 6.72 ; N, 6.06
Calc: C, 59.07 ; H, 6.91 ; N, 6.26

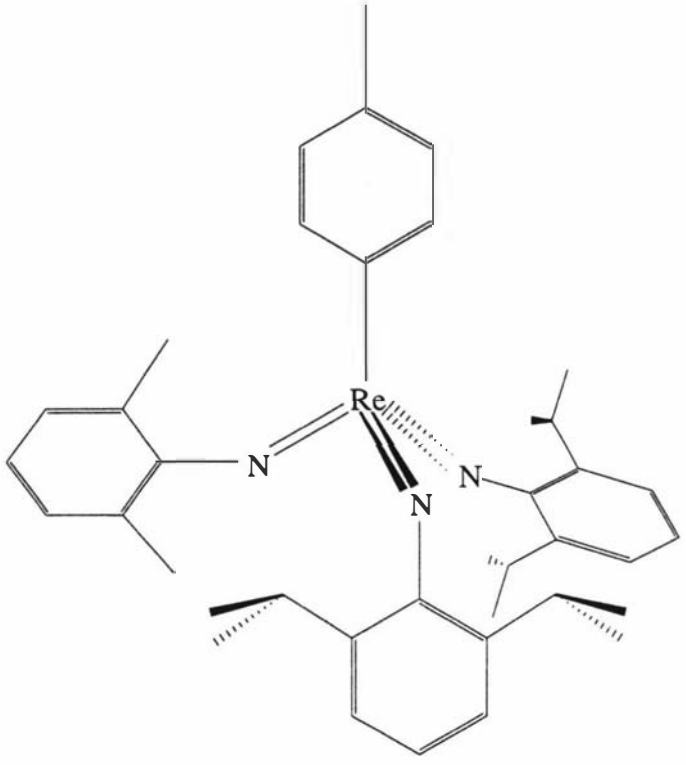

p-tolRe(NAr)$_2$(NAr')

A solution of ClRe(NAr)$_2$(NAr') (0.200g, 0.29mmol) and *p*-tolMgBr (1.0M in diethyl ether, 0.250g, 0.29mmol) in THF was stirred overnight. The reaction mixture was reduced to dryness *in vacuo* and hexane (6mL) was then added. The resulting suspension was filtered through celite, which was then washed with hexane (2x5mL). The filtrates were pumped to dryness, yielding 0.142g (65%) of a red solid.

^{1}H NMR (C_6D_6) : 7.09(d, 4, J=7.1, Ar), 7.02(t, 2, J=7.1, Ar), 7.00(d, 4, J=6.9, $CH_3\underline{C}_6H_4$), 6.98(d, 2, J=7.1, Ar'), 6.79(t, 1, J=7.1, Ar'), 3.86(sept, 4, J=6.8, $C\underline{H}Me_2$), 2.32(s, 6, Ar'$C\underline{H}_3$), 2.01(s, 3, $C_6H_4C\underline{H}_3$), 1.07(d, 24, J=7.0, $CHC\underline{H}_3$).

^{13}C{^{1}H} NMR (C_6D_6) : 152.6(Ar), 152.5(Ar'), 143.8(Ar), 143.0(Ar'), 141.9($\underline{C}_6H_4CH_3$), 140.5($\underline{C}_6H_4CH_3$), 129.3(Ar), 127.0($\underline{C}_6H_4CH_3$), 126.2(Ar'), 125.2($\underline{C}_6H_4CH_3$), 122.0(Ar), 121.9(Ar'), 28.2($\underline{C}HCH_3$), 24.1($CH\underline{C}H_3$), 22.0($C_6H_4\underline{C}H_3$), 18.4($\underline{C}H_3$).

Found: C, 62.10 ; H, 6.88 ; N, 5.51
Calc: C, 62.70 ; H, 6.75 ; N, 5.62

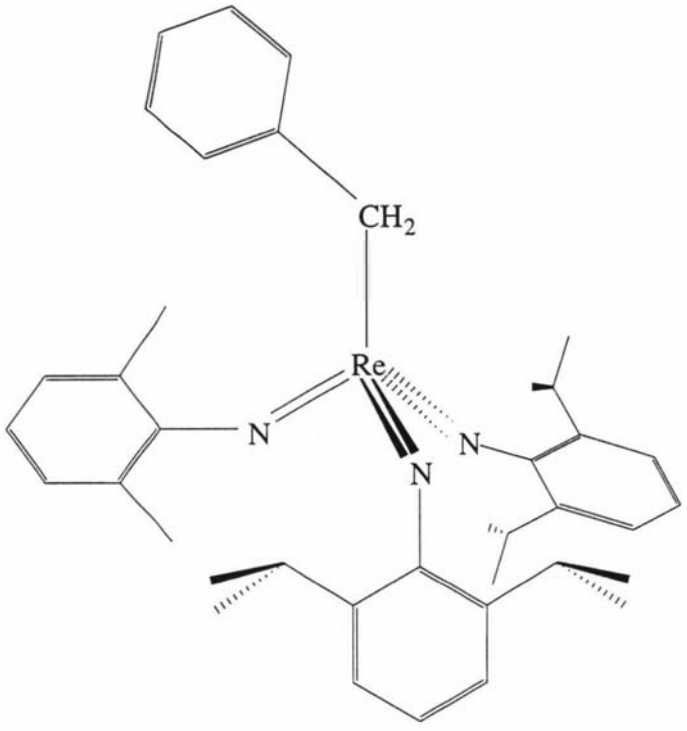

$PhCH_2Re(NAr)_2(NAr')$

A solution of $ClRe(NAr)_2(NAr')$ (0.152g, 0.22mmol) and $PhCH_2MgCl$ (1.0M in diethyl ether, 0.175g, 0.22mmol) in THF was stirred overnight. The reaction mixture was reduced to dryness *in vacuo* and hexane (6mL) was then added. The resulting suspension was filtered through celite, which was then washed with hexane (2x5mL). The filtrates were pumped to dryness, yielding 0.090g (55%) of a red solid.

^1H NMR (C_6D_6) : 7.10-6.96(m, 11, Ar/Ph), 6.92(d, 2, J=7.1, Ar'), 6.79(t, 1, J=7.1, Ar'), 4.91(s, 2, $PhC\underline{H}_2$), 3.62(sept, 4, J=6.8, $C\underline{H}Me_2$), 2.21(s, 6, $Ar'C\underline{H}_3$), 1.05(d, 24, J=7.0, $CHC\underline{H}_3$).

Found: C, 63.68 ; H, 7.04 ; N, 4.94
Calc: C, 62.70 ; H, 6.75 ; N, 5.62

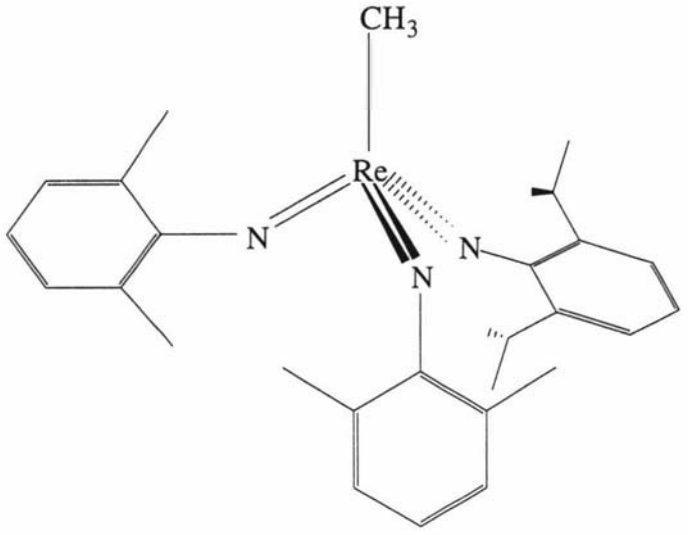

$CH_3Re(NAr')_2(NAr)$

A solution of $ClRe(NAr')_2(NAr)$ (0.145g, 0.23mmol) and MeMgBr (3.0M in diethyl ether, 0.078g, 0.23mmol) in THF was stirred overnight. The reaction mixture was reduced to dryness *in vacuo* and hexane (6mL) was then added. The resulting suspension was filtered through celite, which was then washed with hexane (2x5mL). The filtrates were pumped to dryness, yielding 0.083g (59%) of a red solid.

^1H NMR (C_6D_6) : 7.10(d, 2, J=7.1, Ar), 7.00(t, 1, J=7.1, Ar), 6.92(d, 4, J=7.1, Ar'), 6.79(t, 2, J=7.1, Ar'), 3.71(sept, 2, J=6.8, C<u>H</u>Me_2), 2.59(s, 3, C<u>H</u>$_3$), 2.26(s, 12, Ar'C<u>H</u>$_3$), 1.07(d, 12, J=7.0, CHC<u>H</u>$_3$).

$^{13}C\{^1H\}$ NMR (C_6D_6) : 155.8(Ar), 152.7(Ar'), 141.6(Ar), 141.3(Ar'), 129.8(Ar), 125.1(Ar'), 122.8(Ar), 122.4(Ar'), 27.9(<u>C</u>HCH_3), 22.8(CH<u>C</u>H$_3$), 18.9(Ar'<u>C</u>H$_3$), 7.2(Re<u>C</u>H$_3$).

Found: C, 57.18 ; H, 6.04 ; N, 6.42
Calc: C, 56.65 ; H, 6.23 ; N, 6.83

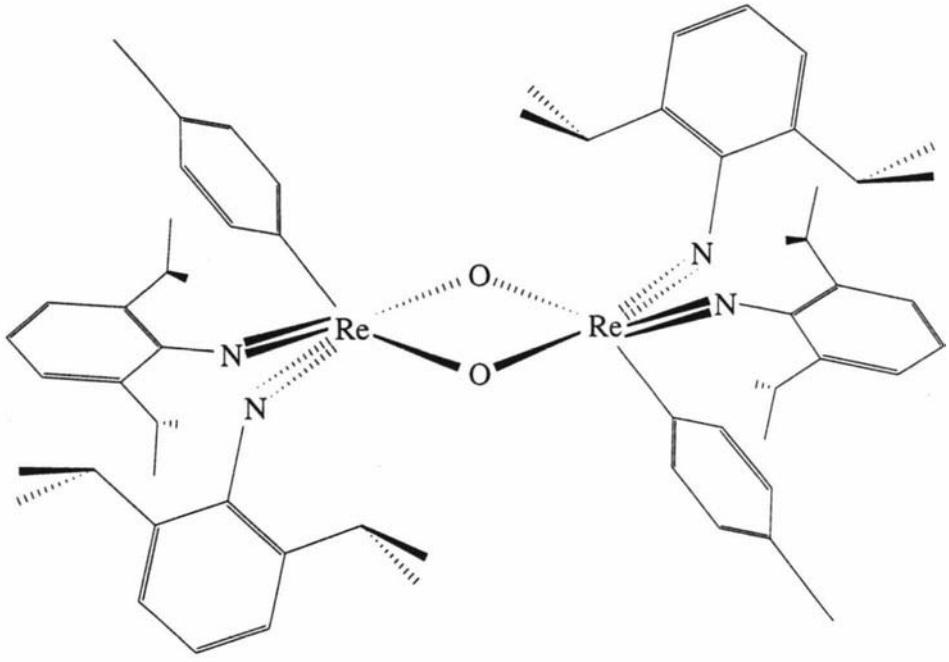

$[Re(NAr)_2(p\text{-tol})(\mu\text{-}O)]_2$

Obtained from *p*-tolRe(NAr)$_2$(NAr') when recrystallized from wet hexamethyldisiloxane.

^{1}H NMR (C_6D_6) : 7.12(d, 8, J=7.1, Ar), 7.02(t, 4, J=7.1, Ar), 6.98(d, 8, J=7.1, $C_6\underline{H}_4CH_3$), 3.63(sept, 8, J=6.8, C$\underline{H}$Me$_2$), 1.88(s, 6, $C_6H_4C\underline{H}_3$), 1.06(d, 48, J=7.0, CHC$\underline{H}_3$).

Mass Spect: M^+ 1288

Found: C, 57.62 ; H, 6.29 ; N, 4.68
Calc: C, 57.83 ; H, 6.42 ; N, 4.35

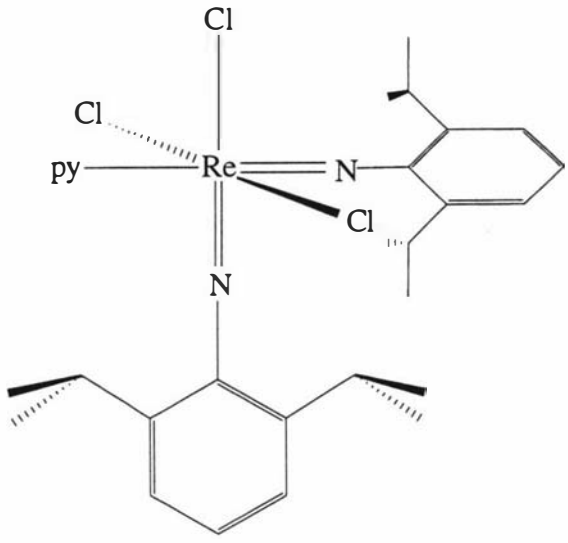

Procedure 1:

$Re(NAr)_2Cl_3(py)$

A solution of $Re(NAr)_3Cl$ (0.160g, 0.21mmol) in THF (5mL) was added to a suspension of pyHCl (0.049g, 0.42mmol) and THF (5mL). The solution was stirred for one hour. The now green solution was filtered to remove any unreacted pyHCl. The filtrate was reduced *in vacuo* and hexane (5mL) was then added. The resulting suspension was filtered and washed thoroughly with pentane to give 0.054g (36%) of a green solid.

^1H NMR (C_6D_6): 9.38(d, 2, py Ho), 7.68(t, 1, py Hp), 7.40(t, 2, py Hm), 6.62(d, 4, imido Hm), 6.35(t, 2, imido Hp), 4.46 and 3.68(v.br, 4, $C\underline{H}Me_2$), 1.08(br, 24, $CHC\underline{H}_3$)

Found: C, 48.72 ; H, 5.62 ; N, 6.04
Calc: C, 48.23 ; H, 5.44 ; N, 5.82

Procedure 2:

$Re(NAr)_2Cl_3(py)$

A solution of $Re(NAr')(NAr)_2Cl$ (0.150g, 0.22mmol) in THF (5mL) was added to a suspension of pyHCl (0.051g, 0.44mmol) and THF (5mL). The solution was stirred for one hour. The now green solution was filtered to remove any unreacted pyHCl. The filtrate was reduced *in vacuo* and hexane (5mL) was then added. The resulting suspension was filtered and washed thoroughly with pentane to give 0.111g (70%) of a green solid.

Found: C, 48.51 ; H, 5.71 ; N, 5.74
Calc: C, 48.23 ; H, 5.44 ; N, 5.82

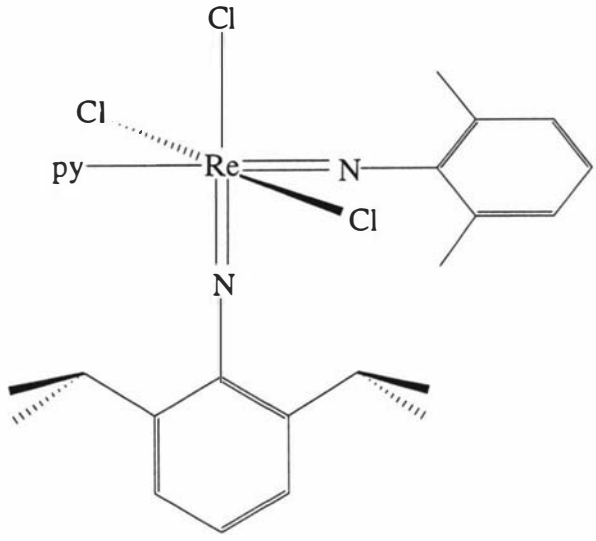

$Re(NAr)(NAr')Cl_3(py)$

A solution of $Re(NAr')_2(NAr)Cl$ (0.170g, 0.27mmol) in THF (5mL) was added to a suspension of pyHCl (0.062g, 0.54mmol) and THF (5mL). The solution was stirred for one hour. The now green solution was filtered to remove any unreacted pyHCl. The filtrate was reduced *in vacuo* and hexane (5mL) was then added. The resulting suspension was filtered and washed thoroughly with pentane to give 0.090g (50%) of a green solid.

^1H NMR (C_6D_6): 9.39(d, 2, py Ho), 7.94(t, 1, py Hp), 7.45(t, 2, py Hm), 6.81(m, 4, imido Hm), 6.52(t, 2, imido Hp), 4.62(br, 2, $C\underline{H}Me_2$), 2.94 and 2.51(each v.br, 6, $C\underline{H}_3$), 1.06(br, 12, $CHC\underline{H}_3$)

Found: C, 44.22 ; H, 5.57 ; N, 6.45
Calc: C, 45.08 ; H, 4.69 ; N, 6.31

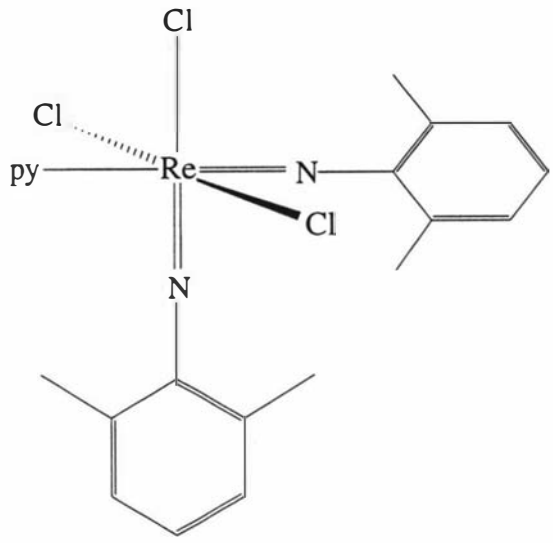

$Re(NAr')_2Cl_3(py)$

A solution of $Me_3SiORe(NAr')_3$ (0.150g, 0.24mmol) in THF (5mL) was added to a suspension of pyHCl (0.056g, 0.48mmol) and THF (5mL). The solution was stirred for one hour. The now green solution was filtered to remove any unreacted pyHCl. The filtrate was reduced *in vacuo* and hexane (5mL) was then added. The resulting suspension was filtered and washed thoroughly with pentane to give 0.112g (76%) of a green solid.

^1H NMR (C_6D_6): 9.28(d, 2, py Ho), 7.79(t, 1, py Hp), 7.42(t, 2, py Hm), 6.72(d, 4, imido Hm), 6.45(t, 2, imido Hp), 2.77 and 2.32(v.br, 12, Ar'C$\underline{H}_3$)

Found: C, 41.68 ; H, 3.49 ; N, 6.90
Calc: C, 41.35 ; H, 3.80 ; N, 6.89

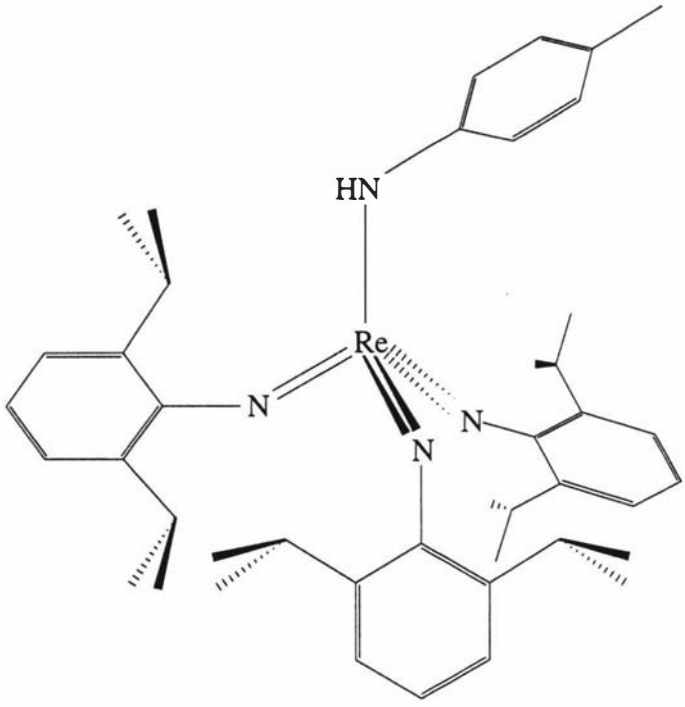

p-tolNHRe(NAr)$_3$

To Re(NAr)$_3$Cl (0.200g, 0.27mmol) in toluene (10mL) precooled to -36°C was slowly added to a solution of *p*-tolNHLi (0.033g, 0.29mmol) in toluene (10mL) also pre-cooled to -36°C. The solution was stirred for 8 hours at room temperature then reduced to dryness *in vacuo*. The residue was extracted into hexane (6mL), the extracts filtered through celite and cooled to -36°C resulting in 0.066g (30%) of a red solid.

^{1}H NMR (C_6D_6) : 7.03(d, 6, J=7.1, Ar), 7.01(s, 1, NH), 6.93(t, 3, J=7.1, Ar), 3.63(sept, 6, J=6.8, C<u>H</u>Me$_2$), 1.06(d, 36, J=7.0, CHC<u>H</u>$_3$).

Found: C, 62.12 ; H, 7.72 ; N, 6.90
Calc: C, 63.13 ; H, 7.27 ; N, 6.85

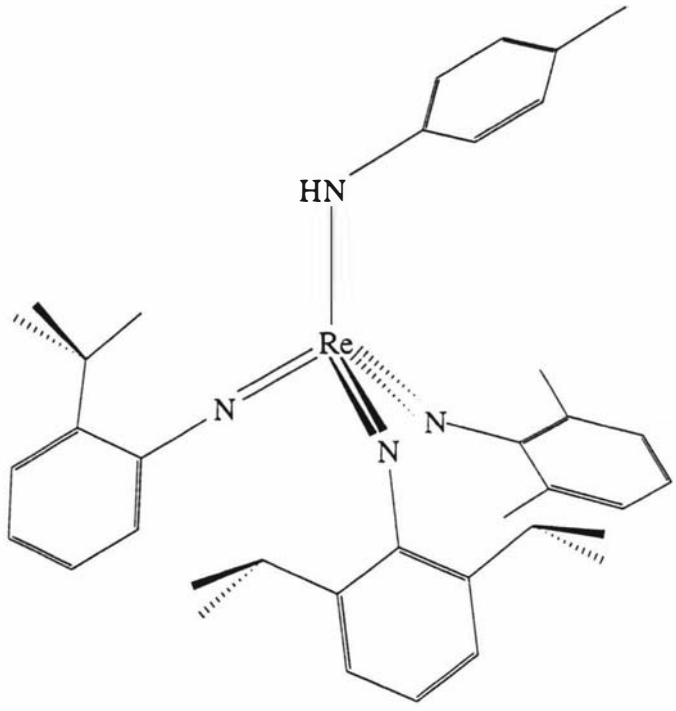

p-tolNHRe(NAr)(NAr')(N-*o*-^{t}Bu)

To Re(NAr)(NAr')(N-*o*-^{t}Bu)Cl (0.090g, 0.14mmol) in toluene (10mL) precooled to -36°C was slowly added to a solution of *p*-tolNHLi (0.018g, 0.16mmol) in toluene (10mL) also pre-cooled to -36°C. The solution was stirred for 8 hours at room temperature then reduced to dryness *in vacuo*. The residue was extracted into hexane (4mL), the extracts filtered through celite and cooled to -36°C resulting in 0.039g (38%) of a red solid.

^{1}H NMR (C_6D_6) : 7.19(d, 1, J=7.2, *t*-butyl), 7.03(d, 2, J=7.0, Ar), 7.01(s, 1, NH), 6.60-6.95(m, 7, Ar/*t*-butyl), 3.74(sept, 2, J=6.8, C$\underline{H}$Me$_2$), 2.24(s, 6, $\underline{C}H_3$), 1.45(s, 9, *t*-butyl), 1.02(d, 12, J=7.0, CHC$\underline{H}_3$)

Found: C, 59.43 ; H, 6.96 ; N, 7.93
Calc: C, 60.55 ; H, 6.45 ; N, 7.63

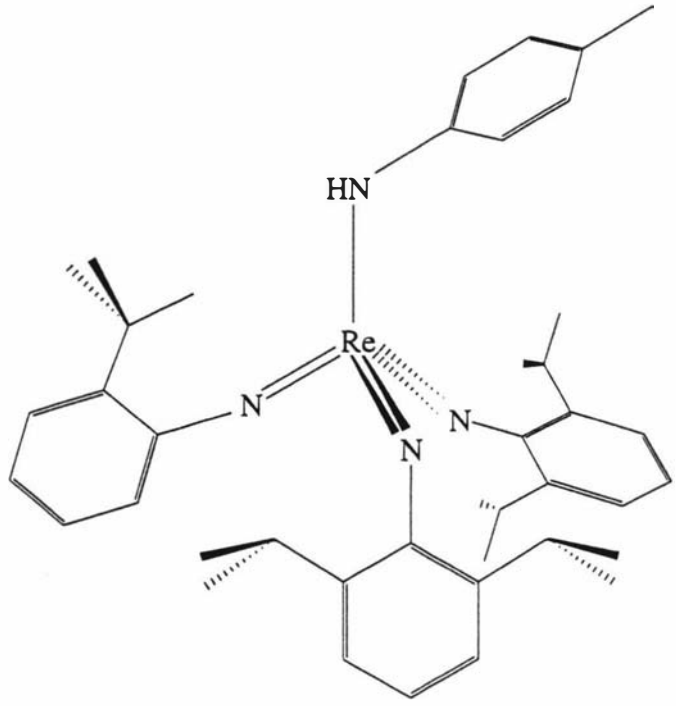

p-tolNHRe(NAr)$_2$(N-*o*-^{t}Bu)

To Re(NAr)$_2$(N-*o*-^{t}Bu)Cl (0.150g, 0.21mmol) in toluene (10mL) precooled to -36°C was slowly added to a solution of *p*-tolNHLi (0.024g, 0.21mmol) in toluene (10mL) also pre-cooled to -36°C. The solution was stirred for 8 hours at room temperature then reduced to dryness *in vacuo*. The residue was extracted into hexane (5mL), the extracts filtered through celite and cooled to -36°C resulting in 0.070g (42%) of a red solid.

^{1}H NMR (C_6D_6); 7.17 (d, 1, J=7.2, *o*-*t*-butylphenyl), 7.02 (d, 4, J=7.0, Ar), 7.00(s, 1, NH), 6.65-6.95 (m, 5, Ar/*o*-*t*-butylphenyl), 3.70 (sept, 4, J=6.8, C<u>H</u>Me$_2$), 1.45 (s, 9, *t*-butyl), 1.06 (d, 24, J=7.0, CHC<u>H</u>$_3$).

Found: C, 61.43 ; H, 7.72 ; N, 7.15
Calc: C, 62.33 ; H, 7.02 ; N, 7.09

Chapter Four

Synthesis and Reactivity of Re(V) Complexes

Introduction

This chapter describes the synthesis of trigonal planar rhenium(V) tris(imido) complexes. The methodology developed involves the use of elemental sodium to reduce tetrahedral Re(VII) tris(imido) complexes to the anionic Re(V) species. Also the reactivity of the anionic complexes towards $ClSnMe_3$ and $ClAuPPh_3$ is presented.

The reaction of d^0 M(VII) tris(imido) complexes with either excess sodium metal or sodium amalgam has lead to the formation of d^1-d^1 M(VI) dimers. For example reduction of $Me_3SiORe(N^tBu)_3$ with 22 equivalents of sodium in an amalgam forms an edge-bridged dimeric complex.[30] An improved synthesis of $[Re(N^tBu)_2(\mu\text{-}N^tBu)]_2$ used 2.5 equivalents of sodium amalgam and $IRe(N^tBu)_3$.[67] However reaction of $Re(NAr)_3Cl$ with 2 equivalents of sodium in an amalgam leads not to the d^1 Re dimer but to a d^2 Re tris(imido) anion.[12] Likewise the technetium anion, $[Tc(NAr)_3]^-$, is formed from 2 equivalents of sodium and the iodo complex, $ITc(NAr)_3$.[17] Interestingly the $[Tc(NAr')_3]^-$ and $[Re(NAr')_3]^-$ anions have never been prepared. Treatment of $ITc(NAr')_3$ with 2 equiv. of sodium leads to uncharacterized products[17] and reduction of $Re(NAr')_3Cl$ using sodium amalgam results in the formation of $[Re(NAr')_2(\mu\text{-}NAr')]_2$, which does not undergo further reduction.[73]

The anionic complex, $[Re(NAr)_3]^-$, was shown to be a good nucleophile reacting with a number of electrophiles.[12] However the reaction of the anion towards $ClSnMe_3$ and $ClAuPPh_3$ has not been explored. The only example of such reactions is the formation of the Tc-Au complex, $(ArN)_3TcAuPPh_3$, made from the anion, $[Tc(NAr)_3]^-$ and $ClAuPPh_3$.[17]

Synthesis from reduction of Re(VII) Complexes

The only synthesis of a d^2 rhenium tris(imido) complex was illustrated in 1993 by Williams and Schrock.[12] They reacted $Re(NAr)_3Cl$ with 2 equivalents of sodium

amalgam (Equation 73). It is believed that the counter ion is $Na(thf)_2^+$. Other salts, $[NEt_4][Re(NAr)_3]$ and $[PPN][Re(NAr)_3]$ have been prepared from $[Re(NAr)_3]^-$ by adding the appropiate salt to the reaction mixture in which $[Re(NAr)_3]^-$ is formed.[12]

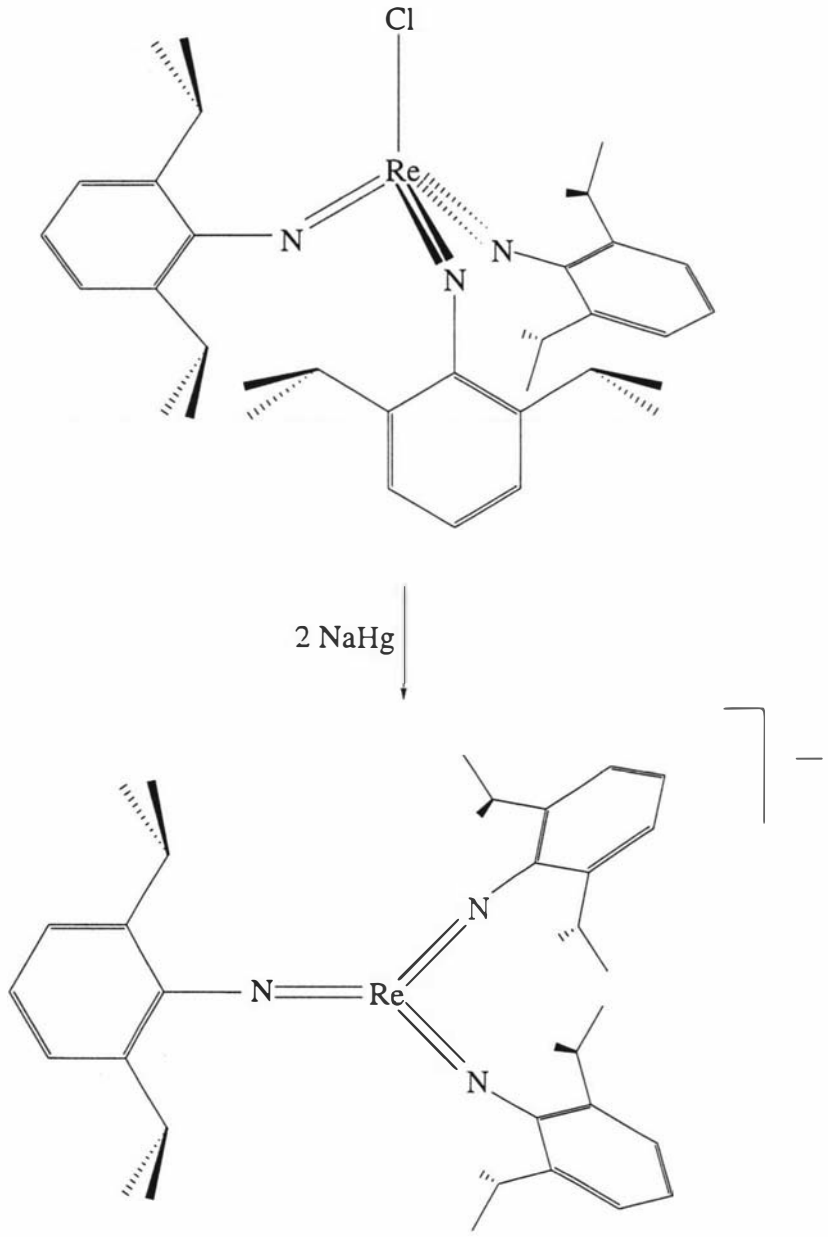

Equation 73

The X-ray structure of $[Re(NAr)_3][PPN]$ showed it to be trigonal planar (as expected for d^2 tris(imido) species, see page 8) where the rhenium is only 0.029Å out of the plane of the imido nitrogen atoms. The mechanism of anion formation is

of anion formation is proposed to occur via 2 possible pathways based on the results of cyclic voltammogram experiments on $Re(NAr)_3Cl$.[12]

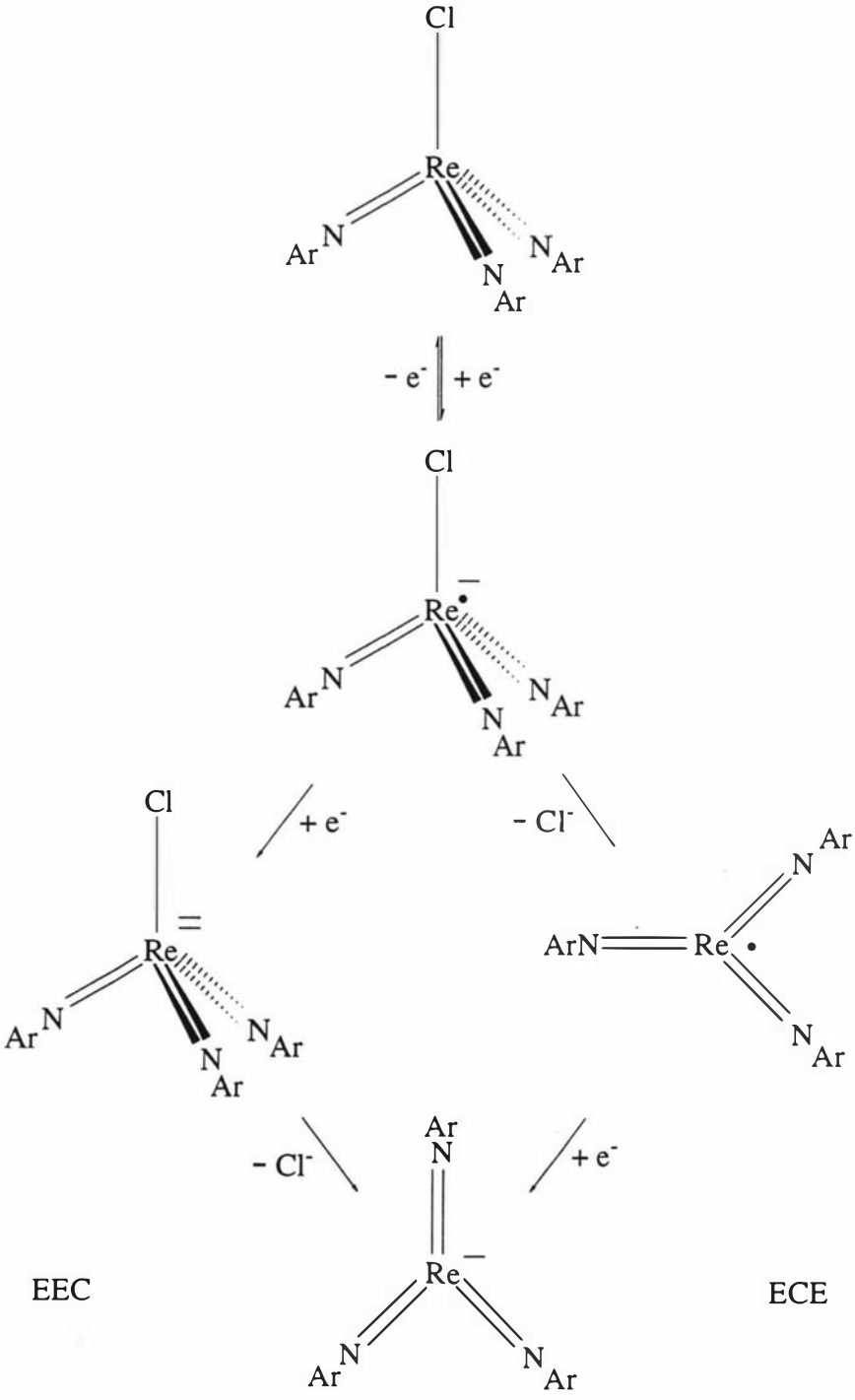

Scheme 19

Schrock *et al.* propose that $[Re(NAr)_3]^{-\bullet}$ is formed, loses Cl^- to give $[Re(NAr)_3]\bullet$,which is immediately reduced to $[Re(NAr)_3]^-$ (an ECE mechanism), or is further reduced at a more negative potential to $[Re(NAr)_3Cl]^{2-}$, which then dissociates Cl^- and forms $[Re(NAr)_3]^-$ (an EEC mechanism) (Scheme 19).[12]

Reactions with Au and Sn compounds

Reactions of both $[Tc(NAr)_3]^-$ and $[Re(NAr)_3]^-$ are illustrated in schemes 20 and 21.[12,17] Reactions of the anions with electrophiles are quite facile. Attempts at protonating $[Tc(NAr)_3]^-$ were unsuccessful, in contrast to rhenium.[12] The reaction of $[Tc(NAr)_3]^-$ with $ClAuPPh_3$ resulted in the first example of a complex containing a Tc-Au bond.[17]

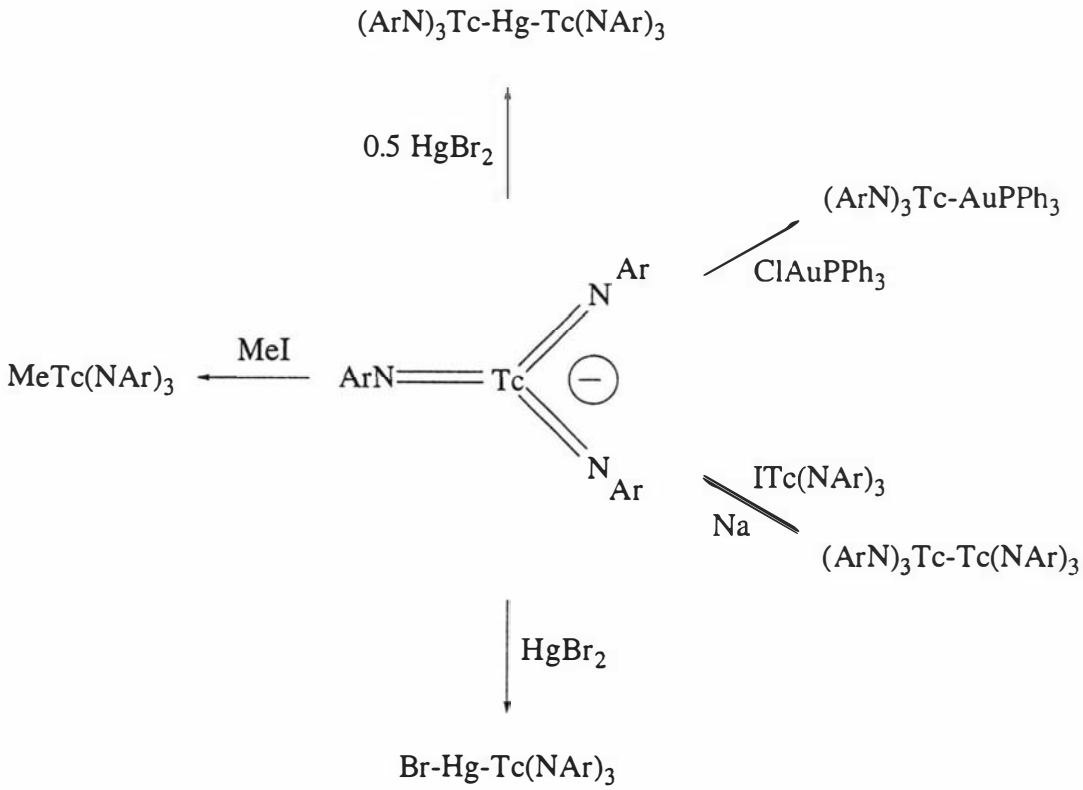

Scheme 20

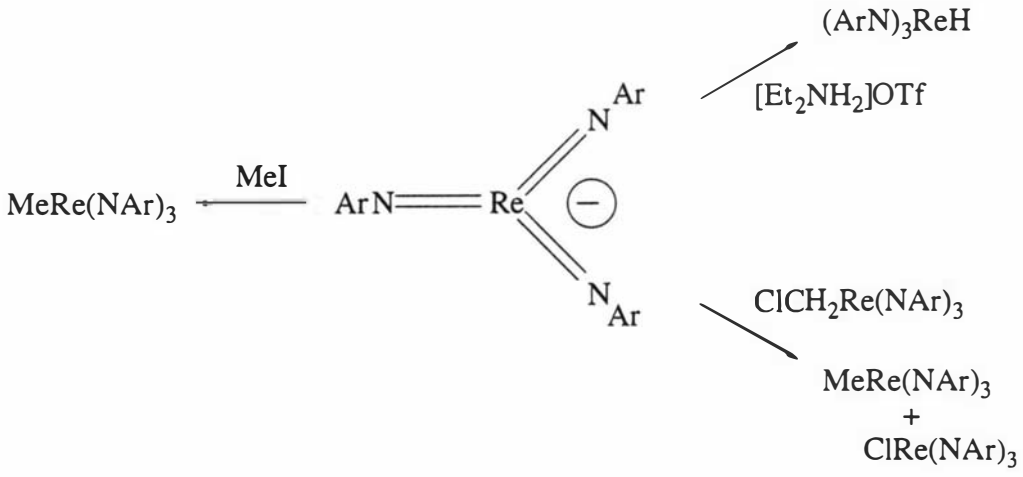

Scheme 21

Results and Discussion

Synthesis of Re(V) anions

It has been shown that the reduction of Re(VII) tris(imido) complexes to the Re(V) complexes can be achieved with elemental sodium or sodium amalgam. Given the potential for the formation of Hg-bridged species,[12,19] elemental sodium was solely employed in the reductions (Scheme 22).

$$XRe(NR)_2(NR') + 2\,Na \longrightarrow [Re(NR)_2(NR')]^-$$

X	R	R'	Complex
Me_3SiO	Ar'	Ar'	$[Re(NAr')_3]^-$
Cl	Ar	Ar	$[Re(NAr)_3]^-$
Cl	Ar	Ar'	$[Re(NAr)_2(NAr')]^-$
Cl	Ar	*o*-^{t}Bu	$[Re(NAr)_2(N\text{-}o\text{-}^t Bu)]^-$

Scheme 22

The nature of the cation is thought to be $[Na(thf)_n]^+$, in the case of $[Re(NAr)_3]^-$, it was found to be $[Na(thf)_2]^+$.[12] Isolation of the anions can be achieved, however handling these complexes results in decompostion to as yet unidentified mixture of compounds that are insoluble in benzene. As such it is very differcult to obtain proton NMR and hence the nature of the cation could not be accurately determined by NMR.

X-ray Structure of $[Re(NAr')_3][Na(thf)_6]$

The steric bulk of the aryl substituents is considered to be an important factor in the stabilization of $[Re(NAr)_3]^-$ and is a possible reason why $[Re(NAr')_3]^-$ and $[Re(N^tBu)_3]^-$ have as yet not been synthesized.[12,30,73]

However moderate yields of $[Re(NAr')_3]^-$ can be prepared with use of elemental sodium. X-ray quality crystals were obtained from thf at -35°C. The final structure is shown in Figure 55. Tables containing complete bond lengths and angles, atomic coordinate and equivalent isotropic displacement parameters, anisotropic displacement parameters and calculated H-atom positions are presented in appendix XIII.

Tables 17 and 18 show selected bond lengths and angles for three tris(imido) trigonal planar complexes. The sodium cation is surrounded by six thf molecules and is well separated from the anion. The structure of $[Re(NAr')_3]^-$ has more in common with $Os(NAr)_3$ as opposed to the analogous anion complex, $[Re(NAr)_3]^-$. All three complexes are trigonal planar, however $[Re(NAr')_3]^-$ has a 2-fold axis passes through Re, N(1), C(11) and C(14) in a similar fashion to $Os(NAr)_3$ as Figure 56 illustrates. The two crystallographically distinct imido ligands are essentially linear (Re-N(1)-C(11)=180.0°, Re-N(2)-C(21)=172.1° with bond lengths of 1.762(3)Å (Re-N(1)) and 1.772(2)Å (Re-N(2)), respectively.

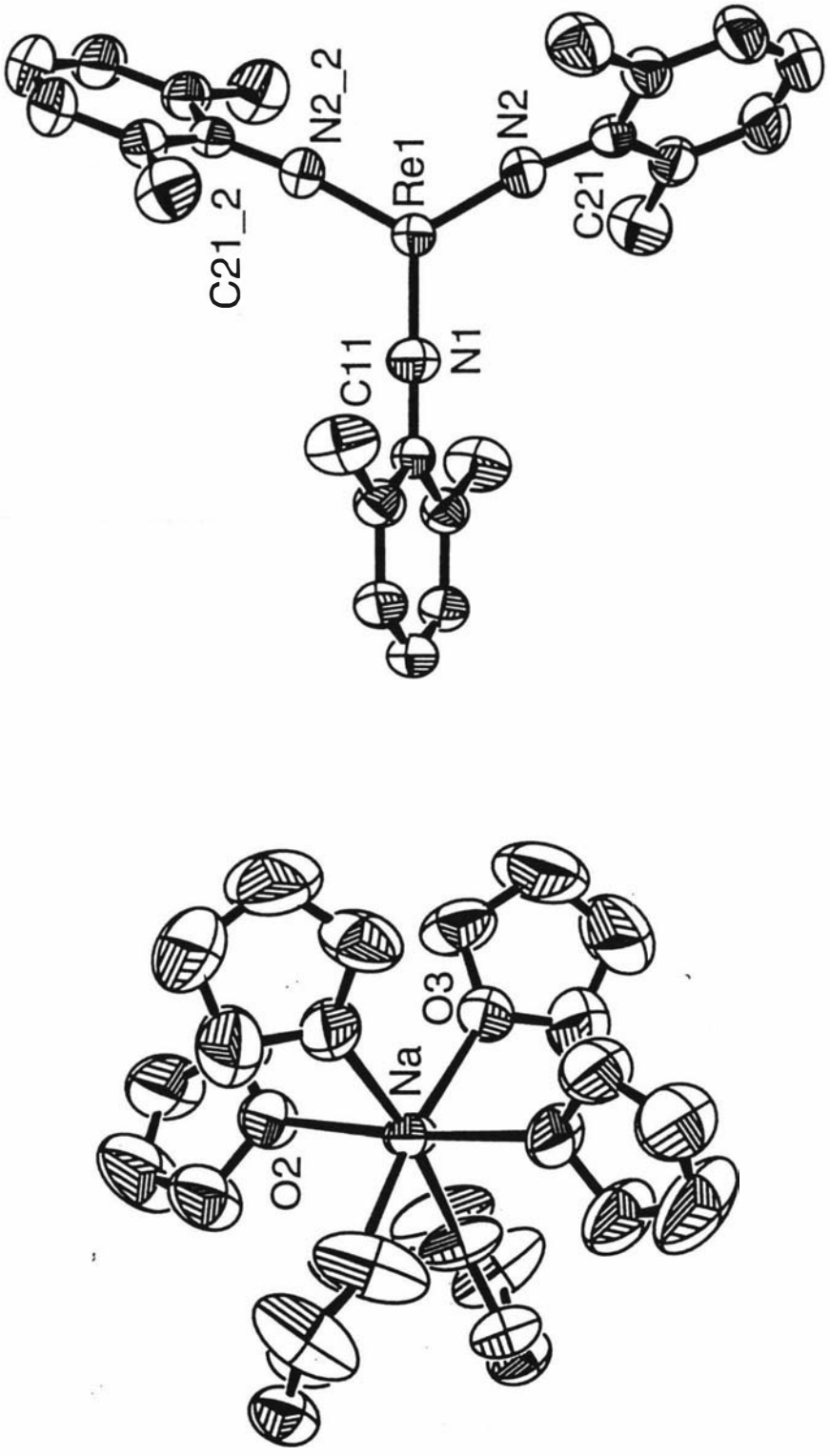

Figure 55

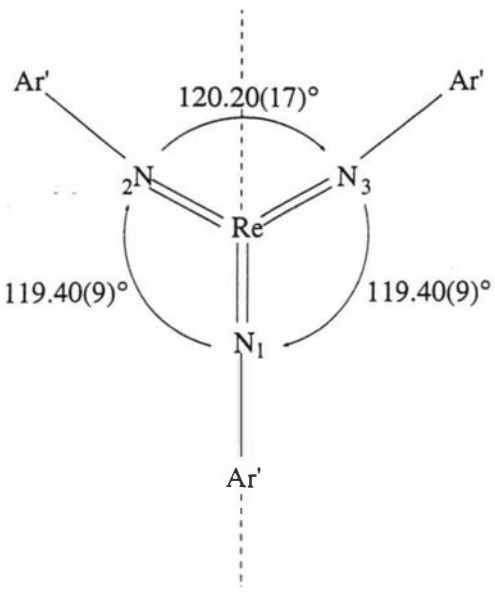

2-fold axis

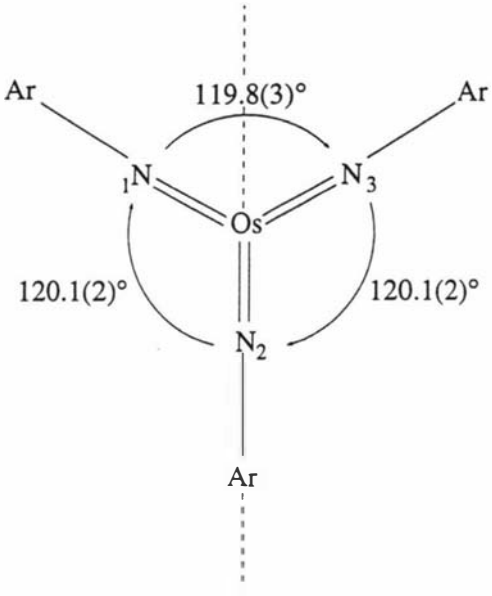

2-fold axis

Figure 56

Complex	#	M-N(#)-C	N(1)-M-N(#)	N(2)-M-N(3)	Ref.	Comments
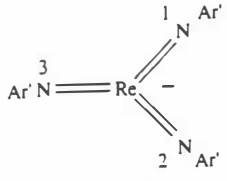	1	180.0		121.20(17)	-	
	2	172.1(2)	119.40(9)			
	3		119.40(9)			
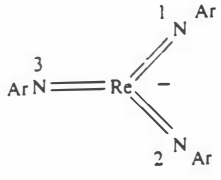	1	168.8(8)		115.8(4)	12	PPN salt, trigonal planar. Aryl rings tilted out of ReN_3 plane
	2	173.6(8)	116.1(4)			
	3	173.2(8)	128.0(4)			
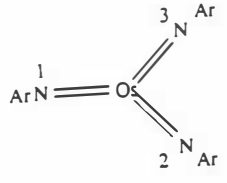	1	178.0(5)		120.1	27	Trigonal planar 2-fold axis through Os-N(2)
	2	180(3)	120.1(2)			
	3		119.8(3)			

Table 17: Selected bond angles for 3 trigonal planer complexes

Complex	M-N(1)	M-N(2)	M-N(3)	Ref.	Comments
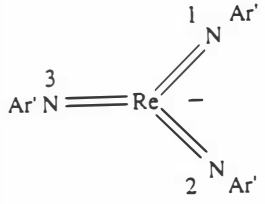	1.762(3)	1.772(2)	1.772(2)	-	
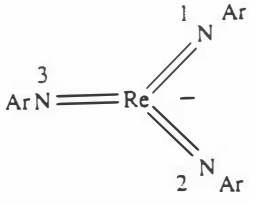	1.60(1)	1.753(8)	1.684(9)	12	PPN salt, Re is 0.029Å out of the ReN_3 plane
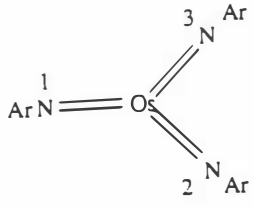	1.736(5)	1.738(7)		27	

Table 18: Selected bond lengths for 3 trigonal planar complexes

Reaction with Au and Sn Compounds

The reaction of $ClAuPPh_3$ and $[Tc(NAr)_3]^-$ was shown to form a Tc-Au complex, $(NAr)_3TcAuPPh_3$ in 89% yield.[17] Reaction of the tin compound, $ClSnMe_3$, with d^2 tris(imido) anions has not been illustrated. Both $ClAuPPh_3$ and $ClSnMe_3$ react with the anions to form Re-Au and Re-Sn complexes respectively as shown in Scheme 23.

$$XRe(NR)_2(NR') \xrightarrow[ii)\ ZCl]{i)\ Na} Z\text{-}Re(NR)_2(NR')$$

X	R	R'	Z	Complex
Me_3SiO	Ar'	Ar'	$AuPPh_3$	$Ph_3PAu\text{-}Re(NAr')_3$
Cl	Ar	Ar	$AuPPh_3$	$Ph_3PAu\text{-}Re(NAr)_3$
Cl	Ar	Ar	$SnMe_3$	$Me_3Sn\text{-}Re(NAr)_3$
Cl	Ar	Ar'	$AuPPh_3$	$Ph_3PAu\text{-}Re(NAr)_2(NAr')$
Cl	Ar	Ar'	$SnMe_3$	$Me_3Sn\text{-}Re(NAr)_2(NAr')$
Cl	Ar	*o*-^{t}Bu	$SnMe_3$	$Me_3Sn\text{-}Re(NAr)_2(N\text{-}o\text{-}^t Bu)$

Scheme 23

When a thf solution of the d^2 tris(imido) anion is added to a thf solution of PPh_3PAuCl or Me_3SnCl, an immediate reaction occurs and the colour of the mixture changes to red.

Due to the difficulties involved in the isolation of the Re(V) tris(imido) anions the formation of the Au and Sn complexes are best accomplished in two steps by first reduction of the Re(VII) tris(imido) complexes to form a reaction mixture containing the anion. Then the reaction mixture is filtered and immediately added to a solution of either the gold or tin compounds.

X-ray Structure of $(NAr)_3ReSnMe_3$ and $(NAr)_2(NAr')ReSnMe_3$

X-ray quality crystals of both tin complexes were obtained from hexane at -35°C. The final structures are shown in figures 57 and 58. Tables containing complete bond lengths and angles, atomic coordinate and equivalent isotropic displacement parameters, anisotropic displacement parameters and calculated H-atom positions are presented in appendices XIV and XV.

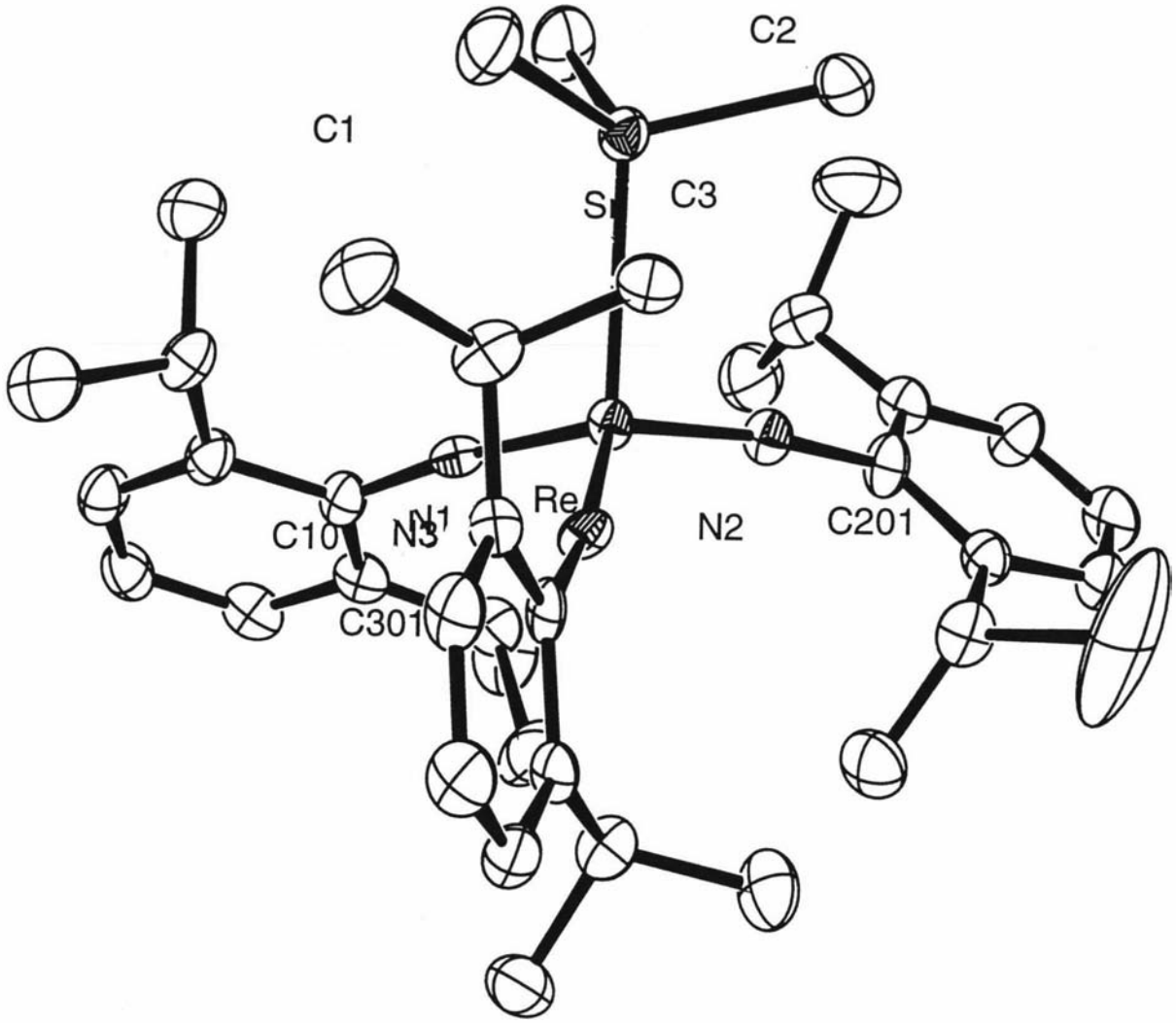

$Me_3SnRe(NAr)_3$

Figure 57

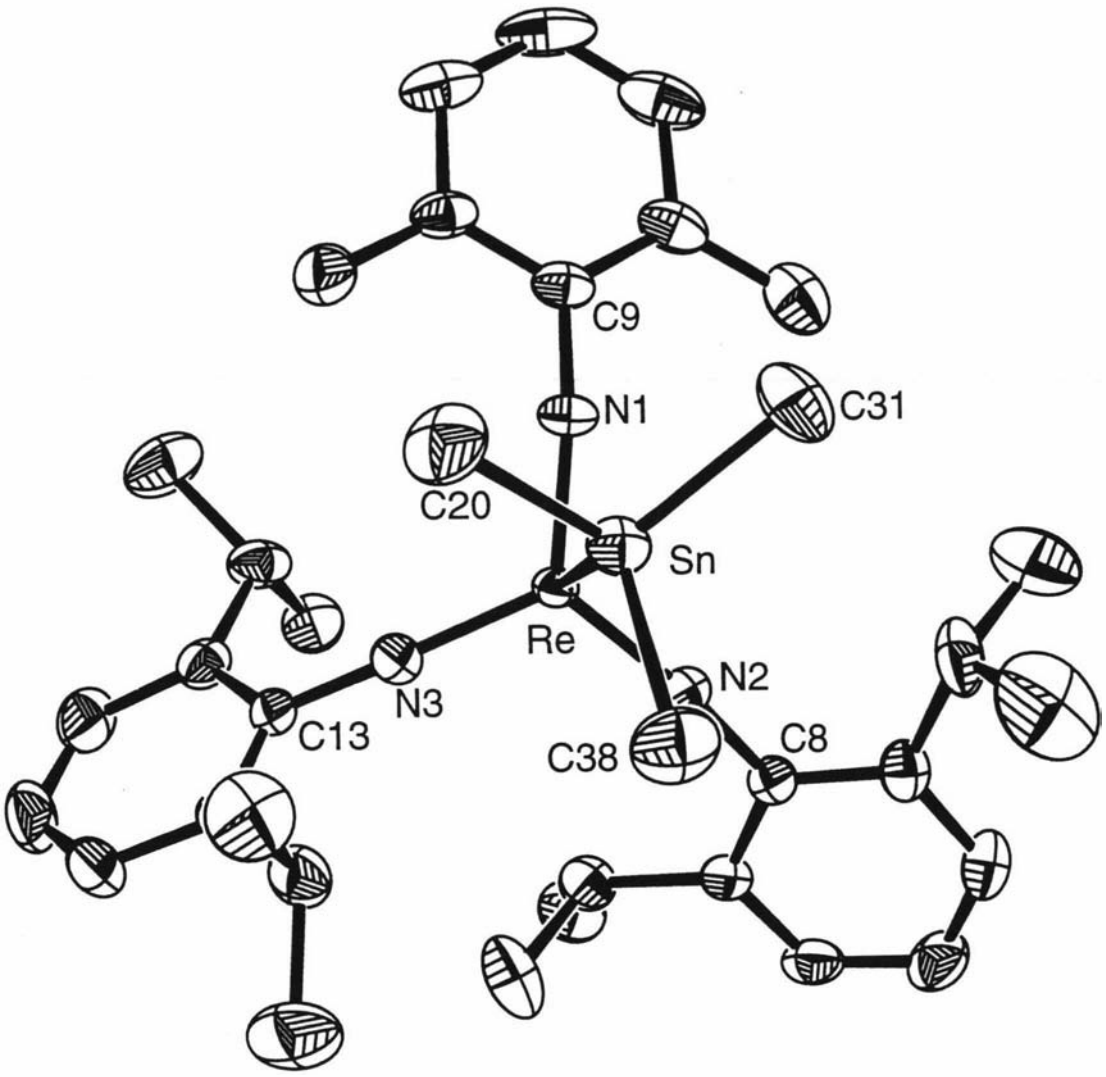

$Me_3SnRe(NAr)_2(NAr')$

Figure 58

Tables 19 and 20 show selected bond lengths and angles for the two complexes and other similar complexes.

Complex	#	X-M-N(#)	M-N(#)-C	N(1)-M-N(#)	Ref	Comments
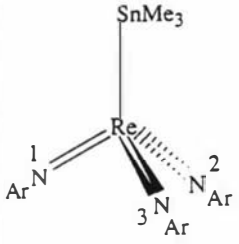	1	92.82(19)	170.2(5)		-	N(2)-Re-N(3) 120.0(2)
	2	93.07(6)	172.5(4)	117.3(2)		N(1)-Re-N(3) 118.6(3)
	3	104.16(18)	172.7(4)	100.4(3)		
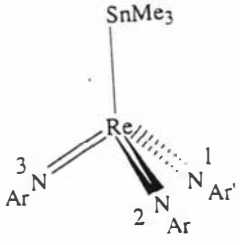	1	90.41(9)	172.9(2)		-	N(2)-Re-N(3)
	2	99.56(8)	171.6(2)	119.58(13)		116.46(13)
	3	104.32(8)	171.0(2)	118.15(13)		
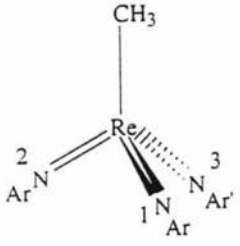	1	103.9(2)	169.1(3)		-	N(2)-Re-N(3)
	2	101.85(19)	171.2(3)	114.75(17)		115.63(17)
	3	102.81(19)	168.5(3)	115.23(18)		
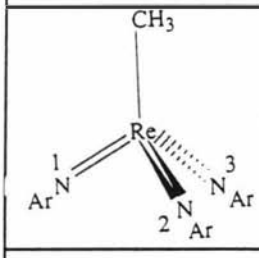	1	102.4(2)	166.3(3)		21	Distorted tetrahedral
	2	101.8(2)	168.8(3)	114.8(2)		N(2)-Re-N(3)
	3	103.0(2)	169.5(3)	116.2(2)		115.6(2)
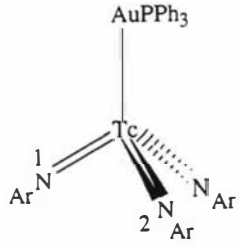	1	97.2(1)		118.4(1)	17	Distorted trigonal based pyramid (Au at apex). 3-fold axis along Tc-Au-P

Table 19: Selected bond angles for $Me_3SnRe(NAr)_2(NAr')$, $Me_3SnRe(NAr)_3$ and 3 other complexes

Complex	M-X	M-N(1)	M-N(2)	M-N(3)	Ref
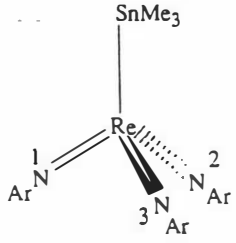	2.7416(8)	1.752(6)	1.760(4)	1.756(6)	-
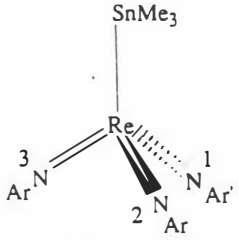	2.7354(6)	1.779(3)	1.766(3)	1.762(3)	-
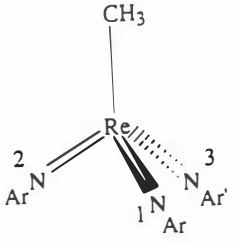	2.113(5)	1.763(4)	1.757(3)	1.753(4)	-
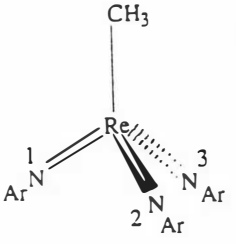	2.109(5)	1.766(3)	1.748(3)	1.758(4)	21
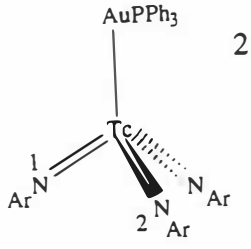	2.589(1)	1.758(5)			17

Table 20: Selected bond lengths for $Me_3SnRe(NAr)_2(NAr')$, $Me_3SnRe(NAr)_3$ and 3 other complexes

Both tin complexes exhibit approximate tetrahedral coordination environments about Re. The X-M-N angle can give an indication of the polarization between the X and $M(NR)_3$ fragments. As the X-M-N angle approaches 90° one can infer that the $M(NR)_3$ moiety is becoming less cationic in nature.[39] The average Sn-Re-N angle for $Me_3SnRe(NAr)_3$ and $Me_3SnRe(NAr)_2(NAr')$ is 96.68(19)° and 98.09(9)° respectively, considerably smaller than the methyl complexes at 102.85(19)° for $CH_3Re(NAr)_2(NAr')$ and 102.4(2)° for $CH_3Re(NAr)_3$[21] and compares well to the Tc(V) gold complex, $PPh_3AuTc(NAr)_3$ at 97.2(1)°.[17] All the Re-N-C angles are essentially linear ranging from 170.2(5) to 172.9(2)° and the Re-N distances ranging from 1.752(6) to 1.779(3)Å are within the expected range for tetrahedral tris(imido) complexes (see appendix III).

Conclusion

Reduction of Re(VII) tris(imido) complexes to Re(V) tris(imido) anions can be achieved in moderate yields with addition of 2 equivalents of elemental sodium. The anions were found to be unstable and as such were differcult to handle once isolated. As a result full characterization of these complexes was not possible. However, their reaction with $ClSnMe_3$ and $ClAuPPh_3$ to produce Re-Sn and Re-Au complexes provided an alternative means of characterizing the Re(V) anions.

The successful synthesis of $[Re(NAr')_3]^-$ calls into question whether the steric bulk of the aryl substituents is a major factor in the stabilization of $[Re(NR)_3]^-$ anions.

The reaction of the anions towards the tin and gold compounds resulted in the expected Re-Sn and Re-Au complexes. The structure of $[Re(NAr')_3]^-$ showed the cation to be Na^+ coordinated to six thf molecules. The presence of a 2-fold axis was surprising given the lack of symmetry found for $[Re(NAr)_3]^-$.[12] The structure of the tin complexes showed small Sn-Re-C angles and compared well with the previously structurally characterized Tc-Au compex, $Ph_3PAuTc(NAr)_3$.[17]

Experimental Section

General

General experimental procedures and details regarding the instrumentation used are given in appendix I. ^{1}H NMR were recorded in d_6-benzene and referenced to benzene at 7.15ppm. ^{13}C NMR were recorded in d_6-benzene and referenced to benzene at 128ppm. Deuterated benzene was purchased from Acros and freeze pumped thawed 3 times before use. THF was distilled from sodium/benzophenone. $ClSnMe_3$ and $ClAuPPh_3$ were purchased from Aldrich. Elemental sodium was purchased from Riedel-de Haen and small quantites of sodium were obtained by stirring sodium metal vigorously in boiling toluene.

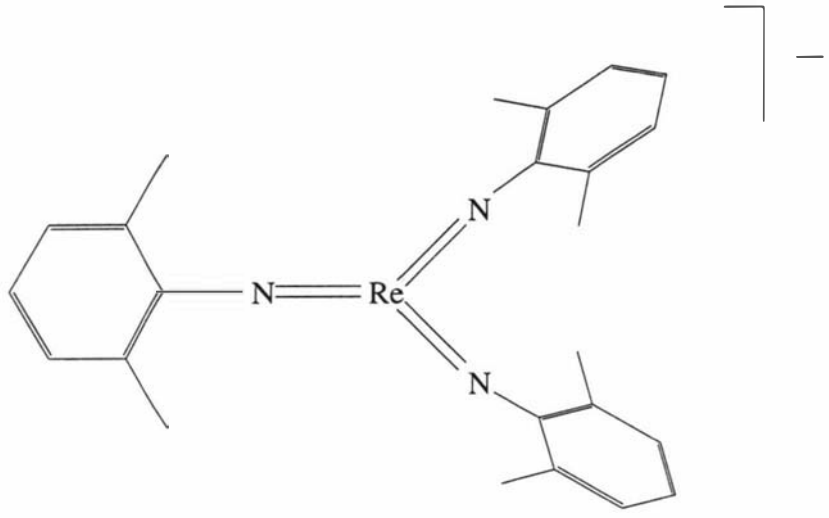

$[Re(NAr')_3][Na(thf)_6]$

Two equivalents of sodium (0.013g, 0.57mmol) was added to a solution of $Me_3SiORe(NAr')_3$ (0.168g, 0.265mmol) in tetrahydrofuran. The solution was then stirred overnight to give a now yellow/brown solution. Unreacted sodium was removed by filtering the solution through celite. The fitrate was then reduced in volume and hexamethyldisiloxane was then added resulting in a precipitate forming. The solid was filtered off and washed with hexane resulting in 0.143g (76%) of a brown powder.

Mass Spect: M^+ 544

Found: C, 57.85 ; H, 7.13 ; N, 4.36
Calc: C, 57.69 ; H, 7.56 ; N, 4.20

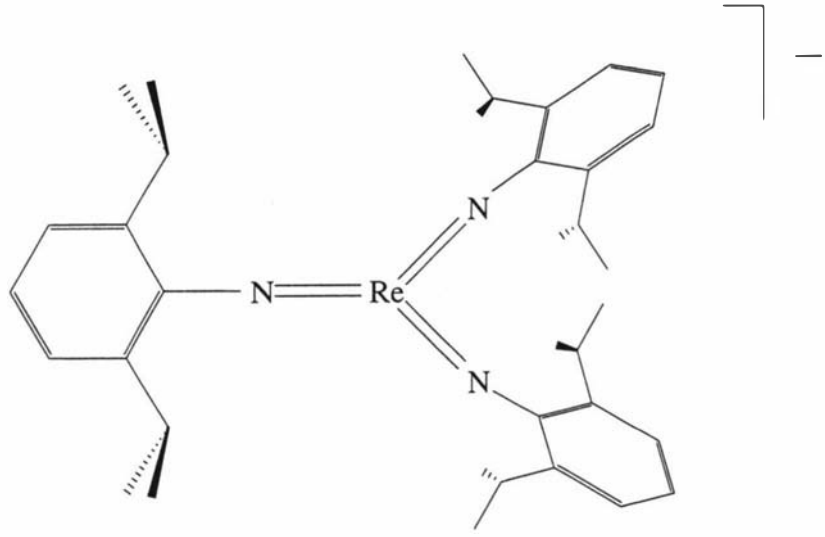

$[Re(NAr)_3][Na(thf)_2]$

To a solution of $Re(NAr)_3Cl$ (0.216g, 0.29mmol) in tetrahydrofuran was added 2 equivalents of sodium (0.014g, 0.61mmol). The solution was stirred overnight to give a now yellow/brown solution. This was then filtered through celite and the filtrate was reduced in volume. A precipitate was formed on addition of hexamethyldisiloxane to the solution. The solid was filtered off and washed with hexane yielding 0.221g (87%) of a brown powder.

Mass Spect: M^+ 712

Found: C, 60.87 ; H, 7.01 ; N, 4.90
Calc: C, 60.11 ; H, 7.68 ; N, 4.78

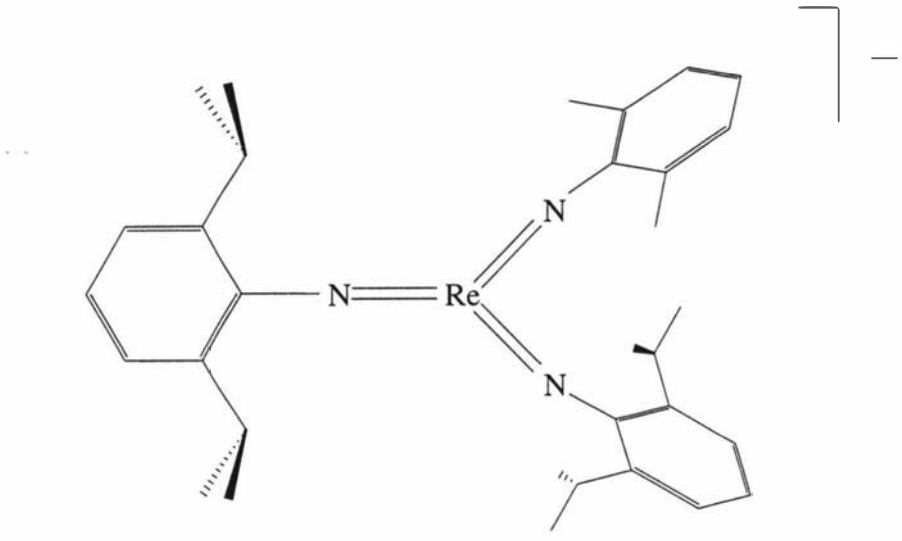

$[Re(NAr)_2(NAr')]^-$

To a solution of $Re(NAr)_2(NAr')Cl$ (0.152g, 0.22mmol) in tetrahydrofuran was added 2 equivalents of sodium (0.011g, 0.48mmol). The solution was stirred overnight to give a now yellow/brown solution. This was then filtered through celite and the filtrate was reduced in volume. A precipitate was formed on addition of hexamethyldisiloxane to the solution. The solid was filtered off and washed with hexane yielding 0.147g (81%) of a brown powder.

Mass Spect: M^+ 656

Found: C, 59.41 ; H, 7.46 ; N, 5.34
Calc: C, 58.32 ; H, 7.22 ; N, 5.11

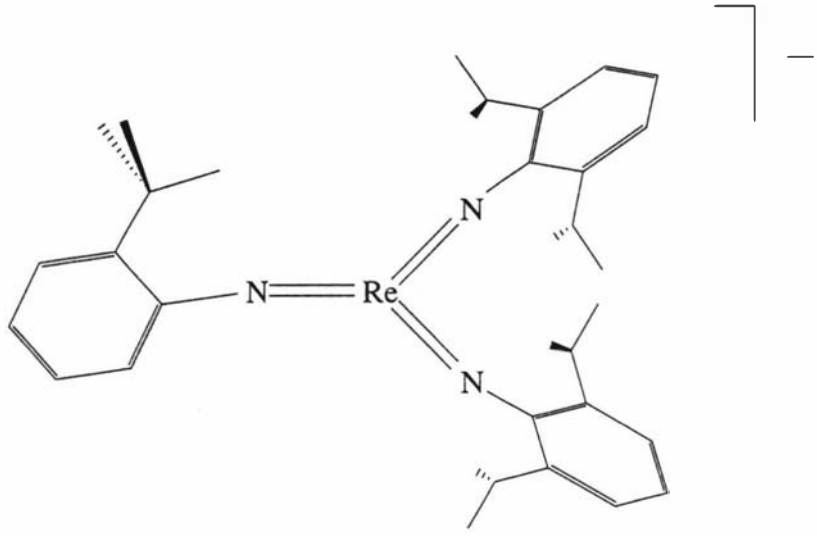

$[Re(NAr)_2(N\text{-}o\text{-}^tBu)]^-$

Two equivalents of sodium (0.010g, 0.44mmol) was added to a solution of $Re(NAr)_2(N\text{-}o\text{-}^tBu)Cl$ (0.151g, 0.211mmol) in tetrahydrofuran. The solution was then stirred overnight to give a now yellow/brown solution. Unreacted sodium was removed by filtering the solution through celite. The fitrate was then reduced in volume and hexamethyldisiloxane was then added resulting in a precipitate forming. The solid was filtered off and washed with hexane resulting in 0.168g (94%) of a brown powder.

Mass Spect: M^+ 684

Found: C, 59.98 ; H, 6.94 ; N, 4.45
Calc: C, 59.27 ; H, 7.46 ; N, 4.94

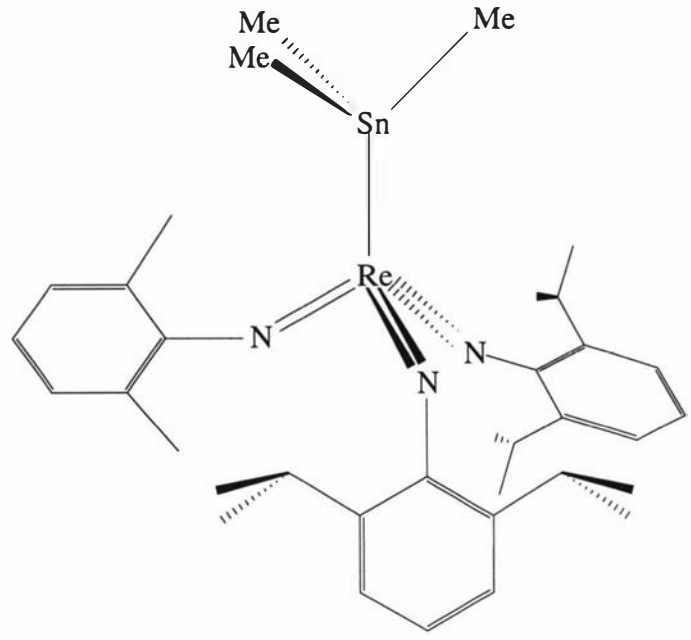

$(NAr)_2(NAr')ReSn(CH_3)_3$

To a solution of $Re(NAr)_2(NAr')Cl$ (0.140g, 0.20mmol) in tetrahydrofuran was added 2 equivalents of sodium (0.010g, 0.43mmol). The solution was stirred overnight. The solution was then filtered through celite into a solution containing $ClSn(CH_3)_3$ (0.040g, 0.20mmol). The solution was stirred for 12 hours to give a now red solution. The solvent was removed *in vacuo* and benzene (10mL) was then added. The resulting solution was filtered through celite and the filtrate was then reduced to dryness in vacuo. Recrystallization from slow evaporation of a hexane solution resulted in 0.102g (62%) of red crystals.

^1H NMR (C_6D_6): 7.13-6.99(m, 6, Ar), 6.90-6.78(m, 3, Ar'), 3.92(sept, 4, J=6.8, $C\underline{H}Me_2$), 2.39(s, 6, $C\underline{H}_3$), 1.21(d, 24, J=7.0, $CHC\underline{H}_3$), 0.68(s, 9, $SnC\underline{H}_3$)

$^{13}C\{^1H\}$ NMR (C_6D_6): 153.0(Ar), 152.9(Ar'), 143.1(Ar), 142.8(Ar'), 130.8(Ar), 127.2(Ar'), 122.5(Ar), 122.4(Ar'), 27.9($\underline{C}HCH_3$), 23.4($CH\underline{C}H_3$), 18.0($\underline{C}H_3$), -1.2($Sn\underline{C}H_3$)

Mass Spect: M^+ 821, M^+-$SnMe_3$ 657, $SnMe_3$ 164

Found: C, 51.53 ; H, 6.42 ; N, 5.24; Calc: C, 51.28 ; H, 6.39 ; N, 5.13

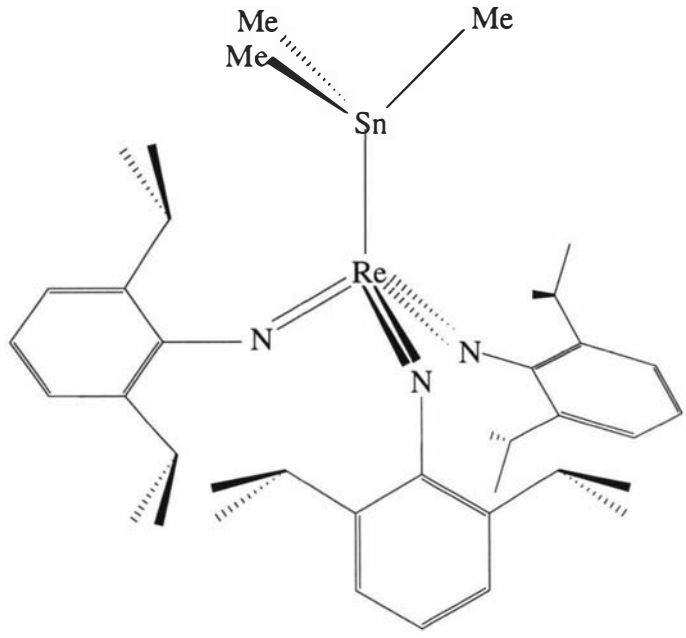

$(NAr)_3ReSn(CH_3)_3$

To a solution of $Re(NAr)_3Cl$ (0.150g, 0.20mmol) in tetrahydrofuran was added 2 equivalents of sodium (0.010g, 0.43mmol). The solution was stirred overnight. The solution was then filtered through celite into a solution containing $ClSn(CH_3)_3$ (0.040 g, 0.20mmol). The solution was stirred for 12 hours to give a now red solution. The solvent was removed *in vacuo* and benzene (10mL) was then added. The resulting solution was filtered through celite and the filtrate was then reduced to dryness in vacuo. Recrystallization from slow evaporation of a hexane solution resulted in 0.121g (69%) of red crystals.

^1H NMR (C_6D_6): 7.12-6.98(m, 9, Ar), 3.87(sept, 6, J=6.8, C$\underline{H}Me_2$), 1.18(d, 36, J=7.0, CHC$\underline{H}_3$), 0.71(s, 9, SnC$\underline{H}_3$)

Mass Spect: M^+ 877, M^+-$SnMe_3$ 713, $SnMe_3$, 164

$^{13}C\{^1H\}$ NMR (C_6D_6): 152.8(Ar), 143.5(Ar), 129.8(Ar), 122.4(Ar), 27.6(C$\underline{C}HCH_3$), 23.8(CH$\underline{C}H_3$), -1.4(Sn$\underline{C}H_3$)

Found: C, 53.24 ; H, 6.65 ; N, 4.97; Calc: C, 53.48 ; H, 6.91 ; N, 4.80

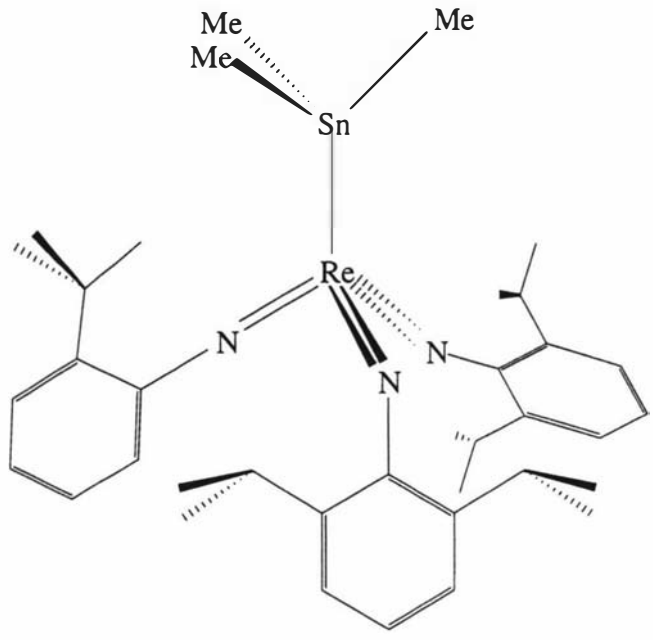

$(NAr)_2(N\text{-}o\text{-}^tBu)ReSn(CH_3)_3$

To a solution of $Re(NAr)_2(N\text{-}o\text{-}^tBu)Cl$ (0.150g, 0.21mmol) in tetrahydrofuran was added 2 equivalents of sodium (0.010g, 0.43mmol). The solution was stirred overnight. The solution was then filtered through celite into a solution containing $ClSn(CH_3)_3$ (0.042g, 0.21mmol). The solution was stirred for 12 hours to give a now red solution. The solvent was removed *in vacuo* and benzene (10mL) was then added. The resulting solution was filtered through celite and the filtrate was then reduced to dryness in vacuo. Recrystallization from slow evaporation of a hexane solution resulted in 0.121g (68%) of red crystals.

^1H NMR (C_6D_6): 7.10-6.80(m, 10, Ar/*o*-^{t}Bu), 3.89(sept, 4, J=6.8, C$\underline{H}$Me$_2$), 1.42(s, 9, *o*-^{t}Bu), 1.14(d, 24, J=7.0, CHC$\underline{H}_3$), 0.68(s, 9, SnC$\underline{H}_3$)

$^{13}C\{^1H\}$ NMR (C_6D_6): 154.0(Ar), 151.1($\underline{C}_6H_5C(CH_3)_3$), 142.2(Ar), 141.8($\underline{C}_6H_5C(CH_3)_3$), 128.4($\underline{C}_6H_5C(CH_3)_3$), 126.4(Ar), 125.7($\underline{C}_6H_5C(CH_3)_3$), 125.0($\underline{C}_6H_5C(CH_3)_3$), 124.7($\underline{C}_6H_5C(CH_3)_3$), 122.5(Ar), 35.5($C_6H_5\underline{C}(CH_3)_3$), 30.2($C_6H_5C(\underline{C}H_3)_3$), 27.8($\underline{C}HCH_3$), 22.9(CH$\underline{C}H_3$), -1.4(Sn$\underline{C}H_3$)

Found: C, 52.84 ; H, 6.24 ; N, 5.13; Calc: C, 52.42 ; H, 6.66 ; N, 4.96

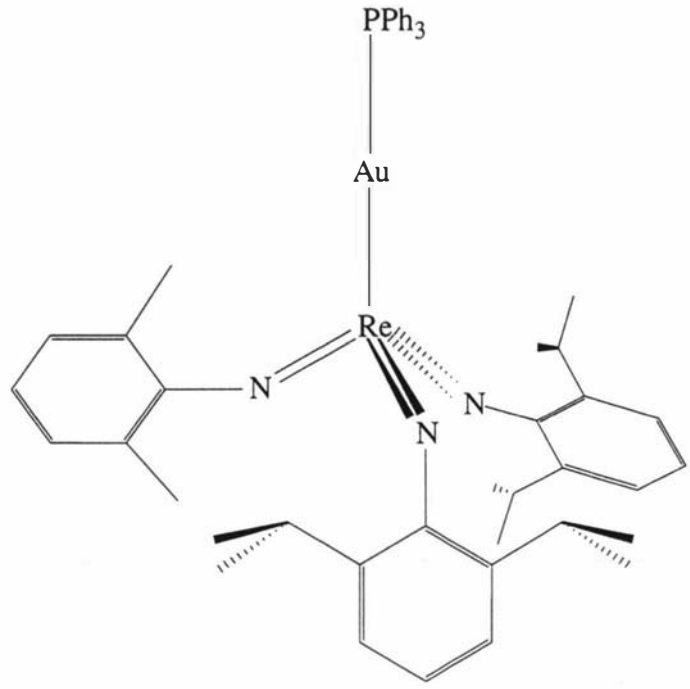

$(NAr)_2(NAr')ReAuPPh_3$

To a solution of $Re(NAr)_2(NAr')Cl$ (0.140g, 0.20mmol) in tetrahydrofuran was added 2 equivalents of sodium (0.010g, 0.43mmol). The solution was stirred overnight. The solution was then filtered through celite into a solution containing $ClAuPPh_3$ (0.099g, 0.20mmol). The solution was stirred for 12 hours to give a now yellow/red solution. The solvent was removed *in vacuo* and benzene (10mL) was then added. The resulting solution was filtered through celite and the filtrate was then reduced in volume. On addition of hexamethyldisiloxane a precipitate was formed. Filtering resulted in 0.148g (66%) of a orange/brown solid.

^1H NMR (C_6D_6): 7.32(br, 6, *o*-phenyl), 7.17(d, 4, J=7.1, Ar), 7.08(t, 2, J=7.1, Ar), 7.00(d, 2, J=7.1, Ar'), 6.82(br, 10, *m/p*-phenyl, Ar'), 4.29(sept, 4, J=6.8, C<u>H</u>Me_2), 2.56(s, 6, C<u>H</u>$_3$), 1.26(d, 24, J=7.0, CHC<u>H</u>$_3$)

Mass Spect: M^+ 1115, PPh_3Au 459

Found: C, 53.46 ; H, 5.46 ; N, 3.68
Calc: C, 53.85 ; H, 5.24 ; N, 3.77

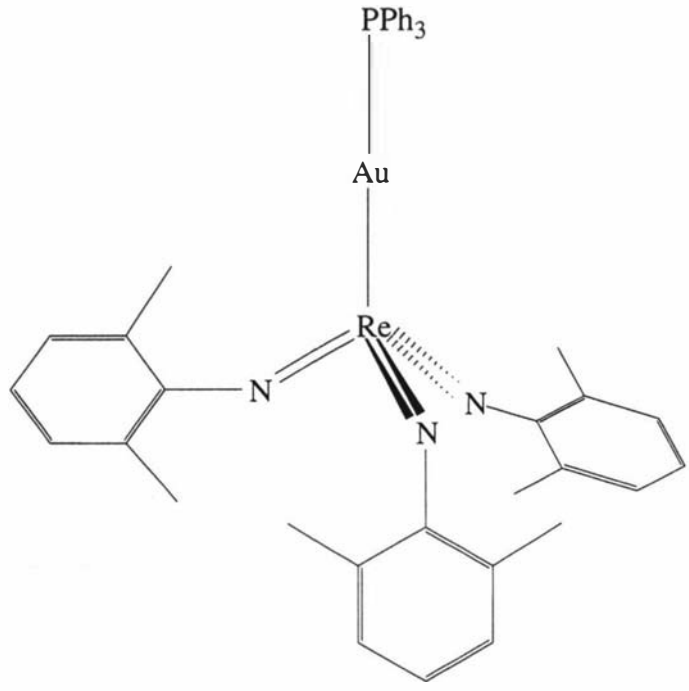

$(NAr')_3ReAuPPh_3$

To a solution of $Me_3SiORe(NAr')_3$ (0.150g, 0.24mmol) in tetrahydrofuran was added 2 equivalents of sodium (0.012g, 0.52mmol). The solution was stirred overnight. The solution was then filtered through celite into a solution containing $ClAuPPh_3$ (0.119g, 0.24mmol). The solution was stirred for 12 hours to give a now yellow/red solution. The solvent was removed *in vacuo* and benzene (10mL) was then added. The resulting solution was filtered through celite and the filtrate was then reduced in volume. On addition of hexamethyldisiloane a precipitate was formed. Filtering resulted in 0.174g (72%) of a brown solid.

^1H NMR (C_6D_6): 7.21-6.61(m, 24, Ar', phenyl), 2.23(s, 18, $C\underline{H}_3$)

Mass Spect: M^+ 1003, M^+-$Re(NAr')_3$ 544, PPh_3Au 459

Found: C, 50.11 ; H, 3.75 ; N, 4.18
Calc: C, 50.30 ; H, 4.22 ; N, 4.19

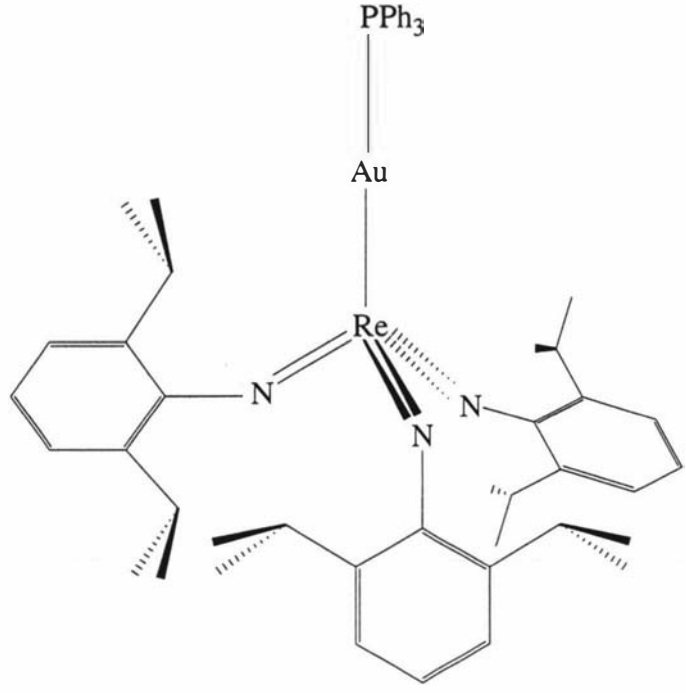

$(NAr)_3ReAuPPh_3$

To a solution of $Re(NAr)_3Cl$ (0.150g, 0.20mmol) in tetrahydrofuran was added 2 equivalents of sodium (0.010g, 0.43mmol). The solution was stirred overnight. The solution was then filtered through celite into a solution containing $ClAuPPh_3$ (0.099g, 0.20mmol). The solution was stirred for 12 hours to give a now yellow/red solution. The solvent was removed *in vacuo* and benzene (10mL) was then added. The resulting solution was filtered through celite and the filtrate was then reduced in volume. On addition of hexamethyldisiloxane a precipitate was formed. Filtering resulted in 0.152g (65%) of a orange solid.

^1H NMR (C_6D_6): 7.41(br, 6, *o*-phenyl), 7.17(d, 6, J=7.1, Ar), 7.04(t, 3, J=7.1, Ar), 6.91(br, 9, *m/p*-phenyl), 4.38(sept, 6, J=6.8, C<u>H</u>Me_2), 1.28(d, 36, J=7.0, CHC<u>H</u>$_3$)

Mass Spect: M^+ 1171, M^+-$Re(NAr)_3$ 712, PPh_3Au 459

Found: C, 55.39 ; H, 5.51 ; N, 3.56
Calc: C, 55.37 ; H, 5.68 ; N, 3.59

Chapter Five

Synthesis of Re(VI) Complexes

Introduction

This chapter describes the synthesis of dimeric rhenium(VI) complexes. The methodology developed involves the one electron oxidation of the rhenium(V) tris(imido) complexes. Evidence of a monomeric rhenium(VII) cation is also discussed.

Transition metal d^1 tris(imido) complexes are known only for manganese,[31,1a] technetium,[33,43] rhenium[48,30,33] and osmium.[54,89] All d^1 tris(imido) complexes are dimeric containing a M-M bond and are hence diamagnetic. In all cases the synthesis of these complexes involves reduction of the d^0 tris(imido) complex (or tetrakis in the case of Os), however, oxidation of a d^2 technetium tris(imido), $[Tc(NAr)_3]^-$, was observed to occur with addition of $ITc(NAr)_3$ resulting in the reduction of the d^0 Tc tris(imido) complex and hence forming the d^1-d^1 dimer, $Tc_2(NAr)_6$.[17] Little is known about the reactivity of M(VI) dimeric tris(imido) complexes. The technetium complex, $Tc_2(NAr)_6$, can be reduced with sodium to the anion, $[Tc(NAr)_3]^-$.[17] The reaction of 2 equivalents of MeMgCl with $Tc_2(NAr')_4(\mu\text{-}NAr')_2$ results in displacement of an imido ligand and formation of $TcMe_2(NAr')(\mu\text{-}NAr')_2Tc(NAr')_2$. Treatment of $TcMe_2(NAr')(\mu\text{-}NAr')_2Tc(NAr')_2$ with a further 2 equivalents of MeMgCl again results in the substitution of an imido ligand and the formation of $Tc_2(NAr')_2(\mu\text{-}NAr')_2Me_4$.[43] This unprecedented substitution of an imido ligand by 2 methyl groups illustrates that reactions of d^1-d^1 dimeric tris(imido) complexes can lead to unexpected results.

Synthesis of Re(VI) Complexes

The interaction of $Me_3SiORe(N^tBu)_3$ with an excess of sodium (or Na/Hg) lead to the diamagnetic complex, $[Re(N^tBu)_2(\mu\text{-}N^tBu)]_2$, in low yield (Equ. 74).[30]

$$Me_3SiORe(N^tBu)_3 + xs\ Na \longrightarrow [Re(N^tBu)_2(\mu\text{-}N^tBu)]_2$$

Equation 74

Williams and Schrock reported that treatment of $Re(NAr)_3Cl$ with 1 equivalent of Na/Hg gives a mercury bridged species (Equ. 75).[12]

$$ClRe(NAr)_3 + NaHg \longrightarrow (ArN)_3Re\text{-}Hg\text{-}Re(NAr)_3$$

Equation 75

A year later Burrell *et al.* described the synthesis of $Re_2(NR)_6$, where R is Ar or Ar' (Equ. 76),[17,73] showing that in the absence of mercury, sodium will reduce $Re(NAr)_3I$ to $Re_2(NAr)_6$. On the basis of proton NMR and comparison with the technetium analogues it is thought that $Re_2(NAr')_6$ adopts an edge-bridged tetrahedral dimeric configuration while $Re_2(NAr)_6$ adopts an ethane-like geometry.[17]

$$IRe(NR)_3 + Na \longrightarrow Re_2(NR)_6$$

Equation 76

Results and Discussion

Synthesis of Re(VI) Complexes

The interaction of $Re(NR)_3Cl$ with 1 equivalent of sodium results in mixtures containing starting material, anion $[Re(NR)_3]^-$ and small amounts of the dimer $Re_2(NR)_6$ indicated by mass spectrometry. Separation of the dimer and $ClRe(NR)_3$ could prove to be difficult and would result in very low yields of the dimer.

Williams and Schrock[12] demonstrated through electrochemical studies of $ClRe(NAr)_3$ that its reduction to $[Re(NAr)_3]^-$ can occur via 2 routes (Scheme 24).

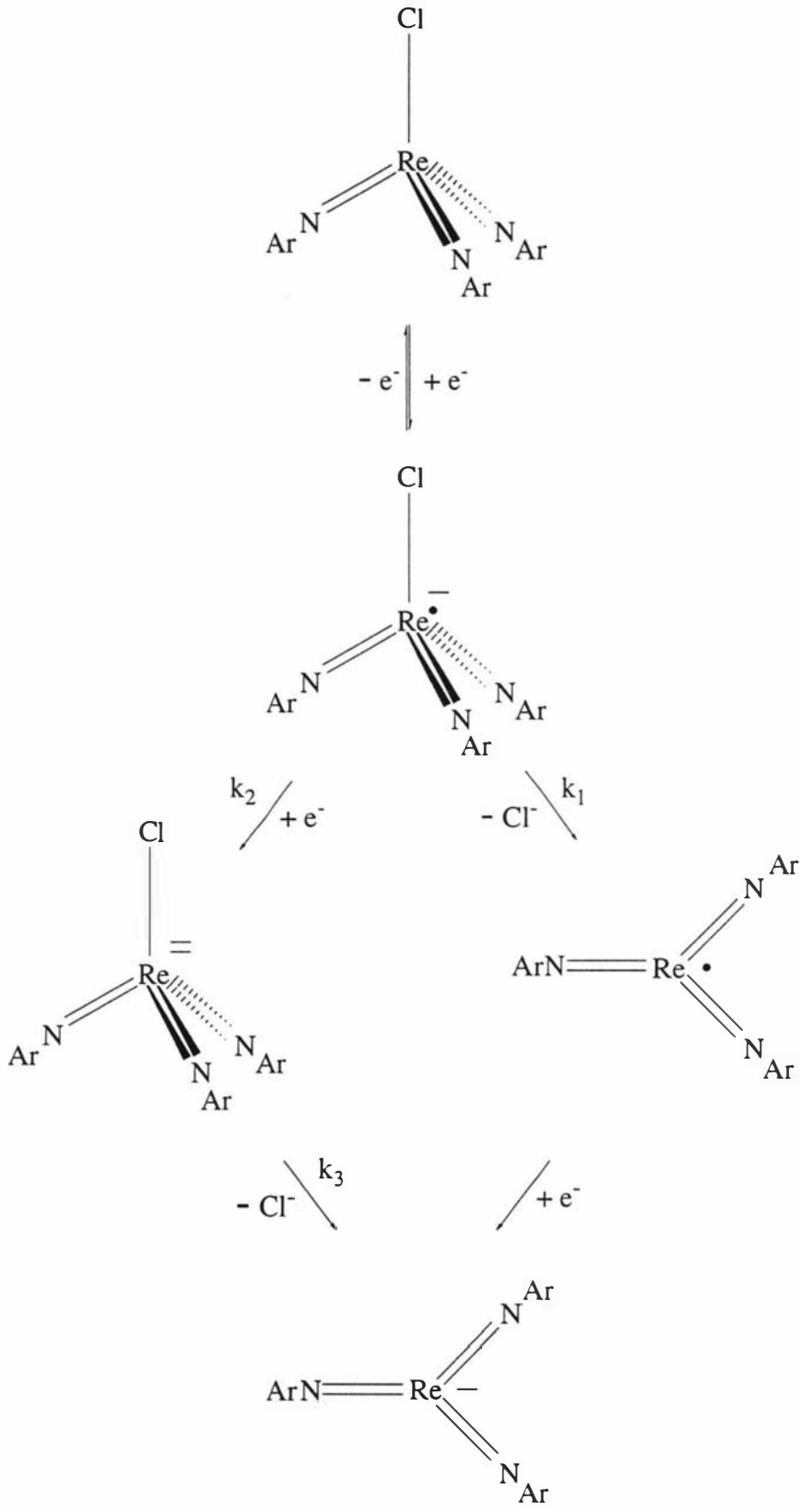
Cl
Re
N
Ar
N
Ar
N
Ar
- e⁻
+ e⁻
Cl
Re
N
Ar
N
Ar
N
Ar
k2
+ e⁻
- Cl⁻
k1
Cl
Re
N
Ar
N
Ar
N
Ar
ArN
Re
N
Ar
N
Ar
k3
- Cl⁻
+ e⁻
ArN
Re
N
Ar
N
Ar

Scheme 24

The first step involves the one electron reduction of $Re(NAr)_3Cl$ to the radical anion. This can then lose Cl^- to form $(NAr)_3Re^{\cdot}$, (slow step) or be reduced further to the $Re(NAr)_3Cl^{2-}$ complex (fast step), which can lose Cl^- to form the anion. Since k_1 is much slower then k_2, reducing $Re(NAr)_3Cl$ by 1 electron leads to mixtures of the anion and $Re(NAr)_3Cl$, as has been confirmed experimentally. In the reduction of $Tc(NAr)_3I$ the dimer is formed in high yield. This may be due to I^- being a better leaving group than Cl^-. Hence for I, k_1 maybe faster than k_2.

Since formation of $Re_2(NR)_6$ via reduction of the Re(VII) species has proved to be problematic then an alternative method is to make use of the Re(V) species.

Hence the 1 electron oxidation of the Re(V) anions with ferrocenium forms the Re(VI) dimers and ferrocene (Scheme 25).

$$2\ [Re(NR)_2(NR')]^- + 2\ Cp_2Fe^+ \longrightarrow Re_2(NR)_4(NR')_2 + 2\ Cp_2Fe$$

R	R'	Complex
Ar'	Ar'	$[Re(NAr')_2(\mu\text{-}NAr')]_2$
Ar	Ar	$(ArN)_3Re\text{-}Re(NAr)_3$
Ar	Ar'	3 compounds in 1:1:1 ratio
Ar	*o*-^{t}Bu	$(ArN)_2(o\text{-}^t BuN)Re\text{-}Re(NAr)_2(N\text{-}o\text{-}^t Bu)$

Scheme 25

The oxidation of $[Re(NAr')_3]^-$ formed a red compound whose ^1H nmr showed two sets of resonances, in a 2:1 ratio, consistent with 4 terminal and 2 bridging aryl imido ligands in an edge-bridged dimeric structure, $Re_2(NAr')_4(\mu\text{-}NAr')_2$. This result was anticipated since the analogous Tc complex, $Tc_2(NAr')_4(\mu\text{-}NAr')_2$ adopts an edge-bridged tetrahedral dimeric structure.[17] The edge-bridged tetrahedral dimeric configuration for the complex is confirmed by a x-ray structural analysis of a single crystal.

X-ray structure of $[Re(NAr')_2(\mu\text{-}NAr')]_2$

X-ray quality crystals of $[Re(NAr')_2(\mu\text{-}NAr')]_2$ were obtained from slow evaporation of a benzene/hexane solution. The final structure is shown in figure 59. Tables containing complete bond lengths and angles, atomic coordinate and equivalent

isotropic displacement parameters, anisotropic displacement parameters and calculated H-atom positions are presented in appendix XVI.

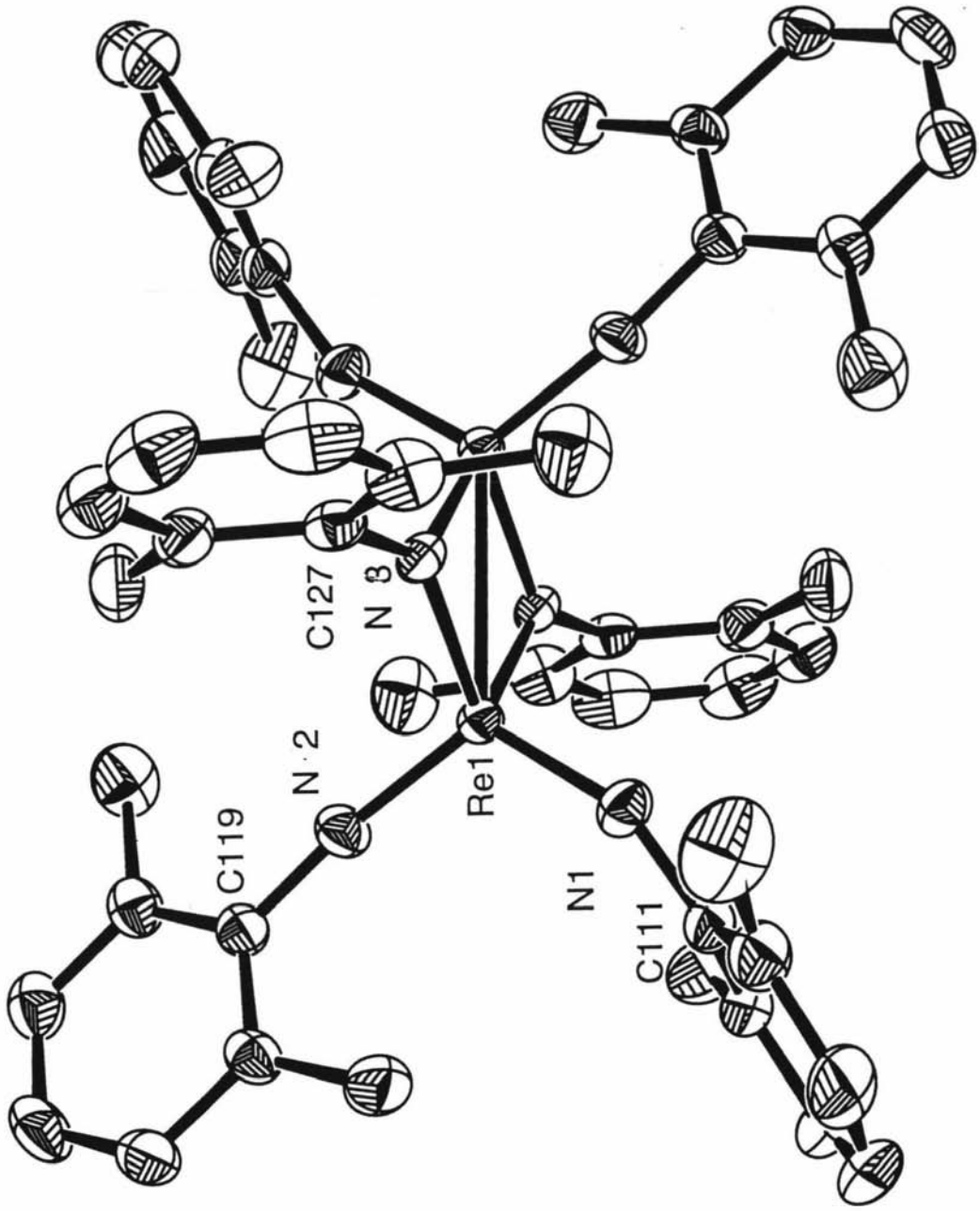

Figure 59

Tables 21 and 22 show selected bond lengths and angles for $[Re(NAr')_2(\mu\text{-}NAr')]_2$ and three other d^1M bridging imido dimers. The dimer comprises two tetrahedral rhenium(VI) atoms with bonds to 2 terminal and 2 bridging imido nitrogens. The structure displays many similarities to $[Re(N^tBu)_2(\mu\text{-}NtBu)]_2$.[30] The bridges are symmetrical with an average Re-N(3)-Re* angle of 88.8(15)°. Generally M-N-M angles in the range 78-84° occur when there is a metal-metal bond, and angles >94° indicate no metal-metal bond. It can be seen the Re-N(bridging imido)-Re angle for $[Re(N^tBu)_2(\mu\text{-}N^tBu)]_2$ is 88.7(7)°, while for the bridging imido/oxo complex it is smaller at 83.8(6)°. The Re-Re bond lengths of 2.7267(3) and 2.7440(3)Å suggest a weak Re-Re interaction. For $[Re(N^tBu)_2(\mu\text{-}N^tBu)]_2$ the Re-Re distance is 2.7Å and for (^{t}BuN)(Br)(mes)Re(μ-N^{t}Bu)(μ-O)Re(N^{t}Bu)($OC_6H_2Me_2CH_2$) (Fig. 60) the Re-Re distance is 2.61Å. Re-Re single bonds have been proposed in the binuclear d^1-d^1, Re(VI) oxo-bridging species $[Me_2(O)Re(\mu\text{-}O)]_2$,[106] $[(Me_3CH_2)_2(O)Re(\mu\text{-}O)]_2$,[107] and $[(PhMe_2CCH_2)_2(O)Re(\mu\text{-}O)]_2$,[108] where the Re-Re distances are 2.593(1), 2.606(1) and 2.6116(7)Å respectively.

The distances between the Re and bridging nitrogen atoms (1.951(3)-1.959(4)Å) are slightly lower then those for $[Re(N^tBu)_2(\mu\text{-}N^tBu)]_2$ but are similar to the Tc dimer, $[Tc(NAr')_2(\mu\text{-}NAr')]_2$ (see table 22). The distances to the terminal imido groups are unremarkable falling within the range for $[Re(N^tBu)_2(\mu\text{-}N^tBu)]_2$ (1.69(3)-1.78(2)Å), $[Tc(NAr')_2(\mu\text{-}NAr')]_2$ (1.737(6)-1.759(6)Å) and (^{t}BuN)(Br)(mes)Re(μ-N^{t}Bu)(μ-O)Re(N^{t}Bu)($OC_6H_2Me_2CH_2$) (1.708(14)-1.695(14)Å) at 1.750(4) to 1.763(3)Å.

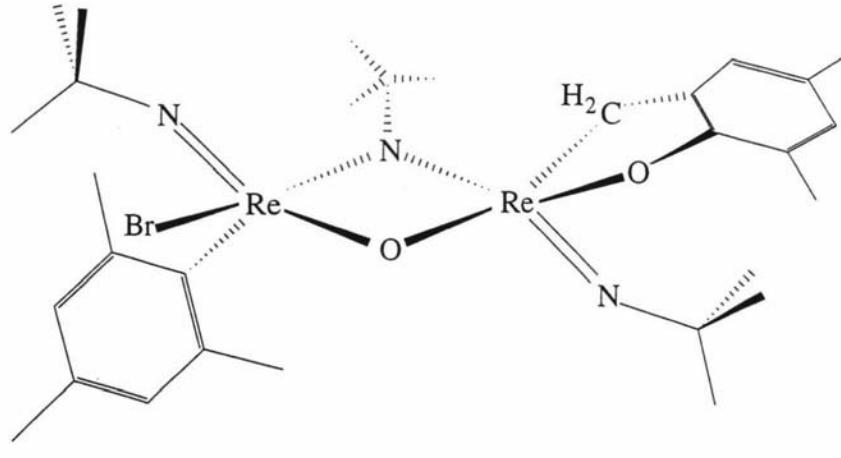

Figure 60

Complex	#	M-N(#)-C	N(1)-M-N(#)	M-M-N(#)	Ref	Comments
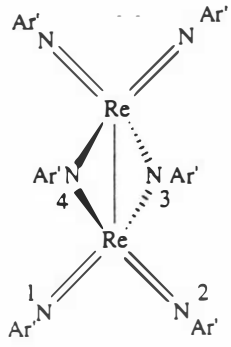	1	156.2(3)		122.26(13)	-	2 independent structures
		168.4(3)		122.95(12)		
	2	168.8(3)	113.48(17)	124.23(12)		N(2)-Re-N(3) 112.18(15)
		166.0(3)	114.10(17)	122.95(12)		112.58(16)
	3	136.7(3)	114.09(16)	45.74(10)		N(3)-Re-N(4) 91.02(15)
		135.3(3)	112.25(15)	45.47(11)		91.40(14)
						Re-N(3)-Re 88.60(14)
						88.98(15)
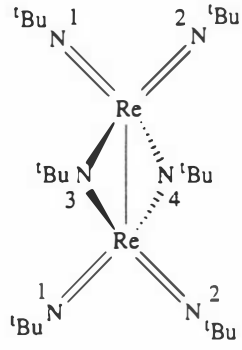	1				30	Tetrahedral about Re
	2		110(1)-112(1)			Re-N(bridg)-Re
						88.4(7)-88.9(7)
						N(3)-Re-N(4)
						91.1(8)-91.6(8)
						Symmetric bridging imido ligands
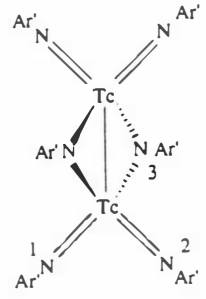	1			121.7(3)	17	2 independent str.
				122.3(2)		Centrosymmetric
	2		115.1(3)	123.3(2)		N(2)-Tc-N(3) 115.1(3)
			116.4(3)	121.3(2)		116.4(3)
	3		111.6(3)			
			111.6(3)			
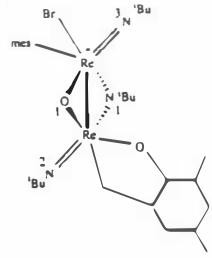	1	138.1(9)			48	Very distorted trigonal bipyramid
		137.0(9)*				
	2	161.9(13)	125.0(6)			Re-O(1)-Re* 87.0(5)
	3	157.8(11)*	108.3(6)			Re-N(1)-Re* 83.8(6)

Table 21: Selected bond angles(°) for $[Re(NAr')_2(\mu\text{-}NAr')]_2$ and 3 other d^1 M bridging imido dimers

Complex	#	M-N(#)	M-M	C-N(#)	Ref.	Comments
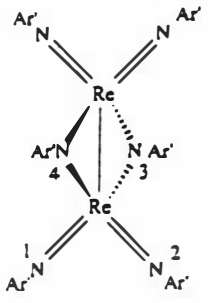	1	1.754(4)	2.7267(3)	1.384(6)	-	2 independent structures
		1.750(4)	2.7440(3)	1.395(6)		
	2	1.763(3)		1.384(5)		Re-N(4) 1.953(3)
		1.756(4)		1.382(5)		1.957(4)
	3	1.951(3)		1.437(5)		
		1.959(4)		1.421(5)		
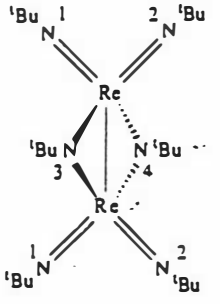	1,2	1.69(3) to 1.78(2)	2.7		30	Weak Re-Re interaction
	3,4	1.85(3) to 1.94(2)				
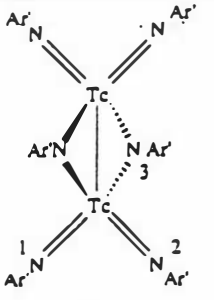	1	1.737(6)	2.696(2)		17	2 independent structures
		1.748(6)	2.667(2)			
	2	1.756(8)				
		1.759(6)				
	3	1.955(7)				
		1.952(6)				
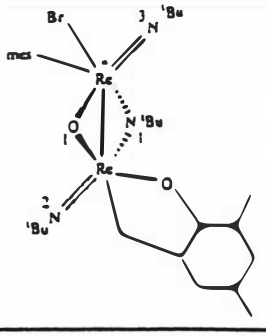	1	1.922(13)	2.61		48	
		1.990(14)*				
	2	1.708(14)				
	3	1.695(14)*				

Table 22: Selected bond lengths(Å) for $[Re(NAr')_2(\mu\text{-}NAr')]_2$ and 3 other d^1 M bridging imido dimers

The oxidation of $[Re(NAr)_3]^-$ also formed a red compound but the ^1H nmr revealed only a single ligand environment. This result is suggestive that an alternative

structure such as the ethane-like dimer found for $Tc_2(NAr)_6$[17] is appropiate for $Re_2(NAr)_6$. This was confirmed by x-ray structural analysis of a single crystal.

X-ray Structure of $Re_2(NAr)_6$

X-ray quality crystals of $Re_2(NAr)_6$ were obtained from slow evaporation of a benzene/hexane solution. The final structure is shown in figure 61. Tables containing complete bond lengths and angles, atomic coordinate and equivalent isotropic displacement parameters, anisotropic displacement parameters and calculated H-atom positions are presented in appendix XVII.

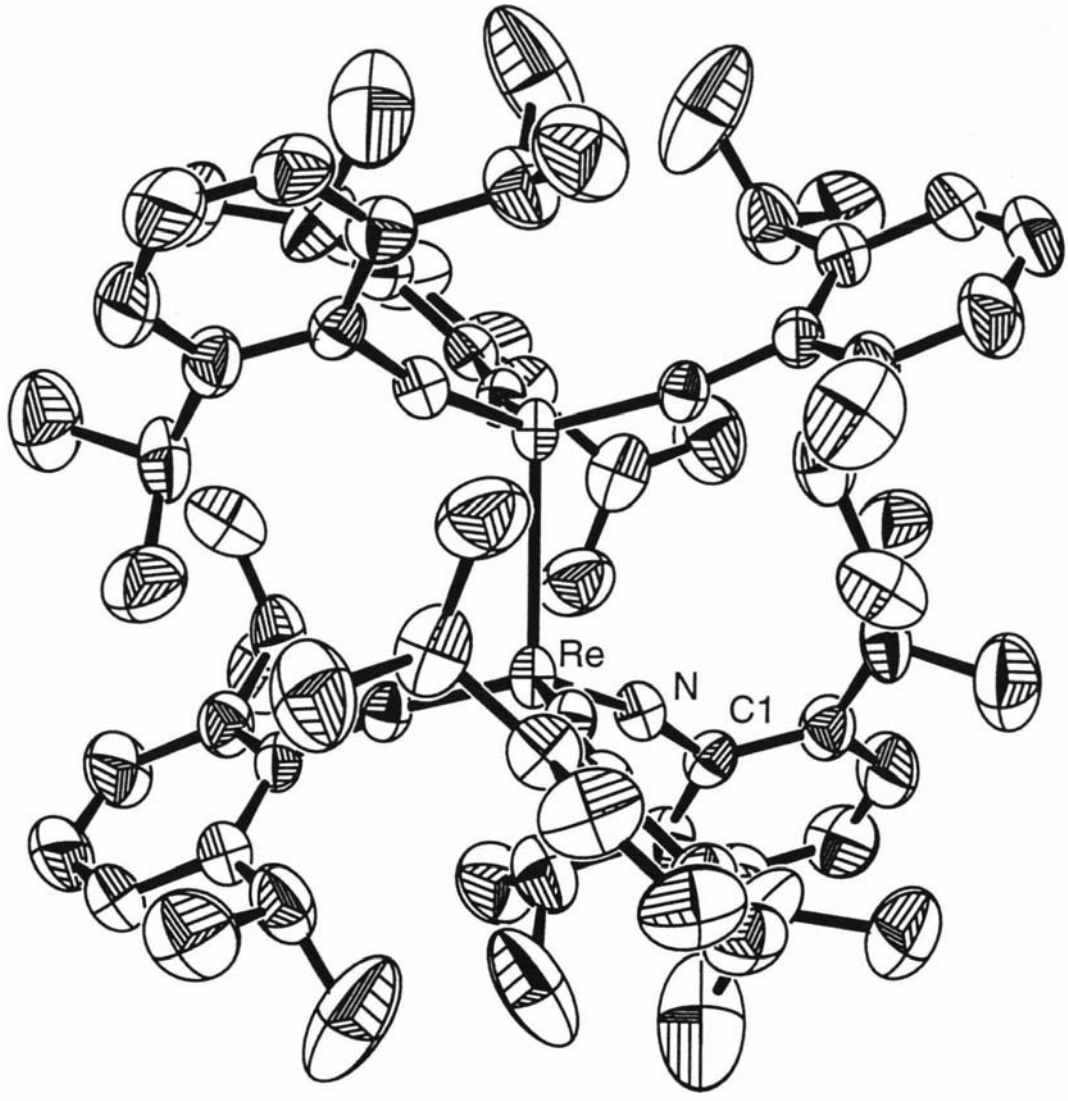

Figure 61

Tables 23 and 24 show selected bond lengths and angles for $Re_2(NAr)_6$, the Tc analogue and IRe(NAr)$_3$. Table 24 also contains bond lengths for $[Re(O)(MeCCMe)_2]_2$.

Just as for $Tc_2(NAr)_6$, the Re dimer adopts an ethane-like geometry with the imido ligands arranged in a staggered orientation. This orientation is also seen in the Re(V) dimer complex, $[Re(C^tBu)(O^tBu)_2]_2$ which contains a Re=Re double bond[109] and the Re(II) dimer, $[Re(O)(MeCCMe)_2]_2$, which contains a Re-Re single bond.[111]

Complex	#	M-N(#)-C	N(1)-M-N(#)	M-M-N(#)	Ref.	Comments
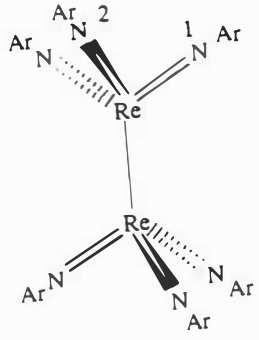	1	168.5(4)		103.80(15)	-	
	2		114.50(12)			
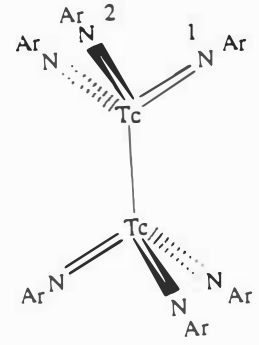	1	167.6(1)		103.6(1)	17	
	2		114.6(1)			
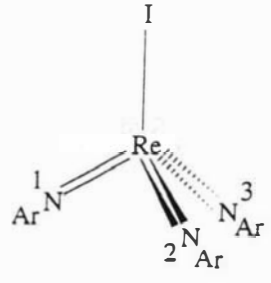	1	165.7(6)		112.2(3)	39	Approx. tetrahedral
	2	169.9(6)	113.8(3)			I-Re-N(1) 106.7(2)
	3	167.5(5)	112.1(3)			I-Re-N(2) 105.9(2)
						I-Re-N(3) 105.4(2)

Table 23: Selected bond angles(°) for $Re_2(NAr)_6$, the Tc analogue and IRe(NAr)$_3$

Complex	#	M-N(#)	M-M	C-N(#)	Ref.	Comments
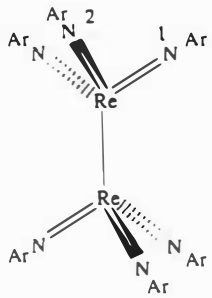	1	1.760(5)	2.7428(7)	1.392(7)	-	
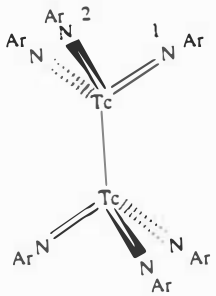	1	1.758(2)	2.744(1)		17	Tc-Tc bond is long
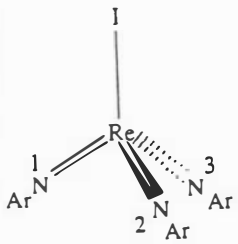	1 2 3	1.770(7) 1.767(6) 1.765(6)			39	I-Re 2.664(1)
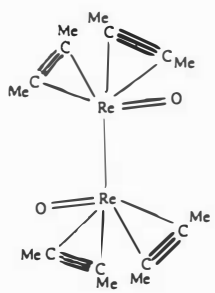			2.686(1)		111	Tetrahedral about Re Staggered ethane-like Single Re-Re bond

Table 24: Selected bond lengths(Å) for $Re_2(NAr)_6$, the Tc analogue, a non-bridging Re(II) dimer and $IRe(NAr)_3$

The terminal imido ligands are essentially linear at 168.5(4)° and compare well to $Tc_2(NAr)_6$ at 167.6(1)° and $IRe(NAr)_3$ ranging from 165.7(6)° to 169.9(6)°.[39] Likewise the N-M-N, M-M-N angles and M-N bond lengths are essentially identical for

both $Re_2(NAr)_6$ and $Tc_2(NAr)_6$ (see tables 23 and 24). The Re-Re bond lies on a crystallographic S_6 axis making all 6 imido ligands symmetry equivalent. The unbridged Re-Re bond of 2.7428(7)Å is longer than that observed in $[Re(NAr')_2(\mu\text{-}NAr')]_2$ (average Re-Re is 2.7354(3)Å) but compares well with $Tc_2(NAr)_6$ (Tc-Tc 2.744(1)Å).[17] The Re(VI)-Re(VI) distances for the oxo-bridging species $[Re(O)(R)_2(\mu\text{-}O)]_2$, R=$CH_2CMe_2Ph$,[108] $CH_2{}^tBu$,[107] CH_2CH_3,[110] and CH_3[106] are 2.6116(7), 2.606(1), 2.6155(6) and 2.593(1)Å respectively, significantly shorter. A Re(II) dimer, $[Re(O)(MeCCMe)_2]_2$ contains a Re-Re bond length of 2.686(1)Å[111] significantly longer than the bridging oxo complexes, but still shorter then found for $Re_2(NAr)_6$. This observation maybe due to steric congestion between the imido groups around the ethane-like structure or to the Re atoms being bridged in the oxo species. The Re(VII)-Re(VII) distances of bridging oxo complexes are much greater ranging from 3.0902(10) to 3.332(4)Å (see table 13 of chapter 3).

On one occasion interaction of $[Re(NAr)_3]^-$ with $Fe(Cp)_2{}^+$ yielded not only the dimer but also a complex containing ferrocene. The complex is thought to be $(NAr)_3Re(C_5H_4FeCp)$ (Fig. 62) formulated by proton NMR (Fig. 63) and mass spect results.

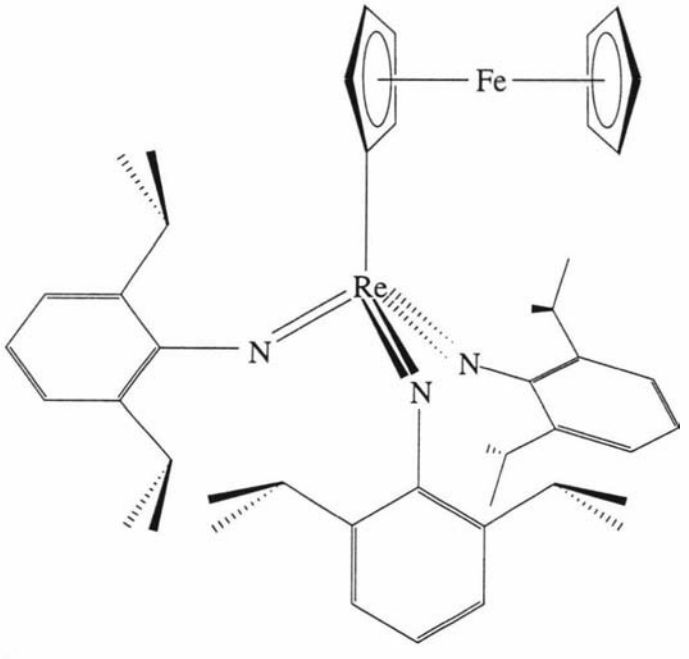

Figure 62

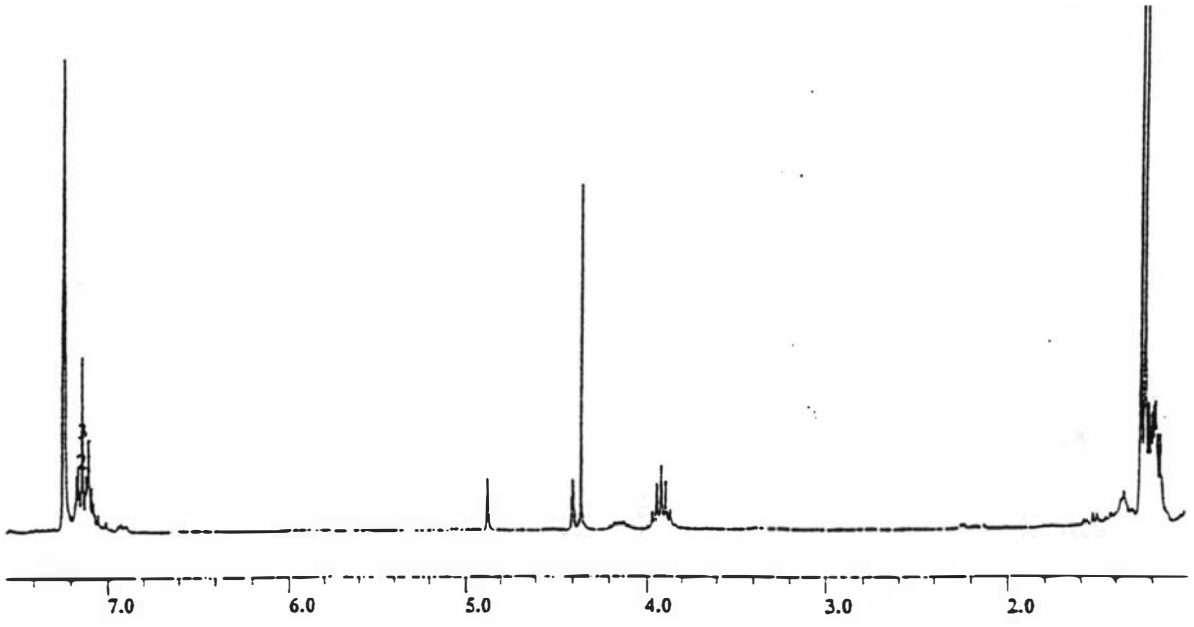

Figure 63

The origin of the ferrocene complex is not established as yet, but it is reasonable to assume it is derived from electrophilic attack of $[Re(NAr)_3]^+$ on ferrocene (Scheme 26). Several attempts to synthesize the complex by interaction of excess $Fe(Cp)_2^+$ with $[Re(NAr)_3]^-$ yielded only the dimers.

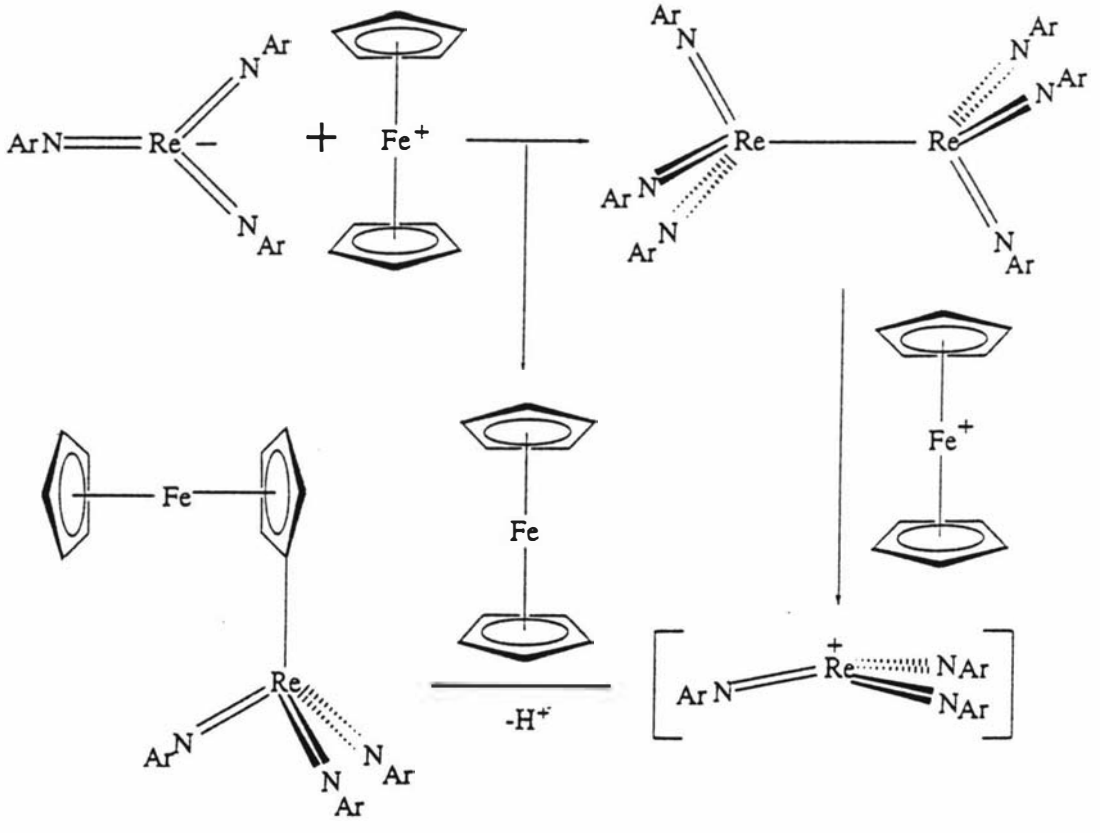

Scheme 26

Three dimers are obtained from the oxidation of $[Re(NAr)_2(NAr')]^-$ in a 1:1:1 ratio rationalised by proton NMR (Fig. 64).

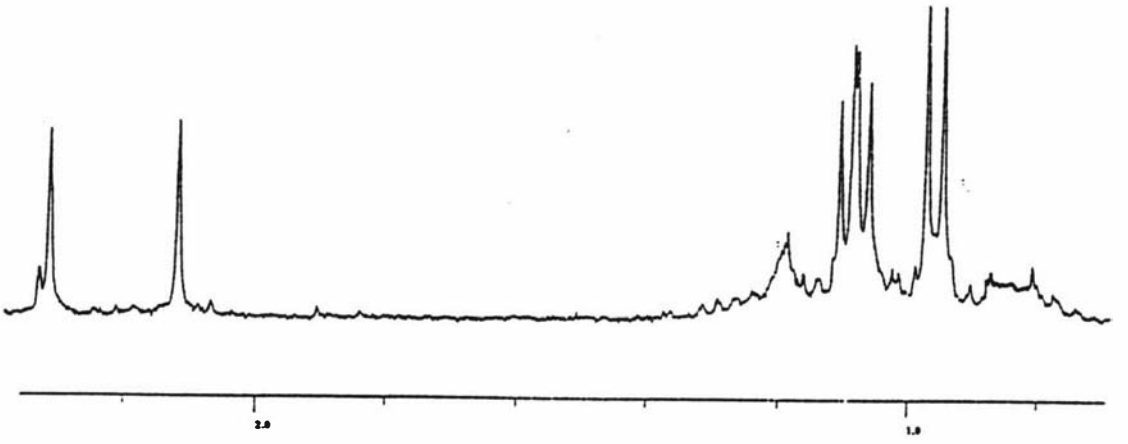

Figure 64

The possible structures of the 3 complexes are given in figure 65. The formation of (I) of figure 65 is perhaps expected given that NAr' is seen to bridge in $[Re(NAr')_2(\mu\text{-}NAr')]_2$. On the basis of the structure of $Re_2(NAr)_6$ which contains no bridging imido ligands, structure (II) and (III) of figure 65 may seem surprising, however the edge-bridged structure is considered to be more stable due, in part, to the greater degree of metal-ligand σ-bonding.[17] Thus it would appear that the steric requirements in the NAr' imido ligand is not great enough to prevent formation of bridging NAr imido ligands.

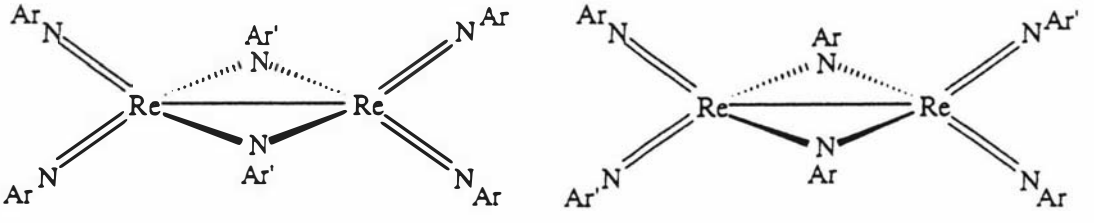

(I) (II)

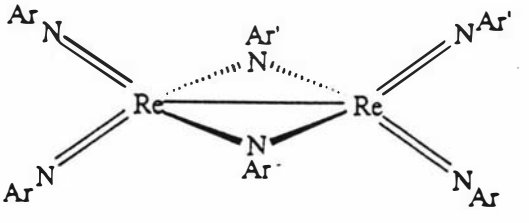

(III)

Figure 65

As the oxidation of $[Re(NAr)_3]^-$ formed the ethane-like, $(ArN)_3Re\text{-}Re(NAr)_3$ it was thought that oxidising $[Re(NAr)_2(N\text{-}o\text{-}^tBu)]^-$ could produce a neutral Re(VI) monomeric complex. This was thought possible on the basis of greater hinderance to forming a Re-Re bond compared with $[Re(NAr)_3]^-$ due to the more sterically demaning *o*-^{t}Bu imido group. However, the ^{1}H nmr of the product revealed it to be diamagnetic, and hence must contain a Re-Re bond. It also revealed a single environment for the iso-propyl and *o*-^{t}Bu imido groups, indicating the structure to be analogous to $Re_2(NAr)_6$, that is $(ArN)_2(o\text{-}^tBuN)Re\text{-}Re(NAr)_2(N\text{-}o\text{-}^tBu)$.

Conclusion

The method of oxidising Re(V) species to the Re(VI) dimeric complexes although successful produces only low yields of product. However without converting the chloro tris(imido) complexes to the iodo derivatives, it is at present the only viable method to produce Re(VI) dimers using the chloro tris(imido) complexes.

The oxidation of $[Re(NAr')_3]^-$ and $[Re(NAr)_3]^-$ produced the expected tetrahedral edge-bridged and ethane-like dimer respectively. The structures of $[Re(NAr')_2(\mu\text{-}NAr')]_2$ and $Re_2(NAr)_6$ were confirmed conclusively by x-ray structural analysis.

X-ray structural analysis of the products from the oxidation of $[Re(NAr)_2(NAr')]^-$ and $[Re(NAr)_2(N\text{-}o\text{-}^tBu)]^-$ was not able to be achieved. However, ^{1}H nmr showed that a mixture of products were obtained from $[Re(NAr)_2(NAr')]^-$ in a 1:1:1 ratio. The complexes contain bridging NAr' and NAr imido ligands. The product from oxidation of $[Re(NAr)_2(N\text{-}o\text{-}^tBu)]^-$ appears to be the ethane-like dimer, $(ArN)_2(o\text{-}^tBuN)Re\text{-}Re(NAr)_2(N\text{-}o\text{-}^tBu)$ on the basis of ^{1}H nmr.

Although a Re(VI) neutral complex, $Re(NR)_3$, was not achieved via oxidation of $[Re(NAr)_2(N\text{-}o\text{-}^tBu)]^-$, evidence of a Re(VII) cation was found when $[Re(NAr)_3]^-$ was oxidised. The complex, $CpFeCpRe(NAr)_3$, is thought to form from electrophilic attack of $[Re(NAr)_3]^+$ towards ferrocene.

Experimental Section

General

General experimental procedures and details regarding the instrumentation used are given in appendix I. ^{1}H NMR were recorded in d_6-benzene and referenced to

benzene at 7.15ppm. ^{13}C NMR were recorded in d_6-benzene and referenced to benzene at 128ppm. Deuterated benzene was purchased from Acros and freeze pumped thawed 3 times before use. THF was distilled from sodium/benzophenone. Pentane and hexane were distilled from sodium. $[Cp_2Fe][BF_4]$ was prepared from literature methods[114] (see appendix I) and freshly prepared before use.

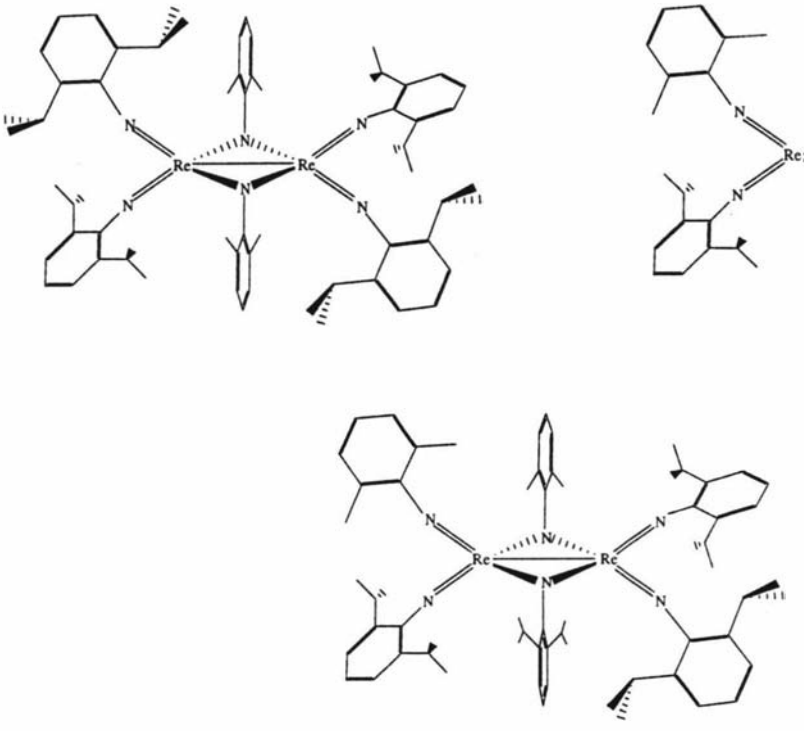

$Re_2(NAr)_4(NAr')_2$

Sodium (0.008g, 0.35mmol) was added to a solution of $ClRe(NAr)_2(NAr')$ (0.111g, 0.16mmol) in THF (10mL). The mixture was stirred until the red colour was no longer evident. The solution was then filtered through celite into a slurry containing $[Cp_2Fe][BF_4]$ (0.100g, 0.37mmol) in THF (10mL). The resulting red solution was then stirred for 4 hours. The solvent was removed *in vacuo* and the residue extracted with pentane (20mL). The pentane solution was filtered through celite and reduced in volume. The filtrate was cooled to -35°C resulting in precipitation of ferrocene which was then filtered off. Any remaining ferrocene was removed by column chromatography with silica gel using hexane as an eluent. Once all the ferrocene is removed the product is obtained by then using benzene as the eluent resulting in a red solution. The benzene is then removed *in vacuo* and a minimal amount of hexane is then added. This hexane solution was cooled to -35°C yielding 0.020g of a red solid.

^{1}H NMR (C_6D_6): 6.70-7.10(m, 54, Ar/Ar'), 3.73(sept, 9, J=6.8, terminal C<u>H</u>Me_2), 3.51(hep, 3, bridging C<u>H</u>Me_2), 2.33(s, 18, bridging *o*-C<u>H</u>$_3$), 2.14(s, 18, terminal *o*-C<u>H</u>$_3$), 1.07-1.18(m, 108, terminal CH(C<u>H</u>$_3$)$_2$), 0.97(d, 36,J=7.0, bridging CH(C<u>H</u>$_3$)$_2$)

Mass Spect. M^+ 1311, M^+-NAr 1136, M^+-Re(NAr)$_2$(NAr') 656, M^+-Re(NAr)$_3$(NAr') 480

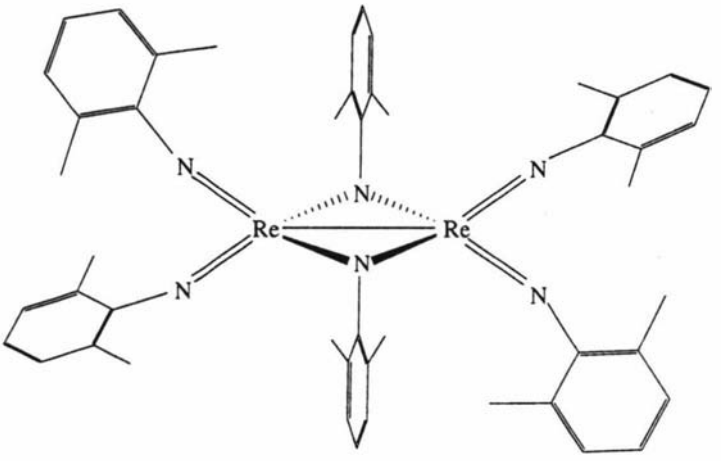

[Re(NAr')$_2$(μ-NAr')]$_2$

Sodium (0.015g, 0.65mmol) was added to a solution of $Me_3SiORe(NAr')_3$ (0.194g, 0.31mmol) in THF (10mL). The mixture was stirred until the red colour was no longer evident. The solution was then filtered through celite into a slurry containing [Cp_2Fe][BF_4] (0.195g, 0.72mmol) in THF (10mL). The resulting red solution was then stirred for 4 hours. The solvent was removed *in vacuo* and the residue extracted with pentane (20mL). The pentane solution was filtered through celite and reduced in volume. The filtrate was cooled to -35°C resulting in precipitation of ferrocene which was then filtered off. Any remaining ferrocene was removed by column chromatography with silica gel using hexane as an eluent. Once all the ferrocene is removed the product is obtained by then using benzene as the eluent resulting in a red solution. The benzene is then removed *in vacuo* and a minimal amount of hexane is then added. This hexane solution was cooled to -35°C yielding 0.032g (19%) of a red solid.

^{1}H NMR (C_6D_6): 6.95-7.15(m, 6, bridging Ar'), 6.60-6.85(m, 12, terminal Ar'), 2.21(s, 12, bridging *o*-C<u>H</u>$_3$), 2.14(s, 24, terminal *o*-C<u>H</u>$_3$)

Mass Spect. M^+ 1087, M^+-NAr' 968, M^+-Re(NAr')$_3$ 544

Found: C, 53.58 ; H, 5.54 ; N, 6.94; Calc: C, 53.02 ; H, 5.01 ; N, 7.73

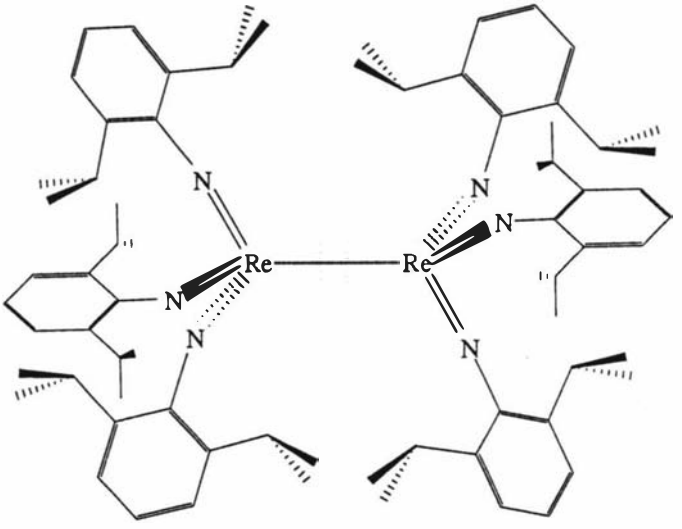

$Re_2(NAr)_6$

Sodium (0.010g, 0.43mmol) was added to a solution of ClRe(NAr)$_3$ (0.152g, 0.20mmol) in THF (10mL). The mixture was stirred until the red colour was no longer evident. The solution was then filtered through celite into a slurry containing [Cp_2Fe][BF_4] (0.124g, 0.46mmol) in THF (10mL). The resulting red solution was then stirred for 4 hours. The solvent was removed *in vacuo* and the residue extracted with pentane (20mL). The pentane solution was filtered through celite and reduced in volume. The filtrate was cooled to -35°C resulting in precipitation of ferrocene which was then filtered off. Any remaining ferrocene was removed by column chromatography with silica gel using hexane as an eluent. Once all the ferrocene is removed the product is obtained by then using benzene as the eluent resulting in a red solution. The benzene is then removed *in vacuo* and a minimal amount of hexane is then added. This hexane solution was cooled to -35°C yielding 0.043g (30%) of a red solid.

^{1}H NMR (C_6D_6): 7.09(d, 12, J=7.1, Ar), 6.97(t, 6, J=7.1, Ar), 3.76(sept, 6, J=6.8, C$\underline{H}$Me$_2$), 1.09(d, 72, J=7.0, CH(C$\underline{H}_3$)$_2$)

Mass Spect. M^+ 1424, M^+-NAr 1249, M^+-Re(NAr)$_3$ 712
Found: C, 60.93 ; H, 7.06 ; N, 5.64; Calc: C, 60.73 ; H, 7.22 ; N, 5.90

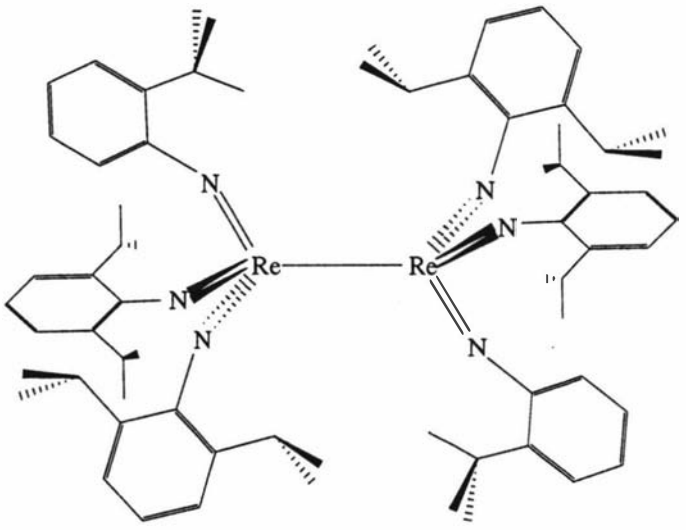

$Re_2(NAr)_4(N\text{-}o\text{-}^tBu)_2$

Sodium (0.010g, 0.43mmol) was added to a solution of $ClRe(NAr)_2(N\text{-}o\text{-}^tBu)$ (0.151g, 0.21mmol) in THF (10mL). The mixture was stirred until the red colour was no longer evident. The solution was then filtered through celite into a slurry containing $[Cp_2Fe][BF_4]$ (0.132g, 0.49mmol) in THF (10mL). The resulting red solution was then stirred for 4 hours. The solvent was removed *in vacuo* and the residue extracted with pentane (20mL). The pentane solution was filtered through celite and reduced in volume. The filtrate was cooled to -35°C resulting in precipitation of ferrocene which was then filtered off. Any remaining ferrocene was removed by column chromatography with silica gel using hexane as an eluent. Once all the ferrocene is removed the product is obtained by then using benzene as the eluent resulting in a red solution. The benzene is then removed *in vacuo* and a minimal amount of hexane is then added. This hexane solution was cooled to -35°C yielding 0.025g (17%) of a red solid.

^1H NMR (C_6D_6): 7.20(d, 2, J=7.2, *o*-*t*-butylphenyl), 6.99(d, 8, J=7.0, Ar), 6.65-6.92(m, 10, Ar/*o*-*t*-butylphenyl), 3.63(sept, 8, J=6.8, C<u>H</u>Me_2), 1.47(s, 18, *o*-*t*-butyl), 1.03(d, 48,J=7.0, $CH(C\underline{H}_3)_2$)

Mass Spect. M^+ 1368, M^+-NAr 1193, M^+-$Re(NAr)_2(N\text{-}o\text{-}^tBu)$ 684

Found: C, 60.48 ; H, 6.57 ; N, 5.84; Calc: C, 59.71 ; H, 6.93 ; N, 6.14

Summary

This thesis described the synthesis of a variety of tetrahedral Re(VII) tris(imido) complexes (Fig. 66).

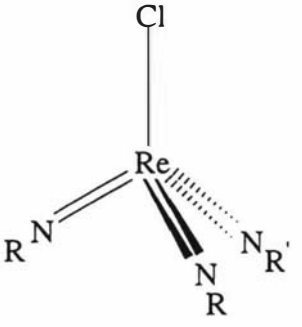

Figure 66

It was found that bis(imido) complexes ($Re(NR)_2Cl_3(py)$) react with anilines in the presence of NEt_3 forming tris(imido) complexes. This methodology allows for control over the choice of R and R', a situation not previously described in the literature. It turns out that the steric bulk of the coordinated imido ligand is a critical factor in the structure and reactivity of imido complexes. Such control over the steric nature of the R and R' groups is very important for determining both stability and reactivity in π-loaded complexes.

The action of pyHCl towards tris(imido) complexes ($XRe(NR)_3$) results in the loss of an imido ligand as H_2NR and formation of bis(imido) complexes, $Re(NR)_2Cl_3(py)$. The imido ligand that is removed is not chosen at random. The reaction of $ClRe(NAr')_2(NAr)$ with 2 equivalents of pyHCl results in only a mixed bis(imido) complex, $Re(NAr)(NAr')Cl_3(py)$, no $Re(NAr')_2Cl_3(py)$ is formed, again providing control in the formation of mixed imido complexes.

Tetrahedral Re(VII) tris(imido) complexes are readily reduced to trigonal planar Re(V) tris(imido) anions (Fig. 67) with elemental sodium.

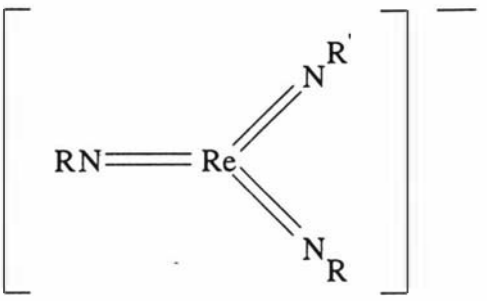

Figure 67

It has been reported previously that reduction of $ClRe(NAr')_3$ using NaHg results in formation of $[Re(NAr')_2(\mu\text{-}NAr')]_2$, which does not undergo further reduction.[12] However, in our hands reaction of $ClRe(NAr')_3$ with 2 equivalents of Na results in good yields of $[Re(NAr')_3]^-$.

The usual route to d^1 Re(VI) tris(imido) complexes involves a 1-electron reduction of the Re(VII) species. However, this method was discarded in favour of 1-electron oxidations of Re(V) anions. This method resulted in isolation of d^1-d^1 dimers whose structures were found to be either edge-bridged (Fig. 68) or ethane-like (Fig.69), depending on the steric bulk of R.

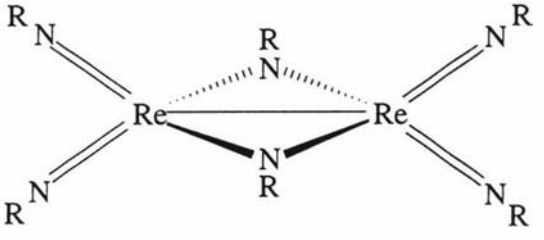

Figure 68

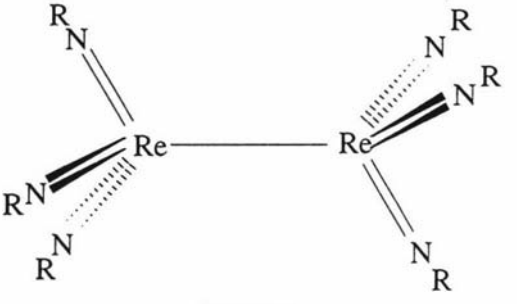

Figure 69

Oxidation of $[Re(NAr')_3]^-$ and $[Re(NAr)_2(NAr')]^-$ resulted in edge-bridged dimers, while oxidation of $[Re(NAr)_3]^-$ and $[Re(NAr)_2(N\text{-}o\text{-}^tBu)]^-$ resulted in the ethane-like configurations.

To conclude the methodology described in this thesis provides the first systematic route to mixed imido complexes. It also confirms that reactivity of π-loaded complexes is highly dependent upon steric factors.

Appendix I

General experimental procedures, details regarding the instrumentation used and preparation of precursors

---

General experimental procedures

Unless otherwise noted all reactions and manipulations were performed in dry glassware under an argon atmosphere in a drybox. All solvents used for preparation described in this thesis were distilled. Solvents and other liquids brought into the drybox were placed in a vessel, which was first purged of air by 3 cycles of evacuation followed by filling with argon, and subsequently purged with argon by 3 cycles of evacuation. Solids brought into the drybox were placed in an oven dried vessel, the opening was then covered with tissue paper, and placed in the antechamber to be evacuated twice. All glassware used was clean, oven dried and free of grease prior to placement in the antechamber. Celite was first oven dried for at least 3 days before placement in the antechamber, followed by evacuation in the antechamber for 24 hours.

Instrumentation and analysis

Nuclear magnetic resonance spectroscopy was preformed at 6.34 Tesla on a JEOL GX270W Spectrometer operating in the fourier transform mode at 270 MHz for ^{1}H and ^{13}C nuclei. Samples were run using deuterated benzene and were referenced to benzene at 7.15ppm (^{1}H) and 128ppm (^{13}C).

Elemental analysis was carried out using standard techniques at the Campbell Microanalytical Laboratory of the University of Otago, Dunedin.

X-ray intensity data was collected either at Canterbury University or the University of Auckland. The structural determination and refinement was carried out at Massey University by Prof. Anthony Burrell. Details on data collection and structural refinement for the complexes are given below.

Crystal data and structure refinement for $Me_3SiORe(NAr')_3$

Empirical formula	C27 H36 N3 O Re Si	
Formula weight	632.88	
Temperature	203(2) K	
Wavelength	0.71073 Å	
Crystal system	P-31c	
Space group	HEXAGONAL	
Unit cell dimensions	a = 12.567(2) Å	α= 90°.
	b = 12.567(2) Å	β= 90°.
	c = 10.084(2) Å	γ = 120°.
Volume	1379.2(4) $Å^3$	
Z	2	
Density (calculated)	1.524 Mg/m^3	
Absorption coefficient	4.471 mm^{-1}	
F(000)	632	
Crystal size	0.37 x 0.27 x 0.24 mm^3	
Theta range for data collection	1.87 to 25.05°.	
Index ranges	-12<=h<=7, -14<=k<=0, -11<=l<=11	
Reflections collected	2471	
Independent reflections	1617 [R(int) = 0.0308]	
Completeness to theta = 0.50°	0.0 %	
Absorption correction	Empirical via scans	
Max. and min. transmission	0.4133 and 0.2885	
Refinement method	Full-matrix least-squares on F^2	
Data / restraints / parameters	1617 / 1 / 100	
Goodness-of-fit on F^2	1.078	
Final R indices [I>2sigma(I)]	R1 = 0.0301, wR2 = 0.0790	
R indices (all data)	R1 = 0.0322, wR2 = 0.0802	
Absolute structure parameter	0.02(2)	
Largest diff. peak and hole	0.917 and -1.499 $e.Å^{-3}$	

Crystal data and structure refinement for $ClRe(NAr)_3$

Empirical formula	C36 H51 Cl N3 Re	
Formula weight	747.45	
Temperature	203(2) K	
Wavelength	0.71073 Å	
Crystal system	Tetragonal	
Space group	Fdd2	
Unit cell dimensions	a = 36.6856(2) Å	α= 90°.
	b = 39.7996(2) Å	β= 90°.
	c = 10.49280(10) Å	γ = 90°.
Volume	15320.25(18) $Å^3$	
Z	16	
Density (calculated)	1.296 Mg/m^3	
Absorption coefficient	3.267 mm^{-1}	
F(000)	6080	
Crystal size	0.55 x 0.32 x 0.20 mm^3	
Theta range for data collection	1.51 to 27.54°.	
Index ranges	-47<=h<=45, -51<=k<=45, -13<=l<=11	
Reflections collected	22168	
Independent reflections	7559 [R(int) = 0.0331]	
Completeness to theta = 0.50°	0.0 %	
Absorption correction	Semi-empirical from equivalents	
Max. and min. transmission	0.5611 and 0.2666	
Refinement method	Full-matrix least-squares on F^2	
Data / restraints / parameters	7559 / 1 / 371	
Goodness-of-fit on F^2	1.197	
Final R indices [I>2sigma(I)]	R1 = 0.0379, wR2 = 0.1099	
R indices (all data)	R1 = 0.0456, wR2 = 0.1182	
Absolute structure parameter	0.314(14)	
Largest diff. peak and hole	1.794 and -0.616 $e.Å^{-3}$	

Crystal data and structure refinement for $ClRe(NAr)_2(NAr')$

Empirical formula	C32 H43 Cl N3 Re	
Formula weight	691.34	
Temperature	203(2) K	
Wavelength	0.71073 Å	
Crystal system	monoclinic	
Space group	P2(1)/c	
Unit cell dimensions	a = 18.622(4) Å	α= 90°.
	b = 21.918(4) Å	β= 103.10(3)°.
	c = 15.955(3) Å	γ = 90°.
Volume	6343(2) $Å^3$	
Z	8	
Density (calculated)	1.448 Mg/m^3	
Absorption coefficient	3.939 mm^{-1}	
F(000)	2784	
Crystal size	0.34 x 0.26 x 0.18 mm^3	
Theta range for data collection	1.46 to 20.02°.	
Index ranges	0<=h<=17, 0<=k<=21, -15<=l<=7	
Reflections collected	5248	
Independent reflections	5122 [R(int) = 0.0845]	
Max. and min. transmission	0.5374 and 0.3477	
Refinement method	Full-matrix least-squares on F^2	
Data / restraints / parameters	5122 / 7 / 593	
Goodness-of-fit on F^2	0.994	
Final R indices [I>2sigma(I)]	R1 = 0.0438, wR2 = 0.1313	
R indices (all data)	R1 = 0.1519, wR2 = 0.2023	
Largest diff. peak and hole	0.826 and -0.871 $e.Å^{-3}$	

Crystal data and structure refinement for $ClRe(NAr)_2(N\text{-}o\text{-}^tBu)$

Empirical formula	C34 H47 Cl N3 Re	
Formula weight	719.40	
Temperature	200(2) K	
Wavelength	0.71073 Å	
Crystal system	Triclinic	
Space group	P-1	
Unit cell dimensions	a = 10.6026(2) Å	α= 80.3510(10)°.
	b = 10.6126(2) Å	β= 72.8540(10)°.
	c = 15.93340(10) Å	γ = 81.98°.
Volume	1681.19(5) $Å^3$	
Z	2	
Density (calculated)	1.421 Mg/m^3	
Absorption coefficient	3.718 mm^{-1}	
F(000)	728	
Crystal size	0.38 x 0.17 x 0.06 mm^3	
Theta range for data collection	1.35 to 27.48°.	
Index ranges	-13<=h<=13, -13<=k<=13, -20<=l<=20	
Reflections collected	16481	
Independent reflections	7301 [R(int) = 0.0205]	
Completeness to theta = 0.50°	0.0 %	
Absorption correction	Semi-empirical from equivalents	
Max. and min. transmission	0.8077 and 0.3323	
Refinement method	Full-matrix least-squares on F^2	
Data / restraints / parameters	7301 / 0 / 352	
Goodness-of-fit on F^2	0.704	
Final R indices [I>2sigma(I)]	R1 = 0.0214, wR2 = 0.0707	
R indices (all data)	R1 = 0.0253, wR2 = 0.0813	
Largest diff. peak and hole	0.628 and -1.051 $e.Å^{-3}$	

Crystal data and structure refinement for $MeRe(NAr)_2(NAr')$

Empirical formula	C33 H46 N3 Re	
Formula weight	670.93	
Temperature	203(2) K	
Wavelength	0.71073 Å	
Crystal system	Monoclinic	
Space group	P2(1)/c	
Unit cell dimensions	a = 9.3838(3) Å	α= 90°.
	b = 39.3038(11) Å	β= 107.7890(10)°.
	c = 9.1197(2) Å	γ = 90°.
Volume	3202.70(15) $Å^3$	
Z	4	
Density (calculated)	1.391 Mg/m^3	
Absorption coefficient	3.818 mm^{-1}	
F(000)	1360	
Crystal size	0.53 x 0.40 x 0.26 mm^3	
Theta range for data collection	1.04 to 27.52°.	
Index ranges	-12<=h<=9, -51<=k<=49, -11<=l<=11	
Reflections collected	19520	
Independent reflections	7073 [R(int) = 0.0279]	
Completeness to theta = 0.50°	0.0 %	
Absorption correction	Semi-empirical from equivalents	
Max. and min. transmission	0.4368 and 0.2368	
Refinement method	Full-matrix least-squares on F^2	
Data / restraints / parameters	7073 / 0 / 334	
Goodness-of-fit on F^2	1.242	
Final R indices [I>2sigma(I)]	R1 = 0.0361, wR2 = 0.0812	
R indices (all data)	R1 = 0.0393, wR2 = 0.0834	
Largest diff. peak and hole	1.514 and -2.595 $e.Å^{-3}$	

Crystal data and structure refinement for $[Re(NAr)_2(p\text{-tol})(\mu\text{-}O)]_2$

Empirical formula	C31 H41 N2 O Re	
Formula weight	643.86	
Temperature	203(2) K	
Wavelength	0.71073 Å	
Crystal system	Monoclinic	
Space group	P2(1)/n	
Unit cell dimensions	a = 13.9361(2) Å	α= 90°.
	b = 15.5442(2) Å	β= 90.6710(10)°.
	c = 14.0110(2) Å	γ = 90°.
Volume	3034.93(7) $Å^3$	
Z	4	
Density (calculated)	1.409 Mg/m^3	
Absorption coefficient	4.027 mm^{-1}	
F(000)	1296	
Crystal size	0.28 x 0.25 x 0.16 mm^3	
Theta range for data collection	1.96 to 26.28°.	
Index ranges	-17<=h<=17, 0<=k<=19, 0<=l<=17	
Reflections collected	6054	
Independent reflections	6054 [R(int) = 0.0000]	
Completeness to theta = 0.50°	0.0 %	
Absorption correction	Semi-empirical from equivalents	
Max. and min. transmission	0.5651 and 0.3985	
Refinement method	Full-matrix least-squares on F^2	
Data / restraints / parameters	6054 / 0 / 316	
Goodness-of-fit on F^2	1.031	
Final R indices [I>2sigma(I)]	R1 = 0.0281, wR2 = 0.0651	
R indices (all data)	R1 = 0.0375, wR2 = 0.0700	
Largest diff. peak and hole	1.042 and -0.835 $e.Å^{-3}$	

Crystal data and structure refinement for $Re(NAr')_2Cl_3(py)$

Empirical formula	C30 H32 Cl3 N3 Re	
Formula weight	727.14	
Temperature	203(2) K	
Wavelength	0.71073 Å	
Crystal system	triclinic	
Space group	P-1	
Unit cell dimensions	a = 8.874(2) Å	α= 73.32(3)°.
	b = 10.735(2) Å	β= 81.45(3)°.
	c = 16.561(3) Å	γ = 73.97(3)°.
Volume	1448.4(5) $Å^3$	
Z	2	
Density (calculated)	1.667 Mg/m^3	
Absorption coefficient	4.496 mm^{-1}	
F(000)	718	
Crystal size	0.28 x 0.14 x 0.13 mm^3	
Theta range for data collection	2.04 to 22.50°.	
Index ranges	0<=h<=9, -11<=k<=11, -17<=l<=17	
Reflections collected	4091	
Independent reflections	3794 [R(int) = 0.1559]	
Completeness to theta = 0.50°	0.0 %	
Max. and min. transmission	0.5926 and 0.3658	
Refinement method	Full-matrix least-squares on F^2	
Data / restraints / parameters	3794 / 0 / 334	
Goodness-of-fit on F^2	1.071	
Final R indices [I>2sigma(I)]	R1 = 0.1205, wR2 = 0.3267	
R indices (all data)	R1 = 0.1239, wR2 = 0.3371	
Largest diff. peak and hole	6.785 and -10.431 $e.Å^{-3}$	

Crystal data and structure refinement for *p*-tolNHRe(NAr)$_3$

Empirical formula	C43 H59 N4 Re	
Formula weight	818.14	
Temperature	203(2) K	
Wavelength	0.71073 Å	
Crystal system	Monoclinic	
Space group	P2(1)/c	
Unit cell dimensions	a = 22.8290(4) Å	α= 90°.
	b = 10.33220(10) Å	β= 110.5910(10)°.
	c = 18.6566(3) Å	γ = 90°.
Volume	4119.47(11) Å^3	
Z	4	
Density (calculated)	1.319 Mg/m^3	
Absorption coefficient	2.982 mm^{-1}	
F(000)	1680	
Crystal size	0.44 x 0.18 x 0.13 mm^3	
Theta range for data collection	1.91 to 27.45°.	
Index ranges	-20<=h<=29, -9<=k<=13, -24<=l<=23	
Reflections collected	22850	
Independent reflections	9057 [R(int) = 0.0358]	
Completeness to theta = 0.50°	0.0 %	
Absorption correction	Semi-empirical from equivalents	
Max. and min. transmission	0.6978 and 0.3537	
Refinement method	Full-matrix least-squares on F^2	
Data / restraints / parameters	9057 / 0 / 433	
Goodness-of-fit on F^2	1.051	
Final R indices [I>2sigma(I)]	R1 = 0.0359, wR2 = 0.0640	
R indices (all data)	R1 = 0.0549, wR2 = 0.0712	
Largest diff. peak and hole	0.909 and -0.921 e.Å^{-3}	

Crystal data and structure refinement for $[Re(NAr')_3][Na(thf)_6]$

Empirical formula	C48 H75 N3 Na O6 Re	
Formula weight	999.30	
Temperature	200(2) K	
Wavelength	0.71073 Å	
Crystal system	Monoclinic	
Space group	C2/c	
Unit cell dimensions	a = 16.009(3) Å	α= 90°.
	b = 19.903(4) Å	β= 107.53(3)°.
	c = 16.524(3) Å	γ = 90°.
Volume	5020.5(17) $Å^3$	
Z	4	
Density (calculated)	1.322 Mg/m^3	
Absorption coefficient	2.475 mm^{-1}	
F(000)	2072	
Crystal size	0.48 x 0.34 x 0.21 mm^3	
Theta range for data collection	1.68 to 27.47°.	
Index ranges	-18<=h<=20, -24<=k<=25, -20<=l<=14	
Reflections collected	15072	
Independent reflections	5528 [R(int) = 0.0163]	
Completeness to theta = 0.50°	0.0 %	
Absorption correction	Semi-empirical from equivalents	
Max. and min. transmission	0.6245 and 0.3829	
Refinement method	Full-matrix least-squares on F^2	
Data / restraints / parameters	5528 / 0 / 269	
Goodness-of-fit on F^2	1.057	
Final R indices [I>2sigma(I)]	R1 = 0.0279, wR2 = 0.0747	
R indices (all data)	R1 = 0.0316, wR2 = 0.0777	
Largest diff. peak and hole	0.776 and -0.762 $e.Å^{-3}$	

Crystal data and structure refinement for $Me_3SnRe(NAr)_3$

Empirical formula	C39 H60 N3 Re Sn	
Formula weight	875.79	
Temperature	168(2) K	
Wavelength	0.71073 Å	
Crystal system	Monoclinic	
Space group	P2(1)/m	
Unit cell dimensions	a = 10.035(2) Å	α= 90°.
	b = 14.976(4) Å	β= 99.816(3)°.
	c = 13.322(3) Å	γ = 90°.
Volume	1972.9(8) $Å^3$	
Z	2	
Density (calculated)	1.474 Mg/m^3	
Absorption coefficient	3.726 mm^{-1}	
F(000)	880	
Crystal size	0.77 x 0.56 x 0.38 mm^3	
Theta range for data collection	2.36 to 26.52°.	
Index ranges	-12<=h<=12, -18<=k<=6, -16<=l<=16	
Reflections collected	12989	
Independent reflections	4191 [R(int) = 0.0532]	
Completeness to theta = 0.50°	0.0 %	
Absorption correction	Semi-empirical from equivalents	
Max. and min. transmission	0.3317 and 0.1615	
Refinement method	Full-matrix least-squares on F^2	
Data / restraints / parameters	4191 / 18 / 382	
Goodness-of-fit on F^2	1.003	
Final R indices [I>2sigma(I)]	R1 = 0.0302, wR2 = 0.0725	
R indices (all data)	R1 = 0.0379, wR2 = 0.0758	
Largest diff. peak and hole	1.750 and -2.863 $e.Å^{-3}$	

Crystal data and structure refinement for $Me_3SnRe(NAr)_2(NAr')$

Empirical formula	C35 H52 N3 Re Sn	
Formula weight	819.69	
Temperature	168(2) K	
Wavelength	0.71073 Å	
Crystal system	Triclinic	
Space group	P1	
Unit cell dimensions	a = 11.078(2) Å	α= 71.892(2)°.
	b = 11.324(2) Å	β= 74.177(2)°.
	c = 16.683(3) Å	γ = 67.195(3)°.
Volume	1805.9(6) $Å^3$	
Z	2	
Density (calculated)	1.507 Mg/m^3	
Absorption coefficient	4.065 mm^{-1}	
F(000)	816	
Crystal size	0.76 x 0.57 x 0.44 mm^3	
Theta range for data collection	2.01 to 26.44°.	
Index ranges	-13<=h<=13, -14<=k<=10, -20<=l<=20	
Reflections collected	23210	
Independent reflections	7326 [R(int) = 0.0293]	
Completeness to theta = 0.50°	0.0 %	
Absorption correction	Semi-empirical from equivalents	
Max. and min. transmission	0.2679 and 0.1482	
Refinement method	Full-matrix least-squares on F^2	
Data / restraints / parameters	7326 / 0 / 361	
Goodness-of-fit on F^2	0.625	
Final R indices [I>2sigma(I)]	R1 = 0.0224, wR2 = 0.0677	
R indices (all data)	R1 = 0.0270, wR2 = 0.0739	
Largest diff. peak and hole	0.350 and -1.491 $e.Å^{-3}$	

Crystal data and structure refinement for $[Re(NAr')_2(\mu\text{-}NAr')]_2$

Empirical formula	C48 H54 N6 Re2	
Formula weight	1087.37	
Temperature	203(2) K	
Wavelength	0.71073 Å	
Crystal system	Monoclinic	
Space group	P2(1)/n	
Unit cell dimensions	a = 10.43990(10) Å	α= 90°.
	b = 20.3130(2) Å	β= 92.48°.
	c = 20.9124(3) Å	γ = 90°.
Volume	4430.66(9) $Å^3$	
Z	4	
Density (calculated)	1.630 Mg/m^3	
Absorption coefficient	5.498 mm^{-1}	
F(000)	2136	
Crystal size	0.54 x 0.32 x 0.26 mm^3	
Theta range for data collection	1.40 to 28.21°.	
Index ranges	-13<=h<=13, 0<=k<=27, 0<=l<=27	
Reflections collected	9956	
Independent reflections	9956 [R(int) = 0.0000]	
Completeness to theta = 0.50°	0.0 %	
Absorption correction	Semi-empirical from equivalents	
Max. and min. transmission	0.3290 and 0.1552	
Refinement method	Full-matrix least-squares on F^2	
Data / restraints / parameters	9956 / 0 / 505	
Goodness-of-fit on F^2	0.752	
Final R indices [I>2sigma(I)]	R1 = 0.0266, wR2 = 0.0845	
R indices (all data)	R1 = 0.0362, wR2 = 0.0956	
Largest diff. peak and hole	0.897 and -1.948 $e.Å^{-3}$	

Crystal data and structure refinement for $Re_2(NAr)_6$

Empirical formula	C36 H51 N3 Re	
Formula weight	712.00	
Temperature	203(2) K	
Wavelength	0.71073 Å	
Crystal system	Rhomohedral	
Space group	R-3	
Unit cell dimensions	a = 13.30190(10) Å	α= 90°.
	b = 13.30190(10) Å	β= 90°.
	c = 33.3445(2) Å	γ = 120°.
Volume	5109.54(6) $Å^3$	
Z	6	
Density (calculated)	1.388 Mg/m^3	
Absorption coefficient	3.594 mm^{-1}	
F(000)	2178	
Crystal size	0.28 x 0.18 x 0.13 mm^3	
Theta range for data collection	1.83 to 26.99°.	
Index ranges	-16<=h<=8, 0<=k<=16, -42<=l<=41	
Reflections collected	4706	
Independent reflections	2465 [R(int) = 0.0160]	
Completeness to theta = 0.50°	0.0 %	
Absorption correction	Semi-empirical from equivalents	
Max. and min. transmission	0.6523 and 0.4327	
Refinement method	Full-matrix least-squares on F^2	
Data / restraints / parameters	2465 / 0 / 121	
Goodness-of-fit on F^2	1.004	
Final R indices [I>2sigma(I)]	R1 = 0.0409, wR2 = 0.1080	
R indices (all data)	R1 = 0.0489, wR2 = 0.1226	
Largest diff. peak and hole	4.320 and -3.087 $e.Å^{-3}$	

Synthesis of precursors

LiNHp-tol

Neat BuLi (0.298g, 4.66mmol) in 7mL of benzene was added to a vigorously stirring solution containing *p*-tolNH_2 (0.510g, 4.76mmol) in 10mL of benzene. The solution was stirred for a further 5 minutes. The white solid was then removed by filtering and washed with generously amounts of benzene, yielding 0.474g (90%) of the lithium amide.

$[Fe(C_5H_5)_2][BF_4]$[114]

To a solution of *p*-benzoquinone (0.43g, 3.98mmol) in diethylether (60mL) was added 1.4mL of a 40% aqueous solution of tetrafluoroboric acid. To this solution was added ferrocene (0.37g, 1.99mmol) in diethylether (60mL). The dark blue solid was then filtered and washed thoroughly with diethylether to yield 0.869g (80%).

Sodium Balls

In order to accurately weigh milligram amounts of sodium the following procedure was developed to obtain small quantities of sodium.

A lump of clean sodium was added to a scintillation vile containing a magnetic flea and enough toluene to cover the lump of sodium. The toluene was heated to boiling and the sodium stirred vigorously, the sodium should melt and form little balls. Let the solution cool down while continuing to stir, before filtering.

Appendix II

Tables of selected bond lengths and angles of structurally characterized complexes reported within this thesis

---

The tables that follow contain selected bond distances (Å) and angles (°) for the following complexes;

$Me_3SiORe(NAr')_3$	chapter 2, page 74
$ClRe(NAr)_3$	chapter 2, page 77
$ClRe(NAr)_2(NAr')$	chapter 2, page 90
$ClRe(NAr)_2(N\text{-}o\text{-}^tBu)$	chapter 2, page 92
$MeRe(NAr)_2(NAr')$	chapter 3, page 121
$[Re(NAr)_2(p\text{-tol})(\mu\text{-}O)]_2$	chapter 3, page 126
$Re(NAr')_2Cl_3(py)$	chapter 3, page 131
p-tolNHRe$(NAr)_3$	chapter 3, page 133
$[Re(NAr')_3][Na(thf)_6]$	chapter 4, page 155
$Me_3SnRe(NAr)_3$	chapter 4, page 159
$Me_3SnRe(NAr)_2(NAr')$	chapter 4, page 159
$[Re(NAr')_2(\mu\text{-}NAr')]_2$	chapter 5, page 179
$Re_2(NAr)_6$	chapter 5, page 184

Statistics involving the bond lengths and angles presented in the following tables are given at the end of table 28.

Complex	Re-X	Re-N(1)	Re-N(2)	Re-N(3)
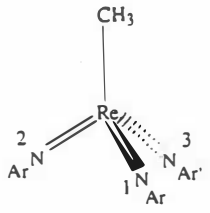	2.113(5)	1.763(4)	1.757(3)	1.753(4)
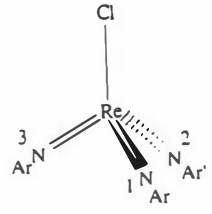	2.271(9) 2.272(9)	1.70(2) 1.72(2)	1.725(18) 1.766(19)	1.71(2) 1.73(2)
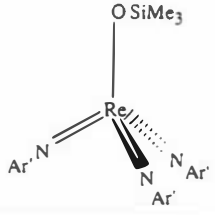	1.840(12)	1.749(6)		
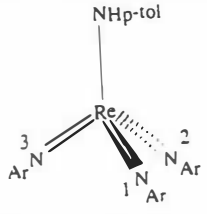	1.969(3)	1.754(3)	1.769(3)	1.757(3)
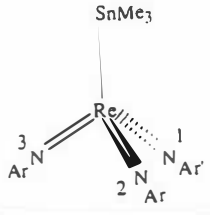	2.7354(6)	1.779(3)	1.766(3)	1.762(3)
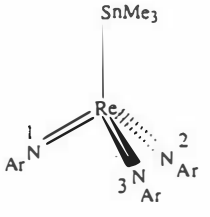	2.7416(8)	1.752(6)	1.760(4)	1.756(6)

Table 25 Selected bond lengths (Å) of $[Re(NAr')_3]^-$ and tetrahedral tris(imido) complexes reported in this thesis

Complex	Re-X	Re-N(1)	Re-N(2)	Re-N(3)
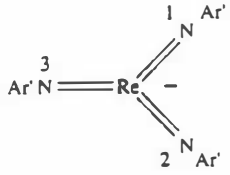		1.762(3)	1.772(2)	1.772(2)
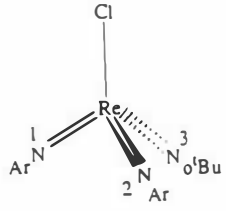	2.2990(8)	1.744(3)	1.751(3)	1.757(3)
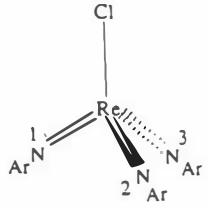	2.292(2)	1.749(6)	1.757(6)	1.769(7)

Table 25 continued

Complex	#	Re-X(#)	Re-N(#)	Re-Re
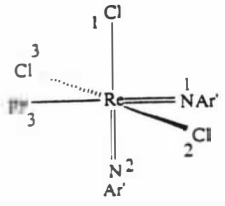	1	2.456(5)	1.734(18)	
	2	2.358(5)	1.760(14)	
	3	2.357(5)	2.305(14)	
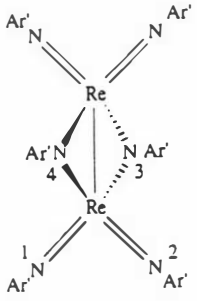	1		1.754(4)	2.7267(3)
			1.750(4)	2.7440(3)
	2		1.763(3)	
			1.756(4)	
	3		1.951(3)	
			1.959(4)	
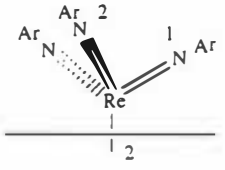	1		1.760(5)	2.7428(7)
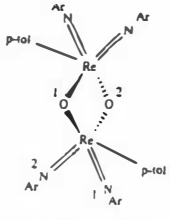	1		1.751(3)	3.1307(3)
	2		1.759(3)	

Table 26 Selected bond lengths (Å) of $Re(NAr')Cl_3(py)$ and dimeric complexes reported in this thesis

Complex	#	X-Re-N(#)	Re-N(#)-C	N(1)-Re-N(#)	N(2)-Re-N(3)
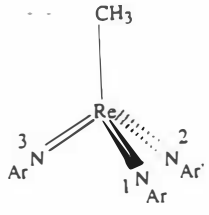	1	103.9(2)	169.1(3)		115.63(17)
	2	101.85(19)	171.2(3)	114.75(17)	
	3	102.81(19)	168.5(3)	115.23(18)	
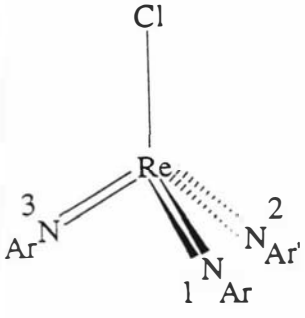	1	107.2(8)	165(2)		112.4(8)
		107.7(8)	166.6(19)		113.5(10)
	2	106.9(8)	165(2)	112.2(10)	
		107.1(7)	170.6(18)	110.0(9)	
	3	107.4(8)	172.5(19)	110.4(10)	
		106.7(8)	162.1(19)	111.6(10)	
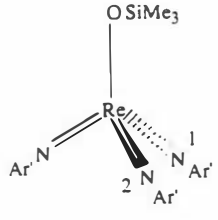	1	109.87(19)	158.8(5)		
	2			109.1(2)	
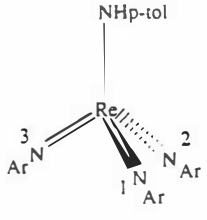	1	100.35(14)	168.8(3)		112.48(15)
	2	107.15(14)	169.8(3)	114.01(15)	
	3	108.12(14)	174.5(3)	113.63(15)	

Table 27 Selected bond angles (°) of $[Re(NAr')_3]^-$ and tetrahedral tris(imido) complexes reported in this thesis

Complex	#	X-Re-N(#)	Re-N(#)-C	N(1)-Re-N(#)	N(2)-Re-N(3)
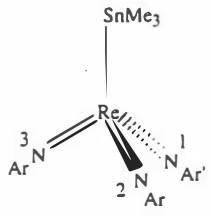	1	90.41(9)	172.9(2)		116.46(13)
	2	99.56(8)	171.6(2)	119.58(13)	
	3	104.32(8)	171.0(2)	118.15(13)	
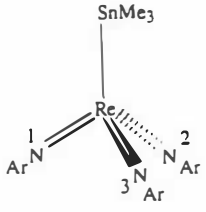	1	92.86(19)	170.2(5)		120.0(2)
	2	93.07(6)	172.5(4)	117.3(2)	
	3	104.16(18)	172.7(4)	100.4(3)	
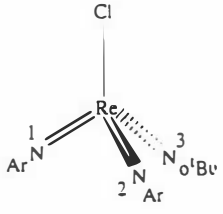	1	107.59(9)	172.4(2)		111.62(12)
	2	107.37(8)	171.2(2)	111.46(13)	
	3	108.10(9)	160.8(2)	110.56(13)	
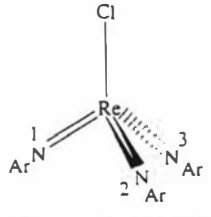	1	106.0(2)	168.9(5)		113.5(3)
	2	106.7(3)	165.9(7)	111.2(3)	
	3	106.0(2)	171.5(7)	112.8(3)	
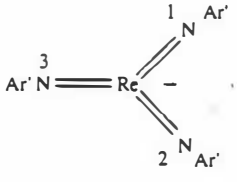	1		180.0		121.20(17)
	2		172.1(2)	119.40(9)	
	3			119.40(9)	

Table 27 continued

Complex	#	X-Re-N(#)	Re-N(#)-C	N(1)-Re-N(#)	N(2)-Re-N(3)
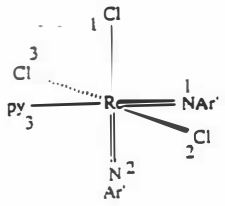	1	95.2(5)*	171.8(12)		*For Cl(2)
	2	92.2(5)*	174.4(13)	106.2(7)	
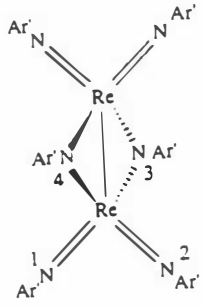	1		156.2(3)		
			168.4(3)		
	2		168.8(3)	113.48(17)	
			166.0(3)	114.10(17)	
	3		136.7(3)	114.09(16)	
			135.3(3)	112.25(15)	
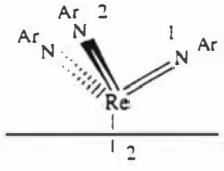	1		168.5(4)		
	2			114.50(12)	
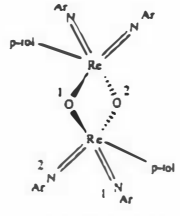	1		145.5(3)		
	2		166.7(3)	107.82(15)	

Table 28 Selected bond angles (°) of Re(NAr')Cl_3(py) and dimeric complexes reported in this thesis

Statistics

The following statistics are concerned with only terminal imido ligands of the complexes given in tables 25 to 28. However, two complexes are excluded, the bis(imido) complex, $Re(NAr')_2Cl_3(py)$ and the oxo-bridging dimer, $[Re(NAr)_2(p\text{-tol})(\mu\text{-}O)]_2$.

Re-N distance (Å):

number of values in sample; **33**
number of complexes in sample; **11**
range; **1.70(2)-1.779(3)**
average; **1.751**
standard deviation; **0.018**

Re-N-C angles (°)

number of values in sample; **32**
number of complexes in sample; **11**
range; **156.2(3)-180.0**
average; **168.9**
standard deviation; **4.7**

N-Re-N angles (°)

number of values in sample; **31**
number of complexes in sample; **11**
range; **100.4(3)-121.20(17)**
average; **113.87**
standard deviation; **4.09**

Appendix III

Tables of selected bond lengths of tetrahedral d^0 tris(imido) complexes, related d^1 complexes and trigonal planar d^2 complexes

---

The tables that follow contain metal-X (where X can be a halide, aryl , alkyl, amine, amide, phosphide, oxygen or sulphur functionality or gold), metal-nitrogen and metal-metal bond distances in Å with esd in brackets. Complexes containing bridging imido ligands to Li or Al are not included. When more than one value is given for the same bond, this indicates 2 or more independent molecules are involved.

Statistics involving the bond lengths presented in the following tables are given at the end of table 30.

Complex	M-X	M-N(1)	M-N(2)	M-N(3)	Ref.
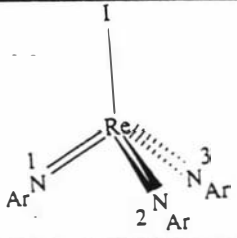	2.664(1)	1.770(7)	1.767(6)	1.765(6)	39
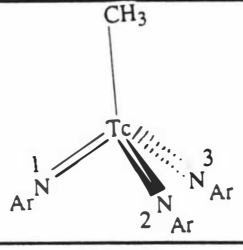	2.136(17)	1.738(11)	1.749(13)	1.743(10)	39
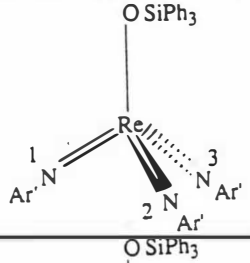	1.902(3)	1.743(3)	1.750(3)	1.726(3)	104
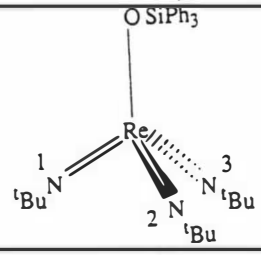	1.902(8)	1.749(8)	1.723(11)	1.735(9)	104
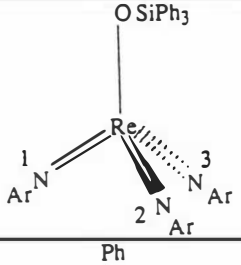	1.891(10) 1.870(8) 1.879(11)	1.741(5) 1.759(4) 1.759(5)	1.741(6) 1.758(6) 1.759(6)	1.742(2) 1.760(3) 1.759(5)	104
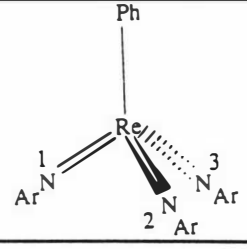	2.088(8)	1.761(5)	1.750(5)	1.750(6)	104

Table 29 Selected bond lengths (Å) of $[Re(NAr)_3]^-$, $Os(NAr)_3$ and tetrahedral tris(imido) complexes reported in the literature

Complex	M-X	M-N(1)	M-N(2)	M-N(3)	Ref.
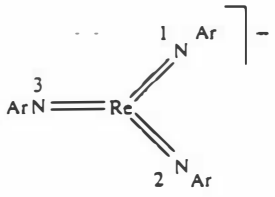		1.60(1)	1.753(8)	1.684(9)	12
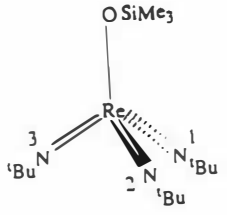	1.899(7)	1.706(9)	1.704(11)	1.740(10)	30
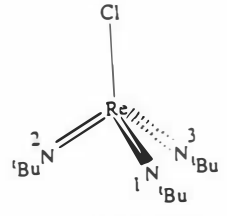	2.301(4)	1.750(15)	1.683(14)	1.719(11)	30
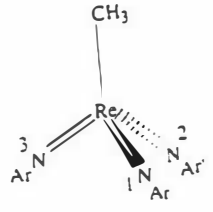	2.109(5)	1.766(3)	1.748(3)	1.758(4)	21
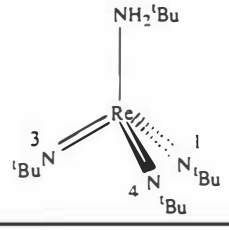	1.849(9)	1.724(8)	1.805(10)	1.761(10)	29
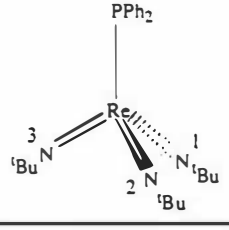	2.446(2) 2.445(2)	1.745(7) 1.743(6)	1.748(8) 1.744(7)	1.732(7) 1.732(7)	29

Table 29 continued

Complex	M-X	M-N(1)	M-N(2)	M-N(3)	Ref.
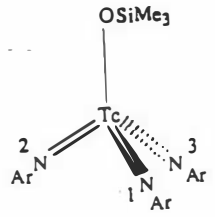	1.909(6)	1.759(6)	1.753(6)	1.749(7)	22
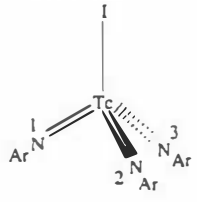	2.654(1)	1.740(7)	1.759(7)	1.763(6)	22
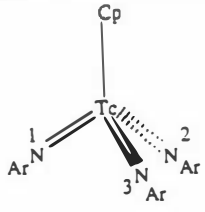	2.156(3)	1.753(2)	1.761(2)	1.748(2)	16
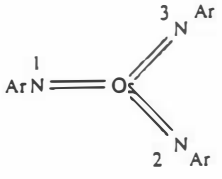		1.736(5)	1.738(7)		27
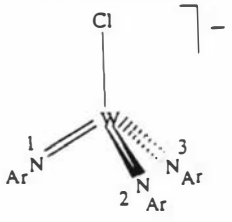	2.343(6)	1.777(15)	1.763(15)	1.805(18)	14
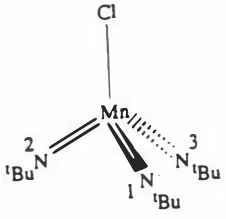	2.222(3)	1.656(5)	1.655(5)	1.656(5)	32

Table 29 continued

Complex	M-X	M-N(1)	M-N(2)	M-N(3)	Ref.
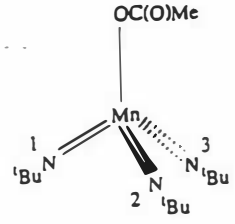	1.91(3)	1.656(5)	1.673(9)	1.65(2)	32
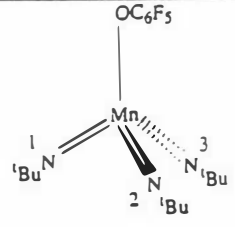	1.896(2)	1.661(2)	1.658(2)	1.652(2)	32
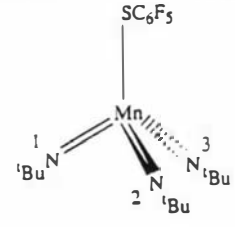	2.289(1)	1.644(3)	1.658(3)	1.651(3)	32
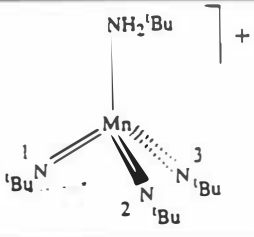	2.028(9)	1.655(7)	1.653(7)	1.655(8)	32
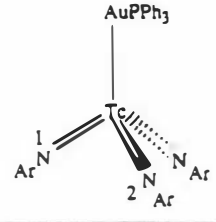	2.589(1)	1.758(5)			17
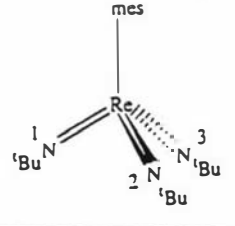	2.097(36)	1.738(29)	1.657(30)	1.769(29)	48

Table 29 continued

Complex	#	M-X(#)	M-N(#)	M-M	Ref.
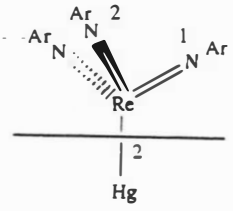	1	2.621(1)	1.76(1)		12
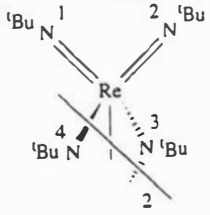	1,2 3,4		1.69(3)-1.78(2) 1.85(3)-1.94(2)	2.7	30
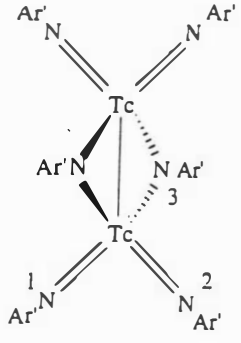	1 2 3		1.955(7) 1.952(6) 1.756(8) 1.759(6) 1.737(6) 1.748(6)	2.696(2) 2.667(2)	17
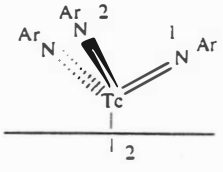	1		1.758(2)	2.744(1)	17

Table 30 Selected bond lengths (Å) of d^1 dimeric complexes containing terminal imido ligands reported in the literature

Complex	#	M-X(#)	M-N(#)	M-M	Ref.
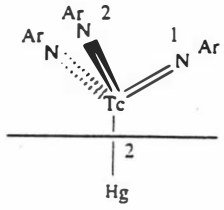	1	2.615(1)	1.718(10)		17
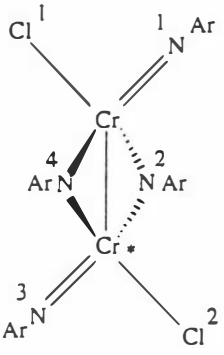	1 2 3 4	2.207(2) 2.204(3) 2.211(2)* 2.202(2)*	1.640(7) 1.646(6) 1.865(8) 1.836(7) 1.654(7)* 1.648(6)* 1.823(7) 1.819(7)	2.476(2) 2.474(2)	99
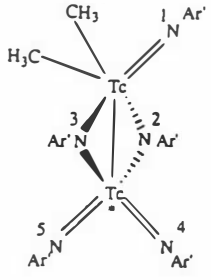	1 2 3 4 5		1.702(11) 1.973(13) 1.974(10) 1.746(11)* 1.76(11)*	2.673(2)	43
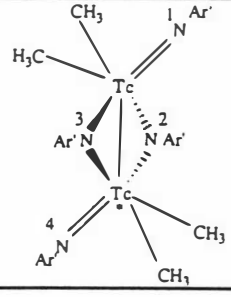	1 2 3 4		1.713(2) 2.001(2) 1.927(2) 1.719(3)*	2.733(1)	43

Table 30 continued

Statistics

The following statistics are concerned with only terminal imido ligands of the complexes given in tables 29 and 30.

M-X distance (Å):

number of values in sample; **31**
number of complexes in sample; **25**
range; **1.849(9)-2.664(1)**
average; **2.179**
standard deviation; **0.264**

M-N distance (Å):

number of values in sample; **96**
number of complexes in sample; **31**
range; **1.60(1)-1.78(2)**
average; **1.725**
standard deviation; **0.045**

M-M distance (Å)

number of values in sample; **8**
number of complexes in sample; **6**
range; **2.474(2)-2.744(1)**
average; **2.645**
standard deviation; **0.108**

Ranges of M-N bond lengths depending on the R group of complexes of the type, $XM(NR)_3$

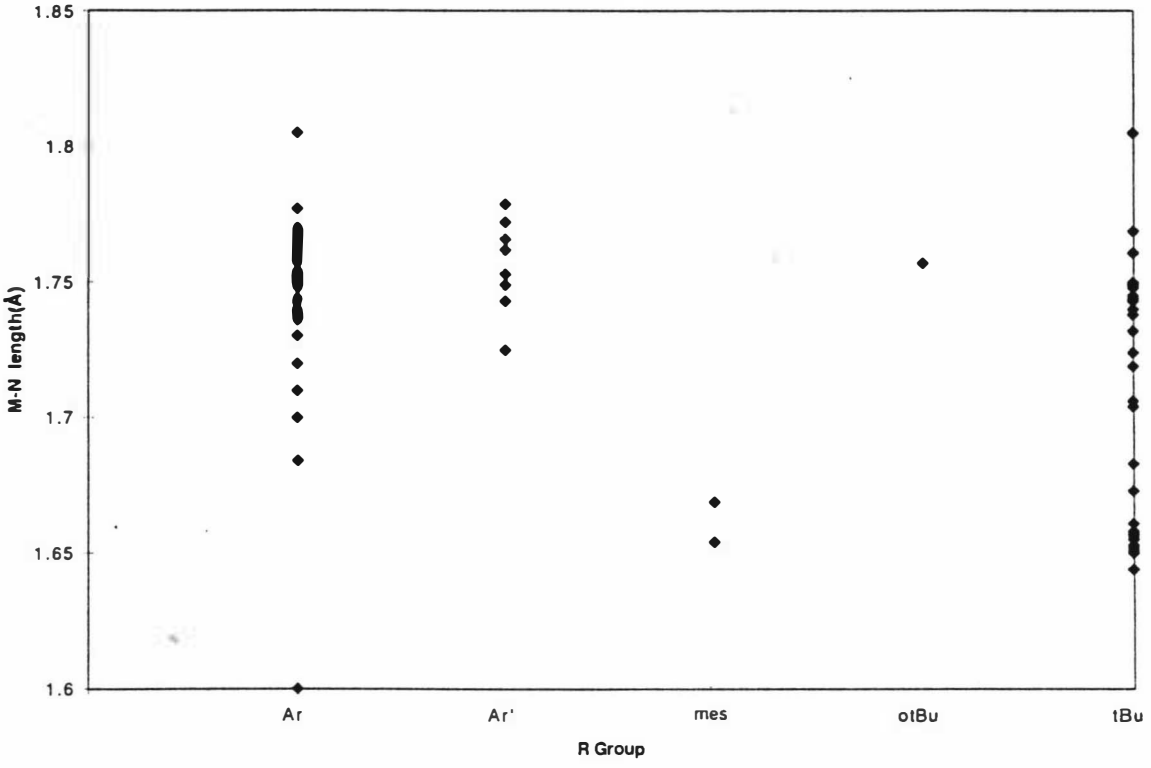

The interesting feature here is although the range of M-N lengths for R=^{t}Bu and Ar are similar, the values for ^{t}Bu are spread out while for Ar they are mostly bunched between 1.684 and 1.805Å. Also all the M-N distaces less than 1.68Å for R=^{t}Bu are complexes of Mn, except in one case ($mesRe(N^tBu)_3$ at 1.657Å).

Ranges of M-N bond lengths depending on the metal of complexes of the type, $XM(NR)_3$

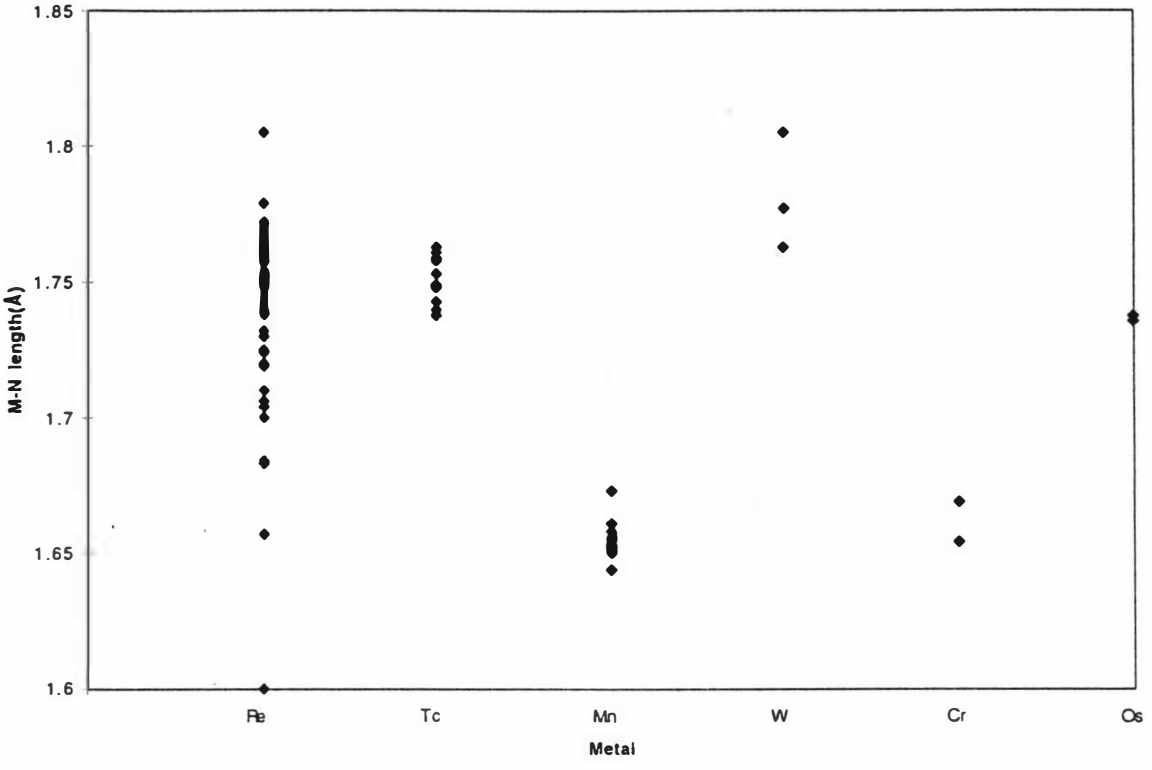

Here we see where the low M-N values (<1.68Å) found for R=^{t}Bu in the previous plot came from. All the Mn-N bond lengths are below 1.68Å. It is also interesting to note the narrow M-N range occupied by Tc, at 1.738 to 1.763Å.

Appendix IV

Tables of selected bond angles of tetrahedral d^0 tris(imido) complexes, related d^1 complexes and trigonal planar d^2 complexes

---

The tables that follow contain X-metal-nitrogen (where X can be a halide, aryl , alkyl, amine, amide, phosphide, oxygen or sulphur functionality or another metal) bond angles, the angles of the imido ligands (M-N-C) and the angles of the imido nitrogens around the metal (N-M-N) in degrees (°) with esd in brackets. Complexes containing bridging imido ligands to Li or Al are not included. When more than one value is given for the same bond, this indicates 2 or more independent molecules are involved.

Statistics involving the bond angles presented in the following tables are given at the end of tables 31 and 32.

Complex	#	X-M-N(#)	M-N(#)-C	N(1)-M-N(#)	N(2)-M-N(3)	Ref.
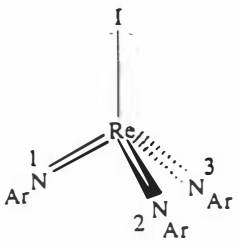	1	106.7(2)	165.7(6)		112.2(3)	39
	2	105.9(2)	169.9(6)	113.8(3)		
	3	105.4(2)	167.5(5)	112.1(3)		
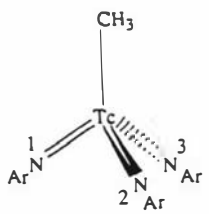	1	101.8(6)	167.0(11)		115.0(5)	39
	2	102.9(6)	163.9(10)	116.6(6)		
	3	101.4(6)	168.0(9)	115.7(5)		
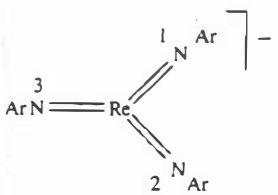	1		168.8(8)		115.8(4)	12
	2		173.6(8)	116.1(4)		
	3		173.2(8)	128.0(4)		
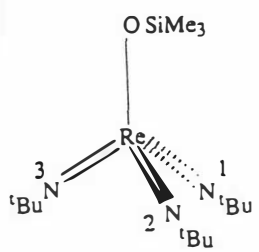	1	109.7(4)	164.8(8)		108.7(6)	30
	2	110.4(5)	160.6(9)	111.1(6)		
	3	108.0(4)	157.7(8)	109.0(6)		

Table 31 Selected bond angles (°) of $[Re(NAr)_3]^-$, $Os(NAr)_3$ and tetrahedral tris(imido) complexes reported in the literature

Complex	#	X-M-N(#)	M-N(#)-C	N(1)-M-N(#)	N(2)-M-N(3)	Ref.
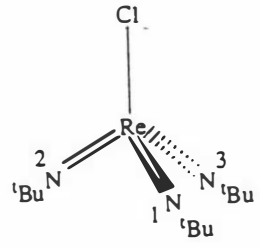	1	104.1(8)	157.5(16)		110.5(9)	30
	2	111.5(7)	159.1(16)	111.9(10)		
	3	109.7(5)	160.3(14)	109.0(9)		
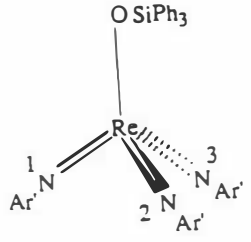	1	106.0(1)	158.4(3)		112.4(2)	104
	2	108.6(1)		112.0(1)		
	3	107.0(1)		110.5(2)		
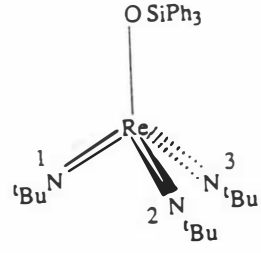	1	111.4(5)	150.6(10)		111.2(7)	104
	2	106.4(4)		110.2(6)		
	3	109.0(6)		108.7(4)		
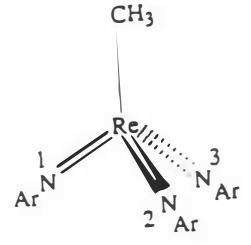	1	102.4(2)	166.3(3)		115.6(2)	21
	2	101.8(2)	168.8(3)	114.8(2)		
	3	103.0(2)	169.5(3)	116.2(2)		

Table 31 continued

Complex	#	X-M-N(#)	M-N(#)-C	N(1)-M-N(#)	N(2)-M-N(3)	Ref.
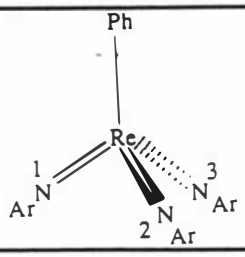	1	104.8(3)	162.6(4)		113.8(2)	104
	2	103.0(3)		114.1(2)		
	3	103.4(3)		115.7(3)		
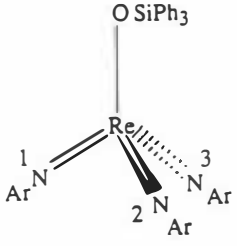	1	108.8(2)			110.1(2)	104
		109.3(2)			109.7(2)	
		109.8(2)			109.1(2)	
	2	108.8(2)		110.1(2)		
		109.3(2)		109.7(2)		
		109.8(2)		109.1(2)		
	3	108.8(2)		110.1(2)		
		109.3(2)		109.6(2)		
		109.8(2)		109.1(2)		
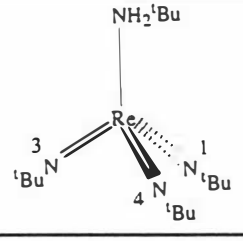	1	102.2(4)	164.6(8)			29
	3	113.5(5)	152.6(8)	113.0(4)		
	4	113.2(4)	146.0(8)	113.2(5)		
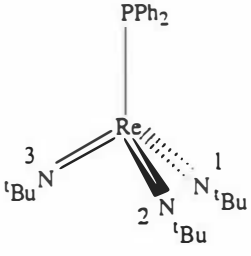	1	107.6(2)	154.9(7)		115.2(3)	29
		100.8(2)	158.7(7)		115.3(3)	
	2	103.2(2)	156.1(6)	114.1(4)		
		107.9(2)	153.2(6)	114.5(3)		
	3	99.7(2)	157.0(7)	114.8(3)		
		99.3(3)	154.1(7)	116.2(3)		

Table 31 continued

Complex	#	X-M-N(#)	M-N(#)-C	N(1)-M-N(#)	N(2)-M-N(3)	Ref.
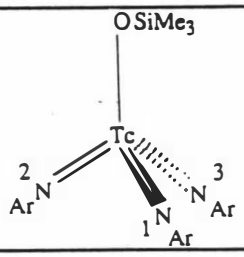	1	111.3(3)	154.3(6)		109.1(3)	22
	2	105.2(3)	158.5(5)	111.3(3)		
	3	109.9(3)	154.7(6)	109.9(3)		
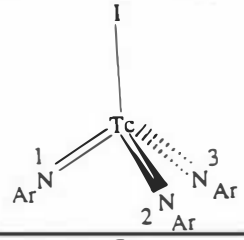	1	107.5(2)	164.8(6)		112.2(3)	22
	2	105.7(2)	169.4(6)	114.3(3)		
	3	105.0(2)	165.6(6)	111.4(3)		
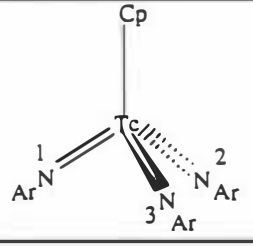	1	105.2(1)	166.2(2)		113.5(1)	16
	2	109.7(1)	157.3(2)	113.2(1)		
	3	102.4(1)	162.0(1)	111.9(1)		
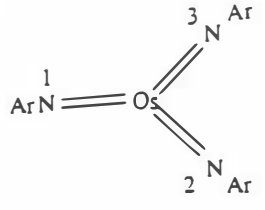	1		178.0(5)			27
	2		180(3)	120.1(2)		
	3			119.8(3)		
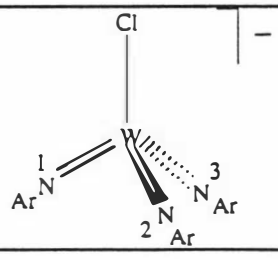	1	106.0(6)	173.4(15)		112.1(7)	14
	2	104.7(5)	167.7(14)	112.5(7)		
	3	107.2(6)	171.4(15)	113.5(7)		

Table 31 continued

Complex	#	X-M-N(#)	M-N(#)-C	N(1)-M-N(#)	N(2)-M-N(3)	Ref.
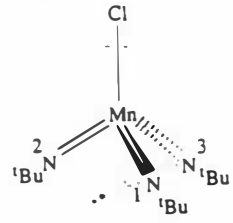	1	108.0(2)	138.5(3)		111.6(3)	32
	2	107.0(2)	141.8(3)	111.1(2)		
	3	106.8(2)	140.6(3)	112.2(3)		
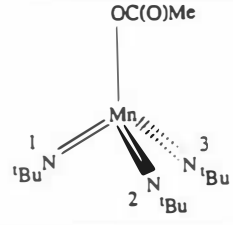	1	105.8(8)	144.6(3)		111.3(7)	32
	2	104.0(3)	140.1(5)	112.8(3)		
	3	110.6(11)	142.2(5)	111.9(3)		
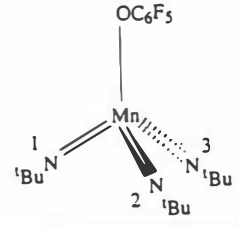	1	109.1(1)	141.9(2)		110.9(1)	32
	2	105.2(1)	139.9(2)	111.7(1)		
	3	108.7(1)	140.7(2)	110.9(1)		
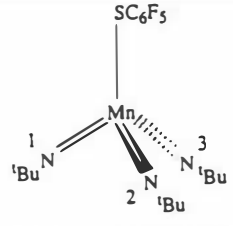	1	106.4(1)	143.1(2)		113.1(1)	32
	2	103.7(1)	142.0(2)	113.0(1)		
	3	107.3(1)	142.2(2)	112.6(1)		
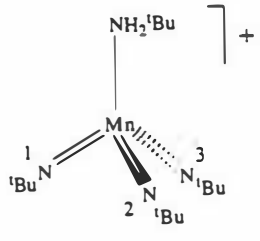	1	103.5(3)	141.0(6)		112.9(4)	32
	2	111.9(4)	141.4(6)	110.4(4)		
	3	106.1(4)	146.5(6)	111.6(4)		
	4		124.5(6)			

Table 31 continued

Complex	#	X-M-N(#)	M-N(#)-C	N(1)-M-N(#)	N(2)-M-N(3)	Ref.
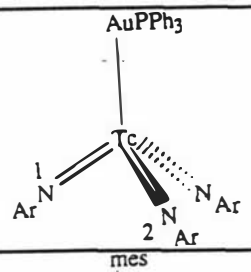	1	97.2(1)		118.4(1)		17
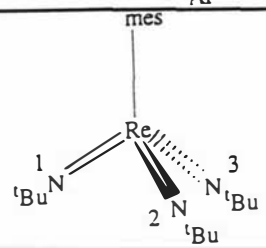	1	94.8(14)	142.4(22)		109.3(14)	48
	2	113.3(14)	161.3(25)	123.1(14)		
	3	105.3(14)	157.1(27)	109.2(13)		

Table 31 continued

Complex	#	X(1)-M-N(#)	M-N(#)-C	N(1)-M-N(#)	Ref.
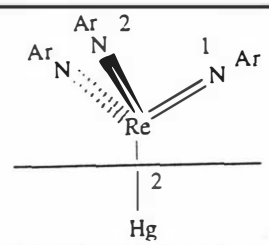	1	97.4(4)	173(1)		12
	2			118.4(2)	
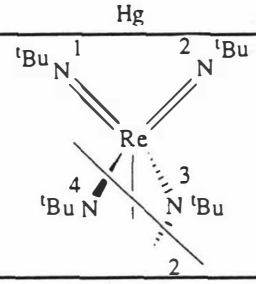	1				30
	2			110(1)-112(1)	

Table 32 Selected bond angles (°) of d^1 dimeric complexes containing terminal imido ligands reported in the literature

Complex	#	X(1)-M-N(#)	M-N(#)-C	N(1)-M-N(#)	Ref.
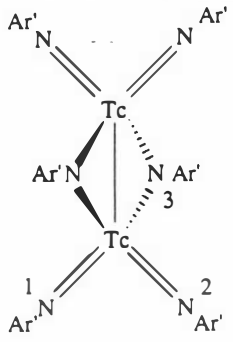	1				17
	2			112.1(3)	
				110.9(3)	
	3			111.6(3)	
				111.6(3)	
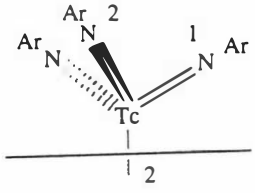	1		167.6(1)		17
	2			114.6(1)	
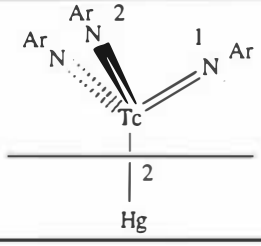	1	97.6(4)			17
	2			118.3(2)	
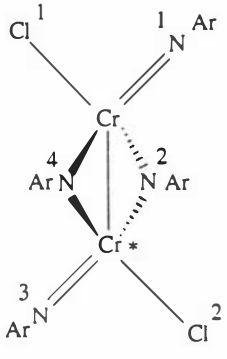	1		176.3(6)		99
			174.9(6)		
	2		138.5(5) 137.2(6)*	112.3(3)	
			138.0(5) 137.2(5)*	111.5(3)	
	3		171.0(6)*		
			172.8(6)*		
	4		136.2(6) 138.4(5)*	112.2(3)	
			139.9(5) 134.7(5)*	112.0(3)	

Table 32 continued

Complex	#	X(1)-M-N(#)	M-N(#)-C	N(1)-M-N(#)	Ref.
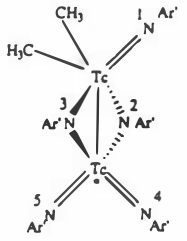	1 4 5		170.8(9) 166.1(10)* 170.3(8)*		43
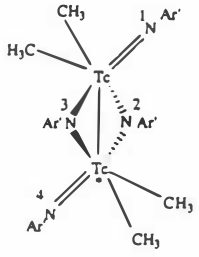	1 4		164.5(2) 175.5(2)*		43

Table 32 continued

Statistics

The following statistics are concerned with only terminal imido ligands of the complexes given in tables 31 and 32.

X-M-N angles (°):

number of values in sample; **75**
number of complexes in sample; **24**
range; **94.8(14)-113.5(5)**
average; **106.2**
standard deviation; **4.0**

M-N-C angles (°):

number of values in sample; **73**
number of complexes in sample; **27**
range; **138.5(3)-180(3)**
average; **159.5**
standard deviation; **11.6**

N-M-N angles (°)

number of values in sample; **86**

number of complexes in sample; **29**

range; **108.7(4)-128.0(4)**

average; **112.9**

standard deviation; **3.6**

Ranges of M-N-R bond angles depending on the R group of complexes of the type, $XM(NR)_3$

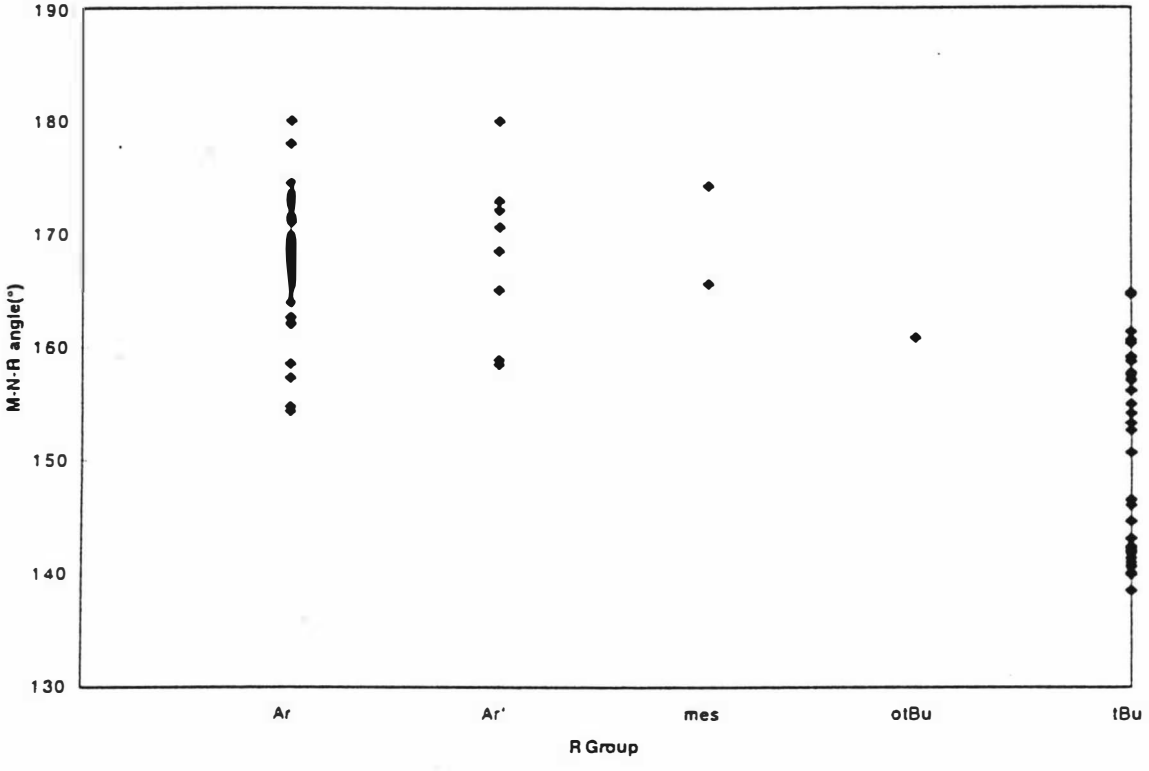

This illustrates the dramatic difference between M-N-R angles of arylimido and ^{t}Bu-imido ligands. However, it should be noted that the M-N-^{t}Bu angles under 150° are all complexes containing Mn with only two exceptions, ^{t}BuNH$_2$Re(N^{t}Bu)$_3$ and mesRe(N^{t}Bu)$_3$.

Ranges of M-N-R bond angles depending on the metal of complexes of the type, $XM(NR)_3$

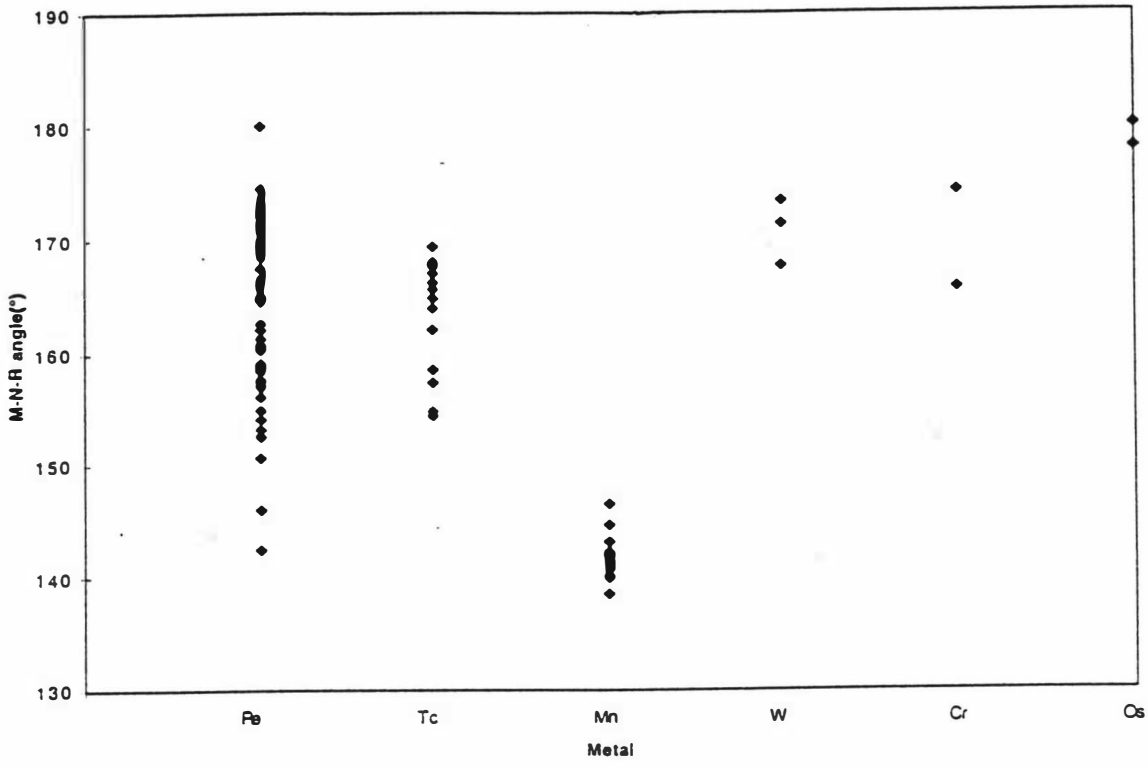

The striking aspect shown above is the exclusively bent M-N-R angles for Mn. Given that all the structurally characterized Mn tris(imido) complexes contain the ^{t}Bu-imido ligand, then perhaps that is the reason for low Mn-N-R values. However, the plot for M-N-R versus R showed that tris(imido) complexes containing the ^{t}Bu-imido ligand do have M-N-R angles greater than 150°. As such it appears to be a property of the metal, rather than the ^{t}Bu group.

Ranges of X-M-N bond angles depending on the R group and the metal of complexes of the type, $XM(NR)_3$

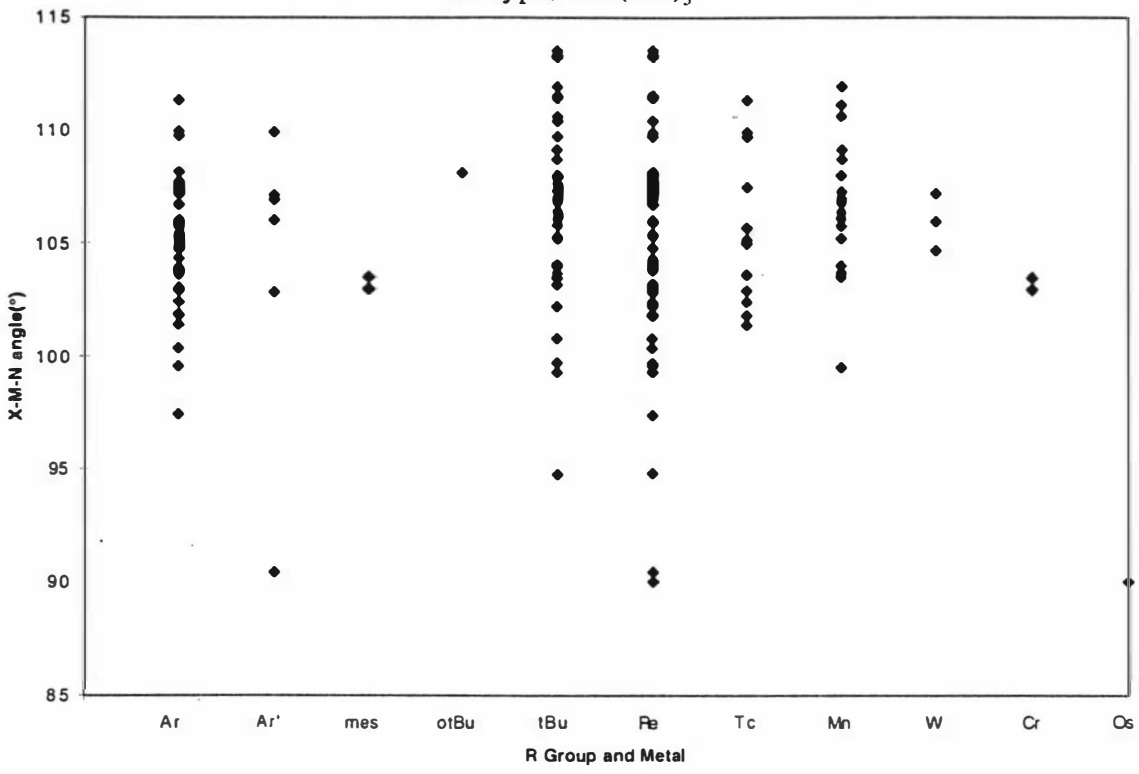

There appears to be little difference between the arylimido and ^{t}Bu-imido complexes or between the metals when it comes to the X-M-N angles.

Appendix V

X-ray data for $Me_3SiORe(NAr')_3$

The tables that follow contain atomic coordinates and equivalent isotropic displacement parameters, complete bond lengths (Å) and angles (°), anisotropic displacement parameters and calculated H-atom positions for $Me_3SiORe(NAr')_3$.

Table 33. Atomic coordinates (x 10^4) and equivalent isotropic displacement parameters ($Å^2$x 10^3). U(eq) is defined as one third of the trace of the orthogonalized U^{ij} tensor.

	x	y	z	U(eq)
Re	3333	6667	2489(1)	19(1)
N	2187(5)	6947(5)	1899(6)	26(1)
C(2)	1806(7)	8636(7)	1542(8)	29(2)
C(6)	931(7)	6841(6)	59(8)	29(2)
C(8)	2576(8)	9295(8)	2725(9)	40(2)
C(1)	1642(6)	7471(6)	1145(7)	25(1)
C(3)	1233(7)	9104(7)	774(8)	37(2)
C(4)	544(7)	8499(7)	-335(8)	36(2)
C(5)	397(7)	7373(8)	-688(8)	37(2)
C(7)	760(8)	5605(8)	-321(8)	42(2)
O	3333	6667	4313(11)	42(2)
Si	3333	6667	5970(4)	28(1)
C(10)	4943(8)	7481(8)	6527(9)	44(2)

Table 34. Bond lengths [Å] and angles [°]

Re-N	1.749(6)	Re-N#1	1.749(6)	Re-N#2	1.749(6)
Re-O	1.840(12)	N-C(1)	1.390(9)	C(2)-C(3)	1.374(11)
C(2)-C(1)	1.429(10)	C(2)-C(8)	1.498(12)	C(6)-C(5)	1.384(11)
C(6)-C(1)	1.384(10)	C(6)-C(7)	1.507(11)	C(3)-C(4)	1.387(11)

C(4)-C(5)	1.378(12)	O-Si	1.671(12)		
Si-C(10)#2	1.840(8)	Si-C(10)	1.840(8)	Si-C(10)#1	1.840(8)
N-Re-N#1	109.1(2)	N-Re-N#2	109.1(2)	N#1-Re-N#2	109.1(2)
N-Re-O	109.87(19)	N#1-Re-O	109.87(19)	N#2-Re-O	109.87(19)
C(1)-N-Re	158.8(5)	C(3)-C(2)-C(1)	116.3(7)	C(3)-C(2)-C(8)	122.9(7)
C(1)-C(2)-C(8)	120.8(7)	C(5)-C(6)-C(1)	119.0(7)	C(5)-C(6)-C(7)	120.4(7)
C(1)-C(6)-C(7)	120.6(7)	N-C(1)-C(6)	119.5(6)	N-C(1)-C(2)	118.6(6)
C(6)-C(1)-C(2)	121.9(7)	C(2)-C(3)-C(4)	122.5(8)	C(5)-C(4)-C(3)	119.8(7)
C(4)-C(5)-C(6)	120.5(8)	Si-O-Re	180.000(1)	O-Si-C(10)#2	107.8(3)
O-Si-C(10)	107.8(3)	C(10)#2-Si-C(10)	111.1(3)		
O-Si-C(10)#1	107.8(3)	C(10)#2-Si-C(10)#1	111.1(3)		
C(10)-Si-C(10)#1		111.1(3)			

Symmetry transformations used to generate equivalent atoms: #1 -x+y,-x+1,z #2 -y+1,x-y+1,z

Table 35. Anisotropic displacement parameters ($Å^2 x\ 10^3$). The anisotropic displacement factor exponent takes the form: $-2\pi^2[\ h^2\ a^{*2}U^{11} + ... + 2\ h\ k\ a^*\ b^*\ U^{12}\ ]$

U^{11}	U^{22}	U^{33}	U^{23}	U^{13}	U^{12}	
Re19(1)	19(1)	19(1)	0	0	10(1)	
N 26(3)	29(3)	22(3)	5(2)	1(2)	13(2)	
C(2)28(4)	24(3)	37(4)	4(3)	14(3)	14(3)	
C(6)25(3)	30(4)	30(4)	2(3)	5(3)	11(3)	
C(8)35(4)	27(4)	53(5)	-6(4)	1(4)	12(4)	
C(1)19(3)	25(3)	34(3)	3(3)	7(3)	12(3)	
C(3)37(4)	32(4)	45(5)	12(4)	14(3)	20(3)	
C(4)32(4)	44(4)	41(4)	16(3)	8(3)	25(4)	
C(5)26(4)	56(5)	34(4)	5(4)	1(3)	23(4)	
C(7)47(5)	45(5)	39(4)	-13(3)	-7(3)	26(4)	
O 45(4)	45(4)	37(6)	0	0	23(2)	
Si32(1)	32(1)	19(2)	0	0	16(1)	
C(10)	37(4)	42(5)	51(5)	-4(4)	-8(4)	20(4)

Table 36. Hydrogen coordinates ($x\ 10^4$) and isotropic displacement parameters ($Å^2 x\ 10^3$).

	x	y	z	U(eq)
H(8A)	2576	10052	2855	48
H(8B)	2252	8791	3500	48
H(8C)	3401	9467	2571	48
H(3A)	1296	9862	1061	44

H(4A)	194	8869	-885	44
H(5A)	-98	6937	-1440	45
H(7A)	1205	5383	287	50
H(7B)	-98	5004	-280	50
H(7C)	1058	5636	-1205	50
H(10A)	4975	7497	7478	52
H(10B)	5349	7061	6194	52
H(10C)	5347	8307	6194	52

Appendix VI

X-ray data for $ClRe(NAr)_3$

The tables that follow contain atomic coordinates and equivalent isotropic displacement parameters, complete bond lengths (Å) and angles (°), anisotropic displacement parameters and calculated H-atom positions for $ClRe(NAr)_3$.

Table 37. Atomic coordinates (x 10^4) and equivalent isotropic displacement parameters ($Å^2$x 10^3). U(eq) is defined as one third of the trace of the orthogonalized U^{ij} tensor.

	x	y	z	U(eq)
Re	3601(1)	1050(1)	2273(1)	35(1)
Cl	3160(1)	1370(1)	3226(3)	65(1)
N(1)	4007(2)	1278(1)	2414(7)	39(1)
N(2)	3472(2)	1004(2)	657(7)	42(2)
N(3)	3611(2)	668(2)	3115(7)	41(1)
C(11)	4356(2)	1398(2)	2575(7)	35(2)
C(12)	4488(3)	1447(2)	3813(9)	50(2)
C(13)	4832(3)	1580(3)	3956(10)	60(2)
C(14)	5037(3)	1652(3)	2918(13)	70(3)
C(15)	4913(3)	1600(3)	1699(10)	60(3)
C(16)	4566(2)	1471(2)	1511(9)	45(2)
C(17)	4254(4)	1384(3)	4961(12)	75(3)
C(18)	4096(5)	1698(5)	5443(16)	113(5)
C(19)	4459(6)	1206(4)	6030(15)	123(6)
C(110)	4421(3)	1400(3)	181(10)	59(2)
C(111)	4500(6)	1062(3)	-336(17)	120(6)
C(112)	4539(5)	1665(3)	-814(13)	103(5)
C(21)	3456(2)	1004(2)	-637(8)	43(2)
C(22)	3485(3)	701(2)	-1334(9)	53(2)
C(23)	3459(3)	709(3)	-2663(14)	74(3)
C(24)	3378(4)	1007(3)	-3279(10)	69(3)
C(25)	3343(3)	1298(3)	-2605(13)	73(3)
C(26)	3391(2)	1311(2)	-1260(9)	49(2)
C(27)	3555(3)	373(2)	-650(12)	72(3)
C(28)	3256(4)	138(3)	-729(16)	110(6)
C(29)	3913(4)	221(5)	-1050(30)	172(13)
C(210)	3353(3)	1639(2)	-533(10)	60(3)
C(211)	2952(3)	1699(3)	-107(18)	86(4)

C(31)	3634(2)	349(2)	3602(8)	41(2)
C(32)	3319(2)	159(2)	3799(8)	47(2)
C(33)	3349(3)	-152(2)	4351(11)	68(3)
C(34)	3685(3)	-286(2)	4670(14)	74(3)
C(35)	3992(3)	-107(2)	4467(11)	67(3)
C(36)	3981(3)	217(2)	3939(10)	53(2)
C(37)	2943(2)	309(2)	3506(11)	61(3)
C(38)	2704(3)	83(3)	2659(13)	89(4)
C(39)	2739(3)	416(4)	4629(15)	107(5)
C(310)	4328(3)	422(2)	3688(11)	63(3)
C(311)	4488(4)	343(4)	2481(15)	103(5)
C(312)	4621(3)	365(4)	4580(20)	113(6)
C(212)	3499(4)	1941(3)	-1239(13)	75(3)

Table 38. Bond lengths [Å] and angles [°].

Re-N(1)	1.749(6)	Re-N(3)	1.757(6)
Re-N(2)	1.769(7)	Re-Cl	2.292(2)
N(1)-C(11)	1.377(9)	N(2)-C(21)	1.358(12)
N(3)-C(31)	1.371(10)	C(11)-C(16)	1.388(11)
C(11)-C(12)	1.401(12)	C(12)-C(13)	1.376(13)
C(12)-C(17)	1.501(16)	C(13)-C(14)	1.354(16)
C(14)-C(15)	1.373(15)	C(15)-C(16)	1.385(12)
C(16)-C(110)	1.520(13)	C(17)-C(18)	1.466(19)
C(17)-C(19)	1.523(19)	C(110)-C(111)	1.478(16)
C(110)-C(112)	1.545(15)	C(21)-C(26)	1.406(12)
C(21)-C(22)	1.414(12)	C(22)-C(23)	1.398(17)
C(22)-C(27)	1.510(13)	C(23)-C(24)	1.384(15)
C(24)-C(25)	1.362(16)	C(25)-C(26)	1.423(16)
C(26)-C(210)	1.520(13)	C(27)-C(28)	1.444(17)
C(27)-C(29)	1.51(2)	C(210)-C(212)	1.508(14)
C(210)-C(211)	1.555(15)	C(31)-C(32)	1.398(11)
C(31)-C(36)	1.422(12)	C(32)-C(33)	1.370(12)
C(32)-C(37)	1.533(13)	C(33)-C(34)	1.385(15)
C(34)-C(35)	1.349(14)	C(35)-C(36)	1.406(12)
C(36)-C(310)	1.536(13)	C(37)-C(39)	1.459(17)
C(37)-C(38)	1.539(15)	C(310)-C(312)	1.446(16)
C(310)-C(311)	1.430(17)		

N(1)-Re-N(3)	112.8(3)
N(1)-Re-N(2)	111.2(3)

N(3)-Re-N(2)	113.5(3)
N(1)-Re-Cl	106.0(2)
N(3)-Re-Cl	106.0(2)
N(2)-Re-Cl	106.7(3)
C(11)-N(1)-Re	168.9(5)
C(21)-N(2)-Re	165.9(7)
C(31)-N(3)-Re	171.5(7)
N(1)-C(11)-C(16)	119.4(7)
N(1)-C(11)-C(12)	119.1(8)
C(16)-C(11)-C(12)	121.5(8)
C(13)-C(12)-C(11)	118.3(9)
C(13)-C(12)-C(17)	120.1(9)
C(11)-C(12)-C(17)	121.4(9)
C(14)-C(13)-C(12)	120.2(9)
C(13)-C(14)-C(15)	122.2(9)
C(14)-C(15)-C(16)	119.5(9)
C(15)-C(16)-C(11)	118.3(8)
C(15)-C(16)-C(110)	121.3(9)
C(11)-C(16)-C(110)	120.3(7)
C(18)-C(17)-C(12)	111.1(10)
C(18)-C(17)-C(19)	109.6(13)
C(12)-C(17)-C(19)	112.7(12)
C(111)-C(110)-C(16)	116.1(11)
C(111)-C(110)-C(112)	108.6(11)
C(16)-C(110)-C(112)	113.3(9)
N(2)-C(21)-C(26)	118.1(8)
N(2)-C(21)-C(22)	121.0(8)
C(26)-C(21)-C(22)	120.9(9)
C(23)-C(22)-C(21)	119.5(9)
C(23)-C(22)-C(27)	120.3(9)
C(21)-C(22)-C(27)	120.2(9)
C(24)-C(23)-C(22)	120.0(11)
C(25)-C(24)-C(23)	120.4(11)
C(24)-C(25)-C(26)	122.3(9)
C(21)-C(26)-C(25)	116.7(9)
C(21)-C(26)-C(210)	122.0(8)
C(25)-C(26)-C(210)	121.2(9)
C(28)-C(27)-C(22)	113.8(10)

C(28)-C(27)-C(29)	112.6(12)
C(22)-C(27)-C(29)	111.2(12)
C(212)-C(210)-C(26)	113.9(9)
C(212)-C(210)-C(211)	110.9(9)
C(26)-C(210)-C(211)	111.2(8)
N(3)-C(31)-C(32)	120.6(8)
N(3)-C(31)-C(36)	119.2(7)
C(32)-C(31)-C(36)	120.1(8)
C(33)-C(32)-C(31)	119.1(9)
C(33)-C(32)-C(37)	120.7(8)
C(31)-C(32)-C(37)	120.0(7)
C(32)-C(33)-C(34)	121.5(9)
C(35)-C(34)-C(33)	120.1(9)
C(34)-C(35)-C(36)	121.5(9)
C(35)-C(36)-C(31)	117.7(8)
C(35)-C(36)-C(310)	122.0(8)
C(31)-C(36)-C(310)	120.3(8)
C(39)-C(37)-C(32)	114.3(10)
C(39)-C(37)-C(38)	110.1(9)
C(32)-C(37)-C(38)	113.6(9)
C(312)-C(310)-C(311)	103.7(12)
C(312)-C(310)-C(36)	115.0(10)
C(311)-C(310)-C(36)	112.0(9)

Symmetry transformations used to generate equivalent atoms:

Table 39. Anisotropic displacement parameters ($Å^2 x\ 10^3$). The anisotropic displacement factor exponent takes the form: $-2\pi^2[\ h^2\ a^{*2}U^{11} + ... + 2\ h\ k\ a^*\ b^*\ U^{12}\ ]$

U^{11}	U^{22}	U^{33}	U^{23}	U^{13}	U^{12}	
Re33(1)	31(1)	39(1)	6(1)	-2(1)	-2(1)	
Cl59(1)	66(1)	70(2)	3(1)	12(1)	19(1)	
N(1)	45(3)	31(3)	41(4)	2(3)	1(3)	-3(2)
N(2)	43(4)	42(4)	40(4)	6(3)	-9(3)	-1(3)
N(3)	38(3)	38(3)	48(4)	9(3)	4(3)	0(3)
C(11)	38(4)	30(3)	37(4)	1(2)	-7(3)	-2(3)
C(12)	59(5)	44(4)	48(5)	-4(4)	-9(4)	0(4)
C(13)	46(5)	74(6)	61(6)	-23(5)	-19(5)	3(4)
C(14)	38(5)	81(7)	90(8)	-28(6)	-14(5)	2(5)
C(15)	41(5)	69(6)	69(6)	-2(5)	20(5)	-4(4)

C(16)	44(4)	41(4)	51(5)	-4(4)	1(4)	-1(3)
C(17)	97(8)	83(7)	46(7)	-12(5)	-1(6)	-23(6)
C(18)	104(11)	139(14)	97(11)	-13(10)	39(9)	19(10)
C(19)	190(20)	104(11)	72(10)	24(8)	-19(11)	-18(13)
C(110)	57(5)	68(6)	51(6)	5(4)	2(4)	-16(5)
C(111)	220(20)	68(7)	70(9)	4(8)	-5(12)	5(8)
C(112)	166(15)	74(8)	69(8)	15(6)	-12(9)	-22(9)
C(21)	38(4)	39(4)	52(5)	6(3)	-11(4)	-2(3)
C(22)	52(5)	50(5)	58(6)	-1(4)	-13(4)	-6(4)
C(23)	98(7)	65(6)	59(6)	-7(6)	-17(8)	-8(5)
C(24)	91(8)	75(7)	40(5)	7(5)	-15(5)	-9(6)
C(25)	92(7)	65(6)	62(7)	23(6)	-21(7)	-3(5)
C(26)	49(5)	50(5)	48(5)	6(4)	-6(4)	0(4)
C(27)	105(9)	39(5)	71(7)	-3(4)	-14(6)	2(5)
C(28)	111(11)	72(8)	147(16)	38(8)	31(10)	-7(7)
C(29)	69(9)	96(12)	350(40)	85(17)	7(14)	10(8)
C(210)	66(6)	43(4)	70(8)	4(4)	-2(5)	1(4)
C(211)	61(6)	80(7)	117(11)	-5(9)	-10(8)	15(5)
C(31)	45(4)	39(4)	41(4)	6(3)	1(3)	-3(3)
C(32)	54(5)	42(4)	46(5)	12(3)	-2(4)	-12(4)
C(33)	67(6)	49(5)	87(8)	19(5)	10(5)	-9(4)
C(34)	100(8)	42(4)	80(7)	26(6)	6(7)	-4(5)
C(35)	65(6)	48(5)	87(9)	16(5)	-17(5)	13(4)
C(36)	48(5)	49(5)	62(6)	12(4)	-6(4)	3(4)
C(37)	39(5)	57(5)	86(7)	10(5)	7(5)	-13(4)
C(38)	83(8)	77(8)	107(12)	-5(7)	-17(7)	5(6)
C(39)	68(7)	167(14)	87(10)	-36(11)	7(8)	28(8)
C(310)	43(5)	47(5)	98(8)	4(5)	-22(5)	-1(4)
C(311)	85(8)	119(10)	104(12)	-10(9)	49(9)	-39(7)
C(312)	65(7)	110(10)	163(16)	7(12)	-47(11)	-3(7)
C(212)	98(8)	49(5)	80(8)	13(5)	9(7)	-4(5)

Table 40. Hydrogen coordinates (x 10^4) and isotropic displacement parameters ($Å^2$x 10^3).

	x	y	z	U(eq)
H(13A)	4925	1622	4776	72
H(14A)	5272	1741	3035	84
H(15A)	5062	1651	997	71
H(17A)	4051	1236	4695	90
H(18A)	3956	1804	4772	170
H(18B)	4290	1847	5715	170
H(18C)	3938	1649	6160	170
H(19A)	4294	1165	6735	185
H(19B)	4659	1347	6317	185
H(19C)	4554	994	5719	185
H(11A)	4153	1416	242	70
H(11B)	4432	893	288	180
H(11C)	4758	1043	-526	180
H(11D)	4360	1027	-1110	180
H(11E)	4441	1605	-1641	154

H(11F)	4803	1673	-860	154
H(11G)	4446	1884	-564	154
H(23A)	3496	511	-3138	89
H(24A)	3348	1009	-4169	83
H(25A)	3285	1497	-3043	87
H(27A)	3581	430	263	86
H(28A)	3323	-69	-297	165
H(28B)	3204	90	-1617	165
H(28C)	3042	234	-327	165
H(29A)	4102	392	-1019	258
H(29B)	3892	137	-1917	258
H(29C)	3975	38	-483	258
H(21A)	3500	1616	254	72
H(21B)	2865	1504	360	129
H(21C)	2800	1734	-852	129
H(21D)	2940	1895	437	129
H(33A)	3137	-278	4516	81
H(34A)	3700	-502	5029	89
H(35A)	4219	-201	4683	80
H(37A)	2990	515	3004	73
H(38A)	2841	15	1913	134
H(38B)	2489	207	2394	134
H(38C)	2631	-114	3136	134
H(39A)	2893	558	5156	161
H(39B)	2665	220	5112	161
H(39C)	2525	541	4365	161
H(31A)	4265	664	3697	75
H(31B)	4705	478	2355	154
H(31C)	4314	390	1808	154
H(31D)	4553	107	2461	154
H(31E)	4828	505	4358	169
H(31F)	4693	131	4558	169
H(31G)	4539	422	5436	169
H(21E)	3750	1899	-1486	113
H(21F)	3489	2136	-690	113
H(21G)	3353	1980	-1994	113

Appendix VII

X-ray data for $ClRe(NAr)_2(NAr')$

The tables that follow contain atomic coordinates and equivalent isotropic displacement parameters, complete bond lengths (Å) and angles (°), anisotropic displacement parameters and calculated H-atom positions for $ClRe(NAr)_2(NAr')$.

Table 41. Atomic coordinates (x 10^4) and equivalent isotropic displacement parameters ($Å^2$x 10^3). U(eq) is defined as one third of the trace of the orthogonalized U^{ij} tensor.

	x	y	z	U(eq)
Re(1)	-8051(1)	1676(1)	3920(1)	51(1)
Re(2)	-1821(1)	3609(1)	5267(1)	53(1)
Cl(1A)	-8930(5)	1498(3)	2704(5)	80(3)
N(1A)	-7266(12)	1326(10)	3797(14)	63(7)
N(3B)	-2181(13)	4063(9)	4387(16)	61(7)
Cl(1B)	-1008(5)	4194(4)	6206(5)	89(3)
N(2B)	-2490(11)	3351(8)	5813(14)	49(6)
N(2A)	-8372(11)	1376(9)	4765(14)	58(7)
N(1B)	-1344(11)	2998(10)	4989(14)	58(6)
C(1B)	-1117(11)	2480(8)	4641(14)	62(9)
C(2B)	-1359(10)	2336(9)	3774(13)	59(7)
C(3B)	-1063(13)	1837(10)	3433(12)	78(10)
C(4B)	-525(13)	1482(8)	3960(18)	180(30)
C(5B)	-284(11)	1626(10)	4826(17)	190(30)
C(6B)	-580(12)	2125(10)	5167(11)	74(10)
C(7B)	-315(19)	2275(17)	6180(30)	128(15)
C(8B)	-1970(20)	2693(14)	3153(18)	123(16)
C(9B)	-3054(10)	3146(10)	6092(13)	82(11)
C(10B)	-3281(12)	2556(9)	5847(12)	108(14)
C(11B)	-3869(13)	2298(8)	6122(15)	104(13)
C(12B)	-4231(10)	2631(11)	6643(16)	116(14)
C(13B)	-4005(12)	3221(11)	6889(14)	129(17)
C(14B)	-3416(12)	3479(8)	6614(14)	77(10)
C(15B)	-3212(19)	4138(16)	6820(30)	96(12)
C(16B)	-3810(20)	4584(17)	6690(30)	170(20)
C(17B)	-2640(30)	4170(30)	7720(40)	250(30)
C(21B)	-2558(19)	4259(10)	3540(20)	57(9)
C(22B)	-2130(20)	4426(11)	2960(20)	75(12)

C(23B)	-2460(20)	4620(13)	2180(20)	90(13)
C(24B)	-3210(20)	4631(15)	1960(20)	95(11)
C(25B)	-3630(20)	4487(14)	2530(20)	93(11)
C(26B)	-3310(20)	4310(13)	3380(20)	72(10)
C(27B)	-3730(20)	4172(15)	3990(30)	114(14)
C(28B)	-4067(19)	3536(17)	3800(30)	134(17)
C(29B)	-4334(19)	4610(20)	4030(20)	133(16)
C(30B)	-1278(15)	4434(11)	3282(16)	50(7)
C(31B)	-1025(16)	4961(12)	3853(18)	81(9)
C(32B)	-870(20)	4415(15)	2540(20)	120(15)
C(1A)	-8434(13)	1103(12)	5523(14)	36(7)
C(2A)	-8305(14)	1448(13)	6279(19)	60(8)
C(3A)	-8368(18)	1162(15)	7058(19)	74(10)
C(4A)	-8640(20)	570(20)	7030(20)	120(15)
C(5A)	-8776(16)	251(14)	6260(20)	73(9)
C(6A)	-8681(18)	512(13)	5511(19)	72(10)
C(7A)	-8070(20)	2078(15)	6290(20)	109(13)
C(8A)	-8868(18)	137(13)	4697(19)	91(11)
C(9A)	-6520(16)	1161(11)	3820(20)	55(9)
C(10A)	-6046(15)	945(12)	4572(18)	49(8)
C(11A)	-5350(20)	795(14)	4560(20)	98(13)
C(12A)	-5120(20)	836(16)	3830(30)	108(14)
C(13A)	-5556(17)	1067(14)	3060(30)	81(12)
C(14A)	-6300(18)	1226(12)	3020(20)	68(11)
C(15A)	-6770(20)	1498(14)	2270(30)	100(16)
C(16A)	-6330(20)	1782(19)	1660(20)	129(15)
C(17A)	-7340(20)	1006(18)	1800(19)	109(13)
C(18A)	-6369(18)	872(14)	5356(18)	71(9)
C(19A)	-5780(30)	973(19)	6160(30)	148(16)
C(20A)	-6730(20)	269(16)	5400(20)	116(14)
C(21A)	-7786(15)	3058(14)	4188(15)	47(8)
C(22A)	-8291(19)	3426(12)	4356(19)	72(11)
C(23A)	-8170(20)	4048(14)	4492(17)	78(11)
C(24A)	-7550(20)	4274(15)	4420(20)	92(12)
C(25A)	-6981(17)	3917(14)	4275(18)	77(10)
C(26A)	-7120(16)	3296(12)	4117(17)	53(7)
C(27A)	-6481(15)	2895(17)	3910(20)	94(12)
C(28A)	-5890(20)	2688(16)	4680(20)	115(12)
C(29A)	-6160(30)	3207(19)	3190(30)	170(20)
C(30A)	-9089(14)	3221(13)	4360(20)	63(9)
C(31A)	-9540(18)	3113(13)	3500(30)	92(12)
C(32A)	-9411(18)	3534(16)	5010(20)	106(12)
N(3A)	-7923(12)	2448(11)	4006(13)	63(7)
C(20B)	-2321(18)	1775(18)	5800(20)	162(18)
C(18B)	-2950(20)	2134(12)	5290(20)	111(12)
C(19B)	-3480(20)	1770(20)	4640(30)	200(20)

Table 42. Bond lengths [Å] and angles [°].

Re(1)-N(1A)	1.70(2)	Re(1)-N(3A)	1.71(2)	Re(1)-N(2A)	1.725(18)
Re(1)-Cl(1A)	2.271(9)	Re(2)-N(1B)	1.72(2)	Re(2)-N(3B)	1.73(2)
Re(2)-N(2B)	1.766(19)	Re(2)-Cl(1B)	2.272(9)	N(1A)-C(9A)	1.43(3)

N(3B)-C(21B)	1.44(3)	N(2B)-C(9B)	1.31(2)	N(2A)-C(1A)	1.38(3)
N(1B)-C(1B)	1.37(2)	C(1B)-C(2B)	1.3900	C(1B)-C(6B)	1.3900
C(2B)-C(3B)	1.3900	C(2B)-C(8B)	1.54(4)	C(3B)-C(4B)	1.3900
C(4B)-C(5B)	1.3900	C(5B)-C(6B)	1.3900	C(6B)-C(7B)	1.61(4)
C(9B)-C(10B)	1.3900	C(9B)-C(14B)	1.3900	C(10B)-C(11B)	1.3900
C(10B)-C(18B)	1.50(3)	C(11B)-C(12B)	1.3900	C(12B)-C(13B)	1.3900
C(13B)-C(14B)	1.3900	C(14B)-C(15B)	1.51(4)	C(15B)-C(16B)	1.46(4)
C(15B)-C(17B)	1.58(6)	C(21B)-C(26B)	1.37(4)	C(21B)-C(22B)	1.41(3)
C(22B)-C(23B)	1.34(4)	C(22B)-C(30B)	1.55(4)	C(23B)-C(24B)	1.35(4)
C(24B)-C(25B)	1.38(4)	C(25B)-C(26B)	1.40(4)	C(26B)-C(27B)	1.41(4)
C(27B)-C(29B)	1.50(4)	C(27B)-C(28B)	1.53(4)	C(30B)-C(31B)	1.48(3)
C(30B)-C(32B)	1.55(3)	C(1A)-C(6A)	1.37(3)	C(1A)-C(2A)	1.40(3)
C(2A)-C(3A)	1.42(4)	C(2A)-C(7A)	1.44(4)	C(3A)-C(4A)	1.39(4)
C(4A)-C(5A)	1.40(4)	C(5A)-C(6A)	1.37(4)	C(6A)-C(8A)	1.51(3)
C(9A)-C(10A)	1.40(4)	C(9A)-C(14A)	1.43(4)	C(10A)-C(11A)	1.34(4)
C(10A)-C(18A)	1.51(3)	C(11A)-C(12A)	1.33(4)	C(12A)-C(13A)	1.40(4)
C(13A)-C(14A)	1.42(4)	C(14A)-C(15A)	1.45(5)	C(15A)-C(16A)	1.53(4)
C(15A)-C(17A)	1.57(5)	C(18A)-C(19A)	1.51(5)	C(18A)-C(20A)	1.49(4)
C(21A)-C(22A)	1.31(3)	C(21A)-C(26A)	1.37(3)	C(21A)-N(3A)	1.38(3)
C(22A)-C(23A)	1.39(3)	C(22A)-C(30A)	1.55(4)	C(23A)-C(24A)	1.29(4)
C(24A)-C(25A)	1.37(4)	C(25A)-C(26A)	1.40(3)	C(26A)-C(27A)	1.58(4)
C(27A)-C(29A)	1.56(4)	C(27A)-C(28A)	1.53(4)	C(30A)-C(31A)	1.45(4)
C(30A)-C(32A)	1.49(4)	C(20B)-C(18B)	1.491(5)	C(18B)-C(19B)	1.490(5)

N(1A)-Re(1)-N(3A)	110.4(10)	N(1A)-Re(1)-N(2A)	112.2(10)
N(3A)-Re(1)-N(2A)	112.4(8)	N(1A)-Re(1)-Cl(1A)	107.2(8)
N(3A)-Re(1)-Cl(1A)	107.4(8)	N(2A)-Re(1)-Cl(1A)	106.9(8)
N(1B)-Re(2)-N(3B)	111.6(10)	N(1B)-Re(2)-N(2B)	110.0(9)
N(3B)-Re(2)-N(2B)	113.5(10)	N(1B)-Re(2)-Cl(1B)	107.7(8)
N(3B)-Re(2)-Cl(1B)	106.7(8)	N(2B)-Re(2)-Cl(1B)	107.1(7)
C(9A)-N(1A)-Re(1)	165(2)	C(21B)-N(3B)-Re(2)	162.1(19)
C(9B)-N(2B)-Re(2)	170.6(18)	C(1A)-N(2A)-Re(1)	165(2)
C(1B)-N(1B)-Re(2)	166.6(19)	N(1B)-C(1B)-C(2B)	122.1(19)
N(1B)-C(1B)-C(6B)	117.7(19)	C(2B)-C(1B)-C(6B)	120.0
C(3B)-C(2B)-C(1B)	120.0	C(3B)-C(2B)-C(8B)	116.6(19)
C(1B)-C(2B)-C(8B)	123.4(19)	C(2B)-C(3B)-C(4B)	120.0
C(3B)-C(4B)-C(5B)	120.0	C(6B)-C(5B)-C(4B)	120.0
C(5B)-C(6B)-C(1B)	120.0	C(5B)-C(6B)-C(7B)	120(2)

C(1B)-C(6B)-C(7B)	120(2)	N(2B)-C(9B)-C(10B)	116.1(17)
N(2B)-C(9B)-C(14B)	123.9(17)	C(10B)-C(9B)-C(14B)	120.0
C(9B)-C(10B)-C(11B)	120.0	C(9B)-C(10B)-C(18B)	127(2)
C(11B)-C(10B)-C(18B)	113(2)	C(12B)-C(11B)-C(10B)	120.0
C(13B)-C(12B)-C(11B)	120.0	C(12B)-C(13B)-C(14B)	120.0
C(13B)-C(14B)-C(9B)	120.0	C(13B)-C(14B)-C(15B)	119.9(17)
C(9B)-C(14B)-C(15B)	119.8(17)	C(16B)-C(15B)-C(14B)	118(3)
C(16B)-C(15B)-C(17B)	115(4)	C(14B)-C(15B)-C(17B)	109(3)
C(26B)-C(21B)-C(22B)	124(4)	C(26B)-C(21B)-N(3B)	118(3)
C(22B)-C(21B)-N(3B)	118(3)	C(23B)-C(22B)-C(21B)	119(4)
C(23B)-C(22B)-C(30B)	123(3)	C(21B)-C(22B)-C(30B)	118(3)
C(22B)-C(23B)-C(24B)	119(3)	C(23B)-C(24B)-C(25B)	122(4)
C(26B)-C(25B)-C(24B)	121(4)	C(21B)-C(26B)-C(25B)	114(3)
C(21B)-C(26B)-C(27B)	123(4)	C(25B)-C(26B)-C(27B)	123(4)
C(26B)-C(27B)-C(29B)	116(3)	C(26B)-C(27B)-C(28B)	109(3)
C(29B)-C(27B)-C(28B)	108(3)	C(31B)-C(30B)-C(22B)	112(2)
C(31B)-C(30B)-C(32B)	110(2)	C(22B)-C(30B)-C(32B)	113(3)
C(6A)-C(1A)-N(2A)	119(2)	C(6A)-C(1A)-C(2A)	121(2)
N(2A)-C(1A)-C(2A)	119(2)	C(1A)-C(2A)-C(3A)	119(3)
C(1A)-C(2A)-C(7A)	121(3)	C(3A)-C(2A)-C(7A)	120(3)
C(4A)-C(3A)-C(2A)	119(3)	C(3A)-C(4A)-C(5A)	119(3)
C(6A)-C(5A)-C(4A)	122(3)	C(1A)-C(6A)-C(5A)	119(3)
C(1A)-C(6A)-C(8A)	123(2)	C(5A)-C(6A)-C(8A)	118(3)
C(10A)-C(9A)-N(1A)	122(3)	C(10A)-C(9A)-C(14A)	123(3)
N(1A)-C(9A)-C(14A)	115(3)	C(11A)-C(10A)-C(9A)	119(3)
C(11A)-C(10A)-C(18A)	124(3)	C(9A)-C(10A)-C(18A)	117(3)
C(12A)-C(11A)-C(10A)	120(4)	C(11A)-C(12A)-C(13A)	124(3)
C(12A)-C(13A)-C(14A)	120(3)	C(9A)-C(14A)-C(13A)	114(4)
C(9A)-C(14A)-C(15A)	123(3)	C(13A)-C(14A)-C(15A)	123(3)
C(14A)-C(15A)-C(16A)	112(3)	C(14A)-C(15A)-C(17A)	109(3)
C(16A)-C(15A)-C(17A)	112(3)	C(19A)-C(18A)-C(20A)	110(3)
C(19A)-C(18A)-C(10A)	110(3)	C(20A)-C(18A)-C(10A)	114(2)
C(22A)-C(21A)-C(26A)	119(3)	C(22A)-C(21A)-N(3A)	122(2)
C(26A)-C(21A)-N(3A)	119(2)	C(21A)-C(22A)-C(23A)	123(3)
C(21A)-C(22A)-C(30A)	124(2)	C(23A)-C(22A)-C(30A)	114(3)
C(24A)-C(23A)-C(22A)	118(3)	C(23A)-C(24A)-C(25A)	123(3)
C(24A)-C(25A)-C(26A)	118(3)	C(21A)-C(26A)-C(25A)	119(2)
C(21A)-C(26A)-C(27A)	123(3)	C(25A)-C(26A)-C(27A)	118(3)

C(29A)-C(27A)-C(28A)	113(3)	C(29A)-C(27A)-C(26A)	110(3)
C(28A)-C(27A)-C(26A)	116(2)	C(31A)-C(30A)-C(32A)	120(3)
C(31A)-C(30A)-C(22A)	114(3)	C(32A)-C(30A)-C(22A)	114(3)
C(21A)-N(3A)-Re(1)	172.5(19)	C(10B)-C(18B)-C(20B)	112(3)
C(10B)-C(18B)-C(19B)	117(3)	C(20B)-C(18B)-C(19B)	113.9(6)

Symmetry transformations used to generate equivalent atoms:

Table 43. Anisotropic displacement parameters ($Å^2 x\ 10^3$). The anisotropic displacement factor exponent takes the form: $-2\pi^2[\ h^2 a^{*2} U^{11} + ... + 2\ h\ k\ a^*\ b^*\ U^{12}\ ]$

	U^{11}	U^{22}	U^{33}	U^{23}	U^{13}	U^{12}
Re(1)	55(1)	52(1)	48(1)	3(1)	14(1)	2(1)
Re(2)	52(1)	50(1)	57(1)	4(1)	14(1)	1(1)
Cl(1A)	76(6)	86(6)	77(6)	1(4)	14(6)	14(5)
N(1A)	36(16)	98(18)	45(17)	13(13)	-8(14)	3(13)
N(3B)	58(17)	48(15)	67(19)	25(14)	-7(16)	24(12)
Cl(1B)	93(7)	87(6)	81(7)	-15(5)	5(6)	-25(5)
N(2B)	33(14)	38(12)	65(17)	5(11)	-14(14)	-4(11)
N(2A)	60(17)	44(13)	83(19)	-18(12)	44(17)	-19(11)
N(1B)	34(14)	60(15)	83(17)	-11(13)	19(14)	6(12)
C(1B)	50(20)	60(20)	80(20)	18(18)	40(20)	-2(17)
C(3B)	50(20)	70(30)	80(30)	0(20)	-40(20)	-7(17)
C(4B)	140(50)	80(30)	320(80)	-100(40)	80(50)	10(30)
C(5B)	140(40)	20(20)	430(90)	-90(40)	110(60)	-10(20)
C(6B)	50(20)	50(20)	130(30)	30(20)	10(30)	-12(16)
C(7B)	70(30)	140(40)	150(40)	70(30)	-10(30)	40(20)
C(8B)	230(50)	90(30)	40(20)	3(19)	30(30)	10(30)
C(9B)	110(30)	50(20)	90(30)	33(18)	40(30)	-40(20)
C(10B)	50(20)	130(30)	160(40)	60(30)	70(30)	0(20)
C(11B)	100(30)	100(30)	110(30)	-40(20)	30(30)	-20(20)
C(12B)	90(30)	110(30)	150(40)	20(30)	30(30)	-60(30)
C(13B)	120(30)	110(30)	200(40)	20(30)	120(40)	10(30)
C(14B)	70(20)	80(30)	90(30)	4(19)	50(20)	20(20)
C(15B)	50(20)	100(30)	150(40)	20(30)	50(30)	10(20)
C(16B)	180(50)	100(30)	280(60)	40(30)	110(50)	50(30)
C(17B)	160(60)	210(70)	310(90)	-90(60)	-80(60)	-10(50)
C(21B)	60(20)	13(15)	90(30)	-21(16)	20(20)	5(14)
C(22B)	120(30)	36(18)	80(30)	-3(17)	60(30)	-15(19)
C(23B)	150(40)	70(20)	70(30)	21(19)	50(30)	0(20)
C(25B)	90(30)	80(30)	80(30)	10(20)	-40(30)	-30(20)
C(26B)	70(30)	60(20)	80(30)	21(19)	20(30)	-4(19)
C(27B)	60(30)	80(30)	200(50)	20(30)	30(30)	-30(20)
C(28B)	70(30)	140(40)	200(50)	50(30)	60(30)	30(30)
C(29B)	60(30)	230(50)	90(30)	-10(30)	-30(20)	50(30)
C(32B)	130(30)	110(30)	140(40)	20(20)	70(30)	-30(30)
C(1A)	31(16)	49(18)	26(17)	-25(14)	1(16)	-19(14)
C(2A)	28(18)	80(20)	70(20)	-8(19)	9(19)	-19(16)
C(3A)	90(30)	80(20)	60(20)	-16(18)	10(20)	-20(20)

C(4A)	130(40)	160(40)	80(30)	20(30)	40(30)	0(30)
C(5A)	60(20)	60(20)	90(30)	10(20)	-10(30)	5(17)
C(6A)	100(30)	50(20)	70(20)	-23(18)	50(20)	-21(19)
C(7A)	140(40)	90(30)	100(30)	-30(20)	30(30)	-50(30)
C(8A)	90(30)	70(20)	80(30)	-10(20)	-50(20)	20(20)
C(9A)	30(19)	31(16)	80(30)	-13(16)	-40(20)	-2(14)
C(10A)	21(17)	70(20)	40(20)	-17(16)	-16(19)	1(15)
C(11A)	80(30)	100(30)	130(30)	10(20)	50(30)	40(20)
C(12A)	50(30)	120(30)	170(40)	10(30)	50(30)	40(20)
C(13A)	30(20)	60(20)	160(40)	-10(20)	20(20)	3(17)
C(14A)	80(30)	50(20)	100(30)	12(18)	60(30)	13(17)
C(15A)	150(40)	60(20)	140(40)	20(20)	130(40)	20(20)
C(16A)	80(30)	230(50)	80(30)	50(30)	10(30)	-10(30)
C(17A)	130(40)	130(40)	50(20)	-30(20)	-10(30)	20(30)
C(18A)	50(20)	100(30)	40(20)	-18(18)	-40(20)	15(19)
C(20A)	120(30)	100(30)	130(40)	-20(20)	40(30)	-30(30)
C(21A)	50(20)	60(20)	30(17)	25(15)	12(16)	7(17)
C(22A)	120(30)	26(18)	80(20)	-21(14)	50(20)	-25(18)
C(23A)	100(30)	80(30)	60(20)	-12(17)	40(20)	-20(20)
C(24A)	120(30)	80(20)	90(30)	-1(19)	50(30)	20(30)
C(25A)	60(20)	80(20)	90(30)	26(19)	30(20)	-30(19)
C(27A)	22(18)	180(40)	60(30)	-20(20)	-20(20)	-30(20)
C(29A)	210(50)	180(40)	180(40)	-50(30)	160(50)	-70(40)
C(30A)	7(15)	80(20)	90(30)	-30(20)	-4(19)	0(15)
C(31A)	70(30)	50(20)	150(40)	-30(20)	20(30)	-9(18)
C(32A)	70(30)	140(30)	110(30)	-10(20)	20(30)	0(20)
N(3A)	77(18)	63(18)	64(16)	-19(12)	49(15)	-22(14)

Table 44. Hydrogen coordinates (x 10^4) and isotropic displacement parameters ($Å^2$x 10^3).

	x	y	z	U(eq)
H(3BA)	-1226	1740	2847	94
H(4BA)	-325	1144	3729	210
H(5BA)	80	1386	5182	225
H(7BA)	-609	2606	6326	192
H(7BB)	200	2392	6311	192
H(7BC)	-378	1915	6510	192
H(8BA)	-2062	2503	2590	184
H(8BB)	-1806	3110	3109	184
H(8BC)	-2413	2691	3369	184
H(11A)	-4023	1899	5956	124
H(12A)	-4630	2457	6829	139
H(13A)	-4250	3446	7241	155
H(15A)	-2921	4255	6393	115
H(16A)	-4135	4525	6127	259
H(16B)	-3607	4993	6728	259
H(16C)	-4089	4529	7131	259
H(17A)	-2509	4590	7857	375
H(17B)	-2205	3937	7690	375
H(17C)	-2866	3997	8158	375

H(23A)	-2187	4747	1782	108
H(24A)	-3443	4741	1390	114
H(25A)	-4150	4509	2357	111
H(27A)	-3387	4160	4564	136
H(28A)	-3681	3244	3775	201
H(28B)	-4424	3541	3254	201
H(28C)	-4309	3419	4254	201
H(29A)	-4128	5015	4168	200
H(29B)	-4581	4481	4476	200
H(29C)	-4686	4620	3482	200
H(30A)	-1139	4060	3629	59
H(31A)	-1297	4974	4305	121
H(31B)	-1111	5335	3521	121
H(31C)	-503	4920	4108	121
H(32A)	-340	4420	2775	180
H(32B)	-1006	4768	2170	180
H(32C)	-1001	4045	2204	180
H(3AA)	-8225	1370	7584	88
H(4AA)	-8737	392	7531	144
H(5AA)	-8936	-156	6248	88
H(7AA)	-8072	2205	5704	164
H(7AB)	-7583	2120	6647	164
H(7AC)	-8415	2332	6510	164
H(8AA)	-8762	371	4224	136
H(8AB)	-9388	32	4571	136
H(8AC)	-8575	-233	4774	136
H(11B)	-5023	661	5063	118
H(12B)	-4643	702	3824	129
H(13B)	-5355	1117	2575	98
H(15B)	-7054	1828	2463	120
H(16D)	-5994	2084	1976	194
H(16E)	-6668	1976	1185	194
H(16F)	-6056	1466	1449	194
H(17D)	-7604	840	2205	164
H(17E)	-7075	680	1586	164
H(17F)	-7682	1194	1323	164
H(18A)	-6748	1193	5330	85
H(19A)	-5992	927	6662	223
H(19B)	-5580	1381	6157	223
H(19C)	-5390	676	6191	223
H(20A)	-6888	239	5940	174
H(20B)	-6384	-56	5371	174
H(20C)	-7157	232	4925	174
H(23B)	-8538	4298	4634	93
H(24B)	-7480	4698	4465	110
H(25C)	-6516	4086	4284	93
H(27B)	-6721	2516	3643	113
H(28D)	-5526	2439	4484	173
H(28E)	-6111	2452	5066	173
H(28F)	-5643	3043	4981	173
H(29D)	-5770	2957	3065	262
H(29E)	-5966	3605	3390	262
H(29F)	-6549	3255	2675	262
H(30B)	-9011	2803	4591	75
H(31D)	-10029	2986	3549	138
H(31E)	-9318	2795	3224	138
H(31F)	-9577	3485	3169	138
H(32D)	-9909	3388	4971	158

H(32E)	-9421	3971	4909	158
H(32F)	-9113	3448	5581	158
H(20D)	-2001	2042	6207	244
H(20E)	-2044	1596	5415	244
H(20F)	-2507	1453	6112	244
H(18B)	-2719	2412	4943	134
H(19D)	-3864	2030	4328	305
H(19E)	-3690	1448	4929	305
H(19F)	-3214	1584	4244	305

Appendix VIII

X-ray data for $ClRe(NAr)_2(N\text{-}o\text{-}^tBu)$

The tables that follow contain atomic coordinates and equivalent isotropic displacement parameters, complete bond lengths (Å) and angles (°), anisotropic displacement parameters and calculated H-atom positions for $ClRe(NAr)_2(N\text{-}o\text{-}^tBu)$.

Table 45. Atomic coordinates (x 10^4) and equivalent isotropic displacement parameters ($Å^2$x 10^3). U(eq) is defined as one third of the trace of the orthogonalized U^{ij} tensor.

	x	y	z	U(eq)
Re(1)	9183(1)	6389(1)	7162(1)	26(1)
Cl(1)	11059(1)	7121(1)	6148(1)	46(1)
N(1)	9030(3)	6962(3)	8155(2)	33(1)
C(1A)	8751(3)	7345(3)	8987(2)	33(1)
C(2A)	7447(4)	7705(3)	9457(2)	38(1)
C(3A)	7234(4)	8095(4)	10279(3)	53(1)
C(4A)	8290(5)	8150(5)	10615(3)	67(1)
C(5A)	9557(5)	7809(6)	10152(4)	74(2)
C(6A)	9845(4)	7382(5)	9317(3)	55(1)
C(7A)	6301(4)	7649(4)	9072(3)	50(1)
C(8A)	5565(5)	6490(5)	9531(5)	81(2)
C(9A)	5362(5)	8877(5)	9127(4)	62(1)
C(10A)	11246(5)	6962(7)	8809(4)	85(2)
C(11A)	11817(8)	5809(8)	9247(8)	174(6)
C(12A)	12123(9)	8048(10)	8583(8)	161(5)
N(2)	7839(3)	6991(2)	6738(2)	30(1)
C(1B)	6656(3)	7424(3)	6534(2)	27(1)
C(2B)	5891(3)	6534(3)	6387(2)	34(1)
C(3B)	4761(4)	7022(4)	6122(3)	48(1)
C(4B)	4392(4)	8321(4)	6012(3)	53(1)
C(5B)	5150(4)	9176(3)	6165(3)	44(1)
C(6B)	6276(3)	8756(3)	6441(2)	32(1)
C(7B)	6256(4)	5106(3)	6547(3)	42(1)
C(8B)	6288(6)	4438(4)	5759(3)	64(1)
C(9B)	5336(6)	4494(4)	7388(3)	64(1)
C(10B)	7096(4)	9694(3)	6625(3)	41(1)
C(11B)	6279(6)	10939(4)	6921(4)	68(1)
C(12B)	8284(5)	9980(5)	5828(3)	61(1)

N(3)	9385(3)	4702(3)	7302(2)	34(1)
C(1)	9166(3)	3437(3)	7641(2)	28(1)
C(2)	8055(3)	3218(3)	8363(2)	38(1)
C(3)	7775(4)	1991(4)	8748(3)	47(1)
C(4)	8608(4)	964(4)	8417(3)	49(1)
C(5)	9691(4)	1168(3)	7701(3)	41(1)
C(6)	10022(3)	2393(3)	7279(2)	30(1)
C(7)	11219(3)	2588(3)	6466(2)	39(1)
C(8)	10760(4)	3273(4)	5667(2)	48(1)
C(9)	11974(5)	1290(4)	6210(3)	61(1)
C(10)	12211(4)	3355(4)	6663(3)	47(1)

Table 46. Bond lengths [Å] and angles [°].

Re(1)-N(1)	1.744(3)	Re(1)-N(2)	1.751(3)	Re(1)-N(3)	1.757(3)
Re(1)-Cl(1)	2.2990(8)	N(1)-C(1A)	1.387(4)	C(1A)-C(2A)	1.399(5)
C(1A)-C(6A)	1.416(5)	C(2A)-C(3A)	1.385(5)	C(2A)-C(7A)	1.525(5)
C(3A)-C(4A)	1.388(7)	C(4A)-C(5A)	1.360(7)	C(5A)-C(6A)	1.411(6)
C(6A)-C(10A)	1.513(7)	C(7A)-C(8A)	1.512(7)	C(7A)-C(9A)	1.525(6)
C(10A)-C(11A)	1.451(10)	C(10A)-C(12A)	1.512(12)	N(2)-C(1B)	1.385(4)
C(1B)-C(6B)	1.410(4)	C(1B)-C(2B)	1.416(4)	C(2B)-C(3B)	1.391(5)
C(2B)-C(7B)	1.508(4)	C(3B)-C(4B)	1.376(5)	C(4B)-C(5B)	1.386(6)
C(5B)-C(6B)	1.383(5)	C(6B)-C(10B)	1.524(5)	C(7B)-C(9B)	1.511(6)
C(7B)-C(8B)	1.532(6)	C(10B)-C(12B)	1.525(6)	C(10B)-C(11B)	1.539(5)
N(3)-C(1)	1.384(4)	C(1)-C(2)	1.398(4)	C(1)-C(6)	1.417(4)
C(2)-C(3)	1.375(5)	C(3)-C(4)	1.377(6)	C(4)-C(5)	1.371(6)
C(5)-C(6)	1.400(4)	C(6)-C(7)	1.532(5)	C(7)-C(8)	1.530(5)
C(7)-C(10)	1.545(5)	C(7)-C(9)	1.547(5)		

N(1)-Re(1)-N(2)	111.46(13)	N(1)-Re(1)-N(3)	110.56(13)
N(2)-Re(1)-N(3)	111.62(12)	N(1)-Re(1)-Cl(1)	107.54(9)
N(2)-Re(1)-Cl(1)	107.37(8)	N(3)-Re(1)-Cl(1)	108.10(9)
C(1A)-N(1)-Re(1)	172.4(2)	N(1)-C(1A)-C(2A)	120.8(3)
N(1)-C(1A)-C(6A)	116.8(3)	C(2A)-C(1A)-C(6A)	122.3(3)
C(3A)-C(2A)-C(1A)	118.1(3)	C(3A)-C(2A)-C(7A)	121.6(3)
C(1A)-C(2A)-C(7A)	120.4(3)	C(4A)-C(3A)-C(2A)	120.7(4)
C(5A)-C(4A)-C(3A)	120.9(4)	C(4A)-C(5A)-C(6A)	121.4(4)
C(5A)-C(6A)-C(1A)	116.5(4)	C(5A)-C(6A)-C(10A)	121.8(4)
C(1A)-C(6A)-C(10A)	121.7(4)	C(8A)-C(7A)-C(2A)	109.9(4)
C(8A)-C(7A)-C(9A)	111.0(4)	C(2A)-C(7A)-C(9A)	112.2(4)

C(11A)-C(10A)-C(6A)	113.2(6)	C(11A)-C(10A)-C(12A)	112.1(7)
C(6A)-C(10A)-C(12A)	111.3(6)	C(1B)-N(2)-Re(1)	171.2(2)
N(2)-C(1B)-C(6B)	118.6(3)	N(2)-C(1B)-C(2B)	119.6(3)
C(6B)-C(1B)-C(2B)	121.7(3)	C(3B)-C(2B)-C(1B)	117.6(3)
C(3B)-C(2B)-C(7B)	121.1(3)	C(1B)-C(2B)-C(7B)	121.3(3)
C(4B)-C(3B)-C(2B)	121.3(3)	C(3B)-C(4B)-C(5B)	120.2(3)
C(6B)-C(5B)-C(4B)	121.5(3)	C(5B)-C(6B)-C(1B)	117.6(3)
C(5B)-C(6B)-C(10B)	121.5(3)	C(1B)-C(6B)-C(10B)	120.8(3)
C(2B)-C(7B)-C(9B)	111.4(3)	C(2B)-C(7B)-C(8B)	112.1(3)
C(9B)-C(7B)-C(8B)	110.5(3)	C(12B)-C(10B)-C(6B)	110.7(3)
C(12B)-C(10B)-C(11B)	111.2(4)	C(6B)-C(10B)-C(11B)	113.4(3)
C(1)-N(3)-Re(1)	160.8(2)	N(3)-C(1)-C(2)	117.4(3)
N(3)-C(1)-C(6)	122.1(3)	C(2)-C(1)-C(6)	120.5(3)
C(3)-C(2)-C(1)	121.1(3)	C(4)-C(3)-C(2)	119.3(4)
C(5)-C(4)-C(3)	120.0(3)	C(4)-C(5)-C(6)	123.2(3)
C(5)-C(6)-C(1)	115.8(3)	C(5)-C(6)-C(7)	121.9(3)
C(1)-C(6)-C(7)	122.2(3)	C(8)-C(7)-C(6)	110.1(3)
C(8)-C(7)-C(10)	110.9(3)	C(6)-C(7)-C(10)	110.3(3)
C(8)-C(7)-C(9)	107.1(3)	C(6)-C(7)-C(9)	111.4(3)
C(10)-C(7)-C(9)	107.0(3)		

Symmetry transformations used to generate equivalent atoms:

Table 47. Anisotropic displacement parameters ($Å^2 x\ 10^3$). The anisotropic displacement factor exponent takes the form: $-2\pi^2[\ h^2\ a^{*2}U^{11} + ... + 2\ h\ k\ a^*\ b^*\ U^{12}\ ]$

U^{11}	U^{22}	U^{33}	U^{23}	U^{13}	U^{12}	
Re(1)	24(1)	23(1)	31(1)	-3(1)	-8(1)	-1(1)
Cl(1)	33(1)	51(1)	47(1)	1(1)	-2(1)	-12(1)
N(1)24(1)	40(1)	38(1)	-9(1)	-10(1)	-3(1)	
C(1A)	35(2)	32(2)	34(2)	-9(1)	-11(1)	-1(1)
C(2A)	38(2)	37(2)	38(2)	-5(1)	-9(1)	-3(1)
C(3A)	52(2)	59(2)	46(2)	-16(2)	-10(2)	3(2)
C(4A)	81(3)	86(3)	45(2)	-25(2)	-27(2)	0(3)
C(5A)	62(3)	113(4)	67(3)	-41(3)	-37(3)	1(3)
C(6A)	48(2)	75(3)	53(2)	-25(2)	-25(2)	3(2)
C(7A)	30(2)	67(3)	56(2)	-26(2)	-7(2)	0(2)
C(8A)	58(3)	49(3)	146(6)	-37(3)	-33(3)	-1(2)
C(9A)	43(2)	62(3)	74(3)	0(2)	-10(2)	-3(2)
C(10A)	40(2)	146(6)	85(4)	-54(4)	-28(3)	6(3)
C(11A)	80(5)	95(6)	258(13)	14(7)	48(6)	39(4)

C(12A)	78(5)	143(9)	190(11)	45(8)	31(6)	4(5)
N(2)31(1)	25(1)	34(1)	2(1)	-9(1)	-5(1)	
C(1B)	25(1)	25(1)	30(1)	-3(1)	-10(1)	-1(1)
C(2B)	31(2)	28(2)	46(2)	-7(1)	-14(1)	-3(1)
C(3B)	37(2)	41(2)	74(3)	-14(2)	-25(2)	-3(2)
C(4B)	39(2)	50(2)	77(3)	-4(2)	-32(2)	5(2)
C(5B)	40(2)	31(2)	59(2)	-5(2)	-17(2)	9(1)
C(6B)	33(2)	27(2)	35(2)	-3(1)	-8(1)	1(1)
C(7B)	38(2)	28(2)	63(2)	-8(2)	-19(2)	-6(1)
C(8B)	95(4)	37(2)	54(3)	-11(2)	-6(2)	-12(2)
C(9B)	90(4)	45(2)	47(2)	-4(2)	-9(2)	-1(2)
C(10B)	55(2)	25(2)	48(2)	-3(1)	-22(2)	-4(1)
C(11B)	108(4)	28(2)	80(3)	-12(2)	-49(3)	10(2)
C(12B)	76(3)	53(2)	61(3)	8(2)	-24(2)	-34(2)
N(3)30(1)	28(1)	37(1)	-3(1)	-4(1)	3(1)	
C(1)28(1)	25(1)	31(1)	-4(1)	-11(1)	0(1)	
C(2)33(2)	40(2)	39(2)	-6(1)	-5(1)	-2(1)	
C(3)42(2)	50(2)	44(2)	4(2)	-7(2)	-13(2)	
C(4)54(2)	35(2)	59(2)	7(2)	-21(2)	-17(2)	
C(5)46(2)	24(2)	53(2)	-6(1)	-18(2)	0(1)	
C(6)31(2)	25(1)	34(2)	-6(1)	-12(1)	2(1)	
C(7)33(2)	41(2)	37(2)	-6(1)	-5(1)	7(1)	
C(8)48(2)	56(2)	35(2)	-9(2)	-7(2)	8(2)	
C(9)50(2)	51(2)	69(3)	-20(2)	-2(2)	18(2)	
C(10)	29(2)	53(2)	54(2)	-2(2)	-9(2)	-1(2)

Table 48. Hydrogen coordinates (x 10^4) and isotropic displacement parameters ($Å^2$x 10^3).

	x	y	z	U(eq)
H(3AA)	6355	8327	10616	63
H(4AA)	8125	8431	11177	81
H(5AA)	10263	7860	10395	89
H(7AA)	6685	7542	8432	60
H(8AA)	6188	5714	9487	121
H(8AB)	4879	6419	9247	121
H(8AC)	5150	6586	10157	121
H(9AA)	5858	9612	8818	93
H(9AB)	4956	8994	9750	93
H(9AC)	4666	8815	8849	93
H(10A)	11196	6745	8233	102
H(11A)	11229	5125	9370	261
H(11B)	11923	5988	9805	261
H(11C)	12685	5535	8861	261
H(12A)	13024	7746	8261	242
H(12B)	12141	8342	9130	242
H(12C)	11771	8760	8212	242
H(3BA)	4233	6446	6014	58
H(4BA)	3615	8632	5832	64
H(5BA)	4889	10071	6078	53
H(7BA)	7169	4975	6624	50

H(8BA)	6889	4845	5220	96
H(8BB)	5394	4513	5685	96
H(8BC)	6602	3529	5869	96
H(9BA)	5333	4926	7886	96
H(9BB)	5641	3583	7500	96
H(9BC)	4436	4576	7323	96
H(10B)	7454	9257	7126	49
H(11D)	5521	10727	7430	102
H(11E)	5958	11424	6432	102
H(11F)	6836	11460	7089	102
H(12D)	8781	9172	5652	92
H(12E)	8861	10491	5987	92
H(12F)	7974	10462	5334	92
H(2A)	7483	3927	8592	46
H(3B)	7014	1854	9237	56
H(4A)	8433	113	8684	58
H(5A)	10243	443	7480	49
H(8A)	10280	4106	5803	73
H(8B)	10172	2746	5534	73
H(8C)	11533	3405	5153	73
H(9A)	11375	774	6078	91
H(9B)	12298	828	6703	91
H(9C)	12727	1446	5685	91
H(10C)	11770	4190	6824	70
H(10D)	12965	3484	6135	70
H(10E)	12529	2876	7155	70

Appendix IX

X-ray data for $MeRe(NAr)_2(NAr')$

The tables that follow contain atomic coordinates and equivalent isotropic displacement parameters, complete bond lengths (Å) and angles (°), anisotropic displacement parameters and calculated H-atom positions for $MeRe(NAr)_2(NAr')$.

Table 49. Atomic coordinates (x 10^4) and equivalent isotropic displacement parameters ($Å^2$x 10^3). U(eq) is defined as one third of the trace of the orthogonalized U^{ij} tensor.

	x	y	z	U(eq)
Re	198(1)	1339(1)	7475(1)	22(1)
C	1905(6)	1538(1)	6657(6)	41(1)
N(1)	1039(4)	982(1)	8575(4)	30(1)
N(2)	-154(4)	1681(1)	8552(4)	25(1)
N(3)	-1230(4)	1245(1)	5771(4)	29(1)
C(11)	1421(5)	682(1)	9366(5)	26(1)
C(12)	2208(5)	434(1)	8791(5)	33(1)
C(13)	2633(7)	137(1)	9631(7)	48(1)
C(14)	2259(8)	79(2)	10958(7)	59(2)
C(15)	1472(7)	318(2)	11492(6)	50(1)
C(16)	1058(6)	627(1)	10734(5)	35(1)
C(17)	2639(7)	503(1)	7348(6)	45(1)
C(18)	4132(9)	694(3)	7765(10)	85(3)
C(19)	2701(13)	187(2)	6413(9)	96(3)
C(110)	218(7)	894(2)	11349(6)	46(1)
C(111)	906(9)	958(3)	13065(9)	97(3)
C(112)	-1400(8)	807(2)	10997(9)	80(3)
C(21)	-586(5)	1918(1)	9458(4)	23(1)
C(22)	-2094(5)	2025(1)	9043(5)	25(1)
C(23)	-2465(6)	2279(1)	9921(6)	37(1)
C(24)	-1386(6)	2420(2)	11170(6)	47(1)
C(25)	72(6)	2308(1)	11580(6)	42(1)
C(26)	509(5)	2052(1)	10756(5)	28(1)
C(27)	-3242(5)	1865(1)	7677(5)	30(1)
C(28)	-3720(6)	1515(2)	8100(7)	45(1)
C(29)	-4617(5)	2088(2)	6976(6)	43(1)
C(210)	2123(5)	1935(1)	11159(5)	34(1)
C(211)	2949(6)	2134(2)	10224(7)	50(1)

C(212)	2968(7)	1955(2)	12873(6)	65(2)
C(31)	-2526(5)	1159(1)	4622(5)	27(1)
C(32)	-3147(6)	1391(2)	3414(5)	40(1)
C(33)	-4435(7)	1286(2)	2255(6)	57(2)
C(34)	-5083(6)	973(2)	2304(7)	67(2)
C(35)	-4471(7)	754(2)	3508(7)	56(2)
C(36)	-3174(6)	838(1)	4673(6)	38(1)
C(37)	-2416(8)	1725(2)	3346(7)	61(2)
C(38)	-2478(8)	593(2)	5956(7)	57(2)

Table 50. Bond lengths [Å] and angles [°].

Re-N(3)	1.753(4)	Re-N(2)	1.757(3)	Re-N(1)	1.763(4)
Re-C	2.113(5)	N(1)-C(11)	1.371(6)	N(2)-C(21)	1.385(5)
N(3)-C(31)	1.384(5)	C(11)-C(12)	1.417(6)	C(11)-C(16)	1.407(6)
C(12)-C(13)	1.386(7)	C(12)-C(17)	1.515(7)	C(13)-C(14)	1.378(8)
C(14)-C(15)	1.372(9)	C(15)-C(16)	1.393(8)	C(16)-C(110)	1.519(7)
C(17)-C(19)	1.517(8)	C(17)-C(18)	1.531(10)	C(110)-C(112)	1.492(9)
C(110)-C(111)	1.520(9)	C(21)-C(26)	1.412(6)	C(21)-C(22)	1.412(6)
C(22)-C(23)	1.390(6)	C(22)-C(27)	1.513(6)	C(23)-C(24)	1.388(7)
C(24)-C(25)	1.377(8)	C(25)-C(26)	1.389(6)	C(26)-C(210)	1.518(6)
C(27)-C(28)	1.531(7)	C(27)-C(29)	1.529(6)	C(210)-C(212)	1.524(6)
C(210)-C(211)	1.532(8)	C(31)-C(36)	1.405(7)	C(31)-C(32)	1.412(7)
C(32)-C(33)	1.403(8)	C(32)-C(37)	1.491(9)	C(33)-C(34)	1.377(12)
C(34)-C(35)	1.375(11)	C(35)-C(36)	1.388(7)	C(36)-C(38)	1.502(8)

N(3)-Re-N(2)	115.63(17)	N(3)-Re-N(1)	115.23(18)	N(2)-Re-N(1)	114.75(17)
N(3)-Re-C	102.81(19)	N(2)-Re-C	101.85(19)	N(1)-Re-C	103.9(2)
C(11)-N(1)-Re	169.1(3)	C(21)-N(2)-Re	171.2(3)	C(31)-N(3)-Re	168.5(3)
N(1)-C(11)-C(12)	118.7(4)	N(1)-C(11)-C(16)	120.3(4)		
C(12)-C(11)-C(16)	121.0(4)	C(13)-C(12)-C(11)	118.0(5)		
C(13)-C(12)-C(17)	121.5(5)	C(11)-C(12)-C(17)	120.4(4)		
C(14)-C(13)-C(12)	121.2(5)	C(15)-C(14)-C(13)	120.5(5)		
C(14)-C(15)-C(16)	121.2(5)	C(15)-C(16)-C(11)	118.0(5)		
C(15)-C(16)-C(110)	121.1(5)	C(11)-C(16)-C(110)	120.9(4)		
C(12)-C(17)-C(19)	114.1(5)	C(12)-C(17)-C(18)	109.8(5)		
C(19)-C(17)-C(18)	110.5(6)	C(112)-C(110)-C(16)	111.8(5)		
C(112)-C(110)-C(111)	110.1(6)	C(16)-C(110)-C(111)	112.9(5)		
N(2)-C(21)-C(26)	118.7(4)	N(2)-C(21)-C(22)	119.5(4)		

C(26)-C(21)-C(22)	121.8(4)	C(23)-C(22)-C(21)	117.8(4)
C(23)-C(22)-C(27)	122.2(4)	C(21)-C(22)-C(27)	120.0(4)
C(24)-C(23)-C(22)	120.8(4)	C(23)-C(24)-C(25)	120.6(5)
C(26)-C(25)-C(24)	121.3(5)	C(25)-C(26)-C(21)	117.7(4)
C(25)-C(26)-C(210)	121.9(4)	C(21)-C(26)-C(210)	120.4(4)
C(22)-C(27)-C(28)	110.8(4)	C(22)-C(27)-C(29)	113.8(4)
C(28)-C(27)-C(29)	110.2(4)	C(26)-C(210)-C(212)	113.6(4)
C(26)-C(210)-C(211)	110.2(4)	C(212)-C(210)-C(211)	110.6(5)
N(3)-C(31)-C(36)	119.0(4)	N(3)-C(31)-C(32)	119.3(4)
C(36)-C(31)-C(32)	121.7(4)	C(33)-C(32)-C(31)	116.9(6)
C(33)-C(32)-C(37)	122.0(5)	C(31)-C(32)-C(37)	121.1(5)
C(34)-C(33)-C(32)	121.7(6)	C(35)-C(34)-C(33)	120.2(5)
C(34)-C(35)-C(36)	121.2(6)	C(35)-C(36)-C(31)	118.3(5)
C(35)-C(36)-C(38)	121.0(6)	C(31)-C(36)-C(38)	120.7(5)

Symmetry transformations used to generate equivalent atoms:

Table 51. Anisotropic displacement parameters ($Å^2 x\ 10^3$). The anisotropic displacement factor exponent takes the form: $-2\pi^2[\ h^2\ a^{*2}U^{11} + ... + 2\ h\ k\ a^*\ b^*\ U^{12}\ ]$

U^{11}	U^{22}	U^{33}	U^{23}	U^{13}	U^{12}	
Re22(1)	24(1)	20(1)	-5(1)	5(1)	1(1)	
C 41(3)	41(3)	46(3)	-5(2)	21(2)	-6(2)	
N(1)32(2)	32(2)	27(2)	-3(2)	11(1)	3(2)	
N(2)25(2)	19(2)	30(2)	-5(1)	6(1)	0(1)	
N(3)32(2)	34(2)	20(2)	-2(2)	6(1)	-4(2)	
C(11)	29(2)	19(2)	26(2)	-2(2)	3(2)	2(2)
C(12)	40(2)	23(2)	35(2)	-4(2)	10(2)	4(2)
C(13)	60(3)	31(3)	53(3)	5(2)	17(3)	16(2)
C(14)	82(5)	38(3)	55(4)	18(3)	20(3)	10(3)
C(15)	72(4)	43(3)	36(3)	7(2)	19(3)	0(3)
C(16)	44(3)	30(3)	31(2)	-4(2)	11(2)	-3(2)
C(17)	64(3)	34(3)	44(3)	0(2)	26(3)	17(3)
C(18)	73(5)	108(7)	91(6)	4(5)	51(5)	-5(5)
C(19)	187(10)	50(5)	68(5)	-12(4)	64(6)	20(5)
C(110)	70(4)	39(3)	39(3)	-2(2)	31(3)	3(3)
C(111)	77(5)	144(9)	63(5)	-60(5)	10(4)	15(5)
C(112)	54(4)	98(7)	82(5)	-38(5)	11(4)	16(4)
C(21)	30(2)	15(2)	23(2)	0(2)	7(2)	2(2)
C(22)	27(2)	23(2)	26(2)	4(2)	10(2)	2(2)
C(23)	36(2)	36(3)	40(3)	-2(2)	14(2)	12(2)
C(24)	51(3)	42(3)	48(3)	-18(2)	17(2)	9(2)
C(25)	44(3)	42(3)	36(3)	-19(2)	6(2)	-3(2)
C(26)	32(2)	26(2)	25(2)	-2(2)	6(2)	2(2)

C(27)	24(2)	39(3)	26(2)	1(2)	7(2)	0(2)
C(28)	38(3)	42(3)	53(3)	-1(3)	12(2)	-11(2)
C(29)	29(2)	55(3)	40(3)	9(2)	4(2)	5(2)
C(210)	32(2)	36(3)	27(2)	-6(2)	0(2)	2(2)
C(211)	34(3)	51(4)	62(4)	2(3)	8(2)	-5(2)
C(212)	58(4)	92(6)	29(3)	-10(3)	-10(2)	28(4)
C(31)	27(2)	33(3)	22(2)	-7(2)	5(2)	0(2)
C(32)	42(3)	51(3)	25(2)	1(2)	8(2)	10(2)
C(33)	44(3)	92(5)	28(3)	-1(3)	0(2)	20(3)
C(34)	36(3)	113(7)	44(3)	-28(4)	1(2)	-11(4)
C(35)	45(3)	71(5)	52(3)	-26(3)	13(3)	-26(3)
C(36)	41(3)	40(3)	32(2)	-12(2)	12(2)	-10(2)
C(37)	85(5)	49(4)	45(3)	18(3)	14(3)	8(3)
C(38)	92(5)	24(3)	55(3)	0(2)	24(3)	-13(3)

Table 52. Hydrogen coordinates (x 10^4) and isotropic displacement parameters ($Å^2$x 10^3).

	x	y	z	U(eq)
H(0A)	2759	1601	7524	61
H(0B)	1534	1738	6031	61
H(0C)	2205	1368	6041	61
H(13A)	3185	-28	9290	58
H(14A)	2546	-126	11502	70
H(15A)	1207	272	12386	60
H(17A)	1867	655	6686	54
H(18A)	4388	743	6834	127
H(18B)	4909	554	8444	127
H(18C)	4044	905	8280	127
H(19A)	3004	250	5524	144
H(19B)	1720	82	6074	144
H(19C)	3419	28	7046	144
H(11A)	276	1110	10812	55
H(11B)	1955	1015	13281	146
H(11C)	813	754	13632	146
H(11D)	388	1145	13376	146
H(11E)	-1832	770	9898	121
H(11F)	-1918	992	11317	121
H(11G)	-1501	601	11547	121
H(23A)	-3459	2356	9666	44
H(24A)	-1654	2594	11743	56
H(25A)	786	2406	12433	50
H(27A)	-2752	1828	6870	36
H(28A)	-2841	1375	8526	67
H(28B)	-4375	1407	7186	67
H(28C)	-4247	1542	8858	67
H(29A)	-4303	2305	6675	64
H(29B)	-5140	2125	7730	64
H(29C)	-5280	1976	6078	64
H(21A)	2109	1693	10850	40
H(21B)	2395	2119	9137	76

H(21C)	3941	2039	10401	76
H(21D)	3032	2371	10542	76
H(21E)	2416	1832	13449	97
H(21F)	3075	2191	13195	97
H(21G)	3951	1853	13067	97
H(33A)	-4866	1432	1423	69
H(34A)	-5947	909	1512	80
H(35A)	-4938	544	3544	68
H(37A)	-3005	1851	2452	91
H(37B)	-1419	1687	3270	91
H(37C)	-2347	1854	4271	91
H(38A)	-3078	388	5815	85
H(38B)	-2431	697	6934	85
H(38C)	-1474	536	5948	85

Appendix X

X-ray data for $[Re(NAr)_2(p\text{-tol})(\mu\text{-}O)]_2$

The tables that follow contain atomic coordinates and equivalent isotropic displacement parameters, complete bond lengths (Å) and angles (°), anisotropic displacement parameters and calculated H-atom positions for $[Re(NAr)_2(p\text{-tol})(\mu\text{-}O)]_2$.

Table 53. Atomic coordinates (x 10^4) and equivalent isotropic displacement parameters ($Å^2$x 10^3). U(eq) is defined as one third of the trace of the orthogonalized U^{ij} tensor.

	x	y	z	U(eq)
Re	313(1)	9085(1)	351(1)	33(1)
O	-726(2)	9920(2)	432(2)	39(1)
N(1)	87(2)	8290(2)	-509(2)	38(1)
N(2)	79(2)	8639(2)	1478(2)	36(1)
C(1)	1841(3)	8973(2)	609(3)	35(1)
C(2)	2495(3)	9364(3)	-2(3)	48(1)
C(3)	3484(3)	9297(3)	176(4)	56(1)
C(4)	3848(3)	8850(3)	956(3)	49(1)
C(5)	3207(3)	8450(4)	1544(3)	62(1)
C(6)	2214(3)	8516(3)	1379(3)	55(1)
C(7)	4917(3)	8802(4)	1160(4)	74(2)
C(8)	-295(3)	7459(3)	-680(3)	40(1)
C(9)	-1307(3)	7356(3)	-670(3)	49(1)
C(10)	-1666(3)	6520(4)	-801(4)	61(1)
C(11)	-1054(4)	5835(3)	-965(4)	69(2)
C(12)	-66(4)	5960(3)	-1018(4)	61(1)
C(13)	336(3)	6773(3)	-874(3)	45(1)
C(14)	-1991(3)	8116(4)	-519(4)	64(1)
C(15)	-2724(6)	8231(5)	-1323(5)	124(3)
C(16)	-2505(6)	8091(7)	393(6)	155(4)
C(17)	1412(3)	6915(3)	-919(4)	55(1)
C(18)	1772(5)	6908(11)	-1904(6)	235(9)
C(19)	1993(5)	6274(7)	-389(7)	167(5)
C(20)	-47(3)	8475(3)	2446(3)	38(1)
C(21)	163(4)	9132(3)	3120(3)	52(1)
C(22)	34(5)	8918(3)	4084(4)	69(2)
C(23)	-283(4)	8119(4)	4362(3)	65(1)
C(24)	-485(3)	7486(3)	3702(3)	54(1)
C(25)	-362(3)	7641(3)	2724(3)	42(1)
C(26)	479(4)	10033(3)	2828(4)	69(2)

C(27)	1337(5)	10361(5)	3417(5)	102(2)
C(28)	-359(6)	10654(4)	2887(5)	102(2)
C(29)	-540(4)	6936(3)	1992(3)	60(1)
C(30)	-1378(5)	6336(4)	2193(5)	93(2)
C(31)	352(5)	6409(5)	1844(6)	106(3)

Table 54. Bond lengths [Å] and angles [°].

Re-N(1)	1.751(3)	Re-N(2)	1.759(3)	Re-O	1.948(2)
Re-O#1	1.985(3)	Re-C(1)	2.163(4)	Re-Re#1	3.1307(3)
O-Re#1	1.985(3)	N(1)-C(8)	1.417(5)	N(2)-C(20)	1.392(5)
C(1)-C(2)	1.397(6)	C(1)-C(6)	1.388(6)	C(2)-C(3)	1.402(6)
C(3)-C(4)	1.386(7)	C(4)-C(5)	1.372(7)	C(4)-C(7)	1.517(6)
C(5)-C(6)	1.404(6)	C(8)-C(13)	1.409(6)	C(8)-C(9)	1.420(5)
C(9)-C(10)	1.403(7)	C(9)-C(14)	1.535(7)	C(10)-C(11)	1.385(7)
C(11)-C(12)	1.393(7)	C(12)-C(13)	1.397(6)	C(13)-C(17)	1.519(6)
C(14)-C(16)	1.473(8)	C(14)-C(15)	1.523(9)	C(17)-C(19)	1.478(8)
C(17)-C(18)	1.473(9)	C(20)-C(21)	1.419(6)	C(20)-C(25)	1.425(6)
C(21)-C(22)	1.405(7)	C(21)-C(26)	1.526(7)	C(22)-C(23)	1.376(8)
C(23)-C(24)	1.377(7)	C(24)-C(25)	1.403(6)	C(25)-C(29)	1.519(6)
C(26)-C(28)	1.516(9)	C(26)-C(27)	1.531(8)	C(29)-C(31)	1.506(8)
C(29)-C(30)	1.523(7)				

N(1)-Re-N(2)	107.82(15)	N(1)-Re-O	112.48(13)	N(2)-Re-O	93.72(13)
N(1)-Re-O#1	102.77(13)	N(2)-Re-O#1	149.41(13)	O-Re-O#1	74.52(12)
N(1)-Re-C(1)	103.12(14)	N(2)-Re-C(1)	90.59(14)	O-Re-C(1)	140.74(13)
O#1-Re-C(1)	82.17(12)	N(1)-Re-Re#1	112.22(11)	N(2)-Re-Re#1	125.89(10)
O-Re-Re#1	37.67(8)	O#1-Re-Re#1	36.85(7)	C(1)-Re-Re#1	113.30(10)
Re-O-Re#1	105.48(12)	C(8)-N(1)-Re	145.5(3)	C(20)-N(2)-Re	166.7(3)
C(2)-C(1)-C(6)	117.2(4)	C(2)-C(1)-Re	120.7(3)	C(6)-C(1)-Re	122.0(3)
C(1)-C(2)-C(3)	120.4(4)	C(4)-C(3)-C(2)	121.8(4)	C(5)-C(4)-C(3)	117.8(4)
C(5)-C(4)-C(7)	120.6(4)	C(3)-C(4)-C(7)	121.6(4)	C(4)-C(5)-C(6)	121.0(4)
C(1)-C(6)-C(5)	121.7(4)	C(13)-C(8)-N(1)	119.2(3)	C(13)-C(8)-C(9)	122.6(4)
N(1)-C(8)-C(9)	118.2(4)	C(10)-C(9)-C(8)	117.1(4)	C(10)-C(9)-C(14)	120.7(4)
C(8)-C(9)-C(14)	122.2(4)	C(11)-C(10)-C(9)	120.9(4)	C(10)-C(11)-C(12)	120.9(4)
C(11)-C(12)-C(13)	120.9(5)	C(8)-C(13)-C(12)	117.5(4)		
C(8)-C(13)-C(17)	121.2(4)	C(12)-C(13)-C(17)	121.3(4)		
C(16)-C(14)-C(9)	114.1(5)	C(16)-C(14)-C(15)	108.4(6)		
C(9)-C(14)-C(15)	113.6(4)	C(13)-C(17)-C(19)	114.7(5)		

C(13)-C(17)-C(18)	112.6(4)	C(19)-C(17)-C(18)	106.0(7)		
N(2)-C(20)-C(21)	119.3(4)	N(2)-C(20)-C(25)	118.4(4)		
C(21)-C(20)-C(25)	122.3(4)	C(20)-C(21)-C(22)	116.3(4)		
C(20)-C(21)-C(26)	122.7(4)	C(22)-C(21)-C(26)	121.0(4)		
C(23)-C(22)-C(21)	122.0(5)	C(24)-C(23)-C(22)	121.3(4)		
C(23)-C(24)-C(25)	120.5(4)	C(24)-C(25)-C(20)	117.7(4)		
C(24)-C(25)-C(29)	121.0(4)	C(20)-C(25)-C(29)	121.4(4)		
C(28)-C(26)-C(21)	110.2(5)	C(28)-C(26)-C(27)	110.9(5)		
C(21)-C(26)-C(27)	112.8(5)	C(25)-C(29)-C(31)	110.9(4)		
C(25)-C(29)-C(30)	115.9(4)	C(31)-C(29)-C(30)	109.2(5)		

Symmetry transformations used to generate equivalent atoms:

#1 -x,-y+2,-z

Table 55. Anisotropic displacement parameters ($Å^2 x\ 10^3$). The anisotropic displacement factor exponent takes the form: $-2\pi^2[\ h^2\ a^{*2}U^{11} + ... + 2\ h\ k\ a^*\ b^*\ U^{12}\ ]$

U^{11}	U^{22}	U^{33}	U^{23}	U^{13}	U^{12}	
Re34(1)	30(1)	35(1)	-1(1)	-3(1)	2(1)	
O 35(1)	37(2)	46(1)	8(1)	4(1)	5(1)	
N(1)30(2)	43(2)	42(2)	-2(2)	-5(1)	0(1)	
N(2)32(2)	35(2)	40(2)	2(1)	0(1)	3(1)	
C(1)36(2)	32(2)	37(2)	-3(2)	-3(2)	0(2)	
C(2)43(2)	53(3)	47(2)	8(2)	7(2)	8(2)	
C(3)41(2)	55(3)	73(3)	7(2)	18(2)	4(2)	
C(4)37(2)	54(3)	56(3)	-8(2)	-3(2)	1(2)	
C(5)40(2)	91(4)	56(3)	17(3)	-11(2)	7(2)	
C(6)38(2)	72(3)	55(3)	20(2)	-3(2)	-3(2)	
C(7)39(3)	94(4)	89(4)	0(3)	-4(2)	2(3)	
C(8)36(2)	44(2)	42(2)	-8(2)	-3(2)	-5(2)	
C(9)42(2)	57(3)	47(2)	-14(2)	2(2)	-6(2)	
C(10)	41(2)	70(3)	72(3)	-16(3)	4(2)	-16(2)
C(11)	64(3)	48(3)	95(4)	-8(3)	2(3)	-21(2)
C(12)	57(3)	39(3)	87(4)	-3(2)	-2(3)	-6(2)
C(13)	41(2)	46(2)	47(2)	-1(2)	-2(2)	-4(2)
C(14)	36(2)	74(3)	83(3)	-37(3)	7(2)	-8(2)
C(15)	167(8)	104(6)	99(5)	-8(5)	-21(5)	60(6)
C(16)	132(7)	221(11)	112(6)	44(6)	50(5)	116(7)
C(17)	40(2)	43(2)	81(3)	-9(2)	-9(2)	1(2)
C(18)	62(4)	540(30)	108(6)	117(10)	-7(4)	-100(9)
C(19)	48(4)	242(12)	210(10)	139(9)	1(5)	12(5)
C(20)	37(2)	39(2)	38(2)	1(2)	0(2)	5(2)
C(21)	68(3)	41(3)	46(2)	-6(2)	5(2)	4(2)
C(22)	109(5)	54(3)	44(3)	-12(2)	12(3)	1(3)
C(23)	85(4)	73(4)	39(2)	4(2)	11(2)	6(3)
C(24)	58(3)	50(3)	54(3)	11(2)	10(2)	3(2)
C(25)	39(2)	40(2)	48(2)	4(2)	2(2)	1(2)

C(26)	112(4)	43(3)	53(3)	-9(2)	3(3)	-8(3)
C(27)	113(6)	75(5)	119(5)	-2(4)	-4(4)	-28(4)
C(28)	156(7)	59(4)	91(5)	-1(4)	-28(5)	18(4)
C(29)	84(4)	45(3)	51(3)	7(2)	0(2)	-14(2)
C(30)	81(4)	76(4)	121(5)	-16(4)	2(4)	-30(3)
C(31)	97(5)	79(5)	144(6)	-52(5)	35(4)	-10(4)

Table 56. Hydrogen coordinates (x 10^4) and isotropic displacement parameters ($Å^2$x 10^3).

	x	y	z	U(eq)
H(2A)	2271	9674	-535	57
H(3A)	3913	9562	-245	67
H(5A)	3436	8126	2066	75
H(6A)	1791	8243	1801	67
H(7A)	5031	8459	1729	111
H(7B)	5169	9377	1259	111
H(7C)	5237	8537	623	111
H(10A)	-2332	6424	-778	73
H(11A)	-1308	5279	-1042	83
H(12A)	335	5490	-1151	73
H(14A)	-1591	8642	-507	77
H(15A)	-3125	8726	-1190	186
H(15B)	-3121	7720	-1371	186
H(15C)	-2393	8320	-1920	186
H(16A)	-2046	8031	915	232
H(16B)	-2942	7606	393	232
H(16C)	-2865	8620	472	232
H(17A)	1553	7488	-643	66
H(18A)	1410	7317	-2287	352
H(18B)	1697	6336	-2172	352
H(18C)	2445	7066	-1901	352
H(19A)	1811	6276	277	250
H(19B)	2668	6418	-439	250
H(19C)	1881	5707	-657	250
H(22A)	169	9334	4554	83
H(23A)	-364	8003	5014	78
H(24A)	-706	6947	3907	65
H(26A)	678	10007	2153	83
H(27A)	1506	10935	3206	153
H(27B)	1879	9978	3330	153
H(27C)	1169	10377	4086	153
H(28A)	-888	10441	2498	153
H(28B)	-163	11214	2655	153
H(28C)	-561	10703	3545	153
H(29A)	-686	7225	1378	72
H(30A)	-1955	6673	2285	139
H(30B)	-1240	6005	2766	139
H(30C)	-1472	5949	1658	139
H(31A)	886	6788	1707	159
H(31B)	251	6018	1312	159
H(31C)	494	6080	2417	159

Appendix XI

X-ray data for $Re(NAr')_2Cl_3(py)$

The tables that follow contain atomic coordinates and equivalent isotropic displacement parameters, complete bond lengths (Å) and angles (°), anisotropic displacement parameters and calculated H-atom positions for $Re(NAr')_2Cl_3(py)$.

Table 57. Atomic coordinates (x 10^4) and equivalent isotropic displacement parameters ($Å^2$x 10^3). U(eq) is defined as one third of the trace of the orthogonalized U^{ij} tensor.

	x	y	z	U(eq)
Re	5626(1)	6995(1)	7244(1)	17(1)
Cl(3)	3776(5)	7784(5)	8275(3)	24(1)
Cl(2)	7104(6)	6650(5)	5986(3)	26(1)
Cl(1)	5728(5)	9347(5)	6643(3)	27(1)
N(2)	5163(16)	5430(14)	7488(9)	22(3)
N	3465(18)	7655(16)	6463(10)	21(4)
N(1)	7244(19)	6747(13)	7796(11)	27(4)
C(22)	5144(19)	3377(18)	8601(11)	24(4)
C(11)	8530(20)	6356(18)	8286(11)	19(4)
C(25)	4200(20)	2353(19)	7493(16)	33(5)
C(16)	8680(20)	7243(19)	8751(10)	23(4)
C(21)	4930(20)	4090(20)	7726(12)	33(6)
C(24)	4380(20)	1620(20)	8264(15)	33(5)
C(26)	4419(19)	3630(20)	7180(12)	27(5)
C(12)	9660(20)	5130(20)	8271(12)	28(5)
C(28)	5690(20)	3982(18)	9208(10)	23(4)
C(13)	10970(20)	4790(20)	8744(12)	30(5)
C(27)	4190(20)	4410(20)	6294(14)	39(5)
C(6)	2190(20)	7304(18)	6796(12)	22(4)
C(5)	820(20)	7658(19)	6335(13)	27(4)
C(2)	3480(20)	8420(20)	5623(11)	30(5)
C(4)	930(20)	8316(18)	5513(11)	23(4)
C(18)	9500(20)	4281(19)	7761(12)	31(4)
C(3)	2300(20)	8717(19)	5161(10)	26(4)
C(400)	8610(20)	7930(20)	3866(12)	33(5)
C(15)	9960(20)	6880(20)	9190(12)	36(5)
C(17)	7470(30)	8460(20)	8738(14)	38(5)
C(23)	4870(20)	2160(20)	8861(15)	43(6)

C(14)	11100(20)	5740(20)	9211(13)	35(5)
C(500)	9950(30)	6930(20)	4072(14)	45(6)
C(300)	8730(20)	9140(20)	3276(12)	34(5)
C(600)	11390(30)	7130(20)	3683(13)	41(5)
C(200)	10120(30)	9300(20)	2900(14)	42(6)
C(100)	11460(30)	8370(30)	3102(15)	51(6)
C(800)	9120(20)	10939(18)	9366(11)	25(4)
C(900)	8430(20)	10580(20)	10159(14)	42(6)
C(700)	10680(20)	10420(20)	9184(13)	39(5)

Table 58. Bond lengths [Å] and angles [°].

Re-N(1)	1.734(18)	Re-N(2)	1.760(14)	Re-N	2.305(14)
Re-Cl(3)	2.357(5)	Re-Cl(2)	2.358(5)	Re-Cl(1)	2.456(5)
N(2)-C(21)	1.44(3)	N-C(6)	1.29(2)	N-C(2)	1.40(2)
N(1)-C(11)	1.40(2)	C(22)-C(23)	1.34(3)	C(22)-C(21)	1.44(3)
C(22)-C(28)	1.54(3)	C(11)-C(12)	1.42(3)	C(11)-C(16)	1.43(3)
C(25)-C(24)	1.30(3)	C(25)-C(26)	1.38(3)	C(16)-C(15)	1.34(3)
C(16)-C(17)	1.44(3)	C(21)-C(26)	1.33(3)	C(24)-C(23)	1.45(3)
C(26)-C(27)	1.48(3)	C(12)-C(13)	1.41(3)	C(12)-C(18)	1.46(3)
C(13)-C(14)	1.48(3)	C(6)-C(5)	1.43(3)	C(5)-C(4)	1.34(3)
C(2)-C(3)	1.30(3)	C(4)-C(3)	1.39(3)	C(400)-C(500)	1.38(3)
C(400)-C(300)	1.40(3)	C(15)-C(14)	1.35(3)	C(500)-C(600)	1.38(3)
C(300)-C(200)	1.33(3)	C(600)-C(100)	1.41(4)	C(200)-C(100)	1.35(3)
C(800)-C(900)	1.36(3)	C(800)-C(700)	1.37(3)		
C(900)-C(700)#1	1.44(3)	C(700)-C(900)#1	1.44(3)		

N(1)-Re-N(2)	106.2(7)	N(1)-Re-N	171.6(6)	N(2)-Re-N	82.2(6)
N(1)-Re-Cl(3)	94.7(5)	N(2)-Re-Cl(3)	94.4(4)	N-Re-Cl(3)	83.3(4)
N(1)-Re-Cl(2)	95.2(5)	N(2)-Re-Cl(2)	92.2(5)	N-Re-Cl(2)	85.5(4)
Cl(3)-Re-Cl(2)	166.10(19)	N(1)-Re-Cl(1)	88.9(5)	N(2)-Re-Cl(1)	164.8(5)
N-Re-Cl(1)	82.8(4)	Cl(3)-Re-Cl(1)	85.78(16)	Cl(2)-Re-Cl(1)	84.66(17)
C(21)-N(2)-Re	174.4(13)	C(6)-N-C(2)	117.5(16)	C(6)-N-Re	120.0(12)
C(2)-N-Re	122.5(12)	C(11)-N(1)-Re	171.8(12)	C(23)-C(22)-C(21)	117(2)
C(23)-C(22)-C(28)	121.0(18)	C(21)-C(22)-C(28)	121.6(18)		
N(1)-C(11)-C(12)	118.8(16)	N(1)-C(11)-C(16)	118.1(15)		
C(12)-C(11)-C(16)	123.0(16)	C(24)-C(25)-C(26)	126(2)		
C(15)-C(16)-C(17)	123.4(18)	C(15)-C(16)-C(11)	117.4(19)		
C(17)-C(16)-C(11)	119.3(16)	C(26)-C(21)-N(2)	120.7(17)		
C(26)-C(21)-C(22)	124(2)	N(2)-C(21)-C(22)	115(2)		

C(25)-C(24)-C(23)	119(2)	C(25)-C(26)-C(21)	115(2)		
C(25)-C(26)-C(27)	123(2)	C(21)-C(26)-C(27)	122(2)		
C(13)-C(12)-C(11)	117.9(19)	C(13)-C(12)-C(18)	120.6(19)		
C(11)-C(12)-C(18)	121.5(17)	C(12)-C(13)-C(14)	117.8(19)		
N-C(6)-C(5)	122.4(17)	C(4)-C(5)-C(6)	117.8(17)	C(3)-C(2)-N	122.7(17)
C(5)-C(4)-C(3)	119.5(17)	C(2)-C(3)-C(4)	119.9(16)		
C(500)-C(400)-C(300)		118.8(19)	C(14)-C(15)-C(16)	124(2)	
C(22)-C(23)-C(24)		119(2)	C(15)-C(14)-C(13)	120.1(19)	
C(600)-C(500)-C(400)	120(2)	C(200)-C(300)-C(400)	120.7(19)		
C(500)-C(600)-C(100)	120(2)	C(300)-C(200)-C(100)	122(2)		
C(200)-C(100)-C(600)	119(2)	C(900)-C(800)-C(700)	121.0(18)		
C(800)-C(900)-C(700)#1	120.5(17)	C(800)-C(700)-C(900)#1	118.4(19)		

Symmetry transformations used to generate equivalent atoms:

#1 -x+2,-y+2,-z+2

Table 59. Anisotropic displacement parameters ($Å^2 x\ 10^3$). The anisotropic displacement factor exponent takes the form: $-2\pi^2[\ h^2\ a^{*2}U^{11} + ... + 2\ h\ k\ a^*\ b^*\ U^{12}\ ]$

U^{11}	U^{22}	U^{33}	U^{23}	U^{13}	U^{12}	
Re11(1)	23(1)	13(1)	-1(1)	2(1)	-2(1)	
Cl(3)	22(2)	29(3)	18(2)	-9(2)	8(2)	-6(2)
Cl(2)	16(2)	37(3)	20(3)	-12(2)	5(2)	1(2)
Cl(1)	22(2)	26(2)	23(2)	3(2)	2(2)	-4(2)
N(2)24(8)	12(8)	21(8)	-3(6)	6(7)	3(6)	
N 17(8)	32(9)	14(8)	3(7)	-12(7)	-8(7)	
N(1)41(10)	0(7)	44(10)	-24(7)	21(8)	-6(7)	
C(22)	14(9)	27(10)	13(9)	11(8)	0(7)	6(7)
C(11)	11(9)	29(10)	15(9)	-2(8)	-3(8)	-2(8)
C(25)	18(10)	16(10)	67(17)	4(10)	-17(11)	-15(8)
C(16)	24(9)	42(11)	10(9)	-7(8)	2(7)	-22(9)
C(21)	6(9)	48(14)	14(10)	14(10)	9(8)	12(9)
C(24)	19(10)	23(10)	59(15)	-9(11)	-8(10)	-7(8)
C(26)	2(8)	60(14)	17(9)	-7(10)	-7(7)	-3(9)
C(12)	13(10)	45(12)	16(10)	9(9)	4(8)	-10(9)
C(28)	19(9)	27(9)	14(9)	0(7)	6(7)	0(7)
C(13)	22(10)	44(12)	19(10)	9(9)	-6(8)	-13(9)
C(27)	22(10)	51(14)	38(12)	-2(11)	-11(9)	-3(10)
C(6)26(10)	21(9)	14(9)	0(7)	9(8)	-10(8)	
C(5)14(9)	33(10)	35(12)	-12(9)	-3(8)	-1(8)	
C(2)21(10)	46(12)	11(9)	-4(8)	13(8)	-1(9)	
C(4)20(10)	27(10)	18(10)	-2(8)	-12(8)	2(8)	
C(18)	19(9)	33(11)	31(11)	1(9)	5(8)	-6(8)
C(3)25(10)	41(11)	1(8)	3(7)	-4(8)	1(8)	
C(400)	21(9)	57(13)	23(10)	-17(10)	-3(8)	-4(9)

C(15)	28(11)	58(14)	24(10)	-1(10)	-1(9)	-24(11)
C(17)	40(13)	50(13)	22(11)	-5(10)	-14(10)	-7(11)
C(23)	11(10)	43(13)	41(13)	22(11)	9(9)	11(9)
C(14)	22(10)	54(13)	29(11)	6(10)	-4(9)	-25(10)
C(500)	69(16)	28(11)	29(12)	0(9)	-7(12)	-1(11)
C(300)	25(11)	45(13)	24(11)	-6(9)	1(9)	0(9)
C(600)	39(12)	52(14)	29(11)	-24(11)	-5(10)	7(10)
C(200)	43(14)	32(12)	34(12)	1(10)	12(11)	-1(11)
C(100)	28(13)	75(19)	42(14)	-20(14)	8(11)	1(13)
C(800)	23(9)	32(10)	18(10)	-4(8)	-4(8)	-5(8)
C(900)	18(11)	60(15)	38(14)	-26(12)	-17(10)	31(10)
C(700)	25(11)	61(15)	29(12)	-18(11)	-2(10)	2(10)

Table 60. Hydrogen coordinates (x 10^4) and isotropic displacement parameters ($Å^2$x 10^3).

	x	y	z	U(eq)
H(25A)	3865	1982	7107	39
H(24A)	4227	728	8437	39
H(28A)	5772	3360	9756	28
H(28B)	6694	4164	8997	28
H(28C)	4936	4802	9249	28
H(13A)	11758	3959	8770	36
H(27A)	3833	3915	5991	47
H(27B)	3412	5238	6291	47
H(27C)	5163	4600	6025	47
H(6A)	2152	6782	7373	26
H(5A)	-135	7427	6606	33
H(2A)	4414	8709	5375	36
H(4A)	56	8514	5178	28
H(18A)	10373	3508	7831	37
H(18B)	8537	3998	7943	37
H(18C)	9478	4770	7177	37
H(3A)	2374	9213	4579	31
H(40A)	7607	7786	4133	39
H(15A)	10066	7447	9523	44
H(17A)	7721	8958	9076	45
H(17B)	7376	9000	8166	45
H(17C)	6488	8232	8960	45
H(23A)	4985	1645	9438	52
H(14A)	12021	5556	9509	42
H(50A)	9906	6098	4477	54
H(30A)	7789	9831	3136	41
H(60A)	12329	6437	3815	49
H(20A)	10172	10131	2489	50
H(10A)	12468	8513	2847	61
H(80A)	8503	11572	8925	30
H(90A)	7338	11036	10172	50
H(70A)	10981	10783	8600	47

Appendix XII

X-ray data for *p*-tolNHRe(NAr)$_3$

The tables that follow contain atomic coordinates and equivalent isotropic displacement parameters, complete bond lengths (Å) and angles (°), anisotropic displacement parameters and calculated H-atom positions for *p*-tolNHRe(NAr)$_3$.

Table 61. Atomic coordinates (x 10^4) and equivalent isotropic displacement parameters (Å^{2}x 10^3). U(eq) is defined as one third of the trace of the orthogonalized U^{ij} tensor.

	x	y	z	U(eq)
Re	2456(1)	1327(1)	4113(1)	27(1)
N(1)	1830(2)	2125(3)	4481(2)	37(1)
N(2)	2246(2)	-319(3)	3923(2)	32(1)
N(3)	2449(1)	2170(3)	3292(2)	30(1)
N(4)	3138(2)	1574(3)	4911(2)	32(1)
C(1)	1186(2)	2280(4)	4104(2)	35(1)
C(2)	868(2)	3258(4)	4333(3)	46(1)
C(3)	230(2)	3421(5)	3952(3)	58(1)
C(4)	-114(2)	2646(5)	3347(3)	54(1)
C(5)	205(2)	1670(5)	3135(3)	49(1)
C(6)	845(2)	1476(4)	3502(2)	41(1)
C(7)	-809(2)	2861(7)	2938(4)	83(2)
C(8)	2500(2)	2785(4)	2656(2)	31(1)
C(9)	3098(2)	3164(4)	2657(2)	36(1)
C(10)	3129(2)	3781(5)	2004(3)	48(1)
C(11)	2602(3)	4064(5)	1396(3)	59(1)
C(12)	2021(2)	3732(5)	1405(2)	51(1)
C(13)	1956(2)	3090(4)	2032(2)	38(1)
C(14)	3687(2)	2855(4)	3328(3)	45(1)
C(15)	4215(2)	3852(6)	3453(4)	71(2)
C(16)	3926(2)	1509(5)	3233(4)	68(2)
C(17)	1310(2)	2747(5)	2035(3)	53(1)
C(18)	897(3)	3925(6)	1947(4)	94(2)
C(19)	974(3)	1749(6)	1432(4)	81(2)
C(20)	2194(2)	-1653(4)	3842(2)	32(1)
C(21)	1843(2)	-2344(4)	4204(2)	38(1)
C(22)	1790(2)	-3679(4)	4094(3)	51(1)
C(23)	2068(3)	-4316(5)	3649(3)	60(1)

C(24)	2416(2)	-3637(4)	3302(3)	50(1)
C(25)	2484(2)	-2297(4)	3385(2)	38(1)
C(26)	1538(2)	-1673(5)	4705(3)	50(1)
C(27)	1813(3)	-2161(6)	5530(3)	86(2)
C(28)	832(3)	-1836(7)	4393(4)	90(2)
C(29)	2842(2)	-1520(4)	2991(3)	45(1)
C(30)	3316(3)	-2303(6)	2761(4)	75(2)
C(31)	2394(2)	-795(5)	2299(3)	53(1)
C(32)	3732(2)	1843(4)	5441(2)	31(1)
C(33)	4124(2)	805(4)	5806(3)	40(1)
C(34)	4704(2)	1110(6)	6354(3)	63(2)
C(35)	4878(2)	2379(6)	6536(4)	73(2)
C(36)	4485(2)	3380(5)	6183(3)	61(2)
C(37)	3903(2)	3148(4)	5627(3)	41(1)
C(38)	3929(2)	-585(4)	5601(3)	47(1)
C(39)	4200(3)	-1084(5)	5017(3)	63(2)
C(40)	4101(3)	-1472(5)	6299(3)	71(2)
C(41)	3449(3)	4232(4)	5274(3)	55(1)
C(42)	3777(3)	5427(5)	5100(4)	95(2)
C(43)	3086(3)	4565(6)	5790(4)	85(2)

Table 62. Bond lengths [Å] and angles [°].

Re-N(3)	1.757(3)	Re-N(4)	1.754(3)		
Re-N(2)	1.769(3)	Re-N(1)	1.969(3)		
N(1)-C(1)	1.399(5)	N(2)-C(20)	1.387(5)		
N(3)-C(8)	1.388(5)	N(4)-C(32)	1.396(5)	C(1)-C(2)	1.394(6)
C(1)-C(6)	1.394(6)	C(2)-C(3)	1.389(6)	C(3)-C(4)	1.382(7)
C(4)-C(5)	1.382(7)	C(4)-C(7)	1.516(6)	C(5)-C(6)	1.393(6)
C(8)-C(9)	1.418(6)	C(8)-C(13)	1.408(6)	C(9)-C(10)	1.399(6)
C(9)-C(14)	1.515(6)	C(10)-C(11)	1.363(7)	C(11)-C(12)	1.376(7)
C(12)-C(13)	1.398(6)	C(13)-C(17)	1.518(6)	C(14)-C(16)	1.527(6)
C(14)-C(15)	1.540(6)	C(17)-C(18)	1.513(7)	C(17)-C(19)	1.520(7)
C(20)-C(21)	1.411(6)	C(20)-C(25)	1.416(6)	C(21)-C(22)	1.393(6)
C(21)-C(26)	1.517(6)	C(22)-C(23)	1.377(7)	C(23)-C(24)	1.378(7)
C(24)-C(25)	1.396(6)	C(25)-C(29)	1.507(6)	C(26)-C(28)	1.517(7)
C(26)-C(27)	1.529(7)	C(29)-C(30)	1.530(6)	C(29)-C(31)	1.531(6)
C(32)-C(33)	1.410(6)	C(32)-C(37)	1.413(6)	C(33)-C(34)	1.393(6)
C(33)-C(38)	1.513(6)	C(34)-C(35)	1.377(7)	C(35)-C(36)	1.375(8)
C(36)-C(37)	1.389(6)	C(37)-C(41)	1.512(6)	C(38)-C(40)	1.526(6)
C(38)-C(39)	1.520(7)	C(41)-C(43)	1.514(7)	C(41)-C(42)	1.537(7)

N(3)-Re-N(4)	113.63(15)	N(3)-Re-N(2)	112.48(15)	N(4)-Re-N(2)	114.01(15)
N(3)-Re-N(1)	108.12(14)	N(4)-Re-N(1)	100.35(14)	N(2)-Re-N(1)	107.15(14)
C(1)-N(1)-Re	129.6(3)	C(20)-N(2)-Re	169.8(3)	C(8)-N(3)-Re	174.5(3)
C(32)-N(4)-Re	168.8(3)	C(2)-C(1)-N(1)	119.8(4)	C(2)-C(1)-C(6)	118.5(4)
N(1)-C(1)-C(6)	121.7(4)	C(3)-C(2)-C(1)	119.7(5)	C(4)-C(3)-C(2)	122.7(5)
C(5)-C(4)-C(3)	116.8(4)	C(5)-C(4)-C(7)	121.8(5)	C(3)-C(4)-C(7)	121.3(5)
C(4)-C(5)-C(6)	122.2(5)	C(5)-C(6)-C(1)	120.1(4)	N(3)-C(8)-C(9)	119.7(4)
N(3)-C(8)-C(13)	119.6(4)	C(9)-C(8)-C(13)	120.6(4)	C(8)-C(9)-C(10)	117.9(4)
C(8)-C(9)-C(14)	121.2(4)	C(10)-C(9)-C(14)	120.9(4)	C(11)-C(10)-C(9)	121.5(4)
C(10)-C(11)-C(12)	120.6(4)	C(11)-C(12)-C(13)	121.0(4)		
C(12)-C(13)-C(8)	118.4(4)	C(12)-C(13)-C(17)	120.2(4)		
C(8)-C(13)-C(17)	121.4(4)	C(9)-C(14)-C(16)	110.2(4)		
C(9)-C(14)-C(15)	113.9(4)	C(16)-C(14)-C(15)	109.5(4)		
C(13)-C(17)-C(18)	112.4(5)	C(13)-C(17)-C(19)	113.2(4)		
C(18)-C(17)-C(19)	109.5(4)	N(2)-C(20)-C(21)	119.5(4)		
N(2)-C(20)-C(25)	119.4(4)	C(21)-C(20)-C(25)	121.0(4)		
C(22)-C(21)-C(20)	117.7(4)	C(22)-C(21)-C(26)	120.6(4)		
C(20)-C(21)-C(26)	121.7(4)	C(23)-C(22)-C(21)	121.8(4)		
C(22)-C(23)-C(24)	120.3(4)	C(23)-C(24)-C(25)	120.9(4)		
C(24)-C(25)-C(20)	118.3(4)	C(24)-C(25)-C(29)	122.2(4)		
C(20)-C(25)-C(29)	119.5(4)	C(28)-C(26)-C(21)	111.6(4)		
C(28)-C(26)-C(27)	110.7(5)	C(21)-C(26)-C(27)	110.8(4)		
C(25)-C(29)-C(30)	114.4(4)	C(25)-C(29)-C(31)	110.9(4)		
C(30)-C(29)-C(31)	110.6(4)	N(4)-C(32)-C(33)	119.0(4)		
N(4)-C(32)-C(37)	118.7(4)	C(33)-C(32)-C(37)	122.2(4)		
C(34)-C(33)-C(32)	117.4(4)	C(34)-C(33)-C(38)	121.3(4)		
C(32)-C(33)-C(38)	121.2(4)	C(35)-C(34)-C(33)	120.9(5)		
C(36)-C(35)-C(34)	121.0(5)	C(35)-C(36)-C(37)	121.2(5)		
C(36)-C(37)-C(32)	117.3(4)	C(36)-C(37)-C(41)	121.8(4)		
C(32)-C(37)-C(41)	120.8(4)	C(33)-C(38)-C(40)	112.9(4)		
C(33)-C(38)-C(39)	110.2(4)	C(40)-C(38)-C(39)	111.1(4)		
C(43)-C(41)-C(37)	109.7(4)	C(43)-C(41)-C(42)	111.6(5)		
C(37)-C(41)-C(42)	112.1(5)				

Symmetry transformations used to generate equivalent atoms:

Table 63. Anisotropic displacement parameters ($Å^2 x\ 10^3$). The anisotropic displacement factor exponent takes the form: $-2\pi^2[\ h^2\ a^{*2}U^{11} + ... + 2\ h\ k\ a^*\ b^*\ U^{12}\ ]$

U^{11}	U^{22}	U^{33}	U^{23}	U^{13}	U^{12}	
Re27(1)	25(1)	27(1)	-1(1)	7(1)	-1(1)	
N(1)37(2)	40(2)	32(2)	-6(2)	11(2)	0(2)	
N(2)37(2)	25(2)	37(2)	-3(1)	15(2)	-2(1)	
N(3)30(2)	28(2)	30(2)	2(1)	7(2)	1(1)	
N(4)32(2)	29(2)	33(2)	-2(1)	9(2)	3(1)	
C(1)33(2)	40(2)	36(2)	3(2)	17(2)	5(2)	
C(2)42(3)	45(3)	52(3)	-1(2)	17(2)	4(2)	
C(3)51(3)	61(3)	68(4)	3(3)	27(3)	17(3)	
C(4)34(3)	68(3)	58(3)	12(3)	13(2)	9(2)	
C(5)34(2)	62(3)	47(3)	-6(2)	9(2)	-7(2)	
C(6)34(2)	48(3)	40(2)	-3(2)	13(2)	3(2)	
C(7)39(3)	111(5)	89(5)	10(4)	10(3)	19(3)	
C(8)39(2)	24(2)	31(2)	-4(2)	15(2)	0(2)	
C(9)42(2)	31(2)	37(2)	0(2)	16(2)	3(2)	
C(10)	54(3)	50(3)	48(3)	3(2)	29(2)	0(2)
C(11)	75(4)	65(3)	45(3)	19(3)	32(3)	6(3)
C(12)	56(3)	65(3)	32(2)	15(2)	15(2)	13(3)
C(13)	41(2)	41(2)	33(2)	0(2)	13(2)	5(2)
C(14)	36(2)	49(3)	52(3)	2(2)	17(2)	-5(2)
C(15)	51(3)	69(4)	86(4)	-7(3)	16(3)	-19(3)
C(16)	49(3)	49(3)	96(4)	12(3)	15(3)	5(2)
C(17)	36(3)	84(4)	34(3)	8(3)	4(2)	2(3)
C(18)	47(3)	91(5)	139(6)	-46(5)	26(4)	0(3)
C(19)	59(4)	63(4)	116(6)	-12(4)	24(4)	-12(3)
C(20)	30(2)	30(2)	30(2)	0(2)	3(2)	-1(2)
C(21)	43(2)	35(2)	31(2)	5(2)	7(2)	-4(2)
C(22)	64(3)	32(2)	54(3)	10(2)	16(2)	-11(2)
C(23)	78(4)	30(3)	63(3)	-1(2)	14(3)	-1(2)
C(24)	59(3)	33(2)	54(3)	-8(2)	17(2)	5(2)
C(25)	34(2)	36(2)	40(2)	-5(2)	8(2)	3(2)
C(26)	56(3)	49(3)	49(3)	9(2)	25(2)	-7(2)
C(27)	134(6)	80(5)	52(4)	10(3)	41(4)	7(4)
C(28)	64(4)	110(6)	105(5)	-6(4)	40(4)	-4(4)
C(29)	37(2)	51(3)	50(3)	-11(2)	19(2)	-3(2)
C(30)	67(4)	79(4)	95(5)	-11(4)	48(4)	8(3)
C(31)	50(3)	69(3)	39(3)	3(2)	17(2)	-6(3)
C(32)	29(2)	32(2)	32(2)	-8(2)	12(2)	-4(2)
C(33)	35(2)	40(2)	43(3)	-6(2)	11(2)	5(2)
C(34)	36(3)	69(4)	67(3)	-12(3)	-2(2)	14(2)
C(35)	32(3)	85(4)	85(4)	-36(4)	0(3)	-6(3)
C(36)	47(3)	58(3)	69(4)	-29(3)	12(3)	-18(2)
C(37)	43(3)	35(2)	44(3)	-9(2)	15(2)	-7(2)
C(38)	43(3)	38(3)	52(3)	1(2)	8(2)	7(2)
C(39)	98(4)	42(3)	49(3)	-3(2)	26(3)	-4(3)
C(40)	102(5)	56(3)	66(4)	17(3)	45(4)	24(3)
C(41)	75(4)	30(2)	55(3)	-4(2)	17(3)	-4(2)
C(42)	136(6)	41(3)	97(5)	4(3)	26(5)	-25(4)
C(43)	99(5)	81(5)	75(4)	1(4)	30(4)	50(4)

Table 64. Hydrogen coordinates (x 10^4) and isotropic displacement parameters ($Å^2$x 10^3).

	x	y	z	U(eq)
H(1A)	1976	2425	4946	44
H(2A)	1086	3805	4743	55
H(3A)	23	4085	4113	70
H(5A)	-16	1120	2729	59
H(6A)	1048	802	3343	49
H(7A)	-969	2230	2531	124
H(7B)	-879	3727	2723	124
H(7C)	-1025	2765	3299	124
H(10A)	3522	4005	1984	57
H(11A)	2636	4489	968	71
H(12A)	1662	3940	983	61
H(14A)	3577	2843	3796	54
H(15A)	4062	4707	3510	106
H(15B)	4352	3845	3016	106
H(15C)	4565	3632	3912	106
H(16A)	3594	881	3156	101
H(16B)	4278	1286	3689	101
H(16C)	4059	1504	2793	101
H(17A)	1367	2361	2541	64
H(18A)	1113	4565	2329	141
H(18B)	511	3676	2017	141
H(18C)	803	4289	1440	141
H(19A)	1240	994	1487	122
H(19B)	882	2118	926	122
H(19C)	587	1496	1498	122
H(22A)	1558	-4158	4331	61
H(23A)	2020	-5216	3581	72
H(24A)	2609	-4083	3006	60
H(26A)	1630	-736	4708	59
H(27A)	1612	-1719	5841	129
H(27B)	2259	-1988	5732	129
H(27C)	1742	-3085	5541	129
H(28A)	667	-1515	3872	135
H(28B)	650	-1352	4708	135
H(28C)	729	-2745	4400	135
H(29A)	3081	-856	3361	54
H(30A)	3595	-2758	3205	112
H(30B)	3558	-1724	2564	112
H(30C)	3097	-2925	2368	112
H(31A)	2097	-304	2455	79
H(31B)	2171	-1412	1906	79
H(31C)	2631	-210	2098	79
H(34A)	4980	441	6601	75
H(35A)	5270	2563	6908	88
H(36A)	4613	4238	6321	73
H(38A)	3467	-597	5356	56
H(39A)	4082	-508	4579	95
H(39B)	4038	-1945	4853	95
H(39C)	4652	-1119	5248	95
H(40A)	3922	-1135	6661	106

H(40B)	4553	-1510	6540	106
H(40C)	3939	-2333	6140	106
H(41A)	3146	3913	4783	66
H(42A)	3470	6097	4875	143
H(42B)	3984	5192	4745	143
H(42C)	4085	5746	5572	143
H(43A)	2881	3794	5884	128
H(43B)	2773	5216	5545	128
H(43C)	3371	4899	6273	128

Appendix XIII

X-ray data for $[Re(NAr')_3][Na(thf)_6]$

The tables that follow contain atomic coordinates and equivalent isotropic displacement parameters, complete bond lengths (Å) and angles (°), anisotropic displacement parameters and calculated H-atom positions for $[Re(NAr')_3][Na(thf)_6]$.

Table 65. Atomic coordinates (x 10^4) and equivalent isotropic displacement parameters ($Å^2$x 10^3). U(eq) is defined as one third of the trace of the orthogonalized U^{ij} tensor.

	x	y	z	U(eq)
Re(1)	0	1308(1)	2500	41(1)
N(1)	0	2194(2)	2500	47(1)
C(11)	0	2882(2)	2500	41(1)
C(12)	-176(2)	3237(2)	1727(2)	49(1)
C(13)	-168(2)	3938(2)	1749(2)	58(1)
C(14)	0	4288(2)	2500	62(1)
C(15)	-363(3)	2864(2)	902(2)	74(1)
N(2)	-1002(2)	871(1)	2084(2)	49(1)
C(21)	-1835(2)	617(1)	1758(2)	44(1)
C(22)	-2311(2)	731(2)	898(2)	54(1)
C(23)	-3149(3)	463(2)	596(3)	75(1)
C(24)	-3523(3)	96(2)	1101(3)	83(1)
C(25)	-3056(3)	-12(2)	1938(3)	72(1)
C(26)	-2215(2)	245(2)	2272(2)	52(1)
C(27)	-1924(4)	1128(2)	330(3)	77(1)
C(28)	-1706(3)	134(3)	3195(3)	80(1)
Na	0	7688(1)	2500	50(1)
O(1)	-326(3)	8533(2)	1440(2)	84(1)
C(1A)	-33(6)	8425(3)	711(4)	124(3)
C(2A)	-484(6)	8839(4)	72(4)	130(3)
C(3A)	-780(3)	9432(2)	491(3)	81(1)
C(4A)	-767(3)	9162(2)	1329(3)	77(1)
O(2)	1436(2)	7630(2)	2318(2)	81(1)
C(1B)	2019(4)	8189(3)	2565(6)	133(3)
C(2B)	2757(5)	8063(4)	2337(8)	188(5)
C(3B)	2623(5)	7468(4)	1849(7)	160(4)
C(4B)	1865(4)	7143(3)	1971(5)	117(2)
O(3)	-552(2)	6881(2)	1377(3)	101(1)

C(1C)	-1379(5)	6973(4)	712(6)	147(3)
C(2C)	-1743(8)	6321(4)	552(8)	188(6)
C(3C)	-1059(8)	5871(4)	1030(9)	277(10)
C(4C)	-255(5)	6260(2)	1286(4)	106(2)

Table 66. Bond lengths [Å] and angles [°].

Re(1)-N(1)	1.762(3)	Re(1)-N(2)	1.772(2)	Re(1)-N(2)#1	1.772(2)
N(1)-C(11)	1.369(5)	C(11)-C(12)#1	1.411(4)	C(11)-C(12)	1.411(4)
C(12)-C(13)	1.396(5)	C(12)-C(15)	1.501(5)	C(13)-C(14)	1.377(5)
C(14)-C(13)#1	1.377(5)	N(2)-C(21)	1.375(4)	C(21)-C(26)	1.398(4)
C(21)-C(22)	1.414(4)	C(22)-C(23)	1.390(5)	C(22)-C(27)	1.496(6)
C(23)-C(24)	1.374(7)	C(24)-C(25)	1.377(7)	C(25)-C(26)	1.390(5)
C(26)-C(28)	1.514(5)	Na-O(1)#1	2.371(3)	Na-O(1)	2.371(3)
Na-O(3)	2.411(3)	Na-O(3)#1	2.411(3)	Na-O(2)	2.410(3)
Na-O(2)#1	2.410(3)	O(1)-C(4A)	1.421(5)	O(1)-C(1A)	1.435(5)
C(1A)-C(2A)	1.362(8)	C(2A)-C(3A)	1.515(7)	C(3A)-C(4A)	1.480(6)
O(2)-C(4B)	1.405(5)	O(2)-C(1B)	1.432(6)	C(1B)-C(2B)	1.368(7)
C(2B)-C(3B)	1.413(9)	C(3B)-C(4B)	1.441(9)	O(3)-C(4C)	1.349(5)
O(3)-C(1C)	1.456(7)	C(1C)-C(2C)	1.414(10)	C(2C)-C(3C)	1.451(12)
C(3C)-C(4C)	1.451(13)				

N(1)-Re(1)-N(2)	119.40(9)	N(1)-Re(1)-N(2)#1	119.40(9)
N(2)-Re(1)-N(2)#1	121.20(17)	C(11)-N(1)-Re(1)	180.0
N(1)-C(11)-C(12)#1	120.04(19)	N(1)-C(11)-C(12)	120.04(19)
C(12)#1-C(11)-C(12)	119.9(4)	C(13)-C(12)-C(11)	118.6(3)
C(13)-C(12)-C(15)	121.0(3)	C(11)-C(12)-C(15)	120.3(3)
C(14)-C(13)-C(12)	121.8(3)	C(13)-C(14)-C(13)#1	119.2(4)
C(21)-N(2)-Re(1)	172.1(2)	N(2)-C(21)-C(26)	120.3(3)
N(2)-C(21)-C(22)	120.0(3)	C(26)-C(21)-C(22)	119.7(3)
C(23)-C(22)-C(21)	117.9(3)	C(23)-C(22)-C(27)	121.0(4)
C(21)-C(22)-C(27)	121.0(3)	C(24)-C(23)-C(22)	122.5(4)
C(25)-C(24)-C(23)	119.3(4)	C(24)-C(25)-C(26)	120.6(4)
C(21)-C(26)-C(25)	120.0(3)	C(21)-C(26)-C(28)	119.3(3)
C(25)-C(26)-C(28)	120.7(4)	O(1)#1-Na-O(1)	89.53(17)
O(1)#1-Na-O(3)	171.59(13)	O(1)-Na-O(3)	87.49(13)
O(1)#1-Na-O(3)#1	87.49(13)	O(1)-Na-O(3)#1	171.59(14)

O(3)-Na-O(3)#1	96.5(2)	O(1)#1-Na-O(2)	96.88(12)
O(1)-Na-O(2)	87.03(13)	O(3)-Na-O(2)	90.81(12)
O(3)#1-Na-O(2)	85.53(13)	O(1)#1-Na-O(2)#1	87.03(13)
O(1)-Na-O(2)#1	96.88(12)	O(3)-Na-O(2)#1	85.53(13)
O(3)#1-Na-O(2)#1	90.81(12)	O(2)-Na-O(2)#1	174.51(16)
C(4A)-O(1)-C(1A)	107.4(3)	C(4A)-O(1)-Na	135.3(2)
C(1A)-O(1)-Na	117.3(3)	C(2A)-C(1A)-O(1)	109.3(5)
C(1A)-C(2A)-C(3A)	106.4(5)	C(4A)-C(3A)-C(2A)	103.1(4)
O(1)-C(4A)-C(3A)	107.9(3)	C(4B)-O(2)-C(1B)	107.2(4)
C(4B)-O(2)-Na	133.3(3)	C(1B)-O(2)-Na	119.4(3)
C(2B)-C(1B)-O(2)	108.8(5)	C(1B)-C(2B)-C(3B)	108.4(6)
C(2B)-C(3B)-C(4B)	106.7(6)	O(2)-C(4B)-C(3B)	106.5(5)
C(4C)-O(3)-C(1C)	107.5(5)	C(4C)-O(3)-Na	129.5(4)
C(1C)-O(3)-Na	122.5(4)	C(2C)-C(1C)-O(3)	104.9(7)
C(1C)-C(2C)-C(3C)	105.3(7)	C(4C)-C(3C)-C(2C)	106.7(8)
O(3)-C(4C)-C(3C)	102.2(7)		

Symmetry transformations used to generate equivalent atoms:

#1 -x,y,-z+1/2

Table 67. Anisotropic displacement parameters ($Å^2 x\ 10^3$). The anisotropic displacement factor exponent takes the form: $-2\pi^2[\ h^2\ a^{*2}U^{11} + ... + 2\ h\ k\ a^*\ b^*\ U^{12}\ ]$

U^{11}	U^{22}	U^{33}	U^{23}	U^{13}	U^{12}	
Re(1)	36(1)	36(1)	51(1)	0	12(1)	0
N(1)52(2)	40(2)	53(2)	0	22(2)	0	
C(11)	33(2)	37(2)	57(2)	0	17(2)	0
C(12)	45(2)	46(2)	58(2)	3(1)	19(1)	-2(1)
C(13)	51(2)	44(2)	76(2)	14(2)	16(2)	-1(1)
C(14)	49(2)	37(2)	94(4)	0	15(2)	0
C(15)	102(3)	68(2)	53(2)	5(2)	26(2)	-5(2)
N(2)41(1)	50(1)	55(1)	-3(1)	12(1)	-3(1)	
C(21)	40(1)	34(1)	57(2)	-8(1)	13(1)	2(1)
C(22)	50(2)	48(2)	58(2)	-8(1)	8(1)	4(1)
C(23)	58(2)	70(2)	79(2)	-13(2)	-7(2)	1(2)
C(24)	45(2)	76(3)	117(4)	-11(2)	8(2)	-12(2)
C(25)	55(2)	59(2)	110(3)	-9(2)	36(2)	-9(2)
C(26)	48(2)	46(2)	66(2)	-4(1)	23(1)	-2(1)
C(27)	94(3)	75(3)	56(2)	3(2)	13(2)	-6(2)
C(28)	86(3)	83(3)	71(2)	17(2)	23(2)	-15(2)
Na51(1)	39(1)	68(1)	0	29(1)	0	
O(1)145(3)	58(2)	70(2)	15(1)	64(2)	34(2)	
C(1A)	227(8)	91(3)	88(3)	20(3)	101(5)	58(5)

C(2A)	185(7)	140(5)	98(4)	54(4)	93(5)	90(5)
C(3A)	91(3)	71(3)	85(3)	23(2)	34(2)	14(2)
C(4A)	108(3)	57(2)	76(2)	7(2)	44(2)	20(2)
O(2)60(2)	73(2)	129(3)	-19(2)	54(2)	-6(1)	
C(1B)	91(4)	99(4)	237(8)	-58(5)	93(5)	-28(3)
C(2B)	98(5)	148(7)	357(14)	-118(8)	127(7)	-49(5)
C(3B)	111(5)	110(5)	299(11)	-54(6)	124(7)	-1(4)
C(4B)	87(3)	78(3)	210(7)	-37(4)	79(4)	0(3)
O(3)73(2)	69(2)	142(3)	-39(2)	6(2)	2(2)	
C(1C)	97(4)	126(6)	178(7)	-42(5)	-18(4)	14(4)
C(2C)	148(9)	136(8)	208(11)	-25(6)	-56(8)	-33(5)
C(3C)	271(14)	79(5)	318(15)	-12(7)	-158(13)	-24(7)
C(4C)	141(6)	73(3)	96(4)	-19(2)	22(4)	28(3)

Table 68. Hydrogen coordinates (x 10^4) and isotropic displacement parameters ($Å^2$x 10^3).

	x	y	z	U(eq)
H(13A)	-283	4180	1232	69
H(14A)	0	4765	2500	74
H(15A)	-464	3186	434	111
H(15B)	-886	2584	822	111
H(15C)	138	2578	912	111
H(23A)	-3476	536	20	90
H(24A)	-4097	-81	875	99
H(25A)	-3312	-264	2291	87
H(27A)	-2346	1154	-239	116
H(27B)	-1387	909	298	116
H(27C)	-1786	1583	560	116
H(28A)	-2060	-131	3470	120
H(28B)	-1564	569	3482	120
H(28C)	-1162	-109	3232	120
H(1AA)	602	8520	857	148
H(1AB)	-132	7951	526	148
H(2AA)	-996	8603	-310	156
H(2AB)	-102	8992	-265	156
H(3AA)	-371	9816	553	97
H(3AB)	-1376	9579	161	97
H(4AA)	-457	9477	1785	92
H(4AB)	-1373	9103	1354	92
H(1BA)	1730	8603	2281	159
H(1BB)	2175	8257	3186	159
H(2BA)	3267	8010	2850	226
H(2BB)	2876	8443	2000	226
H(3BA)	3142	7171	2041	192
H(3BB)	2520	7574	1242	192
H(4BA)	1473	6978	1423	141
H(4BB)	2044	6757	2363	141
H(1CA)	-1771	7276	904	176
H(1CB)	-1280	7164	195	176
H(2CA)	-1909	6216	-62	225

H(2CB)	-2270	6283	744	225
H(3CA)	-1200	5697	1535	333
H(3CB)	-997	5485	674	333
H(4CA)	148	6092	1827	127
H(4CB)	47	6252	844	127

Appendix XIV

X-ray data for $Me_3SnRe(NAr)_3$

The tables that follow contain atomic coordinates and equivalent isotropic displacement parameters, complete bond lengths (Å) and angles (°), anisotropic displacement parameters and calculated H-atom positions for $Me_3SnRe(NAr)_3$.

Table 69. Atomic coordinates (x 10^4) and equivalent isotropic displacement parameters ($Å^2$x 10^3). U(eq) is defined as one third of the trace of the orthogonalized U^{ij} tensor.

	x	y	z	U(eq)
Re	9654(1)	2500	2200(1)	20(1)
N(1)	10955(6)	2189(4)	3188(5)	24(1)
N(2)	10023(5)	2500	955(3)	25(1)
N(3)	8325(6)	1841(4)	2493(4)	22(1)
Sn	8600(1)	4193(1)	2011(1)	26(1)
C(1)	8711(11)	4767(7)	3501(7)	49(2)
C(2)	9833(9)	4902(5)	1112(6)	34(2)
C(3)	6553(9)	4275(7)	1231(8)	47(2)
C(101)	11891(7)	2028(5)	4096(5)	23(2)
C(102)	12621(8)	1206(6)	4195(5)	24(2)
C(103)	13543(8)	1071(6)	5111(6)	29(2)
C(104)	13734(9)	1713(6)	5869(6)	35(2)
C(105)	13023(6)	2500	5745(4)	32(1)
C(106)	12073(7)	2683(5)	4876(5)	23(3)
C(107)	11299(8)	3544(5)	4747(6)	31(2)
C(108)	11031(10)	3941(6)	5746(7)	42(2)
C(109)	12055(10)	4210(6)	4169(7)	32(2)
C(110)	12425(9)	534(5)	3347(6)	31(2)
C(111)	12395(10)	-428(6)	3735(7)	40(2)
C(112)	13550(10)	614(6)	2701(7)	42(2)
C(201)	10391(7)	2388(6)	-6(5)	29(2)
C(202)	9398(6)	2500	-894(4)	28(1)
C(203)	9805(8)	2380(30)	-1846(5)	37(7)
C(204)	11119(10)	2167(5)	-1916(6)	39(2)
C(205)	12088(9)	2069(5)	-1049(7)	36(2)
C(206)	11761(8)	2164(5)	-78(5)	27(2)
C(207)	7917(8)	2678(7)	-844(6)	33(4)
C(208)	7495(13)	3561(8)	-1359(11)	66(3)
C(209)	6972(12)	1933(8)	-1314(10)	56(3)
C(210)	12801(8)	2022(6)	885(6)	32(2)
C(211)	14268(8)	2500	759(7)	146(7)
C(212)	12700(10)	1069(6)	1278(7)	42(2)
C(301)	7381(7)	1222(5)	2747(5)	25(2)
C(302)	6793(8)	1363(5)	3632(6)	29(2)
C(303)	5830(8)	768(6)	3839(6)	33(2)
C(304)	5461(9)	38(6)	3212(7)	35(2)
C(305)	6069(9)	-105(5)	2370(6)	33(2)
C(306)	7030(8)	482(5)	2109(6)	27(2)
C(307)	7745(9)	307(5)	1221(6)	31(2)
C(308)	9135(10)	-150(7)	1616(8)	48(2)
C(309)	6921(11)	-244(8)	375(7)	53(3)
C(310)	7163(9)	2188(5)	4289(6)	32(2)
C(311)	6166(11)	2931(6)	3903(7)	45(2)
C(312)	7150(10)	2028(7)	5420(6)	48(2)

Table 70. Bond lengths [Å] and angles [°].

Re-N(1)	1.752(6)	Re-N(1)#1	1.752(6)	Re-N(3)	1.756(6)
Re-N(3)#1	1.756(6)	Re-N(2)	1.760(4)	Re-Sn#1	2.7416(8)
Re-Sn	2.7416(8)	N(1)-N(1)#1	0.933(11)	N(1)-C(101)	1.420(9)
N(1)-C(101)#1	1.826(9)	N(2)-C(201)#1	1.402(7)	N(2)-C(201)	1.402(7)
N(3)-C(301)	1.406(9)	N(3)-Sn#1	1.716(6)	Sn-C(307)#1	1.448(8)
Sn-C(308)#1	1.648(10)	Sn-C(306)#1	1.676(8)	Sn-N(3)#1	1.716(6)
Sn-C(301)#1	1.803(7)	Sn-C(3)	2.142(9)	Sn-C(2)	2.145(8)
Sn-C(1) 2.149(9)		C(2)-C(308)#1	1.113(12)	C(3)-C(306)#1	1.240(12)
C(3)-C(307)#1	1.352(12)	C(3)-C(309)#1	1.921(14)	C(101)-C(106)#1	1.111(9)
C(101)-C(106)	1.417(10)	C(101)-C(102)	1.428(11)	C(101)-C(107)#1	1.419(9)
C(101)-C(101)#1	1.412(15)	C(101)-N(1)#1	1.826(9)	C(101)-C(109)#1	1.863(11)
C(102)-C(109)#1	0.841(10)	C(102)-C(103)	1.414(11)	C(102)-C(110)	1.502(11)
C(102)-C(107)#1	1.665(11)	C(102)-C(106)#1	2.016(11)	C(103)-C(104)	1.384(11)
C(103)-C(109)#1	1.828(13)	C(104)-C(105)	1.372(9)	C(105)-C(104)#1	1.372(9)
C(105)-C(106)	1.395(9)	C(105)-C(106)#1	1.395(9)	C(106)-C(106)#1	0.548(14)
C(106)-C(101)#1	1.111(9)	C(106)-C(107)	1.499(10)	C(106)-C(107)#1	1.990(11)
C(106)-C(102)#1	2.016(11)	C(107)-C(101)#1	1.419(9)	C(107)-C(108)	1.524(11)
C(107)-C(109)	1.537(11)	C(107)-C(102)#1	1.665(11)	C(107)-C(106)#1	1.990(11)
C(109)-C(102)#1	0.841(10)	C(109)-C(110)#1	1.275(11)	C(109)-C(103)#1	1.828(13)
C(109)-C(101)#1	1.863(11)	C(109)-C(111)#1	1.961(12)	C(110)-C(109)#1	1.275(11)
C(110)-C(111)	1.532(12)	C(110)-C(112)	1.536(11)	C(111)-C(109)#1	1.961(12)
C(201)-C(201)#1	0.334(17)	C(201)-C(206)	1.434(10)	C(201)-C(202)	1.420(9)
C(201)-C(206)#1	1.547(10)	C(202)-C(203)	1.409(10)	C(202)-C(201)#1	1.420(9)
C(202)-C(203)#1	1.409(10)	C(202)-C(207)#1	1.522(10)	C(202)-C(207)	1.522(10)
C(203)-C(203)#1	0.35(9)	C(203)-C(204)	1.377(16)	C(203)-C(204)#1	1.50(2)
C(204)-C(204)#1	0.997(16)	C(204)-C(205)	1.385(13)	C(204)-C(203)#1	1.50(2)
C(204)-C(205)#1	1.790(12)	C(205)-C(205)#1	1.291(16)	C(205)-C(206)	1.396(10)
C(205)-C(206)#1	1.802(11)	C(205)-C(204)#1	1.790(12)	C(206)-C(206)#1	1.006(14)
C(206)-C(201)#1	1.547(10)	C(206)-C(210)	1.524(11)	C(206)-C(205)#1	1.802(11)
C(206)-C(210)#1	1.940(11)	C(207)-C(207)#1	0.53(2)	C(207)-C(209)#1	1.196(14)
C(207)-C(208)	1.517(14)	C(207)-C(209)	1.528(14)	C(207)-C(208)#1	1.999(16)
C(208)-C(209)#1	0.915(15)	C(208)-C(207)#1	1.999(16)	C(209)-C(208)#1	0.915(15)
C(209)-C(207)#1	1.196(14)	C(209)-C(209)#1	1.70(2)	C(210)-C(210)#1	1.430(17)
C(210)-C(212)	1.530(12)	C(210)-C(211)	1.671(11)	C(210)-C(206)#1	1.94011)
C(211)-C(210)#1	1.671(11)	C(301)-C(302)	1.422(10)	C(301)-C(306)	1.405(10)
C(301)-Sn#1	1.803(7)	C(302)-C(311)#1	1.311(12)	C(302)-C(303)	1.377(11)
C(302)-C(310)	1.523(11)	C(303)-C(304)	1.388(12)	C(303)-C(311)#1	1.976(13)
C(304)-C(305)	1.382(12)	C(305)-C(306)	1.392(11)	C(306)-C(3)#1	1.240(12)
C(306)-C(307)	1.507(11)	C(306)-Sn#1	1.676(8)	C(307)-C(3)#1	1.352(12)
C(307)-Sn#1	1.448(8)	C(307)-C(309)	1.523(11)	C(307)-C(308)	1.563(13)
C(308)-C(2)#1	1.113(12)	C(308)-Sn#1	1.648(10)	C(309)-C(3)#1	1.921(14)
C(310)-C(310)#1	0.934(16)	C(310)-C(311)#1	1.058(12)	C(310)-C(311)	1.525(11)
C(310)-C(312)	1.528(11)	C(310)-C(312)#1	1.912(12)	C(311)-C(310)#1	1.058(12)
C(311)-C(311)#1	1.292(18)	C(311)-C(302)#1	1.311(12)	C(311)-C(303)#1	1.976(13)
C(312)-C(312)#1	1.41(2)	C(312)-C(310)#1	1.912(12)	N(1)-Re-N(1)#1	30.9(4)
N(1)-Re-N(3)	100.4(3)	N(1)#1-Re-N(3)	118.6(3)	N(1)-Re-N(3)#1	118.6(3)
N(1)#1-Re-N(3)#1	100.4(3)	N(3)-Re-N(3)#1	68.4(4)	N(1)-Re-N(2)	117.3(2)
N(1)#1-Re-N(2)	117.3(2)	N(3)-Re-N(2)	120.0(2)	N(3)#1-Re-N(2)	120.0(2)
N(1)-Re-Sn#1	92.82(19)	N(1)#1-Re-Sn#1	122.77(19)	N(3)-Re-Sn#1	37.33(18)
N(3)#1-Re-Sn#1	104.16(18)	N(2)-Re-Sn#1	93.07(6)	N(1)-Re-Sn	122.77(19)
N(1)#1-Re-Sn	92.82(19)	N(3)-Re-Sn	104.16(18)	N(3)#1-Re-Sn	37.33(18)
N(2)-Re-Sn	93.07(6)	Sn#1-Re-Sn	135.22(3)	N(1)#1-N(1)-C(101)	99.7(4)
N(1)#1-N(1)-Re	74.57(19)	C(101)-N(1)-Re	170.2(5)	N(1)#1-N(1)-C(101)#1	50.0(3)
C(101)-N(1)-C(101)#1	49.7(5)	Re-N(1)-C(101)#1	124.1(4)	C(201)#1-N(2)-C(201)	13.7(7)
C(201)#1-N(2)-Re	172.5(4)	C(201)-N(2)-Re	172.5(4)	C(301)-N(3)-Sn#1	69.7(4)
C(301)-N(3)-Re	172.7(4)	Sn#1-N(3)-Re	104.3(3)	C(307)#1-Sn-C(308)#1	60.2(5)
C(307)#1-Sn-C(306)#1	57.1(4)	C(308)#1-Sn-C(306)#1	97.7(5)	C(307)#1-Sn-N(3)#1	128.7(4)
C(308)#1-Sn-N(3)#1	170.4(4)	C(306)#1-Sn-N(3)#1	91.1(3)	C(307)#1-Sn-C(301)#1	101.6(4)
C(308)#1-Sn-C(301)#1	139.6(4)	C(306)#1-Sn-C(301)#1	47.5(3)	N(3)#1-Sn-C(301)#1	47.0(3)
C(307)#1-Sn-C(3)	38.5(4)	C(308)#1-Sn-C(3)	97.6(5)	C(306)#1-Sn-C(3)	35.3(4)
N(3)#1-Sn-C(3)	91.8(3)	C(301)#1-Sn-C(3)	66.4(3)	C(307)#1-Sn-C(2)	70.4(4)
C(308)#1-Sn-C(2)	30.7(4)	C(306)#1-Sn-C(2)	122.7(4)	N(3)#1-Sn-C(2)	143.2(3)
C(301)#1-Sn-C(2)	169.6(3)	C(3)-Sn-C(2)	107.3(4)	C(307)#1-Sn-C(1)	113.3(4)
C(308)#1-Sn-C(1)	88.8(5)	C(306)#1-Sn-C(1)	73.3(4)	N(3)#1-Sn-C(1)	90.1(3)
C(301)#1-Sn-C(1)	64.5(3)	C(3)-Sn-C(1)	108.7(4)	C(2)-Sn-C(1)	112.0(4)
C(307)#1-Sn-Re	135.7(3)	C(308)#1-Sn-Re	133.8(4)	C(306)#1-Sn-Re	127.9(3)
N(3)#1-Sn-Re	38.4(2)	C(301)#1-Sn-Re	85.3(2)	C(3)-Sn-Re	114.9(3)
C(2)-Sn-Re	105.0(2)	C(1)-Sn-Re	109.1(3)	C(308)#1-C(2)-Sn	49.2(6)
C(306)#1-C(3)-C(307)#1	71.0(7)	C(306)#1-C(3)-C(309)#1	104.8(8)		
C(307)#1-C(3)-C(309)#1	52.0(6)	C(306)#1-C(3)-Sn	51.4(5)		
C(307)#1-C(3)-Sn	41.8(4)	C(309)#1-C(3)-Sn	93.8(5)		

C(106)#1-C(101)-C(106)	20.9(6)	C(106)#1-C(101)-C(102)	104.4(7)
C(106)-C(101)-C(102)	121.9(6)	C(106)#1-C(101)-C(107)#1	71.5(6)
C(106)-C(101)-C(107)#1	89.1(6)	C(102)-C(101)-C(107)#1	71.6(6)
C(106)#1-C(101)-C(101)#1	67.1(5)	C(106)-C(101)-C(101)#1	46.2(4)
C(102)-C(101)-C(101)#1	149.6(4)	C(107)#1-C(101)-C(101)#1	127.2(5)
C(106)#1-C(101)-N(1)	135.3(8)	C(106)-C(101)-N(1)	119.4(7)
C(102)-C(101)-N(1)	118.6(6)	C(107)#1-C(101)-N(1)	109.7(6)
C(101)#1-C(101)-N(1)	80.3(4)	C(106)#1-C(101)-N(1)#1	110.7(7)
C(106)-C(101)-N(1)#1	91.7(5)	C(102)-C(101)-N(1)#1	144.4(6)
C(107)#1-C(101)-N(1)#1	124.8(5)	C(101)#1-C(101)-N(1)#1	50.0(3)
N(1)-C(101)-N(1)#1	30.2(4)	C(106)#1-C(101)-C(109)#1	109.9(6)
C(106)-C(101)-C(109)#1	130.6(6)	C(102)-C(101)-C(109)#1	25.5(4)
C(107)#1-C(101)-C(109)#1	53.8(5)	C(101)#1-C(101)-C(109)#1	174.6(4)
N(1)-C(101)-C(109)#1	104.6(6)	N(1)#1-C(101)-C(109)#1	134.8(5)
C(109)#1-C(102)-C(103)	105.5(10)	C(109)#1-C(102)-C(101)	107.6(10)
C(103)-C(102)-C(101)	117.0(7)	C(109)#1-C(102)-C(110)	58.0(8)
C(103)-C(102)-C(110)	122.4(7)	C(101)-C(102)-C(110)	120.6(7)
C(109)#1-C(102)-C(107)#1	66.5(8)	C(103)-C(102)-C(107)#1	96.0(6)
C(101)-C(102)-C(107)#1	53.9(4)	C(110)-C(102)-C(107)#1	118.1(7)
C(109)#1-C(102)-C(106)#1	113.3(9)	C(103)-C(102)-C(106)#1	85.4(5)
C(101)-C(102)-C(106)#1	32.3(4)	C(110)-C(102)-C(106)#1	151.8(6)
C(107)#1-C(102)-C(106)#1	46.9(4)	C(102)-C(103)-C(104)	121.2(8)
C(102)-C(103)-C(109)#1	26.3(4)	C(104)-C(103)-C(109)#1	131.0(7)
C(103)-C(104)-C(105)	120.3(7)	C(104)#1-C(105)-C(106)	101.5(5)
C(104)#1-C(105)-C(104)	118.3(8)	C(106)-C(105)-C(104)	122.4(5)
C(104)#1-C(105)-C(106)#1	122.4(5)	C(106)-C(105)-C(106)#1	22.6(6)
C(104)-C(105)-C(106)#1	101.5(5)	C(106)#1-C(106)-C(101)#1	112.9(5)
C(106)#1-C(106)-C(105)	78.7(3)	C(101)#1-C(106)-C(105)	146.3(7)
C(106)#1-C(106)-C(101)	46.2(4)	C(101)#1-C(106)-C(101)	66.7(7)
C(105)-C(106)-C(101)	117.2(6)	C(106)#1-C(106)-C(107)	149.3(4)
C(101)#1-C(106)-C(107)	63.8(6)	C(105)-C(106)-C(107)	122.1(6)
C(101)-C(106)-C(107)	120.7(6)	C(106)#1-C(106)-C(107)#1	22.6(3)
C(101)#1-C(106)-C(107)#1	106.2(6)	C(105)-C(106)-C(107)#1	95.3(4)
C(101)-C(106)-C(107)#1	45.5(4)	C(107)-C(106)-C(107)#1	126.6(7)
C(106)#1-C(106)-C(102)#1	145.6(3)	C(101)#1-C(106)-C(102)#1	43.3(5)
C(105)-C(106)-C(102)#1	109.5(5)	C(101)-C(106)-C(102)#1	104.6(5)
C(107)-C(106)-C(102)#1	54.2(4)	C(107)#1-C(106)-C(102)#1	148.8(5)
C(101)#1-C(107)-C(106)	44.7(4)	C(101)#1-C(107)-C(108)	157.5(8)
C(106)-C(107)-C(108)	113.6(7)	C(101)#1-C(107)-C(109)	78.0(6)
C(106)-C(107)-C(109)	109.0(7)	C(108)-C(107)-C(109)	111.1(7)
C(101)#1-C(107)-C(102)#1	54.4(5)	C(106)-C(107)-C(102)#1	78.9(5)
C(108)-C(107)-C(102)#1	124.8(7)	C(109)-C(107)-C(102)#1	30.1(4)
C(101)#1-C(107)-C(106)#1	45.4(4)	C(106)-C(107)-C(106)#1	8.1(2)
C(108)-C(107)-C(106)#1	114.2(6)	C(109)-C(107)-C(106)#1	115.1(6)
C(102)#1-C(107)-C(106)#1	85.3(5)	C(102)#1-C(109)-C(110)#1	87.9(10)
C(102)#1-C(109)-C(107)	83.4(9)	C(110)#1-C(109)-C(107)	150.1(8)
C(102)#1-C(109)-C(103)#1	48.2(8)	C(110)#1-C(109)-C(103)#1	109.6(8)
C(107)-C(109)-C(103)#1	85.5(6)	C(102)#1-C(109)-C(101)#1	46.9(7)
C(110)#1-C(109)-C(101)#1	106.9(7)	C(107)-C(109)-C(101)#1	48.1(4)
C(103)#1-C(109)-C(101)#1	82.0(5)	C(102)#1-C(109)-C(111)#1	123.5(10)
C(110)#1-C(109)-C(111)#1	51.4(5)	C(107)-C(109)-C(111)#1	151.3(7)
C(103)#1-C(109)-C(111)#1	104.7(6)	C(101)#1-C(109)-C(111)#1	158.3(6)
C(109)#1-C(110)-C(102)	34.0(5)	C(109)#1-C(110)-C(111)	88.1(7)
C(102)-C(110)-C(111)	112.6(7)	C(109)#1-C(110)-C(112)	143.9(9)
C(102)-C(110)-C(112)	110.8(7)	C(111)-C(110)-C(112)	108.7(7)
C(110)-C(111)-C(109)#1	40.5(4)	C(201)#1-C(201)-C(206)	103.6(4)
C(201)#1-C(201)-C(202)	83.2(3)	C(206)-C(201)-C(202)	121.1(6)
C(201)#1-C(201)-N(2)	83.2(3)	C(206)-C(201)-N(2)	119.6(6)

C(202)-C(201)-N(2)	119.3(6)
C(206)-C(201)-C(206)#1	39.2(6)
N(2)-C(201)-C(206)#1	112.3(6)
C(201)-C(202)-C(201)#1	13.5(7)
C(201)-C(202)-C(203)#1	119.6(6)
C(201)#1-C(202)-C(203)#1	117.7(7)
C(203)-C(202)-C(207)#1	116.9(7)
C(203)#1-C(202)-C(207)#1	119.8(6)
C(203)-C(202)-C(207)	119.8(6)
C(203)#1-C(202)-C(207)	116.9(7)
C(203)#1-C(203)-C(204)	103.5(17)
C(204)-C(203)-C(202)	121.3(8)
C(204)-C(203)-C(204)#1	40.3(7)
C(204)#1-C(204)-C(203)	76.5(18)
C(203)-C(204)-C(205)	120.8(7)
C(203)-C(204)-C(203)#1	13(3)
C(204)#1-C(204)-C(205)#1	50.3(4)
C(205)-C(204)-C(205)#1	45.8(6)
C(205)#1-C(205)-C(206)	84.1(5)
C(206)-C(205)-C(204)	121.3(8)
C(206)-C(205)-C(206)#1	33.7(5)
C(205)#1-C(205)-C(204)#1	50.3(4)
C(204)-C(205)-C(204)#1	33.6(6)
C(206)#1-C(206)-C(205)	95.9(5)
C(205)-C(206)-C(201)	117.7(7)
C(205)-C(206)-C(201)#1	117.0(7)
C(206)#1-C(206)-C(210)	98.0(4)
C(201)-C(206)-C(210)	120.2(6)
C(206)#1-C(206)-C(205)#1	50.4(3)
C(201)-C(206)-C(205)#1	101.1(6)
C(210)-C(206)-C(205)#1	120.7(6)
C(205)-C(206)-C(210)#1	119.5(6)
C(201)#1-C(206)-C(210)#1	94.0(5)
C(205)#1-C(206)-C(210)#1	86.1(5)
C(207)#1-C(207)-C(208)	150.7(6)
C(207)#1-C(207)-C(202)	79.9(4)
C(208)-C(207)-C(202)	109.4(8)
C(209)#1-C(207)-C(209)	76.1(12)
C(202)-C(207)-C(209)	113.4(8)
C(209)#1-C(207)-C(208)#1	99.8(9)
C(202)-C(207)-C(208)#1	88.5(6)
C(209)#1-C(208)-C(207)	52.0(10)
C(207)-C(208)-C(207)#1	7.5(3)
C(208)#1-C(209)-C(207)	107.1(14)
C(208)#1-C(209)-C(209)#1	143.9(11)
C(207)-C(209)-C(209)#1	43.1(6)
C(210)#1-C(210)-C(206)	82.0(4)
C(210)#1-C(210)-C(211)	64.7(3)
C(206)-C(210)-C(211)	110.1(6)
C(212)-C(210)-C(206)#1	138.8(7)
C(211)-C(210)-C(206)#1	92.8(5)
C(302)-C(301)-C(306)	121.5(7)
C(306)-C(301)-N(3)	119.0(7)
C(306)-C(301)-Sn#1	61.5(4)
C(311)#1-C(302)-C(301)	129.3(7)
C(301)-C(302)-C(303)	118.4(7)
C(301)-C(302)-C(310)	120.1(7)
C(302)-C(303)-C(304)	120.9(8)
C(201)#1-C(201)-C(206)#1	64.3(4)
C(202)-C(201)-C(206)#1	113.7(5)
C(201)-C(202)-C(203)	117.7(7)
C(203)-C(202)-C(201)#1	119.6(6)
C(203)-C(202)-C(203)#1	14(3)
C(201)-C(202)-C(207)#1	119.7(5)
C(201)#1-C(202)-C(207)#1	122.4(5)
C(201)-C(202)-C(207)	122.4(5)
C(201)#1-C(202)-C(207)	119.7(5)
C(207)#1-C(202)-C(207)	20.1(8)
C(203)#1-C(203)-C(202)	82.8(17)
C(203)#1-C(203)-C(204)#1	63.2(15)
C(202)-C(203)-C(204)#1	113.1(16)
C(204)#1-C(204)-C(205)	96.1(5)
C(204)#1-C(204)-C(203)#1	63.2(15)
C(205)-C(204)-C(203)#1	119.7(7)
C(203)-C(204)-C(205)#1	103.2(14)
C(203)#1-C(204)-C(205)#1	93.4(12)
C(205)#1-C(205)-C(204)	83.9(5)
C(205)#1-C(205)-C(206)#1	50.4(3)
C(204)-C(205)-C(206)#1	110.1(7)
C(206)-C(205)-C(204)#1	110.2(6)
C(206)#1-C(205)-C(204)#1	84.9(5)
C(206)#1-C(206)-C(201)	76.4(4)
C(206)#1-C(206)-C(201)#1	64.3(4)
C(201)-C(206)-C(201)#1	12.1(6)
C(205)-C(206)-C(210)	122.1(7)
C(201)#1-C(206)-C(210)	119.8(6)
C(205)-C(206)-C(205)#1	45.5(6)
C(201)#1-C(206)-C(205)#1	92.3(6)
C(206)#1-C(206)-C(210)#1	51.1(3)
C(201)-C(206)-C(210)#1	102.9(5)
C(210)-C(206)-C(210)#1	46.9(6)
C(207)#1-C(207)-C(209)#1	119.2(7)
C(209)#1-C(207)-C(208)	37.1(7)
C(209)#1-C(207)-C(202)	139.1(9)
C(207)#1-C(207)-C(209)	43.1(6)
C(208)-C(207)-C(209)	110.2(9)
C(207)#1-C(207)-C(208)#1	21.8(5)
C(208)-C(207)-C(208)#1	128.9(11)
C(209)-C(207)-C(208)#1	26.0(6)
C(209)#1-C(208)-C(207)#1	47.0(10)
C(208)#1-C(209)-C(207)#1	90.9(14)
C(207)#1-C(209)-C(207)	17.7(7)
C(207)#1-C(209)-C(209)#1	60.8(7)
C(210)#1-C(210)-C(212)	159.0(5)
C(212)-C(210)-C(206)	110.0(7)
C(212)-C(210)-C(211)	123.0(7)
C(210)#1-C(210)-C(206)#1	51.1(3)
C(206)-C(210)-C(206)#1	30.9(5)
C(210)-C(211)-C(210)#1	50.7(6)
C(302)-C(301)-N(3)	119.6(7)
C(302)-C(301)-Sn#1	156.6(5)
N(3)-C(301)-Sn#1	63.2(4)
C(311)#1-C(302)-C(303)	94.6(7)
C(311)#1-C(302)-C(310)	43.1(6)
C(303)-C(302)-C(310)	121.4(7)
C(302)-C(303)-C(311)#1	41.4(5)

C(304)-C(303)-C(311)#1	146.0(7)	C(305)-C(304)-C(303)	120.1(8)
C(306)-C(305)-C(304)	121.7(8)	C(3)#1-C(306)-C(305)	104.4(8)
C(3)#1-C(306)-C(301)	110.8(8)	C(305)-C(306)-C(301)	117.4(7)
C(3)#1-C(306)-C(307)	58.0(6)	C(305)-C(306)-C(307)	121.9(7)
C(301)-C(306)-C(307)	120.5(7)	C(3)#1-C(306)-Sn#1	93.3(6)
C(305)-C(306)-Sn#1	154.6(6)	C(301)-C(306)-Sn#1	71.0(5)
C(307)-C(306)-Sn#1	53.8(4)	C(3)#1-C(307)-Sn#1	99.7(6)
C(3)#1-C(307)-C(309)	83.6(7)	Sn#1-C(307)-C(309)	176.6(8)
C(3)#1-C(307)-C(306)	51.1(6)	Sn#1-C(307)-C(306)	69.0(4)
C(309)-C(307)-C(306)	113.8(7)	C(3)#1-C(307)-C(308)	160.1(8)
Sn#1-C(307)-C(308)	66.2(5)	C(309)-C(307)-C(308)	110.6(8)
C(306)-C(307)-C(308)	109.2(6)	C(2)#1-C(308)-C(307)	105.6(9)
C(2)#1-C(308)-Sn#1	100.1(8)	C(307)-C(308)-Sn#1	53.5(4)
C(307)-C(309)-C(3)#1	44.4(5)	C(310)#1-C(310)-C(311)#1	99.7(7)
C(310)#1-C(310)-C(311)	43.1(5)	C(311)#1-C(310)-C(311)	56.6(10)
C(310)#1-C(310)-C(302)	144.2(4)	C(311)#1-C(310)-C(302)	57.8(7)
C(311)-C(310)-C(302)	108.5(7)	C(310)#1-C(310)-C(312)	99.0(5)
C(311)#1-C(310)-C(312)	106.7(9)	C(311)-C(310)-C(312)	109.4(7)
C(302)-C(310)-C(312)	113.4(7)	C(310)#1-C(310)-C(312)#1	52.1(4)
C(311)#1-C(310)-C(312)#1	110.7(9)	C(311)-C(310)-C(312)#1	74.1(5)
C(302)-C(310)-C(312)#1	156.5(7)	C(312)-C(310)-C(312)#1	46.9(7)
C(310)#1-C(311)-C(311)#1	80.3(7)	C(310)#1-C(311)-C(302)#1	79.2(9)
C(311)#1-C(311)-C(302)#1	143.7(5)	C(310)#1-C(311)-C(310)	37.1(7)
C(311)#1-C(311)-C(310)	43.1(5)	C(302)#1-C(311)-C(310)	111.3(8)
C(310)#1-C(311)-C(303)#1	109.2(9)	C(311)#1-C(311)-C(303)#1	170.3(4)
C(302)#1-C(311)-C(303)#1	44.0(5)	C(310)-C(311)-C(303)#1	146.2(7)
C(312)#1-C(312)-C(310)	81.0(5)	C(312)#1-C(312)-C(310)#1	52.1(4)
C(310)-C(312)-C(310)#1	28.8(5)		

Symmetry transformations used to generate equivalent atoms:
#1 x,-y+1/2,z

Table 71. Anisotropic displacement parameters ($Å^2 x\ 10^3$). The anisotropic displacement factor exponent takes the form: $-2\pi^2[\ h^2\ a^{*2}U^{11} + ...\ + 2\ h\ k\ a^*\ b^*\ U^{12}\ ]$

	U^{11}	U^{22}	U^{33}	U^{23}	U^{13}	U^{12}
Re	22(1)	25(1)	11(1)	0	0(1)	0
N(1)11(3)	30(3)	28(3)	0(2)	0(2)	4(2)	
N(2)23(2)	33(2)	17(2)	0	1(2)	0	
N(3)19(3)	19(3)	25(3)	-3(2)	0(2)	4(2)	
Sn	26(1)	30(1)	22(1)	2(1)	5(1)	3(1)
C(1)54(6)	51(6)	47(6)	-9(4)	25(5)	1(5)	
C(2)39(5)	34(4)	28(4)	6(3)	6(4)	1(4)	
C(3)28(5)	65(6)	48(6)	13(5)	4(4)	6(5)	
C(101)	20(4)	41(4)	9(3)	3(3)	3(3)	-1(3)
C(102)	25(4)	34(4)	12(3)	2(3)	1(3)	0(4)
C(103)	22(4)	43(4)	21(4)	4(3)	2(3)	7(3)
C(104)	37(5)	51(5)	15(4)	2(3)	-3(3)	5(4)
C(105)	30(3)	49(3)	15(3)	0	1(2)	0
C(106)	25(4)	24(8)	21(3)	-3(3)	4(3)	-5(3)
C(107)	28(4)	36(4)	27(4)	-10(3)	-1(3)	2(3)
C(108)	49(6)	47(5)	30(5)	-12(4)	6(4)	8(4)
C(109)	38(6)	23(4)	38(5)	-1(4)	10(4)	0(4)
C(110)	30(5)	34(4)	27(4)	-8(3)	3(3)	-2(3)
C(111)	43(5)	35(4)	41(5)	8(4)	5(4)	2(4)
C(112)	56(6)	45(5)	29(5)	-9(4)	15(4)	-8(5)
C(201)	31(3)	43(6)	14(3)	-3(4)	7(2)	-3(5)
C(202)	35(3)	34(3)	15(3)	0	0(2)	0
C(203)	38(4)	50(20)	18(3)	2(5)	5(3)	10(7)
C(204)	61(6)	45(5)	14(4)	3(3)	13(4)	3(4)
C(205)	38(5)	36(4)	37(5)	-1(4)	20(4)	1(4)
C(206)	33(4)	28(3)	19(4)	0(3)	6(3)	-1(3)
C(207)	37(4)	40(11)	18(3)	-7(3)	-2(3)	9(4)
C(208)	51(8)	47(7)	96(10)	11(7)	1(7)	11(6)
C(209)	50(7)	50(7)	71(8)	-4(6)	18(6)	-8(6)
C(210)	26(4)	42(4)	27(4)	-4(4)	1(3)	-3(4)
C(211)	23(5)	360(20)	53(6)	0	1(4)	0
C(212)	44(6)	48(5)	31(5)	9(4)	3(4)	2(4)

C(301)	24(4)	34(4)	17(4)	0(3)	2(3)	1(3)
C(302)	30(5)	36(4)	21(4)	0(3)	6(3)	5(3)
C(303)	22(4)	44(5)	32(4)	3(4)	7(3)	3(4)
C(304)	29(5)	36(4)	39(5)	8(4)	7(4)	-5(4)
C(305)	35(5)	33(4)	29(4)	1(3)	-4(4)	-4(4)
C(306)	25(4)	33(4)	18(4)	3(3)	-8(3)	2(3)
C(307)	38(5)	33(4)	20(4)	-5(3)	0(3)	-4(4)
C(308)	48(6)	57(6)	42(5)	-5(5)	17(5)	13(5)
C(309)	60(7)	69(7)	30(5)	-20(5)	5(5)	-17(6)
C(310)	32(5)	39(5)	26(4)	-9(3)	7(4)	2(3)
C(311)	67(7)	42(5)	26(5)	-4(4)	10(5)	12(5)
C(312)	63(7)	54(5)	24(4)	-7(4)	0(4)	10(5)

Table 72. Hydrogen coordinates (x 10^4) and isotropic displacement parameters ($Å^2$x 10^3).

	x	y	z	U(eq)
H(1A)	8342	5359	3433	58
H(1B)	8194	4407	3892	58
H(1C)	9634	4792	3842	58
H(2A)	9513	5505	1017	40
H(2B)	10756	4904	1455	40
H(2C)	9779	4616	461	40
H(3A)	6266	4887	1198	57
H(3B)	6494	4042	553	57
H(3C)	5981	3931	1594	57
H(10A)	14043	521	5192	35
H(10B)	14368	1604	6482	42
H(10C)	13157	2943	6276	38
H(10D)	10443	3420	4327	37
H(10E)	10551	3516	6090	51
H(10F)	11872	4090	6174	51
H(10G)	10494	4471	5602	51
H(10H)	12212	3933	3550	39
H(10I)	11527	4742	4010	39
H(10J)	12905	4362	4581	39
H(11A)	11579	656	2913	37
H(11B)	11680	-506	4122	48
H(11C)	12278	-841	3176	48
H(11D)	13250	-535	4165	48
H(11E)	13588	1201	2420	51
H(11F)	14385	488	3149	51
H(11G)	13412	183	2160	51
H(20A)	9133	2428	-2450	44
H(20B)	11370	2089	-2575	47
H(20C)	13007	1930	-1104	43
H(20D)	7835	2714	-137	39
H(20E)	8080	4028	-1047	79
H(20F)	7543	3531	-2072	79
H(20G)	6582	3686	-1276	79
H(20H)	6051	2069	-1262	68
H(20I)	7054	1878	-2019	68
H(20J)	7230	1380	-969	68
H(21A)	12464	2379	1386	39
H(21B)	14890	2395	1379	175
H(21C)	14619	2241	198	175
H(21D)	14152	3131	652	175
H(21E)	11772	909	1274	50
H(21F)	13088	666	846	50
H(21G)	13193	1031	1960	50
H(30A)	5412	863	4427	39
H(30B)	4800	-378	3373	41
H(30C)	5825	-616	1942	40
H(30D)	7910	876	933	37
H(30E)	9570	-257	1039	57
H(30F)	9689	240	2086	57
H(30G)	9011	-706	1946	57
H(30H)	6065	45	166	64
H(30I)	7384	-291	-197	64
H(30J)	6777	-831	627	64
H(31A)	8047	2379	4197	39
H(31B)	6150	3027	3188	54
H(31C)	5280	2764	4015	54
H(31D)	6440	3471	4269	54
H(31E)	7396	2574	5783	57
H(31F)	6270	1844	5529	57
H(31G)	7799	1573	5663	57

Appendix XV

X-ray data for $Me_3SnRe(NAr)_2(NAr')$

The tables that follow contain atomic coordinates and equivalent isotropic displacement parameters, complete bond lengths (Å) and angles (°), anisotropic displacement parameters and calculated H-atom positions for $Me_3SnRe(NAr)_2(NAr')$.

Table 73. Atomic coordinates (x 10^4) and equivalent isotropic displacement parameters ($Å^2$x 10^3). U(eq) is defined as one third of the trace of the orthogonalized U^{ij} tensor.

	x	y	z	U(eq)
Re	7367(1)	9179(1)	2126(1)	21(1)
Sn	4756(1)	9905(1)	1994(1)	33(1)
C(3)	8257(4)	12336(4)	3493(2)	38(1)
N(3)	7619(3)	7751(3)	2963(2)	26(1)
N(2)	7341(3)	10615(3)	2350(2)	26(1)
N(1)	7869(3)	8983(3)	1054(2)	28(1)
C(7)	6789(4)	12943(3)	2219(2)	34(1)
C(8)	7452(3)	11613(3)	2603(2)	25(1)
C(9)	8375(3)	8684(4)	259(2)	29(1)
C(10)	8218(3)	11302(3)	3246(2)	29(1)
C(11)	8688(3)	9645(4)	-457(2)	37(1)
C(12)	7151(4)	6406(3)	4380(2)	34(1)
C(13)	8027(3)	6609(3)	3586(2)	27(1)
C(14)	6857(4)	13928(4)	2520(3)	42(1)
C(15)	9310(4)	5660(3)	3424(2)	33(1)
C(16)	8567(3)	7412(4)	186(2)	34(1)
C(18)	8971(4)	9871(4)	3635(2)	36(1)
C(19)	7574(4)	13637(4)	3163(3)	44(1)
C(20)	4258(5)	8271(5)	1976(3)	59(1)
C(21)	5790(4)	7412(4)	4555(2)	40(1)
C(22)	9129(4)	7113(5)	-618(3)	48(1)
C(23)	10360(4)	9668(5)	3770(3)	48(1)
C(24)	8833(5)	4309(4)	4831(3)	51(1)
C(25)	10269(4)	5910(4)	2595(2)	40(1)
C(26)	9675(4)	4537(4)	4074(3)	46(1)
C(27)	9256(5)	9273(5)	-1235(3)	55(1)
C(28)	11285(4)	6402(4)	2711(3)	48(1)
C(29)	6041(4)	13276(4)	1498(3)	47(1)

C(31)	4459(5)	11297(5)	789(3)	56(1)
C(32)	7572(5)	5224(4)	4986(3)	45(1)
C(33)	9484(5)	8007(6)	-1308(3)	61(1)
C(35)	8427(5)	10997(5)	-378(3)	51(1)
C(37)	8128(5)	6433(4)	933(3)	47(1)
C(38)	3487(5)	10792(5)	3022(3)	57(1)
C(39)	8154(5)	9339(5)	4450(3)	59(1)
C(44)	10962(5)	4680(5)	2226(3)	60(1)
C(45)	4723(5)	7015(6)	4409(4)	67(1)
C(46)	5456(5)	7639(6)	5458(3)	66(1)
C(49)	6765(6)	13871(6)	641(3)	73(2)
C(60)	4599(5)	14151(7)	1693(5)	94(2)

Table 74. Bond lengths [Å] and angles [°].

Re-N(3)	1.762(3)	Re-N(2)	1.766(3)		
Re-N(1)	1.779(3)				
Re-Sn	2.7354(6)	Sn-C(20)	2.137(4)	Sn-C(31)	2.151(4)
Sn-C(38)	2.142(4)	C(3)-C(19)	1.380(6)	C(3)-C(10)	1.375(5)
N(3)-C(13)	1.388(4)	N(2)-C(8)	1.380(4)	N(1)-C(9)	1.384(4)
C(7)-C(14)	1.391(5)	C(7)-C(8)	1.420(5)	C(7)-C(29)	1.515(5)
C(8)-C(10)	1.423(5)	C(9)-C(16)	1.412(5)	C(9)-C(11)	1.411(5)
C(10)-C(18)	1.529(5)	C(11)-C(27)	1.396(6)	C(11)-C(35)	1.486(6)
C(12)-C(32)	1.401(5)	C(12)-C(13)	1.425(5)	C(12)-C(21)	1.513(5)
C(13)-C(15)	1.426(5)	C(14)-C(19)	1.391(6)	C(15)-C(26)	1.393(5)
C(15)-C(25)	1.521(5)	C(16)-C(22)	1.401(5)	C(16)-C(37)	1.499(6)
C(18)-C(39)	1.508(6)	C(18)-C(23)	1.534(5)	C(21)-C(45)	1.515(6)
C(21)-C(46)	1.529(6)	C(22)-C(33)	1.358(7)	C(24)-C(26)	1.369(7)
C(24)-C(32)	1.392(7)	C(25)-C(28)	1.512(6)	C(25)-C(44)	1.534(5)
C(27)-C(33)	1.394(7)	C(29)-C(49)	1.529(7)	C(29)-C(60)	1.527(7)
N(3)-Re-N(2)	116.46(13)	N(3)-Re-N(1)	118.15(13)	N(2)-Re-N(1)	119.58(13)
N(3)-Re-Sn	104.32(8)	N(2)-Re-Sn	99.56(8)	N(1)-Re-Sn	90.41(9)
C(20)-Sn-C(31)	106.8(2)	C(20)-Sn-C(38)	110.2(2)	C(31)-Sn-C(38)	109.8(2)
C(20)-Sn-Re	111.67(14)	C(31)-Sn-Re	107.85(13)	C(38)-Sn-Re	110.41(13)
C(19)-C(3)-C(10)	123.4(4)	C(13)-N(3)-Re	171.0(2)		
C(8)-N(2)-Re	171.6(2)	C(9)-N(1)-Re	172.9(2)		
C(14)-C(7)-C(8)	118.1(3)	C(14)-C(7)-C(29)	121.1(3)		
C(8)-C(7)-C(29)	120.8(3)	N(2)-C(8)-C(7)	119.3(3)		
N(2)-C(8)-C(10)	119.9(3)	C(7)-C(8)-C(10)	120.8(3)		
N(1)-C(9)-C(16)	118.7(3)	N(1)-C(9)-C(11)	119.8(3)		

C(16)-C(9)-C(11)	121.4(3)	C(3)-C(10)-C(8)	117.3(3)
C(3)-C(10)-C(18)	122.0(3)	C(8)-C(10)-C(18)	120.7(3)
C(27)-C(11)-C(9)	117.5(4)	C(27)-C(11)-C(35)	121.6(4)
C(9)-C(11)-C(35)	120.9(3)	C(32)-C(12)-C(13)	117.8(3)
C(32)-C(12)-C(21)	120.9(3)	C(13)-C(12)-C(21)	121.3(3)
N(3)-C(13)-C(12)	119.1(3)	N(3)-C(13)-C(15)	119.7(3)
C(12)-C(13)-C(15)	121.2(3)	C(7)-C(14)-C(19)	121.6(3)
C(26)-C(15)-C(13)	117.4(4)	C(26)-C(15)-C(25)	121.5(3)
C(13)-C(15)-C(25)	121.0(3)	C(22)-C(16)-C(9)	117.8(4)
C(22)-C(16)-C(37)	121.0(4)	C(9)-C(16)-C(37)	121.1(3)
C(39)-C(18)-C(10)	110.8(3)	C(39)-C(18)-C(23)	111.6(3)
C(10)-C(18)-C(23)	113.3(3)	C(3)-C(19)-C(14)	118.6(4)
C(12)-C(21)-C(45)	110.9(4)	C(12)-C(21)-C(46)	112.5(4)
C(45)-C(21)-C(46)	109.9(4)	C(33)-C(22)-C(16)	121.6(4)
C(26)-C(24)-C(32)	120.5(3)	C(28)-C(25)-C(15)	111.6(3)
C(28)-C(25)-C(44)	110.5(3)	C(15)-C(25)-C(44)	111.7(4)
C(24)-C(26)-C(15)	122.2(4)	C(33)-C(27)-C(11)	121.4(4)
C(7)-C(29)-C(49)	111.6(4)	C(7)-C(29)-C(60)	112.2(4)
C(49)-C(29)-C(60)	111.7(4)	C(24)-C(32)-C(12)	120.8(4)
C(22)-C(33)-C(27)	120.1(4)		

Symmetry transformations used to generate equivalent atoms:

Table 75. Anisotropic displacement parameters ($Å^2 x\ 10^3$). The anisotropic displacement factor exponent takes the form: $-2\pi^2[\ h^2\ a^{*2}U^{11} + \ldots + 2\ h\ k\ a^*\ b^*\ U^{12}\ ]$

U^{11}	U^{22}	U^{33}	U^{23}	U^{13}	U^{12}	
Re22(1)	22(1)	18(1)	-5(1)	-5(1)	-6(1)	
Sn26(1)	40(1)	34(1)	-10(1)	-10(1)	-10(1)	
C(3)45(2)	47(2)	26(2)	-14(2)	4(2)	-23(2)	
N(3)21(1)	28(1)	26(1)	-6(1)	-3(1)	-6(1)	
N(2)22(1)	27(1)	29(1)	-8(1)	-8(1)	-5(1)	
N(1)26(1)	39(2)	22(1)	-12(1)	-4(1)	-11(1)	
C(7)34(2)	29(2)	37(2)	-3(1)	-5(1)	-12(1)	
C(8)23(1)	27(2)	25(2)	-6(1)	-1(1)	-10(1)	
C(9)21(1)	42(2)	26(2)	-12(1)	-6(1)	-7(1)	
C(10)	33(2)	31(2)	24(2)	-7(1)	-4(1)	-11(1)
C(11)	27(2)	55(2)	29(2)	-7(2)	-7(1)	-15(2)
C(12)	46(2)	33(2)	25(2)	-2(1)	-10(2)	-16(2)
C(13)	35(2)	23(2)	25(2)	-6(1)	-9(1)	-9(1)
C(14)	44(2)	26(2)	53(2)	-6(2)	-11(2)	-12(2)

C(15)	36(2)	31(2)	36(2)	-12(1)	-16(1)	-4(1)
C(16)	26(2)	44(2)	34(2)	-19(2)	-10(1)	-3(1)
C(18)	36(2)	38(2)	36(2)	-8(2)	-17(2)	-8(2)
C(19)	56(2)	37(2)	49(2)	-17(2)	-4(2)	-24(2)
C(20)	64(3)	62(3)	72(3)	-21(2)	-20(2)	-32(2)
C(21)	42(2)	40(2)	32(2)	-6(2)	3(2)	-14(2)
C(22)	36(2)	67(3)	47(2)	-37(2)	-7(2)	-8(2)
C(23)	42(2)	58(3)	47(2)	-10(2)	-19(2)	-14(2)
C(24)	72(3)	32(2)	48(2)	8(2)	-32(2)	-15(2)
C(25)	36(2)	44(2)	34(2)	-18(2)	-11(2)	4(2)
C(26)	51(2)	33(2)	52(2)	-9(2)	-29(2)	1(2)
C(27)	51(2)	91(4)	26(2)	-10(2)	2(2)	-36(2)
C(28)	51(2)	45(2)	44(2)	-14(2)	-3(2)	-13(2)
C(29)	52(2)	28(2)	61(3)	7(2)	-33(2)	-11(2)
C(31)	52(3)	64(3)	50(3)	5(2)	-33(2)	-14(2)
C(32)	66(3)	42(2)	29(2)	1(2)	-13(2)	-24(2)
C(33)	48(2)	108(4)	41(2)	-48(3)	10(2)	-27(3)
C(35)	51(2)	56(3)	45(2)	3(2)	-13(2)	-25(2)
C(37)	61(3)	39(2)	47(2)	-11(2)	-22(2)	-14(2)
C(38)	40(2)	67(3)	59(3)	-27(2)	2(2)	-9(2)
C(39)	61(3)	52(3)	53(3)	15(2)	-13(2)	-25(2)
C(44)	48(3)	59(3)	71(3)	-41(3)	-4(2)	-1(2)
C(45)	54(3)	76(3)	76(4)	-17(3)	-21(3)	-20(3)
C(46)	58(3)	90(4)	50(3)	-32(3)	18(2)	-31(3)
C(49)	84(4)	94(4)	49(3)	-12(3)	-27(3)	-31(3)
C(60)	39(3)	118(5)	99(5)	-9(4)	-31(3)	2(3)

Table 76. Hydrogen coordinates (x 10^4) and isotropic displacement parameters ($Å^2$x 10^3).

	x	y	z	U(eq)
H(3A)	8624	12155	3994	45
H(14A)	6383	14829	2279	50
H(18A)	9084	9369	3234	43
H(19A)	7674	14319	3340	53
H(20A)	3333	8590	1933	71
H(20B)	4783	7925	1487	71
H(20C)	4405	7587	2488	71
H(21A)	5776	8242	4164	49
H(22A)	9257	6256	-681	57
H(23A)	10894	9966	3244	58
H(23B)	10251	10163	4175	58
H(23C)	10791	8750	3998	58
H(24A)	9092	3498	5250	61
H(25A)	9755	6572	2182	48
H(26A)	10571	3940	4001	55
H(27A)	9538	9881	-1728	66
H(28A)	10838	7188	2923	57
H(28B)	11810	5735	3115	57
H(28C)	11853	6589	2173	57
H(29A)	6024	12452	1463	56

H(31A)	3542	11554	743	67
H(31B)	4661	12057	771	67
H(31C)	5014	10909	321	67
H(32A)	6980	5063	5516	54
H(33A)	9870	7778	-1851	73
H(35A)	8694	11526	-922	61
H(35B)	7503	11408	-172	61
H(35C)	8947	10917	24	61
H(37A)	8337	5617	779	57
H(37B)	8572	6279	1394	57
H(37C)	7184	6790	1111	57
H(38A)	2578	11037	2962	69
H(38B)	3634	10169	3558	69
H(38C)	3671	11560	3008	69
H(39A)	7298	9465	4344	71
H(39B)	8586	8421	4678	71
H(39C)	8046	9833	4855	71
H(44A)	11543	4873	1696	72
H(44B)	11477	4017	2637	72
H(44C)	10334	4366	2132	72
H(45A)	3877	7675	4523	81
H(45B)	4881	6931	3831	81
H(45C)	4722	6187	4798	81
H(46A)	6151	7890	5524	79
H(46B)	4614	8308	5567	79
H(46C)	5449	6820	5857	79
H(49A)	7676	13312	560	88
H(49B)	6342	13896	202	88
H(49C)	6728	14745	610	88
H(60A)	4202	14317	1207	113
H(60B)	4136	13704	2193	113
H(60C)	4542	14972	1779	113

Appendix XVI

X-ray data for $[Re(NAr')_2(\mu\text{-}NAr')]_2$

The tables that follow contain atomic coordinates and equivalent isotropic displacement parameters, complete bond lengths (Å) and angles (°), anisotropic displacement parameters and calculated H-atom positions for $[Re(NAr')_2(\mu\text{-}NAr')]_2$.

Table 77. Atomic coordinates (x 10^4) and equivalent isotropic displacement parameters ($Å^2$x 10^3). U(eq) is defined as one third of the trace of the orthogonalized U^{ij} tensor.

	x	y	z	U(eq)
Re(1)	5424(1)	9604(1)	491(1)	22(1)
N(11)	6936(3)	9705(2)	877(2)	30(1)
N(12)	4553(3)	8933(2)	784(2)	30(1)
N(13)	4402(3)	10407(2)	436(2)	24(1)
C(111)	7998(4)	9524(2)	1255(2)	35(1)
C(112)	8658(4)	8941(3)	1116(2)	41(1)
C(113)	9666(5)	8753(3)	1533(3)	55(2)
C(114)	10030(6)	9114(4)	2059(4)	69(2)
C(115)	9416(6)	9694(4)	2176(3)	66(2)
C(116)	8393(5)	9927(3)	1778(3)	45(1)
C(117)	8285(5)	8530(3)	541(3)	53(1)
C(118)	7730(7)	10571(4)	1887(3)	68(2)
C(119)	3970(4)	8444(2)	1129(2)	28(1)
C(120)	2893(4)	8109(2)	874(2)	34(1)
C(121)	2329(5)	7631(2)	1242(3)	41(1)
C(122)	2811(5)	7491(2)	1856(3)	44(1)
C(123)	3869(5)	7821(2)	2113(2)	39(1)
C(124)	4485(4)	8304(2)	1755(2)	31(1)
C(125)	2334(5)	8258(3)	211(3)	51(1)
C(126)	5638(5)	8661(3)	2026(2)	42(1)
C(127)	3621(4)	10779(2)	854(2)	28(1)
C(128)	2389(4)	10553(3)	987(2)	36(1)
C(129)	1647(5)	10928(3)	1383(2)	46(1)
C(130)	2086(6)	11507(3)	1644(3)	54(2)
C(131)	3297(6)	11734(3)	1497(3)	51(1)
C(132)	4085(5)	11376(2)	1102(2)	41(1)
C(133)	1859(5)	9924(3)	700(3)	47(1)
C(134)	5365(6)	11642(3)	920(3)	57(2)

Re(2)	6090(1)	4930(1)	385(1)	25(1)
N(21)	6911(3)	4179(2)	478(2)	31(1)
N(22)	4251(3)	4844(2)	516(2)	27(1)
N(23)	6783(3)	5580(2)	826(2)	30(1)
C(211)	7770(4)	3682(2)	636(2)	30(1)
C(212)	7566(5)	3276(2)	1173(2)	39(1)
C(213)	8438(6)	2776(3)	1311(3)	56(2)
C(214)	9499(6)	2679(3)	944(4)	63(2)
C(215)	9697(5)	3087(3)	437(3)	57(2)
C(216)	8859(5)	3595(3)	263(3)	43(1)
C(217)	6456(6)	3399(3)	1578(3)	52(1)
C(218)	9110(6)	4051(4)	-283(3)	65(2)
C(219)	3493(4)	4683(2)	1042(2)	31(1)
C(220)	3287(4)	5162(2)	1512(2)	36(1)
C(221)	2551(5)	4983(3)	2028(2)	43(1)
C(222)	2045(5)	4359(3)	2079(3)	50(1)
C(223)	2244(4)	3896(3)	1615(3)	46(1)
C(224)	2976(4)	4047(2)	1090(2)	38(1)
C(225)	3855(5)	5834(3)	1468(3)	45(1)
C(226)	3207(5)	3540(3)	583(3)	47(1)
C(227)	7527(4)	6006(2)	1211(2)	31(1)
C(228)	7194(5)	6679(2)	1254(2)	40(1)
C(229)	7993(5)	7082(3)	1645(3)	48(1)
C(230)	9064(6)	6849(3)	1966(3)	54(1)
C(231)	9355(5)	6187(3)	1927(3)	47(1)
C(232)	8615(4)	5751(2)	1553(2)	37(1)
C(233)	6021(5)	6959(3)	916(3)	53(1)
C(234)	8947(6)	5037(3)	1518(3)	54(2)

Table 78. Bond lengths [Å] and angles [°].

Re(1)-N(11)	1.754(4)	Re(1)-N(12)	1.763(3)	Re(1)-N(13)	1.951(3)
Re(1)-N(13)#1	1.953(3)	Re(1)-Re(1)#1	2.7267(3)	N(11)-C(111)	1.384(6)
N(12)-C(119)	1.384(5)	N(13)-C(127)	1.437(5)	N(13)-Re(1)#1	1.953(3)
C(111)-C(112)	1.405(7)	C(111)-C(116)	1.414(7)	C(112)-C(113)	1.390(7)
C(112)-C(117)	1.501(8)	C(113)-C(114)	1.362(10)	C(114)-C(115)	1.369(11)
C(115)-C(116)	1.406(8)	C(116)-C(118)	1.502(9)	C(119)-C(120)	1.400(6)
C(119)-C(124)	1.423(6)	C(120)-C(121)	1.386(6)	C(120)-C(125)	1.511(7)
C(121)-C(122)	1.387(7)	C(122)-C(123)	1.380(7)	C(123)-C(124)	1.406(6)
C(124)-C(126)	1.496(7)	C(127)-C(132)	1.396(7)	C(127)-C(128)	1.405(6)
C(128)-C(129)	1.386(7)	C(128)-C(133)	1.507(7)	C(129)-C(130)	1.368(8)
C(130)-C(131)	1.391(9)	C(131)-C(132)	1.396(7)	C(132)-C(134)	1.506(8)
Re(2)-N(23)	1.750(4)	Re(2)-N(21)	1.756(4)	Re(2)-N(22)#2	1.957(4)
Re(2)-N(22)	1.959(4)	Re(2)-Re(2)#2	2.7440(3)	N(21)-C(211)	1.382(5)
N(22)-C(219)	1.421(5)	N(22)-Re(2)#2	1.957(4)	N(23)-C(227)	1.395(6)
C(211)-C(216)	1.416(7)	C(211)-C(212)	1.418(7)	C(212)-C(213)	1.385(7)

C(212)-C(217)	1.485(8)	C(213)-C(214)	1.388(10)	C(214)-C(215)	1.368(10)
C(215)-C(216)	1.391(8)	C(216)-C(218)	1.502(8)	C(219)-C(224)	1.404(7)
C(219)-C(220)	1.406(7)	C(220)-C(221)	1.399(7)	C(220)-C(225)	1.493(7)
C(221)-C(222)	1.379(9)	C(222)-C(223)	1.374(8)	C(223)-C(224)	1.400(7)
C(224)-C(226)	1.506(8)	C(227)-C(228)	1.415(7)	C(227)-C(232)	1.414(6)
C(228)-C(229)	1.405(7)	C(228)-C(233)	1.499(7)	C(229)-C(230)	1.364(8)
C(230)-C(231)	1.382(9)	C(231)-C(232)	1.394(7)	C(232)-C(234)	1.493(8)

N(11)-Re(1)-N(12)	113.48(17)	N(11)-Re(1)-N(13)	114.09(16)
N(12)-Re(1)-N(13)	112.18(15)	N(11)-Re(1)-N(13)#1	109.72(15)
N(12)-Re(1)-N(13)#1	114.09(15)	N(13)-Re(1)-N(13)#1	91.40(14)
N(11)-Re(1)-Re(1)#1	122.26(13)	N(12)-Re(1)-Re(1)#1	124.23(12)
N(13)-Re(1)-Re(1)#1	45.74(10)	N(13)#1-Re(1)-Re(1)#1	45.66(10)
C(111)-N(11)-Re(1)	156.2(3)	C(119)-N(12)-Re(1)	168.8(3)
C(127)-N(13)-Re(1)	136.7(3)	C(127)-N(13)-Re(1)#1	133.6(3)
Re(1)-N(13)-Re(1)#1	88.60(14)	N(11)-C(111)-C(112)	119.6(4)
N(11)-C(111)-C(116)	119.2(5)	C(112)-C(111)-C(116)	121.2(5)
C(113)-C(112)-C(111)	117.9(5)	C(113)-C(112)-C(117)	120.8(5)
C(111)-C(112)-C(117)	121.4(4)	C(114)-C(113)-C(112)	122.3(6)
C(113)-C(114)-C(115)	119.4(5)	C(114)-C(115)-C(116)	122.2(6)
C(115)-C(116)-C(111)	116.8(6)	C(115)-C(116)-C(118)	123.1(6)
C(111)-C(116)-C(118)	120.0(5)	N(12)-C(119)-C(120)	120.9(4)
N(12)-C(119)-C(124)	117.8(4)	C(120)-C(119)-C(124)	121.2(4)
C(121)-C(120)-C(119)	118.8(4)	C(121)-C(120)-C(125)	119.5(4)
C(119)-C(120)-C(125)	121.6(4)	C(120)-C(121)-C(122)	120.8(5)
C(123)-C(122)-C(121)	120.9(4)	C(122)-C(123)-C(124)	120.5(5)
C(123)-C(124)-C(119)	117.8(4)	C(123)-C(124)-C(126)	121.1(4)
C(119)-C(124)-C(126)	121.1(4)	C(132)-C(127)-C(128)	121.1(4)
C(132)-C(127)-N(13)	119.1(4)	C(128)-C(127)-N(13)	119.8(4)
C(129)-C(128)-C(127)	118.6(5)	C(129)-C(128)-C(133)	119.9(5)
C(127)-C(128)-C(133)	121.5(4)	C(130)-C(129)-C(128)	121.6(5)
C(129)-C(130)-C(131)	119.3(5)	C(132)-C(131)-C(130)	121.5(5)
C(131)-C(132)-C(127)	117.9(5)	C(131)-C(132)-C(134)	121.0(5)
C(127)-C(132)-C(134)	121.0(4)	N(23)-Re(2)-N(21)	114.10(17)
N(23)-Re(2)-N(22)#2	112.56(16)	N(21)-Re(2)-N(22)#2	112.23(16)
N(23)-Re(2)-N(22)	112.25(15)	N(21)-Re(2)-N(22)	112.58(16)
N(22)#2-Re(2)-N(22)	91.02(15)	N(23)-Re(2)-Re(2)#2	122.95(12)
N(21)-Re(2)-Re(2)#2	122.95(12)	N(22)#2-Re(2)-Re(2)#2	45.54(10)

N(22)-Re(2)-Re(2)#2	45.47(11)	C(211)-N(21)-Re(2)	166.0(3)
C(219)-N(22)-Re(2)#2	135.7(3)	C(219)-N(22)-Re(2)	135.3(3)
Re(2)#2-N(22)-Re(2)	88.98(15)	C(227)-N(23)-Re(2)	168.4(3)
N(21)-C(211)-C(216)	119.2(4)	N(21)-C(211)-C(212)	119.8(4)
C(216)-C(211)-C(212)	121.0(4)	C(213)-C(212)-C(211)	118.1(5)
C(213)-C(212)-C(217)	121.8(5)	C(211)-C(212)-C(217)	120.1(4)
C(214)-C(213)-C(212)	121.4(6)	C(215)-C(214)-C(213)	119.6(5)
C(214)-C(215)-C(216)	122.5(6)	C(215)-C(216)-C(211)	117.4(5)
C(215)-C(216)-C(218)	121.8(5)	C(211)-C(216)-C(218)	120.8(5)
C(224)-C(219)-C(220)	121.1(4)	C(224)-C(219)-N(22)	119.7(4)
C(220)-C(219)-N(22)	119.2(4)	C(221)-C(220)-C(219)	117.7(5)
C(221)-C(220)-C(225)	121.2(5)	C(219)-C(220)-C(225)	121.1(4)
C(222)-C(221)-C(220)	121.6(5)	C(221)-C(222)-C(223)	120.3(5)
C(222)-C(223)-C(224)	120.5(5)	C(223)-C(224)-C(219)	118.9(5)
C(223)-C(224)-C(226)	120.8(5)	C(219)-C(224)-C(226)	120.4(4)
N(23)-C(227)-C(228)	120.3(4)	N(23)-C(227)-C(232)	118.7(4)
C(228)-C(227)-C(232)	121.0(4)	C(229)-C(228)-C(227)	117.3(5)
C(229)-C(228)-C(233)	120.4(5)	C(227)-C(228)-C(233)	122.3(5)
C(230)-C(229)-C(228)	122.5(5)	C(229)-C(230)-C(231)	119.1(5)
C(230)-C(231)-C(232)	122.2(5)	C(231)-C(232)-C(227)	117.7(5)
C(231)-C(232)-C(234)	121.4(5)	C(227)-C(232)-C(234)	120.9(4)

Symmetry transformations used to generate equivalent atoms:

#1 -x+1,-y+2,-z #2 -x+1,-y+1,-z

Table 79. Anisotropic displacement parameters ($Å^2 x\ 10^3$). The anisotropic displacement factor exponent takes the form: $-2\pi^2[\ h^2\ a^{*2}U^{11} + ... + 2\ h\ k\ a^*\ b^*\ U^{12}\ ]$

	U^{11}	U^{22}	U^{33}	U^{23}	U^{13}	U^{12}
Re(1)	22(1)	23(1)	22(1)	2(1)	-2(1)	0(1)
N(11)	26(2)	37(2)	28(2)	-1(2)	-4(1)	0(2)
N(12)	33(2)	23(2)	33(2)	3(2)	3(1)	-3(1)
N(13)	19(2)	25(2)	28(2)	-1(1)	-2(1)	3(1)
C(111)	24(2)	48(3)	31(2)	9(2)	-5(2)	-8(2)
C(112)	24(2)	50(3)	48(3)	16(2)	3(2)	1(2)
C(113)	27(2)	64(4)	74(4)	31(3)	-5(2)	2(2)
C(114)	36(3)	84(5)	84(5)	40(4)	-31(3)	-16(3)
C(115)	49(3)	100(6)	46(3)	12(3)	-24(3)	-33(4)
C(116)	38(3)	56(3)	41(3)	6(2)	-8(2)	-15(2)
C(117)	47(3)	46(3)	66(4)	4(3)	3(3)	16(2)

C(118)	66(4)	84(5)	54(4)	-27(4)	-10(3)	-5(4)
C(119)	30(2)	23(2)	33(2)	1(2)	7(2)	4(2)
C(120)	35(2)	30(2)	37(2)	-1(2)	4(2)	-5(2)
C(121)	36(2)	34(2)	53(3)	-3(2)	9(2)	-5(2)
C(122)	51(3)	27(2)	56(3)	9(2)	20(2)	-4(2)
C(123)	44(3)	38(3)	36(2)	10(2)	11(2)	9(2)
C(124)	36(2)	23(2)	34(2)	3(2)	10(2)	4(2)
C(125)	52(3)	58(4)	42(3)	-5(3)	-5(2)	-17(3)
C(126)	41(3)	54(3)	32(2)	7(2)	-1(2)	4(2)
C(127)	32(2)	30(2)	22(2)	1(2)	0(2)	8(2)
C(128)	31(2)	44(3)	32(2)	6(2)	4(2)	8(2)
C(129)	38(3)	69(4)	31(2)	6(2)	10(2)	16(2)
C(130)	57(3)	68(4)	38(3)	-9(3)	6(2)	28(3)
C(131)	71(4)	38(3)	42(3)	-12(2)	-3(3)	14(3)
C(132)	48(3)	35(3)	40(3)	-9(2)	0(2)	3(2)
C(133)	32(3)	52(3)	59(3)	1(3)	11(2)	-6(2)
C(134)	56(3)	41(3)	73(4)	-17(3)	1(3)	-11(3)
Re(2)	22(1)	23(1)	30(1)	2(1)	-2(1)	0(1)
N(21)	31(2)	23(2)	39(2)	2(2)	2(2)	2(1)
N(22)	25(2)	26(2)	30(2)	3(1)	-2(1)	-2(1)
N(23)	24(2)	29(2)	36(2)	2(2)	-1(1)	1(1)
C(211)	29(2)	23(2)	37(2)	-4(2)	-10(2)	2(2)
C(212)	52(3)	26(2)	36(2)	-2(2)	-15(2)	-1(2)
C(213)	78(4)	29(3)	59(4)	-4(2)	-37(3)	8(3)
C(214)	56(3)	42(3)	89(5)	-17(3)	-40(3)	23(3)
C(215)	32(3)	55(3)	82(4)	-29(3)	-18(3)	13(2)
C(216)	32(2)	39(3)	58(3)	-12(2)	-6(2)	-2(2)
C(217)	69(4)	46(3)	41(3)	7(2)	5(3)	-5(3)
C(218)	49(3)	80(5)	67(4)	-2(4)	22(3)	-1(3)
C(219)	21(2)	41(2)	31(2)	7(2)	-3(2)	4(2)
C(220)	29(2)	41(3)	38(3)	4(2)	-2(2)	6(2)
C(221)	28(2)	68(4)	33(3)	0(2)	-1(2)	9(2)
C(222)	30(2)	77(4)	42(3)	20(3)	0(2)	-5(2)
C(223)	30(2)	59(3)	48(3)	18(3)	-4(2)	-13(2)
C(224)	25(2)	40(3)	48(3)	14(2)	-5(2)	-5(2)
C(225)	52(3)	37(3)	45(3)	-8(2)	6(2)	5(2)
C(226)	46(3)	38(3)	57(3)	8(2)	-7(2)	-18(2)
C(227)	35(2)	31(2)	28(2)	0(2)	1(2)	-6(2)
C(228)	40(3)	37(3)	43(3)	-4(2)	5(2)	-4(2)
C(229)	58(3)	36(3)	51(3)	-12(2)	7(2)	-11(2)
C(230)	54(3)	53(3)	53(3)	-15(3)	-6(3)	-20(3)
C(231)	41(3)	54(3)	45(3)	-4(2)	-13(2)	-12(2)
C(232)	28(2)	38(3)	46(3)	2(2)	-3(2)	-3(2)
C(233)	53(3)	32(3)	73(4)	-7(3)	3(3)	4(2)
C(234)	49(3)	46(3)	65(4)	-3(3)	-25(3)	4(2)

Table 80. Hydrogen coordinates (x 10^4) and isotropic displacement parameters ($Å^2$x 10^3).

	x	y	z	U(eq)
H(11B)	10112	8363	1448	66
H(11C)	10697	8966	2339	83
H(11D)	9687	9946	2534	79

H(11E)	8848	8151	525	79
H(11F)	8361	8791	156	79
H(11G)	7406	8383	571	79
H(11H)	8119	10785	2261	102
H(11I)	6829	10491	1954	102
H(11J)	7812	10852	1516	102
H(12A)	1611	7399	1074	49
H(12B)	2413	7167	2099	53
H(12C)	4180	7721	2530	47
H(12D)	1595	7978	121	76
H(12E)	2974	8175	-101	76
H(12F)	2074	8716	188	76
H(12G)	5851	8500	2454	63
H(12H)	5455	9129	2044	63
H(12I)	6356	8587	1756	63
H(12J)	822	10780	1475	55
H(13B)	1576	11750	1918	65
H(13C)	3591	12137	1669	61
H(13D)	1000	9851	845	71
H(13E)	2405	9558	835	71
H(13F)	1831	9957	237	71
H(13G)	5530	12056	1139	85
H(13H)	5358	11712	461	85
H(13I)	6033	11329	1043	85
H(21A)	8308	2496	1660	68
H(21B)	10078	2336	1044	76
H(21C)	10427	3021	197	68
H(21D)	6459	3079	1922	78
H(21E)	5667	3359	1319	78
H(21F)	6519	3839	1756	78
H(21G)	9888	3916	-484	97
H(21H)	9210	4497	-123	97
H(21I)	8394	4033	-594	97
H(22B)	2397	5296	2347	52
H(22C)	1563	4251	2433	60
H(22D)	1885	3474	1651	55
H(22E)	3616	6095	1833	67
H(22F)	3538	6045	1076	67
H(22G)	4782	5800	1466	67
H(22H)	2787	3131	691	71
H(22I)	4121	3465	558	71
H(22J)	2862	3697	172	71
H(22K)	7782	7529	1686	58
H(23A)	9598	7136	2210	64
H(23B)	10077	6026	2162	57
H(23C)	5967	7426	1006	79
H(23D)	5265	6739	1065	79
H(23E)	6073	6893	459	79
H(23F)	9713	4952	1785	81
H(23G)	9101	4920	1079	81
H(23H)	8243	4777	1669	81

Appendix XVII

X-ray data for $Re_2(NAr)_6$

The tables that follow contain atomic coordinates and equivalent isotropic displacement parameters, complete bond lengths (Å) and angles (°), anisotropic displacement parameters and calculated H-atom positions for $Re_2(NAr)_6$.

Table 81. Atomic coordinates (x 10^4) and equivalent isotropic displacement parameters ($Å^2$x 10^3). U(eq) is defined as one third of the trace of the orthogonalized U^{ij} tensor.

	x	y	z	U(eq)
Re	6667	3333	3745(1)	34(1)
N	7015(4)	2259(4)	3871(1)	39(1)
C(1)	7336(5)	1511(5)	4046(2)	40(1)
C(2)	6776(6)	342(6)	3935(2)	53(2)
C(3)	7177(9)	-358(7)	4096(3)	77(2)
C(4)	8061(10)	51(8)	4370(3)	81(3)
C(5)	8567(8)	1186(8)	4493(2)	64(2)
C(6)	8240(6)	1942(6)	4336(2)	49(1)
C(7)	5786(7)	-171(6)	3628(3)	62(2)
C(8)	4785(10)	-1342(8)	3759(4)	99(3)
C(9)	6214(10)	-292(9)	3229(3)	84(3)
C(10)	8843(8)	3190(7)	4470(3)	71(2)
C(11)	10144(9)	3708(10)	4536(3)	94(3)
C(12)	8300(11)	3298(13)	4848(5)	143(6)

Table 82. Bond lengths [Å] and angles [°].

Re-N	1.760(5)	Re-N#1	1.760(5)	Re-N#2	1.760(5)
Re-Re#3	2.7428(7)	N-C(1)	1.392(7)	C(1)-C(2)	1.396(9)
C(1)-C(6)	1.421(9)	C(2)-C(3)	1.393(10)	C(2)-C(7)	1.531(10)
C(3)-C(4)	1.367(13)	C(4)-C(5)	1.372(12)	C(5)-C(6)	1.383(9)
C(6)-C(10)	1.505(10)	C(7)-C(9)	1.489(13)	C(7)-C(8)	1.521(12)
C(10)-C(12)	1.495(16)	C(10)-C(11)	1.525(13)		
N-Re-N#1	114.50(12)	N-Re-N#2	114.50(12)	N#1-Re-N#2	114.50(11)
N-Re-Re#3	103.80(15)	N#1-Re-Re#3	103.80(15)	N#2-Re-Re#3	103.80(15)
C(1)-N-Re	168.5(4)	N-C(1)-C(2)	120.0(5)	N-C(1)-C(6)	119.8(5)
C(2)-C(1)-C(6)	120.2(6)	C(1)-C(2)-C(3)	118.2(7)	C(1)-C(2)-C(7)	122.3(6)
C(3)-C(2)-C(7)	119.4(7)	C(4)-C(3)-C(2)	122.1(8)	C(5)-C(4)-C(3)	119.3(7)
C(4)-C(5)-C(6)	121.8(7)	C(5)-C(6)-C(1)	118.3(6)	C(5)-C(6)-C(10)	120.1(7)
C(1)-C(6)-C(10)	121.6(6)	C(9)-C(7)-C(8)	109.4(8)	C(9)-C(7)-C(2)	110.8(7)
C(8)-C(7)-C(2)	112.5(8)	C(12)-C(10)-C(6)	109.9(9)		
C(12)-C(10)-C(11)	109.2(9)	C(6)-C(10)-C(11)	113.6(8)		

Symmetry transformations used to generate equivalent atoms:

#1 -y+1,x-y,z #2 -x+y+1,-x+1,z #3 -x+4/3,-y+2/3,-z+2/3

Table 83. Anisotropic displacement parameters ($Å^2 x\ 10^3$). The anisotropic displacement factor exponent takes the form: $-2\pi^2[\ h^2\ a^{*2}U^{11} + ... + 2\ h\ k\ a^*\ b^*\ U^{12}\ ]$

U^{11}	U^{22}	U^{33}	U^{23}	U^{13}	U^{12}	
Re27(1)	27(1)	49(1)	0	0	13(1)	
N 33(2)	37(2)	46(2)	-4(2)	-1(2)	18(2)	
C(1)41(3)	39(3)	46(3)	6(2)	6(2)	25(2)	
C(2)61(4)	42(3)	60(4)	3(3)	1(3)	30(3)	
C(3)115(7)	52(4)	82(5)	0(4)	-14(5)	56(5)	
C(4)121(8)	80(6)	75(5)	8(4)	-12(5)	75(6)	
C(5)77(5)	80(5)	56(4)	6(3)	-7(3)	56(5)	
C(6)52(4)	55(4)	51(3)	1(3)	-3(3)	34(3)	
C(7)62(4)	34(3)	92(5)	-7(3)	-13(4)	25(3)	
C(8)80(7)	61(6)	129(9)	-4(6)	12(6)	14(5)	
C(9)92(7)	84(6)	70(5)	10(4)	-14(5)	39(6)	
C(10)	76(5)	65(5)	82(5)	-17(4)	-35(4)	42(4)
C(11)	69(6)	97(8)	99(7)	-17(6)	-24(5)	28(5)
C(12)	94(9)	120(11)	207(16)	-92(11)	-4(9)	48(8)

Table 84. Hydrogen coordinates (x 10^4) and isotropic displacement parameters ($Å^2$x 10^3).

	x	y	z	U(eq)
H(3A)	6829	-1138	4015	92
H(4A)	8319	-439	4472	97
H(5A)	9152	1457	4689	77
H(7A)	5486	373	3600	75
H(8A)	4184	-1633	3555	149
H(8B)	4470	-1253	4010	149
H(8C)	5063	-1885	3795	149
H(9A)	5573	-623	3040	127
H(9B)	6543	-796	3252	127
H(9C)	6805	466	3134	127
H(10A)	8732	3650	4259	86
H(11A)	10480	4510	4620	142
H(11B)	10506	3674	4288	142
H(11C)	10274	3270	4742	142
H(12A)	7471	2965	4807	214
H(12B)	8640	4112	4918	214
H(12C)	8435	2889	5062	214

Appendix XVIII

Is there correlation between terminal imido bond lengths and angles?

There has been much discussion in the literature about the correlation between M-N(imido) bond lengths and M-N(imido)-C angles and its implications for the nature of the metal-imido bond. Bent and linear imido coordination are often taken to represent metal-nitrogen double and triple bonds respectively. However, inspection of the experimental imido bond angles and lengths suggests that trends in M-N(imido) bond lengths and M-N(imido)-C bond angles are not so clear cut. In figure 70 experimental M-N(imido)-C angles are plotted against M-N(imido) bond lengths for the complexes reported within this thesis (appendix II) and for the complexes of appendices III and IV (this excludes bis(imido) complexes and dimers containing bridging imido ligands).

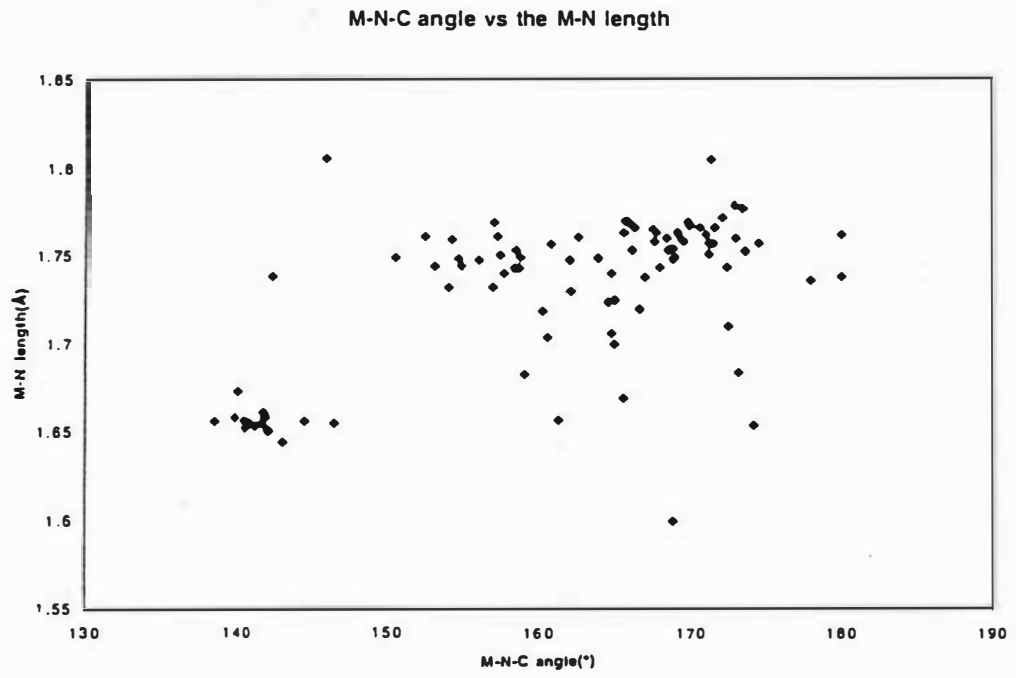

Figure 70

It is obvious that there is no correlation between the two parameters. Most M-N(imido) bond lengths lie between 1.7 and 1.8Å regardless of the M-N(imido)-C angle. The small cluster of points below M-N(imido)-C angles of 150° are all Mn tris(imido) complexes (apart from 2 Re complexes) which contain the shorter M-N(imido) lengths (~1.64Å), but also have the most bent imido ligands (138 to 150°).

References

1. (a) Wigley, D.E. *Prog. Inorg. Chem.* **1994,** *42,* 239.
   (b) Nugent, W.A.; Mayer, J.M. "Metal-Ligand Multiple Bonds" John Wiley and Sons, New York, **1988.**
   (c) Romao, C.C.; Kuhn, F.E.; Herrmann, W.A. *Chem. Rev.* **1997,** *97,* 3197.
2. Walsh, P.J.; Baranger, A.M.; Bergman, R.G. *J. Am. Chem. Soc.* **1992,** *114,* 1708.
3. McGrane, P.L.; Jensen, M.; Livinghouse, T. *J. Am. Chem. Soc.* **1992,** *114,* 5459.
4. McGrane, P.L.; Livinghouse, T. *J. Am. Chem. Soc.* **1993,** *115,* 11485.
5. Schaller, C.P.; Bonanno, J.B.; Wolczanski, P.T. *J. Am. Chem. Soc.* **1994,** *116,* 4133.
6. Walsh, P.J.; Hollander, F.J.; Bergman, R.G. *J. Am. Chem. Soc.* **1988,** *110,* 8729.
7. Doxsee, K.M.; Farahi, J.B.; Hope, H. *J. Am. Chem. Soc.* **1991,** *113,* 8889.
8. Blake, A.J.; Mountford, P.; Nikonov, G.I.; Swallow, D. *J. Chem. Soc., Chem. Comm.* **1996,** 1835.
9. Glueck, D.S.; Wu, J.; Hollander, F.J.; Bergman, R.G. *J. Am. Chem. Soc.* **1991,** *113,* 2041.
10. Bennett, J.L.; Wolczanski, P.T. *J. Am. Chem. Soc.* **1994,** *116,* 2179.
11. Walsh, P.J.; Hollander, F.J.; Bergman, R.G. *Organometallics* **1993,** *12,* 3705.
12. Williams, D.S.; Schrock, R.R. *Organometallics* **1993,** *12,* 1148.
13. Huber, S.H.; Baldwin, T.C.; Wigley, D.E. *Organometallics* **1993,** *12,* 91.
14. Chao, Y-W.; Rodgers, P.M.; Wigley, D.E.; Alexander, S.J.; Rheingold, A.L. *J. Am. Chem. Soc.* **1991,** *113,* 6326.

15. Cundari, T.R. *J. Am. Chem. Soc.* **1992,** *114*, 7879.

16. Burrell, A.K.; Bryan, J.C. *Organometallics* **1992,** *11*, 3501.

17. Burrell, A.K.; Clark, D.L.; Gordon, P.L.; Sattelberger, A.P.; Byran, J.C. *J. Am. Chem. Soc.* **1994,** *116*, 3813.

18. Wolf, J.R.; Bazan, G.C.; Schrock, R.R. *Inorg. Chem.* **1993,** *32*, 4155.

19. Williams, D.S.; Anhaus, J.T.; Schofield, M.H.; Schrock, R.R.; Davis, W.M. *J. Am. Chem. Soc.* **1991,** *113*, 5480.

20. Schafer II, D.F.; Wolczanski, P.T. *J. Am. Chem. Soc.* **1998,** *120*, 4881.

21. Herrmann, W.A.; Ding, H.; Kuhn, F.E.; Scherer, W. *Organometallics* **1998,** *17*, 2751.

22. Bryan, J.C.; Burrell, A.K.; Miller, M.M.; Smith, W.H.; Burns, C.J.; Sattelberger, A.P. *Polyhedron* **1993,** *12*, 1769.

23. Schaller, C.P.; Wolczanski, P.T. *Inorg. Chem.* **1993,** *32*, 131.

24. Horton, A.D.; de With, J. *Angew. Chem., Int. Ed. Engl.* **1993,** *32*, 903.

25. Cundari, T.R. *Organometallics* **1994,** *13*, 2987.

26. Anhaus, J.T.; Kee, T.P.; Schofield, M.H.; Schrock, R.R. *J. Am. Chem. Soc.* **1990,** *112*, 1642.

27. Schofield, M.H.; Kee, T.P.; Anhaus, J.T.; Schrock, R.R.; Johnson, K.; Davis, W.M. *Inorg. Chem.* **1991,** *30*, 3595.

28. Morrison, D.L.; Wigley, D.E. *Inorg. Chem.* **1995,** *34*, 2610.

29. Saboonchian, V.; Danopoulos, A.A.; Gutierrez, A.; Wilkinson, G.; Williams, D.J. *Polyhedron* **1991,** *10*, 2241.

30. Danopoulos, A.A.; Longley, C.J.; Wilkinson, G.; Hussain, B.; Hursthouse, M.B. *Polyhedron* **1989,** *8*, 2657.

31. Danopoulos, A.A.; Wilkinson, G.; Sweet, T.; Hursthouse, M.B. *J. Chem. Soc., Chem. Comm.* **1993,** 495.

32. Danopoulos, A.A.; Wilkinson, G.; Sweet, T.K.N.; Hursthouse, M.B. *J. Chem. Soc., Dalton Trans.* **1994,** 1037.

33. Burrell, A.K.; Bryan, J.C. *Angew. Chem., Int. Ed. Engl.* **1993,** *32*, 94.

34. Chong, A.O.; Oshima, K.; Sharpless, K.B. *J. Am. Chem. Soc.* **1977,** *99*, 3420.

35. Benson, M.T.; Cundari, T.R.; Moody, E.W. *J. Organometal. Chem.* **1995,** *504*, 2995.

36. Boatz, J.A.; Gordon, M.S. *J. Phys. Chem.* **1989,** *93,* 1819.

37. Mayer, I. *Theoret. Chim. Acta* **1985,** *67,* 315.

38. Cundari, T.R. *Organometallics* **1993,** *12*, 1998.

39. Benson, M.T.; Bryan, J.C.; Burrell, A.K.; Cundari, T.R. *Inorg. Chem.* **1995,** *34*, 2348.

40. Maatta, E.A.; Wentworth, R.A.D. *Inorg. Chem.* **1979,** *18*, 2409.

41. Herrmann, W.A.; Weichselbaumer, G.; Paciello, R.A.; Fischer, R.A.; Herdtweck, E.; Okuda, J.; Marz, D.W. *Organometallics* **1990,** *9,* 489.

42. Szyperski, T.; Schwerdtfeger, P. *Angew. Chem., Int. Ed. Engl.* **1989,** *28*, 1228.

43. Burrell, A.K.; Bryan, J.C. *Organometallics* **1993,** *12*, 2426.

44. Smith, D.P.; Allen, K.D.; Carducci, M.D.; Wigley, D.E. *Inorg. Chem.* **1992,** *31*, 1319.

45. Deutsch, E.; Libson, K.; Jurisson, S. *Prog. Inorg. Chem.* **1983,** *30,* 75.

46. Haymore, B.L.; Maatta, E.A.; Wentworth, R.A.D. *J. Am. Chem. Soc.* **1979,** *101*, 2063.

47. Danopoulos, A.A.; Wilkinson, G. *Polyhedron* **1990,** *9*, 1009.

48. Gutierrez, A.; Wilkinson, G.; Hussain-Bates, B.; Hursthouse, M.B. *Polyhedron* **1990,** *9*, 2081.

49. Legzdins, P.; Phillips, E.C.; Rettig, S.J.; Trotter, J.; Veltheer, J.E.; Yee, V.C. *Organometallics* **1992,** *11*, 3104.

50. Arnold, R.G.; Nelson, J.A.; Verbanc, J.J. *Chem. Rev.* **1957,** *57,* 47.

51. Horton, A.D.; Schrock, R.R. *Polyhedron* **1988,** *7*, 1841.

52. Lu, Y-j.; Ansari, M.A.; Ibers, J.A. *Inorg. Chem.* **1989,** *28,* 4049.

53. Hadjikyriacou, A.I.; Coucouvanis, D. *Inorg. Chem.* **1987,** *26,* 2400.

54. Danopoulos, A.A.; Wilkinson, G.; Hussain-Bates, B.; Hursthouse, M.B. *J. Chem. Soc., Dalton Trans.* **1991,** 269.

55. Chisholm, M.H.; Corning, J.F.; Folting, K.; Huffman, J.C. *Polyhedron* **1985,** *4*, 383.

56. Summerville, R.H.; Hoffmann, R. *J. Am. Chem. Soc.* **1976,** *98*, 7240.

57. Arney, D.J.; Bruck, M.A.; Huber, S.R.; Wigley, D.E. *Inorg. Chem.* **1992,** *31*, 3749.

58. Kee, T.P.; Park, L.Y.; Robbins, J.; Schrock, R.R. *J. Chem. Soc., Chem. Comm.* **1991,** 121.

59. Arney, D.S.J.; Burns, C.J. *J. Am. Chem. Soc.* **1995,** *117*, 9448.

60. de With, J.; Horton, A.D. *Organometallics* **1993,** *12*, 1493.

61. Nugent, W.A.; Harlow, R.L. *J. Chem. Soc., Chem. Comm.* **1979,** 1105.

62. Danopoulos, A.A.; Wilkinson, G.; Hussain, B.; Hursthouse, M.B. *J. Chem. Soc., Chem. Comm.* **1989,** 896.

63. Cook, M.R.; Herrmann, W.A.; Kiprof, P.; Takacs, J. *J. Chem. Soc., Dalton Trans.* **1991,** 797.

64. Toreki, R.; Schrock, R.R.; Davis, W.M. *J. Am. Chem. Soc.* **1992,** *114*, 3367.

65. Mealli, C.; Lopez, J.A.; Calhorda, M.J.; Romao, C.C.; Herrmann, W.A. *Inorg. Chem.* **1994,** *33*, 1139.

66. Gobbi, A.; Frenking, G. *J. Am. Chem. Soc.* **1994,** *116*, 9275.

67. Danopoulos, A.A.; Wilkinson, G.; Sweet, T.K.N.; Hursthouse, M.B. *J. Chem. Soc., Dalton Trans.* **1996,** 2995.

68. Danopoulos, A.A.; Wilkinson, G.; Sweet, T.K.N.; Hursthouse, M.B. *J. Chem. Soc., Dalton Trans.* **1995,** 937.

69. Danopoulos, A.A.; Wilkinson, G.; Hussain, B.; Hursthouse, M.B. *Polyhedron* **1989,** *8*, 2947.

70. Danopoulos, A.A.; Wilkinson, G.; Hussain-Bates, B.; Hursthouse, M.B. *J. Chem. Soc., Dalton Trans.* **1990,** 2753.

71. Longley, C.J.; Savage, P.D.; Wilkinson, G.; Hussain, B.; Hursthouse, M.B. *Polyhedron* **1988,** *7*, 1079.

72. Edwards, D.S.; Biondi, L.V.; Ziller, J.W.; Churchill, M.R.; Schrock, R.R. *Organometallics* **1983,** *2*, 1505.

73. $Re_2(NAr')_4(\mu\text{-}NAr')_2$ has previously been mentioned, see reference 12.

74. Gibson, V.C. *J. Chem. Soc., Dalton Trans.* **1994,** 1607.

75. Green, M.L.H.; Hogarth, G.; Konidaris, P.C.; Mountford, P. *J. Organometal. Chem.* **1990,** *394*, C9.

76. Hogarth, G.; Konidaris, P.C. *J. Organometal. Chem.* **1990,** *399*, 149.

77. Ashcroft, B.R.; Nielson, A.J.; Bradley, D.C.; Hursthouse, M.B.; Short, R.L.; Errington, R.J. *J. Chem. Soc., Dalton Trans.* **1987,** 2059.

78. Ashcroft, B.R.; Bradley, D.C.; Clark, G.R.; Errington, R.J.; Nielson, A.J.; Rickard, C.E.F. *J. Chem. Soc., Chem. Comm.* **1987,** 170.

79. Clark, G.R.; Nielson, A.J.; Rickard, C.E.F. *Polyhedron* **1988,** *7*, 117.

80. Dyer, P.W.; Howard, J.A.K.; Gibson, V.C.; Whittle, B.; Wilson, C. *J. Chem. Soc., Chem. Comm.* **1992,** 1666.

81. Bell, A.; Clegg, W.; Dyer, P.W.; Elsegood, M.R.J.; Gibson, V.C.; Marshall, E.L. *J. Chem. Soc., Chem. Comm.* **1994,** 2547.

82. Bell, A.; Clegg, W.; Dyer, P.W.; Elsegood, M.R.J.; Gibson, V.C.; Marshall, E.L. *J. Chem. Soc., Chem. Comm.* **1994,** 2247.

83. Copley, R.C.B.; Dyer, P.W.; Gibson, V.C.; Howard, J.A.K.; Marshall, E.L.; Wang, W.; Whittle, B. *Polyhedron* **1996,** *15*, 3001.

84. Jernakoff, P.; Geoffroy, G.L.; Rheingold, A.L.; Geib, S.J. *J. Chem. Soc., Chem. Comm.* **1987,** 1610.

85. Schrock, R.R.; Murdzek, J.S.; Bazan, G.C.; Robbins, J.; DiMare, M.; O'Regan, M. *J. Am. Chem. Soc.* **1990,** *112*, 3875.

86. Jolly, M.; Mitchell, J.P.; Gibson, V.C. *J. Chem. Soc., Dalton Trans.* **1992,** 1329.

87. Jolly, M.; Mitchell, J.P.; Gibson, V.C. *J. Chem. Soc., Dalton Trans.* **1992,** 1331.

88. Rankin, D.W.H.; Robertson, H.E.; Danopoulos, A.A.; Lyne, P.D.; Mingos, M.P.; Wilkinson, G. *J. Chem. Soc., Dalton Trans.* **1994,** 1563.

89. Danopoulos, A.A.; Wilkinson, G.; Hussain-Bates, B.; Hursthouse, M.B. *J. Chem. Soc., Dalton Trans.* **1991,** 1855.

90. Cummins, C.C.; Baxter, S.M.; Wolczanski, P.T. *J. Am. Chem. Soc.* **1988,** *110*, 8731.

91. Toreki, R.; Schrock, R.R. *J. Am. Chem. Soc.* **1990,** *112*, 2448.

92. Schrock, R.R.; DePue, R.T.; Feldman, J.; Yap, K.B.; Yang, D.C.; Davis, W.M.; Park, L.; DiMare, M.; Schofield, M.; Anhaus, J.; Walborsky, E.; Evitt, E.; Kruger, C.; Betz, P. *Organometallics* **1990,** *9*, 2262.

93. Fox, H.H.; Yap, K.B.; Schrock, R.R.; Robbins, J.; Cai, S. *Inorg. Chem.* **1992,** *31*, 2287.

94. Nugent, W.A. *Inorg. Chem.* **1983,** *22*, 965.

95. Sullivan, A.C.; Wilkinson, G.; Motevalli, M.; Hursthouse, M.B. *J. Chem. Soc., Dalton Trans.* **1988,** 53.

96. Ehrenfeld, D.; Kress, J.; Moore, B.D.; Osborn, J.A.; Schoettel, G. *J. Chem. Soc., Chem. Comm.* **1987,** 129.

97. Weinstock, I.A.; Schrock, R.R.; Davis, W.M. *J. Am. Chem. Soc.* **1991,** *113*, 135.

98. de With, J.; Horton, A.D.; Orpen, A.G. *Organometallics* **1990,** *9*, 2207.

99. Chew, K.C.; Clegg, W.; Coles, M.P.; Elsegood, M.R.J.; Williams, D.J.; Gibson, V.C.; White, A.J.P. *J. Chem. Soc., Dalton Trans.* **1999,** 2633.

100. Cheng, J.Y.K.; Cheung, K-K.; Chan, M.C.W.; Wong, K-Y.; Che, C-M. *Inorg. Chim. Acta* **1998,** *272*, 176.

101. Nugent, W.A.; Harlow, R.L. *Inorg. Chem.* **1980,** *19*, 777.

102. Danopoulos, A.A.; Wilkinson, G.; Williams, D.J. *J. Chem. Soc., Chem. Comm.* **1991,** 181.

103. Danopoulos, A.A.; Hankin, D.M.; Wilkinson, G.; Cafferkey, S.M.; Sweet, T.N.K.; Hursthouse, M.B. *Polyhedron* **1997,** *16*, 3879.

104. Schoop, T.; Roesky, H.W.; Noltemeyer, M.; Schmidt, H-G. *Organometallics* **1993,** *12*, 571.

105. Bradley, D.C.; Errington, R.J.; Hursthouse, M.B.; Short, R.L.; Ashcroft, B.R.; Clark, G.R.; Nielson, A.J.; Rickard, C.E.F. *J. Chem. Soc., Dalton Trans.* **1987,** 2067.

106. Herrmann, W.A.; Kuchler, J.G.; Felixberger, J.K.; Herdtweck, E.; Wagner, W. *Angew. Chem., Int. Ed. Engl.* **1988,** *27*, 394.

107. Cai, S.; Hoffman, D.M.; Huffman, J.C.; Wierda, D.A.; Woo, H-G. *Inorg. Chem.* **1987,** *26*, 3693.

108. Huggins, J.M.; Whitt, D.R.; Lebioda, L. *J. Organometal. Chem.* **1986,** *312*, C15.

109. Toreki, R.; Schrock, R.R.; Vale, M.G. *J. Am. Chem. Soc.* **1991,** *113*, 3610.

110. Herrmann, W.A.; Romao, C.C.; Kiprof, P.; Behm, J.; Cook, M.R.; Taillefer, M. *J. Organometal. Chem.* **1991,** *413*, 11.

111. Valencia, E.; Santarsiero, B.D.; Geib, S.J.; Rheingold, A.L.; Mayer, J.M. *J. Am. Chem. Soc.* **1987,** *109*, 6896.

112. Bryson, N.; Youinou, M-T.; Osborn, J.A. *Organometallics* **1991,** *10*, 3389.

113. Takacs, J.; Kiprof, P.; Riede, J.; Herrmann, W.A. *Organometallics* **1990,** *9*, 782.

114. Hendrikson, Sohn, Gray. *Inorg. Chem.* **1971,** *10*, 1559.

115. Schofield, M.H.; Schrock, R.R.; Park, L.Y. *Organometallics* **1991,** *10*, 1844.